



EVOLUTION OF GENETIC MECHANISMS OF ANTIBIOTIC RESISTANCE

EDITED BY: Silvia Buroni, Simona Pollini, Gian Maria Rossolini and Elena Perrin
PUBLISHED IN: *Frontiers in Genetics* and *Frontiers in Microbiology*



frontiers

Frontiers eBook Copyright Statement

The copyright in the text of individual articles in this eBook is the property of their respective authors or their respective institutions or funders. The copyright in graphics and images within each article may be subject to copyright of other parties. In both cases this is subject to a license granted to Frontiers.

The compilation of articles constituting this eBook is the property of Frontiers.

Each article within this eBook, and the eBook itself, are published under the most recent version of the Creative Commons CC-BY licence.

The version current at the date of publication of this eBook is CC-BY 4.0. If the CC-BY licence is updated, the licence granted by Frontiers is automatically updated to the new version.

When exercising any right under the CC-BY licence, Frontiers must be attributed as the original publisher of the article or eBook, as applicable.

Authors have the responsibility of ensuring that any graphics or other materials which are the property of others may be included in the CC-BY licence, but this should be checked before relying on the CC-BY licence to reproduce those materials. Any copyright notices relating to those materials must be complied with.

Copyright and source acknowledgement notices may not be removed and must be displayed in any copy, derivative work or partial copy which includes the elements in question.

All copyright, and all rights therein, are protected by national and international copyright laws. The above represents a summary only. For further information please read Frontiers' Conditions for Website Use and Copyright Statement, and the applicable CC-BY licence.

ISSN 1664-8714

ISBN 978-2-88963-222-0

DOI 10.3389/978-2-88963-222-0

About Frontiers

Frontiers is more than just an open-access publisher of scholarly articles: it is a pioneering approach to the world of academia, radically improving the way scholarly research is managed. The grand vision of Frontiers is a world where all people have an equal opportunity to seek, share and generate knowledge. Frontiers provides immediate and permanent online open access to all its publications, but this alone is not enough to realize our grand goals.

Frontiers Journal Series

The Frontiers Journal Series is a multi-tier and interdisciplinary set of open-access, online journals, promising a paradigm shift from the current review, selection and dissemination processes in academic publishing. All Frontiers journals are driven by researchers for researchers; therefore, they constitute a service to the scholarly community. At the same time, the Frontiers Journal Series operates on a revolutionary invention, the tiered publishing system, initially addressing specific communities of scholars, and gradually climbing up to broader public understanding, thus serving the interests of the lay society, too.

Dedication to Quality

Each Frontiers article is a landmark of the highest quality, thanks to genuinely collaborative interactions between authors and review editors, who include some of the world's best academicians. Research must be certified by peers before entering a stream of knowledge that may eventually reach the public - and shape society; therefore, Frontiers only applies the most rigorous and unbiased reviews.

Frontiers revolutionizes research publishing by freely delivering the most outstanding research, evaluated with no bias from both the academic and social point of view. By applying the most advanced information technologies, Frontiers is catapulting scholarly publishing into a new generation.

What are Frontiers Research Topics?

Frontiers Research Topics are very popular trademarks of the Frontiers Journals Series: they are collections of at least ten articles, all centered on a particular subject. With their unique mix of varied contributions from Original Research to Review Articles, Frontiers Research Topics unify the most influential researchers, the latest key findings and historical advances in a hot research area! Find out more on how to host your own Frontiers Research Topic or contribute to one as an author by contacting the Frontiers Editorial Office: researchtopics@frontiersin.org

EVOLUTION OF GENETIC MECHANISMS OF ANTIBIOTIC RESISTANCE

Topic Editors:

Silvia Buroni, University of Pavia, Italy

Simona Pollini, University of Florence, Italy

Gian Maria Rossolini, University of Florence, Italy

Elena Perrin, University of Florence, Italy

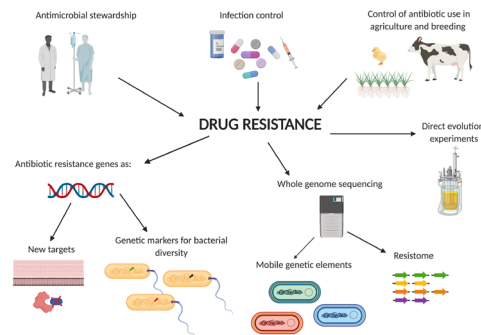


Image: created by Silvia Buroni with BioRender.com

Since the first introduction of antibiotics into clinical practice, microbial drug resistance has emerged as a major obstacle in the treatment of infections. Recently, the combination of emergence of a complex variety of multidrug resistant strains and the dearth of newly discovered molecules to effectively target and eliminate these strains, has made antibiotic resistance one of the major public health problems of this century.

Although different strategies can be adopted to contain the emergence and spread of antibiotic resistance, including (i) antimicrobial stewardship, (ii) infection control, and (iii) tighter control over the use of antibiotics in agriculture and breeding, a better understanding of the dynamics that lead to the evolution of antibiotic resistance remains essential for the development of more efficient strategies to combat this phenomenon.

The recent developments in genomics have greatly contributed to expand our knowledge on the mechanisms of microbial resistance, and of the processes by which they emerge, develop and spread. Different approaches and expertise can be used to accelerate advances in this area, ranging from clinical studies on the evolution of resistance in vivo, to theoretical modeling and the study of evolution in the laboratory.

Citation: Buroni, S., Pollini, S., Rossolini, G. M., Perrin, E., eds. (2019). Evolution of Genetic Mechanisms of Antibiotic Resistance. Lausanne: Frontiers Media SA.

doi: 10.3389/978-2-88963-222-0

Table of Contents

05 Editorial: Evolution of Genetic Mechanisms of Antibiotic Resistance

Silvia Buroni, Simona Pollini, Gian Maria Rossolini and Elena Perrin

CHAPTER 1

ANTIBIOTIC RESISTANCE GENES AS NEW ANTIBIOTIC TARGET

08 *Mycobacterial Aminoglycoside Acetyltransferases: A Little of Drug Resistance, and a Lot of Other Roles*

Fernando Sanz-García, Ernesto Anoz-Carbonell, Esther Pérez-Herrán, Carlos Martín, Ainhoa Lucía, Liliana Rodrigues and José A. Aínsa

19 *Insights on Mycobacterium leprae Efflux Pumps and Their Implications in Drug Resistance and Virulence*

Diana Machado, Emmanuel Lecorche, Faiza Mougari, Emmanuelle Cambau and Miguel Viveiros

29 *Effect of a Point Mutation in *mprF* on Susceptibility to Daptomycin, Vancomycin, and Oxacillin in an MRSA Clinical Strain*

Feng-Jui Chen, Tsai-Ling Lauderdale, Chen-Hsiang Lee, Yu-Chieh Hsu, I-Wen Huang, Pei-Chi Hsu and Chung-Shi Yang

CHAPTER 2

ANTIBIOTIC RESISTANCE GENES AS GENETIC MARKERS FOR BACTERIAL POPULATION DIVERSITY AND FOR MONITORING ANTIBIOTIC RESISTANCE

41 *Genetic Diversity of *norA*, Coding for a Main Efflux Pump of Staphylococcus aureus*

Sofia Santos Costa, Benjamin Sobkowiak, Ricardo Parreira, Jonathan D. Edgeworth, Miguel Viveiros, Taane G. Clark and Isabel Couto

52 *Occurrence and Distribution of Tetracycline Antibiotics and Resistance Genes in Longshore Sediments of the Three Gorges Reservoir, China*

Lunhui Lu, Jie Liu, Zhe Li, Zhiping Liu, Jinsong Guo, Yan Xiao and Jixiang Yang

64 *Genetic Differentiation, Diversity, and Drug Susceptibility of Candida krusei*

Jie Gong, Meng Xiao, He Wang, Timothy Kudinha, Yu Wang, Fei Zhao, Weiwei Wu, Lihua He, Ying-Chun Xu and Jianzhong Zhang

CHAPTER 3

WHOLE GENOME SEQUENCING ANALYSIS OF MOBILE GENETIC ELEMENTS ASSOCIATED WITH ANTIBIOTIC RESISTANCE

74 *Characterization of NDM-Encoding Plasmids From Enterobacteriaceae Recovered From Czech Hospitals*

Veronika Paskova, Matej Medvecký, Anna Skalova, Katerina Chudejova, Ibrahim Bitar, Vladislav Jakubu, Tamara Bergerova, Helena Zemlickova, Costas C. Papagiannitsis and Jaroslav Hrabak

- 86 Identification of a Novel Plasmid Lineage Associated With the Dissemination of Metallo- β -Lactamase Genes Among *Pseudomonads***
Vincenzo Di Pilato, Alberto Antonelli, Tommaso Giani, Lucia Henrici De Angelis, Gian Maria Rossolini and Simona Pollini
- 97 Characterization of a Multiresistance Plasmid Carrying the *optrA* and *cfr* Resistance Genes From an *Enterococcus faecium* Clinical Isolate**
Gianluca Morroni, Andrea Brenciani, Alberto Antonelli, Marco Maria D'Andrea, Vincenzo Di Pilato, Simona Fioriti, Marina Mingoia, Carla Vignaroli, Oscar Cirioni, Francesca Biavasco, Pietro E. Varaldo, Gian Maria Rossolini and Eleonora Giovanetti
- 105 Excision and Circularization of Integrative Conjugative Element Tn5253 of *Streptococcus pneumoniae***
Francesco Santoro, Alessandra Romeo, Gianni Pozzi and Francesco Iannelli

CHAPTER 4

WHOLE GENOME SEQUENCING ANALYSIS AND RESISTOME

- 112 The Versatile Mutational Resistome of *Pseudomonas aeruginosa***
Carla López-Causapé, Gabriel Cabot, Ester del Barrio-Tofiño and Antonio Oliver
- 121 Genome Sequencing and Comparative Analysis of *Stenotrophomonas acidaminiphila* Reveal Evolutionary Insights Into Sulfamethoxazole Resistance**
Yao-Ting Huang, Jia-Min Chen, Bing-Ching Ho, Zong-Yen Wu, Rita C. Kuo and Po-Yu Liu

CHAPTER 5

DIRECT EVOLUTION EXPERIMENTS TO STUDY HOW ANTIBIOTIC RESISTANCE EMERGES, EVOLVES AND SPREADS

- 134 Mutational Evolution of *Pseudomonas aeruginosa* Resistance to Ribosome-Targeting Antibiotics**
Fernando Sanz-García, Sara Hernando-Amado and José L. Martínez
- 147 Insights Into the Evolution of *Staphylococcus aureus* Daptomycin Resistance From an in vitro Bioreactor Model**
Erica Lasek-Nesselquist, Jackson Lu, Ryan Schneider, Zhuo Ma, Vincenzo Russo, Smruti Mishra, Manjunath P. Pai, Janice D. Pata, Kathleen A. McDonough and Meenakshi Malik
- 158 Construction and Characterization of Synthetic Bacterial Community for Experimental Ecology and Evolution**
Johannes Cairns, Roosa Jokela, Jenni Hultman, Manu Tamminen, Marko Virta and Teppo Hiltunen



Editorial: Evolution of Genetic Mechanisms of Antibiotic Resistance

Silvia Buroni¹, Simona Pollini^{2,3}, Gian Maria Rossolini^{2,3} and Elena Perrin^{4*}

¹ Department of Biology and Biotechnology, University of Pavia, Italy, ² Department of Experimental and Clinical Medicine, University of Florence, Italy, ³ Microbiology and Virology Unit, Careggi University Hospital, Italy, ⁴ Department of Biology, University of Florence, Italy

Keywords: antibiotic resistance, evolution, genetic mechanisms, mobile genetic elements, whole genome sequencing

Editorial on the Research Topic

Evolution of Genetic Mechanisms of Antibiotic Resistance

Almost simultaneously with the introduction of antibiotics into clinical practice, antibiotic resistance (AR) emerged as a crucial problem for the treatment of infections (Gould, 2016; Podolsky, 2018). While initially the problem could be solved by new antibiotics, it became relevant with the dearth of the discovery of new classes of molecules (Podolsky, 2018), up to the present days in which, accordingly to World Health Organization (WHO), we are close to a “Post-Antibiotic” era (Reardon, 2014).

While different strategies could be used to try to counteract AR (Lee et al., 2013), a better understanding of the dynamics that lead to its evolution remains essential for the development of more efficient strategies to combat this phenomenon (Davies and Davies, 2010; Lukacisinova and Bollenbach, 2017).

This Research Topic collects 15 articles focused on different aspects of the genetic mechanisms and on the evolution and spread of AR. Starting from the analysis of single genes related to resistance, the topic moves to the analysis of resistance at whole genome and population levels thanks to the recent advances in genome sequencing and analysis, and also covers direct evolution experiments that allowed to follow the emergence, evolution and spread of resistance in defined laboratory conditions.

An in-depth knowledge of the genetic mechanisms of AR allows, for example, to identify new possible antibiotic targets. Two different examples have been reported for mycobacterial species (Machado et al.; Sanz-Garcia et al.). In both cases, characterization of the physiological function of an AR determinant revealed an important role that goes beyond resistance. Sanz-Garcia et al., through a review of the literature on aminoglycoside acetyltransferases in mycobacteria, highlighted the roles of these enzymes in resistance to muramidase enzymes, thanks to their contribution to acetylation of peptidoglycan, and as virulence determinants, since, for example, they control the production of pro-inflammatory cytokines. The authors suggested that these enzymes are promising drug targets rather than a resistance mechanism to aminoglycoside. The work by Machado et al. is instead focused on efflux systems of *Mycobacterium leprae*. The fact that several efflux systems are conserved, despite the drastic genome reduction occurred in this species, indicates a probable role in intracellular survival, making them suitable as possible new antibiotic targets.

OPEN ACCESS

Edited and reviewed by:

Ludmila Chistoserdova,
University of Washington,
United States

*Correspondence:

Elena Perrin
elena.perrin@unifi.it

Specialty section:

This article was submitted to
Evolutionary and Genomic
Microbiology,
a section of the journal
Frontiers in Genetics

Received: 30 July 2019

Accepted: 17 September 2019

Published: 11 October 2019

Citation:

Buroni S, Pollini S, Rossolini GM
and Perrin E (2019) Editorial:
Evolution of Genetic Mechanisms of
Antibiotic Resistance.
Front. Genet. 10:983.
doi: 10.3389/fgene.2019.00983

Another example of the roles of AR genes in cell biology is reported in the work of Chen et al. They demonstrated that a mutation in the *mprF* gene conferring resistance to daptomycin and vancomycin in methicillin-resistant *Staphylococcus aureus* (MRSA), not only decreases the resistance to oxacillin, but has also a pleiotropic effect on cell membrane and cell wall and on the doubling time.

AR genes can also be used as genetic markers for bacterial population diversity and to monitor AR at different levels. For example, three different alleles of the gene coding for the *norA* efflux pump have been identified in *S. aureus*, and an analysis of the variability of these genes in 112 strains suggests that different variants reflect the population structure of this species (Costa et al.). Three different tetracycline resistance genes together with three tetracyclines molecules have been instead used to monitor the presence of antibiotics and of AR in the longshore sediments of the Three Gorges Reservoir in China (Lu et al.), revealing a significant seasonal variation of both that correlates with a higher use of antibiotics in winter. Finally, Gong et al. developed genetic markers that can be used for population structure analysis and to identify the populations which are most frequently associated with AR.

Beyond single genes involved in AR, it is well known that a fundamental role in the evolution and spread of resistance is played by mobile genetic elements (MGE) that are often associated to more than one mechanism of resistance to different classes of antibiotics. The next-generation and third generation sequencing (long reads sequencing) technologies allowed a better characterization of these elements.

For example, in three different works reported in this research topic, whole genome sequencing (WGS) analysis of different plasmids from clinical isolates allowed a better understanding of the mechanisms of resistance of the associate strains and of the evolution and spread of resistance in hospital environments. In the first article, Paskova et al. reconstructed the important role played by IncX3 plasmids in the dissemination of *bla*_{NDM}-like (New Delhi Metallo-Beta-lactamases) genes in both sporadic cases and in an outbreak of NDM-like-producing *Enterobacteriales* in Czech hospitals. Di Pilato et al. have instead identified a plasmid lineage that, circulating for over 20 years in different countries in various environmental and clinical *Pseudomonas* spp., contributed to the spread of different Metallo-Beta-lactamases (MBL) encoding genes. Finally, Morroni et al. identified and sequenced a plasmid in *Enterococcus faecium* isolated from a patient in Italy, which is a serious concern since it carries and could co-spread two genes involved in resistance to last resort agents such as oxazolidinones.

Among MGE, also integrative conjugative elements (ICE) have an important role in AR, like for example the Tn5253 ICE that confers resistance to tetracycline and chloramphenicol in *Streptococcus pneumoniae*. Santoro et al. elucidated the mechanisms of excision and circularization that allowed the transfer of this ICE.

WGS data are useful not only to study MGE associated with AR genes, but also to study the complete resistome of a certain species. A review of the WGS data obtained in different

kind of experiments in *Pseudomonas aeruginosa*, for example, highlighted how these data not only allowed to understand the evolutionary dynamics of AR, but are also useful to design specific therapeutic strategies (Lopez-Causape et al.). Similar results have been obtained in a comparative analysis between the genomes of some *Stenotrophomonas acidaminiphila* strains that revealed the evolution of sulfamethoxazole resistance in this species (Huang et al.).

WGS and all the recent -omic technologies have also been the driving force for the development of several direct evolution experiments that allowed to follow and study in a controlled laboratory environment how AR emerges, evolves and spreads. Two examples of these experiments are reported in this research topic. The first one suggested that the development of resistance is in some ways predictable, since *P. aeruginosa* populations evolved in parallel in the presence of antibiotics showed similar patterns of resistance mutations (Sanz-Garcia et al.). Moreover the authors demonstrated that bacteria are able to develop higher levels of resistance to antibiotics to which they are considered intrinsically resistant (Sanz-Garcia et al.). Similar results have been obtained by Lasek-Nesselquist et al. that, using a continuous culture bioreactor model to avoid the problem of nutrients depletion, found that daptomycin resistance in *S. aureus* arises from a combination of mutations localized in few loci, and that most of these mutations appeared early, at low frequency, within the population.

A further step forward in this field is the construction of synthetic bacterial communities to be used for evolution experiments closer to real natural conditions than the use of single strains. An example of the construction and the characterization of a synthetic bacterial community for studies of experimental evolution is reported in the work of Cairns et al.

To conclude, in this Research Topic different aspects of the genetic mechanisms of AR have been addressed. New possible antibiotic targets have been identified and new information on how AR appears and diffuses have been obtained. We think that this aspect of AR is important and need to be further investigated, since trying to avoid the emergence and spread of AR could be essential to face the “Post-Antibiotic” era.

AUTHOR CONTRIBUTIONS

EP wrote the manuscript; SB, SP, and GMR participated in manuscript correction.

FUNDING

EP was funded by an “Assegno Premiale” from the Department of Biology, University of Florence. SB is supported by the Italian Ministry of Education, University and Research (MIUR): Dipartimenti di Eccellenza Program (2018–2022) – Department of Biology and Biotechnology “L. Spallanzani,” University of Pavia.

REFERENCES

- Davies, J., and Davies, D. (2010). Origins and evolution of antibiotic resistance. *Microbiol. Mol. Biol. Rev.* 74, 417–433. doi: 10.1128/MMBR.00016-10
- Gould, K. (2016). Antibiotics: from prehistory to the present day. *J. Antimicrob. Chemother.* 71, 572–575. doi: 10.1093/jac/dkv484
- Lee, C. R., Cho, I. H., Jeong, B. C., and Lee, S. H. (2013). Strategies to minimize antibiotic resistance. *Int. J. Environ. Res. Public Health* 10, 4274–4305. doi: 10.3390/ijerph10094274
- Lukacisinova, M., and Bollenbach, T. (2017). Toward a quantitative understanding of antibiotic resistance evolution. *Curr. Opin. Biotechnol.* 46, 90–97. doi: 10.1016/j.copbio.2017.02.013
- Podolsky, S. H. (2018). The evolving response to antibiotic resistance (1945–2018). *Palgrave Commun.* 4, 124. doi: 10.1057/s41599-018-0181-x
- Reardon, S. (2014). WHO warns against "post-antibiotic" era. *Nature News*. doi: 10.1038/nature.2014.15135

Conflict of Interest: The authors declare that the research was conducted in the absence of any commercial or financial relationships that could be construed as a potential conflict of interest.

Copyright © 2019 Buroni, Pollini, Rossolini and Perrin. This is an open-access article distributed under the terms of the Creative Commons Attribution License (CC BY). The use, distribution or reproduction in other forums is permitted, provided the original author(s) and the copyright owner(s) are credited and that the original publication in this journal is cited, in accordance with accepted academic practice. No use, distribution or reproduction is permitted which does not comply with these terms.



OPEN ACCESS

Edited by:

Silvia Buroni,
University of Pavia, Italy

Reviewed by:

Peter Sander,
University of Zurich, Switzerland
Roland Brosch,
Institut Pasteur, France

*Correspondence:

José A. Ainsa
ainsa@unizar.es

† Present address:

Fernando Sanz-García,
Departamento de Biotecnología
Microbiana, Centro Nacional
de Biotecnología, Consejo Superior
de Investigaciones Científicas,
Madrid, Spain
Esther Pérez-Herrán,
GlaxoSmithKline, Tres Cantos
Medicines Development Campus,
Tres Cantos, Spain
Liliana Rodrigues,
Unit of Medical Microbiology, Global
Health and Tropical Medicine, Instituto
de Higiene e Medicina Tropical,
Universidade Nova de Lisboa, Lisbon,
Portugal

‡ These authors have contributed
equally to this work

Specialty section:

This article was submitted to
Evolutionary and Genomic
Microbiology,
a section of the journal
Frontiers in Microbiology

Received: 05 October 2018

Accepted: 11 January 2019

Published: 30 January 2019

Citation:

Sanz-García F, Anoz-Carbonell E,
Pérez-Herrán E, Martín C, Lucía A,
Rodrigues L and Ainsa JA (2019)
Mycobacterial Aminoglycoside
Acetyltransferases: A Little of Drug
Resistance, and a Lot of Other Roles.
Front. Microbiol. 10:46.
doi: 10.3389/fmicb.2019.00046

Mycobacterial Aminoglycoside Acetyltransferases: A Little of Drug Resistance, and a Lot of Other Roles

Fernando Sanz-García^{1†‡}, Ernesto Anoz-Carbonell^{1,2‡}, Esther Pérez-Herrán^{1†},
Carlos Martín^{1,3}, Ainhoa Lucía^{1,3}, Liliana Rodrigues^{1,3,4†} and José A. Ainsa^{1,3*}

¹ Departamento de Microbiología, Facultad de Medicina – Instituto Universitario de Investigación de Biocomputación y Física de Sistemas Complejos, Instituto de Investigación Sanitaria Aragón, Universidad de Zaragoza, Zaragoza, Spain,

² Departamento de Bioquímica y Biología Molecular y Celular, Facultad de Ciencias – Instituto Universitario de Investigación de Biocomputación y Física de Sistemas Complejos, Universidad de Zaragoza, Zaragoza, Spain, ³ Centro de Investigación Biomédica en Red Enfermedades Respiratorias, Instituto de Salud Carlos III, Madrid, Spain, ⁴ Fundación Agencia Aragonesa para la Investigación y el Desarrollo, Zaragoza, Spain

Aminoglycoside acetyltransferases are important determinants of resistance to aminoglycoside antibiotics in most bacterial genera. In mycobacteria, however, aminoglycoside acetyltransferases contribute only partially to aminoglycoside susceptibility since they are related with low level resistance to these antibiotics (while high level aminoglycoside resistance is due to mutations in the ribosome). Instead, aminoglycoside acetyltransferases contribute to other bacterial functions, and this can explain its widespread presence along species of genus *Mycobacterium*. This review is focused on two mycobacterial aminoglycoside acetyltransferase enzymes. First, the aminoglycoside 2'-N-acetyltransferase [AAC(2')], which was identified as a determinant of weak aminoglycoside resistance in *M. fortuitum*, and later found to be widespread in most mycobacterial species; AAC(2') enzymes have been associated with resistance to cell wall degradative enzymes, and bactericidal mode of action of aminoglycosides. Second, the Eis aminoglycoside acetyltransferase, which was identified originally as a virulence determinant in *M. tuberculosis* (enhanced intracellular survival); Eis protein in fact controls production of pro-inflammatory cytokines and other pathways. The relation of Eis with aminoglycoside susceptibility was found after the years, and reaches clinical significance only in *M. tuberculosis* isolates resistant to the second-line drug kanamycin. Given the role of AAC(2') and Eis proteins in mycobacterial biology, inhibitory molecules have been identified, more abundantly in case of Eis. In conclusion, AAC(2') and Eis have evolved from a marginal role as potential drug resistance mechanisms into a promising future as drug targets.

Keywords: mycobacteria, aminoglycoside antibiotics, aminoglycoside acetyltransferase, drug target, pathogenicity, aminoglycoside resistance

BACTERIAL RESISTANCE TO AMINOGLYCOSIDE ANTIBIOTICS

Aminoglycoside (AG) antibiotics (**Box 1**) have not been an exception to the fact that after their introduction in clinical practice, resistance has been recorded (Waglechner and Wright, 2017). In fact, the three classes of aminoglycoside-modifying enzymes, aminoglycoside acetyltransferases (AACs), aminoglycoside phosphotransferases (APHs), and aminoglycoside nucleotidyltransferases

(ANTs), have been widely detected in most pathogenic bacteria as a major determinant of resistance; in these bacteria the presence of aminoglycoside-modifying enzymes correlated with patterns of AG susceptibility (Smith and Baker, 2002). The modified AG (either by acetylation, phosphorylation or nucleotidylation) fails to inhibit their bacterial target, the 30S ribosomal subunit (Smith and Baker, 2002). Most genes encoding aminoglycoside-modifying enzymes are plasmid-located (indicative of a potential acquisition by horizontal gene transfer processes) and confer the bacterial hosts with high levels of AG resistance (Davies and Wright, 1997).

In mycobacteria, however, resistance to AGs resulted mainly from mutations of the ribosome components that prevent the drugs from inhibiting its function (Jugheli et al., 2009; Zhang and Yew, 2009; Shcherbakov et al., 2010). This is due to the fact that most mycobacterial species have either one (like *Mycobacterium tuberculosis*) or two (like *Mycobacterium fortuitum*) ribosomal operons, hence making dominant those mutations acquired in their components (Magnet and Blanchard, 2005; Shi et al., 2013). The presence of aminoglycoside-modifying enzymes, mostly AAC, in mycobacterial species has been reported over the years (as detailed in the following sections), and the role of such AACs has been explored, originally for their contribution to AG resistance, and more recently for their role in other bacterial processes, which has resulted in the interest of developing inhibitors of these enzymes (Jana and Deb, 2005; Labby and Garneau-Tsodikova, 2013). In this review, we will summarize major findings on two mycobacterial AACs, the AAC(2')-I and Eis enzymes, that have resulted in a Copernican turn for AACs in mycobacteria, from being putative drug resistance mechanisms, to reach the status of novel drug targets.

AACs IN NON-TUBERCULOUS MYCOBACTERIA

The first detection of AACs in mycobacteria (Hull et al., 1984) was reported in a group of *M. fortuitum* isolates, an opportunistic fast-growing mycobacteria. Biochemical assays of crude extracts from *M. fortuitum* strains revealed the presence of AAC activity, strongly acetylating gentamicin and kanamycin A, along with other AGs. This substrate profile was consistent with that of AAC(3) enzymes that had been previously described in *Pseudomonas* and *Enterobacteriaceae* (Angelatou et al., 1982), although confirmation at the genetic or molecular levels were not done at that time. Surprisingly, the AG susceptibility profile of *M. fortuitum* could not be correlated with the activity of AACs, indicating that in this species AACs were not the major responsible for AG resistance; it was neither correlated with the presence of plasmids, hence suggesting a chromosomal location (Hull et al., 1984). In fact, the frequency of resistant mutants to kanamycin and amikacin in *M. fortuitum* and the related species *Mycobacterium chelonae* ranged between 10^{-4} and 10^{-7} (Wallace et al., 1985). This relatively high frequency of mutations, along with the fact that AAC activity was detected at similar levels between susceptible and resistant strains, led the authors to suggest that ribosome alterations were the main

factor responsible of AG resistance in these species (Wallace et al., 1985). In another study (Udou et al., 1986), altered transport or permeability of AGs was identified as a contributor to AG resistance in *M. fortuitum*, since ribosomes from a clinical isolate were inhibited by one tenth of the MIC of AGs: for example, the MIC of kanamycin for *M. fortuitum* was 50 $\mu\text{g/ml}$, and in cell-free systems, 5 $\mu\text{g/ml}$ of kanamycin reduced the activity of ribosomes to 13% in comparison with drug-free controls; similar results were obtained when using gentamicin or paromomycin (Udou et al., 1986).

The biochemical analysis of crude extracts from other non-tuberculous mycobacteria such as *Mycobacterium smegmatis*, *Mycobacterium phlei*, *Mycobacterium vaccae*, and *Mycobacterium kansasii*, from both clinical and environmental origins, revealed similar characteristics to those found in *M. fortuitum*: crude extracts from all strains contained AAC enzymatic activity, but no correlation with AG susceptibility profile could be established (Udou et al., 1987; Ho et al., 2000). In other mycobacterial species such as *Mycobacterium avium* and *Mycobacterium intracellulare*, however, AAC activity could not be detected (Ho et al., 2000). In a recent study, using cell-free translation assays, ribosomes of *Mycobacterium abscessus* and *M. smegmatis* were inhibited by both AGs having a 2'-amino group (tobramycin, dibekacin, and kanamycin B) and by those having a 2'-hydroxyl group (amikacin, and kanamycin A). However, in *M. abscessus*, those AGs having a 2'-amino group (tobramycin, dibekacin, and kanamycin B) were less efficient in killing the cells and inhibiting its ribosomes, which is consistent with the presence of a highly active AAC(2') activity in this species. These findings suggested that in *M. abscessus*, AACs could somewhat mitigate the bactericidal effect of its AGs substrates (Maurer et al., 2015).

Interestingly, when characterizing the enzymatic activity of crude extracts, early reports detected that substrates such as amino sugars, malonyl-CoA, propionyl-CoA or butyryl-CoA inhibited the enzymatic activity of AACs from mycobacterial species. Such effect of non-acetyl CoA donors had never been described for the AAC(3) enzymes from other bacteria (Udou et al., 1987). Altogether, these findings strongly suggested for the very first time that, in mycobacteria, AACs could have important metabolic functions, and their contribution to AG resistance could be marginal (Udou et al., 1989).

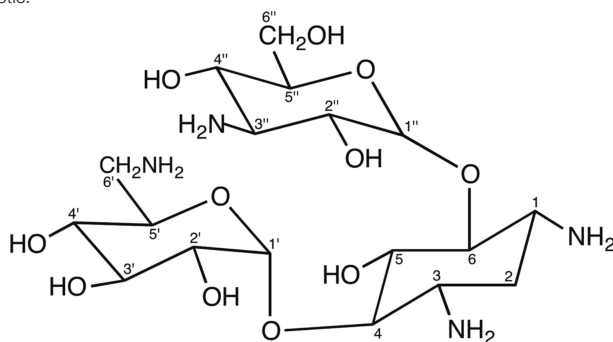
AAC(2'), A NEW ENZYME COMES INTO SCENE

In *Providencia stuartii*, a Gram-negative species, phylogenetically distant from mycobacteria, a novel class of AAC was identified as AAC(2'), because of its acetylating activity against gentamicin and lack of enzymatic activity against kanamycin A. The gene encoding AAC(2')-Ia was cloned from *P. stuartii* (Rather et al., 1993) and found to be present in the chromosome of all isolates of this bacteria. In *P. stuartii*, the expression of the *aac(2')-Ia* gene was controlled by several transcriptional regulators (Macinga and Rather, 1999), suggesting that this enzyme could play an important role, beyond its contribution to drug resistance (Franklin and Clarke, 2001). In fact, AAC(2')-Ia contributes to

BOX 1 | Aminoglycosides: origins, structure, mode of action, resistance and clinical use.

Most aminoglycoside antibiotics are produced by bacterial species of the genus *Streptomyces*, such as the antitubercular streptomycin that is produced by *S. griseus* being the first antibiotic identified from bacteria. Other genera producing aminoglycosides are *Micromonospora* and *Bacillus*. Many semi-synthetic aminoglycosides, such as amikacin, have also been produced (Mingeot-Leclercq et al., 1999; Magnet and Blanchard, 2005; Shi et al., 2013).

Structurally, aminoglycosides are formed by an aminocyclitol (commonly, 2-deoxystreptamine) with additional amino sugars bound by glycosidic bonds. There are two large families of 2-deoxystreptamine aminoglycosides, those carrying substitutions at positions 4 and 5 of the 2-deoxystreptamine ring (including neomycin, paromomycin, lividomycin, ribostamycin and butirosin) and those being substituted at positions 4 and 6 of the 2-deoxystreptamine (including kanamycin, amikacin, tobramycin, dibekacin, arbekacin, gentamicin, isepamicin, sisomicin, and netilmicin). The carbon atoms in the sugar bound to position 4 of the 2-deoxystreptamine ring are named with primed numbers ('), and those in the sugar bound to positions 5 or 6 of the 2-deoxystreptamine ring are named with double-primed numbers (''). Other aminoglycosides contain aminocyclitols distinct to 2-deoxystreptamine (this is the case of streptomycin or apramycin) or are formed by fused amino sugar rings (i.e., spectinomycin) (Magnet and Blanchard, 2005; Shi et al., 2013). The following figure shows the structure of kanamycin A, an example of 4,6 di-substituted 2-deoxystreptamine aminoglycoside antibiotic.



The bacterial target of aminoglycosides is the 30S small ribosomal subunit, and their global effect is the interference with protein synthesis. In bacterial cells, translation is initiated when the 30S ribosomal subunit binds the Shine-Dalgarno sequence (because of sequence complementarity between the Shine-Dalgarno sequence and the 16S rRNA molecule of the 30S ribosomal subunit), which is normally present in the 5' untranslated region of mRNAs. Next, initiation factors and fMet-tRNA will join the complex that finally will recruit the 50S ribosomal subunit in order to start translation. Aminoglycoside binding to the 30S subunit does not affect the binding of mRNA and the large 50S subunit, so translation can proceed. However, aminoglycosides differ in their binding site at the 30S subunit, hence affecting the protein production at different levels. Whereas spectinomycin blocks translocation (hence being bacteriostatic), streptomycin and most 2-deoxystreptamine aminoglycosides lock the ribosome in a conformation that is prone to introducing erroneous aminoacyl-tRNAs. The accumulation of aberrant proteins in the bacteria results in cell death (Davies and Wright, 1997; Magnet and Blanchard, 2005; Shell et al., 2015).

Resistance to aminoglycosides may be due to several mechanisms (Davies and Wright, 1997; Magnet and Blanchard, 2005). Reduced uptake (which can be a consequence of alterations in the composition of bacterial membrane or to metabolic conditions like anaerobiosis) or the action of efflux pumps can lead to limited intracellular concentration of aminoglycosides, hence causing resistance. Mutations in 16S ribosomal RNA or certain ribosomal proteins such as S12 (encoded by *rpsL* gene) lead to aminoglycoside resistance through target modification; this is also achieved after the action of methyltransferases, which introduce methyl groups in guanine or adenine nucleotides of 16S ribosomal RNA. The presence of aminoglycoside-modifying enzymes is, however, the most prevalent mechanism of aminoglycoside resistance; there are three types of aminoglycoside-modifying enzymes: aminoglycoside *N*-acetyltransferases (AAC), *O*-phosphotransferases (APH), and *O*-nucleotidyltransferases (ANT). Aminoglycoside-modifying enzymes are named by using the aforementioned abbreviations, followed by a number in brackets indicating the site of modification in the aminoglycoside molecule (as explained above), a Roman numeral related with substrate profile, and a lower-case letter for differentiating isoenzymes, i.e., AAC(2')-Ib.

Clinically, due to their oto- and nephrotoxicity and the rising prevalence of resistance, aminoglycosides are commonly reserved as a second line of treatment of serious infections. Due to their low absorption when given orally, aminoglycosides need to be administered through injections. Streptomycin was a first-line drug in the treatment of tuberculosis, and in our days, kanamycin and amikacin are listed as second line drugs against this disease. Spectinomycin is used against *Neisseria gonorrhoeae* infections (Suay-García and Perez-Gracia, 2018). *Pseudomonas aeruginosa* infections in cystic fibrosis patients, septicemia, endocarditis and several other infections caused by non-tuberculous mycobacteria, Gram-positive or Gram-negative bacteria can be treated efficiently by using aminoglycosides, either alone or in combinations with other antibacterials such as the beta-lactam antibiotics (Mingeot-Leclercq et al., 1999; Magnet and Blanchard, 2005; Bassetti et al., 2018).

O-acetylation of peptidoglycan affecting cell morphology and the expression of autolysins, and can use acetylated peptidoglycan precursors as donors of acetyl groups, another indication about the role of this enzyme beyond resistance (Payie et al., 1995, 1996; Clarke et al., 1996; Payie and Clarke, 1997).

AAC(2') in Mycobacteria

Given the high AG acetylating activity against gentamicin, tobramycin, netilmicin and its derivatives 2'-*N*-ethyl- and 6'-*N*-ethyl-netilmicin, kanamycin A and kanamycin B found in *M. fortuitum* (Hull et al., 1984; Ainsa et al., 1996), we launched a molecular approach aimed at characterizing the determinant of AG resistance in this species. A genomic library of *M. fortuitum* was transformed in *M. smegmatis*, and characterization of AG

resistant clones allowed the identification of a *M. fortuitum* gene showing sequence similarity to *aac(2')-Ia* of *P. stuartii*. The enzyme of *M. fortuitum* was named AAC(2')-Ib (Ainsa et al., 1996) and was capable of acetylating gentamicin, but not kanamycin A, hence indicating that another AAC enzyme should be present in *M. fortuitum*. Similarly to *P. stuartii*, the *aac(2')-Ib* gene was found in all strains of *M. fortuitum* regardless of the phenotype of AG resistance, suggesting other roles for the AAC(2')-Ib in this species. Further studies (done by database searching or by southern blot analysis using the probe of *aac(2')-Ib* gene) demonstrated the presence of *aac(2')-I* genes in other mycobacterial species, including *M. tuberculosis* (the major pathogenic species in this genus), *Mycobacterium leprae*, and *M. smegmatis*, indicating thus that the presence

of *aac(2′)-I* genes in mycobacteria could be universal (Ainsa et al., 1997). Interestingly, the expression of the *aac(2′)-Id* gene in *M. smegmatis* was driven from two promoters, and the strongest one produced a leaderless transcript having a GTG translation start codon at its 5′ end (Mick et al., 2008). Leaderless transcripts are those in which the transcription start site coincides with the translation start codon; although representing a rather unusual feature in the model organism *E. coli*, they are quite common in mycobacteria, where 25% of all transcripts are predicted to be leaderless (Shell et al., 2015); in fact, *eis* gene of *M. tuberculosis* (see the section “The Eis Protein Becomes a Novel Aminoglycoside Acetyltransferase,” below) is transcribed also as a leaderless mRNA (Zaunbrecher et al., 2009). In leaderless mRNAs, there is no Shine-Dalgarno sequence, and 70S ribosomes bind directly to the 5′-end of the mRNA in order to initiate translation (Shell et al., 2015).

New Roles for AAC(2′) in Mycobacteria

Two major evidences supported that in mycobacteria, AAC(2′)-I enzymes could have additional roles other than acetylation of AGs containing 2′-amino group: first, the capability of amino sugars and diverse acyl-CoA molecules to inhibit the acetylating activity of mycobacterial crude extracts (Udou et al., 1989); and second, the implication of AAC(2′)-Ia (an enzyme of the same class) in acetylation of cell wall substrates in *P. stuartii*. In a series of laboratory mutants of *P. stuartii* expressing *aac(2′)-Ia* gene at different levels, it was found that the extent of peptidoglycan acetylation correlated with the activity of AAC(2′)-Ia, hence suggesting a partial contribution of this enzyme (along with other enzymes) to peptidoglycan acetylation. Many bacterial pathogens acetylate their peptidoglycan as a way to resist the action of muramidase enzymes. Under *in vitro* conditions, AAC(2′)-Ia was able to acetylate tobramycin having acetylated peptidoglycan as donor of acetyl groups (Payie et al., 1995, 1996; Payie and Clarke, 1997).

We investigated the hypothesis of mycobacterial AAC(2′)-I enzymes having also a role in cell wall metabolism, and a gene knock-out mutant of *M. smegmatis* deleted in *aac(2′)-Id* gene was constructed. This mutant (named EP-10) defective in AAC(2′)-I activity was more susceptible to gentamicin, tobramycin, dibekacin, and netilmicin than the parental wild-type strain, and crude extracts of *M. smegmatis* EP-10 failed to acetylate 2′-amino group containing AGs, whereas wild-type strains of *M. smegmatis* readily acetylated such AGs (Ainsa et al., 1997; Maurer et al., 2015). *M. smegmatis* EP-10 was also twofold more susceptible to lysozyme, a feature that has been associated with the extent of peptidoglycan acetylation (Ainsa et al., 1997). Hence, we concluded that in *M. smegmatis*, AAC(2′)-Id enzyme could also contribute to acetylation of peptidoglycan, since a less extensively acetylated peptidoglycan in the knock-out strain would be more susceptible to lysozyme degradation affecting cell viability.

Biochemical Analysis of Mycobacterial AAC(2′)-I Enzymes

The presence of an AG (2′)-N-acetyltransferase gene in the genome of *M. tuberculosis* was intriguing. In this species, AAC

activity had never been reported (Mitsuhashi et al., 1977) and the expression of the *aac(2′)-Ic* gene [annotated as Rv1258c gene in the *M. tuberculosis* H37Rv genome (Cole et al., 1998)] in the surrogate host *M. smegmatis* could not be associated with any change in the levels of susceptibility to AGs (Ainsa et al., 1997). We constructed a knock-out mutant of *M. tuberculosis* H37Rv deleted in the *aac(2′)-Ic* gene and observed that the mutant (named *M. tuberculosis* B1) was twofold more susceptible than the original wild-type strain to AGs containing a 2′-amino group such as gentamicin, tobramycin and dibekacin, and fourfold more susceptible to 6′-N-ethyl-netilmicin. This indicated that the *aac(2′)-Ic* gene was being expressed in *M. tuberculosis* although at a very low level, and that the AAC(2′)-Ic enzyme in *M. tuberculosis* would acetylate all these four AGs in the wild type strain; hence, acetylated AGs would bind less efficiently to the ribosome, and the AAC(2′)-Ic enzyme would contribute to basal AG resistance in this species.

In order to find the physiological role of this enzyme in *M. tuberculosis*, recombinant *E. coli*-produced AAC(2′)-Ic enzyme from *M. tuberculosis* was studied and found to efficiently acetylate AG antibiotics containing an amino group at the 2′ position (as expected; for example, K_m for kanamycin B was 1.4 μ M), and surprisingly, it was also capable of acetylating (although to a much lesser extent) other AGs such as kanamycin A (K_m 320 μ M) and amikacin (K_m 968 μ M) that have a hydroxyl group in the 2′ position, hence suggesting this enzyme to be capable of both N- and O-acetylation (Hegde et al., 2001; Draker et al., 2003). This residual activity of AAC(2′)-Ic against kanamycin A and amikacin does not affect their bactericidal activity, and these two antibiotics are used as second line drugs against drug resistant *M. tuberculosis* (World Health Organization [WHO], 2010). The activity of *M. tuberculosis* AAC(2′)-Ic is dependent on metal ions, being inhibited by Cu^{2+} and Au^{3+} (Li et al., 2015).

Another study consisted in binding covalently the AGs kanamycin A, tobramycin, neamine and neomycin B to an agarose matrix in order to quantify the extent of AG acetylation by AAC enzymes and their subsequent ability to bind an artificial probe mimicking the A-site of the ribosome (Barrett et al., 2008). In such experimental model system, the AGs acetylated by *M. tuberculosis* AAC(2′)-Ic enzyme (only tobramycin, neamine and neomycin B) maintained their binding affinity with the probe mimicking A-site of the ribosome at detectable levels, maybe because the percent of AG acetylation by AAC(2′)-Ic was low. In contrast, these AGs were very efficiently acetylated by *E. coli* AAC(3) (at a different amino group) and had readily lost their affinity for binding this artificial probe. These experiments suggested that subtle differences in the structure of modified AGs (i.e., acetylation at the amino group in 2′ or 3 position) are sufficient to drastically affect their capability of binding to the A-site probe, and this would be expected to correlate with their activity as ribosome inhibitors. In consequence, in mycobacteria, AAC(2′)-I enzymes would not play a major role in resistance to these drugs (Barrett et al., 2008). High resolution crystal structures of AAC(2′)-Ic complexed with AGs demonstrated that this enzyme is a member of the GNC5 acetyltransferase superfamily and suggested a role in the synthesis of mycothiol,

a metabolite that has a key role in regulating redox potential in mycobacteria (Vetting et al., 2002, 2003).

In agreement with the preferential *N*-acetylating activity over the *O*-acetylating activity that was found in the *M. tuberculosis* enzyme (Hegde et al., 2001; Draker et al., 2003), *M. abscessus* clinical isolates were found to be more susceptible to AGs containing a hydroxyl group at the 2' position (such as amikacin and kanamycin A) than to AGs with a 2'-amino group (such as tobramycin, dibekacin and kanamycin B), as the latter group would be substrates of *M. abscessus* AAC(2')-I enzyme (Maurer et al., 2015). In fact, crude extracts of *M. abscessus* efficiently acetylated kanamycin B, whereas kanamycin A was not acetylated at detectable levels. In this species, deletion of the *aac(2')-I* gene resulted in increased susceptibility to kanamycin B, tobramycin, dibekacin and gentamicin C (all of them containing a 2'-amino group) (Rominski et al., 2017). These two reports demonstrate that in *M. abscessus*, the presence of an AAC(2')-I enzyme contributes to decreased innate susceptibility to AGs containing a 2'-amino group (Luthra et al., 2018).

Becoming a Drug Target: Developing Inhibitors of AAC(2')-I

The interest in developing inhibitors against AAC(2')-I enzymes came from a study in the non-tuberculous species *M. abscessus* (Maurer et al., 2014). It was found that AGs such as amikacin, gentamicin or tobramycin, which are normally bactericidal against *E. coli*, do not have such activity against *M. abscessus* or *M. smegmatis*. However, disruption of the chromosomally encoded *aac(2')-I* gene in these species restored the bactericidal activity of these AGs (Maurer et al., 2014). Given that AGs are used as second-line drugs in treatment of multidrug resistant (MDR) tuberculosis infections, and also in the treatment of other infections caused by non-tuberculous mycobacteria, the possibility of developing compounds that could enhance bactericidal activity of current antimycobacterial treatments became an interesting approach.

To date, the only putative inhibitor of *M. tuberculosis* AAC(2')-Ic is andrographolide, a natural product that was identified in methanolic extracts of a plant that were capable of inhibiting growth of *M. tuberculosis* strains (Prabu et al., 2015). *In silico* analysis predicted that this compound could potentially bind with a high affinity the AAC(2')-Ic enzyme, as well as isocitrate lyase (a metabolic enzyme of the glyoxylate shunt, involved in persistence and virulence of *M. tuberculosis*) and other *M. tuberculosis* proteins (Prabu et al., 2015). However, the specificity of this binding and the ability to really inhibit such putative target proteins were not tested. Given that the gene encoding AAC(2')-Ic is not essential in *M. tuberculosis*, a direct link between AAC(2')-Ic inhibition and bacterial growth inhibition could be discarded. Hence, the ability of plant extracts containing andrographolide to inhibit growth of *M. tuberculosis* could be due to the presence of additional compounds in the extract, or to multiple effects on *M. tuberculosis* cells. Other *in silico* analysis revealed that AAC(2')-Ic enzyme from *M. tuberculosis* could interact with ten other proteins (including a protein of a putative RND-like efflux pump), suggesting that

inhibition of AAC(2')-Ic could also impact many other metabolic processes, hence conferring this enzyme with a relevant role in drug discovery of antituberculosis agents (Joshi et al., 2013).

THE Eis PROTEIN BECOMES A NOVEL AMINOGLYCOSIDE ACETYLTRANSFERASE

Investigation of *M. tuberculosis* virulence factors lead to the identification of a protein, that was required for infecting and survival in human macrophages; this protein was named Eis for enhanced intracellular survival (Box 2) (Wei et al., 2000). Bioinformatic analysis revealed that Eis protein of *M. tuberculosis* was an acetyltransferase of the GCN-5 family (Samuel et al., 2007).

Later on, the analysis of kanamycin resistant *M. tuberculosis* laboratory and clinical strains revealed mutations in the –10 and –35 regions of the *eis* gene promoter, which resulted in increased levels of *eis* mRNA and Eis protein. These mutations were related to low-level resistance to kanamycin (MIC 25 µg/ml), but not to amikacin (MIC < 4 µg/ml), whereas 16S rRNA mutations confer higher levels of resistance to kanamycin (MIC > 80 µg/ml) and frequently cross-resistance to amikacin. These *eis* mutants also displayed increased levels of AAC activity, hence demonstrating that Eis was a novel class of AAC, highly divergent from all other previously known AACs. Eis is capable of acetylating kanamycin more efficiently than amikacin, and streptomycin was not found to be a substrate of Eis (Zaunbrecher et al., 2009). From then on, detection of mutations in *eis* promoter has become a relevant assay in clinical microbiology laboratories for determining susceptibility to kanamycin (Georghiou et al., 2012); the diagnostic and clinical implications of these tests are beyond the scope of this review.

Formation of stable hexamers by Eis is required for its AAC activity (Ganaie et al., 2011; Anand and Sharma, 2018), which can acetylate multiple amine groups of different AG antibiotics, including netilmicin, sisomicin, neamine, ribostamycin, paromomycin, neomycin B, kanamycin, amikacin, tobramycin and hygromycin, resulting in mono-, di-, tri, and tetraacetylated products (Chen et al., 2011; Houghton et al., 2013a), being able to use not only acetyl-CoA but also other acyl-CoA derivatives (Chen et al., 2012a). The Eis protein works by a random-sequential bisubstrate mechanism of acetylation (Tsodikov et al., 2014). Interestingly, Eis is also able to acetylate capreomycin, a polypeptide second-line antituberculosis drug commonly used in the treatment of MDR tuberculosis infections (Reeves et al., 2013). Several metal ions such as Au³⁺, Cd²⁺ and Zn²⁺ inhibited Eis activity *in vitro* (Li et al., 2015).

Other mycobacterial species such as *M. smegmatis* and *M. abscessus* have ortholog (and even paralog) *eis* genes, although the Eis proteins have distinct biochemical features and impact on AG susceptibility in comparison with Eis of *M. tuberculosis* (Chen et al., 2012b; Rominski et al., 2017). For example, *M. abscessus* has two *eis* genes, and the deletion of one (but not the other one) resulted in altered AG susceptibility (Rominski et al., 2017; Luthra et al., 2018). Consistently with these findings, mutational

BOX 2 | Discovery and characterization of enhanced intracellular survival (Eis) protein of *M. tuberculosis*.

A genome wide investigation of the ability of *M. tuberculosis* for infecting macrophages resulted in the identification of a coding sequence that, once cloned in the non-pathogenic *M. smegmatis* species, conferred capacity for infecting the human macrophage-like cell line U937. This gene was named *eis* (Rv2416c in the *M. tuberculosis* genome; Cole et al., 1998) for enhanced intracellular survival (Wei et al., 2000), and was detected only in pathogenic species of mycobacteria. The promoter of the *eis* gene is similar to consensus *E. coli* sigma-70 dependent promoters (Roberts et al., 2004) and it is recognized by *M. tuberculosis* SigA sigma factor (Wu et al., 2009). The Eis protein was found to be mostly hydrophilic, but having a hydrophobic N-terminal end, so that it could be found in the cytosolic but also in other cell fractions such as the membrane, cell wall or among the secreted proteins of *M. tuberculosis* (Dahl et al., 2001). In fact, antibodies against Eis could detect this protein in the sera of tuberculosis patients (Dahl et al., 2001) and in the cytoplasm of infected macrophages (Samuel et al., 2007). Also, it was found that Eis protein, directly added to cultures of human monocytes, modulated the secretion of pro-inflammatory cytokines in a similar way to that found in *M. tuberculosis* infected cells (Samuel et al., 2007), hence suggesting a role of Eis as an effector protein. Further studies demonstrated that Eis inhibits the extra-cellular signal-regulated kinase 1/2 (ERK1/2) and JAK pathways, and in consequence it inhibited the production of TNF-alpha and IL-4, and stimulated the production of IFN-gamma and IL-10 (Lella and Sharma, 2007). The effect of Eis in increasing production of IL-10 was found to be related to Eis-mediated acetylation of histone H3, which binds the promoter of the human IL-10 gene (Duan et al., 2016). Hence, by disturbing cross-regulation of T-cells and impairing TH1 and TH2 response, Eis could mediate *M. tuberculosis* pathogenicity (Lella and Sharma, 2007). In fact, an isolate of the Beijing family (which are more transmissible and virulent than other *M. tuberculosis* genetic lineages (Hanekom et al., 2011) was found to contain elevated levels of Eis protein, mediated by increased expression of SigA (Wu et al., 2009). Other key factors in host immune response to tuberculosis are also mediated by Eis, which increased production of ROS and consequently modulated processes such as autophagy, inflammation, and cell death (Shin et al., 2010). These processes are started by Eis-dependent acetylation of dual-specificity phosphatase-16 (DUSP16)-mitogen-activated protein kinase phosphatase-7 (MKP-7), which dephosphorylates the JNK protein leading to its inactivation (Kim et al., 2012; Yoon et al., 2013). Other studies have revealed the activity of Eis for acetylating arylalkylamines such as histamine, octopamine, or tyramine, suggesting novel roles for this protein in *M. tuberculosis* pathogenicity (Pan et al., 2018).

changes in the amino acid residues lining the substrate binding site of *M. tuberculosis* Eis altered its substrate specificity (Jennings et al., 2013).

It is important to note that in *M. tuberculosis*, transcription of the *eis* gene is activated by the regulator WhiB7 (Reeves et al., 2013). Mutations in the promoter of *whiB7* gene that led to increase in the mRNA of this gene resulted in increased expression of *eis* gene, along with other genes such as *rv1258c* (encoding the Tap efflux pump; Ainsa et al., 1998), hence resulting in cross resistance to several drugs including kanamycin (mediated by Eis protein) or streptomycin (mediated by Tap efflux pump). Similarly, in *M. abscessus*, WhiB7 controlled the expression of one of the two *eis* genes in this species and also that of the *erm(41)* gene, which encodes a ribosomal methyltransferase that by altering target structure is associated with resistance to macrolide antibiotics (Pryjma et al., 2017; Luthra et al., 2018). Subinhibitory concentrations of clarithromycin induced the *whiB7* gene and consequently decreased Eis-mediated susceptibility to AGs, such as amikacin that is currently used in the treatment of *M. abscessus* infections (Pryjma et al., 2017).

Aminoglycosides and Beyond...

The unusual properties of Eis acetyltransferase include its capability for acetylating peptides and proteins (Kim et al., 2012; Houghton et al., 2013b; Yoon et al., 2013), in contrast with other AACs. The *M. tuberculosis* nucleoid-associated protein HU (encoded by Rv2986c gene) can be acetylated by Eis on multiple lysine residues, hence decreasing its ability to interact with DNA, and altering its DNA compaction activity (Ghosh et al., 2016; Green et al., 2018). Overexpression of Eis led to a hyperacetylation of HU protein, and consequently, to a decompaction of the genome (Ghosh et al., 2016). The reverse effect (condensation of relaxed DNA) could be reached through the deacetylation of HU protein, which is mediated by a Sir2 family protein from *M. tuberculosis* encoded by the Rv1155c gene (Anand et al., 2017; Green et al., 2018). Controlling the architecture of DNA is a key process in any bacteria, and so, the

HU protein is essential for *M. tuberculosis*. In fact, inhibitors of HU have been discovered (Bhowmick et al., 2014), which could act in synergy with potential inhibitors of Eis, as described in the next section.

Finding Inhibitors of Eis Protein

The crystal structure of *M. tuberculosis* Eis protein was determined by several groups (Chen et al., 2011; Kim et al., 2012), which has been useful for determining docking properties of potential inhibitory compounds; also, its comparison with the crystal structure of *M. smegmatis* Eis protein revealed several distinct structural features that may account for the biochemical and substrate differences between the two proteins (Kim et al., 2014). A first screening of potential inhibitors of Eis from *M. tuberculosis* resulted in the identification of 25 molecules (including the antiseptic chlorhexidine) that inhibited Eis with IC₅₀ values in the low micromolar range. In addition, this inhibition was specific to the *M. tuberculosis* Eis protein, since these molecules could not inhibit significantly AACs from AAC(2'), AAC(3), and AAC(6') families (Green et al., 2012), nor Eis protein from *Bacillus anthracis* (Green et al., 2015a). Later studies revealed the presence of *eis*-like genes in many pathogenic and non-pathogenic bacteria (remarkably, many mycobacterial species have two or even three paralogs of the *eis* gene), and chlorhexidine was capable of inhibiting (to different levels) all Eis proteins that were capable of acetylating AGs (Green et al., 2015b).

A second screening of a larger collection of small-molecule compounds resulted in the identification of several families of compounds capable of inhibiting Eis activity. These contained diverse chemical scaffolds (Garzan et al., 2016a,b, 2017; Willby et al., 2016; Ngo et al., 2018). Besides, these inhibitors were highly selective for Eis, and did not inhibited AACs from other families (Garzan et al., 2016b). More importantly, as these inhibitors bound in the AG pocket of the Eis protein, they were able to reverse kanamycin resistance of a *M. tuberculosis* isolate (Garzan et al., 2016b; Willby et al., 2016; Ngo et al., 2018).

Some of these inhibitors, such as those based on a pyrrolo[1,5-a]pyrazine scaffold, also lacked any toxicity on mammalian cell lines (Garzan et al., 2017).

OTHER AMINOGLYCOSIDE-MODIFYING ENZYMES IN MYCOBACTERIA

Genome-wide analysis of *M. tuberculosis* genome identified only one other potential AAC (encoded by the Rv1347c gene), although such enzymatic activity could not be detected on the recombinant protein (Draker et al., 2003). Later studies related the product of the Rv1347c gene with a role in the synthesis of mycobactin, the mycobacterial siderophore (Card et al., 2005).

Leaving apart AACs, only a few reports of other classes of aminoglycoside-modifying enzymes have been done in mycobacteria. An APH enzyme of the APH(3'') family, conferring resistance to the AG streptomycin only, has been characterized in *M. fortuitum* (Ramon-Garcia et al., 2006) and *M. abscessus* (Dal Molin et al., 2018; Luthra et al., 2018); the latter species encodes up to 11 additional putative APH enzymes (Ripoll et al., 2009). Furthermore, a putative APH of the APH(3') class, encoded by the Rv3168 gene of *M. tuberculosis*, was identified and expressed as a recombinant enzyme in *E. coli*, being related to kanamycin phosphotransferase activity (Ahn and Kim, 2013).

BACK TO THE START POINT: Eis IN *M. fortuitum*

We started this review referring to previous work that has shown that crude extracts of *M. fortuitum* harbored AAC activity having gentamicin, tobramycin, netilmicin and its derivatives 2'-N-ethyl- and 6'-N-ethyl-netilmicin, kanamycin A and kanamycin B as substrates. So far, the only AG acetyltransferase identified in this species has been AAC(2')-Ib (Ainsa et al., 1996), which cannot explain the acetyltransferase activity against kanamycin A and 2'-N-ethyl-netilmicin detected in *M. fortuitum* crude extracts. Later studies characterized Eis AAC in diverse mycobacterial species, but no report were been done on a putative Eis protein in *M. fortuitum*. In view of the universal presence of Eis proteins in mycobacteria, and its activity as AAC, we hypothesized that *M. fortuitum* could also have a putative Eis protein that would be responsible for the acetyltransferase activity against kanamycin A and 2'-N-ethyl-netilmicin detected in crude extracts of this species, as it was reported earlier (Hull et al., 1984; Ainsa et al., 1996).

Thus, we first ascertained the existence of an *eis* gene in the genome of *M. fortuitum* (Ho et al., 2012), which presented a 94% of identity with respect to the one reported in *M. tuberculosis*; the sequence of both Eis proteins from *M. tuberculosis* and *M. fortuitum* also presented high levels of identity (Figure 1). We designed two oligonucleotides for amplifying specifically a DNA fragment from *M. fortuitum* genome containing *eis* gene. This DNA fragment was subsequently cloned in pMV261 vector (Stover et al., 1991), which expresses genes constitutively under

the control of the *hsp60* gene promoter, resulting in plasmid pFS2. Given that this plasmid still contains the Tn903-derived aminoglycoside-3'-phosphotransferase (*aph*) gene (present in the original pMV261 cloning vector) conferring kanamycin resistance as selection marker, we anticipated that *M. smegmatis* strains harboring pMV261 vector or its derivatives would be intrinsically resistant to kanamycin A; this would prevent from determining whether this antibiotic is a substrate of the *M. fortuitum* Eis protein. Additionally, the selection marker could have cross-effect with other AGs and thus interfering with the resistance phenotype conferred by *eis* gene. To circumvent these problems, we generated a derivative of pFS2 through the disruption of the *aph* gene with the ampicillin resistance cassette (*bla* gene) from pGEM®-T easy (Promega). The resistance to 2'-N-ethylnetilmicin conferred by *eis* gene, as demonstrated for the parental plasmid pFS2 (see Table 1) was used as resistance marker for transformant selection and plasmid maintenance. This process resulted in plasmid pEAC which contains the *M. fortuitum eis* gene and no other determinant of AG resistance.

The three plasmids [original empty vector pMV261 as a control, and the two plasmids (pFS2 and pEAC) containing *M. fortuitum eis* gene] were introduced in *M. smegmatis* mc² 155 in order to over-express the ortholog *eis* gene from *M. fortuitum* and to elucidate its hypothetical implication in AG susceptibility. The antibiotic susceptibility assay was made, based on a double dilution protocol with the addition of resazurin dye (Palomino et al., 2002).

We observed that plasmids pFS2 and pEAC produced detectable changes in AG susceptibility of *M. smegmatis* mc² 155, which can be attributed to the expression of the plasmid-borne *M. fortuitum eis* gene. The major shift in the MICs was detected for 2'-N-ethylnetilmicin (Table 1), since the MIC increased from 3.12 to 6.25 µg/ml in the control strains to 50–100 µg/ml in the strains containing *M. fortuitum* Eis, accounting for a 8- to 32-fold increase; similar changes were observed for 6'-N-ethylnetilmicin (8-fold increase in the MIC). A moderate decrease in the susceptibility to kanamycin A (fivefold), hygromycin (twofold to fourfold) and gentamicin (twofold to fourfold) was also observed. Finally, slight changes (twofold) in the MICs were detected for kanamycin B and capreomycin; this finding is consistent with previous reports on the activity of *M. tuberculosis* Eis against capreomycin (Reeves et al., 2013). The levels of susceptibility to the AGs amikacin, streptomycin and spectinomycin, and to other non-AG compounds tested (isoniazid, rifampicin, ethambutol, ciprofloxacin, tetracycline, chloramphenicol) were not altered significantly by the presence of the plasmid-encoded *eis* gene (Table 1 and data not shown), suggesting that either these antimicrobials are not substrates of the Eis enzyme or the corresponding acetylations (if any) might just not affect antibacterial activity.

CONCLUDING REMARKS

The presence and activity of AAC(2')-I and Eis AACs in mycobacteria have clearly demonstrated that their primary role is little related with susceptibility to AGs.

Mfortuitum	MAGKSVALVGGDGVALSVSVIDDAASTTTTLTLDVTVDADWAGMALLGNTAFGETNHPDSMA	60
Mtuberculosis	MA-----QSDSVTVTLCSPTEDDWPGMFLAAASFTDFIGPESAT	40
	** :.:.*:** : *: **.* ** .:* : *.* :	
Mfortuitum	AWQQMVPPGGGVVMRAGGSDG-DIVGQSIYLDMSLTVPGGVVLPAAGLSYVAVAPTHRRR	119
Mtuberculosis	AWRTLVPDTGAVVVRDAGGPGSEVVGMALYMDLRLTVPGEVVLPAGLSFVAVAPTHRRR	100
	** : **..*.*:* *..* :.* :*:.*: ***** :*:.*.*:*****	
Mfortuitum	GILRSMYGELHQRIADAQYPVAALTASEGGIYGRFGYGPATTVHLMTIDRRFAQFHASVP	179
Mtuberculosis	GLLRAMCAELHRRRIADSGYPVAALHASEGGIYGRFGYGPATTLHELTVDRRFARFHADAP	160
	:.:* .**:*.**: ***** :***** :*:.*.*:*****:***..*	
Mfortuitum	DP--GG--VRLVKPAEHRDTLAEIYDRWRRQTPGGLVCP TALWDDVLADREDARDGGSAL	235
Mtuberculosis	GGGLGGSSVRLVRPTEHRGEFEAIYERWRQQVPGGLLRPQVLWDELLAECKAAPGGDRES	220
	. ** *****:.*.*: : *:*.*.*:.*.**: * .*****: : * .*	
Mfortuitum	FAFLHPDGYALYRVHGEESRTLVRREVTAVTTDAYIALWRALLGMDLMEKVSIIWTHPGDP	295
Mtuberculosis	FALLHPDGYALYRVDRITDLKLARVSELRAVTADAHCALWRALIGLDSMERISIIITHQDP	280
	** :***** . : : ** *: *:*.**: *****:.* ** :.* ** *	
Mfortuitum	LPYLLTNPRLARVTSSDDLWIRIMNIPAALEARRYQADLDVVLEVADGFRSDGGRFALQ	355
Mtuberculosis	LPHLLTDTRLARTTWRQDGLWLRIMNVPAALEARGYAHEVGEFSTVLE--VSDGGRFALK	338
	** :.**: .****.* .*.**:*.**:***** * :.: . * : *****:	
Mfortuitum	IRDGGAQCTPTDAPADVELDLVLGSLYLGTHRPDAFVTANRLCSKDPVAVQGLGAAFAS	415
Mtuberculosis	IGDGRARCTPTDAAAEIEMDRDVLGSLYLGHAHRASTLAAANRLRTKDSQLLRRLDAAAFAS	398
	* ** *:*****.*:.*:* *****:.*..:.*:***** :*. :.: *.*****	
Mfortuitum	EVPAELGYSF	425
Mtuberculosis	DVPVQTAFEF	408
	:**.: :.*	

FIGURE 1 | Comparison of the amino acid sequences of Eis proteins from *M. fortuitum* and *M. tuberculosis*. Symbols under the sequence alignment: Asterisks (*) indicate positions with identical amino acid in both proteins. Colons (:) indicate positions which have amino acids with strongly similar properties. Periods (.) indicate positions which have amino acids with weakly similar properties.

TABLE 1 | MICs ($\mu\text{g/ml}$) of antibiotics of different structural families in the *M. smegmatis* mc² 155 strains that overexpress *eis* gene from *M. fortuitum*.

Strain	<i>M. smegmatis</i> mc ² 155			
Plasmid	None	pMV261	pFS2	pEAC
Marker gene on plasmid	None	<i>aph</i>	<i>aph</i>	<i>bla</i>
<i>M. fortuitum</i> eis gene	—	—	+	+
Gentamicin	0.78–1.56	0.78	3.12	3.12
2'- <i>N</i> -ethyl netilmicin	6.25	3.12–6.25	50–100	50
6'- <i>N</i> -ethyl netilmicin	3.12	3.12	3.12–6.25	25
Kanamycin A	1.56	>100	>100	7.8
Kanamycin B	6.25	>100	>100	12.5
Hygromycin	15.6	15.6	31.2–62.5	62.5
Amikacin	0.39	0.39	0.39	0.39
Capreomycin	1.95	1.95	3.9	3.9
Streptomycin	0.25	0.25	0.25	0.25
Spectinomycin	62.5	31.2–62.5	62.5	62.5

The values separated by a dash indicate that growth was detected in both concentrations. The range of antibiotic concentrations spanned from 0.78 µg/ml to 100 µg/ml, and from 0.25 µg/ml to 125 µg/ml; a twofold difference in the MIC was not considered as significant. aph: aminoglycoside 3'-phosphotransferase from *Tn903*; bla: beta-lactamase.

In the case of AAC(2')-I enzymes, its presence in phylogenetically distant genera as *Providencia* and *Mycobacterium* remains to be an evolutionary mystery.

In contrast with this restricted distribution of AAC(2')-I enzymes among bacteria, Eis enzymes seem to be more widely distributed, being present even in non-pathogenic and environmental species, which suggest a general function of Eis-like enzymes in bacterial metabolism, and virtually excludes any potential selection of *eis* genes due to the use of AGs, or its horizontal transfer from other species.

It is clear that in mycobacteria ribosomal modifications constitute the major mechanism of AG resistance, given that only one or two copies of ribosomal RNA operons are present in these species, hence making likely the acquisition of mutations conferring high levels of AG resistance. Then, AAC(2')-I enzymes only contribute modestly to innate low level susceptibility to AGs, and despite other roles have been suggested in the literature for mycobacterial AAC(2')-I enzymes, their relevance as potential drug targets is still modest, especially in comparison with Eis acetyltransferase. The contribution of Eis acetyltransferase to virulence of *M. tuberculosis*, and the finding that Eis is related with resistance to kanamycin (a second line drug for the treatment of tuberculosis) in clinical isolates has greatly attracted the attention and promoted the interest in developing Eis inhibitors. In some way, Eis inhibitors would fall into the class of anti-virulence and anti-resistance mechanisms compounds, which is a trending topic

in the age of antimicrobial resistance. Globally, antimicrobial resistance is a major public health threat, and multi and extensively drug resistant (MDR, XDR) tuberculosis is a case of particular concern, so progress and major advances that can be expected from the coming years will be greatly welcomed.

AUTHOR CONTRIBUTIONS

JA, LR, and CM contributed to the conception and design of the study. FS-G, EA-C, AL, LR, and EP-H carried out the experimental work. FS-G, EA-C, and JA wrote the manuscript. All authors contributed to manuscript revision, read and approved the submitted version.

REFERENCES

- Ahn, J. W., and Kim, K. J. (2013). Rv3168 phosphotransferase activity mediates kanamycin resistance in *Mycobacterium tuberculosis*. *J. Microbiol. Biotechnol.* 23, 1529–1535. doi: 10.4014/jmb.1306.06048
- Ainsa, J. A., Blokpoel, M. C., Otal, I., Young, D. B., De Smet, K. A., and Martin, C. (1998). Molecular cloning and characterization of Tap, a putative multidrug efflux pump present in *Mycobacterium fortuitum* and *Mycobacterium tuberculosis*. *J. Bacteriol.* 180, 5836–5843.
- Ainsa, J. A., Martin, C., Gicquel, B., and Gomez-Lus, R. (1996). Characterization of the chromosomal aminoglycoside 2'-N-acetyltransferase gene from *Mycobacterium fortuitum*. *Antimicrob. Agents Chemother.* 40, 2350–2355. doi: 10.1128/AAC.40.10.2350
- Ainsa, J. A., Perez, E., Pelicic, V., Berthet, F. X., Gicquel, B., and Martin, C. (1997). Aminoglycoside 2'-N-acetyltransferase genes are universally present in mycobacteria: characterization of the aac(2')-Ic gene from *Mycobacterium tuberculosis* and the aac(2')-Id gene from *Mycobacterium smegmatis*. *Mol. Microbiol.* 24, 431–441. doi: 10.1046/j.1365-2958.1997.3471717.x
- Anand, C., Garg, R., Ghosh, S., and Nagaraja, V. (2017). A Sir2 family protein Rv1151c deacetylates HU to alter its DNA binding mode in *Mycobacterium tuberculosis*. *Biochem. Biophys. Res. Commun.* 493, 1204–1209. doi: 10.1016/j.bbrc.2017.09.087
- Anand, S., and Sharma, C. (2018). Glycine-rich loop encompassing active site at interface of hexameric *M. tuberculosis* Eis protein contributes to its structural stability and activity. *Int. J. Biol. Macromol.* 109, 124–135. doi: 10.1016/j.ijbiomac.2017.12.058
- Angelatou, F., Litsas, S. B., and Kontomichalou, P. (1982). Purification and properties of two gentamicin-modifying enzymes, coded by a single plasmid pPK237 originating from *Pseudomonas aeruginosa*. *J. Antibiot.* 35, 235–244. doi: 10.7164/antibiotics.35.235
- Barrett, O. J., Pushechnikov, A., Wu, M., and Disney, M. D. (2008). Studying aminoglycoside modification by the acetyltransferase class of resistance-causing enzymes via microarray. *Carbohydr. Res.* 343, 2924–2931. doi: 10.1016/j.carres.2008.08.018
- Basseti, M., Vena, A., Croxatto, A., Righi, E., and Guery, B. (2018). How to manage *Pseudomonas aeruginosa* infections. *Drugs Context* 7:212527. doi: 10.7573/dic.212527
- Bhowmick, T., Ghosh, S., Dixit, K., Ganesan, V., Ramagopal, U. A., Dey, D., et al. (2014). Targeting *Mycobacterium tuberculosis* nucleoid-associated protein HU with structure-based inhibitors. *Nat. Commun.* 5:4124. doi: 10.1038/ncomms5124
- Card, G. L., Peterson, N. A., Smith, C. A., Rupp, B., Schick, B. M., and Baker, E. N. (2005). The crystal structure of Rv1347c, a putative antibiotic resistance protein from *Mycobacterium tuberculosis*, reveals a GCN5-related fold and suggests an alternative function in siderophore biosynthesis. *J. Biol. Chem.* 280, 13978–13986. doi: 10.1074/jbc.M413904200
- Chen, W., Biswas, T., Porter, V. R., Tsodikov, O. V., and Garneau-Tsodikova, S. (2011). Unusual regioversatility of acetyltransferase Eis, a cause of drug

FUNDING

FS-G and EA-C are recipients of FPU fellowships from the Spanish Ministry of Economy and Competitiveness. JA acknowledges funding from the European Commission [More Medicines for Tuberculosis (MM4TB) grant 260872] and the Spanish Ministry of Economy and Competitiveness (grants SAF-2013-48971-C2-2-R and SAF2017-84839-C2-1-R).

ACKNOWLEDGMENTS

Dessi Marinova was acknowledged for critical reading of the manuscript.

- resistance in XDR-TB. *Proc. Natl. Acad. Sci. U.S.A.* 108, 9804–9808. doi: 10.1073/pnas.1105379108
- Chen, W., Green, K. D., and Garneau-Tsodikova, S. (2012a). Cosubstrate tolerance of the aminoglycoside resistance enzyme Eis from *Mycobacterium tuberculosis*. *Antimicrob. Agents Chemother.* 56, 5831–5838. doi: 10.1128/AAC.00932-12
- Chen, W., Green, K. D., Tsodikov, O. V., and Garneau-Tsodikova, S. (2012b). Aminoglycoside multiacetylating activity of the enhanced intracellular survival protein from *Mycobacterium smegmatis* and its inhibition. *Biochemistry* 51, 4959–4967. doi: 10.1021/bi3004473
- Clarke, A. J., Francis, D., and Keenleyside, W. J. (1996). The prevalence of gentamicin 2'-N-acetyltransferase in the Proteaceae and its role in the O-acetylation of peptidoglycan. *FEMS Microbiol. Lett.* 145, 201–207.
- Cole, S. T., Brosch, R., Parkhill, J., Garnier, T., Churcher, C., Harris, D., et al. (1998). Deciphering the biology of *Mycobacterium tuberculosis* from the complete genome sequence. *Nature* 393, 537–544. doi: 10.1038/31159
- Dahl, J. L., Wei, J., Moulder, J. W., Laal, S., and Friedman, R. L. (2001). Subcellular localization of the intracellular survival-enhancing Eis protein of *Mycobacterium tuberculosis*. *Infect. Immun.* 69, 4295–4302. doi: 10.1128/IAI.69.7.4295-4302.2001
- Dal Molin, M., Gut, M., Rominski, A., Haldimann, K., Becker, K., and Sander, P. (2018). Molecular mechanisms of intrinsic streptomycin resistance in *Mycobacterium abscessus*. *Antimicrob. Agents Chemother.* 62:e001427-17. doi: 10.1128/AAC.01427-17
- Davies, J., and Wright, G. D. (1997). Bacterial resistance to aminoglycoside antibiotics. *Trends Microbiol.* 5, 234–240. doi: 10.1016/S0966-842X(97)01033-0
- Draker, K. A., Boehr, D. D., Elowe, N. H., Noga, T. J., and Wright, G. D. (2003). Functional annotation of putative aminoglycoside antibiotic modifying proteins in *Mycobacterium tuberculosis* H37Rv. *J. Antibiot.* 56, 135–142. doi: 10.7164/antibiotics.56.135
- Duan, L., Yi, M., Chen, J., Li, S., and Chen, W. (2016). *Mycobacterium tuberculosis* EIS gene inhibits macrophage autophagy through up-regulation of IL-10 by increasing the acetylation of histone H3. *Biochem. Biophys. Res. Commun.* 473, 1229–1234. doi: 10.1016/j.bbrc.2016.04.045
- Franklin, K., and Clarke, A. J. (2001). Overexpression and characterization of the chromosomal aminoglycoside 2'-N-acetyltransferase of *Providencia stuartii*. *Antimicrob. Agents Chemother.* 45, 2238–2244. doi: 10.1128/AAC.45.8.2238-2244.2001
- Ganaie, A. A., Lella, R. K., Solanki, R., and Sharma, C. (2011). Thermostable hexameric form of Eis (Rv2416c) protein of *M. tuberculosis* plays an important role for enhanced intracellular survival within macrophages. *PLoS One* 6:e27590. doi: 10.1371/journal.pone.0027590
- Garzan, A., Willby, M. J., Green, K. D., Gajadeera, C. S., Hou, C., Tsodikov, O. V., et al. (2016a). Sulfonamide-based inhibitors of aminoglycoside acetyltransferase Eis abolish resistance to kanamycin in *Mycobacterium tuberculosis*. *J. Med. Chem.* 59, 10619–10628. doi: 10.1021/acs.jmedchem.6b01161
- Garzan, A., Willby, M. J., Green, K. D., Tsodikov, O. V., Posey, J. E., and Garneau-Tsodikova, S. (2016b). Discovery and optimization of two Eis inhibitor families

- as kanamycin adjuvants against drug-resistant *M. tuberculosis*. *ACS Med. Chem. Lett.* 7, 1219–1221. doi: 10.1021/acsmedchemlett.6b00261
- Garzan, A., Wilby, M. J., Ngo, H. X., Gajadeera, C. S., Green, K. D., Holbrook, S. Y., et al. (2017). Combating enhanced intracellular survival (Eis)-mediated kanamycin resistance of *Mycobacterium tuberculosis* by novel pyrrolo[1,5-a]pyrazine-based Eis inhibitors. *ACS Infect. Dis.* 3, 302–309. doi: 10.1021/acsinfecdis.6b00193
- Georgiou, S. B., Magana, M., Garfein, R. S., Catanzaro, D. G., Catanzaro, A., and Rodwell, T. C. (2012). Evaluation of genetic mutations associated with *Mycobacterium tuberculosis* resistance to amikacin, kanamycin and capreomycin: a systematic review. *PLoS One* 7:e33275. doi: 10.1371/journal.pone.0033275
- Ghosh, S., Padmanabhan, B., Anand, C., and Nagaraja, V. (2016). Lysine acetylation of the *Mycobacterium tuberculosis* HU protein modulates its DNA binding and genome organization. *Mol. Microbiol.* 100, 577–588. doi: 10.1111/mmi.13339
- Green, K. D., Biswas, T., Chang, C., Wu, R., Chen, W., Janes, B. K., et al. (2015a). Biochemical and structural analysis of an Eis family aminoglycoside acetyltransferase from bacillus anthracis. *Biochemistry* 54, 3197–3206. doi: 10.1021/acs.biochem.5b00244
- Green, K. D., Pricer, R. E., Stewart, M. N., and Garneau-Tsodikova, S. (2015b). Comparative study of Eis-like enzymes from pathogenic and nonpathogenic bacteria. *ACS Infect. Dis.* 1, 272–283. doi: 10.1021/acsinfecdis.5b00036
- Green, K. D., Biswas, T., Pang, A. H., Wilby, M. J., Reed, M. S., Stuchlik, O., et al. (2018). Acetylation by Eis and deacetylation by Rv1151c of *Mycobacterium tuberculosis* HupB: biochemical and structural insight. *Biochemistry* 57, 781–790. doi: 10.1021/acs.biochem.7b01089
- Green, K. D., Chen, W., and Garneau-Tsodikova, S. (2012). Identification and characterization of inhibitors of the aminoglycoside resistance acetyltransferase Eis from *Mycobacterium tuberculosis*. *ChemMedChem* 7, 73–77. doi: 10.1002/cmdc.201100332
- Hanekom, M., Gey van Pittius, N. C., McEvoy, C., Victor, T. C., Van Helden, P. D., and Warren, R. M. (2011). *Mycobacterium tuberculosis* Beijing genotype: a template for success. *Tuberculosis* 91, 510–523. doi: 10.1016/j.tube.2011.07.005
- Hegde, S. S., Javid-Majd, F., and Blanchard, J. S. (2001). Overexpression and mechanistic analysis of chromosomally encoded aminoglycoside 2'-N-acetyltransferase (AAC(2')-Ic) from *Mycobacterium tuberculosis*. *J. Biol. Chem.* 276, 45876–45881. doi: 10.1074/jbc.M108810200
- Ho, I. I., Chan, C. Y., and Cheng, A. F. (2000). Aminoglycoside resistance in *Mycobacterium kansasii*, *Mycobacterium avium-M. intracellulare*, and *Mycobacterium fortuitum*: are aminoglycoside-modifying enzymes responsible? *Antimicrob. Agents Chemother.* 44, 39–42. doi: 10.1128/AAC.44.1.39-42.2000
- Ho, Y. S., Adroub, S. A., Aleisa, F., Mahmood, H., Othoum, G., Rashid, F., et al. (2012). Complete genome sequence of *Mycobacterium fortuitum* subsp. *fortuitum* type strain DSM46621. *J. Bacteriol.* 194, 6337–6338. doi: 10.1128/JB.01461-12
- Houghton, J. L., Biswas, T., Chen, W., Tsodikov, O. V., and Garneau-Tsodikova, S. (2013a). Chemical and structural insights into the regioversatility of the aminoglycoside acetyltransferase Eis. *Chembiochem* 14, 2127–2135. doi: 10.1002/cbic.201300359
- Houghton, J. L., Green, K. D., Pricer, R. E., Mayhoub, A. S., and Garneau-Tsodikova, S. (2013b). Unexpected N-acetylation of capreomycin by mycobacterial Eis enzymes. *J. Antimicrob. Chemother.* 68, 800–805. doi: 10.1093/jac/dks497
- Hull, S. I., Wallace, R. J. Jr., Bobey, D. G., Price, K. E., Goodhines, R. A., Swenson, J. M., et al. (1984). Presence of aminoglycoside acetyltransferase and plasmids in *Mycobacterium fortuitum*. Lack of correlation with intrinsic aminoglycoside resistance. *Am. Rev. Respir. Dis.* 129, 614–618.
- Jana, S., and Deb, J. K. (2005). Molecular targets for design of novel inhibitors to circumvent aminoglycoside resistance. *Curr. Drug Targets* 6, 353–361. doi: 10.2174/1389450053765860
- Jennings, B. C., Labby, K. J., Green, K. D., and Garneau-Tsodikova, S. (2013). Redesign of substrate specificity and identification of the aminoglycoside binding residues of Eis from *Mycobacterium tuberculosis*. *Biochemistry* 52, 5125–5132. doi: 10.1021/bi4002985
- Joshi, R. S., Jamdhade, M. D., Sonawane, M. S., and Giri, A. P. (2013). Resistome analysis of *Mycobacterium tuberculosis*: identification of aminoglycoside 2'-N-acetyltransferase (AAC) as co-target for drug designing. *Bioinformation* 9, 174–181. doi: 10.6026/97320630009174
- Jugheli, L., Bzekalava, N., de Rijk, P., Fissette, K., Portaels, F., and Rigouts, L. (2009). High level of cross-resistance between kanamycin, amikacin, and capreomycin among *Mycobacterium tuberculosis* isolates from Georgia and a close relation with mutations in the *rrs* gene. *Antimicrob. Agents Chemother.* 53, 5064–5068. doi: 10.1128/AAC.00851-09
- Kim, K. H., An, D. R., Song, J., Yoon, J. Y., Kim, H. S., Yoon, H. J., et al. (2012). *Mycobacterium tuberculosis* Eis protein initiates suppression of host immune responses by acetylation of DUSP16/MKP-7. *Proc. Natl. Acad. Sci. U.S.A.* 109, 7729–7734. doi: 10.1073/pnas.1120251109
- Kim, K. H., An, D. R., Yoon, H. J., Yang, J. K., and Suh, S. W. (2014). Structure of *Mycobacterium smegmatis* Eis in complex with paromomycin. *Acta Crystallogr. F Struct. Biol. Commun.* 70(Pt 9), 1173–1179. doi: 10.1107/S2053230X14017385
- Labby, K. J., and Garneau-Tsodikova, S. (2013). Strategies to overcome the action of aminoglycoside-modifying enzymes for treating resistant bacterial infections. *Future Med. Chem.* 5, 1285–1309. doi: 10.4155/fmc.13.80
- Lella, R. K., and Sharma, C. (2007). Eis (enhanced intracellular survival) protein of *Mycobacterium tuberculosis* disturbs the cross regulation of T-cells. *J. Biol. Chem.* 282, 18671–18675. doi: 10.1074/jbc.C600280200
- Li, Y., Green, K. D., Johnson, B. R., and Garneau-Tsodikova, S. (2015). Inhibition of aminoglycoside acetyltransferase resistance enzymes by metal salts. *Antimicrob. Agents Chemother.* 59, 4148–4156. doi: 10.1128/AAC.00885-15
- Luthra, S., Rominski, A., and Sander, P. (2018). The role of antibiotic-target-modifying and antibiotic-modifying enzymes in *Mycobacterium abscessus* drug resistance. *Front. Microbiol.* 9:2179. doi: 10.3389/fmicb.2018.02179
- Macinga, D. R., and Rather, P. N. (1999). The chromosomal 2'-N-acetyltransferase of *Providencia stuartii*: physiological functions and genetic regulation. *Front. Biosci.* 4, D132–D140. doi: 10.2741/Macinga
- Magnet, S., and Blanchard, J. S. (2005). Molecular insights into aminoglycoside action and resistance. *Chem. Rev.* 105, 477–498. doi: 10.1021/cr0301088
- Maurer, F. P., Bruderer, V. L., Castelberg, C., Ritter, C., Scherbakov, D., Bloemberg, G. V., et al. (2015). Aminoglycoside-modifying enzymes determine the innate susceptibility to aminoglycoside antibiotics in rapidly growing mycobacteria. *J. Antimicrob. Chemother.* 70, 1412–1419. doi: 10.1093/jac/dku550
- Maurer, F. P., Bruderer, V. L., Ritter, C., Castelberg, C., Bloemberg, G. V., and Bottger, E. C. (2014). Lack of antimicrobial bactericidal activity in *Mycobacterium abscessus*. *Antimicrob. Agents Chemother.* 58, 3828–3836. doi: 10.1128/AAC.02448-14
- Mick, V., Rebollo, M. J., Lucia, A., Garcia, M. J., Martin, C., and Ainsa, J. A. (2008). Transcriptional analysis of and resistance level conferred by the aminoglycoside acetyltransferase gene *aac(2')-Id* from *Mycobacterium smegmatis*. *J. Antimicrob. Chemother.* 61, 39–45. doi: 10.1093/jac/dkm440
- Mingeot-Leclercq, M. P., Glupczynski, Y., and Tulkens, P. M. (1999). Aminoglycosides: activity and resistance. *Antimicrob. Agents. Chemother.* 43, 727–737. doi: 10.1128/AAC.43.4.727
- Mitsuhashi, S., Tanaka, T., Kawabe, H., and Umezawa, H. (1977). Biochemical mechanism of kanamycin resistance in *Mycobacterium tuberculosis*. *Microbiol. Immunol.* 21, 325–327. doi: 10.1111/j.1348-0421.1977.tb00294.x
- Ngo, H. X., Green, K. D., Gajadeera, C. S., Wilby, M. J., Holbrook, S. Y. L., Hou, C., et al. (2018). Potent 1,2,4-triazino[5,6 b]indole-3-thioether inhibitors of the kanamycin resistance enzyme Eis from *Mycobacterium tuberculosis*. *ACS Infect. Dis.* 4, 1030–1040. doi: 10.1021/acsinfecdis.8b00074
- Palomino, J. C., Martin, A., Camacho, M., Guerra, H., Swings, J., and Portaels, F. (2002). Resazurin microtiter assay plate: simple and inexpensive method for detection of drug resistance in *Mycobacterium tuberculosis*. *Antimicrob. Agents Chemother.* 46, 2720–2722. doi: 10.1128/AAC.46.8.2720-2722.2002
- Pan, Q., Zhao, F. L., and Ye, B. C. (2018). Eis, a novel family of arylalkylamine N-acetyltransferase (EC 2.3.1.87). *Sci. Rep.* 8:2435. doi: 10.1038/s41598-018-20802-6
- Payie, K. G., and Clarke, A. J. (1997). Characterization of gentamicin 2'-N-acetyltransferase from *Providencia stuartii*: its use of peptidoglycan metabolites for acetylation of both aminoglycosides and peptidoglycan. *J. Bacteriol.* 179, 4106–4114. doi: 10.1128/jb.179.13.4106-4114.1997

- Paye, K. G., Rather, P. N., and Clarke, A. J. (1995). Contribution of gentamicin 2'-N-acetyltransferase to the O acetylation of peptidoglycan in *Providencia stuartii*. *J. Bacteriol.* 177, 4303–4310. doi: 10.1128/jb.177.15.4303-4310.1995
- Paye, K. G., Strating, H., and Clarke, A. J. (1996). The role of O-acetylation in the metabolism of peptidoglycan in *Providencia stuartii*. *Microb. Drug Resist.* 2, 135–140. doi: 10.1089/mdr.1996.2.135
- Prabu, A., Hassan, S., Prabuseenivasan, Shainaba, A. S., Hanna, L. E., and Kumar, V. (2015). Andrographolide: a potent antituberculosis compound that targets Aminoglycoside 2'-N-acetyltransferase in *Mycobacterium tuberculosis*. *J. Mol. Graph. Model.* 61, 133–140. doi: 10.1016/j.jmgm.2015.07.001
- Pryjma, M., Burian, J., Kuchinski, K., and Thompson, C. J. (2017). Antagonism between front-line antibiotics clarithromycin and amikacin in the treatment of *Mycobacterium abscessus* infections is mediated by the *whiB7* gene. *Antimicrob. Agents Chemother.* 61:e01353-17. doi: 10.1128/AAC.01353-17
- Ramon-Garcia, S., Ota, I., Martin, C., Gomez-Lus, R., and Ainsa, J. A. (2006). Novel streptomycin resistance gene from *Mycobacterium fortuitum*. *Antimicrob. Agents Chemother.* 50, 3920–3922. doi: 10.1128/AAC.00223-06
- Rather, P. N., Orosz, E., Shaw, K. J., Hare, R., and Miller, G. (1993). Characterization and transcriptional regulation of the 2'-N-acetyltransferase gene from *Providencia stuartii*. *J. Bacteriol.* 175, 6492–6498. doi: 10.1128/jb.175.20.6492-6498.1993
- Reeves, A. Z., Campbell, P. J., Sultana, R., Malik, S., Murray, M., Plikaytis, B. B., et al. (2013). Aminoglycoside cross-resistance in *Mycobacterium tuberculosis* due to mutations in the 5' untranslated region of *whiB7*. *Antimicrob. Agents Chemother.* 57, 1857–1865. doi: 10.1128/AAC.02191-12
- Ripoll, F., Pasek, S., Schenowitz, C., Dossat, C., Barbe, V., Rottman, M., et al. (2009). Non mycobacterial virulence genes in the genome of the emerging pathogen *Mycobacterium abscessus*. *PLoS One* 4:e5660. doi: 10.1371/journal.pone.0005660
- Roberts, E. A., Clark, A., McBeth, S., and Friedman, R. L. (2004). Molecular characterization of the *Eis* promoter of *Mycobacterium tuberculosis*. *J. Bacteriol.* 186, 5410–5417. doi: 10.1128/JB.186.16.5410-5417.2004
- Rominski, A., Selchow, P., Becker, K., Brulle, J. K., Dal Molin, M., and Sander, P. (2017). Elucidation of *Mycobacterium abscessus* aminoglycoside and capreomycin resistance by targeted deletion of three putative resistance genes. *J. Antimicrob. Chemother.* 72, 2191–2200. doi: 10.1093/jac/dkx125
- Samuel, L. P., Song, C. H., Wei, J., Roberts, E. A., Dahl, J. L., Barry, C. E., et al. (2007). Expression, production and release of the *Eis* protein by *Mycobacterium tuberculosis* during infection of macrophages and its effect on cytokine secretion. *Microbiology* 153(Pt 2), 529–540. doi: 10.1099/mic.0.2006/002642-0
- Shcherbakov, D., Akbergenov, R., Matt, T., Sander, P., Andersson, D. I., and Bottger, E. C. (2010). Directed mutagenesis of *Mycobacterium smegmatis* 16S rRNA to reconstruct the in vivo evolution of aminoglycoside resistance in *Mycobacterium tuberculosis*. *Mol. Microbiol.* 77, 830–840. doi: 10.1111/j.1365-2958.2010.07218.x
- Shell, S. S., Wang, J., Lapierre, P., Mir, M., Chase, M. R., Pyle, M. M., et al. (2015). Leaderless transcripts and small proteins are common features of the mycobacterial translational landscape. *PLoS Genet.* 11:e1005641. doi: 10.1371/journal.pgen.1005641
- Shi, K., Caldwell, S. J., Fong, D. H., and Berghuis, A. M. (2013). Prospects for circumventing aminoglycoside kinase mediated antibiotic resistance. *Front. Cell. Infect. Microbiol.* 3:22. doi: 10.3389/fcimb.2013.00022
- Shin, D. M., Jeon, B. Y., Lee, H. M., Jin, H. S., Yuk, J. M., Song, C. H., et al. (2010). *Mycobacterium tuberculosis* *Eis* regulates autophagy, inflammation, and cell death through redox-dependent signaling. *PLoS Pathog.* 6:e1001230. doi: 10.1371/journal.ppat.1001230
- Smith, C. A., and Baker, E. N. (2002). Aminoglycoside antibiotic resistance by enzymatic deactivation. *Curr. Drug Targets Infect. Disord.* 2, 143–160. doi: 10.2174/1568005023342533
- Stover, C. K., de la Cruz, V. F., Fuerst, T. R., Burlein, J. E., Benson, L. A., Bennett, L. T., et al. (1991). New use of BCG for recombinant vaccines. *Nature* 351, 456–460. doi: 10.1038/351456a0
- Suay-Garcia, B., and Perez-Gracia, M. T. (2018). Future prospects for *Neisseria gonorrhoeae* treatment. *Antibiotics* 7:E49. doi: 10.3390/antibiotics7020049
- Tsodikov, O. V., Green, K. D., and Garneau-Tsodikova, S. (2014). A random sequential mechanism of aminoglycoside acetylation by *Mycobacterium tuberculosis* *Eis* protein. *PLoS One* 9:e92370. doi: 10.1371/journal.pone.0092370
- Udou, T., Mizuguchi, Y., and Wallace, R. J. Jr. (1987). Patterns and distribution of aminoglycoside-acetylating enzymes in rapidly growing mycobacteria. *Am. Rev. Respir. Dis.* 136, 338–343. doi: 10.1164/ajrccm/136.2.338
- Udou, T., Mizuguchi, Y., and Wallace, R. J. Jr. (1989). Does aminoglycoside-acetyltransferase in rapidly growing mycobacteria have a metabolic function in addition to aminoglycoside inactivation? *FEMS Microbiol. Lett.* 48, 227–230. doi: 10.1111/j.1574-6968.1989.tb03304.x
- Udou, T., Mizuguchi, Y., and Yamada, T. (1986). Biochemical mechanisms of antibiotic resistance in a clinical isolate of *Mycobacterium fortuitum*. Presence of beta-lactamase and aminoglycoside-acetyltransferase and possible participation of altered drug transport on the resistance mechanism. *Am. Rev. Respir. Dis.* 133, 653–657. doi: 10.1164/arrd.1986.133.4.653
- Vetting, M., Roderick, S. L., Hegde, S., Magnet, S., and Blanchard, J. S. (2003). What can structure tell us about in vivo function? The case of aminoglycoside-resistance genes. *Biochem. Soc. Trans.* 31(Pt 3), 520–522. doi: 10.1042/bst0310520
- Vetting, M. W., Hegde, S. S., Javid-Majd, F., Blanchard, J. S., and Roderick, S. L. (2002). Aminoglycoside 2'-N-acetyltransferase from *Mycobacterium tuberculosis* in complex with coenzyme A and aminoglycoside substrates. *Nat. Struct. Biol.* 9, 653–658. doi: 10.1038/nsb830
- Waglechner, N., and Wright, G. D. (2017). Antibiotic resistance: it's bad, but why isn't it worse? *BMC Biol.* 15:84. doi: 10.1186/s12915-017-0423-1
- Wallace, R. J. Jr., Hull, S. I., Bobey, D. G., Price, K. E., Swenson, J. M., Steele, L. C., et al. (1985). Mutational resistance as the mechanism of acquired drug resistance to aminoglycosides and antibacterial agents in *Mycobacterium fortuitum* and *Mycobacterium chelonae*. Evidence is based on plasmid analysis, mutational frequencies, and aminoglycoside-modifying enzyme assays. *Am. Rev. Respir. Dis.* 132, 409–416. doi: 10.1164/arrd.1985.132.2.409
- Wei, J., Dahl, J. L., Moulder, J. W., Roberts, E. A., O'Gaora, P., Young, D. B., et al. (2000). Identification of a *Mycobacterium tuberculosis* gene that enhances mycobacterial survival in macrophages. *J. Bacteriol.* 182, 377–384. doi: 10.1128/JB.182.2.377-384.2000
- Willby, M. J., Green, K. D., Gajadeera, C. S., Hou, C., Tsodikov, O. V., Posey, J. E., et al. (2016). Potent inhibitors of acetyltransferase *Eis* overcome kanamycin resistance in *Mycobacterium tuberculosis*. *ACS Chem. Biol.* 11, 1639–1646. doi: 10.1021/acscchembio.6b00110
- World Health Organization [WHO] (2010). *Treatment of Tuberculosis Guidelines*. Geneva: World Health Organization. doi: 10.1099/mic.0.024638-0
- Wu, S., Barnes, P. F., Samten, B., Pang, X., Rodrigue, S., Ghanny, S., et al. (2009). Activation of the *Eis* gene in a W-Beijing strain of *Mycobacterium tuberculosis* correlates with increased SigA levels and enhanced intracellular growth. *Microbiology* 155(Pt 4), 1272–1281. doi: 10.1099/mic.0.024638-0
- Yoon, H. J., Kim, K. H., Yang, J. K., Suh, S. W., Kim, H., and Jang, S. (2013). A docking study of enhanced intracellular survival protein from *Mycobacterium tuberculosis* with human DUSP16/MKP-7. *J. Synchrotron Radiat.* 20(Pt 6), 929–932. doi: 10.1107/S0909049513021341
- Zaunbrecher, M. A., Sikes, R. D. Jr., Metchock, B., Shinnick, T. M., and Posey, J. E. (2009). Overexpression of the chromosomally encoded aminoglycoside acetyltransferase *Eis* confers kanamycin resistance in *Mycobacterium tuberculosis*. *Proc. Natl. Acad. Sci. U.S.A.* 106, 20004–20009. doi: 10.1073/pnas.0907925106
- Zhang, Y., and Yew, W. W. (2009). Mechanisms of drug resistance in *Mycobacterium tuberculosis*. *Int. J. Tuberc. Lung Dis.* 13, 1320–1330.

Conflict of Interest Statement: The authors declare that the research was conducted in the absence of any commercial or financial relationships that could be construed as a potential conflict of interest.

Copyright © 2019 Sanz-García, Anoz-Carbonell, Pérez-Herrán, Martín, Lucía, Rodrigues and Ainsa. This is an open-access article distributed under the terms of the Creative Commons Attribution License (CC BY). The use, distribution or reproduction in other forums is permitted, provided the original author(s) and the copyright owner(s) are credited and that the original publication in this journal is cited, in accordance with accepted academic practice. No use, distribution or reproduction is permitted which does not comply with these terms.



Insights on *Mycobacterium leprae* Efflux Pumps and Their Implications in Drug Resistance and Virulence

Diana Machado^{1,2}, Emmanuel Lecorche^{3,4,5}, Faiza Mougari^{3,4,5}, Emmanuelle Cambau^{2,3,4,5*} and Miguel Viveiros^{1,2*}

¹ Global Health and Tropical Medicine, Instituto de Higiene e Medicina Tropical, Universidade Nova de Lisboa, Lisbon, Portugal, ² Study Group for Mycobacterial Infections (ESGMYC), European Society for Clinical Microbiology and Infectious Diseases (ESCMID), Basel, Switzerland, ³ Université Paris Diderot, INSERM IAME UMR1137, Sorbonne Paris Cité, Paris, France, ⁴ APHP, Groupe Hospitalier Lariboisière Fernand-Widal, Laboratoire de Bactériologie, Paris, France, ⁵ Centre National de Référence des Mycobactéries et Résistance des Mycobactéries aux Antituberculeux, Paris, France

OPEN ACCESS

Edited by:

Silvia Buroni,
University of Pavia, Italy

Reviewed by:

Katiany Rizzieri Caleffi Ferracioli,
Universidade Estadual de Maringá,
Brazil

Yusuf Akhter,
Babasaheb Bhimrao Ambedkar
University, India

*Correspondence:

Emmanuelle Cambau
emmanuelle.cambau@aphp.fr
Miguel Viveiros
mviveiros@ihmt.unl.pt

Specialty section:

This article was submitted to
Evolutionary and Genomic
Microbiology,
a section of the journal
Frontiers in Microbiology

Received: 18 July 2018

Accepted: 28 November 2018

Published: 13 December 2018

Citation:

Machado D, Lecorche E, Mougari F,
Cambau E and Viveiros M (2018)
Insights on *Mycobacterium leprae*
Efflux Pumps and Their Implications in
Drug Resistance and Virulence.
Front. Microbiol. 9:3072.
doi: 10.3389/fmicb.2018.03072

Drug resistance in *Mycobacterium leprae* is assumed to be due to genetic alterations in the drug targets and reduced cell wall permeability. However, as observed in *Mycobacterium tuberculosis*, drug resistance may also result from the overactivity of efflux systems, which is mostly unexplored. In this perspective, we discuss known efflux pumps involved in *M. tuberculosis* drug resistance and virulence and investigate similar regions in the genome of *M. leprae*. *In silico* analysis reveals that the major *M. tuberculosis* efflux pumps known to be associated with drug resistance and virulence have been retained during the reductive evolutionary process that *M. leprae* underwent, e.g., RND superfamily, the ABC transporter BacA, and the MFS P55. However, some are absent (DinF, MATE) while others are derepressed (Mmr, SMR) in *M. leprae* reflecting the specific environment where *M. leprae* may live. The occurrence of several multidrug resistance efflux transporters shared between *M. leprae* and *M. tuberculosis* reveals potential implications in drug resistance and virulence. The conservation of the described efflux systems in *M. leprae* upon genome reduction indicates that these systems are potentially required for its intracellular survival and lifestyle. They potentially are involved in *M. leprae* drug resistance, which could hamper leprosy treatment success. Studying *M. leprae* efflux pumps as new drug targets is useful for future leprosy therapeutics, enhancing the global efforts to eradicate endemic leprosy, and prevent the emergence of drug resistance in afflicted countries.

Keywords: antimicrobial resistance, efflux pumps, leprosy, mycobacteria, tuberculosis, virulence

INTRODUCTION

Leprosy and tuberculosis are public health threatening infectious diseases with similar problems of ongoing human-to-human transmission, inherent drug resistance to several antimicrobial agents, propensity to develop resistance to antimycobacterial drugs, and virulence (Singh et al., 2016; Dheda et al., 2017). Whilst there is extensive knowledge about the mechanisms of *M. tuberculosis* drug resistance, less is known about the mechanisms by which *M. leprae* develops drug resistance. *M. leprae* is an obligate intracellular pathogen and one of the few known microorganisms that still cannot be cultured *in vitro*

which have been hindering the study of the mechanisms of drug resistance by biochemical and functional studies. The overexpression of multidrug (MDR) efflux pump genes is a common mechanism of antimicrobial resistance in *M. tuberculosis* (da Silva et al., 2016; Machado et al., 2017). Likewise, efflux pumps certainly contribute to drug resistance in *M. leprae*, which is mostly unexplored.

Efflux pumps are one of the most widespread resistance determinants in bacteria. Usually, they are chromosomally encoded and are greatly conserved at both gene and protein level across bacterial species. More than 50 putative efflux pumps have been associated with the transport of several drugs in *M. tuberculosis* (De Rossi et al., 2006; Louw et al., 2009; Kapopoulou et al., 2011; Black et al., 2014; da Silva et al., 2016). Although they are mostly known due to their role in the efflux of antimicrobials, efflux pumps are mainly involved in physiological processes such as cell-to-cell communication, bacterial virulence, cellular homeostasis, detoxification of intracellular metabolites, and intracellular signal trafficking (De Rossi et al., 2006; Martinez et al., 2009; Viveiros et al., 2012; Black et al., 2014; da Silva et al., 2016; Li et al., 2016; Sandhu and Akhter, 2018). Recently, it was shown that the loss of the efflux pump AcrAB in *Salmonella enterica* serovar Typhimurium reduces virulence leading to the accumulation of noxious molecules inside the bacteria reducing the bacterial factors required for infection (Wang-Kan et al., 2017). From a biological point of view, drug resistance and virulence are required for pathogen survival. In normal conditions, the expression of these systems is tightly downregulated by specific transcriptional regulators (Grkovic et al., 2001) and their overexpression is achieved only in the presence of specific stressors capable of binding to the transcriptional regulators. The induction of efflux systems in the presence of inducers such as antimicrobials or host factors during infection promote a low-level resistance phenotype that allows the bacteria to survive during prolonged periods in the presence of drugs contributing for the development and stabilization of resistant phenotypes (Machado et al., 2012; Schmalstieg et al., 2012).

In this perspective, we compared *in silico* *M. tuberculosis* efflux pumps involved in drug resistance and virulence with those of *M. leprae* investigating their possible involvement in antimicrobial resistance and virulence in *M. leprae*.

REDUCTIVE EVOLUTION

The genome of the non-pathogenic *Mycobacterium smegmatis* mc²155 has 7 Mb in size; the genomes of the pathogenic *M. tuberculosis* and *M. leprae* are much smaller in length and for *M. leprae* this is even more dramatic with almost 2000 genes lost in comparison with *M. tuberculosis*. Compared to non-pathogenic mycobacteria, *M. tuberculosis* and *M. leprae* evolved by extensive reductive evolution suggesting that pathogenic mycobacteria evolved toward pathogenicity by the loss of genetic material as the result of niche adaptation. Contrary to *M. tuberculosis*, *M. leprae* is an obligate intracellular pathogen. Adaptation to a permanent pathogenic lifestyle in constant association with the

host led to gene loss toward a minimal gene set, such as those coding for metabolism and respiration, needed for a successful obligate intracellular parasitism (Moran, 2002; Scollard et al., 2006) and limited capacity to survive extracellularly (Cole et al., 2001; Eiglmeier et al., 2001). Of interest is the fact that the G+C content is lower in *M. leprae* pseudogenes (56.5%) than in its active ORFs (60.1%) (Cole et al., 2001). Changes in G+C content during the path of evolution may confer an advantage in response to environmental changes (Mann and Chen, 2010). Free-living organisms have an average G+C content higher than obligatory pathogens and symbionts. The shift toward lower G+C contents and smaller genomes in obligate pathogenic mycobacteria seems to occur in response to environmental adaptation where they encounter low selective pressure (Mann and Chen, 2010). In this context some genes became inactivated, as they are not required in these highly specialized niches meeting the theoretical principles of Morris, Lenski, and Zinser's Black Queen Hypothesis for the symbiotic reductive genome evolution of microorganisms (Morris et al., 2012), now applied to a bacterium and his long-lasting and almost exclusive host—the human being. In this case, *M. leprae* relies on his host functions to live efficiently, losing burdensome genes for functions it does not have to perform for itself (Morris et al., 2012). Nevertheless, it is not clear why *M. leprae* maintains such high number of pseudogenes in the genome. It has been hypothesized that the maintenance of pseudogenes is due to the slow-growth rate (McLeod et al., 2004) or lack of recombination (Bolotin and Hershberg, 2015). Additionally, pseudogene maintenance may allow the bacteria to revert back and forward from a non-functional protein to a functional one (Bolotin and Hershberg, 2015). If true, this may explain why some genes are lost and others are maintained as pseudogenes in *M. leprae* genome.

In this evolutionary context, where an obligate intracellular pathogen evolved to become dependent on his host, the central question of this work is the impact of *M. leprae* genome downsizing on antimicrobial resistance. This can be viewed as the time when the host decides that he no longer wants to maintain this intimate relation and starts antibiotic treatment with the assistance of his clinician and the health system.

DRUG RESISTANCE AND EFFLUX SYSTEMS IN *M. LEPRAE*

Several mycobacterial drug efflux pumps have been described in *M. tuberculosis* (Table 1). Comparative analysis of *M. leprae* genome shows the presence of approximately half of these transporters while several others are inactivated or absent, probably lost as consequence of reductive evolution. *In silico*, *M. tuberculosis* H37Rv genome encodes 267 putative transporters, of which 129 belong to the ATP-binding cassette (ABC) superfamily, 31 to the major facilitator superfamily (MFS), 14 to the resistance nodulation and cell division (RND) superfamily, 1 to the small multidrug resistance (SMR) family, and 1 to the multidrug and toxic compound extrusion (MATE) family. *M. leprae* genome encodes for 114 transporters, of which 62 corresponds to ABC transporters, 6 MFS, 5 RND, and 1 SMR

TABLE 1 | Putative drug membrane transporters encoded by *M. tuberculosis* H37Rv and its orthologous in *M. leprae* TN.

Efflux pump family	Gene	Gene locus tag*		Identity (%)**	<i>M. tuberculosis</i>	
		<i>M. tuberculosis</i>	<i>M. leprae</i>		Antimicrobial substrates	Main references
ABC						
“One gene”	<i>bacA</i>	Rv1819c	ML2084	75	RIF, INH, BL, CHL, TET, VAN, MAC, NOV, AGs, AP	Daniilchanka et al., 2008; Domenech et al., 2009; Gupta et al., 2010a; Kapopoulou et al., 2011; Li et al., 2015
	<i>Rv0194</i>	Rv0194	Absent	-	BL, CHL, STR, TET, VAN, MAC, NOV, EMB, EtBr	Daniilchanka et al., 2008; Kapopoulou et al., 2011; Garima et al., 2015
	<i>pstB</i>	Rv0933	<u>ML0741c</u>	-	FQs, INH, RIF, EMB	Banerjee et al., 1996, 2000; Braibant et al., 1996; Gupta et al., 2006; Srivastava et al., 2010; Kapopoulou et al., 2011; Brandis and Hughes, 2013; Lu et al., 2014
	<i>Rv1473</i>	Rv1473	ML1816c	88	MAC	Kapopoulou et al., 2011
	<i>Rv2477c</i>	Rv2477c	ML1248	92	MAC, FQs	Gupta et al., 2010a; Kapopoulou et al., 2011
“Two-genes”	<i>Rv1218c-Rv1217c</i>	Rv1218c- Rv1217c	<u>ML1073c-ML1072c</u>	-	BL, NOV, BP, PD, PR, BSP, PA, INH, RIF	Balganesh et al., 2010; Kapopoulou et al., 2011; Dinesh et al., 2013; Wang et al., 2013
	<i>Rv1273c-Rv1272c</i>	Rv1273c- Rv1272c	<u>ML1114c-ML1113c</u>	78	Unknown	Kapopoulou et al., 2011
	<i>Rv1668c-Rv1667c</i>	Rv1668c- Rv1667c	<u>ML1240c-ML1239c</u>	75		
	<i>Rv1668c-Rv1667c</i>	Rv1668c- Rv1667c	<u>ML1240c-ML1239c</u>	-	MAC	Kapopoulou et al., 2011
	<i>Rv1687c-Rv1686c</i>	Rv1687c- Rv1686c	<u>ML1350c-ML1349c</u>	-	MAC	Kapopoulou et al., 2011
	<i>Rv1687c-Rv1686c</i>	Rv1687c- Rv1686c	<u>ML1350c-ML1349c</u>	-	MAC	Kapopoulou et al., 2011
“Three-genes”	<i>Rv1458c-Rv1457c</i>	Rv1458c- Rv1457c	ML0590c-ML0589c	88	RIF, INH, STR, EMB	Hao et al., 2011; Kapopoulou et al., 2011; Caleffi-Ferracioli et al., 2016
	<i>Rv1456c-Rv2688c</i>	Rv1456c- Rv2688c	ML0587c-Absent	83	FQs	Pasca et al., 2004; Gupta et al., 2010a; Kapopoulou et al., 2011
	<i>Rv2687c-Rv2686c</i>	Rv1687c- Rv1686c	<u>ML1035</u> <u>ML1034</u>	-		
	<i>drvA-drrB-drrC</i>	Rv2936- Rv2937- Rv2938	ML2352c-ML2351c-ML2350c	85	TET, EMB, MAC, AGs, CHL, RIF, EtBr, NOR, PUR, BCECF, DAU, DOX	Choudhuri et al., 2002; Kapopoulou et al., 2011; Pang et al., 2013; Li et al., 2015
	<i>drvA-drrB-drrC</i>	Rv2936- Rv2937- Rv2938	ML2352c-ML2351c-ML2350c	64		
	<i>drvA-drrB-drrC</i>	Rv2936- Rv2937- Rv2938	ML2352c-ML2351c-ML2350c	79		
	<i>drvA-drrB-drrC</i>	Rv2936- Rv2937- Rv2938	ML2352c-ML2351c-ML2350c	-		
	<i>drvA-drrB-drrC</i>	Rv2936- Rv2937- Rv2938	ML2352c-ML2351c-ML2350c	-		
MFS						
	<i>Rv0037c</i>	Rv0037c	<u>ML0027c</u>	-	Unknown	Kapopoulou et al., 2011
	<i>Rv0191</i>	Rv0191	<u>ML2610</u>	-	RIF	Kapopoulou et al., 2011; Li et al., 2015
	<i>emrB</i>	Rv0783c	<u>ML2224</u>	-	Multiple drugs	De Rossi et al., 2002; Gupta et al., 2010a; Kapopoulou et al., 2011; Brandis and Hughes, 2013; Li et al., 2015
	<i>Rv0842</i>	Rv0842	Absent	-	RIF	Kapopoulou et al., 2011; Li et al., 2015
	<i>Rv0849</i>	Rv0849	Absent	-	BL, INH, RIF	Kapopoulou et al., 2011; Balganesh et al., 2012
	<i>Rv0876c</i>	Rv0876c	ML2143	81	Unknown	Kapopoulou et al., 2011
	<i>Rv1250</i>	Rv1250	<u>ML1097</u>	-	INH	Kapopoulou et al., 2011; Garima et al., 2015; Li et al., 2015
	<i>Rv1258c</i>	Rv1258c	<u>ML1104c</u>	-	TET, FQs, RIF, CFZ, INH, EMB, ERY, EtBr, SPE	Ainsa et al., 1998; Siddiqi et al., 2004; Gupta et al., 2006; Ramón-García et al., 2006, 2012; Jiang et al., 2008; Kapopoulou et al., 2011; Balganesh et al., 2012; Machado et al., 2012, 2017
	<i>p55</i>	Rv1410c	ML0556c	82	TET, AGs, RIF, INH, CFZ	da Silva et al., 2001; Jiang et al., 2008; Ramón-García et al., 2009; Bianco et al., 2011a,b; Kapopoulou et al., 2011; Machado et al., 2012, 2017; Li et al., 2015
	<i>Rv1634</i>	Rv1634	<u>ML1388</u>	-	FQs; SKI	De Rossi et al., 2002; Kapopoulou et al., 2011; Harris et al., 2014
	<i>Rv1672c</i>	Rv1672c	Absent	-	Unknown	Kapopoulou et al., 2011
	<i>Rv1877</i>	Rv1877	Absent	-	RIF, EtBr, ACR, ERY, KAN, TET	De Rossi et al., 2002; Li et al., 2004; Kapopoulou et al., 2011; Louw et al., 2011
	<i>Rv2265</i>	Rv2265	Absent	-	Unknown	Kapopoulou et al., 2011
	<i>stp</i>	Rv2333c	Absent	-	SPE, TET, RIF	Ramón-García et al., 2007; Kapopoulou et al., 2011; Li et al., 2015

(Continued)

TABLE 1 | Continued

Efflux pump family	Gene	Gene locus tag*		Identity (%)**	<i>M. tuberculosis</i>	
		<i>M. tuberculosis</i>	<i>M. leprae</i>		Antimicrobial substrates	Main references
	<i>Rv2456c</i>	Rv2456c	Absent	-	Unknown	Kapopoulou et al., 2011
	<i>Rv2459</i>	Rv2459	Absent	-	INH, EMB, RIF, EtBr	De Rossi et al., 2002; Gupta et al., 2010b; Kapopoulou et al., 2011; Machado et al., 2012; Li et al., 2015
	<i>efpA</i>	Rv2846c	ML1562c	81	INH, RIF, EtBr, ACR, ERY, FQs	Doran et al., 1997; Wilson et al., 1999; Li et al., 2004, 2015; Gupta et al., 2010a; Kapopoulou et al., 2011; Machado et al., 2012, 2017
	<i>Rv2994</i>	Rv2994	<u>ML1690</u>	-	STR, RIF	Gupta et al., 2010a; Kapopoulou et al., 2011; Louw et al., 2011
	<i>Rv3239c</i>	Rv3239c	Absent	-	Unknown	Kapopoulou et al., 2011
	<i>Rv3728</i>	Rv3728	<u>ML2340</u>	-	RIF	Gupta et al., 2010a; Kapopoulou et al., 2011
RND						
	<i>mmpS1-mmpL1</i>	Rv0403c-Rv0402c	Absent	-	Unknown	Kapopoulou et al., 2011
	<i>mmpS2-mmpL2</i>	Rv0506-Rv0507	Absent	-	Unknown	Kapopoulou et al., 2011
	<i>mmpL3</i>	Rv0206c	ML2620c	76	SQ109, BM212, AU, IA	Kapopoulou et al., 2011; La Rosa et al., 2012; Tahlan et al., 2012; Li et al., 2014
	<i>mmpS4-mmpL4</i>	Rv0451c-Rv0450c	ML2377 ML2378	75 79	CMB, MB, RIF	Kapopoulou et al., 2011; de Knecht et al., 2013; Wells et al., 2013
	<i>mmpS5-mmpL5</i>	Rv0677c-Rv0676c	Absent	-	AZ, BDQ, CFZ, TET	Milano et al., 2009; Kapopoulou et al., 2011; Hartkoorn et al., 2014
	<i>mmpL6</i>	Rv1557	Absent	-	Unknown	Kapopoulou et al., 2011
	<i>mmpL7</i>	Rv2942	ML0137c	69	INH	Choudhuri et al., 1999; Domenech et al., 2005; Kapopoulou et al., 2011; Machado et al., 2012
	<i>mmpL8</i>	Rv3823c	Absent	-	SQ109	Pasca et al., 2005
	<i>mmpL9</i>	Rv2339	Absent	-	SQ109	Domenech et al., 2004; Kapopoulou et al., 2011; Li et al., 2014
	<i>mmpL10</i>	Rv1183	ML1231	71	Unknown	Kapopoulou et al., 2011
	<i>mmpL11</i>	Rv0202c	ML2617c	73	Unknown	Kapopoulou et al., 2011
	<i>mmpL12</i>	Rv1522c	Absent	-	Unknown	Kapopoulou et al., 2011
	<i>mmpL13a</i>	Rv1145	<u>ML0971</u>	-	Unknown	Kapopoulou et al., 2011
	<i>mmpL13b</i>	Rv1146	<u>ML0972</u>	-	Unknown	Kapopoulou et al., 2011
	<i>mmpS3</i>	Rv2198c	ML0877	68	-	Kapopoulou et al., 2011
SMR						
	<i>mmr</i>	Rv3065	ML1756	79	ACR, EtBr, INH, MAC, FQs, TPP, PY	De Rossi et al., 1998; Kapopoulou et al., 2011; Balganesi et al., 2012; Machado et al., 2012; Rodrigues et al., 2013
MATE						
	<i>dinF</i>	Rv2836c	Absent	-	AGs, Phleo, sulpha drugs, CPC	Kapopoulou et al., 2011; Mishra and Daniels, 2013

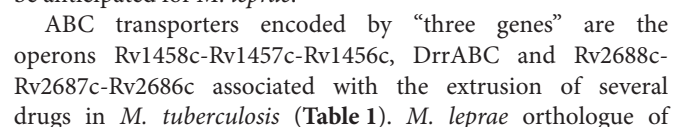
* CDS, coding DNA sequence; ** determined at protein level; pseudogenes are underlined. ABC, ATP-binding cassette; ACR, acriflavine; AGs, aminoglycosides; AP, antimicrobial peptides; AU, adamantyl ureas; AZ, azoles; BCECF, 2',7'-bis-(2-carboxyethyl)-5(6)-carboxyfluorescein; BDQ, bedaquiline; BL, β -lactams; BP, biarylpyrazines; BSP, bisanilinopyrimidines; CFZ, cefazolin; CHL, chloramphenicol; CMB, carboxymycobactins; CPC, cetylpyridinium chloride; DAU, daunorubicin; DOX, doxorubicin; EMB, ethambutol; ERY, erythromycin; EtBr, ethidium bromide; FQs, fluoroquinolones; IA, indoleamides; INH, isoniazid; KAN, kanamycin; MAC, macrolides; MATE, multidrug and toxic compound extrusion; MB, mycobactins; MFS, major facilitator superfamily; NOR, norfloxacin; NOV, novobiocin; PA, pyrazolones; PD, pyridines; Phleo, phleomycin; PR, pyrroles; PUR, puromycin; PY, pyronin Y; RIF, rifampicin; RND, resistance nodulation division; SKI, imidazole SKI-356313; SMR, small multidrug resistance; SPE, spectinomycin; STR, streptomycin; TET, tetracycline; TPP, tetraphenylphosphonium; VAN, vancomycin.

(Elbourne et al., 2017). Those that have been associated with drug resistance in *M. tuberculosis* are discussed below. Alignment visualization of the *M. tuberculosis* and the *M. leprae* whole genome sequences, with the predicted CDS regions of the efflux transporters of *M. leprae* highlighted is shown in **Figure 1**.

ABC Transporters

ABC transporters can be divided in those encoded by “one,” “two,” and “three genes” (**Table 1**). Among those coded by “one gene” in *M. leprae* is ML2084, homologue of BacA that

is involved in virulence of *M. tuberculosis* (Domenech et al., 2009) and in the active transport of drugs across the membrane (**Table 1**). Absent from *M. leprae* genome is the transporter Rv0194, which was the first to be associated with β -lactam transport in *M. tuberculosis* -important taking into account since β -lactams can be useful in *M. leprae* chemotherapy (Danilchanka et al., 2008; Garima et al., 2015). The phosphate-specific ABC transporter (PstB) is known to be operative in *M. tuberculosis* during phosphate limiting conditions during infection (Banerjee et al., 2000). The *pst* operon encodes pseudogenes in *M.*



Rv1458c-Rv1457c-Rv1456c is ML0590c-ML0589c-ML0587c, which encodes a functional efflux transporter. In relation to Rv2688c-Rv2687c-Rv2686c, *M. leprae* chromosome has non-functional orthologues of two components, ML1034-ML1035 (positive strand), while the orthologue of Rv2688c is absent. The genes Rv2686c, Rv2687c, and Rv2688c are co-transcribed. Rv2686c and Rv2687c proteins possess six transmembrane segments, whereas Rv2688c has a nucleotide-binding domain and is likely involved in ATP hydrolysis. In consequence, Rv2688c probably coordinates the functionality of the whole operon. In this case, it is not surprising that the absence of the Rv2688c orthologue in *M. leprae* renders non-functional the other genes within this operon, contributing to the increased susceptibility of *M. leprae* to fluoroquinolones.

MFS Transporters

M. leprae genome possess 11 MFS drug transporters, whereas 20 can be detected in *M. tuberculosis* (Table 1). Among the nine transporters absent from *M. leprae* genome, nothing is known about their role in *M. tuberculosis* for five of them, while for the remaining four it has been described an association with resistance to several drugs (Table 1). Concerning the 11 MFS efflux transporters present in *M. leprae*, eight are non-functional of which some were found to be upregulated in *M. tuberculosis* in response to antibiotics (Table 1). Among these is noted that Rv1258c, also known as Tap-like efflux pump, is a pseudogene (ML1104c) in *M. leprae* presenting 58.4% similarity at nucleotide level with Rv1258c. Rv1258c is associated with reduced susceptibility to several drugs, namely to rifampicin and clofazimine (Table 1) and has an essential role in physiology, growth, and cell morphology (Ramón-García et al., 2012). These findings emphasize the important role of the Rv1258c efflux pump in the oxidative stress response, cell wall assembly and growth, intrinsic drug resistance (Ramón-García et al., 2012) and macrophage tolerance (Adams et al., 2011). Since *M. leprae* orthologue is non-functional, it is unlikely that Rv1258c play any role in *M. leprae* intrinsic drug resistance and virulence. This can be one more genomic trait of *M. leprae* that contributes to its notable susceptibility to rifampicin and clofazimine *in vivo*.

M. leprae chromosome encodes only three functional MFS efflux pumps associated with drug transport in *M. tuberculosis* (Table 1). Of these, the *M. tuberculosis* P55 efflux pump (Rv1410c), orthologue of *M. leprae* ML0556c, is one of the most relevant and well-studied efflux pumps of *M. tuberculosis* and has been associated with the resistance to several drugs (Table 1) and virulence. P55 forms an operon with LprG (Rv1411c), a conserved lipoprotein, which is required for *in vivo* growth of *M. tuberculosis* (Bigi et al., 2004; Farrow and Rubin, 2008), virulence (Bianco et al., 2011a) and accurate cell-wall assembly (Bigi et al., 2004; Bianco et al., 2011b). *M. leprae* encodes both proteins presenting high similarity with those of *M. tuberculosis*. P55 is also associated with cholesterol transport, carbon metabolism, and oxidative stress, which are of major importance for mycobacterial optimal survival and pathogenesis (Ramón-García et al., 2015). Contrary to that observed for Rv1258c (Tap-like efflux pump), the presence of P55 in *M. leprae*

genome indicates a vital role of this transporter in *M. leprae* for which a significant contribution in providing intrinsic antibiotic resistance is plausible.

MATE Transporters

DinF (Rv2836c) is the only MATE transporter that *M. tuberculosis* genome encodes. The *M. tuberculosis* homologue in *M. smegmatis* (Mmp) is involved in the resistance to multiple drugs (Table 1). Importantly, DinF is absent from *M. leprae* genome which can be related with the Na⁺-dependent nature of the MATE transporters that may not exist in the environment where *M. leprae* resides. Youm and Saier (2012) also noted the absence of other Na⁺ transporters in *M. leprae* that are present in *M. tuberculosis* and suggested that these facilitators probably contribute to the maintenance of ion homeostasis and adaptation to several stress conditions.

SMR Transporters

M. tuberculosis genome harbors only one gene belonging to the SMR family, the *mmr* gene, orthologue of ML1756 of *M. leprae*. Mmr overexpression was showed to decrease susceptibility of *M. smegmatis* and *M. tuberculosis* to intercalating dyes, quaternary ammonium compounds and antibiotics (Table 1). Mmr is controlled by the TetR-like transcriptional repressor Rv3066 (Bolla et al., 2012) whose orthologue in *M. leprae* is ML1757. In both species, the transcriptional repressor is located immediately downstream of *mmr* or ML1756. However, while in *M. tuberculosis* the Rv3066 gene encodes a 202-aminoacidic protein, its orthologue in *M. leprae* is a pseudogene. This means that *mmr* transcription is no longer repressed in *M. leprae*. Nothing is known about *M. leprae* susceptibility to biocides and dyes thus the significance of *mmr* depression cannot be unveiled.

RND Transporters

M. tuberculosis genome contains 13 genes that encode MmpLs (Mycobacterial membrane protein, Large), and five auxiliary proteins, the MmpSs (Mycobacterial membrane protein, Small) (Table 1). The MmpLs efflux pumps are responsible for the transport of lipids, mainly mycolic acids, essential for mycobacterial survival and pathogenesis, and heme transport (Cox et al., 1999; Camacho et al., 2001; Converse et al., 2003; Domenech et al., 2005; Tullius et al., 2011; Grzegorzewicz et al., 2012; Tahlan et al., 2012; Rodríguez et al., 2013). The expression of *M. tuberculosis* MmpL proteins is controlled by a complex regulatory network that includes orthologues of TetR (Rv1816 and Rv3249c) and MarR (Rv0678) transcriptional regulators (Radhakrishnan et al., 2014; Delmar et al., 2015). The transcriptional regulator Rv0678 has no orthologue in *M. leprae* and Rv3249c and Rv1816, whose *M. leprae* counterparts are ML0770 and ML0933, are non-functional. This indicate that some of the *M. leprae* *mmpL* genes are out of regulation and are being constitutively expressed or MmpLs regulation in *M. leprae* involves a different regulatory network from that found in *M. tuberculosis*. Of the 13 MmpLs encoded in *M. tuberculosis*, only MmpL3, MmpL4, MmpL7, MmpL10, and MmpL11 are functional proteins in *M. leprae*, while the remaining are absent or non-functional (Table 1). Of these, only MmpL3 is essential

for *M. tuberculosis* survival (Domenech et al., 2005). Moreover, MmpL3 has emerged as a novel therapeutic target in *M. tuberculosis* (Li et al., 2014). Due to high degree of similarity between *M. leprae* MmpL7, MmpL11, and MmpL3 and their orthologous in *M. tuberculosis* (Table 1), we can anticipate a similar function for both proteins in *M. leprae*.

MmpS5-MmpL5, one of the most important RND transporters of *M. tuberculosis*, is absent in the *M. leprae* genome. During the reductive evolutionary process that *M. leprae* experienced, the MmpS5-MmpL5 efflux transporter was eliminated probably to maintain only the pathways required for a strict intracellular lifestyle, typical of *M. leprae*. The overexpression of the MmpS5-MmpL5 efflux transporter was shown to be associated with resistance of *M. tuberculosis* to azoles (Milano et al., 2009) and bedaquiline and cross-resistance to clofazimine (Andries et al., 2014). The absence of the MmpS5-MmpL5 explains why clofazimine is so efficient against *M. leprae*. So far, very rare *M. leprae* strains were described with clofazimine resistance reinforcing the connection between MmpS5-MmpL5 and clofazimine resistance as well as its unique hypersusceptibility in *M. leprae*.

CONCLUSIONS AND FUTURE PERSPECTIVES

The occurrence of shared multidrug resistance efflux transporters between *M. leprae* and *M. tuberculosis* reveals implications for drug resistance and virulence. Multidrug resistance efflux pumps are ubiquitous in nature. Some efflux pumps exhibit a dual role in *M. tuberculosis* contributing to both drug resistance and virulence. Here, we have shown that the major *M. tuberculosis* efflux pumps that are associated with drug efflux and virulence have been retained during the reductive evolutionary process that *M. leprae* underwent. These efflux pumps are not only important for substrate transport across the inner membrane but are also responsible for drug resistance by extruding drugs from the periplasm to the outside of the cell. They may confer a selective advantage in hostile environments, therefore contributing to *M. leprae* pathogenicity and acquired drug resistance to therapy as seen in *M. tuberculosis*. It has been recently shown that resistance to effective multidrug therapy, especially in the high burden countries such as Brazil and India, is on rise, with

noteworthy rates of resistance especially against rifampicin and dapsone (Cambau et al., 2018). Rifampicin resistance was found in new cases of leprosy that may relate to individual abuse of this antibiotic usage for treating other bacterial infections as it was also seen with ofloxacin resistance although an antibiotic not used for the first-line treatment of leprosy (Cambau et al., 2018). Future work should focus on efflux pumps, as those mentioned above, as new drug targets for new leprosy therapeutics. A comparative transcriptomic profile of these transporters may provide additional insights, since differences are expected in the efflux pump expression due to pathogen specificity as consequence of the obligate intracellular lifecycle of *M. leprae*. The modulation of these novel targets will enhance the eradication efforts of endemic leprosy and prevent emergence of drug resistance in afflicted countries. This comparative and perspective study identified these new targets using biological information gathered from *M. tuberculosis* and constitutes the first step for a more detailed computational studies to bring more mechanistic insights and biological analyses to be applied to *M. leprae*, susceptible and drug resistant clinical strains, similar to what have been done for *M. tuberculosis* (Sandhu and Akhter, 2016). The increase in the number of available sequenced genomes and structural data of these proteins together with the advances on experimental and computational biology will improve our knowledge on the relationship between *M. leprae* protein sequence, structure, dynamics and function (Li et al., 2017).

AUTHOR CONTRIBUTIONS

DM and MV designed this conceptual study. DM performed the analyses. DM, EL, FM, EC and MV have made substantial contributions to the work and approved its final version.

FUNDING

DM and MV work is partially supported by the Global Health and Tropical Medicine (GHTM) Research Center (Grant UID/Multi/04413/2013) from Fundação para a Ciência e a Tecnologia (FCT), Portugal and own funding. DM is supported by grant SFRH/BPD/100688/2014 from FCT, Portugal. EL, FM, and EC work on leprosy is supported by the 2016-2022 grant from Santé Publique France.

REFERENCES

- Adams, K. N., Takaki, K., Connolly, L. E., Wiedenhoft, H., Winglee, K., Humbert, O., et al. (2011). Drug tolerance in replicating mycobacteria mediated by a macrophage-induced efflux mechanism. *Cell* 145, 39–53. doi: 10.1016/j.cell.2011.02.022
- Ainsa, J., Blokhoel, M., Otal, I., Young, D., De Smet, K., and Martin, C. (1998). Molecular cloning and characterization of Tap, a putative multidrug efflux pump present in *Mycobacterium fortuitum* and *Mycobacterium tuberculosis*. *J. Bacteriol.* 80, 5836–5843.
- Alikhan, N.-F., Petty, N. K., Zakour, N. L., and Beatson, S. A. (2011). BLAST ring image generator (BRIG): simple prokaryote genome comparisons. *BMC Genomics* 12:402. doi: 10.1186/1471-2164-12-402
- Andries, K., Villellas, C., Coeck, N., Thys, K., Gevers, T., Vranckx, L., et al. (2014). Acquired resistance of *Mycobacterium tuberculosis* to bedaquiline. *PLoS ONE* 9:e102135. doi: 10.1371/journal.pone.0102135
- Balganesh, M., Dinesh, N., Sharma, S., Kuruppath, S., Nair, A. V., and Sharma, U. (2012). Efflux pumps of *Mycobacterium tuberculosis* play a significant role in antituberculosis activity of potential drug candidates. *Antimicrob. Agents Chemother.* 56, 2643–2651. doi: 10.1128/AAC.06003-11
- Balganesh, M., Kuruppath, S., Marcel, N., Sharma, S., Nair, A., and Sharma, U. (2010). Rv1218c, an ABC transporter of *Mycobacterium tuberculosis* with implications in drug discovery. *Antimicrob. Agents Chemother.* 54, 5167–5172. doi: 10.1128/AAC.00610-10
- Banerjee, S. K., Bhatt, K., Misra, P., and Chakraborti, P. (2000). Involvement of a natural transport system in the process of efflux-mediated drug

- resistance in *Mycobacterium smegmatis*. *Mol. Gen. Genet.* 262, 949–956. doi: 10.1007/PL00008663
- Banerjee, S. K., Bhatt, K., Rana, S., Misra, P., and Chakraborti, P. (1996). Involvement of an efflux system in mediating high level of fluoroquinolone resistance in *Mycobacterium smegmatis*. *Biochem. Biophys. Res. Commun.* 226, 362–368. doi: 10.1006/bbrc.1996.1362
- Bianco, M. V., Blanco, F., Forrellad, M., Aguilar, D., Campos, E., Klepp, L., et al. (2011a). Knockout mutation of *p27-p55* operon severely reduces replication of *Mycobacterium bovis* in a macrophagic cell line and survival in a mouse model of infection. *Virulence* 2, 233–237. doi: 10.4161/viru.2.3.15888
- Bianco, M. V., Blanco, F., Imperiale, B., Forrellad, M., Rocha, R., Klepp, L., et al. (2011b). Role of P27-P55 operon from *Mycobacterium tuberculosis* in the resistance to toxic compounds. *BMC Infect. Dis.* 11:195. doi: 10.1186/1471-2334-11-195
- Bigi, F., Gioffré, A., Klepp, L., de la Paz Santangelo, M., Alito, A., Caimi, K., et al. (2004). The knockout of the *lprG-Rv1410* operon produces strong attenuation of *Mycobacterium tuberculosis*. *Microbes Infect.* 6, 182–187. doi: 10.1016/j.micinf.2003.10.010
- Black, P. A., Warren, R., Louw, G., van Helden, P., Victor, T., and Kana, B. (2014). Energy metabolism and drug efflux in *Mycobacterium tuberculosis*. *Antimicrob. Agents Chemother.* 58, 2491–2503. doi: 10.1128/AAC.02293-13
- Bolla, J. R., Do, S., Long, F., Dai, L., Su, C., Lei, H., et al. (2012). Structural and functional analysis of the transcriptional regulator Rv3066 of *Mycobacterium tuberculosis*. *Nucleic Acids Res.* 40, 9340–9355. doi: 10.1093/nar/gks677
- Bolotin, E., and Hershberg, R. (2015). Gene loss dominates as a source of genetic variation within clonal pathogenic bacterial species. *Genome Biol. Evol.* 7, 2173–2187. doi: 10.1093/gbe/evv135
- Braibant, M., Lefevre, P., de Wit, L., Peirs, P., Ooms, J., Huygen, K., et al. (1996). A *Mycobacterium tuberculosis* gene cluster encoding proteins of a phosphate transporter homologous to the *Escherichia coli* Pst system. *Gene* 176, 171–176. doi: 10.1016/0378-1119(96)00242-9
- Brandis, G., and Hughes, D. (2013). Genetic characterization of compensatory evolution in strains carrying *rpoB* Ser531Leu, the rifampicin resistance mutation most frequently found in clinical isolates. *J. Antimicrob. Chemother.* 68, 2493–2497. doi: 10.1093/jac/dkt224
- Caleffi-Ferracioli, K. R., Amaral, R., Demitto, F., Maltempe, F., Canezin, P., Scodro, R., et al. (2016). Morphological changes and differentially expressed efflux pump genes in *Mycobacterium tuberculosis* exposed to a rifampicin and verapamil combination. *Tuberculosis* 97, 65–72. doi: 10.1016/j.tube.2015.12.010
- Camacho, L., Constant, P., Raynaud, C., Laneelle, M., Triccas, J., Gicquel, B., et al. (2001). Analysis of the phthiocerol dimycocerosate locus of *Mycobacterium tuberculosis*. Evidence that this lipid is involved in the cell wall permeability barrier. *J. Biol. Chem.* 276, 19845–19854. doi: 10.1074/jbc.M100662200
- Cambau, E., Saunderson, P., Matsuoka, M., Cole, S., Kai, M., Suffys, P., et al. (2018). WHO surveillance network of antimicrobial resistance in leprosy. Antimicrobial resistance in leprosy: results of the first prospective open survey conducted by a WHO surveillance network for the period 2009–15. *Clin. Microbiol. Infect.* 24, 1305–1310. doi: 10.1016/j.cmi.2018.02.022
- Choudhuri, B. S., Bhakta, S., Barik, R., Basu, J., Kundu, M., and Chakrabarti, P. (2002). Overexpression and functional characterization of an ABC (ATP-binding cassette) transporter encoded by the genes *drdA* and *drdB* of *Mycobacterium tuberculosis*. *Biochem. J.* 367, 279–285. doi: 10.1042/bj20020615
- Choudhuri, B. S., Sen, S., and Chakrabarti, P. (1999). Isoniazid accumulation in *Mycobacterium smegmatis* is modulated by proton motive force-driven and ATP-dependent extrusion systems. *Biochem. Biophys. Res. Commun.* 256, 682–684. doi: 10.1006/bbrc.1999.0357
- Cole, S. T., Eiglmeier, K., Parkhill, J., James, K., Thomson, N., Wheeler, P., et al. (2001). Massive gene decay in the leprosy bacillus. *Nature* 409, 1007–1011. doi: 10.1038/35059006
- Converse, S. E., Mougous, J., Leavell, M., Leary, J., Bertozzi, C., and Cox, J. (2003). MmpL8 is required for sulfolipid-1 biosynthesis and *Mycobacterium tuberculosis* virulence. *Proc. Natl. Acad. Sci. U.S.A.* 100, 6121–6126. doi: 10.1073/pnas.1030024100
- Cox, J. S., Chen, B., McNeil, M., and Jacobs, W. R. Jr. (1999). Complex lipid determines tissue-specific replication of *Mycobacterium tuberculosis* in mice. *Nature* 402:79–83.
- da Silva, P., Bigi, F., Santangelo, M., Romano, M., Martín, C., Cataldi, A., et al. (2001). Characterization of P55, a multidrug efflux pump in *Mycobacterium bovis* and *Mycobacterium tuberculosis*. *Antimicrob. Agents Chemother.* 45, 800–804. doi: 10.1128/AAC.45.3.800-804.2001
- da Silva, P. E., Machado, D., Ramos, D., Couto, I., von Groll, A., and Viveiros, M. (2016). “Efflux pumps in mycobacteria: antimicrobial resistance, physiological functions, and role in pathogenicity,” in *Efflux-Mediated Antimicrobial Resistance in Bacteria*, 1st Edn. eds Li X-Z., Elkins C. A., and Zgurskaya H. I. (Cham: Springer International Publishing), 527–559.
- Danilchanka, O., Mailaender, C., and Niederweis, M. (2008). Identification of a novel multidrug efflux pump of *Mycobacterium tuberculosis*. *Antimicrob. Agents Chemother.* 52, 2503–2511. doi: 10.1128/AAC.00298-08
- de Knecht, G. J., Bruning, O., Marian, T., de Jong, M., van Belkum, A., Endtz, H. P., et al. (2013). Rifampicin-induced transcriptome response in rifampicin-resistant *Mycobacterium tuberculosis*. *Tuberculosis* 93, 96–101. doi: 10.1016/j.tube.2012.10.013
- De Rossi, E., Ainsa, J., and Ricardi, G. (2006). Role of mycobacterial efflux transporters in drug resistance: and unresolved question. *FEMS Microbiol. Rev.* 30, 36–52. doi: 10.1111/j.1574-6976.2005.00002.x
- De Rossi, E., Arrigo, P., Bellinzoni, M., da Silva, P., Martin, C., Ainsa, J., et al. (2002). The multidrug transporters belonging to major facilitator superfamily in *Mycobacterium tuberculosis*. *Mol. Med.* 8, 714–724. doi: 10.1007/BF03402035
- De Rossi, E., Branzoni, M., Cantoni, R., Milano, A., Riccardi, G., and Ciferri, O. (1998). *mmr*, a *Mycobacterium tuberculosis* gene conferring resistance to small cationic dyes and inhibitors. *J. Bacteriol.* 180, 6068–6071.
- Delmar, J., Chou, T., Wright, C., Licon, M., Doh, J., Radhakrishnan, A., et al. (2015). Structural basis for the regulation of the MmpL transporters of *Mycobacterium tuberculosis*. *J. Biol. Chem.* 290, 28559–28574. doi: 10.1074/jbc.M115.683797
- Dheda, K., Gumbo, T., Maartens, G., Dooley, K. E., McNerney, R., Murray, M., et al. (2017). The epidemiology, pathogenesis, transmission, diagnosis, and management of multidrug-resistant, extensively drug-resistant, and incurable tuberculosis. *Lancet Respir. Med.* 5, 291–360. doi: 10.1016/S2213-2600(17)30079-6
- Dinesh, N., Sharma, S., and Balganes, M. (2013). Involvement of efflux pumps in the resistance to peptidoglycan synthesis inhibitors in *Mycobacterium tuberculosis*. *Antimicrob. Agents Chemother.* 57, 1941–1943. doi: 10.1128/AAC.01957-12
- Domenech, P., Kobayashi, H., LeVier, K., Walker, G., and Barry, C. (2009). BAcA, an ABC transporter involved in maintenance of chronic murine infections with *Mycobacterium tuberculosis*. *J. Bacteriol.* 191, 477–485. doi: 10.1128/JB.01132-08
- Domenech, P., Reed, M., and Barry, C. (2005). Contribution of the *Mycobacterium tuberculosis* MmpL protein family to virulence and drug resistance. *Infect. Immun.* 73, 3492–3501. doi: 10.1128/IAI.73.6.3492-3501.2005
- Domenech, P., Reed, M., Dowd, C., Manca, C., Kaplan, G., and Barry, C. (2004). The role of MmpL8 in sulfatide biogenesis and virulence of *Mycobacterium tuberculosis*. *J. Biol. Chem.* 279, 21257–21265. doi: 10.1074/jbc.M400324200
- Doran, J. L., Pang, Y., Mdluli, K., Moran, A., Victor, T., Stokes, R., et al. (1997). *Mycobacterium tuberculosis* *effA* encodes an efflux protein of the QacA transporter family. *Clin. Diagn. Lab. Immunol.* 4, 23–32.
- Eiglmeier, K., Parkhill, J., Honore, N., Garnier, T., Tekaia, F., Telenti, A., et al. (2001). The decaying genome of *Mycobacterium leprae*. *Lepr. Rev.* 72, 387–398.
- Elbourne, L. D., Tetu, S., Hassan, K., and Paulsen, I. (2017). TransportDB 2.0: a database for exploring membrane transporters in sequenced genomes from all domains of life. *Nucleic Acids Res.* 45, D320–D324. doi: 10.1093/nar/gkw1068
- Farrow, M. F., and Rubin, E. (2008). Function of a mycobacterial major facilitator superfamily pump requires a membrane-associated lipoprotein. *J. Bacteriol.* 190, 1783–1791. doi: 10.1128/JB.01046-07
- Garima, K., Pathak, R., Tandon, R., Rathor, N., Sinha, R., Bose, M., et al. (2015). Differential expression of efflux pump genes of *Mycobacterium tuberculosis* in response to varied subinhibitory concentrations of antituberculosis agents. *Tuberculosis* 95, 155–161. doi: 10.1016/j.tube.2015.01.005
- Grkovic, S., Brown, M., and Skurray, R. (2001). Transcriptional regulation of multidrug efflux pumps in bacteria. *Semin. Cell Dev. Biol.* 12, 225–237. doi: 10.1006/scdb.2000.0248
- Grzegorzewicz, A. E., Pham, H., Gundi, V., Scherman, M., North, E., Hess, T., et al. (2012). Inhibition of mycolic acid transport across the *Mycobacterium tuberculosis* plasma membrane. *Nat. Chem. Biol.* 8, 334–341. doi: 10.1038/nchembio.794

- Gupta, A. K., Chauhan, D., Srivastava, K., Das, R., Batra, S., Mittal, M., et al. (2006). Estimation of efflux mediated multi-drug resistance and its correlation with expression levels of two major efflux pumps in mycobacteria. *J. Commun. Dis.* 38, 246–254.
- Gupta, A. K., Katoch, V., Chauhan, D., Sharma, R., Singh, M., Venkatesan, K., et al. (2010a). Microarray analysis of efflux pump genes in multidrug-resistant *Mycobacterium tuberculosis* during stress induced by common anti-tuberculous drugs. *Microb. Drug Resist.* 16, 21–28. doi: 10.1089/mdr.2009.0054
- Gupta, A. K., Reddy, V., Lavania, M., Chauhan, D., Venkatesan, K., Sharma, V., et al. (2010b). *jefA* (Rv2459), a drug efflux gene in *Mycobacterium tuberculosis* confers resistance to isoniazid and ethambutol. *Indian J. Med. Res.* 132, 176–188.
- Hao, P., Shi-Liang, Z., Ju, L., Ya-Xin, D., Biao, H., Xu, W., et al. (2011). The role of ABC efflux pump, Rv1456c-Rv1457c-Rv1458c, from *Mycobacterium tuberculosis* clinical isolates in China. *Folia Microbiol.* 56, 549–553. doi: 10.1007/s12223-011-0080-7
- Harris, K. K., Fay, A., Yan, G. H., Kunwar, P., Socci, N. D., Pottabathini, N., et al. (2014). Novel imidazoline antimicrobial scaffold that inhibits DNA replication with activity against mycobacteria and drug resistant Gram-positive cocci. *ACS Chem. Biol.* 9, 2572–2583. doi: 10.1021/cb500573z
- Hartkoorn, R. C., Uplekar, S., and Cole, S. (2014). Cross-resistance between clofazimine and bedaquiline through upregulation of MmpL5 in *Mycobacterium tuberculosis*. *Antimicrob. Agents Chemother.* 58, 2979–2981. doi: 10.1128/AAC.00037-14
- Jiang, X., Zhang, W., Zhang, Y., Gao, F., Lu, C., Zhang, X., et al. (2008). Assessment of efflux pump gene expression in a clinical isolate *Mycobacterium tuberculosis* by real-time reverse transcription PCR. *Microb. Drug Resist.* 14, 7–11. doi: 10.1089/mdr.2008.0772
- Kapopoulou, A., Lew, J., and Cole, S. (2011). The MycoBrowser portal: a comprehensive and manually annotated resource for mycobacterial genomes. *Tuberculosis* 91, 8–13. doi: 10.1016/j.tube.2010.09.006
- La Rosa, V., Poce, G., Canseco, J. O., Buroni, S., Pasca, M. R., Biava, M., et al. (2012). MmpL3 is the cellular target of the antitubercular pyrrole derivative BM212. *Antimicrob. Agents Chemother.* 56, 324–331. doi: 10.1128/AAC.05270-11
- Li, G., Zhang, J., Guo, Q., Wei, J., Jiang, Y., Zhao, X., et al. (2015). Study of efflux pump gene expression in rifampicin-mono-resistant *Mycobacterium tuberculosis* clinical isolates. *J. Antibiot.* 68, 431–435. doi: 10.1038/ja.2015.9
- Li, P., Gu, Y., Li, J., Xie, L., Li, X. Z., and Xie, J. (2017). *Mycobacterium tuberculosis* Major Facilitator superfamily transporters. *J. Membrane Biol.* 250, 573–585. doi: 10.1007/s00232-017-9982-x
- Li, W., Upadhyay, A., Fontes, F., North, E., Wang, Y., Crans, D., et al. (2014). Novel insights into the mechanism of inhibition of MmpL3, a target of multiple pharmacophores in *Mycobacterium tuberculosis*. *Antimicrob. Agents Chemother.* 58, 6413–6423. doi: 10.1128/AAC.03229-14
- Li, X., Zhang, L., and Nikaido, H. (2004). Efflux pump-mediated intrinsic drug resistance in *Mycobacterium smegmatis*. *Antimicrob. Agents Chemother.* 48, 2415–2423. doi: 10.1128/AAC.48.7.2415-2423.2004
- Li, X.-Z., Elkins, C., and Zgurskaya, H. (2016). *Efflux-Mediated Antimicrobial Resistance in Bacteria*, 1st Edn. Cham: Springer International Publishing, 1–848.
- Louw, G. E., Warren, R., van Pittius, N., Leon, R., Jimenez, A., Hernandez-Pando, R., et al. (2011). Rifampicin reduces susceptibility to ofloxacin in rifampicin-resistant *Mycobacterium tuberculosis* through efflux. *Am. J. Respir. Crit. Care Med.* 184, 269–276. doi: 10.1164/rccm.201011-1924OC
- Louw, G. E., Warren, R., van Pittius, N., McEvoy, C., van Helden, P., and Victor, T. (2009). A balancing act: efflux/influx in mycobacterial drug resistance. *Antimicrob. Agents Chemother.* 53, 3181–3189. doi: 10.1128/AAC.01577-08
- Lu, J., Liu, M., Wang, Y., Pang, Y., and Zhao, Z. (2014). Mechanisms of fluoroquinolone mono-resistance in *Mycobacterium tuberculosis*. *FEMS Microbiol. Lett.* 353, 40–48. doi: 10.1111/1574-6968.12401
- Machado, D., Coelho, T., Perdigão, J., Pereira, C., Couto, I., Portugal, I., et al. (2017). Interplay between mutations and efflux in drug resistant clinical isolates of *Mycobacterium tuberculosis*. *Front. Microbiol.* 8:711. doi: 10.3389/fmicb.2017.00711
- Machado, D., Couto, I., Perdigão, J., Rodrigues, L., Baptista, P., Portugal, I., et al. (2012). Contribution of efflux to the emergence of isoniazid and multidrug resistance in *Mycobacterium tuberculosis*. *PLoS ONE* 7:e34538. doi: 10.1371/journal.pone.0034538
- Mann, S., and Chen, Y.-P. (2010). Bacterial genomic G+C composition-eliciting environmental adaptation. *Gemonics* 95, 7–15. doi: 10.1016/j.ygeno.2009.09.002
- Martinez, J. L., Sánchez, M., Martinez-Solano, L., Hernandez, A., Garmendia, L., Fajardo, A., et al. (2009). Functional role of bacterial multidrug efflux pumps in microbial natural ecosystems. *FEMS Microbiol. Rev.* 33, 430–449. doi: 10.1111/j.1574-6976.2008.00157.x
- McLeod, M. P., Qin, X., Karpathy, S., Gioia, J., Highlander, S., Fox, G., et al. (2004). Complete genome sequence of *Rickettsia typhi* and comparison with sequences of other *Rickettsiae*. *J. Bacteriol.* 186, 5842–5855. doi: 10.1128/JB.186.17.5842-5855.2004
- Milano, A., Pasca, M., Provvedi, R., Lucarelli, A., Manina, G., Ribeiro, A., et al. (2009). Azole resistance in *Mycobacterium tuberculosis* is mediated by the MmpS5-MmpL5 efflux system. *Tuberculosis* 89, 84–90. doi: 10.1016/j.tube.2008.08.003
- Mishra, M., and Daniels, L. (2013). Characterization of the MSMEG_2631 gene (*mmp*) encoding a multidrug and toxic compound extrusion (MATE) family protein in *Mycobacterium smegmatis* and exploration of its polyspecific nature using biollog phenotype microarray. *J. Bacteriol.* 195, 1610–1621. doi: 10.1128/JB.01724-12
- Moran, N. (2002). Microbial minimalism: genome reduction in bacterial pathogens. *Cell* 108, 583–586. doi: 10.1016/S0092-8674(02)00665-7
- Morris, J. J., Lenski, R., and Zinser, E. (2012). The black queen hypothesis: evolution of dependencies through adaptive gene loss. *mBio* 3, e00036–e00012. doi: 10.1128/mBio.00036-12
- Pang, Y., Lu, J., Wang, Y., Song, Y., Wang, S., and Zhao, Y. (2013). Study of the rifampin mono-resistance mechanism in *Mycobacterium tuberculosis*. *Antimicrob. Agents Chemother.* 5, 893–900. doi: 10.1128/AAC.01024-12
- Pasca, M. R., Gugliera, P., Arcesi, F., Bellinzoni, M., De Rossi, E., and Riccardi, G. (2004). Rv2686c-Rv2687c-Rv2688c, an ABC fluoroquinolone efflux pump in *Mycobacterium tuberculosis*. *Antimicrob. Agents Chemother.* 48, 3175–3178. doi: 10.1128/AAC.48.8.3175-3178.2004
- Pasca, M. R., Gugliera, P., De Rossi, E., Zara, F., and Riccardi, G. (2005). *mmpL7* gene of *Mycobacterium tuberculosis* is responsible for isoniazid efflux in *Mycobacterium smegmatis*. *Antimicrob. Agents Chemother.* 49, 4775–4777. doi: 10.1128/AAC.49.11.4775-4777.2005
- Radhakrishnan, A., Kumar, N., Wright, C. C., Chou, T. H., Bolla, J. R., Tringides, M. L., et al. (2014). Crystal structure of the transcriptional regulator Rv0678 of *Mycobacterium tuberculosis*. *J. Biol. Chem.* 289, 16526–16540. doi: 10.1074/jbc.M113.538959
- Ramón-García, S., Martín, C., Ainsa, J. A., and De Rossi, E. (2006). Characterization of tetracycline resistance mediated by the efflux pump Tap from *Mycobacterium fortuitum*. *J. Antimicrob. Chemother.* 57, 252–259. doi: 10.1093/jac/dki436
- Ramón-García, S., Martín, C., De Rossi, E., and Ainsa, J. A. (2007). Contribution of the Rv2333c efflux pump (the Stp protein) from *Mycobacterium tuberculosis* to intrinsic antibiotic resistance in *Mycobacterium bovis* BCG. *J. Antimicrob. Chemother.* 59, 544–547. doi: 10.1093/jac/dkl510
- Ramón-García, S., Martín, C., Thompson, C. J., and Ainsa, J. A. (2009). Role of the *Mycobacterium tuberculosis* P55 efflux pump in intrinsic drug resistance, oxidative stress responses, and growth. *Antimicrob. Agents Chemother.* 53, 3675–3682. doi: 10.1128/AAC.00550-09
- Ramón-García, S., Mick, V., Dainese, E., Martín, C., Thompson, C., De Rossi, E., et al. (2012). Functional and genetic characterization of the Tap efflux pump in *Mycobacterium bovis* BCG. *Antimicrob. Agents Chemother.* 56, 2074–2083. doi: 10.1128/AAC.05946-11
- Ramón-García, S., Stewart, G., Hui, Z., Mohn, W., and Thompson, C. (2015). The mycobacterial P55 efflux pump is required for optimal growth on cholesterol. *Virulence* 6, 444–448. doi: 10.1080/21505594.2015.1044195
- Rodrigues, L., Villellas, C., Bailo, R., Viveiros, M., and Ainsa, J. (2013). Role of the Mmr efflux pump in drug resistance in *Mycobacterium tuberculosis*. *Antimicrob. Agents Chemother.* 57, 751–757. doi: 10.1128/AAC.01482-12
- Rodríguez, J. E., Ramírez, A., Salas, L., Helguera-Repetto, C., Gonzalez-y-Merchand, J., Soto, C., et al. (2013). Transcription of genes involved in sulfolipid and polyacyltrehalose biosynthesis of *Mycobacterium tuberculosis*

- in experimental latent tuberculosis infection. *PLoS ONE* 8:e58378. doi: 10.1371/journal.pone.0058378
- Sandhu, P., and Akhter, Y. (2016). The drug binding sites and transport mechanism of the RND pumps from *Mycobacterium tuberculosis*: insights from molecular dynamics simulations. *Arch. Biochem. Biophys.* 592, 38–49. doi: 10.1016/j.abb.2016.01.007
- Sandhu, P., and Akhter, Y. (2018). Evolution of structural fitness and multifunctional aspects of mycobacterial RND family transporters. *Arch. Microbiol.* 200, 19–31. doi: 10.1007/s00203-017-1434-6
- Schmalstieg, A. M., Srivastava, S., Belkaya, S., Deshpande, D., Meek, C., Leff, R., et al. (2012). The antibiotic resistance arrow of time: efflux pump induction is a general first step in the evolution of mycobacterial drug resistance. *Antimicrob. Agents Chemother.* 56, 4806–4815. doi: 10.1128/AAC.05546-11
- Scollard, D. M., Adams, L., Gillis, T., Krahenbuhl, J., Truman, R., and Williams, D. (2006). The continuing challenges of leprosy. *Clin. Microbiol. Rev.* 19, 338–381. doi: 10.1128/CMR.19.2.338-381.2006
- Siddiqi, N., Das, R., Pathak, N., Banerjee, S., Ahmed, N., Katoch, V., et al. (2004). *Mycobacterium tuberculosis* isolate with a distinct genomic identity overexpresses a Tap-like efflux pump. *Infection* 32, 109–111. doi: 10.1007/s15010-004-3097-x
- Singh, I., Lavania, M., Nigam, A., Turankar, R., Ahuja, M., John, A., et al. (2016). Symposium on emerging needs in leprosy research in the post elimination era: The Leprosy Mission Trust India. *Lepr. Rev.* 87, 132–143.
- Srivastava, S., Musuka, S., Sherman, C., Meek, C., Leff, R., and Gumbo, T. (2010). Efflux-pump-derived multiple drug resistance to ethambutol monotherapy in *Mycobacterium tuberculosis* and the pharmacokinetics and pharmacodynamics of ethambutol. *J. Infect. Dis.* 201, 1225–1231. doi: 10.1086/651377
- Tahlan, K., Wilson, R., Kastrinsky, D., Arora, K., Nair, V., Fischer, E., et al. (2012). SQ109 targets MmpL3, a membrane transporter of trehalose monomycolate involved in mycolic acid donation to the cell wall core of *Mycobacterium tuberculosis*. *Antimicrob. Agents Chemother.* 56, 1797–1809. doi: 10.1128/AAC.05708-11
- Tullius, M. V., Harmston, C. A., Owens, C. P., Chim, N., Morse, R. P., McMath, L. N. M., et al. (2011). Discovery and characterization of a unique mycobacterial heme acquisition system. *Proc. Natl. Acad. Sci. U.S.A.* 108, 5051–5056. doi: 10.1073/pnas.1009516108
- Viveiros, M., Martins, M., Rodrigues, L., Machado, D., Couto, I., Ainsa, J., et al. (2012). Inhibitors of mycobacterial efflux pumps as potential boosters for anti-tubercular drugs. *Expert Rev. Anti. Infect. Ther.* 10, 983–998. doi: 10.1586/eri.12.89
- Wang, K., Pei, H., Huang, B., Zhu, X., Zhang, J., Zhou, B., et al. (2013). The expression of ABC efflux pump, Rv1217c–Rv1218c, and its association with multidrug resistance of *Mycobacterium tuberculosis* in China. *Curr. Microbiol.* 66, 222–226. doi: 10.1007/s00284-012-0215-3
- Wang-Kan, X., Blair, J., Chirullo, B., Betts, J., La Ragione, R. M., Ivens, A., et al. (2017). Lack of AcrB efflux function confers loss of virulence on *Salmonella enterica* serovar Typhimurium. *mBio* 8, e00968–e00917. doi: 10.1128/mBio.00968-17
- Wells, R. M., Jones, C., Xi, Z., Speer, A., Danilchanka, O., Doornbos, K., et al. (2013). Discovery of a siderophore export system essential for virulence of *Mycobacterium tuberculosis*. *PLoS Pathog.* 9:e1003120. doi: 10.1371/journal.ppat.1003120
- Wilson, M., DeRisi, J., Kristensen, H.-H., Imboden, P., Rane, S., Brown, P., et al. (1999). Exploring drug induced alterations in gene expression in *Mycobacterium tuberculosis* by microarray hybridization. *Proc. Natl. Acad. Sci. U.S.A.* 96, 12833–12838. doi: 10.1073/pnas.96.22.12833
- Youm, J., and Saier, M. (2012). Comparative analyses of transport proteins encoded within the genomes of *Mycobacterium tuberculosis* and *Mycobacterium leprae*. *Biochim. Biophys. Acta Biomembranes.* 1818, 776–797. doi: 10.1016/j.bbmem.2011.11.015

Conflict of Interest Statement: The authors declare that the research was conducted in the absence of any commercial or financial relationships that could be construed as a potential conflict of interest.

Copyright © 2018 Machado, Lecorche, Mougari, Cambau and Viveiros. This is an open-access article distributed under the terms of the Creative Commons Attribution License (CC BY). The use, distribution or reproduction in other forums is permitted, provided the original author(s) and the copyright owner(s) are credited and that the original publication in this journal is cited, in accordance with accepted academic practice. No use, distribution or reproduction is permitted which does not comply with these terms.



Effect of a Point Mutation in *mprF* on Susceptibility to Daptomycin, Vancomycin, and Oxacillin in an MRSA Clinical Strain

Feng-Jui Chen^{1*}, Tsai-Ling Lauderdale¹, Chen-Hsiang Lee², Yu-Chieh Hsu¹, I-Wen Huang¹, Pei-Chi Hsu¹ and Chung-Shi Yang³

¹ National Institute of Infectious Diseases and Vaccinology, National Health Research Institutes, Zhunan, Taiwan, ² Division of Infectious Diseases, Kaohsiung Chang Gung Memorial Hospital, College of Medicine, Chang Gung University, Kaohsiung, Taiwan, ³ Institute of Biomedical Engineering and Nanomedicine, National Health Research Institutes, Zhunan, Taiwan

OPEN ACCESS

Edited by:

Elena Perrin,
Università degli Studi di Firenze, Italy

Reviewed by:

Daniel Haeusser,
Canisius College, United States
Balaji Veeraraghavan,
Christian Medical College & Hospital,
India

*Correspondence:

Feng-Jui Chen
frchen@nhri.org.tw

Specialty section:

This article was submitted to
Evolutionary and Genomic
Microbiology,
a section of the journal
Frontiers in Microbiology

Received: 28 February 2018

Accepted: 07 May 2018

Published: 25 May 2018

Citation:

Chen F-J, Lauderdale T-L, Lee C-H,
Hsu Y-C, Huang I-W, Hsu P-C and
Yang C-S (2018) Effect of a Point
Mutation in *mprF* on Susceptibility
to Daptomycin, Vancomycin,
and Oxacillin in an MRSA Clinical
Strain. *Front. Microbiol.* 9:1086.
doi: 10.3389/fmicb.2018.01086

We previously reported the sequential recovery of daptomycin-nonsusceptible MRSA clinical isolates with an L431F substitution in the MprF protein. The aim of the present study is to determine the effect of this mutation by replacing the *mprF* gene on the chromosome of a daptomycin-susceptible progenitor strain, CGK5, to obtain CGK5mut having the L431F MprF mutation. Compared to CGK5, the daptomycin and vancomycin MICs of CGK5mut increased from 0.5 to 3 μ g/ml and from 1.5 to 3 μ g/ml, respectively; however, its oxacillin MIC decreased from 128 to 1 μ g/ml in medium without added 2% NaCl. The expression levels of *vraSR* and several other cell-wall synthesis-related genes were significantly increased in CGK5mut, and the mutant also had significantly reduced negative cell membrane charge, thicker cell wall, and longer doubling time. These features were abolished in the reverse mutant carrying F431L MprF, confirming the pleiotropic effects of the L431F MprF mutation. We believe that this is the first work that shows a single MprF missense mutation can lead to not only changes in the cell membrane but also increased expression of *vraSR* and subsequently increased resistance to daptomycin and vancomycin while simultaneously conferring increased susceptibility to oxacillin in an isogenic MRSA strain.

Keywords: MRSA, evolution, drug resistance, daptomycin, vancomycin, oxacillin

INTRODUCTION

Daptomycin, a cyclic lipopeptide antibiotic, is one of the last-line agents for the treatment of certain severe multidrug-resistant *Staphylococcus aureus* infections, including those caused by methicillin-resistant *S. aureus* (MRSA) (Enoch et al., 2007). Daptomycin functions by inserting itself into the bacterial cell membrane in a calcium-dependent manner to cause membrane depolarization, leading to cell death (Enoch et al., 2007; Baltz, 2009). Daptomycin-nonsusceptible (DAP-NS) MRSA isolates, although still uncommon, have emerged during daptomycin treatment of patients (Lee et al., 2010; Boyle-Vavra et al., 2011). DAP-NS MRSA mutants have also been generated in the laboratory by serial passage of isolates in sublethal concentrations of daptomycin (Enoch et al., 2007; Camargo et al., 2008; Mishra et al., 2009, 2012; Rubio et al., 2012).

The exact mechanisms giving rise to daptomycin-non-susceptibility in *S. aureus* are not fully elucidated but appear to involve diverse genetic events and several genetic loci, including

mprF, *ycgG* (*walK*), *vraSR*, *tagA*, and *dltABCD* (Friedman et al., 2006; Baltz, 2009; Bertsche et al., 2011; Song et al., 2013). These loci are all part of the cell wall stimulon in *S. aureus* and include genes encoding proteins involved in the production of membrane phospholipids. The *mprF* (multiple peptide resistance factor) gene seems to be especially critical, as *mprF* mutations are the most frequently reported genetic lesions in DAP-NS MRSA isolates (Friedman et al., 2006; Lee et al., 2010; Boyle-Vavra et al., 2011; Mehta et al., 2012a). MprF is a bi-functional membrane protein with lysylphosphatidylglycerol (LPG) synthase and flippase activities (Peschel et al., 2001; Ernst et al., 2009; Ernst and Peschel, 2011). Different point mutations in *mprF* have been associated with elevated LPG synthesis. This results in increased amounts of LPG relative to phosphatidylglycerol (PG) on the outer leaflet of the cytoplasmic membrane and an accompanying reduction in cell membrane negative charge (Baltz, 2009; Rubio et al., 2012).

A feature that has been seen in both clinical and laboratory-generated DAP-NS MRSA isolates is a concomitant vancomycin intermediate or heterogeneous intermediate resistance (VISA or hVISA) phenotype (Camargo et al., 2008; Mishra et al., 2009); VISA has moderate resistance to vancomycin and hVISA has varying sub-population of cells resistant to vancomycin, thus exhibit mixed susceptibility to vancomycin. Mutations in the *vraSR*, *graSR*, or *walKR* (*ycgG*) two-component systems have been associated with the VISA/hVISA phenotype (Howden et al., 2010). Among these 3 two-component systems, the *VraSR* system is particularly important in maintaining cell wall integrity. It serves as a sentinel in response to cell wall damage by positively regulating a unique set of genes involved in cell wall synthesis, resulting in the generation of a resistant phenotype (Kuroda et al., 2003; Gardete et al., 2006; McAleese et al., 2006). Another unusual feature is the so-called “seesaw” effect on β -lactam susceptibility, wherein DAP-NS isolates exhibit reduced β -lactam MICs (Mishra et al., 2009; Lee et al., 2010; Yang et al., 2010; Mehta et al., 2012a). However, these phenomena are not observed in all DAP-NS MRSA isolates.

Our previous study of eight sequential clinical MRSA isolates from a patient with persistent bacteremia revealed an L431F amino acid substitution in the MprF protein of DAP-NS isolates (Lee et al., 2010). Since this mutation had not been reported previously, we undertook the present study to determine the effect of this mutation on the cellular response to daptomycin. To eliminate the possibility of unknown genetic changes that might have occurred in paired clinical strains, we used a base-substitution method to replace a single nucleotide (from CTT to TTT) within the chromosomal *mprF* gene of the daptomycin-susceptible (DAP-S) progenitor of the DAP-NS strains. To confirm the results obtained by this single amino acid exchange (L431F) in MprF, we also constructed a reverse mutant carrying F431L MprF as well as a silent EcoRV site. Our study demonstrated that this single amino acid change (L431F) confers increased resistance to both daptomycin and vancomycin, with a concurrent decrease in oxacillin MIC. The phenotype and genetic factors associated with these changes were investigated.

MATERIALS AND METHODS

Bacterial Strains

The bacterial strains, plasmids, and primers used are listed in **Tables 1, 2**. Unless stated otherwise, Luria-Bertani (LB) broth and plates were used for growth of *Escherichia coli* and *S. aureus* at 37°C. *E. coli* strain XL10-Gold (Stratagene, La Jolla, CA, United States) and GeneHogs® (Invitrogen, Carlsbad, CA, United States) were used for cloning. *S. aureus* cells were transformed by electroporation, as described previously (Schenk and Laddaga, 1992). Ampicillin (100 μ g/ml), chloramphenicol (5 μ g/ml), erythromycin (5 μ g/ml), spectinomycin (100 μ g/ml), and tetracycline (5 μ g/ml) were used for plasmid selection in *E. coli* and *S. aureus*.

Construction of MprF Mutant Derivatives

To add new selection markers and cloning sites, the *bgaB* cassette located between the HindIII sites was removed from pMAD by digesting with HindIII, and religated. A modified *bgaB*, with extra restriction sites, was cloned by PCR (using primers *bgaBnew-F* and *bgaBnew-R*) from the original pMAD into the pMAD lacking the *bgaB* cassette to generate new pMAD. Two selection markers, as *sat4* and *tetM* cassettes, were incorporated by cloning PCR fragments of the *sat4* and *tetM* genes from the chromosomal DNA of 2V076 and RN6911, respectively, into the StuI-SalI sites of the new pMAD using primers *sat4-F* and *sat4-R*, and *tetM-F* and *tetM-R* to produce pMAD-SAT4-tetM, which confers resistance to noursoethricin and tetracycline. To assess the effect of MprF L431F on daptomycin non-susceptibility, an *mprF*-bearing fragment from CGK6 (the first DAP-NS isolate containing the MprF F431 mutant) was amplified by PCR using the primers *mprF-F* and *mprF-R*, and ligated into the BamHI-SmaI sites of pMAD-SAT4-tetM. This recombinant plasmid, pMprFmut, was used as the allelic exchange vector for mutation of the *mprF* gene in CGK5 to create CGK5mut. To validate the phenotypes in CGK5mut, the mutant strain was reverted to wild type by allelic exchange again. The *mprF* fragment was amplified from CGK5 and then cloned into pMAD-SAT4-tetM. This recombinant plasmid, pMprF5, was used as the template DNA for site-directed mutagenesis to introduce a new EcoRV site¹ into the complementation construct (and without altering the coding sequence) to allow it to be differentiated from the CGK5 parental strain. After PCR using the mutant primers *mprF*(EcoRV)-F and *mprF*(EcoRV)-R, the *mprF* reverse mutant was treated with DpnI, ligated into a circle with T4 DNA ligase, and then used as the template DNA. The entire *mprF* gene was then cloned from the mutated plasmid into the pMAD-SAT4-tetM vector again to eliminate potential mutation of the vector sequence. The constructs were verified by restriction analysis and DNA sequencing. Sequencing was performed at the DNA Sequencing Core Lab of our institutes.

The allele replacement procedure was applied to create a single base replacement in the *mprF* gene of CGK5, as described previously (Arnaud et al., 2004). Briefly, the pMprFmut plasmid was electroporated into *S. aureus* strain RN4220, and then

¹<http://emboss.bioinformatics.nl/cgi-bin/emboss/silent>

electroporated into CGK5. Transformants were selected at 30°C on LB plates containing tetracycline and X-Gal (150 µg/ml). One blue colony was inoculated in Trypticase Soy broth (TSB) containing tetracycline and incubated with shaking for 2 h at 30°C followed by 6 h at 43°C, serially diluted then plated on Trypticase Soy agar (TSA) plates containing tetracycline and X-Gal and incubated at 43°C overnight to obtain light blue colonies caused by a single crossover event. One light blue colony was inoculated in TSB without antibiotic and incubated with shaking at 30°C overnight, then diluted 1:100 and incubated at 43°C for 6 h; serial dilutions were plated on TSA plates in the absence of antibiotics and incubated at 37°C overnight. Several white colonies were selected to verify for tetracycline sensitivity, which indicates loss of the integrated vector resulting from a double crossover event. To confirm the double crossover, PCR amplifications were performed with multiplex primers hybridizing outside and inside of the *mprF* gene and vector sequences. A colony with a single crossover was used as a negative control. The resulting mutant was verified by DNA sequencing, including the adjacent region of the *mprF* gene. The complementation construct (CGK5mutR) was constructed by the same procedure.

Antimicrobial Susceptibility Testing

The MICs of daptomycin, oxacillin and vancomycin were determined by Etest® (bioMérieux SA, Marcy l'Étoile, France) following the manufacturer's instructions and using Mueller Hinton II agar (MHA) (Becton Dickinson, Cockeysville, MD, United States). The daptomycin Etest strips were overlaid with

40 µg/ml of calcium (Package insert) and the MHA contained 2.9–5.9 µg/ml of calcium. The MICs of oxacillin were also determined by broth microdilution (BMD) (CLSI, 2013). The BMD method was performed in Mueller Hinton II broth (MHB) (Becton Dickinson) with and without 2% NaCl from an inoculum of 5×10^5 CFU/ml, and the MIC was read after incubation at 35°C for 24 h. *S. aureus* ATCC 29213 and *Enterococcus faecalis* ATCC 29212 were used as quality control organisms for Etest. *S. aureus* ATCC 29213 and ATCC 43300 were used as quality control organisms for BMD.

Population Analysis Profiles

A population analysis profile (PAP) for vancomycin was performed on CGK5 and CGK5 mutant derivatives following protocols previously described (Hiramatsu et al., 1997; Howden et al., 2006). Briefly, overnight cultures of test isolates were serially diluted in TSB and inoculated onto brain–heart infusion (BHI) agar plates containing 0–8 µg/ml vancomycin. After 48 h incubation at 35°C, colonies were counted and plotted. Mu3 (ATCC 700698) and N315 *S. aureus* strains were tested in parallel as hVISA positive and negative controls, respectively. The area under the curve (AUC) values of the test strains were compared to that of Mu3.

Cell Wall Thickness

Bacterial cells for transmission electron microscopy were prepared following previously described protocols (Hanaki et al., 1998). Photographic images were obtained at a final magnification of 15,000× using a Hitachi H-7650

TABLE 1 | Bacterial strains and plasmids used in this study.

Strain/plasmid	Description	Source or Reference
Strains		
<i>E. coli</i>		
XL10-Gold	Ultra-competent cell for site-directed mutagenesis	Stratagene
Genehogs	Electrocompetent cells	Invitrogen
<i>S. aureus</i>		
RN4220	Restriction-deficient derivative of 8325-4	Novick, 1991
RN6911	RN6390B <i>agr::tetM</i> (<i>agr</i> -null)	Novick et al., 1993
Z172	Clinical VISA isolate with <i>spc</i> gene	Chen et al., 2013
CGK5	Daptomycin-susceptible MRSA	Lee et al., 2010
CGK5mut	MprF L431F derivative of CGK5	This study
CGK5mutR	Reversed derivative of CGK5mut with MprF containing F431L and a new EcoRV site	This study
CGK6	Daptomycin-non-susceptible MRSA	Lee et al., 2010
<i>E. faecium</i>		
2V076	Clinical isolate with <i>aadE-sat4-aphA-3</i> gene cluster	This study
Plasmids		
pMAD	pE194 ^{ts} derivative for gene replacement in Gram-positive bacteria	Arnaud et al., 2004
pMAD-SAT4-tetM	Modified pMAD with <i>sat4</i> and <i>tetM</i> markers	This study
pMprFmut	The <i>mprF</i> fragment amplified from CGK6 and cloned into pMAD-SAT4-tetM for allelic exchange in CGK5	This study
pMprF5	The <i>mprF</i> fragment amplified from CGK5 and cloned into pMAD-SAT4-tetM for site-directed mutagenesis	This study
pMprFmutR	A silent EcoRV site was introduced into the middle of the <i>mprF</i> fragment amplified from pMprF5 and cloned into pMAD-SAT4-tetM for allelic exchange in CGK5mut	This study
pluxT2	pSK5630 derivative containing <i>luxABCDE</i> with T2 terminator	Chen et al., 2014
pluxT2-SPC	pluxT2 with <i>spc</i> marker	This study

^{ts}Stands for thermosensitive.

microscope (Hitachi High-Technologies Corporation, Tokyo, Japan). Fifty measurements of equatorially cut cells were taken for the calculation of cell wall thickness, and results were expressed as mean \pm SD following previously described protocols (Cui et al., 2000).

Growth Rate

Overnight fresh cultures of bacteria were adjusted in 0.85% NaCl to 0.5 McFarland turbidity, then diluted 1:200 in MHB to obtain 5×10^5 CFU/ml starting inoculum. The inoculum was dispensed at 120 μ l per well in triplicates into a 100-well plate and incubated at 37°C in Bioscreen C MBR (Oy Growth Curves Ab Ltd, Helsinki, Poland) (Richardson et al., 2008). Triplicate medium-only blank wells were included in each plate. The OD₆₀₀

of each well was read every 30 min for 24 h. The average OD of the blank wells was subtracted from the average of the triplicate test wells at each time point and plotted. Doubling times were calculated using the exponential growth phase following a previously described protocol (Cui et al., 2003). To verify the OD measurements, the CFU counts were checked by the shaker flask method.

Cytochrome c Binding Assay

Cytochrome *c* binding assay was performed following an approach similar to that of Mukhopadhyay et al. (2007) with slight modification. Briefly, bacteria grown overnight at 35°C were harvested and washed twice with 20 mM MOPS buffer (pH 7.0) and resuspended in the same buffer to a final OD₅₇₈ of 7.

TABLE 2 | Primers used in this study.

Primers	Nucleotide sequence (5'–3') ^a
Cloning of new pMAD	
<i>bgaB</i> new-F	CGGGATCCAGGAATTCGCTCCCGGGCATGCCATGGGTCTAGTTAATGTGTAACGTAACA
<i>bgaB</i> new-R	ACGCGTCGACGTAAGGCCCTTCACTAAACCTTCCCGGCTTC
<i>sat4</i> -F	P-AGAGAGGCGGGAACAGTG
<i>sat4</i> -R	ACGCGTCGACTGCAGGCCCTTCAGATCTAAGACGAACCTCCAATTCAT
<i>tetM</i> -F	P-GGAGATTCCTTTACAAATATG
<i>tetM</i> -R	ACGCGTCGACGTAAGGCCCTATAACAACATAAAACGCACTA
Cloning of <i>mprF</i> gene for allelic exchange	
<i>mprF</i> -F	CGGGATCCCTAGAAATTGATGTGAAAAAATGA
<i>mprF</i> -R	TCCCGCGGGCGCATCAGGCATAACTGTATA
Site-directed mutagenesis	
<i>mprF</i> (EcoRV)-F	P-ATCATTGCTAAAATCCATCATTGTC
<i>mprF</i> (EcoRV)-R	ATCCTTTTGATAAGACATTAAAA
Real-time qPCR	
<i>mprF</i> -QF	TCATTATTGCTGCATTATCTGGA
<i>mprF</i> -QR	TTTTCCTCAGGGACACCTAAAG
<i>vraSR</i> -QF	GCCAGATTCAGGTACACG
<i>vraSR</i> -QR	TCTGAGTCGTCGCTTC
<i>fmtA</i> -QF	AAAACATCTAAGCCTATCCCATTG
<i>fmtA</i> -QR	TTTGAATCGCTTTAACTGCTTGAT
<i>murZ</i> -QF	AAAATAAGAGGTGGACGCACA
<i>murZ</i> -QR	ACTGTTTTTCGCGCCACT
<i>pbp2</i> -QF	TCCGTGCAATTGGTAAGAACT
<i>pbp2</i> -QR	TTAATGTTGAGGCACCTTCAGA
<i>sgtB</i> -QF	TAGCGACAGAGATGTGC
<i>sgtB</i> -QR	TTGTGACATAGCCTGTTG
<i>tagA</i> -QF	AATAAATCAAGCGAGCTATATTGTTG
<i>tagA</i> -QR	ACGATGCGAAGCTTTGACTAC
<i>gyrB</i> -QF	CGTTAATTGAAGCAGGCTATGTG
<i>gyrB</i> -QR	TGGTGTTGGATTCAATTCAGATT
Cloning of promoter-reporter	
<i>spc</i> -F	P-AAAGTTCTCGTTCGGAGG
<i>spc</i> -R	TCCCGCGGGAAAGTAAGCACCTGTTATTGC
<i>PmprF</i> -F	CGGGATCCGAAAAATAAAACAAGTGGTAT
<i>PmprF</i> -R	ACGCGTCGACTTAACTTCCTGATTCATT
<i>PvraSR</i> -F	CGGGATCCCGTTTATCTCATCAAATG
<i>PvraSR</i> -R	ACGCGTCGACTAGTTCATAACTATCACCTTT

^aRestriction enzyme sites are underlined. P represents phosphorylation. Boldface type indicates a mutant nucleotide.

Cytochrome *c* (Sigma Chemicals, St. Louis, MO, United States) was prepared in the same buffer. The bacterial suspension was incubated with 1 mg/ml cytochrome *c* for 10 min, and then centrifuged at 3000 *g* at 4°C for 10 min. The supernatant containing unbound cytochrome *c* was collected and measured spectrophotometrically at OD₅₃₀. The cytochrome *c* was serially diluted (0.1–0.6 mg/ml) to create a standard curve to measure the cytochrome *c* concentration of the supernatant.

Western Blot Analysis for PBP2a Detection

Detailed descriptions of mouse monoclonal anti-PBP2a antibody (2F6F) production and detection of PBP2a were presented previously (Chen et al., 2014). However, in that study, PBP2a was detected in the total protein preparation. In the present study, for more precise detection of PBP2a in the membrane, membrane fraction was prepared following previously described protocol with slight modifications (Downer et al., 2002). Briefly, strains were grown in TSB overnight at 37°C with shaking at 200 rpm, then diluted 1/100 in 50 ml fresh medium and further incubated until cells reached an OD₆₀₀ of 1. Ten milliliter of the bacterial cultures was then centrifuged, and the pellet was resuspended in 1 ml lysis buffer. Cells were disrupted by FastProtein™ Blue Matrix using a FastPrep-24 homogenizer (MP Biomedicals) at 6 M/s for 4 cycles of 20 s with a 2-min ice incubation in between each cycle. Protein samples (1 µg of protein per lane) were separated in 10% sodium dodecyl sulfate polyacrylamide gel electrophoresis (SDS-PAGE), and then transferred to a polyvinylidene difluoride membrane (Immobilon, Millipore Corp., Bedford, MA, United States). PBP2a was probed with mouse monoclonal anti-PBP2a antibody (2F6F), and bands were visualized with HRP-conjugated secondary antibodies (Abcam Inc., Cambridge, MA, United States) followed by incubation in Western lightning chemiluminescence reagent plus (Perkin Elmer Life Sciences, Boston, MA, United States). Sortase A, a transpeptidase, was used as an internal control, identified by rabbit polyclonal anti-Sortase A primary antibody (Abcam Inc.).

Real-Time Quantitative PCR Analysis for *mprF*, *vraSR*, and Cell Wall Synthesis-Related Genes

For RNA isolation, strains were grown overnight with shaking at 37°C in MHB and diluted with 5 ml fresh medium to 1/100. They were then grown at 37°C with shaking at 200 rpm, and samples were collected from four time points (2, 3, 4, 5 h) for analysis. Approximately 2×10^9 cells were harvested for RNA isolation. Total RNA isolation was performed as described previously (Chen et al., 2009). Real-time quantitative PCR analysis was performed using Maxima SYBR Green qPCR Master Mix (Thermo Fisher Scientific, United States) on a Roche LightCycler 480 II Real-Time PCR System (Roche). Results were normalized to the expression of *gyrB*. The expression levels of *mprF*, *vraSR*, and several selected cell wall synthesis-related genes (*fntA*, *murZ*, *pbp2*, *sgtB*, *tagA*) were determined using the primers listed in Table 2. The expression of *ldh1*, a gene involved in nitric oxide resistance in *S. aureus* (Richardson et al., 2008),

was used as a negative control. The target gene transcripts were quantified by using the basic relative quantification method of the LightCycler 480 Software v1.5.1.62 (Roche). Three independent experiments were performed in duplicate and results are shown as mean \pm SD. The mRNA expression levels of genes from CGK5 were defined as 1.

Construction of *mprF* and *vraSR* Promoter-Reporter Plasmids

For introducing the *luxT2* reporter into CGK5, the selection marker *spc* was amplified by PCR from the Z172 strain (Chen et al., 2013), digested with *Sma*I and then cloned into *luxT2* (Chen et al., 2014) to generate *luxT2*-SPC. The *mprF* and *vraSR* promoter fragments were PCR-amplified from the chromosome of CGK5 using the primers *PmprF*-F, *PmprF*-R and *PvraSR*-F, *PvraSR*-R. These amplified promoter fragments were fused upstream of the *lux* reporter genes of *luxT2*-SPC using the *Bam*HI and *Sal*I sites, and the resulting plasmids were used for transformation of the *S. aureus* strain RN4220 and then of CGK5 and CGK5 mutant derivatives. The resulting promoter-reporter fusion constructs were confirmed by restriction enzyme analysis and DNA sequencing.

Luciferase Reporter Assays

Bioluminescence was measured with a SpectraMax L microplate reader (Molecular Devices, Sunnyvale, CA, United States) to determine the transcriptional level of the *mprF* and *vraSR* promoter constructs. Three independent transformants harboring promoter-reporter fusion plasmids were grown overnight with shaking at 37°C in TSB containing spectinomycin for reporter plasmid maintenance, diluted 1:100 in the same medium, and aliquots (200 µl) of the cultures were transferred into 96-well plates in duplicate and incubated at 37°C. Both OD₅₉₅ and bioluminescence (in relative light units, RLU) were monitored every hour for 7 h.

Statistical Analysis

Assay results are reported as mean \pm SD where appropriate. For comparison of differences between CGK5 and CGK5 mutant derivatives, the Student's *t*-test was performed using GraphPad Prism 6 software (GraphPad, La Jolla, CA, United States). A *P* value less than 0.05 was considered statistically significant.

RESULTS

To examine the effects of the *MprF* L431F amino acid substitution in an isogenic background, we replaced the chromosomal wild-type *mprF* gene of the DAP-S parental strain CGK5 with the mutant *mprF* gene from the CGK6 DAP-NS strain, creating the new strain CGK5mut. A single base change (from CTT to TTT) causes the L431F mutation in *MprF*. Furthermore, we generated a reverse mutation complementation construct from CGK5mut, called CGK5mutR, which carries a wild-type *mprF* with a new *EcoRV* restriction site that can be used to differentiate CGK5mutR from CGK5. CGK5mut and CGK5mutR were verified by PCR and sequencing of the entire

mprF gene. We then carried out a phenotypic analysis to compare CGK5mut and CGK5mutR against their parental strain CGK5.

The daptomycin MIC of CGK5mut was 6-fold higher (3 μ g/ml) compared to that of the wild-type parental strain CGK5 (0.5 μ g/ml), a level of increase similar to what we previously reported for DAP-NS clinical isolates (Lee et al., 2010). To our surprise, the vancomycin MIC of CGK5mut was also increased compared to CGK5 (3 μ g/ml vs. 1.5 μ g/ml). The reverse complementation construct, CGK5mutR, showed the same level of susceptibility as CGK5. PAP results showed that, of the three strains, only CGK5mut displayed a hVISA phenotype (Figure 1A). The bacterial feature that is often associated with DAP-NS and VISA or hVISA strains is increased cell wall thickness (Camargo et al., 2008; Mehta et al., 2012a). Transmission electron microscopy analysis revealed that CGK5mut has a significantly thicker cell wall (38.09 ± 5.67 nm) than CGK5 (30.65 ± 2.58 nm) and CGK5mutR (25.94 ± 3.75 nm) ($p < 0.05$) (Figure 1B). It has also been reported that clinical and *in vitro*-derived *S. aureus* strains exhibiting increased vancomycin MICs grow slower than their progenitors (Cui et al., 2003; Camargo et al., 2008). This phenomenon has been

attributed to increased cell wall synthesis at a biological cost to the resistant strains (Cui et al., 2003). We also found that CGK5mut (doubling time = 240 ± 9.5 min) grows slower than both CGK5 (doubling time = 158 ± 3.5 min) and CGK5mutR (doubling time = 170 ± 4.2 min) in MHB (Figure 2).

Altered cell membrane charge has been found in some DAP-NS *S. aureus* isolates with point mutations in *mprF* (Peschel et al., 2001; Oku et al., 2004). Cytochrome *c* is a cationic protein that has been used to estimate the relative bacterial cell surface charge of *S. aureus* (Mukhopadhyay et al., 2007). We detected a significant increase in unbound cytochrome *c* for CGK5mut (0.676 ± 0.056 mg/ml) compared to CGK5 (0.393 ± 0.058 mg/ml) and CGK5mutR (0.417 ± 0.02 mg/ml) ($p < 0.05$) (Figure 3), indicating an increased positive charge density on the cell surface of CGK5mut and suggesting a mechanism by which the L431F mutation of MprF might contribute to daptomycin resistance.

The mechanism of oxacillin resistance in MRSA is thought to be mainly due to the production of penicillin-binding protein 2a (PBP2a, encoded by the *mecA* gene) with reduced affinity for β -lactams (Hiramatsu et al., 2001). Although first observed

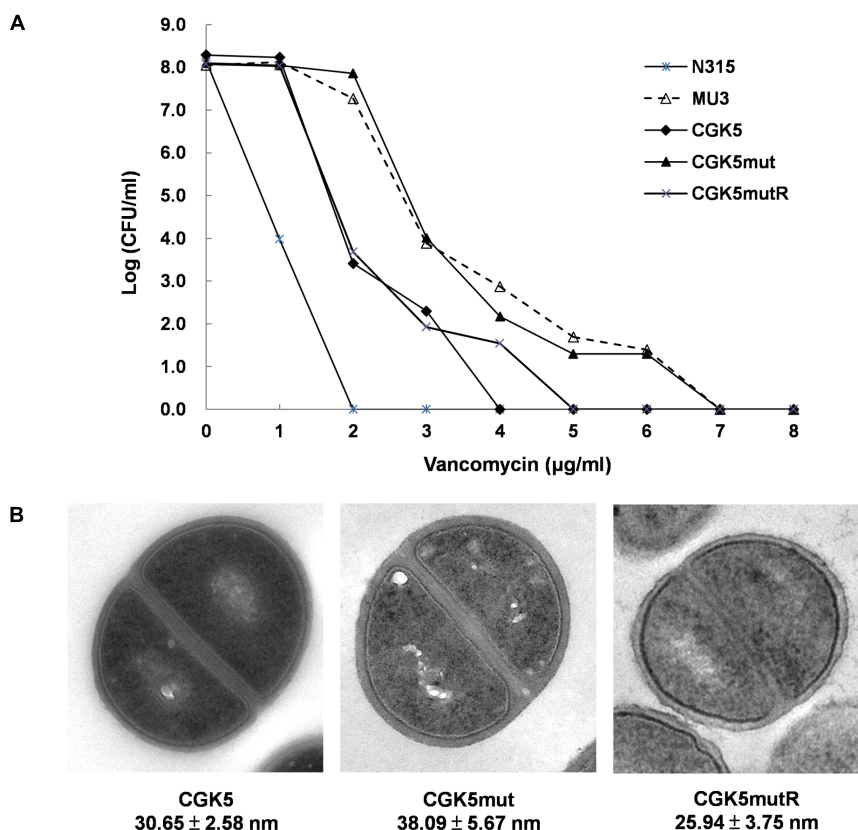


FIGURE 1 | Detection of hVISA features. **(A)** Population analysis profile of vancomycin on CGK5 and its mutant derivatives. Overnight cultures of test isolates were serially diluted in Trypticase Soy broth (TSB) and inoculated onto brain heart infusion (BHI) agar plates containing 0 to 8 μ g/ml of vancomycin. After 48 h incubation at 35°C, colonies were counted and the results were plotted on a graph. Mu3 (ATCC 700698) and N315 *S. aureus* strains were tested in parallel as hVISA positive and negative controls, respectively. **(B)** Transmission electron microscopy images of CGK5 and its mutant derivatives. Cell wall thickness (in nanometers) was measured at 150,000 \times magnification. Fifty measurements of equatorially cut cells were taken for calculation of cell wall thickness, and results are expressed as mean \pm SD. CGK5, progenitor of CGK5mut; CGK5mut, derivatives of CGK5 with L431F mutation in *mprF*; CGK5mutR, reverse complementation construct of CGK5mut.

between glycopeptide and β -lactams (Sieradzki and Tomasz, 1999), the “seesaw” inverse relationship between daptomycin and β -lactam susceptibility has been reported by several groups (Mishra et al., 2009; Lee et al., 2010; Yang et al., 2010; Mehta et al., 2012a). We determined the level of PBP2a production in CGK5mut and found it to be comparable to that of CGK5 and CGK5mutR (Figure 4A).

However, concurrent to the increased daptomycin MIC, the oxacillin MIC of CGK5mut decreased to 1 μ g/ml from 128 μ g/ml in CGK5, as determined by the BMD method in medium without 2% NaCl, whereas CGK5mutR showed a similar MIC as CGK5 (Figure 4B). Thus, CGK5mut exhibits the “seesaw-like” effect similar to which we and others have previously observed in DAP-NS *in vitro*-selected and clinical *S. aureus* isolates (Lee et al., 2010; Mehta et al., 2012a,b). Interestingly, the oxacillin MICs of CGK5, CGK5mut and CGK5mutR were the same (256 μ g/ml) in medium containing 2% NaCl (Figure 4B). Therefore, we further measured the level of PBP2a of these strains grown in oxacillin (0.25 μ g/ml) containing medium with and without 2% NaCl. The level of PBP2a of CGK5mut showed a marked reduction after exposure to oxacillin, and 2% NaCl counteracted this effect (Figure 4A).

Mutation of *mprF* has been shown to impact the expression of *mprF* itself (Yang et al., 2009b). In addition, *VraSR*, a two-component regulatory system that plays a major role in cell wall synthesis and is a key player in the cell-wall stress response, has often been implicated in vancomycin and daptomycin resistance (Kuroda et al., 2003; Camargo et al., 2008; Muthaiyan et al., 2008; Mehta et al., 2012a). We therefore compared the expression of *mprF* and *vraSR*-related genes in CGK5 and its mutant derivatives by real-time quantitative PCR analysis. We found there was no significant difference in the *mprF* expression among them (Figure 5). However, significant increases (>4 -fold increase, $P < 0.01$) in the expression of *vraSR* were seen in CGK5mut compared to CGK5 and CGK5mutR at the 4-h time point. In addition, the expression levels of four examined cell wall synthesis-related genes (*fmtA*, *murZ*, *pbp2*, *sgtB*) were also significantly increased in CGK5mut ($>2\sim3$ -fold increase, $P < 0.01$) at this time point.

To clarify whether the up-regulation of gene expression in CGK5mut is due to promoter activity, we constructed *mprF* and *vraSR* promoter-reporters. The transcriptional activity of the *mprF* and *vraSR* promoters was compared in CGK5 and its mutant derivatives by using a bioluminescence assay. *mprF* promoter activity among the tested strains showed no obvious differences (Figure 6A). However, the *vraSR* promoter showed significantly higher promoter activity in CGK5mut compared to the other two strains and the maximum discrepancy was at the 4-h time point (Figure 6A), indicating that the up-expression of *vraSR* in CGK5mut was mediated by its promoter.

To determine whether the reduced oxacillin MIC of CGK5mut was caused by increased expression of *vraSR*, and how this might be related to the fact that 2% NaCl could restore the oxacillin MIC of CGK5mut to wild-type levels, we examined whether the high salt concentration could inhibit the expression of *vraSR* in CGK5mut. A *vraSR* promoter activity assay showed that NaCl does indeed inhibit *vraSR* promoter activity (Figure 6B). The

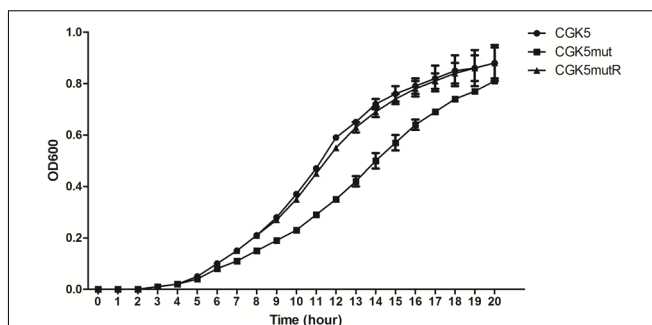


FIGURE 2 | Growth curve of CGK5, CGK5mut, and CGK5mutR in Mueller Hinton II broth (MHB). Overnight fresh cultures of the bacteria were adjusted in 0.85% NaCl to 0.5 McFarland turbidity, then diluted 1:200 in MHB to obtain $\sim 5 \times 10^5$ CFU/ml starting inoculum. The inoculum was dispensed at 120 μ l per well in triplicates to a 100-well plate and incubated at 37°C in Bioscreen C MBR. The OD₆₀₀ of each well was read every 30 min for 24 h. The average OD of the blank wells was subtracted from the average of the triplicate test wells at each time point and plotted.

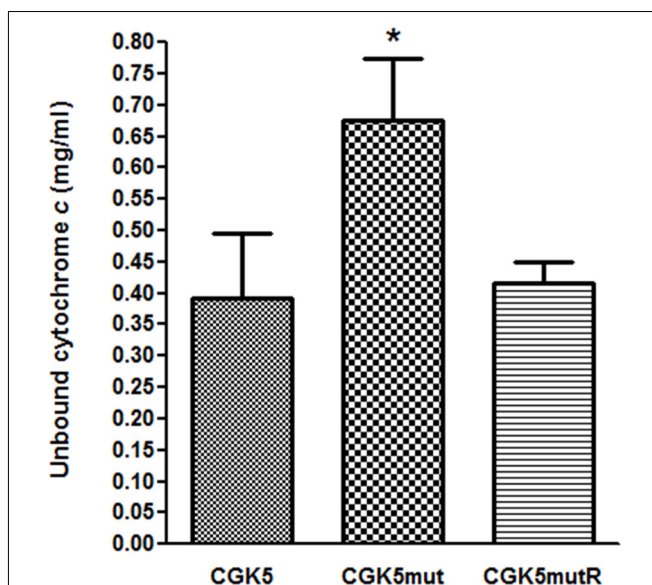


FIGURE 3 | Binding of cationic cytochrome c to CGK5, CGK5mut, and CGK5mutR whole cells. The graph represents the unbound concentrations of cytochrome c after 10 min of incubation with CGK5 and CGK5 mutant derivatives. Results are expressed as mean \pm SD from three independent experiments. * $p < 0.05$.

effect is dose-dependent and 2% NaCl is the critical concentration for inhibition.

DISCUSSION

Daptomycin is an important last-line agent against serious *S. aureus* infection, particularly in patients with persistent MRSA bacteremia and endocarditis (Boucher and Sakoulas, 2007; Marco et al., 2008). Daptomycin non-susceptibility in *S. aureus*, albeit still rare, can emerge during treatment and usually in

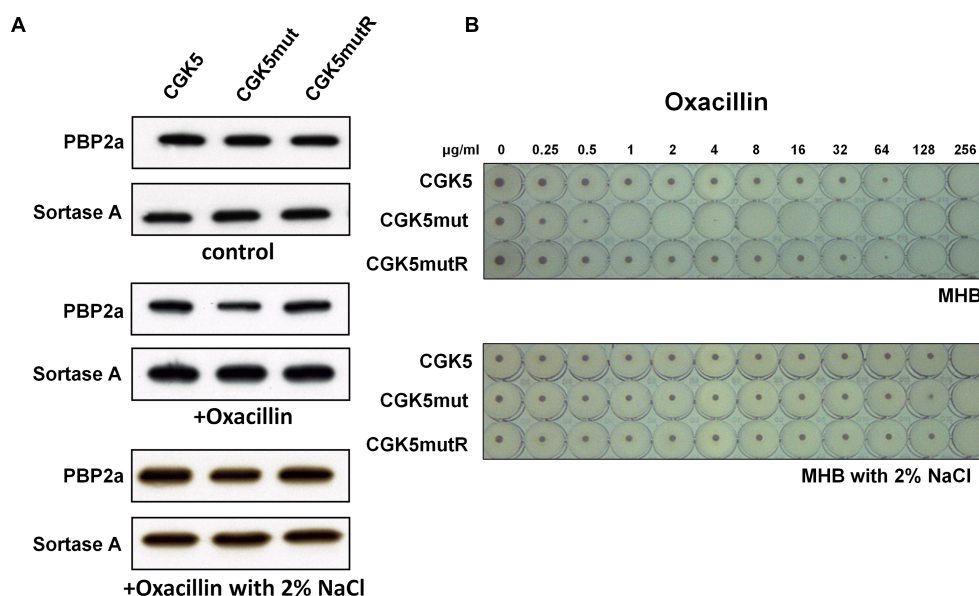


FIGURE 4 | PBP2a production and the “seesaw-like” effect. **(A)** Production of penicillin-binding protein 2a (PBP2a) by CGK5 and CGK5 mutant derivatives was measured by Western blot analysis. Membrane protein was extracted from strains grown in medium alone (control) and in oxacillin (0.25 µg/ml)-containing medium with and without 2% NaCl. PBP2a was probed with mouse monoclonal anti-PBP2a antibody (2F6F), and sortase A was used as an internal control by using rabbit polyclonal anti-Sortase A primary antibody. **(B)** Oxacillin MICs of CGK5 and CGK5 mutant derivatives were determined by broth microdilution (BMD) in Mueller Hinton II broth (MHB; containing 2% NaCl or not) from an inoculum of 5×10^5 CFU/ml.

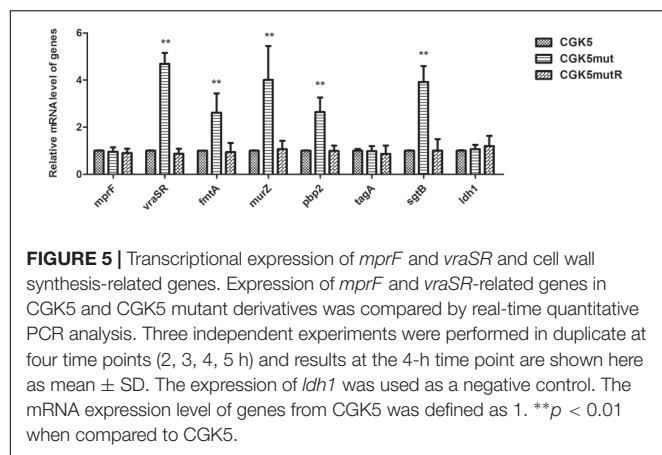
patients with severe deep-seated infections (Julian et al., 2007; Lee et al., 2010; Boyle-Vavra et al., 2011). The mechanism of daptomycin-non-susceptibility is still not fully understood but has been associated with multiple genetic changes on the bacterial chromosome, with single point mutations in the *mprF* gene being the most frequently identified alteration (Friedman et al., 2006; Julian et al., 2007; Mehta et al., 2012a; Mishra et al., 2012). Although a few hot spots have been associated with daptomycin resistance, such as L826F, S295L, and S337L, there is considerable variation in the locations of the mutations in the MprF polypeptide structure (Friedman et al., 2006; Julian et al., 2007; Yang et al., 2009a; Lee et al., 2010; Boyle-Vavra et al., 2011; Mehta et al., 2012a; Peleg et al., 2012). A study just published by Yang et al. (2018) investigated the impact of laboratory generated single or dual point mutations within the hot spot loci of *mprF* and found that extra point mutation in *mprF* resulted in diminished characteristics associated with DAP-NS, which may explain why no clinically derived DAP-NS strains contained multiple point mutations within the *mprF* gene.

Our previous study on sequential clinical MRSA isolates from a patient with persistent bacteremia revealed an L431F amino acid substitution in the 3 DAP-NS isolates we characterized (Lee et al., 2010). Since this mutation had not been seen in other DAP-NS isolates reported to date, we carried out the present study to verify its contribution to daptomycin resistance. Because some DAP-NS isolates are also vancomycin non-susceptible, and a few DAP-NS isolates (including our own; Mishra et al., 2009; Lee et al., 2010; Yang et al., 2010; Mehta et al., 2012a) have been reported to exhibit a reduced oxacillin MIC, we also investigated the effects of this L431F MprF change on vancomycin and

oxacillin MICs. The approach we employed differed from those of other studies in that we used a single-base-substitution (from CTT to TTT) method to create the L431F mutant (CGK5mut) from CGK5, the wild-type progenitor of our DAP-NS strains. We also generated a reverse mutant from CGK5mut, CGK5mutR, to verify our findings for CGK5mut. This approach ensured that the strains we tested and compared were isogenic, except for the single nucleotide difference at the site corresponding to codon 431 of MprF (and a mutated silent EcoRV site in CGKmutR which has no effect on the sequence of the polypeptide).

The increased daptomycin MIC observed in CGK5mut confirmed that the L431F missense mutation contributes to daptomycin resistance. We also showed that CGK5mut has reduced binding of cytochrome *c*. Since the L431 amino acid is located in the C-terminal LPG synthase domain of MprF (Ernst et al., 2009), the daptomycin-non-susceptibility in CGK5mut might be an effect of a reduced PG:LPG ratio (Ernst et al., 2009; Yang et al., 2009b). A lower PG:LPG ratio has been shown to reduce the negative charge of the cell membrane (Baltz, 2009; Rubio et al., 2012), thus diminishing the access of calcium-dependent daptomycin to its cellular target.

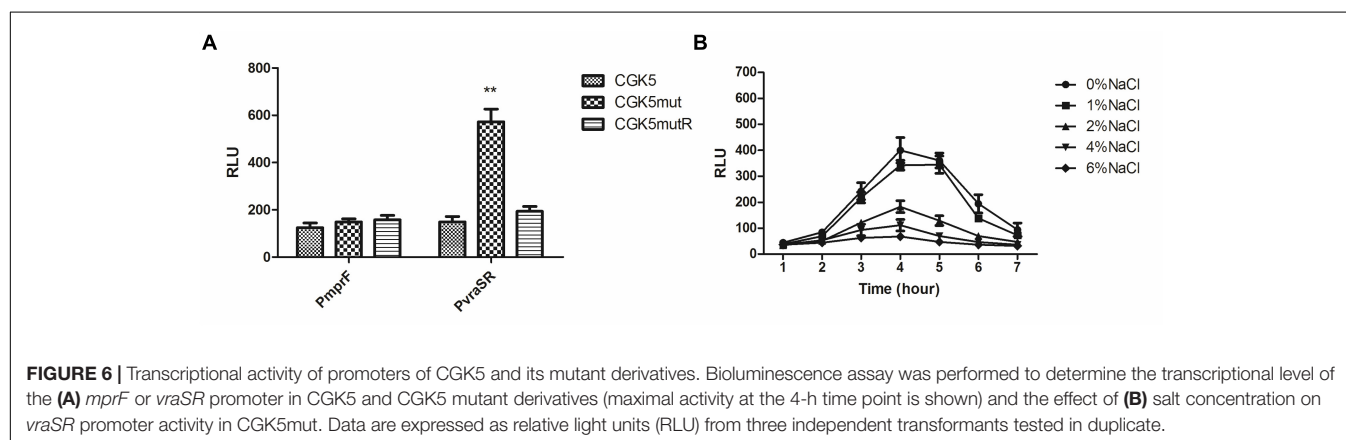
Another factor that is commonly associated with daptomycin-non-susceptibility is VraSR (Camargo et al., 2008; Mehta et al., 2012a), a two-component system that positively regulates the cell wall biosynthesis pathway and is involved in the cell wall stimulon (Kuroda et al., 2003; Gardete et al., 2006). The VraSR system was originally identified as a key regulator of vancomycin resistance in VISA and hVISA isolates (Kuroda et al., 2000; Cui et al., 2005). We found that the expression levels of *vraSR* and several *vraSR*-regulated genes were significantly



increased in CGK5mut compared to CGK5 and CGK5mutR. In addition to the increased daptomycin MICs, the vancomycin MIC of CGK5mut was also increased, and population analysis showed that more CGK5mut isolates were able to grow in higher concentrations of vancomycin compared to CGK5 and CGK5mutR. CGK5mut cells also have a thicker cell wall and grow slower than CGK5 and CGK5mutR cells. These cellular features have been associated with both DAP-NS *S. aureus* and hVISA/VISA (Camargo et al., 2008; Song et al., 2013). The changes in CGK5mut vancomycin MIC and cell wall thickness likely arise from the upregulated *vraSR*-dependent system. But how the L431F mutant protein brings about the increased expression of *vraSR* and the cell wall-related genes is unknown. However, CGK5mut had significant increased *vraSR* promoter activity compared to CGK5 and CGK5mutR using *vraSR* promoter-reporter assay, indicating that the up-expression of *vraSR* in CGK5mut was mediated by its promoter. A previous study observed the mutual presence of both *mprF* point mutations and increased expression levels of *vraSR* in DAP-NS strains compared to their DAP-susceptible counterparts, and hypothesized that both genes were mechanistically linked to the DAP-NS phenotype (Mehta et al., 2012a). However, our results suggest a causal relationship between *mprF* point mutation and increased expression of *vraSR*, which may explain why the

daptomycin resistance is often concomitant with vancomycin resistance in clinical isolates. There are a plethora of pathways to heterogeneous and intermediate resistance to vancomycin in *S. aureus* (Howden et al., 2010). In addition to *VraSR*, two other two-component systems, *GraSR* and *WalKR*, have also been associated with reduced susceptibility of *S. aureus* to both daptomycin and vancomycin. It has been reported that *GraSR* also plays an important role in *S. aureus* resistance to cationic antimicrobial peptides via altered expression of *mprF* and *dltABCD* resulting in increased electrostatic repulsion of cationic antimicrobial peptides. *GraSR* has also been shown to interact with the *WalKR* system and have significant regulatory overlap (Li et al., 2007; Meehl et al., 2007; Dubrac et al., 2008; Falord et al., 2011). However, we found no significant differences in the expression of *mprF* and *mprF* promoter activity among the tested strains. Therefore, it appears unlikely that reduced susceptibility of CGK5mut to both daptomycin and vancomycin are associated with these two two-component systems.

Although expression of PBP2a (encoded by the *mecA* gene) is thought to play a major role in oxacillin-resistance, several studies have reported that the amount of PBP2a expressed does not correlate with the level of methicillin-resistance (Chambers and Hackbarth, 1987; Murakami and Tomasz, 1989; De Lencastre et al., 1994), and other auxiliary genes have been reported to be essential for the optimal expression of methicillin-resistance (De Lencastre and Tomasz, 1994). When we determined the production level of PBP2a in CGK5mut and found it to be comparable to that of CGK5 and CGK5mutR in the normal condition, we thought its “seesaw-like” effect may be caused by other factors. This indicated that the expression of *mecA* gene in CGK5mut was not altered by the *mprF* point mutation. Since the oxacillin MIC of CGK5mut was reduced in medium lacking 2% NaCl, we measured the levels of PBP2a in these strains in the presence of oxacillin with and without 2% NaCl and found that the level of PBP2a production in CGK5mut reduced after exposure to oxacillin and 2% NaCl could abolish this effect. According to the CLSI guideline, 2% NaCl should be added to the medium in determining the oxacillin MIC for staphylococci (CLSI, 2013). Interestingly, our results also showed that the expression of *vraSR* decreased in the presence of



2% NaCl, with a concurrent restoration of oxacillin resistance in CGK5mut, indicating that the effect of upregulation of *vraSR* in CGK5mut could be abolished by adding 2% NaCl. Since the “seesaw” effect has been observed in only a few DAP-NS MRSA isolates (Mehta et al., 2012b), the factors associated with this phenomenon warrant further investigation. However, *mprF* point mutation in CGK5mut only exhibits the “seesaw-like” effect (meaning the seesaw effect was only observed in the absence of NaCl), we speculate that additional mutations at other genes are required to achieve truly “seesaw” effect observed in clinical isolates. In addition, how 2% NaCl counteracts the up-regulation effect of *vraSR* caused by MprF L431F mutation requires further research.

In fact, Mehta et al. (2012a) previously observed the phenotype in DAP-non-susceptible strains with upregulation of the two-component regulatory system *vraSR*; however, they did not prove this was caused by the MprF mutation. By contrast, they introduced an overexpression of *vraSR* in DAP-susceptible strains to show a reduction in oxacillin resistance. In their latest study, they found that introducing an overexpression of *vraSR* in DAP-susceptible strains triggering MprF mutation and result in impairment of PrsA chaperone functions, both events are required for β -lactam resistance via PBP2a maturation (Renzoni et al., 2017). It has long been recommended that 2% NaCl (or KCl) be added to the culture medium to reliably detect oxacillin resistance in staphylococci (Thornsberry and McDougal, 1983; Huang et al., 1993). When salt is placed in solvent, the solid salt dissolves into its component ions, sodium (Na^+), potassium (K^+), chloride (Cl^-), which are the primary ions of electrolytes in physiology. It is plausible to speculate that these ions maintain the phosphorylation state of *VraS* in respond to *mprF* point mutation and/or β -lactam stimulon to precisely regulate its downstream genes for the generation of resistant phenotype.

CONCLUSION

The present study demonstrated that a single amino acid substitution (L431F) in the MprF protein contributes to

both daptomycin and vancomycin resistance as well as increased oxacillin susceptibility in an isogenic MRSA strain. This point mutation in CGK5 also causes up-expression of *vraSR*. Further studies on the mechanisms contributing to these phenomena may lead to discovery of potential therapeutics against multidrug-resistant staphylococci.

AUTHOR CONTRIBUTIONS

F-JC contributed to the study design, data analysis, and manuscript preparation. T-LL performed the data analysis and prepared the manuscript. C-HL, Y-CH, I-WH, P-CH, and C-SY performed the work and data analysis.

FUNDING

This project was supported by intramural grants from the National Health Research Institutes to the National Institute of Infectious Diseases and Vaccinology (IV-101-SP-10, IV-102-SP-10, and IV-101-SP-11), and grants from the Ministry of Science and Technology in Taiwan (MOST 104-2320-B-400-013-). The transmission electron microscopy analysis was supported by an NHRI intramural grant to the Center for Nanomedicine Research (NM-101-PP-04).

ACKNOWLEDGMENTS

We wish to thank Ms. Yu-Ching Chen, Hsin-Ying Huang (Research Assistant, Center for Nanomedicine Research), and Yu-Lin Chen (Research Assistant, NIIDV) for their technical assistance. We are also grateful to Prof. Paul Williams (University of Nottingham, United Kingdom) for kindly providing many of important bacterial strains and plasmids used in this study.

REFERENCES

- Arnaud, M., Chastanet, A., and Debarbouille, M. (2004). New vector for efficient allelic replacement in naturally nontransformable, low-GC-content, gram-positive bacteria. *Appl. Environ. Microbiol.* 70, 6887–6891. doi: 10.1128/AEM.70.11.6887-6891.2004
- Baltz, R. H. (2009). Daptomycin: mechanisms of action and resistance, and biosynthetic engineering. *Curr. Opin. Chem. Biol.* 13, 144–151. doi: 10.1016/j.cbpa.2009.02.031
- Bertsche, U., Weidenmaier, C., Kuehner, D., Yang, S. J., Baur, S., Wanner, S., et al. (2011). Correlation of daptomycin resistance in a clinical *Staphylococcus aureus* strain with increased cell wall teichoic acid production and D-alanylation. *Antimicrob. Agents Chemother.* 55, 3922–3928. doi: 10.1128/AAC.01226-10
- Boucher, H. W., and Sakoulas, G. (2007). Perspectives on Daptomycin resistance, with emphasis on resistance in *Staphylococcus aureus*. *Clin. Infect. Dis.* 45, 601–608. doi: 10.1086/520655
- Boyle-Vavra, S., Jones, M., Gourley, B. L., Holmes, M., Ruf, R., Balsam, A. R., et al. (2011). Comparative genome sequencing of an isogenic pair of USA800 clinical methicillin-resistant *Staphylococcus aureus* isolates obtained before and after daptomycin treatment failure. *Antimicrob. Agents Chemother.* 55, 2018–2025. doi: 10.1128/AAC.01593-10
- Camargo, I. L., Neoh, H. M., Cui, L., and Hiramoto, K. (2008). Serial daptomycin selection generates daptomycin-nonsusceptible *Staphylococcus aureus* strains with a heterogeneous vancomycin-intermediate phenotype. *Antimicrob. Agents Chemother.* 52, 4289–4299. doi: 10.1128/AAC.00417-08
- Chambers, H. F., and Hackbarth, C. J. (1987). Effect of NaCl and nafcillin on penicillin-binding protein 2a and heterogeneous expression of methicillin resistance in *Staphylococcus aureus*. *Antimicrob. Agents Chemother.* 31, 1982–1988. doi: 10.1128/AAC.31.12.1982
- Chen, F. J., Lauderdale, T. L., Wang, L. S., and Huang, I. W. (2013). Complete genome sequence of *Staphylococcus aureus* Z172, a vancomycin-intermediate and daptomycin-nonsusceptible methicillin-resistant strain isolated in Taiwan. *Genome Announc.* 1:e01011-13. doi: 10.1128/genomeA.01011-13
- Chen, F. J., Wang, C. H., Chen, C. Y., Hsu, Y. C., and Wang, K. T. (2014). Role of the *mecA* gene in oxacillin resistance in a *Staphylococcus aureus* clinical strain with a pvl-positive ST59 genetic background. *Antimicrob. Agents Chemother.* 58, 1047–1054. doi: 10.1128/AAC.02045-13

- Chen, L. C., Tsou, L. T., and Chen, F. J. (2009). Ligand-receptor recognition for activation of quorum sensing in *Staphylococcus aureus*. *J. Microbiol.* 47, 572–581. doi: 10.1007/s12275-009-0004-2
- CLSI (2013). *Performance Standards for Antimicrobial Susceptibility Testing: 23rd Informational Supplement M100-S23*. Wayne, PA: Clinical and Laboratory Standards Institute.
- Cui, L., Lian, J. Q., Neoh, H. M., Reyes, E., and Hiramatsu, K. (2005). DNA microarray-based identification of genes associated with glycopeptide resistance in *Staphylococcus aureus*. *Antimicrob. Agents Chemother.* 49, 3404–3413. doi: 10.1128/AAC.49.8.3404-3413.2005
- Cui, L., Ma, X., Sato, K., Okuma, K., Tenover, F. C., Mamizuka, E. M., et al. (2003). Cell wall thickening is a common feature of vancomycin resistance in *Staphylococcus aureus*. *J. Clin. Microbiol.* 41, 5–14. doi: 10.1128/JCM.41.1.5-14.2003
- Cui, L., Murakami, H., Kuwahara-Arai, K., Hanaki, H., and Hiramatsu, K. (2000). Contribution of a thickened cell wall and its glutamine nonamidated component to the vancomycin resistance expressed by *Staphylococcus aureus* Mu50. *Antimicrob. Agents Chemother.* 44, 2276–2285. doi: 10.1128/AAC.44.9.2276-2285.2000
- De Lencastre, H., De Jonge, B. L., Matthews, P. R., and Tomasz, A. (1994). Molecular aspects of methicillin resistance in *Staphylococcus aureus*. *J. Antimicrob. Chemother.* 33, 7–24. doi: 10.1093/jac/33.1.7
- De Lencastre, H., and Tomasz, A. (1994). Reassessment of the number of auxiliary genes essential for expression of high-level methicillin resistance in *Staphylococcus aureus*. *Antimicrob. Agents Chemother.* 38, 2590–2598. doi: 10.1128/AAC.38.11.2590
- Downer, R., Roche, F., Park, P. W., Mecham, R. P., and Foster, T. J. (2002). The elastin-binding protein of *Staphylococcus aureus* (EbpS) is expressed at the cell surface as an integral membrane protein and not as a cell wall-associated protein. *J. Biol. Chem.* 277, 243–250. doi: 10.1074/jbc.M107621200
- Dubrac, S., Bisicchia, P., Devine, K. M., and Msadek, T. (2008). A matter of life and death: cell wall homeostasis and the WalK (YycG) essential signal transduction pathway. *Mol. Microbiol.* 70, 1307–1322. doi: 10.1111/j.1365-2958.2008.06483.x
- Enoch, D. A., Bygott, J. M., Daly, M. L., and Karas, J. A. (2007). Daptomycin. *J. Infect.* 55, 205–213. doi: 10.1016/j.jinf.2007.05.180
- Ernst, C. M., and Peschel, A. (2011). Broad-spectrum antimicrobial peptide resistance by MprF-mediated aminoacylation and flipping of phospholipids. *Mol. Microbiol.* 80, 290–299. doi: 10.1111/j.1365-2958.2011.07576.x
- Ernst, C. M., Staubitz, P., Mishra, N. N., Yang, S. J., Hornig, G., Kalbacher, H., et al. (2009). The bacterial defensin resistance protein MprF consists of separable domains for lipid lysinylation and antimicrobial peptide repulsion. *PLoS Pathog.* 5:e1000660. doi: 10.1371/journal.ppat.1000660
- Falord, M., Mader, U., Hiron, A., Debarbouille, M., and Msadek, T. (2011). Investigation of the *Staphylococcus aureus* GraSR regulon reveals novel links to virulence, stress response and cell wall signal transduction pathways. *PLoS One* 6:e21323. doi: 10.1371/journal.pone.0021323
- Friedman, L., Alder, J. D., and Silverman, J. A. (2006). Genetic changes that correlate with reduced susceptibility to daptomycin in *Staphylococcus aureus*. *Antimicrob. Agents Chemother.* 50, 2137–2145. doi: 10.1128/AAC.00039-06
- Gardete, S., Wu, S. W., Gill, S., and Tomasz, A. (2006). Role of VraSR in antibiotic resistance and antibiotic-induced stress response in *Staphylococcus aureus*. *Antimicrob. Agents Chemother.* 50, 3424–3434.
- Hanaki, H., Kuwahara-Arai, K., Boyle-Vavra, S., Daum, R. S., Labischinski, H., and Hiramatsu, K. (1998). Activated cell-wall synthesis is associated with vancomycin resistance in methicillin-resistant *Staphylococcus aureus* clinical strains Mu3 and Mu50. *J. Antimicrob. Chemother.* 42, 199–209. doi: 10.1093/jac/42.2.199
- Hiramatsu, K., Aritaka, N., Hanaki, H., Kawasaki, S., Hosoda, Y., Hori, S., et al. (1997). Dissemination in Japanese hospitals of strains of *Staphylococcus aureus* heterogeneously resistant to vancomycin. *Lancet* 350, 1670–1673. doi: 10.1016/S0140-6736(97)07324-8
- Hiramatsu, K., Cui, L., Kuroda, M., and Ito, T. (2001). The emergence and evolution of methicillin-resistant *Staphylococcus aureus*. *Trends Microbiol.* 9, 486–493. doi: 10.1016/S0966-842X(01)02175-8
- Howden, B. P., Davies, J. K., Johnson, P. D., Stinear, T. P., and Grayson, M. L. (2010). Reduced vancomycin susceptibility in *Staphylococcus aureus*, including vancomycin-intermediate and heterogeneous vancomycin-intermediate strains: resistance mechanisms, laboratory detection, and clinical implications. *Clin. Microbiol. Rev.* 23, 99–139. doi: 10.1128/CMR.00042-09
- Howden, B. P., Johnson, P. D., Ward, P. B., Stinear, T. P., and Davies, J. K. (2006). Isolates with low-level vancomycin resistance associated with persistent methicillin-resistant *Staphylococcus aureus* bacteremia. *Antimicrob. Agents Chemother.* 50, 3039–3047. doi: 10.1128/AAC.00422-06
- Huang, M. B., Gay, T. E., Baker, C. N., Banerjee, S. N., and Tenover, F. C. (1993). Two percent sodium chloride is required for susceptibility testing of staphylococci with oxacillin when using agar-based dilution methods. *J. Clin. Microbiol.* 31, 2683–2688.
- Julian, K., Kosowska-Shick, K., Whitener, C., Roos, M., Labischinski, H., Rubio, A., et al. (2007). Characterization of a daptomycin-nonsusceptible vancomycin-intermediate *Staphylococcus aureus* strain in a patient with endocarditis. *Antimicrob. Agents Chemother.* 51, 3445–3448. doi: 10.1128/AAC.00559-07
- Kuroda, M., Kuroda, H., Oshima, T., Takeuchi, F., Mori, H., and Hiramatsu, K. (2003). Two-component system VraSR positively modulates the regulation of cell-wall biosynthesis pathway in *Staphylococcus aureus*. *Mol. Microbiol.* 49, 807–821. doi: 10.1046/j.1365-2958.2003.03599.x
- Kuroda, M., Kuwahara-Arai, K., and Hiramatsu, K. (2000). Identification of the up- and down-regulated genes in vancomycin-resistant *Staphylococcus aureus* strains Mu3 and Mu50 by cDNA differential hybridization method. *Biochem. Biophys. Res. Commun.* 269, 485–490. doi: 10.1006/bbrc.2000.2277
- Lee, C. H., Wang, M. C., Huang, I. W., Chen, F. J., and Lauderdale, T. L. (2010). Development of daptomycin nonsusceptibility with heterogeneous vancomycin-intermediate resistance and oxacillin susceptibility in methicillin-resistant *Staphylococcus aureus* during high-dose daptomycin treatment. *Antimicrob. Agents Chemother.* 54, 4038–4040. doi: 10.1128/AAC.00533-10
- Li, M., Cha, D. J., Lai, Y., Villaruz, A. E., Sturdevant, D. E., and Otto, M. (2007). The antimicrobial peptide-sensing system aps of *Staphylococcus aureus*. *Mol. Microbiol.* 66, 1136–1147. doi: 10.1111/j.1365-2958.2007.05986.x
- Marco, F., De La Maria, C. G., Armero, Y., Amat, E., Soy, D., Moreno, A., et al. (2008). Daptomycin is effective in treatment of experimental endocarditis due to methicillin-resistant and glycopeptide-intermediate *Staphylococcus aureus*. *Antimicrob. Agents Chemother.* 52, 2538–2543. doi: 10.1128/AAC.00510-07
- McAleese, F., Wu, S. W., Sieradzki, K., Dunman, P., Murphy, E., Projan, S., et al. (2006). Overexpression of genes of the cell wall stimulon in clinical isolates of *Staphylococcus aureus* exhibiting vancomycin-intermediate- *S. aureus*-type resistance to vancomycin. *J. Bacteriol.* 188, 1120–1133. doi: 10.1128/JB.188.3.1120-1133.2006
- Meehl, M., Herbert, S., Gotz, F., and Cheung, A. (2007). Interaction of the GraRS two-component system with the VraFG ABC transporter to support vancomycin-intermediate resistance in *Staphylococcus aureus*. *Antimicrob. Agents Chemother.* 51, 2679–2689. doi: 10.1128/AAC.00209-07
- Mehta, S., Cui, L., Plata, K. B., Riosa, S., Silverman, J. A., Rubio, A., et al. (2012a). VraSR two-component regulatory system contributes to mprF-mediated decreased susceptibility to daptomycin in *in vivo*-selected clinical strains of methicillin-resistant *Staphylococcus aureus*. *Antimicrob. Agents Chemother.* 56, 92–102. doi: 10.1128/AAC.00432-10
- Mehta, S., Singh, C., Plata, K. B., Chanda, P. K., Paul, A., Riosa, S., et al. (2012b). beta-lactams increase the antibacterial activity of daptomycin against clinical methicillin-resistant *Staphylococcus aureus* strains and prevent selection of daptomycin-resistant derivatives. *Antimicrob. Agents Chemother.* 56, 6192–6200. doi: 10.1128/AAC.01525-12
- Mishra, N. N., Rubio, A., Nast, C. C., and Bayer, A. S. (2012). Differential adaptations of methicillin-resistant *Staphylococcus aureus* to serial *in vitro* passage in daptomycin: evolution of daptomycin resistance and role of membrane carotenoid content and fluidity. *Int. J. Microbiol.* 2012:683450. doi: 10.1155/2012/683450
- Mishra, N. N., Yang, S. J., Sawa, A., Rubio, A., Nast, C. C., Yeaman, M. R., et al. (2009). Analysis of cell membrane characteristics of *in vitro*-selected daptomycin-resistant strains of methicillin-resistant *Staphylococcus aureus*. *Antimicrob. Agents Chemother.* 53, 2312–2318. doi: 10.1128/AAC.01682-08
- Mukhopadhyay, K., Whitmire, W., Xiong, Y. Q., Molden, J., Jones, T., Peschel, A., et al. (2007). *In vitro* susceptibility of *Staphylococcus aureus* to thrombin-induced platelet microbicidal protein-1 (tPMP-1) is influenced by cell membrane phospholipid composition and asymmetry. *Microbiology* 153, 1187–1197. doi: 10.1099/mic.0.2006/003111-0

- Murakami, K., and Tomasz, A. (1989). Involvement of multiple genetic determinants in high-level methicillin resistance in *Staphylococcus aureus*. *J. Bacteriol.* 171, 874–879. doi: 10.1128/jb.171.2.874-879.1989
- Muthaiyan, A., Silverman, J. A., Jayaswal, R. K., and Wilkinson, B. J. (2008). Transcriptional profiling reveals that daptomycin induces the *Staphylococcus aureus* cell wall stress stimulon and genes responsive to membrane depolarization. *Antimicrob. Agents Chemother.* 52, 980–990. doi: 10.1128/AAC.01121-07
- Novick, R. P. (1991). Genetic systems in staphylococci. *Methods Enzymol.* 204, 587–636. doi: 10.1016/0076-6879(91)04029-N
- Novick, R. P., Ross, H. F., Projan, S. J., Kornblum, J., Kreiswirth, B., and Moghazeh, S. (1993). Synthesis of staphylococcal virulence factors is controlled by a regulatory RNA molecule. *EMBO J.* 12, 3967–3975.
- Oku, Y., Kurokawa, K., Ichihashi, N., and Sekimizu, K. (2004). Characterization of the *Staphylococcus aureus* *mprF* gene, involved in lysinylation of phosphatidylglycerol. *Microbiology* 150, 45–51. doi: 10.1099/mic.0.26706-0
- Peleg, A. Y., Miyakis, S., Ward, D. V., Earl, A. M., Rubio, A., Cameron, D. R., et al. (2012). Whole genome characterization of the mechanisms of daptomycin resistance in clinical and laboratory derived isolates of *Staphylococcus aureus*. *PLoS One* 7:e28316. doi: 10.1371/journal.pone.0028316
- Peschel, A., Jack, R. W., Otto, M., Collins, L. V., Staubitz, P., Nicholson, G., et al. (2001). *Staphylococcus aureus* resistance to human defensins and evasion of neutrophil killing via the novel virulence factor MprF is based on modification of membrane lipids with l-lysine. *J. Exp. Med.* 193, 1067–1076. doi: 10.1084/jem.193.9.1067
- Renzoni, A., Kelley, W. L., Rosato, R. R., Martinez, M. P., Roch, M., Fatouraie, M., et al. (2017). Molecular bases determining daptomycin resistance-mediated resensitization to beta-lactams (seesaw effect) in methicillin-resistant *Staphylococcus aureus*. *Antimicrob. Agents Chemother.* 61:e1634-16. doi: 10.1128/AAC.01634-16
- Richardson, A. R., Libby, S. J., and Fang, F. C. (2008). A nitric oxide-inducible lactate dehydrogenase enables *Staphylococcus aureus* to resist innate immunity. *Science* 319, 1672–1676. doi: 10.1126/science.1155207
- Rubio, A., Moore, J., Varoglu, M., Conrad, M., Chu, M., Shaw, W., et al. (2012). LC-MS/MS characterization of phospholipid content in daptomycin-susceptible and -resistant isolates of *Staphylococcus aureus* with mutations in *mprF*. *Mol. Membr. Biol.* 29, 1–8. doi: 10.3109/09687688.2011.640948
- Schenk, S., and Laddaga, R. A. (1992). Improved method for electroporation of *Staphylococcus aureus*. *FEMS Microbiol. Lett.* 73, 133–138. doi: 10.1111/j.1574-6968.1992.tb05302.x
- Sieradzki, K., and Tomasz, A. (1999). Gradual alterations in cell wall structure and metabolism in vancomycin-resistant mutants of *Staphylococcus aureus*. *J. Bacteriol.* 181, 7566–7570.
- Song, Y., Rubio, A., Jayaswal, R. K., Silverman, J. A., and Wilkinson, B. J. (2013). Additional routes to *Staphylococcus aureus* daptomycin resistance as revealed by comparative genome sequencing, transcriptional profiling, and phenotypic studies. *PLoS One* 8:e58469. doi: 10.1371/journal.pone.0058469
- Thornsberry, C., and McDougal, L. K. (1983). Successful use of broth microdilution in susceptibility tests for methicillin-resistant (heteroresistant) staphylococci. *J. Clin. Microbiol.* 18, 1084–1091.
- Yang, S. J., Kreiswirth, B. N., Sakoulas, G., Yeaman, M. R., Xiong, Y. Q., Sawa, A., et al. (2009a). Enhanced expression of *dltABCD* is associated with the development of daptomycin nonsusceptibility in a clinical endocarditis isolate of *Staphylococcus aureus*. *J. Infect. Dis.* 200, 1916–1920. doi: 10.1086/648473
- Yang, S. J., Mishra, N. N., Kang, K. M., Lee, G. Y., Park, J. H., and Bayer, A. S. (2018). Impact of multiple single-nucleotide polymorphisms within *mprF* on daptomycin resistance in *Staphylococcus aureus*. *Microb. Drug Resist.* doi: 10.1089/mdr.2017.0156. [Epub ahead of print].
- Yang, S. J., Xiong, Y. Q., Boyle-Vavra, S., Daum, R., Jones, T., and Bayer, A. S. (2010). Daptomycin-oxacillin combinations in treatment of experimental endocarditis caused by daptomycin-nonsusceptible strains of methicillin-resistant *Staphylococcus aureus* with evolving oxacillin susceptibility (the “seesaw effect”). *Antimicrob. Agents Chemother.* 54, 3161–3169. doi: 10.1128/AAC.00487-10
- Yang, S. J., Xiong, Y. Q., Dunman, P. M., Schrenzel, J., Francois, P., Peschel, A., et al. (2009b). Regulation of *mprF* in daptomycin-nonsusceptible *Staphylococcus aureus* strains. *Antimicrob. Agents Chemother.* 53, 2636–2637. doi: 10.1128/AAC.01415-08

Conflict of Interest Statement: The authors declare that the research was conducted in the absence of any commercial or financial relationships that could be construed as a potential conflict of interest.

Copyright © 2018 Chen, Lauderdale, Lee, Hsu, Huang, Hsu and Yang. This is an open-access article distributed under the terms of the Creative Commons Attribution License (CC BY). The use, distribution or reproduction in other forums is permitted, provided the original author(s) and the copyright owner are credited and that the original publication in this journal is cited, in accordance with accepted academic practice. No use, distribution or reproduction is permitted which does not comply with these terms.



Genetic Diversity of *norA*, Coding for a Main Efflux Pump of *Staphylococcus aureus*

Sofia Santos Costa¹, Benjamin Sobkowiak², Ricardo Parreira¹, Jonathan D. Edgeworth³, Miguel Viveiros¹, Taane G. Clark^{2,4*} and Isabel Couto^{1*}

¹ Global Health and Tropical Medicine, Instituto de Higiene e Medicina Tropical, Universidade NOVA de Lisboa, Lisbon, Portugal, ² Faculty of Infectious and Tropical Diseases, London School of Hygiene and Tropical Medicine, London, United Kingdom, ³ Department of Infectious Diseases, Centre for Clinical Infection and Diagnostics Research, Guy's and St Thomas' NHS Foundation Trust, King's College London, London, United Kingdom, ⁴ Faculty of Epidemiology and Population Health, London School of Hygiene and Tropical Medicine, London, United Kingdom

OPEN ACCESS

Edited by:

Silvia Buroni,
University of Pavia, Italy

Reviewed by:

Maria José Saavedra,
Universidade de Trás os Montes e
Alto Douro, Portugal
Teruo Kuroda,
Hiroshima University, Japan

*Correspondence:

Taane G. Clark
taane.clark@lshtm.ac.uk
Isabel Couto
icouto@ihmt.unl.pt

Specialty section:

This article was submitted to
Evolutionary and Genomic
Microbiology,
a section of the journal
Frontiers in Genetics

Received: 28 August 2018

Accepted: 18 December 2018

Published: 09 January 2019

Citation:

Costa SS, Sobkowiak B,
Parreira R, Edgeworth JD, Viveiros M,
Clark TG and Couto I (2019) Genetic
Diversity of *norA*, Coding for a Main
Efflux Pump of *Staphylococcus*
aureus. *Front. Genet.* 9:710.
doi: 10.3389/fgene.2018.00710

NorA is the best studied efflux system of *Staphylococcus aureus* and therefore frequently used as a model for investigating efflux-mediated resistance in this pathogen. NorA activity is associated with resistance to fluoroquinolones, several antiseptics and disinfectants and several reports have pointed out the role of efflux systems, including NorA, as a first-line response to antimicrobials in *S. aureus*. Genetic diversity studies of the gene *norA* have described three alleles; *norAI*, *norAII* and *norAIII*. However, the epidemiology of these alleles and their impact on NorA activity remains unclear. Additionally, increasing studies do not account for *norA* variability when establishing relations between resistance phenotypes and *norA* presence or reported absence, which actually corresponds, as we now demonstrate, to different *norA* alleles. In the present study we assessed the variability of the *norA* gene present in the genome of over 1,000 *S. aureus* isolates, corresponding to 112 *S. aureus* strains with whole genome sequences publicly available; 917 MRSA strains sourced from a London-based study and nine MRSA isolates collected in a major Hospital in Lisbon, Portugal. Our analyses show that *norA* is part of the core genome of *S. aureus*. It also suggests that occurrence of *norA* variants reflects the population structure of this major pathogen. Overall, this work highlights the ubiquitous nature of *norA* in *S. aureus* which must be taken into account when studying the role played by this important determinant on *S. aureus* resistance to antimicrobials.

Keywords: *Staphylococcus aureus*, *norA*, alleles, variability, efflux

INTRODUCTION

Staphylococcus aureus is one of the major human pathogens in the hospital and community settings, causing a wide array of clinical manifestations, from mild skin infections to life-threatening systemic infections (Chambers and DeLeo, 2009; Tong et al., 2015). Development and acquisition of resistance to antibiotics and other antimicrobials is of paramount importance in *S. aureus*, as exemplified by the common occurrence and dissemination of strains displaying a phenotype of multidrug resistance (MDR), including methicillin-resistant

Staphylococcus aureus (MRSA) strains (Chambers and DeLeo, 2009). MRSA are spread worldwide and are a public health threat, ranked amongst the major nosocomial pathogens (Lee et al., 2018; Tacconelli et al., 2018). MRSA epidemiology has revealed the local or global dissemination of a few number of clones, namely the lineages in clonal complexes CC1, CC5, CC8, CC22, CC30, CC45, CC59, and CC80 (Lee et al., 2018).

In recent years, several studies have supported drug efflux as a player in the emergence of resistance toward antibiotics and other antimicrobials in *S. aureus* (DeMarco et al., 2007; Furi et al., 2013; Kwak et al., 2013; Costa et al., 2015). Of particular interest are multidrug efflux pumps (MDR EPs), which extrude a wide range of chemically dissimilar antimicrobials, being frequently associated with MDR phenotypes in bacteria (Piddock, 2006; Poole, 2007). In *S. aureus*, more than twenty putative MDR EPs are encoded in the chromosome (Schindler et al., 2015), of which several have already been characterized (Costa et al., 2013b). Among these, NorA is the most well studied, being frequently used as a model for studying efflux-mediated resistance in this pathogen.

NorA is a 388 aminoacid protein with 12 transmembrane segments (TMS) that belongs to the Major Facilitator Superfamily (MFS) of secondary transporters. This MDR EP uses the proton motive force to extrude from the cell fluoroquinolones, ethidium bromide, quaternary ammonium compounds, and other antimicrobials (Yoshida et al., 1990; Kaatz et al., 1993; Neyfakh et al., 1993). Several reports have associated NorA activity to low-level resistance to fluoroquinolones and reduced susceptibility to biocides (DeMarco et al., 2007; Huet et al., 2008; Kosmidis et al., 2010; Costa et al., 2011, 2015; Furi et al., 2013). Other studies support a broader substrate range for NorA, including siderophores (Deng et al., 2012) and fusaric acid (Marchi et al., 2015).

The NorA encoding gene, *norA*, was first identified in the chromosome of a fluoroquinolone-resistant *S. aureus* isolate, collected in 1986 at a Japanese hospital (Ubukata et al., 1989). Early studies have shown that genetic diversity of this gene can be captured by three alleles, differing up to 10% at the level of the nucleotide sequence and 5% in the polypeptide sequence; *norAI* (Yoshida et al., 1990), *norAII* (also described as *norA23*) (Noguchi et al., 2004) and *norAIII* (also described as *norA1199*) (Kaatz et al., 1993). The occurrence of *norA* variants is also strengthened by a recent study by Brooks et al. (2018) that refers to the variability of this gene in a set of over 150 *S. aureus* strains. Although some studies have been conducted to ascertain the impact of this genetic diversity on the efflux activity of NorA (Schmitz et al., 1998; Sierra et al., 2000; Noguchi et al., 2004), this effect remains unclear.

Despite this early characterization, there are still contradictory reports in literature on the role of NorA in *S. aureus* efflux-mediated antimicrobial resistance. Several studies have reported on the putative absence of *norA*, most probably due to failure to amplify this gene with primers directed to only one of the possible *norA* alleles. The present study aims at clarifying some of these aspects, by demonstrating that the *norA* gene is part of the core genome of *S. aureus*, reflecting on the genetic variability of the gene, its distribution amongst *S. aureus* clonal lineages, including

both methicillin-resistant and -susceptible strains and possible impact on NorA function.

MATERIALS AND METHODS

Study Datasets

Four sets of nucleotide sequences of the *norA* structural gene and the corresponding polypeptide sequences were used in this study, comprising (i) the sequences of the three *norA* alleles described to date in literature; (ii) the *norA* sequences from 112 *S. aureus* whole genome sequences retrieved from the GenBank database; (iii) the *norA* sequences from 917 MRSA strains sourced from a London-based study (Auguet et al., 2018) (ENA accession PRJEB11177); (iv) the *norA* sequences of nine MRSA isolates collected in a major Hospital in Lisbon, Portugal, representative of the circulating *norA* alleles in that hospital at the time (Costa et al., 2011, 2016), which were deposited in GenBank.

A detailed list of all the sequences comprised in this study and respective accession numbers can be found in **Supplementary Information S1**. The Lisbon MRSA isolates were previously characterized for their susceptibility toward fluoroquinolones and biocides and presence of mutations in the quinolone-resistance determining region of *glaA/gyrA* genes (Costa et al., 2011, 2013a) – **Supplementary Information S1**. Information on the remaining *S. aureus* strains was gathered from the GenBank database and relevant published papers.

Whenever sequence types (ST) were not provided, *in silico* MLST was performed using the MLST 1.8 (Larsen et al., 2012) and SRST2 (Inouye et al., 2014) softwares. The datasets were used to construct a pan-genome (set of all genes within a given species), and a core genome (set of genes found in all strains of that species) for *S. aureus* (Tettelin et al., 2005; van Tonder et al., 2014).

Sequence Analysis of *norA* and MLST Alleles

De novo assemblies were performed for all London samples using Velvet (Zerbino and Birney, 2008) and VelvetOptimiser (Zerbino, 2010). Resulting contig FASTA files and FASTA files of the *S. aureus* samples obtained from GenBank were annotated using Prokka (Seemann, 2014). The pan-genome of these samples was then constructed with Roary (Page et al., 2015), and the sequences of the *norA* and MLST genes (*arcC*, *aroE*, *glpF*, *gmk*, *pta*, *tpi*, and *yqiL*) isolated using custom R scripts (R Core Team, 2016).

For the set of the nine Portuguese MRSA clinical isolates, *norA* was amplified by PCR using three pairs of primers (**Table 1**). PCR reaction mixtures were prepared in 0.05 mL containing 2.5 U Taq Polymerase (Thermo Scientific, Waltham, MA, United States); 1X Taq buffer (Thermo Scientific); 30 pmol of each primer (Invitrogen, Carlsbad, CA, United States); 0.2 mM dNTPs (GE Healthcare, Chicago, IL, United States); 1.75 mM MgCl₂ (Thermo Scientific). The amplification conditions were the following: initial DNA denaturation step at 95°C for 3 min, followed by 35 cycles of denaturation at 94°C for 1 min, annealing at 52°C [*norA*(a)], 45°C [*norA*(b)] or 50°C [*norA*(c)] for 1 min,

TABLE 1 | Primers used to sequence the *norA* promoter and coding region of *Staphylococcus aureus* clinical strains.

Primer	Sequence (5' – 3')	Amplicon size	Location ^a	Reference
<i>norA_fw(a)</i>	TGTTAAGTCTT GGTCATCTGCA	761	706005–706026	Couto et al., 2008
<i>norA_nv(a)</i>	CCATAATCCA CCAATCCC		706765–706747	This study ^b
<i>norA_fw(b)</i>	TTCACCAAGCC ATCAAAAAG	620	706671–706690	Sierra et al., 2000
<i>norA_nv(b)</i>	CTTGCCTTTCT CCAGCAATA		707290–707271	Couto et al., 2008
<i>norA_fw(c)</i>	GGTCATTATTA TATTCAGTTGTTG	419	707135–707158	Schmitz et al., 1998
<i>norA_nv(c)</i>	GTAAGAAAAAC GATGCTAAT		707553–707534	

^aPosition of the primers in the genome of *S. aureus* DSM20231 (accession no. CP011526.1). ^bThe primer was designed with the aid of the free software Primer3 (<http://primer3.sourceforge.net/>) and tested in silico (<http://insilico.ehu.es/PCR/>).

and extension at 72°C for 1 min, followed by a final extension step at 72°C for 5 min. The PCR products were sequenced using the same set of primers and the sequences analyzed and assembled to make up the entire fragment using the software MAFFT v. 6¹ and BioEdit v. 7.0.9.0².

The *norA* and MLST gene sequences from all four datasets were aligned using custom R scripts. Samples that shared identical *norA* and MLST sequences were grouped together and representative sequences used for phylogenetic reconstruction. Maximum-likelihood (ML) tree construction was performed on the aligned *norA* and concatenated MLST gene sequences separately using RAXML (Stamatakis, 2014) with a GTRGAMMA evolutionary model. The resulting phylogenetic trees were displayed and annotated using FigTree³.

Analysis of the Impact of *norA* Variability on NorA Activity

The tridimensional structure of the NorA efflux pump was predicted via the *in silico* platform PHYRE2 (Protein Homology/analogY Recognition Engine v2.0⁴) (Kelley et al., 2015) based on the nucleotide sequences of the three *norA* variants described in literature. A mutational analysis based on the predicted tridimensional structure was conducted with the Phyre2 Investigator tools, using the SuSPect algorithm (Yates et al., 2014). This algorithm produces a table of scores from 0 to 100 according to predicted deleteriousness (0 = neutral to 100 = deleterious). A score of 50 is recommended as a cut-off between neutral and deleterious variants, with extreme scores being more confident predictions (Yates et al., 2014). In this work, a score of ≥ 75 was used as cut-off value.

¹mafft.cbrc.jp/alignment/software/

²<https://bioedit.software.informer.com/>

³<http://tree.bio.ed.ac.uk/software/figtree/>

⁴<http://www.sbg.bio.ic.ac.uk/phyre2>

RESULTS AND DISCUSSION

norA Is Part of the Core Genome of *S. aureus*

Our study sought to establish if *norA* is part of the core genome of *S. aureus*. This is a relevant question since a significant part of the studies on efflux-mediated resistance in this pathogen focus mainly on the activity of NorA and some studies have reported the absence of the *norA* gene in several *S. aureus* strains (Monecke and Enricht, 2005; Vali et al., 2008; Conceição et al., 2015; Hasanvand et al., 2015; Liu et al., 2015; Ammar et al., 2016; Taheri et al., 2016; Antiabong et al., 2017; Hassanzadeh et al., 2017; Hadadi et al., 2018; Kernberger-Fischer et al., 2018). This reported absence could be explained by the genetic diversity

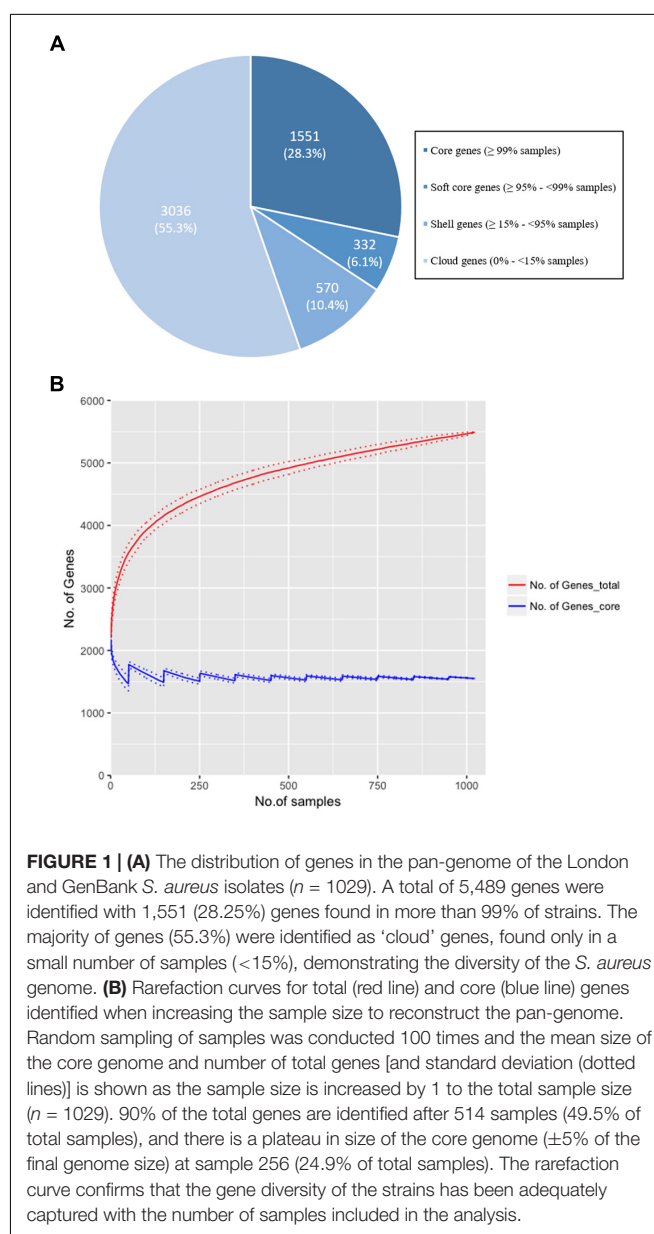


FIGURE 1 | (A) The distribution of genes in the pan-genome of the London and GenBank *S. aureus* isolates ($n = 1029$). A total of 5,489 genes were identified with 1,551 (28.25%) genes found in more than 99% of strains. The majority of genes (55.3%) were identified as 'cloud' genes, found only in a small number of samples ($<15\%$), demonstrating the diversity of the *S. aureus* genome. **(B)** Rarefaction curves for total (red line) and core (blue line) genes identified when increasing the sample size to reconstruct the pan-genome. Random sampling of samples was conducted 100 times and the mean size of the core genome and number of total genes [and standard deviation (dotted lines)] is shown as the sample size is increased by 1 to the total sample size ($n = 1029$). 90% of the total genes are identified after 514 samples (49.5% of total samples), and there is a plateau in size of the core genome ($\pm 5\%$ of the final genome size) at sample 256 (24.9% of total samples). The rarefaction curve confirms that the gene diversity of the strains has been adequately captured with the number of samples included in the analysis.

of the gene and a consequent primer failure during *norA* PCR screening. To test if *norA* is part of the core genome of *S. aureus*, we constructed the pan-genome from the 1029 *S. aureus* isolates whole genome sequence datasets (112 GenBank; 917 London *S. aureus* isolates). The core genome of *S. aureus* consists of 1551 genes (found in $\geq 99\%$ of individuals with 95% BLAST identity; **Figure 1A**) with the genome of each individual isolate containing a median of 2196 genes (with a range of 1955 to 2469), marginally lower than the number of genes found in *S. aureus* reference strains (Li et al., 2011). Rarefaction curves were calculated and determined that the number of samples used was adequate to accurately reconstruct the pan-genome of the population; 90% of the total gene diversity was present when considering just 49.5% (514/1029) of the samples and there was a stabilization of the core genome size after 24.9% (256/1029) of the total samples (**Figure 1B**). The *norA* gene was found to be present in all London and GenBank samples and thus is part of the core genome, with each sample containing a single gene variant. Additionally, we performed a Blastn search using as query the nucleotide sequence of the *norAI* allele (GenBank accession no. D90119.1) against all *S. aureus* genome sequences (complete, scaffold or contig

formats) deposited in GenBank⁵, corresponding to more than 8,000 (circa 8,150) sequences. All the Blastn searched sequences retrieved hits with $\geq 90\%$ identity to *norAI* allele. This result supports the notion that *norA* is a *S. aureus* core gene, occurring in all *S. aureus* genomes. The finding that *norA* is part of *S. aureus* core genome and thus is present in all *S. aureus* strains, implies that reporting the detection of this gene is not sufficient to make a direct association with a particular resistance phenotype. To make such a correlation, one must carry out expression analysis of the *norA* gene as well as of other efflux pump genes, as it has been shown that *S. aureus* strains can display different efflux pump gene expression patterns (DeMarco et al., 2007; Kosmidis et al., 2010, 2012), even under pressure of the same antimicrobial (Huet et al., 2008; Costa et al., 2011, 2015).

Genetic Diversity of the *norA* Gene

One of the goals of this study was to determine the distribution of the *norA* variants amongst the several *S. aureus* clonal lineages. A phylogenetic analysis was performed with the three

⁵www.ncbi.nlm.nih.gov/genome/genomes/154

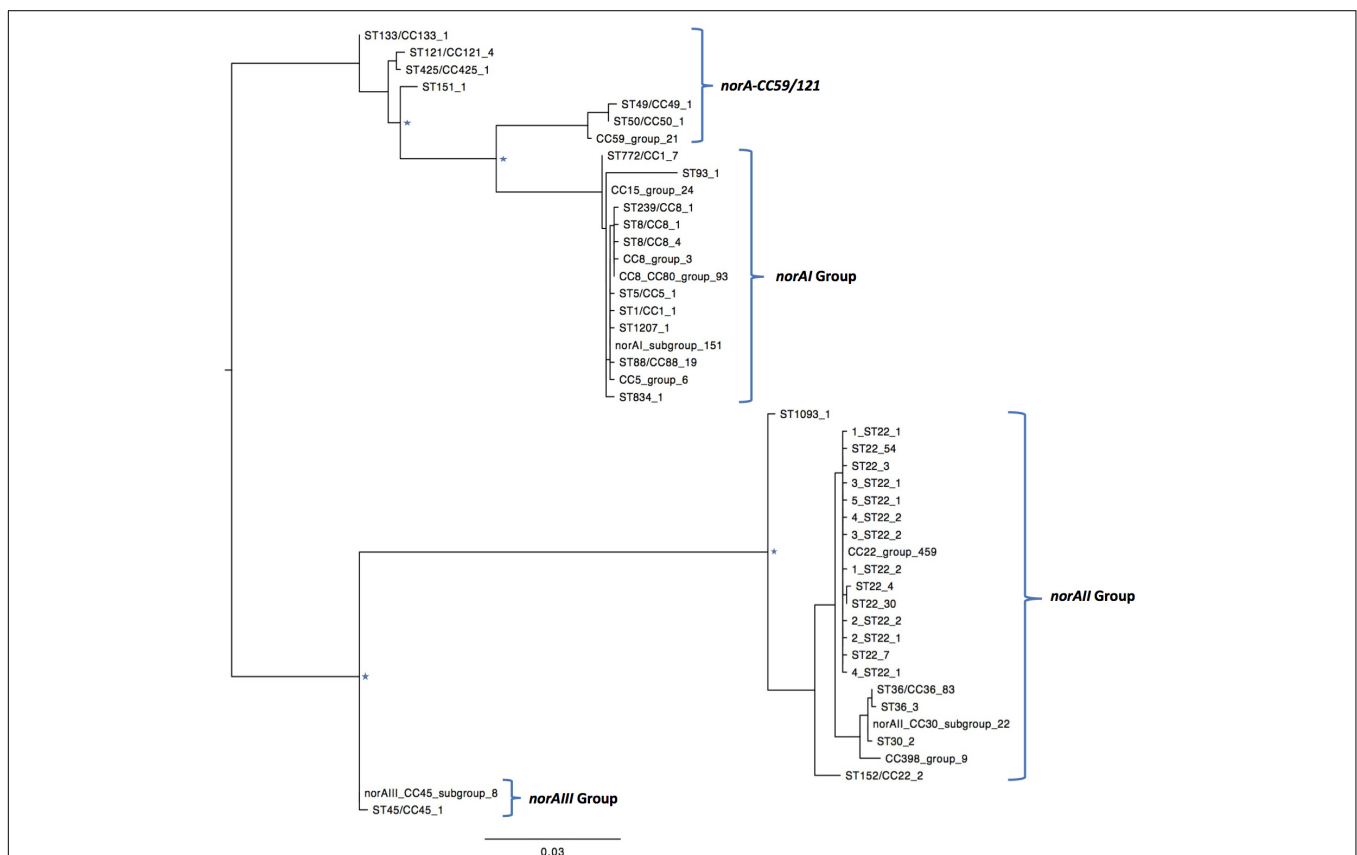


FIGURE 2 | Maximum likelihood phylogeny of the *norA* sequences analyzed in this study. Identical *norA* sequences among all samples used in this study have been collapsed and represented by a single label, which denotes a representative ST/CC of that group. The number of sequences is denoted by the last number of the tip label. Four major groups are found, clustering with the *norA* alleles described in literature, *norAI* (D90119.1), *norAII* (AB019536.1), *norAIII* (M97169.1), and the allelic variant *norA*-CC59/121. The *norAI* associated group is the most diverse, including samples belonging to CC1, CC5, CC8, CC15, CC80, and a wide range of sequence types. The *norAII* associated group contains samples belonging to clonal complexes CC22, CC30, CC36, and CC398. Major nodes supported with bootstrap values above 75% are denoted with a star.

norA alleles and *norA* nucleotide sequences retrieved from complete *S. aureus* genomes available in GenBank and from the Portuguese and London-based *S. aureus* collections (Figure 2). As expected, a certain degree of genetic variability was revealed by the maximum-likelihood tree obtained, despite this gene being relatively conserved. Figure 3 shows the distribution of the pairwise genetic distance within *norA* across the samples used to construct the phylogenetic tree, with a maximum of 143 SNP differences between samples (12.3% of the total gene length of 1164 bp).

A global analysis showed a clear correlation between occurrence of *norA* alleles and specific *S. aureus* clonal lineages. The *norAI* allele was mainly associated with genetic backgrounds of the clonal complexes CC1, CC5, CC8, and CC80 or closely related lineages. On the other hand, *norAII* and close variants appear to be restricted to strains belonging to CC30, CC398, and CC22 (Figure 2). The *norAIII* allele is only associated with the *S. aureus* lineage CC45 and novel but related STs.

Among the sequences retrieved from GenBank, the *norAI* allele is the most frequent (76 out of 112 strains) and the *norAII* allele the second most frequent allele (21 out of 112 strains), whereas *norAIII* occurs in just two CC45 strains. We also detected 13 more divergent variants, most closely related to the *norAI* allele, that were associated with other lineages, such as CC59 and CC121 (Figures 2, 3). Although these findings may be biased as the dataset analyzed reflects the current epidemiologically *S. aureus* relevant clones, with a frequency of ~70% MRSA strains (78 out of 112 genomes), it clearly shows that *norAI* and related variants are the most prevalent alleles

across lineages, as suggested by earlier studies (Schmitz et al., 1998; Sierra et al., 2000; Noguchi et al., 2004). Interestingly, a sample isolated in Brazil in 2010 (FCFHV36) carried a *norAI* type variant of the *norA* gene that included a frameshift mutation in codon 129. This mutation caused a premature stop codon at codon number 147, resulting in potential pseudogenization of *norA* in this isolate.

Regarding the London isolates, we found the *norAII* allele to be the most common allele, identified in 671/917 samples, due to the high number of CC22 strains in the study samples (539/917). As with the GenBank samples, the *norAIII* allele was the least common variant found in the London isolates, with only the three CC45 and four novel ST strains carrying closely related variants. The *norAI* allele was found in 220/917 strains consisting of the broadest range of lineages, comprising 21 different STs. Additionally, one ST22 sample possessed a *norA* variant with a frameshift mutation at codon 365 that results in a premature stop codon at codon number 367 and, again, possible pseudogenization.

Nine MRSA isolates, representative of a collection of 53 *S. aureus* clinical isolates isolated at a major Portuguese Hospital and previously characterized for efflux activity and clonal lineage (Costa et al., 2011, 2013a, 2015, 2016) were added to the study to ascertain their *norA* allele. The full sequence of the *norA* gene was determined for these isolates and compared with *norA* alleles from major clonal lineages (Figure 4). Both the *norAI* and *norAII* alleles were found amongst the Portuguese isolates and their distribution reflects the findings for the other datasets analyzed. Eight isolates from

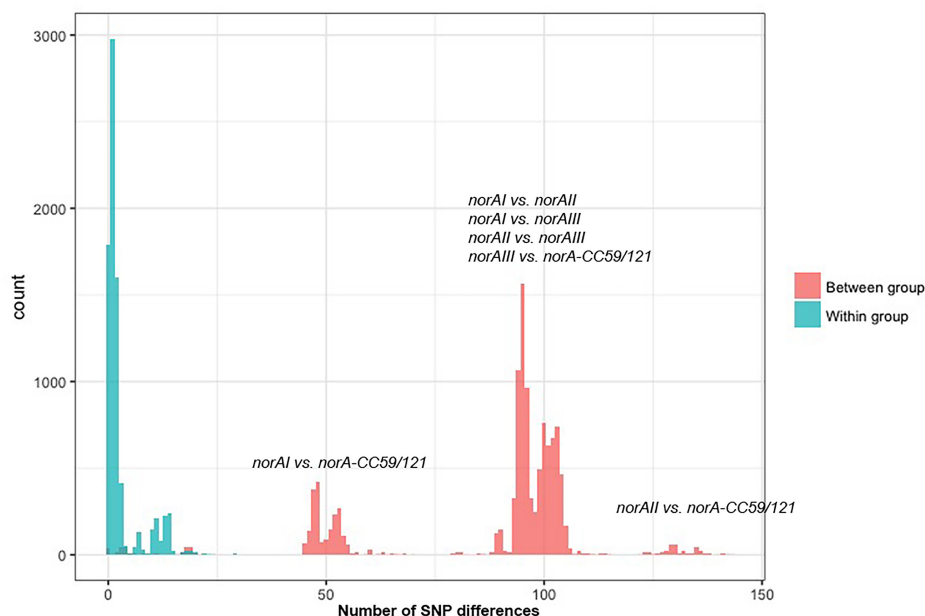


FIGURE 3 | Distribution of the pairwise SNP distance within *norA* sequences used in this study. The *norA* sequences include *norAI* (D90119.1), *norAII* (AB019536.1) and *norAIII* (M97169.1), the nine Portuguese isolates, 112 complete assemblies from GenBank, and 75 representative sequences of London isolates. The figure is annotated to show the pairwise SNP distance between isolates both within (blue) and between (red) each of the four major *norA* groups described in the main text: *norAI* group, *norAII* group, *norAIII* group, and CC121/CC59 group.

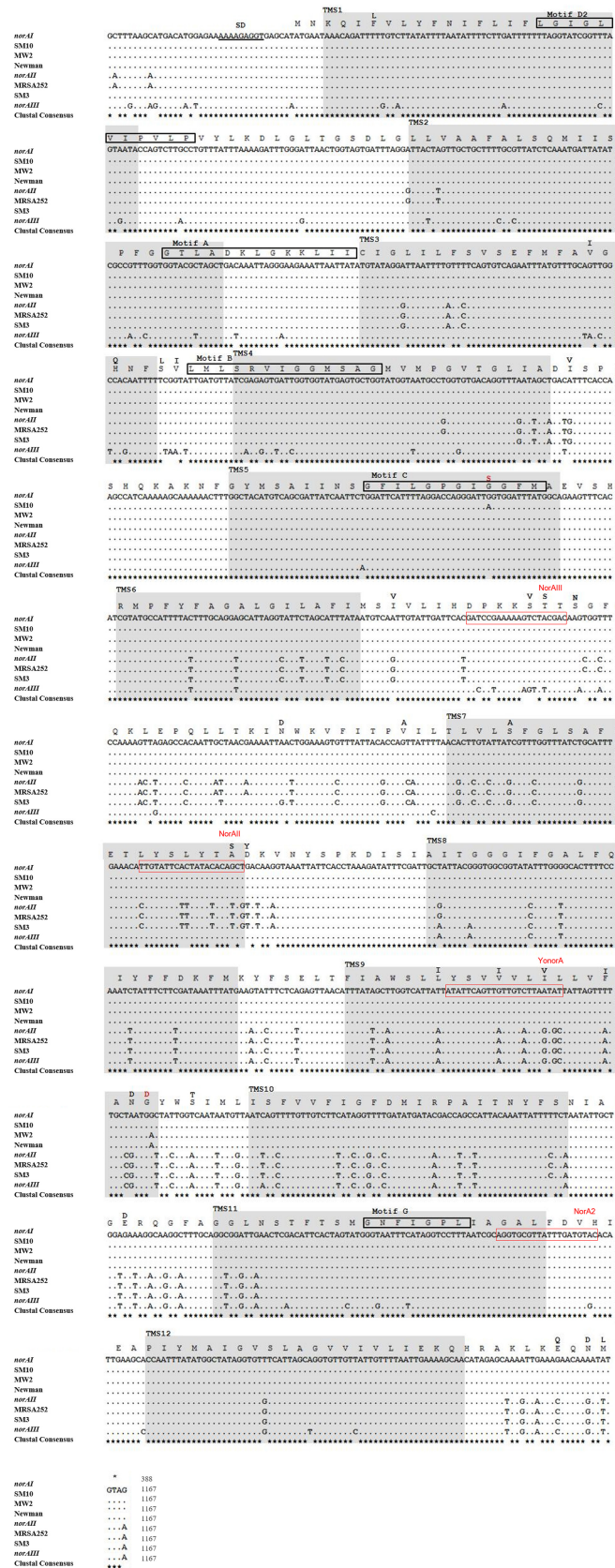


FIGURE 4 | Continued

FIGURE 4 | Multiple alignment of *norA* sequences of the three *norA* alleles, from selected Portuguese MRSA clinical isolates (SM) and from strains of representative clonal lineages. The MRSA strains displayed were selected to represent the main clones found, namely SM10 – CC5; SM3 – CC22; MW2 – CC1; Newman – CC8; MRSA252 – CC30. The Shine-Dalgarno (SD) sequence is underlined in black. The shaded regions correspond to the putative TMS of NorA as suggested by Paulsen et al. (1996). The amino acid regions inside the boxes are relative to the conserved motifs described for MFS transporters with 12 TMS. The black residues shown above the main polypeptide sequence represent the variations present in the various NorA polypeptide sequences relatively to the NorAI variant. The red residues represent alterations found among the SM collection of Portuguese MRSA clinical isolates. The red boxes indicate the primers described in **Table 2** for distinction of *norA* alleles.

clonal lineages CC5, CC8, and CC88 carried *norAI* and a single isolate from clonal lineage CC22 harboured the *norAII* allele (**Figure 4**). Combining information on *norA* allele, clonal lineage and previous characterization of these isolates (Costa et al., 2011) showed no correlation between *norA* allele, *norA* expression levels, efflux capacity, or antimicrobial resistance levels (**Supplementary Information S1**).

A wet lab PCR-based strategic approach is proposed for detection and differentiation of the several *norA* alleles occurring in *S. aureus*. The *norAI* and *norAII* alleles can be easily distinguished using two sets of specific primers (**Table 2** and **Figure 4**). To amplify and differentiate *norAIII* from the *norA* allele associated with CC59/CC121, an approach consisting in PCR amplification followed by restriction of the PCR product with HindIII can be applied (**Table 2** and **Figure 4**).

Impact of Genetic Variability on NorA Function

A mutational analysis was performed *in silico* via the PHYRE2 platform to construct a NorA structural model, using the SuSPect algorithm to predict the effect of each residue substitution on

NorA function. This analysis is limited because of the lack of available structural data for bacterial MFS pumps, mostly limited to substrate-specific transporters. Nevertheless, the polypeptide sequences encoded by the three *norAI* alleles were used to predict a tri-dimensional structure of NorA. All three NorA variants showed the highest identity with the putative MFS transporter YajR of *Escherichia coli* (Jiang et al., 2013). A second NorA *in silico* model, based on the structure of glycerol-3-phosphate MFS transporter from *E. coli*, described by Bhaskar et al. (2016) was taken into account for comparison purposes. The SuSPect-derived mutational analysis revealed 42 residues for which particular mutations could potentially impair NorA activity (**Supplementary Information S2**). Of these, residues Pro110, Pro158, Pro311, and Gly326 were particularly susceptible to mutations.

Analysis of the polypeptide sequence corresponding to the three *norA* variants revealed a total of 43 amino acid alterations. **Figure 5** summarizes these alterations, their location in NorA and their distribution amongst *S. aureus* lineages. There was no overlap between these alterations and the residues identified by SuSPect. We also compared the *S. aureus* NorAI variant with the NorA efflux pump encoded in the *Staphylococcus epidermidis* ATCC 12228 chromosome, which presents the same substrate profile (Costa et al., 2018; **Supplementary Information S2**). The differences encountered between the two polypeptide sequences correspond to residues that were not highlighted as pivotal for the protein activity by SuSPect. These results suggest conservation of NorA function in these two main staphylococcal species.

One alteration, Gly147Ser located within putative TMS 5, may affect NorA function (**Figure 4**). This alteration was detected in all four strains belonging to ST105 (three of which are of Portuguese origin) and in one of the strains belonging to ST225 (Portuguese origin) (**Supplementary Information S2**), but was absent from strains from other CC5 lineages, such as ST5. Residue 147 is predicted to be located within the conserved motif C (gxxxGPxiGGxl) (Paulsen et al., 1996) on the TMS 5, facing a water-filled channel. This motif is conserved among MFS drug-H⁺ antiporters and has been implicated in the binding of the substrate, with the glycines being essential for that function (Ginn et al., 2000; Tamura et al., 2001). In fact, in a mutagenesis study in *S. aureus* efflux pump TetA(K), also a 12-TMS member of the MFS family, the mutation Gly147Ser was responsible for the loss of 80% of the activity of that efflux pump (Ginn et al., 2000). Although Tet transporters and NorA are distinct in their substrate specificity, these pumps share abundance of glycines in TMS 5, a trait that has been postulated to confer conformational plasticity to EPs (Ginn et al., 2000). Thus, the

TABLE 2 | List of primers proposed to amplify and differentiate the *norA* alleles by conventional PCR.

Primer	Sequence (5' – 3')	Amplified <i>norA</i> allele	Amplicon size (nt)	Reference
<i>norA_fw(b)</i>	TTCACCAAGC CATCAAAAAG	all	704	Sierra et al., 2000
NorA2	GCACATCAAA TAACGCACCT			
YonorA	ATATTGAGTTGT TGTCTTAATAT	<i>norAI</i>	230	Sierra et al., 2000
NorA2	GCACATCAAA TAACGCACCT			
NorAII	CTGTATTCTTT ATATACATCG	<i>norAII</i>	391	This study ^a
NorA2	GCACATCAAA AAGGCACCT			Sierra et al., 2000
NorAIII	GACCCTAAAA AAGTTTCGAC	<i>norAIII</i>	526	This study ^a
NorA2	GCACATCAATA ACGCACCT	<i>norA</i> - CC59/CC121 Plus HindIII restriction: <i>norAIII</i> : 166 nt + 360 nt; <i>norA</i> -CC59/121: no cut (526 nt)		Sierra et al., 2000

^aThe primers were designed with the aid of the free software Primer3 (<http://primer3.sourceforge.net/>). The primers and the HindIII restriction were tested *in silico* (<http://insilico.ehu.es/>) against several *S. aureus* genome sequences of representative clonal lineages.

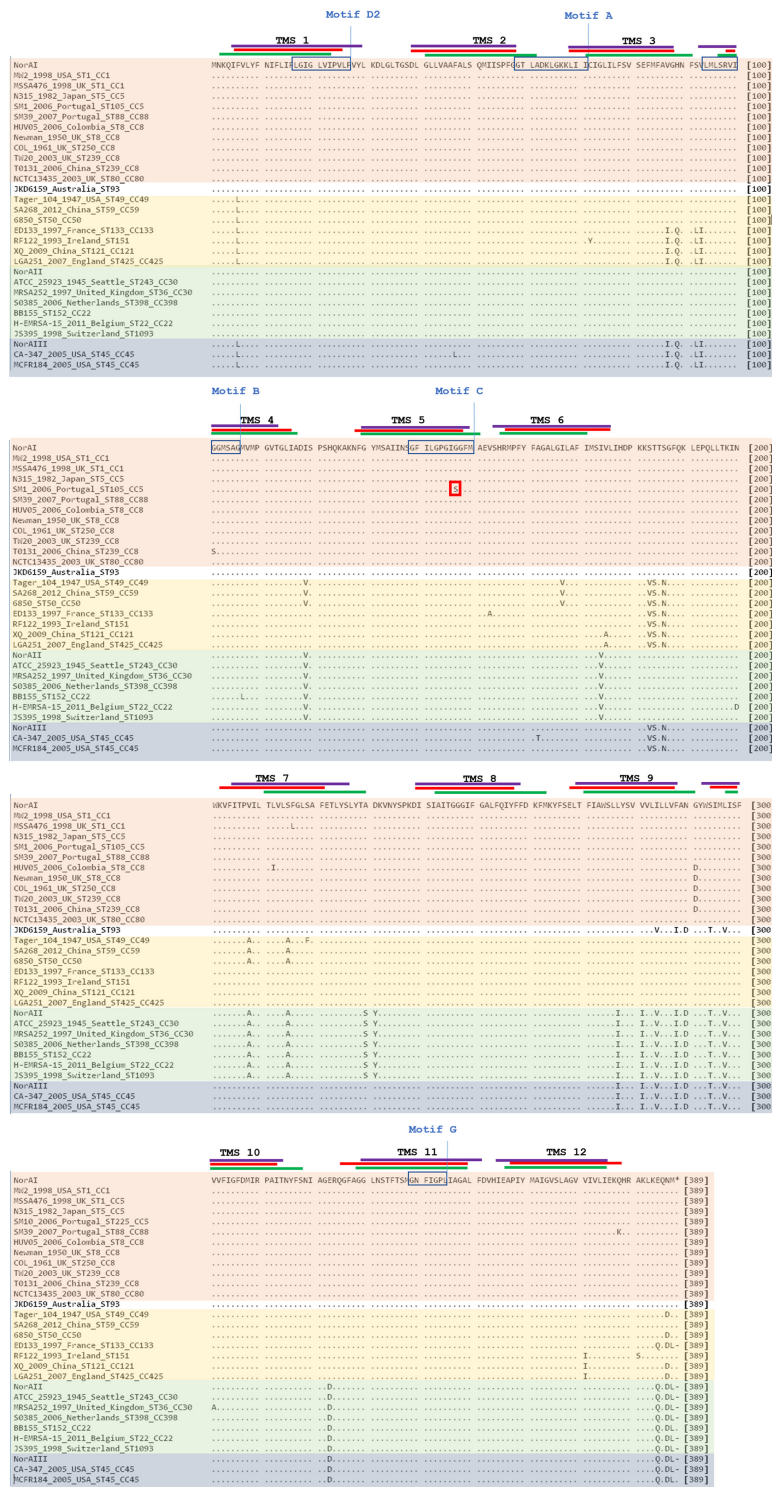


FIGURE 5 | Multiple alignment of *NorA* polypeptide sequences derived from alleles *norAI* (Yoshida et al., 1990), *norAll* (Noguchi et al., 2004), and *norAllI* (Kaatz et al., 1993) and from the *norA* alleles from selected *S. aureus* strains. The MRSA strains displayed were selected to represent the main *S. aureus* clonal lineages found for the strains with genomes publicly available and for the Portuguese strains (SM10 – CC5; SM39 – CC88). Sequences are grouped according to the respective *norA* allele (orange – *norAI*; green – *norAll*; blue – *norAllI*; yellow – *norA-CC59/121*). The lines correspond to the transmembrane segments (TMS) of *NorA*, as predicted by Paulsen et al. (1996) (green), by the HMMTOP method as presented in Bhaskar et al. (2016) (red) and as predicted by the Phyre2-based *NorA* model (purple). The amino acid regions inside the boxes are relative to the conserved motifs described for MFS transporters with 12 TMS (Paulsen et al., 1996). The red box corresponds to the amino acid substitution likely to affect *NorA* function.

mutation Gly147Ser may have a deleterious effect on NorA activity. Additional studies are necessary to fully ascertain the impact of this alteration in the efflux capacity of NorA. The same applies to the full understanding of possible correlations between a given *norA* allele and corresponding NorA efflux capacity, probably requiring carefully controlled genetic systems because of overlapping substrates between many staphylococcal multidrug efflux systems and the redundancy in their response to antimicrobials (Costa et al., 2013b; Schindler and Kaatz, 2016).

CONCLUSION

In this study we provide evidence that the efflux pump gene *norA* is part of core genome of *S. aureus*. This gene presents some genetic variability which may impair its detection by conventional laboratorial techniques, such as PCR, due to potential primer mismatch. Strikingly, a correlation was observed between the several *norA* alleles and specific *S. aureus* lineages, suggesting that the occurrence of *norA* variants reflects the population structure of this major pathogen.

DATA AVAILABILITY

The sequences analyzed in this study are available in GenBank and their accession numbers detailed in **Supplementary Information S1**, except for WGS data for the London-based strains that are available from the European Nucleotide Archive database under accession number PRJEB11177.

AUTHOR CONTRIBUTIONS

IC, SC, and TC conceived and designed the study. SC performed the wet lab *norA* analysis and the *in silico* mutational analysis. BS

conducted the pan-genome analysis. SC and BS performed the phylogenetic analysis. JE provided genomic data on the London-based MRSA strains. RP, JE, MV, TC, and IC contributed to the analysis of these data. SC, BS, TC, and IC wrote the first draft of the manuscript. All authors have reviewed the final version of the manuscript.

FUNDING

This work was partially supported by Fundação para a Ciência e a Tecnologia (FCT, Portugal), through funds to GHTM – UID/Multi/04413/2013. SC was supported by grant SFRH/BPD/97508/2013 from FCT, Portugal. TC was funded by the Medical Research Council United Kingdom (Grant Nos. MR/K000551/1, MR/M01360X/1, MR/N010469/1, and MR/R020973/1) and BBSRC United Kingdom (BB/R013063/1). BS was funded by the Medical Research Council United Kingdom (Grant No. MR/N010469/1).

ACKNOWLEDGMENTS

The MRC eMedLab computing resource was used for bioinformatics and statistical analysis. The authors deeply acknowledge Professor José Melo-Cristino for providing the Portuguese *S. aureus* strains analyzed in this study.

SUPPLEMENTARY MATERIAL

The Supplementary Material for this article can be found online at: <https://www.frontiersin.org/articles/10.3389/fgene.2018.00710/full#supplementary-material>

REFERENCES

- Ammar, A. M., Attia, A. M., Abd El-Hamid, M. I., El-Shorbagy, I. M., and Abd El-Kader, S. A. (2016). Genetic basis of resistance waves among methicillin resistant *Staphylococcus aureus* isolates recovered from milk and meat products in Egypt. *Cell Mol. Biol.* 62, 7–15.
- Antibong, J. F., Kock, M. M., Bellea, N. M., and Ehlers, M. M. (2017). Diversity of multidrug efflux genes and phenotypic evaluation of the *in vitro* resistance dynamics of clinical *Staphylococcus aureus* isolates using methicillin; a model β -lactam. *Open Microbiol. J.* 11, 132–141. doi: 10.2174/1874285801711010132
- Auguet, O. T., Stabler, R. A., Betley, J., Preston, M. D., Dhaliwal, M., Gaunt, M., et al. (2018). Frequent undetected MRSA ward-based transmission linked to patient sharing between hospitals. *Clin. Infect. Dis.* 66, 840–848. doi: 10.1093/cid/cix901
- Bhaskar, B. V., Babu, T. M., Reddy, N. V., and Rajendra, W. (2016). Homology modeling, molecular dynamics, and virtual screening of NorA efflux pump inhibitors of *Staphylococcus aureus*. *Drug Des. Dev. Ther.* 10, 3237–3252. doi: 10.2147/DDDT.S113556
- Brooks, L. E., Ul-Hasan, S., Chan, B. K., and Siström, M. J. (2018). Quantifying the evolutionary conservation of genes encoding multidrug efflux pumps in the ESKAPE pathogens to identify antimicrobial drug targets. *mSystems* 3:e00024-18. doi: 10.1128/mSystems.00024-18
- Chambers, H. F., and DeLeo, F. R. (2009). Waves of resistance: *Staphylococcus aureus* in the antibiotic era. *Nat. Rev. Microbiol.* 7, 629–641. doi: 10.1038/nrmicro2200
- Conceição, T., Coelho, C., de Lencastre, H., and Aires-de-Sousa, M. (2015). High prevalence of biocide resistance determinants in *Staphylococcus aureus* isolates from three african countries. *Antimicrob. Agents Chemother.* 60, 678–681. doi: 10.1128/AAC.02140-15
- Costa, S. S., Falcão, C., Viveiros, M., Machado, D., Martins, M., Melo-Cristino, J., et al. (2011). Exploring the contribution of efflux on the resistance to fluoroquinolones in clinical isolates of *Staphylococcus aureus*. *BMC Microbiol.* 11:e241. doi: 10.1186/1471-2180-11-241
- Costa, S. S., Palma, C., Kadlec, K., Fessler, A. T., Viveiros, M., Melo-Cristino, J., et al. (2016). Plasmid-borne antimicrobial resistance of *Staphylococcus aureus* isolated in a Hospital in Lisbon, Portugal. *Microb. Drug Resist.* 22, 617–626. doi: 10.1089/mdr.2015.0352
- Costa, S. S., Junqueira, E., Palma, C., Viveiros, M., Melo-Cristino, J., Amaral, L., et al. (2013a). Resistance to antimicrobials mediated by efflux pumps in *Staphylococcus aureus*. *Antibiotics* 2, 83–99. doi: 10.3390/antibiotics2010083
- Costa, S. S., Viveiros, M., Amaral, L., and Couto, I. (2013b). Multidrug efflux pumps in *Staphylococcus aureus*: an update. *Open Microbiol. J.* 7, 59–71. doi: 10.2174/1874285801307010059
- Costa, S. S., Viveiros, M., Pomba, C., and Couto, I. (2018). Active antimicrobial efflux in *Staphylococcus epidermidis*: building up of resistance to

- fluoroquinolones and biocides in a major opportunistic pathogen. *J. Antimicrob. Chemother.* 73, 320–324. doi: 10.1093/jac/dkx400
- Costa, S. S., Viveiros, M., Rosato, A. E., Melo-Cristino, J., and Couto, I. (2015). Impact of efflux in the development of multidrug resistance phenotypes in *Staphylococcus aureus*. *BMC Microbiol.* 15:232. doi: 10.1186/s12866-015-0572-578
- Couto, I., Costa, S. S., Viveiros, M., Martins, M., and Amaral, L. (2008). Efflux-mediated response of *Staphylococcus aureus* exposed to ethidium bromide. *J. Antimicrob. Chemother.* 62, 504–513. doi: 10.1093/jac/dkn217
- DeMarco, C. E., Cushing, L. A., Frempong-Manso, E., Seo, S. M., Jaravaza, T. A. A., and Kaatz, G. W. (2007). Efflux-related resistance to norfloxacin, dyes, and biocides in bloodstream isolates of *Staphylococcus aureus*. *Antimicrob. Agents Chemother.* 51, 3235–3239. doi: 10.1128/AAC.00430-07
- Deng, X., Ji, Q., Liang, H., Missiakas, D., Lan, L., and He, C. (2012). Expression of multidrug resistance efflux pump gene *norA* is iron responsive in *Staphylococcus aureus*. *J. Bacteriol.* 194, 1753–1762. doi: 10.1128/JB.06582-11
- Furi, L., Ciusa, M. L., Knight, S., Di Lorenzo, V., Tocci, N., Cirasola, D., et al. (2013). Evaluation of reduced susceptibility to quaternary ammonium compounds and bisguanidines in clinical isolates and laboratory-generated mutants of *Staphylococcus aureus*. *Antimicrob. Agents Chemother.* 57, 3488–3497. doi: 10.1128/AAC.00498-13
- Ginn, S. L., Brown, M. H., and Skurray, R. A. (2000). The TetA(K) tetracycline/H⁺ antiporter from *Staphylococcus aureus*: mutagenesis and functional analysis of motif C. *J. Bacteriol.* 182, 1492–1498. doi: 10.1128/JB.182.6.1492-1498.2000
- Hadadi, M., Heidari, H., Ebrahim-Saraie, H. S., and Motamedifar, M. (2018). Molecular characterization of vancomycin, mupirocin and antiseptic resistant *Staphylococcus aureus* strains. *Mediterr. J. Hematol. Infect. Dis.* 10:e2018053. doi: 10.4084/MJHID.2018.053
- Hasanvand, A., Ghafourian, S., Taherikalani, M., Jalilian, F. A., Sadeghifard, N., and Pakzad, I. (2015). Antiseptic resistance in methicillin sensitive and methicillin resistant *Staphylococcus aureus* isolates from some major hospitals, Iran. *Recent Pat. Antiinfect. Drug Discov.* 10, 105–112. doi: 10.2174/1574891X10666150623093259
- Hassanzadeh, S., Mashhadi, R., Yousefi, M., Askari, E., Saniei, M., and Pourmand, M. R. (2017). Frequency of efflux pump genes mediating ciprofloxacin and antiseptic resistance in methicillin-resistant *Staphylococcus aureus* isolates. *Microb. Pathog.* 111, 71–74. doi: 10.1016/j.micpath.2017.08.026
- Huet, A. A., Raygada, J. L., Mendiratta, K., Seo, S. M., and Kaatz, G. W. (2008). Multidrug efflux pump overexpression in *Staphylococcus aureus* after single and multiple in vitro exposures to biocides and dyes. *Microbiology* 154, 3144–3153. doi: 10.1099/mic.0.2008/021188-0
- Inouye, M., Dashnow, H., Raven, L.-A., Schultz, M. B., Pope, B. J., Tomita, T., et al. (2014). SRST2: rapid genomic surveillance for public health and hospital microbiology labs. *Genome Med.* 6:90. doi: 10.1186/s13073-014-0090-6
- Jiang, D., Zhao, Y., Wang, X., Fan, J., Heng, J., Liu, X., et al. (2013). Structure of the YajR transporter suggests a transport mechanism based on the conserved motif A. *Proc. Natl. Acad. Sci. U.S.A.* 110, 14664–14669. doi: 10.1073/pnas.1308127110
- Kaatz, G. W., Seo, S. M., and Ruble, C. A. (1993). Efflux-mediated fluoroquinolone resistance in *Staphylococcus aureus*. *Antimicrob. Agents Chemother.* 37, 1086–1094. doi: 10.1128/AAC.37.5.1086
- Kelley, L. A., Mezulis, S., Yates, C. M., Wass, M. N., and Sternberg, M. J. (2015). The Phyre2 web portal for protein modeling, prediction and analysis. *Nat. Protoc.* 10, 845–858. doi: 10.1038/nprot.2015.053
- Kernberger-Fischer, I. A., Krischek, C., Strommenger, B., Fiegen, U., Beyerbach, M., Kreienbrock, L., et al. (2018). Susceptibility of methicillin-resistant and -susceptible *Staphylococcus aureus* isolates of various clonal lineages from Germany to eight biocides. *Appl. Environ. Microbiol.* 84, e799–e718. doi: 10.1128/AEM.00799-18
- Kosmidis, C., DeMarco, C. E., Frempong-Manso, E., Seo, S. M., and Kaatz, G. W. (2010). In silico genetic correlations of multidrug efflux pump gene expression in *Staphylococcus aureus*. *Int. J. Antimicrob. Agents* 36, 222–229. doi: 10.1016/j.ijantimicag.2010.05.015
- Kosmidis, C., Schindler, B. D., Jacinto, P. L., Patel, D., Bains, K., Seo, S. M., et al. (2012). Expression of multidrug resistance efflux pump genes in clinical and environmental isolates of *Staphylococcus aureus*. *Int. J. Antimicrob. Agents* 40, 204–209. doi: 10.1016/j.ijantimicag.2012.04.014
- Kwak, Y. G., Truong-Bolduc, Q. C., Kim, H. B., Song, K. H., Kim, E. S., and Hooper, D. C. (2013). Association of *norB* overexpression and fluoroquinolone resistance in clinical isolates of *Staphylococcus aureus* from Korea. *J. Antimicrob. Chemother.* 68, 2766–2772. doi: 10.1093/jac/dkt286
- Larsen, M. V., Cosentino, S., Rasmussen, S., Friis, C., Hasman, H., Marvig, R. L., et al. (2012). Multilocus sequence typing of total genome sequenced bacteria. *J. Clin. Microbiol.* 50, 1355–1361. doi: 10.1128/JCM.06094-11
- Lee, A. S., de Lencastre, H., Garau, J., Kluytmans, J., Malhotra-Kumar, S., Peschel, A., et al. (2018). Methicillin-resistant *Staphylococcus aureus*. *Nat. Rev. Dis. Primers* 4:18033. doi: 10.1038/nrdp.2018.33
- Li, Y., Cao, B., Zhang, Y., Zhgou, J., Yang, B., and Wang, L. (2011). Complete genome sequence of *Staphylococcus aureus* T0131, an ST239-MRSA-SCCmec type III clone isolated in China. *J. Bacteriol.* 193, 3411–3412. doi: 10.1128/JB.05135-11
- Liu, Q., Zhao, H., Han, L., Shu, W., Wu, Q., and Ni, Y. (2015). Frequency of biocide-resistant genes and susceptibility to chlorhexidine in high-level mupirocin-resistant, methicillin-resistant *Staphylococcus aureus* (MuH MRSA). *Diagn. Microbiol. Infect. Dis.* 82, 278–283. doi: 10.1016/j.diagmicrobio.2015.03.023
- Marchi, E., Furi, L., Arioli, S., Morrissey, I., Di Lorenzo, V., Mora, D., et al. (2015). Novel insight into antimicrobial resistance and sensitivity phenotypes associated to *qac* and *norA* genotypes in *Staphylococcus aureus*. *Microbiol. Res.* 170, 184–194. doi: 10.1016/j.micres.2014.07.001
- Monecke, S., and Enricht, R. (2005). Rapid genotyping of methicillin-resistant *Staphylococcus aureus* (MRSA) isolates using miniaturized oligonucleotide arrays. *Clin. Microbiol. Infect.* 11, 825–833. doi: 10.1111/j.1469-0691.2005.01243.x
- Neyfakh, A. A., Borsch, C. M., and Kaatz, G. W. (1993). Fluoroquinolone resistance protein NorA of *Staphylococcus aureus* is a multidrug efflux transporter. *Antimicrob. Agents Chemother.* 37, 128–129. doi: 10.1128/AAC.37.1.128
- Noguchi, N., Okada, H., Narui, K., and Sasatsu, M. (2004). Comparison of the nucleotide sequence and expression of *norA* genes and microbial susceptibility in 21 strains of *Staphylococcus aureus*. *Microb. Drug Resist.* 10, 197–203. doi: 10.1089/mdr.2004.10.197
- Page, A. J., Cummins, C. A., Hunt, M., Wong, V. K., Reuter, S., Holden, M. T. G., et al. (2015). Roary: rapid large-scale prokaryote pan genome analysis. *Bioinformatics* 31, 3691–3693. doi: 10.1093/bioinformatics/btv421
- Paulsen, I. T., Brown, M. H., and Skurray, R. A. (1996). Proton-dependent multidrug efflux systems. *Microbiol. Rev.* 60, 575–608.
- Piddock, L. J. V. (2006). Clinically relevant chromosomally encoded multidrug resistance efflux pumps in bacteria. *Clin. Microbiol. Rev.* 19, 382–402. doi: 10.1128/CMR.19.2.382-402.2006
- Poole, K. (2007). Efflux pumps as antimicrobial resistance mechanisms. *Ann. Med.* 39, 162–176. doi: 10.1080/07853890701195262
- R Core Team (2016). *R: A Language and environment for statistical computing*. Vienna: R Foundation for Statistical Computing.
- Schindler, B. D., Frempong-Manso, E., DeMarco, C. E., Kosmidis, C., Matta, V., Seo, S. M., et al. (2015). Analyses of multidrug efflux pump-like proteins encoded on the *Staphylococcus aureus* chromosome. *Antimicrob. Agents Chemother.* 59, 747–748. doi: 10.1128/AAC.04678-14
- Schindler, B. D., and Kaatz, G. W. (2016). Multidrug efflux pumps of Gram-positive bacteria. *Drug Resist. Updat.* 27, 1–13. doi: 10.1016/j.drup.2016.04.003
- Schmitz, F. J., Hertel, B., Hofmann, B., Scheuring, S., Verhoeve, J., Fluit, A. C., et al. (1998). Relationship between mutations in the coding and promoter regions of the *norA* genes in 42 unrelated clinical isolates of *Staphylococcus aureus* and the MICs of norfloxacin for these strains. *J. Antimicrob. Chemother.* 42, 561–563. doi: 10.1093/jac/42.4.561
- Seemann, T. (2014). Prokka: rapid prokaryotic genome annotation. *Bioinformatics* 30, 2068–2069. doi: 10.1093/bioinformatics/btu153
- Sierra, J. M., Ruiz, J., de Anta, M. T. J., and Vila, J. (2000). Prevalence of two different genes encoding NorA in 23 clinical strains of *Staphylococcus aureus*. *J. Antimicrob. Chemother.* 46, 145–146. doi: 10.1093/jac/46.1.145
- Stamatakis, A. (2014). RAxML version 8: a tool for phylogenetic analysis and post-analysis of large phylogenies. *Bioinformatics* 30, 1312–1313. doi: 10.1093/bioinformatics/btu033
- Tacconelli, E., Carrara, E., Savoldi, A., Harbarth, S., Mendelson, M., Monnet, D. L., et al. (2018). Discovery, research, and development of new antibiotics: the WHO priority list of antibiotic-resistant bacteria and tuberculosis. *Lancet Infect. Dis.* 18, 318–327. doi: 10.1016/S1473-3099(17)30753-3

- Taheri, N., Ardebili, A., Amouzandeh-Nobaveh, A., and Ghaznavi-Rad, E. (2016). Frequency of antiseptic resistance among *Staphylococcus aureus* and coagulase-negative Staphylococci isolated from a university hospital in central Iran. *Oman Med. J.* 31, 426–432. doi: 10.5001/omj.2016.86
- Tamura, N., Konishi, S., Iwaki, S., Kimura-Someya, T., Nada, S., and Yamaguchi, A. (2001). Complete cysteine-scanning mutagenesis and site-directed chemical modification of the Tn10-encoded metal-tetracycline/H⁺ antiporter. *J. Biol. Chem.* 276, 20330–20339. doi: 10.1074/jbc.M007993200
- Tettelin, H., Massignani, V., Cieslewicz, M. J., Donati, C., Medini, D., Ward, N. L., et al. (2005). Genome analysis of multiple pathogenic isolates of *Streptococcus agalactiae*: implications for the microbial “pan-genome”. *Proc. Natl. Acad. Sci. U.S.A.* 102, 13950–13955. doi: 10.1073/pnas.0506758102
- Tong, S. Y. C., Davis, J. S., Eichenberger, E., Holland, T. L., and Fowler, V. G. Jr. (2015). *Staphylococcus aureus* infections: epidemiology, pathophysiology, clinical manifestations, and management. *Clin. Microbiol. Rev.* 28, 603–661. doi: 10.1128/CMR.00134-14
- Ubukata, K., Itoh-Yamashita, N., and Konno, M. (1989). Cloning and expression of the *norA* gene for fluoroquinolone resistance in *Staphylococcus aureus*. *Antimicrob. Agents Chemother.* 33, 1535–1539. doi: 10.1128/AAC.33.9.1535
- Vali, L., Davies, S. E., Lai, L. L. G., Dave, J., and Amyes, S. G. B. (2008). Frequency of biocide resistance genes, antibiotic resistance and the effect of chlorhexidine exposure on clinical methicillin-resistant *Staphylococcus aureus* isolates. *J. Antimicrob. Chemother.* 61, 524–532. doi: 10.1093/jac/dkm520
- van Tonder, A. J., Mistry, S., Bray, J. E., Hill, D. M., Cody, A. J., Farmer, C. L., et al. (2014). Defining the estimated core genome of bacterial populations using a Bayesian decision model. *PLoS Comput. Biol.* 10:e1003788. doi: 10.1371/journal.pcbi.1003788
- Yates, C. M., Filippis, I., Kelley, L. A., and Sternberg, M. J. (2014). SuSPect: enhanced prediction of single amino acid variant (SAV) phenotype using network features. *J. Mol. Biol.* 426, 2692–2701. doi: 10.1016/j.jmb.2014.04.026
- Yoshida, H., Bogaki, M., Nakamura, S., Ubukata, K., and Konno, M. (1990). Nucleotide sequence and characterization of the *Staphylococcus aureus* *norA* gene, which confers resistance to quinolones. *J. Bacteriol.* 172, 6942–6949. doi: 10.1128/jb.172.12.6942-6949.1990
- Zerbino, D. R. (2010). Using the Velvet de novo assembler for short-read sequencing technologies. *Curr. Protoc. Bioinformatics* Chapter 11:Unit 11.5. doi: 10.1002/0471250953.bi1105s31
- Zerbino, D. R., and Birney, E. (2008). Velvet: algorithms for de novo short read assembly using de Bruijn graphs. *Genome Res.* 18, 821–829. doi: 10.1101/gr.074492.107

Conflict of Interest Statement: The authors declare that the research was conducted in the absence of any commercial or financial relationships that could be construed as a potential conflict of interest.

Copyright © 2019 Costa, Sobkowiak, Parreira, Edgeworth, Viveiros, Clark and Couto. This is an open-access article distributed under the terms of the Creative Commons Attribution License (CC BY). The use, distribution or reproduction in other forums is permitted, provided the original author(s) and the copyright owner(s) are credited and that the original publication in this journal is cited, in accordance with accepted academic practice. No use, distribution or reproduction is permitted which does not comply with these terms.



Occurrence and Distribution of Tetracycline Antibiotics and Resistance Genes in Longshore Sediments of the Three Gorges Reservoir, China

Lunhui Lu^{1†}, Jie Liu^{2†}, Zhe Li^{1,2*}, Zhiping Liu^{2*}, Jinsong Guo², Yan Xiao¹ and Jixiang Yang¹

¹ CAS Key Laboratory of Reservoir Aquatic Environment, Chongqing Institute of Green and Intelligent Technology, Chinese Academy of Sciences, Chongqing, China, ² Key Laboratory of the Three Gorges Reservoir Region's Eco-Environment, Ministry of Education, Chongqing University, Chongqing, China

OPEN ACCESS

Edited by:

Gian Maria Rossolini,
Università degli Studi di Firenze, Italy

Reviewed by:

Andrea Di Cesare,
Università di Genova, Italy
Luciana Migliore,
Università degli Studi di Roma Tor
Vergata, Italy

*Correspondence:

Zhe Li
lizhe@cigit.ac.cn
Zhiping Liu
liulqs@163.com

[†]These authors have contributed
equally to this work and share first
authorship

Specialty section:

This article was submitted to
Evolutionary and Genomic
Microbiology,
a section of the journal
Frontiers in Microbiology

Received: 16 April 2018

Accepted: 30 July 2018

Published: 17 August 2018

Citation:

Lu L, Liu J, Li Z, Liu Z, Guo J, Xiao Y
and Yang J (2018) Occurrence
and Distribution of Tetracycline
Antibiotics and Resistance Genes
in Longshore Sediments of the Three
Gorges Reservoir, China.
Front. Microbiol. 9:1911.
doi: 10.3389/fmicb.2018.01911

The widespread use of antibiotics and the induced antibiotic resistance genes have attracted much attention in recent years. The longshore sediments in the water-level-fluctuating zone of the Three Gorges Reservoir were selected to investigate the spatial-temporal distribution of antibiotics and antibiotic resistance genes in two different operation stages (low-water level in summer and high-water level in winter). Three kinds of tetracycline antibiotics (tetracycline, oxytetracycline, and chlortetracycline) and three kinds of tetracycline resistance genes [*tet*(A), *tet*(C), and *tet*(M)] were analyzed and quantified. The results showed that the distribution of tetracyclines and resistance genes in riverine, transition and lacustrine zones showed a certain regularity, and the tetracycline antibiotics concentration and the total abundance of the tetracycline resistance genes were highest in the transition zone, and then the riverine zone. Meanwhile, there were significant seasonal variations of tetracycline and the resistance genes. The concentrations of the tetracycline and resistance genes were higher in summer than those in winter, while the relative abundance of resistance genes was higher in winter. It was suggested that the different seasonal distribution of antibiotics and resistance genes may be correlated with the reservoir operation in the Three Gorges Reservoir and the higher use of antibiotics in winter. In addition, Pearson correlation analysis showed that the concentrations of the tetracycline, class 1 integron and 16S rRNA were positively correlated with the abundance of the tetracycline resistance genes.

Keywords: Three Gorges Reservoir, longshore sediments, tetracycline antibiotics, antibiotic resistance genes, spatial-temporal distribution

INTRODUCTION

In recent years, with the widespread abuse of antibiotics in human medicine and animal husbandry, exogenous antibiotics and antibiotic resistance genes (ARGs) in the environment have become an increasingly global problem (Sarmah et al., 2006). China leads the world in antibiotic production capacity, with a significant percentage of antibiotics utilized in animal agriculture and medicine

(Luo et al., 2010). In general, after the consumption, only a small portion of antibiotics can be bio-degraded, most antibiotics are discharged into the environment without being metabolized (Xiong et al., 2018). As the most commonly applied antibiotics, tetracyclines (TCs), such as tetracycline (TC), oxytetracycline (OTC), and chlortetracycline (CTC), are broad-spectrum and affordable (Patterson et al., 2007). Accordingly, TCs are used extensively in medical treatment, as well as for veterinary drugs and growth promoter in poultry farming and aquaculture, particularly in developing countries (Chopra and Roberts, 2001; Roberts, 2003). Remarkably, compared with other antibiotics, TCs are more persistent, highly adsorptive and hardly degradable in soils and sediments (Chee-Sanford et al., 2009). Thus, they are also more easily accumulated (Rabolle and Spliid, 2000; Sarmah et al., 2006; Jiang et al., 2011), posing a potential threat to ecosystems and human health.

TCs may trigger the production of tetracycline resistance genes, which directly cause environmental pollution (Kim, 2004). A typical feature of ARGs is that they can be transferred horizontally between microorganisms using mobile genetic elements as carriers, such as plasmids and transposons (Zhou et al., 2014; Lin et al., 2015). As a type of genetic assembly platform, integrons associated with these mobile genetic elements are considered as the key players in horizontal gene transfer, particularly class 1 integrons (Gaze et al., 2011; Berglund et al., 2014). Through this horizontal gene transfer, ARGs can migrate and transform from different environmental media, and are likely to be introduced into the food chain along with the resistant plasmid and finally enter the human body to increase human antibiotic resistance (Ghosh et al., 2009; Stoll et al., 2012; Sengupta et al., 2013). The aquatic environment is an important pool for ARGs because many pollutants from wastewater treatment plants, industries, hospitals and swine farms finally circulate in water environments and drive the propagation of ARGs (Zhang et al., 2009; Lupo et al., 2012; Yan et al., 2014a,b; Yang et al., 2017). Sediments may act as a sink but also as a secondary source of various contaminants including antibiotics and ARGs (Su et al., 2014), constituting a great potential danger for aquatic organisms (Siedlewicz et al., 2017). Hence, the diversity of antibiotics and ARGs in sediments of the watershed is important for us to understand the diffusion of antibiotic resistance at the catchment scale. To date, reports on the pollution of antibiotics and ARGs in sediments are mainly concentrated in the coastal areas, some rivers and lakes (Pei et al., 2006; Luo et al., 2010; Su et al., 2014; Yang et al., 2016; Calero-Caceres et al., 2017; Siedlewicz et al., 2017). However, there are relatively few studies on longshore sediments in the large reservoir.

As the largest reservoir in China, the Three Gorges Reservoir (TGR) performs several functions, such as flood control, power generation, navigation, irrigation and aquaculture, and its ecological functions are crucial. Since the completion of the Three Gorges Project, the operation of the reservoir has been implemented as an anti-seasonal artificial water level regulation and management method for “winter storage and summer drainage.” The water level rises to 175 m in October and begins to decline in May of the following year. From June to September, the

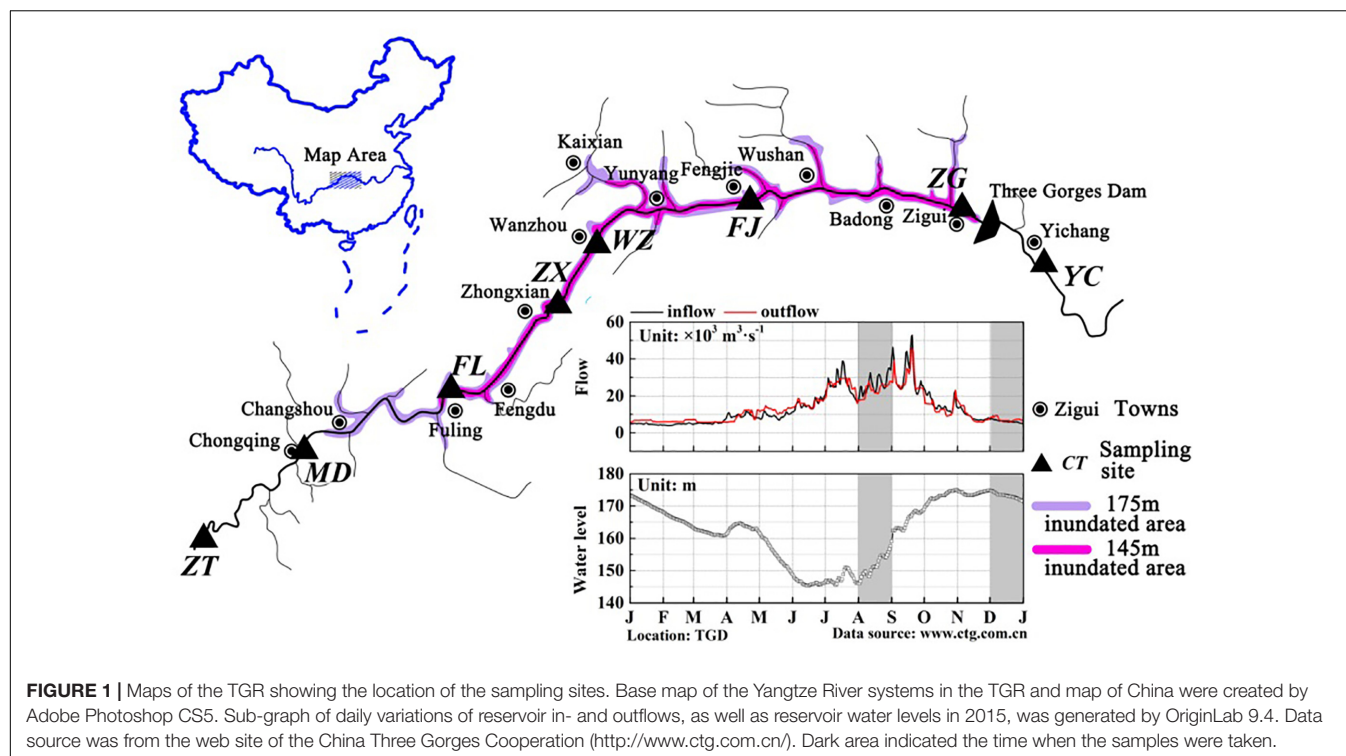
reservoir water level is maintained at the lowest level of 145 m. Periodic changes in reservoir water level affect the sediment deposition in the riparian zone (Wang et al., 2016), which inevitably leads to a change in the transport characteristics of pollutants adsorbed on sediment. Hence, the purpose of this study was to focus on detecting and discussing the spatial-temporal distribution of TCs and tetracycline resistance genes in the longshore sediments of the TGR.

In this study, eight sampling sites were selected in the sediments of the water-level-fluctuating zone of the TGR. Three tetracycline antibiotics (TC, OTC, and CTC) were determined by liquid chromatography-mass spectrometry (LC-MS). Three tetracycline resistance genes [*tet(A)*, *tet(C)*, and *tet(M)*], one genetic element (class 1 integron, *intI1*) and 16S rRNA gene abundance were assessed by real-time quantitative PCR to reveal the presence of the tetracycline resistance genes in the TGR. This study would give insight into further research on assessment of antibiotics and antibiotic resistance genes pollution in the TGR.

MATERIALS AND METHODS

Site Selection and Sampling

The TGR is formed after the completion of the Three Gorges hydropower station, with a water surface area of 1084 km². This reservoir is from Chongqing (west) to Yichang of Hubei province (east), and the distance is approximately 662.9 km (Chang et al., 2010). According to Thornton et al. (1990), a pure river-like reservoir can be divided into three longitudinal zones: riverine zone, transition zone and lacustrine zone. A riverine zone is located at the upper domain that has a narrow and channelized basin with relatively high flow rates; the lower part immediately upstream of the dam is often described as the lacustrine zone, which has a broad, deep and lake-like basin with low flow rates; a transitional zone is defined between the riverine and lacustrine zones that has a relatively broader and deeper basin with modest flow rates (Kimmel and Groeger, 1984; Thornton et al., 1990). Longitudinal zonation in a reservoir changes in the zone extension due to the difference in hydrodynamic conditions. TGR is periodically regulated by dam operations, and thus exhibits the characteristics of both rivers and lakes, showing the same zonation characteristics. The TGR is a typical reservoir containing three typical zones (riverine zone, transition zone and lacustrine zone) according to the differences in hydrological characteristics, and these three zones are distinguishable along the longitudinal axis (Li et al., 2017). The average water velocity in the sites Zhutuo, Mudong and Fuling (about 0.6~1.05 m/s in August and 0.30 in December), Fengjie and Zigui (about 0.2 m/s in August and <0.1 m/s in December) (**Supplementary Figure S1**). Moreover, the hydraulic retention time in the TGR varied from 6~19 days between the sites ZT and FL, from 11~36 days between Zhongxian and Wanzhou, from 35~110 days between the sites FJ and ZG. According to the hydraulic retention time and average water velocity calculated, the sampling sites were classified qualitatively. For this reason, eight sampling sites were established along the reservoir: three sites belong to the riverine zone (ZT, MD, and



FL), two sites belong to the transition zone (ZX and WZ), two sites belong to the lacustrine zone (FJ and ZG), and one site YC after the dam (**Figure 1**). Detailed information of these sampling sites was summarized in **Table 1**. According to its regulation plan, the water level in the TGR is impounded to 175 m for power generation during the winter and discharged to 145 m for flood control during the summer (Li et al., 2010). Water residence time in August and December represented two periods of the reservoir, i.e., the lotic and lentic periods throughout the year. In this case, sediment samples were collected in the TGR during periods of low-water level (August 2015) and high-water level (December 2015).

Sampling sites were located along the riparian zone within a distance of 10 m from the water edge, which were subjected to alternate inundation and exposure due to the fluctuation of water level. At each sampling site, three surface sediment subsamples (0–20 cm) were randomly collected by a small shovel. After mixing and splitting into about 1 kg by quartering technique, samples were taken to the laboratory in sterile containers and stored at -80°C for further treatment and analysis (Zhang et al., 2012).

Physicochemical Properties of the Samples

Sediment samples were air-dried and sieved through a mesh screen (<0.149 mm) and then stored at 4°C before use. Nitrate (NO_3^- -N), nitrite (NO_2^- -N) and ammonium (NH_4^+ -N) were extracted from the sediments using 2 M KCl. The extracted NO_3^- -N was then determined by a UV spectrophotometry method (Song et al., 2007); the extraction liquid containing

NO_2^- -N and NH_4^+ -N was subsequently analyzed according to previously published methods (International Organization for Standardization [ISO], 2003). Water-soluble organic carbon (WSOC) was measured using a Vario TOC Cube analyzer (Elementar, Hanau, Germany). All the above determinations were carried out in triplicate, and the average results were calculated.

Extraction and Determination of Tetracyclines

Sediment samples were extracted using the most common solid-phase extraction method (Kim and Carlson, 2007a). First, the freeze-dried samples were broken into 0.3 mm particles, and 20 mL McIlvaine buffer was added to 4 g samples. The upper extract of the mixed sample after 30 min of shaking was filtered through a $0.45\ \mu\text{m}$ filter. Then, the filtrate was extracted by an OASIS hydrophilic-lipophilic balance solid-phase extraction column (Waters, Milford, MA, United States), and 5 mL of methanol was added to elute the antibiotics. The eluent was dried by a nitrogen blower, then sealed with 1 mL of methanol and stored at -20°C for LC-MS.

The target compounds TC, OTC and CTC in the extracts were determined by LC-MS. First, analyses were carried out using a Waters ACQUITY UPLCTM system (Waters, Milford, MA, United States). The chromatographic conditions were as follows: chromatographic column, Waters ACQUITY UPLC BEH C18 column ($1.7\ \mu\text{m}$; $2.1\ \text{mm} \times 100\ \text{mm}$); mobile phase, acetonitrile (A) and 0.1% formic acid (formic acid/ultrapure water, V/V) (B); flow rate, 0.2 mL/min; injection volume, 2 μL ; column temperature, 30°C . Then, mass spectrometry was performed.

The mass spectrometry system consisted of a Waters Micromass Quattro Premier XE (triple-quadrupole) detector and an ion source. The mass spectrometry conditions were as follows: ion source, ESI (+); source temperature, 110°C; desolvation temperature, 400°C; capillary voltage, 2.80 kV; desolvation gas flow, 600 L/h; cone gas flow, 50 L/h. The detailed mass spectrometric operating conditions are found in reference (Jia et al., 2009). For each sample, three replicate assays were performed for LC-MS analysis. The tetracyclines concentrations were all determined based on a dry weight.

DNA Extraction and PCR

The DNA in the longshore sediment samples was extracted in triplicate with the PowerWater DNA Extraction Kit (Mo Bio, CA, United States) according to the manufacturer's protocol. The DNA extracts were pooled for each sample to reduce sample variability for the following research. The content and purity of the extracted DNA were detected by 1% (weight/volume) agarose gel and Nanodrop ND-1000 (Nanodrop, United States). The A260/A280 values ranged from 1.8 to 2.0, and A260/230 ranged from 2.2 to 2.5, indicating that the purity of the DNA obtained was high.

Three *tet* genes [*tet*(A), *tet*(C), and *tet*(M)], one genetic element (class 1 integron, *intI1*) and the 16S rRNA gene were investigated. Information about the primers and the annealing temperature is listed in **Table 2**. PCR mixtures contained 25 μ L of 2 \times Power Taq PCR MasterMix (TIANGEN, Beijing, China), 1 μ L of each primer (25 μ M), and 10 ng of the DNA extracts in a total volume of 50 μ L. PCR amplification was run on a MyCycler (Bio-Rad, Hercules, CA, United States) with an initial cycle of denaturation (3 min at 95°C) followed by 30 cycles (30 s at 94°C, 30 s at the annealing temperature (**Table 2**) and 60 s at 72°C), and a final elongation step (5 min at 72°C).

The above PCR amplification products were analyzed using electrophoresis with a Bio-Rad Gel Doc2000 on 2% agarose gel electrophoresis. The universal DNA purification and recovery kit (centrifugal column) was then used to purify the sediment DNA in the PCR reaction solution.

Gene Quantification With Real-time Quantitative PCR

Quantitative PCR (qPCR) was used to quantify the target genes. The 16S rRNA gene was included to quantify the total bacterial load and to normalize the abundance of ARGs (ARG copies/16S rRNA gene copies, defined as relative abundance) in the collected samples. Real-time QPCR was performed on an iCycler iQ5 thermocycler (Bio-Rad, Hercules, CA, United States) to determine the abundance of the target genes in the samples. Standard plasmids carrying target genes were obtained by TA clones and extracted using a TIAPure Mini Plasmid kit (TIANGEN, Beijing, China) (Yu et al., 2005). Concentrations of the standard plasmids (ng/ μ L) were determined with the Nanodrop ND-1000 spectrophotometer (Nanodrop, United States). Copy concentrations (copies/ μ L) were then calculated by the following formula (Pei et al., 2006).

copy concentration (copies/g)=

$$\frac{\text{DNA mass concentration (ng/g)}}{\text{DNA molecular weight (g/mol)}}$$

The 25 μ L qPCR mix contained 2 ng of sediment microbial DNA, 0.75 μ L of each primer (25 μ M), 10 μ L of 2.5 \times RealMasterMix (TIANGEN, Beijing, China) and 1.5 μ L of 20 \times SYBR solution (TIANGEN, Beijing, China). The protocol was as follows: 15 min at 95°C; 40 cycles consisting of 10 s at 95°C, 20 s at the annealing temperature and 30 s at 72°C; followed by a final

TABLE 1 | Detailed information about the eight sampling sites.

Sampling sites	Abbreviation	Site characteristics	Location		Distance to the Three Gorges Dam (km)
			Latitude (N)	Longitude (E)	
Zhutuo	ZT	Riverine zone	N29°00'47.40"	E105°51'10.20"	778
Mudong	MD		N 29°34'16.20"	E 106°50'22.80"	592
Fuling	FL		N 29°47'31.80"	E 107°27'43.80"	493
Zhongxian	ZX	Transition zone	N 30°25'11.40"	E 108°10'36.60"	352
Wanzhou	WZ		N 30°42'08.40"	E 108°23'15.00"	310
Fengjie	FJ	Lacustrine zone	N 31°02'36.60"	E 109°31'51.00"	164
Zigui	ZG		N 30°51'12.60"	E 110°58'30.00"	2
Yichang	YC	After the dam	N 30°40'31.00"	E 111°18'31.20"	−30

TABLE 2 | Information of the PCR primers and amplification conditions.

Target genes	Forward primers	Reverse primers	Amplicon length (bp)	Annealing temperature (°C)	Reference
<i>tet</i> (A)	GCTACATCCTGCTTGCCTTC	CATAGATCGCGGTGAAGAGG	210	55	Ng et al., 2001
<i>tet</i> (C)	CTTGAGAGCCTTCAACCCAG	ATGGTCGTATCTACCTGCC	278	55	Aminov et al., 2001
<i>stet</i> (M)	GCAATTCTACTGATTCTGC	CTGTTTGATTACAATTTCCGC	171	45	Aminov et al., 2001
<i>intI1</i>	CCTCCCGCACGATGATC	TCCACGCATCGTCAGGC	280	55	Goldstein et al., 2001
<i>338F/518R</i>	CCTACGGGAGGCAGCAG	ATTACCGCGGCTGCTGG	174	55	Koike et al., 2007

extension of 30 s at 72°C. The fluorescent signal was measured at the end of each extension step (Bustin et al., 2009). The melting process was automatically generated by the iCycler iQ5 system.

For the generation of the standards for all qPCR assays, a plasmid construct was used containing the inset of each ARG obtained by conventional PCR. The following requirements were satisfied to obtain reliable quantification (**Supplementary Table S1**): R^2 was higher than 0.99 for all standard curves over five orders of magnitude. Amplification efficiencies based on slopes were between 95 and 110%. The specificity was assured by the melting curves and gel electrophoresis. The minimum quantification limits for all target genes were within the range of 1.0×10^2 to 1.0×10^3 copies per μL DNA. The qPCR performed included two sets of standards and no-template negative (sterile water) controls on all samples and standards. The presence of PCR inhibitors in the DNA extracted from sediment samples was examined by diluting the DNA extract and mixing a known amount of standard DNA to a DNA extract before qPCR. In none of these cases was inhibition detected. The target genes concentrations were all determined based on a dry weight.

Statistical Analysis

Pearson correlation analysis was conducted to detect significant differences between physicochemical parameters and the target genes. Differences with $p < 0.05$ were considered statistically significant. The distribution map of antibiotics and resistance genes was completed by Origin 8.0. To understand the distribution characteristics of resistance genes at different sites, principal component analysis (PCA) was performed with Canoco 4.5. Linear-regression analysis was used to assess the association between TCs, *intI1*, 16S rRNA and ARGs.

Statistical analyses were performed using SPSS 19.0 (IBM, United States).

RESULTS

Physicochemical Parameters of Sediment Samples

The variation of the physicochemical parameters of longshore sediments at the eight sampling sites is presented in **Table 3**. There were significant differences between the parameters at different sites. The mean values of all physicochemical descriptors at site WZ were higher in winter than those in summer. For the other sampling sites, most parameters at the upstream locations of ZT, MD, FL, and ZX appeared analogous distribution characteristics, while only $\text{NH}_4^+\text{-N}$ at the downstream locations of FJ, ZG, and YC were higher in winter than those in summer. In terms of the physicochemical parameters, the mean values of organic matter were higher in summer than in winter. In contrast, WSOC, $\text{NH}_4^+\text{-N}$, $\text{NO}_2^-\text{-N}$, and $\text{NO}_3^-\text{-N}$ were higher in winter. Briefly, seasonal differences were noticed between these parameters ($p > 0.05$).

Pearson correlation analysis of these indicators at each site showed that the conductivity and WSOC were significantly correlated with $\text{NO}_3^-\text{-N}$, with p values of 0.023 and 0.040, respectively, while there was no obvious correlation between other physicochemical indicators (**Supplementary Table S2**).

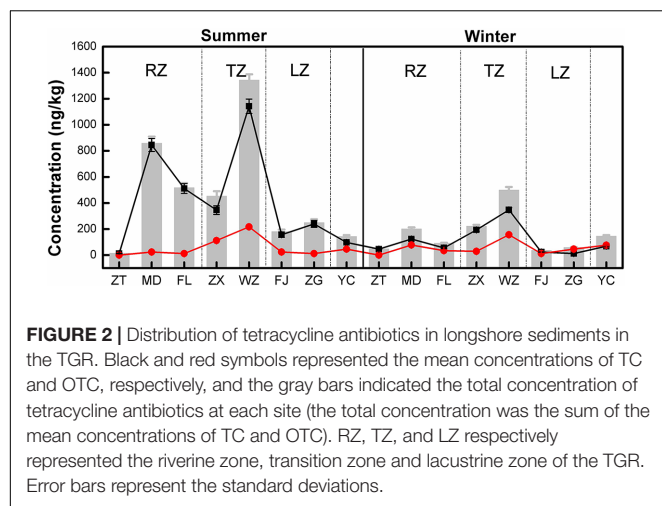
Spatial-Temporal Distributions of Tetracyclines

Of the three tetracycline antibiotic compounds, CTC was only detected at Wanzhou site in the summer. TC and OTC were

TABLE 3 | The physicochemical parameters of the sediments in the TGR.

Time	Sampling site	pH		C^b (mS/cm)		OM^c (%)		WSOC^d (mg/kg)		$\text{NH}_4^+\text{-N}$ (mg/kg)		$\text{NO}_2^-\text{-N}$ (mg/kg)		$\text{NO}_3^-\text{-N}$ (mg/kg)	
		Average	SD^a	Average	SD	Average	SD	Average	SD	Average	SD	Average	SD	Average	SD
2015.8	ZT	7.14	0.05	0.38	0.05	5.46	0.46	9.08	0.66	8.60	0.82	18.56	1.02	3.98	0.70
	MD	7.16	0.06	0.16	0.02	2.93	0.23	7.88	0.60	8.01	0.57	7.72	0.77	11.05	0.86
	FL	6.53	0.25	0.06	0.00	7.82	0.71	8.93	0.71	9.41	0.81	9.27	0.75	3.06	0.23
	ZX	6.58	0.17	0.57	0.06	8.53	0.70	10.59	0.42	8.12	0.53	15.34	0.94	9.53	0.31
	WZ	6.88	0.11	0.22	0.02	4.79	0.52	13.90	1.45	8.21	0.28	7.41	0.59	1.43	0.15
	FJ	6.40	0.31	0.74	0.05	11.22	1.05	19.38	1.67	7.61	0.62	10.21	0.83	25.50	2.29
	ZG	7.56	0.27	0.74	0.04	6.84	0.72	17.70	1.11	7.69	0.58	13.05	1.02	14.04	0.54
	YC	7.46	0.17	0.11	0.04	5.11	0.43	26.20	1.90	5.95	0.22	10.54	0.93	8.24	0.66
2015.12	ZT	7.24	0.36	0.89	0.10	2.89	0.27	17.86	1.27	10.67	0.63	12.51	0.81	23.24	0.48
	MD	6.64	0.25	0.48	0.08	3.79	0.59	22.40	2.26	9.37	0.53	11.22	0.84	5.45	0.45
	FL	6.85	0.28	0.41	0.04	4.51	0.49	14.16	1.81	8.56	0.50	16.30	0.87	5.12	0.44
	ZX	6.96	0.00	0.26	0.05	10.75	0.98	36.24	2.34	10.72	0.57	22.51	1.09	23.07	0.55
	WZ	7.07	0.32	0.39	0.04	5.54	0.44	17.79	1.96	11.18	0.96	14.34	0.60	10.03	0.57
	FJ	6.11	0.22	0.22	0.03	6.81	0.45	25.59	1.58	9.84	0.64	19.75	1.13	16.17	0.48
	ZG	6.59	0.18	0.22	0.03	4.15	0.28	12.41	1.42	8.05	0.82	8.27	0.72	3.31	0.30
	YC	6.52	0.17	0.18	0.02	3.32	0.28	21.89	1.80	8.24	0.50	10.40	0.82	6.29	0.49

Abbreviations: a, standard deviation; b, conductivity; c, organic matter; d, water-soluble organic carbon.



detected at all sampling sites in both sampling seasons. The results of the concentrations of all detected tetracyclines are shown in **Figure 2**. The TC concentration ranged from 12.11 to 1142.67 ng/kg in the summer, 11.74 to 347.21 ng/kg in the winter. For OTC, the concentration ranged from 0.33 to 216.93 ng/kg in the summer and 0.12 to 156.44 ng/kg in the winter. In addition, the mean concentrations of TC and OTC were 263.60 and 54.73 ng/kg, respectively. Clearly, TC was the dominant tetracycline antibiotic in the TGR, contributing 20.45–99.74% to the total tetracycline antibiotic detected. Except for ZT and TC concentrations at all sites were noticeably higher in the summer. For OTC, only the concentrations at ZT, ZX, WZ, and FJ were slightly higher in summer, indicating that the distribution of OTC did not have a clear seasonal variation. On the other hand, the concentrations of TC and OTC in WZ were the highest, followed by MD and FL. The concentrations of TC and OTC were added together as the sum of the concentrations of tetracyclines at each site, and recorded as TCs (the gray bars in **Figure 2**). It was found that the concentration of TCs in the transition zone (ZX and WZ) was the highest, followed by the riverine zone (ZT, MD, and FL), and the lacustrine zone (FJ and ZG) was the lowest.

Distribution of Tetracycline Resistance Genes

Figure 3 shows the occurrences and quantities of ARGs and *intI1* in the sediments of the TGR. Of tetracycline resistance genes analyzed, *tet(C)* and *tet(M)* had 100% detection frequency in all eight sediment samples of the TGR, followed by *tet(A)* (87.5%). The concentrations of these three genes varied greatly by five orders of magnitude, ranging from 2.11×10^2 copies/g [*tet(M)* of site MD in the winter] to 3.23×10^7 copies/g [*tet(A)* of site MD in the summer]. Additionally, among the three investigated genes, the absolute and relative abundance of *tet(A)* was the highest, while the *tet(M)* gene was found with the lowest average absolute abundance and relative abundance. *IntI1* was also detected in sediment samples; however, the detection frequency (75%) was lower than that of *tet* genes, with mean absolute abundance of 1.91×10^5 copies/g and

mean relative abundance of 7.14×10^5 copies/16S rRNA. On the other hand, from the time perspective, the absolute concentration of ARGs and *intI1* in summer was higher than that in winter, while the relative abundance of ARGs and *intI1* was the opposite.

The principle component analysis (PCA) was carried out to reveal the distribution characteristics of the target genes at different sites (**Figure 4**). As shown in the figure, ZT was located at the end of the PCA graphs. Principal components 1 and 2 accounted for 87.2% of the total sample variability (64.2 and 23.0% for PC1 and PC2, respectively). PCA coordinates showed comparatively high discrepancies between the different sites and periods in the TGR. In summer, WZ and MD had a highly similar distribution of resistance genes, and it was probably due to the sites affected by human activities seriously. Sites of the lacustrine zone (FJ and ZG) clustered together in the PCA plot, showing a certain similarity. However, the riverine and transition zone did not show similarity between the sites in the same zone. In winter, the two sites of the riverine zone (MD and FL) and the two sites of the transition zone (ZX and WZ) were clustered together.

Distribution of TCs and ARGs in Relation to Environmental Variables Within the TGR

To explore the factors influencing the distribution characteristics of TCs and ARGs, some environmental factors (physicochemical indicators detected in this study) and social factors (population density, GDP per capita, GDP, land area, and permanent population¹) were selected for Pearson correlation analysis. In summer, no correlation was found between any factors (**Supplementary Table S3**). But in winter, there was a significant correlation between *intI1* and organic matter, $\text{NH}_4^+\text{-N}$, $\text{NO}_2^-\text{-N}$, and $\text{NO}_3^-\text{-N}$ (**Supplementary Table S4**). Besides, an obvious correlation was found between *intI1* and permanent population, land area, population density, organic matter, which indicating that *intI1* was greatly affected by these factors in winter. When all data in both seasons were grouped together, as shown in **Supplementary Table S5**, correlation analysis demonstrated that only *tet(A)* had negative correlation relationship with $\text{NO}_2^-\text{-N}$ ($p = 0.047$).

Correlation Between ARGs Abundances and Antibiotic Concentrations

As shown in **Figure 5**, significant correlations existed between TC concentration and the three *tet* genes abundance at the $p < 0.01$ level. The correlation between OTC concentration and tetracycline resistance genes was different. It was noteworthy that no correlation was found between *tet(A)*, *tet(C)* abundance and OTC concentration, but there was a significant correlation between *tet(M)* abundance and OTC concentration. In addition, Pearson correlation analysis also showed that *intI1* and 16S rRNA abundance had positive correlation relationships with the three *tet* genes abundance at the $p < 0.01$ level.

¹<http://www.cqjt.gov.cn/>

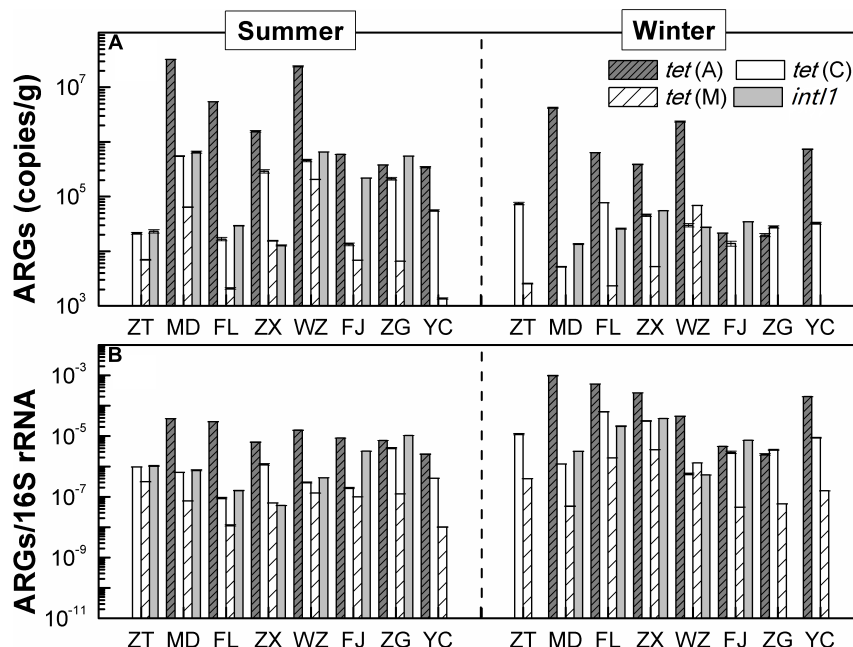


FIGURE 3 | The distribution of ARGs. **(A)** The absolute abundance distribution of ARGs. **(B)** The distribution of ARGs/16S rRNA (relative abundance of ARGs), copies/16S gene copies. Each value is the mean \pm SD of three replicates.

DISCUSSION

Relationships Between TCs, *int11*, 16S rRNA, and ARGs

Tet genes can be classified into four categories according to their different resistance mechanisms: efflux genes, ribosomal protection genes, enzymatic genes and other genes (Roberts, 2005). The three *tet* genes detected in this study cover two of them: the efflux genes [*tet*(A) and *tet*(C)] and the ribosome protection genes [*tet*(M)]. Previous studies had shown that efflux genes were more common in the environment compared with ribosomal protection genes (Borjesson et al., 2010). This may be the reason why the abundance (absolute and relative) of *tet*(M) was quite different from that of *tet*(A) and *tet*(C). Chopra and Roberts (2001) pointed out that ribosomal protection protein conferred a wider spectrum of resistance to TCs than those carrying tetracycline efflux proteins, with the exception of *tet*(B). Correlation analysis with antibiotics in this study showed that *tet*(A) and *tet*(C) had a relatively consistent correlation, while *tet*(M) was opposite. This difference may be caused by different mechanisms of the genes. However, due to the limited number of genes selected in this study, the above phenomenon may be accidental, and further research is needed to verify it.

Apart from the possible internal factors of the resistance mechanism, many external factors were also the key factors affecting the distribution of antibiotics and resistance genes, like environmental conditions (Siedlewicz et al., 2017) and human activities (Pruden et al., 2006; Zhou et al., 2011; Su et al., 2014; Yang et al., 2016). However, the sampling location and

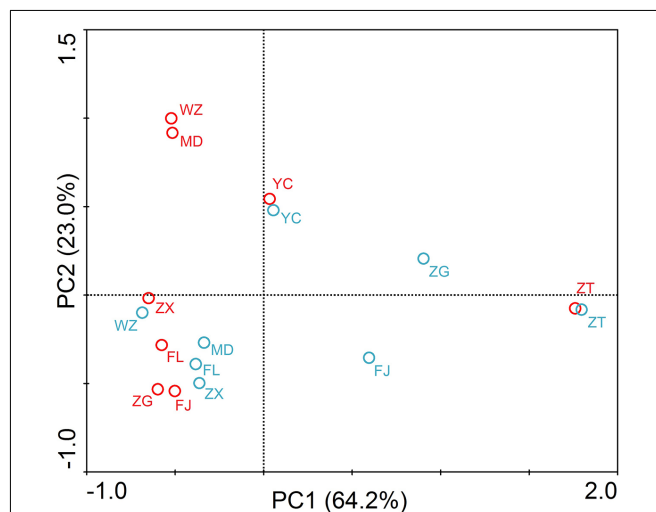
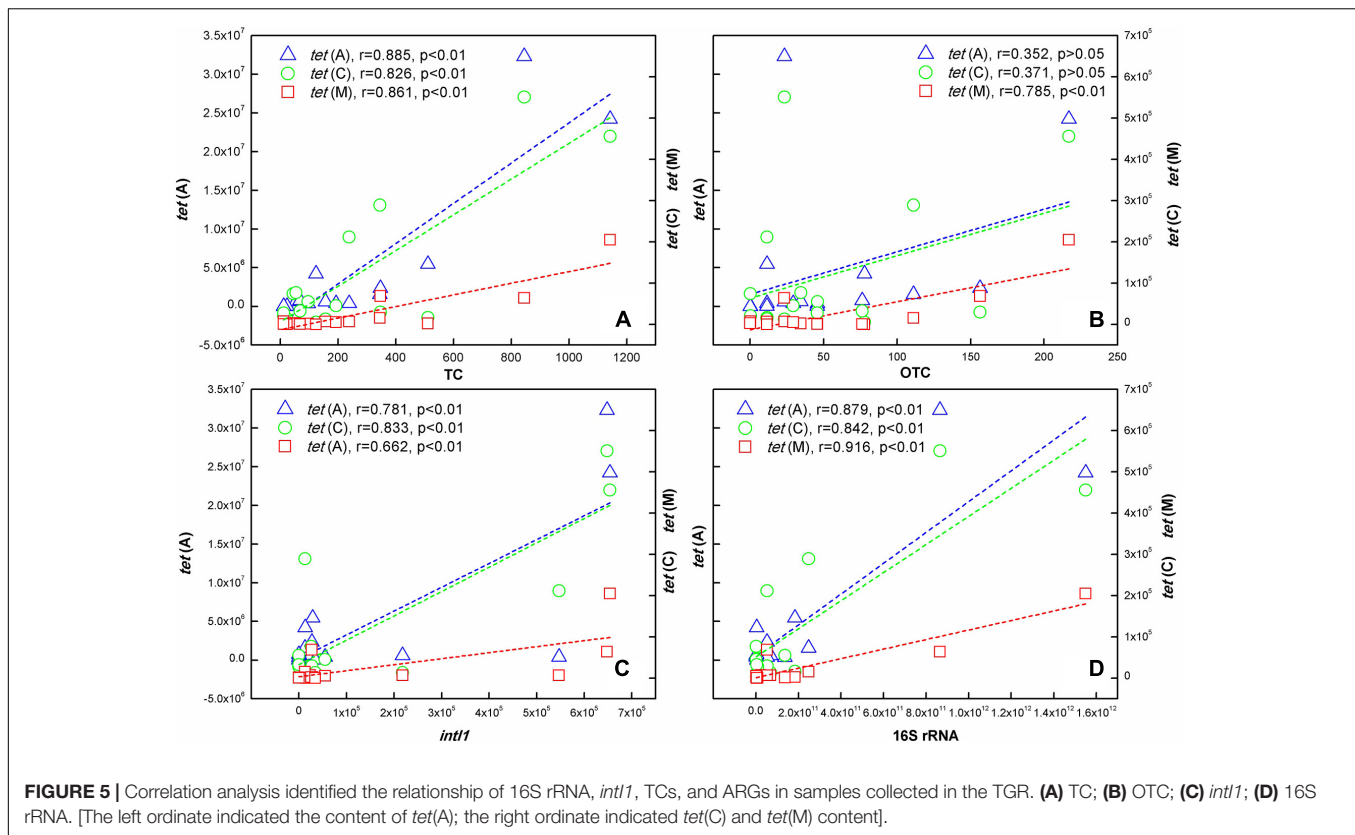


FIGURE 4 | Principle component analysis (PCA) of absolute concentrations of three *tet* genes, 16S rRNA and *int11* in the TGR. The circle in the graph represented the sampling site. Red circle and blue circle represented the samples in summer and winter, respectively. The PC1 and PC2 explained 64.2 and 23.0% of the total variance, respectively. Seven sampling sites along the longitudinal axis in the TGR were selected from upstream to downstream: riverine zone consisted of sites ZT, MD, and FL; the transition zone consisted of sites ZX and WZ; the lacustrine zone consisted of FJ and ZG. YC belonged to the site after the dam.

sampling strategy selected by different research institutes were inconsistent, which may be the reason for the lack of correlation between antibiotics, ARGs and other factors chosen in this study.



Except for the above elements, other factors also affected the abundance of resistance genes, such as antibiotics (Luo et al., 2010), *int11* (Zhu et al., 2013) and 16S rRNA (Chen and Zhang, 2013). In theory, as the direct selection pressure of ARGs, the abundance of ARGs in the environment was consistent with the corresponding concentration of induced antibiotics (Wang et al., 2014; Niu et al., 2016). However, some articles suggested that there was no correlation between some antibiotics and their corresponding ARGs (Niu et al., 2016). Because in addition to the above factors, light (Pei et al., 2007), temperature (Engemann et al., 2008), heavy metals (Baker-Austin et al., 2006; Gillings and Stokes, 2012) and other factors also affect the abundance of ARGs, especially antibiotic resistance can be co-selected by heavy metals (Zhu et al., 2013). Nevertheless, antibiotic residues are still considered to be the direct and primary selection pressures for acceleration of the expansion of the bacterial resistance (Caucci et al., 2016). In general, such a significant difference existed in the association of antibiotics with ARGs, one of which may be due to the different habits of antibiotic use in different regions and the different chemical properties of different ARGs. *int11* was known to play a key role in horizontal gene transfer, leading to widespread antibiotic resistance (Zhu et al., 2013). Meanwhile, *int11* was also regarded as an environmental marker of anthropogenic pollution (Gillings et al., 2015). The high correlation between the *tet* genes and *int11* revealed the potential horizontal gene transfer in these samples. The characteristics of the bacterial abundance were analyzed based on 16S rRNA. As the potential hosts of ARGs,

bacteria would amplify or attenuate under different conditions, so the persistence and proliferation of ARGs were also closely associated with the bacterial abundance (Su et al., 2017). The above results indicated that the higher abundance of bacteria in sediments in summer than that in winter may play an important role in the horizontal spread of *tet(A)*, *tet(C)* and *tet(M)* genes in the TGR.

Spatial-Temporal Variation of TCs and ARGs in the Sediments of the TGR

The TGR is different from other basins, with a low-water level in summer and a high-water level in winter. The seasonal distribution of TGR antibiotics and resistance genes was also different from other basins that was, the concentration of TC and the abundance of ARGs were higher in summer than those in winter. In general, many factors would cause antibiotics to present different distribution characteristics in different seasons, such as temperature and water flow rate (Kim and Carlson, 2007b; Loftin et al., 2008). For example, photo degradation and biodegradation were less effective at low temperature in winter (Cheng et al., 2014). At the same time, TCs were commonly administered to livestock for the prevention and treatment of most respiratory infection and diarrhea (Matsui et al., 2008) and their usage tended to increase in winter (Cheng et al., 2014). Under the influence of these factors, most studies found that the concentration of antibiotics in the water body was higher in the dry season (Yan et al., 2013;

Chen et al., 2018). The seasonal variation in antibiotics would produce a selective pressure, so the abundance of ARG in winter would be higher (Caucci et al., 2016; Sui et al., 2017). But the opposite phenomenon were also found in other literatures (Arikan et al., 2008; Jiang et al., 2011; Knapp et al., 2012; Calero-Caceres et al., 2017), which indicating that the seasonal distribution of antibiotics and ARGs was controversial. It was suggested that the hydrological conditions of different basins may be inconsistent, therefore we speculate that the seasonal distribution in this study may be caused by unique hydrological conditions of the TGR.

It had been reported that the sediment could act as a significant secondary source of antibiotics and could release pollutants into the water if the aquatic environment changed (Cheng et al., 2014), with the antibiotics strongly bonding in the sediments. This tended to protect them from potential degradation processes, which resulted in a greater persistence and a longer-term fate of the antibiotics (Chen and Zhou, 2014). In summer, the TGR is no longer at the high-water level, but operates stably at the low-water level of 145 m. The aquatic environment was changed, sediments in the riparian zone were also changed, and fluctuation of the water level turned the original bottom sediment in winter into the longshore sediment in summer. Previously, the antibiotics in water bodies were adsorbed and accumulated in sediments by natural sedimentation, which resulting in an increase in the concentration of TCs in these sediments. On the other hand, heavy rainfall occurred in the summer, and rainfall runoff carried a large amount of antibiotics into the water, leading to an increase in external input. As the main selection pressure of ARGs, the concentration of TCs in the water during the summer was higher and thus the absolute abundance of ARGs was also higher. In addition, as the rainfall increased, the velocity of the flowing water in the reservoir also increased. ARGs could migrate among different environmental compartments (Chen et al., 2013). Hence, it was reasonable to assume that aqueous-phase mechanical agitation should be enhanced, possibly resulting in the increased exchange of ARGs between the longshore sediments and the water phase (Fang et al., 2017), thereby resulting in a higher concentration of ARGs in the longshore sediments. Meanwhile, we also hypothesized that more frequent exchanges of ARGs may likely occur in the summer than in the winter, bringing about higher concentrations of ARGs in the sediments. This was maybe because the warmer temperatures may promote the survival of bacteria in sediments, and thus lead to a greater number of copies of ARGs (Luo et al., 2010). This assumption was supported by our findings that the abundance of 16S rRNA in sediments was higher in the summer than in the winter and that massive microbial carriers of the ARGs provided the fundamental conditions for the exchange of ARGs (Fang et al., 2017). In December, the reservoir operated at a high-water level and the water flow rate slowed down, which in turn accelerated the sedimentation of antibiotics in the water, leading to a lower concentration of TCs and ARGs in the longshore sediments.

The distribution of TCs and ARGs exhibited clear spatial heterogeneity. Reservoirs are created ecosystems that behave as

"hybrids" of river and lake ecosystems (Scott et al., 2009). The riverine, transition and lacustrine zones are three typical zones in the TGR. These longitudinal gradients influence the physical, chemical and biological processes that affect sedimentation (Liu et al., 2012). Along the longitudinal axis, sites MD, FL, and WZ were near a large metropolitan area with a large population and sizeable industries (Li et al., 2017), which resulted in more external antibiotics and ARGs flowing into the TGR. The sediments in the riverine zone were mainly exogenous (Cooke et al., 2011), so the concentrations of antibiotics and resistance genes in the riverine zone were relatively high. However, the riverine zone was close to the inlet of the reservoir, where the fastest water flow rate led to a degree of dilution of the antibiotics and resistance genes. The sediments in the transition zone were exogenous and endogenous (Filstrup and Lind, 2010). Due to the large input of WZ, the content of antibiotics and ARGs in the transition zone were also highest among the eight sites in this study. Moreover, and the decrease in the reservoir flow rate in the transition zone resulted in the residence of the antibiotics and ARGs. Besides, it was worth noting that, in addition to ZT, the concentrations of antibiotics and ARGs at upstream sites (ZT, MD, FL, ZX, and WZ) were higher than those at downstream sites (ZG and FJ), in agreement with previous studies on the Liao River (Dong et al., 2016). Our previous work indicated that anthropogenic activities might lead to the different characteristics of the upstream and downstream sites (Li et al., 2017). Hence, fewer exogenous inputs at FJ and ZG may also result in lower concentrations of antibiotics and ARGs at the downstream sites. In addition, the relatively low antibiotic concentration at the downstream sites could be mainly attributed to dilution of the water from the TGR (Loftin et al., 2008).

CONCLUSION

This study demonstrated the occurrence and distribution of antibiotic and ARGs in the longshore sediments of the TGR, China. The differences in hydrological conditions and surrounding environmental conditions also probably led to different distribution characteristics of antibiotic and resistance genes in three typical zones of the TGR (riverine, transition, and lacustrine zones). Statistical analyses revealed that both antibiotics and 16S rRNA played a role in the distribution of ARGs within the TGR. Besides, the concentration of *tet* genes was significantly correlated with *intI1* ($p < 0.05$) implying horizontal transfer of ARGs, which posed a great threat to public health. It is necessary to conduct further researches on the environmental effects and migration transformation mechanisms of the ARGs.

AUTHOR CONTRIBUTIONS

LL, ZL, ZPL, and JG conceived and designed the study. JL, YX, and JY performed the experiments. LL, ZL, JL, ZPL, and JG analyzed the data and wrote the paper. All authors contributed to the editing of the manuscript.

FUNDING

This study was supported by the National Key Research and Development Plan of China (No. 2017YFC0404705), the National Natural Science Foundation of China (No. 51509233, 51679226, 51779240, and 51861125204), Chongqing Science and Technology Commission (No. cstc2017jcyjAX0243) and Key Research Program of Frontier Sciences, CAS (QYZDJSSWDQC008). All the data in the manuscript are

accessible and can be requested from the corresponding author.

SUPPLEMENTARY MATERIAL

The Supplementary Material for this article can be found online at: <https://www.frontiersin.org/articles/10.3389/fmicb.2018.01911/full#supplementary-material>

REFERENCES

- Aminov, R. I., Garrigues-Jeanjean, N., and Mackie, R. I. (2001). Molecular ecology of tetracycline resistance: Development and validation of primers for detection of tetracycline resistance genes encoding ribosomal protection proteins. *Appl. Environ. Microb.* 67, 22–32. doi: 10.1128/aem.67.1.22-32.2001
- Arikan, O. A., Rice, C., and Codling, E. (2008). Occurrence of antibiotics and hormones in a major agricultural watershed. *Desalination* 226, 121–133. doi: 10.1016/j.desal.2007.01.238
- Baker-Austin, C., Wright, M. S., Stepanauskas, R., and McArthur, J. V. (2006). Co-selection of antibiotic and metal resistance. *Trends Microbiol.* 14, 176–182. doi: 10.1016/j.tim.2006.02.006
- Berglund, B., Khan, G. A., Lindberg, R., Fick, J., and Lindgren, P.-E. (2014). Abundance and dynamics of antibiotic resistance genes and integrons in lake sediment microcosms. *PLoS One* 9:e108151. doi: 10.1371/journal.pone.0108151
- Borjesson, S., Mattsson, A., Lindgren, P. E., and Lindgren, P. E. (2010). Genes encoding tetracycline resistance in a full-scale municipal wastewater treatment plant investigated during one year. *J. Water Health* 8, 247–256. doi: 10.2166/wh.2009.159
- Bustin, S. A., Benes, V., Garson, J. A., Hellems, J., Huggett, J., Kubista, M., et al. (2009). The MIQE Guidelines: minimum information for publication of quantitative real-time PCR experiments. *Clin. Chem.* 55, 611–622. doi: 10.1373/clinchem.2008.112797
- Calero-Caceres, W., Mendez, J., Martin-Diaz, J., and Muniesa, M. (2017). The occurrence of antibiotic resistance genes in a Mediterranean river and their persistence in the riverbed sediment. *Environ. Pollut.* 223, 384–394. doi: 10.1016/j.envpol.2017.01.035
- Cauci, S., Karkman, A., Cacace, D., Rybicki, M., Timpel, P., Voolaid, V., et al. (2016). Seasonality of antibiotic prescriptions for outpatients and resistance genes in sewers and wastewater treatment plant outflow. *FEMS Microbiol. Ecol.* 92:fiw060. doi: 10.1093/femsec/fiw060
- Chang, X., Meyer, M. T., Liu, X., Zhao, Q., Chen, H., Chen, J., et al. (2010). Determination of antibiotics in sewage from hospitals, nursery and slaughter house, wastewater treatment plant and source water in Chongqing region of Three Gorge Reservoir in China. *Environ. Pollut.* 158, 1444–1450. doi: 10.1016/j.envpol.2009.12.034
- Chee-Sanford, J. C., Mackie, R. I., Koike, S., Krapac, I. G., Lin, Y.-F., Yannarell, A. C., et al. (2009). Fate and transport of antibiotic residues and antibiotic resistance genes following land application of manure waste. *J. Environ. Qual.* 38, 1086–1108. doi: 10.2134/jeq2008.0128
- Chen, B., Liang, X., Huang, X., Zhang, T., and Li, X. (2013). Differentiating anthropogenic impacts on ARGs in the Pearl River Estuary by using suitable gene indicators. *Water Res.* 47, 2811–2820. doi: 10.1016/j.watres.2013.02.042
- Chen, H., Jing, L., Teng, Y., and Wang, J. (2018). Characterization of antibiotics in a large-scale river system of China: occurrence pattern, spatiotemporal distribution and environmental risks. *Sci. Total Environ.* 618, 409–418. doi: 10.1016/j.scitotenv.2017.11.054
- Chen, H., and Zhang, M. (2013). Occurrence and removal of antibiotic resistance genes in municipal wastewater and rural domestic sewage treatment systems in eastern China. *Environ. Int.* 55, 9–14. doi: 10.1016/j.envint.2013.01.019
- Chen, K., and Zhou, J. L. (2014). Occurrence and behavior of antibiotics in water and sediments from the Huangpu River, Shanghai, China. *Chemosphere* 95, 604–612. doi: 10.1016/j.chemosphere.2013.09.119
- Cheng, D., Liu, X., Wang, L., Gong, W., Liu, G., Fu, W., et al. (2014). Seasonal variation and sediment-water exchange of antibiotics in a shallower large lake in North China. *Sci. Total Environ.* 47, 266–275. doi: 10.1016/j.scitotenv.2014.01.010
- Chopra, I., and Roberts, M. (2001). Tetracycline antibiotics: mode of action, applications, molecular biology, and epidemiology of bacterial resistance. *Microbiol. Mol. Biol. Rev.* 65, 232–260. doi: 10.1128/MMBR.65.2.232-260.2001
- Cooke, G. D., Welch, E. B., and Jones, J. R. (2011). Eutrophication of Tenkiller Reservoir, Oklahoma, from nonpoint agricultural runoff. *Lake Reserv. Manage.* 27, 256–270. doi: 10.1080/07438141.2011.607552
- Dong, D., Zhang, L., Liu, S., Guo, Z., and Hua, X. (2016). Antibiotics in water and sediments from Liao River in Jilin Province, China: occurrence, distribution, and risk assessment. *Environ. Earth Sci.* 75:1202. doi: 10.1007/s12665-016-6008-4
- Engemann, C. A., Keen, P. L., Knapp, C. W., Hall, K. J., and Graham, D. W. (2008). Fate of tetracycline resistance genes in aquatic systems: migration from the water column to peripheral biofilms. *Environ. Sci. Technol.* 42, 5131–5136. doi: 10.1021/es800238e
- Fang, H., Zhang, Q., Nie, X., Chen, B., Xiao, Y., Zhou, Q., et al. (2017). Occurrence and elimination of antibiotic resistance genes in a long-term operation integrated surface flow constructed wetland. *Chemosphere* 173, 99–106. doi: 10.1016/j.chemosphere.2017.01.027
- Filstrup, C. T., and Lind, O. T. (2010). Sediment transport mechanisms influencing spatiotemporal resuspension patterns in a shallow, polymictic reservoir. *Lake Reserv. Manage.* 26, 85–94. doi: 10.1080/07438141.2010.490771
- Gaze, W. H., Zhang, L., Abdouslam, N. A., Hawkey, P. M., Calvo-Bado, L., Royle, J., et al. (2011). Impacts of anthropogenic activity on the ecology of class 1 integrons and integron-associated genes in the environment. *ISME J.* 5, 1253–1261. doi: 10.1038/ismej.2011.15
- Ghosh, S., Ramsden, S. J., and LaPara, T. M. (2009). The role of anaerobic digestion in controlling the release of tetracycline resistance genes and class 1 integrons from municipal wastewater treatment plants. *Appl. Microbiol. Biotechnol.* 84, 791–796. doi: 10.1007/s00253-009-2125-2
- Gillings, M. R., Gaze, W. H., Pruden, A., Smalla, K., Tiedje, J. M., and Zhu, Y.-G. (2015). Using the class 1 integron-integrase gene as a proxy for anthropogenic pollution. *ISME J.* 9, 1269–1279. doi: 10.1038/ismej.2014.226
- Gillings, M. R., and Stokes, H. W. (2012). Are humans increasing bacterial evolvability? *Trends Ecol. Evol.* 27, 346–352. doi: 10.1016/j.tree.2012.02.006
- Goldstein, C., Lee, M. D., Sanchez, S., Hudson, C., Phillips, B., Register, B., et al. (2001). Incidence of class 1 and 2 integrons in clinical and commensal bacteria from livestock, companion animals, and exotics. *Antimicrob. Agents Chemother.* 45, 723–726. doi: 10.1128/aac.45.3.723-726.2001
- International Organization for Standardization [ISO] (2003). Soil Quality-Determination of Nitrate, Nitrite, and Ammonium in Field-Moist Soils by Extraction with Potassium Chloride Solution-Part 1: Manual Method (ISO/TS 14256-1: 2003). Available at: <https://www.iso.org/standard/36706.html> [accessed March 28, 2018].
- Jia, A., Xiao, Y., Hu, J., Asami, M., and Kunikane, S. (2009). Simultaneous determination of tetracyclines and their degradation products in environmental waters by liquid chromatography-electrospray tandem mass spectrometry. *J. Chromatogr. A* 1216, 4655–4662. doi: 10.1016/j.chroma.2009.03.073
- Jiang, L., Hu, X., Yin, D., Zhang, H., and Yu, Z. (2011). Occurrence, distribution and seasonal variation of antibiotics in the Huangpu River, Shanghai, China. *Chemosphere* 82, 822–828. doi: 10.1016/j.chemosphere.2010.11.028

- Kim, S. (2004). Occurrence of tetracycline resistance genes tet(M) and tet(S) in bacteria from marine aquaculture sites. *FEMS Microbiol. Lett.* 237, 147–156. doi: 10.1111/j.1574-6968.2004.tb09690.x
- Kim, S. C., and Carlson, K. (2007a). Quantification of human and veterinary antibiotics in water and sediment using SPE/LC/MS/MS. *Anal. Bioanal. Chem.* 387, 1301–1315. doi: 10.1007/s00216-006-0613-0
- Kim, S. C., and Carlson, K. (2007b). Temporal and spatial trends in the occurrence of human and veterinary antibiotics in aqueous and river sediment matrices. *Environ. Sci. Technol.* 41, 50–57.
- Kimmel, B. L., and Groeger, A. W. (1984). Factors controlling primary production in lakes and reservoirs: a perspective. *Lake Reservoir Manag.* 1, 277–281. doi: 10.1080/07438148409354524
- Knapp, C. W., Lima, L., Olivares-Rieumont, S., Bowen, E., Werner, D., and Graham, D. W. (2012). Seasonal variations in antibiotic resistance gene transport in the almedares river, havana, cuba. *Front. Microbiol.* 3:396. doi: 10.3389/fmicb.2012.00396
- Koike, S., Krapac, I. G., Oliver, H. D., Yannarell, A. C., Chee-Sanford, J. C., Aminov, R. I., et al. (2007). Monitoring and source tracking of tetracycline resistance genes in lagoons and groundwater adjacent to swine production facilities over a 3-year period. *Appl. Environ. Microbiol.* 73, 4813–4823. doi: 10.1128/aem.00665-07
- Li, X., Guo, S., Liu, P., and Chen, G. (2010). Dynamic control of flood limited water level for reservoir operation by considering inflow uncertainty. *J. Hydrol.* 391, 126–134. doi: 10.1016/j.jhydrol.2010.07.011
- Li, Z., Lu, L., Guo, J., Yang, J., Zhang, J., He, B., et al. (2017). Responses of spatial-temporal dynamics of bacterioplankton community to large-scale reservoir operation: a case study in the Three Gorges Reservoir. China. *Sci. Rep.* 7:42469. doi: 10.1038/srep42469
- Lin, L., Yuan, K., Liang, X., Chen, X., Zhao, Z., Yang, Y., et al. (2015). Occurrences and distribution of sulfonamide and tetracycline resistance genes in the Yangtze River Estuary and nearby coastal area. *Mar. Pollut. Bull.* 100, 304–310. doi: 10.1016/j.marpolbul.2015.08.036
- Liu, J., Lin, Z., Zhang, H., and Han, B.-P. (2012). Hydrodynamic change recorded by diatoms in sediments of Liuxihe Reservoir, southern China. *J. Paleolimnol.* 47, 17–27. doi: 10.1007/s10933-011-9543-8
- Loftin, K. A., Adams, C. D., Meyer, M. T., and Surampalli, R. (2008). Effects of ionic strength, temperature, and pH on degradation of selected antibiotics. *J. Environ. Qual.* 37, 378–386. doi: 10.2134/jeq2007.0230
- Luo, Y., Mao, D., Rysz, M., Zhou, Q., Zhang, H., Xu, L., et al. (2010). Trends in Antibiotic Resistance Genes Occurrence in the Haihe River. China. *Environ. Sci. Technol.* 44, 7220–7225. doi: 10.1021/es100233w
- Lupo, A., Coyne, S., and Berendonk, T. U. (2012). Origin and evolution of antibiotic resistance: the common mechanisms of emergence and spread in water bodies. *Front. Microbiol.* 3:18. doi: 10.3389/fmicb.2012.00018
- Matsui, Y., Ozu, T., Inoue, T., and Matsushita, T. (2008). Occurrence of a veterinary antibiotic in streams in a small catchment area with livestock farms. *Desalination* 226, 215–221. doi: 10.1016/j.desal.2007.01.243
- Ng, L. K., Martin, I., Alfa, M., and Mulvey, M. (2001). Multiplex PCR for the detection of tetracycline resistant genes. *Mol. Cell. Probes.* 15, 209–215. doi: 10.1006/mcpr.2001.0363
- Niu, Z. G., Zhang, K., and Zhang, Y. (2016). Occurrence and distribution of antibiotic resistance genes in the coastal area of the Bohai Bay, China. *Mar. Pollut. Bull.* 107, 245–250. doi: 10.1016/j.marpolbul.2016.03.064
- Patterson, A. J., Colangeli, R., Spigaglia, P., and Scott, K. P. (2007). Distribution of specific tetracycline and erythromycin resistance genes in environmental samples assessed by microarray detection. *Environ. Microbiol.* 9, 703–715. doi: 10.1111/j.1462-2920.2006.01190.x
- Pei, R., Cha, J., Carlson, K. H., and Pruden, A. (2007). Response of antibiotic resistance genes (ARG) to biological treatment in dairy lagoon water. *Environ. Sci. Technol.* 41, 5108–5113. doi: 10.1021/es070051x
- Pei, R., Kim, S.-C., Carlson, K. H., and Pruden, A. (2006). Effect of River Landscape on the sediment concentrations of antibiotics and corresponding antibiotic resistance genes (ARG). *Water Res.* 40, 2427–2435. doi: 10.1016/j.watres.2006.04.017
- Pruden, A., Pei, R., Storteboom, H., and Carlson, K. H. (2006). Antibiotic resistance genes as emerging contaminants: studies in Northern Colorado. *Environ. Sci. Technol.* 40, 7445–7450. doi: 10.1021/es0604131
- Rabolle, M., and Spliid, N. H. (2000). Sorption and mobility of metronidazole, olaquinox, oxytetracycline and tylosin in soil. *Chemosphere* 40, 715–722. doi: 10.1016/s0045-6535(99)00442-7
- Roberts, M. C. (2003). Tetracycline therapy: update. *Clin. Infect. Dis.* 36, 462–467. doi: 10.1086/367622
- Roberts, M. C. (2005). Update on acquired tetracycline resistance genes. *FEMS Microbiol. Lett.* 245, 195–203. doi: 10.1016/j.femsle.2005.02.034
- Sarmah, A. K., Meyer, M. T., and Boxall, A. B. (2006). A global perspective on the use, sales, exposure pathways, occurrence, fate and effects of veterinary antibiotics (VAs) in the environment. *Chemosphere* 65, 725–759. doi: 10.1016/j.chemosphere.2006.03.026
- Scott, J. T., Stanley, J. K., Doyle, R. D., Forbes, M. G., and Brooks, B. W. (2009). River-reservoir transition zones are nitrogen fixation hot spots regardless of ecosystem trophic state. *Hydrobiologia* 625, 61–68. doi: 10.1007/s10750-008-9696-2
- Sengupta, S., Chattopadhyay, M. K., and Grossart, H.-P. (2013). The multifaceted roles of antibiotics and antibiotic resistance in nature. *Front. Microbiol.* 4:47. doi: 10.3389/fmicb.2013.00047
- Siedlewicz, G., Bialk-Bielinska, A., Borecka, M., Winogradow, A., Stepnowski, P., and Pazdro, K. (2017). Presence, concentrations and risk assessment of selected antibiotic residues in sediments and near-bottom waters collected from the Polish coastal zone in the southern Baltic Sea - summary of 3 years of studies. *Mar. Pollut. Bull.* 129, 787–801. doi: 10.1016/j.marpolbul.2017.10.075
- Song, G., Sun, B., and Jiao, J. Y. (2007). Comparison between ultraviolet spectrophotometry and other methods in determination of soil nitrate-n. *Acta Pedol. Sin.* 44, 288–293. doi: 10.3321/j.issn:0564-3929.2007.02.014
- Stoll, C., Sidhu, J. P. S., Tiehm, A., and Toze, S. (2012). Prevalence of clinically relevant antibiotic resistance genes in surface water samples collected from Germany and Australia. *Environ. Sci. Technol.* 46, 9716–9726. doi: 10.1021/es302020s
- Su, H.-C., Pan, C.-G., Ying, G.-G., Zhao, J.-L., Zhou, L.-J., Liu, Y.-S., et al. (2014). Contamination profiles of antibiotic resistance genes in the sediments at a catchment scale. *Sci. Total Environ.* 490, 708–714. doi: 10.1016/j.scitotenv.2014.05.060
- Su, Y., Wang, J., Huang, Z., and Xie, B. (2017). On-site removal of antibiotics and antibiotic resistance genes from leachate by aged refuse bioreactor: effects of microbial community and operational parameters. *Chemosphere* 178, 486–495. doi: 10.1016/j.chemosphere.2017.03.063
- Sui, Q., Zhang, J., Tong, J., Chen, M., and Wei, Y. (2017). Seasonal variation and removal efficiency of antibiotic resistance genes during wastewater treatment of swine farms. *Environ. Sci. Pollut. Res. Int.* 24, 9048–9057. doi: 10.1007/s11356-015-5891-7
- Thornton, K. W., Kimmel, B. L., and Payne, F. E. (1990). *Reservoir Limnology: Ecological Perspectives*. Somerset, NJ: John Wiley & Sons, Inc.
- Wang, B.-Y., Yan, D.-C., Wen, A.-B., and Chen, J.-C. (2016). Influencing factors of sediment deposition and their spatial variability in riparian zone of the Three Gorges Reservoir. China. *J. Mt. Sci.* 13, 1387–1396. doi: 10.1007/s11629-015-3806-1
- Wang, F.-H., Qiao, M., Su, J.-Q., Chen, Z., Zhou, X., and Zhu, Y.-G. (2014). High throughput profiling of antibiotic resistance genes in urban park soils with reclaimed water irrigation. *Environ. Sci. Technol.* 48, 9079–9085. doi: 10.1021/es502615e
- Xiong, W., Wang, M., Dai, J., Sun, Y., and Zeng, Z. (2018). Application of manure containing tetracyclines slowed down the dissipation of tet resistance genes and caused changes in the composition of soil bacteria. *Ecotoxicol. Environ. Saf.* 147, 455–460. doi: 10.1016/j.ecoenv.2017.08.061
- Yan, C., Yang, Y., Zhou, J., Liu, M., Nie, M., Shi, H., et al. (2013). Antibiotics in the surface water of the Yangtze Estuary: occurrence, distribution and risk assessment. *Environ. Pollut.* 175, 22–29. doi: 10.1016/j.envpol.2012.12.008
- Yan, Q., Gao, X., Chen, Y.-P., Peng, X.-Y., Zhang, Y.-X., Gan, X.-M., et al. (2014a). Occurrence, fate and ecotoxicological assessment of pharmaceutically active compounds in wastewater and sludge from wastewater treatment plants in Chongqing, the Three Gorges Reservoir Area. *Sci. Total Environ.* 470, 618–630. doi: 10.1016/j.scitotenv.2013.09.032
- Yan, Q., Gao, X., Huang, L., Gan, X.-M., Zhang, Y.-X., Chen, Y.-P., et al. (2014b). Occurrence and fate of pharmaceutically active compounds in the

- largest municipal wastewater treatment plant in Southwest China: mass balance analysis and consumption back-calculated model. *Chemosphere* 99, 160–170. doi: 10.1016/j.chemosphere.2013.10.062
- Yang, Y., Cao, X., Lin, H., and Wang, J. (2016). Antibiotics and antibiotic resistance genes in sediment of Honghu Lake and East Dongting Lake, China. *Microb. Ecol.* 72, 791–801. doi: 10.1007/s00248-016-0814-9
- Yang, Y., Liu, W., Xu, C., Wei, B., and Wang, J. (2017). Antibiotic resistance genes in lakes from middle and lower reaches of the Yangtze River, China: effect of land use and sediment characteristics. *Chemosphere* 178, 19–25. doi: 10.1016/j.chemosphere.2017.03.041
- Yu, Z. T., Michel, F. C., Hansen, G., Wittum, T., and Morrison, M. (2005). Development and application of real-time PCR assays for quantification of genes encoding tetracycline resistance. *Appl. Environ. Microbiol.* 71, 6926–6933. doi: 10.1128/aem.71.11.6926-6933.2005
- Zhang, B., Fang, F., Guo, J., Chen, Y., Li, Z., and Guo, S. (2012). Phosphorus fractions and phosphate sorption-release characteristics relevant to the soil composition of water-level-fluctuating zone of Three Gorges Reservoir. *Ecol. Eng.* 40, 153–159. doi: 10.1016/j.ecoleng.2011.12.024
- Zhang, W., Sturm, B. S. M., Knapp, C. W., and Graham, D. W. (2009). Accumulation of tetracycline resistance genes in aquatic biofilms due to periodic waste loadings from swine lagoons. *Environ. Sci. Technol.* 43, 7643–7650. doi: 10.1021/es9014508
- Zhou, L. J., Ying, G. G., Zhao, J. L., Yang, J. F., Wang, L., Yang, B., et al. (2011). Trends in the occurrence of human and veterinary antibiotics in the sediments of the Yellow River, Hai River and Liao River in northern China. *Environ. Pollut.* 159, 1877–1885. doi: 10.1016/j.envpol.2011.03.034
- Zhou, T., Lu, J., Tong, Y., Li, S., and Wang, X. (2014). Distribution of antibiotic resistance genes in Bosten Lake, Xinjiang, China. *Water Sci. Technol.* 70, 925–931. doi: 10.2166/wst.2014.321
- Zhu, Y. G., Johnson, T. A., Su, J. Q., Qiao, M., Guo, G. X., Stedtfeld, R. D., et al. (2013). Diverse and abundant antibiotic resistance genes in Chinese swine farms. *Proc. Natl. Acad. Sci. U.S.A.* 110, 3435–3440. doi: 10.1073/pnas.1222743110

Conflict of Interest Statement: The authors declare that the research was conducted in the absence of any commercial or financial relationships that could be construed as a potential conflict of interest.

Copyright © 2018 Lu, Liu, Li, Liu, Guo, Xiao and Yang. This is an open-access article distributed under the terms of the Creative Commons Attribution License (CC BY). The use, distribution or reproduction in other forums is permitted, provided the original author(s) and the copyright owner(s) are credited and that the original publication in this journal is cited, in accordance with accepted academic practice. No use, distribution or reproduction is permitted which does not comply with these terms.



Genetic Differentiation, Diversity, and Drug Susceptibility of *Candida krusei*

Jie Gong^{1†}, Meng Xiao^{2,3†}, He Wang^{2,3}, Timothy Kudinha^{4,5}, Yu Wang⁶, Fei Zhao¹, Weiwei Wu⁷, Lihua He¹, Ying-Chun Xu^{2,3*} and Jianzhong Zhang^{1*}

¹ State Key Laboratory of Infectious Disease Prevention and Control, Collaborative Innovation Center for Diagnosis and Treatment of Infectious Diseases, National Institute for Communicable Disease Control and Prevention, Chinese Center for Disease Control and Prevention, Beijing, China, ² Department of Clinical Laboratory, Peking Union Medical College Hospital, Chinese Academy of Medical Sciences, Beijing, China, ³ Beijing Key Laboratory for Mechanisms Research and Precision Diagnosis of Invasive Fungal Diseases, Beijing, China, ⁴ School of Biomedical Science, Charles Sturt University, Orange, NSW, Australia, ⁵ Central West Pathology Laboratory, Orange, NSW, Australia, ⁶ Key Laboratory of Wildlife Biotechnology, Conservation and Utilization of Zhejiang Province, Zhejiang Normal University, Jinhua, China, ⁷ Department of Dermatology, Hainan Provincial Center for Skin Disease and STI Control, Haikou, China

OPEN ACCESS

Edited by:

Silvia Buroni,
University of Pavia, Italy

Reviewed by:

Paula Sampaio,
University of Minho, Portugal
Avi Peretz,
The Baruch Padeh Medical Center,
Poriya, Israel
Sona Kucharikova,
University of Trnava, Slovakia

*Correspondence:

Ying-Chun Xu
xycpumch@139.com
Jianzhong Zhang
Zhangjianzhong@icdc.cn

[†]These authors have contributed
equally to this work

Specialty section:

This article was submitted to
Evolutionary and Genomic
Microbiology,
a section of the journal
Frontiers in Microbiology

Received: 19 July 2018

Accepted: 24 October 2018

Published: 20 November 2018

Citation:

Gong J, Xiao M, Wang H, Kudinha T,
Wang Y, Zhao F, Wu W, He L, Xu Y-C
and Zhang J (2018) Genetic
Differentiation, Diversity, and Drug
Susceptibility of *Candida krusei*.
Front. Microbiol. 9:2717.
doi: 10.3389/fmicb.2018.02717

Candida krusei is a notable pathogenic fungus that causes invasive candidiasis, mainly due to its natural resistance to fluconazole. However, to date, there is limited research on the genetic population features of *C. krusei*. We developed a set of microsatellite markers for this organism, with a cumulative discriminatory power of 1,000. Using these microsatellite loci, 48 independent *C. krusei* strains of clearly known the sources, were analyzed. Furthermore, susceptibility to 9 antifungal agents was determined for each strain, by the Clinical and Laboratory Standards Institute broth microdilution method. Population structure analyses revealed that *C. krusei* could be separated into two clusters. The cluster with the higher genetic diversity had wider MIC ranges for six antifungal agents. Furthermore, the highest MIC values of the six antifungal agents belonged to the cluster with higher genetic diversity. The higher genetic diversity cluster might have a better adaptive capacity when *C. krusei* is under selection pressure from antifungal agents, and thus is more likely to develop drug resistance.

Keywords: *Candida krusei*, invasive candidiasis, genetic differentiation, genetic diversity, microsatellites, drug susceptibility

INTRODUCTION

Invasive candidiasis is the most common fungal disease among hospitalized patients, and affects more than 250,000 people worldwide annually, with more than 50,000 deaths reported (Kullberg and Arendrup, 2015). In the *Candida* genus, *Candida krusei* attracts much medical attention because it is intrinsically resistant to fluconazole (Akova et al., 1991; Schuster et al., 2013). In addition, *C. krusei* exhibits resistance to other antifungal drugs such as voriconazole, echinocandins, and amphotericin B (Fukuoka et al., 2003; Hakki et al., 2006; Pfaller et al., 2008). It has been known for some time that mutations in *ERG11* and *FKS 1* genes are the major mechanisms responsible for azole- and echinocandin-resistance in *Candida* species, including *C. krusei* (Jensen et al., 2014; Forastiero et al., 2015; Feng et al., 2016; Perlin et al., 2017). In addition, antifungal resistance can be acquired by over-expression of efflux pump e.g., Abc1p (Lamping et al., 2009; Ricardo et al., 2014). However, there have been some *C. krusei* antifungal resistant phenotypes, including resistance to azoles other than fluconazole and to echinocandins e.g., caspofungin, that cannot be explained by currently known mechanisms of resistance (Hakki et al., 2006; Whaley et al., 2017).

From an evolutionary perspective, drug resistance in a microorganism is part of the adaptive evolutionary response of a species to environmental pressures (Salmond and Welch, 2008). Nowadays, the environmental pressure of antifungal drugs comes not only from the use of clinical drugs, but also from the use of agricultural drugs (Sanglard, 2016).

The adaptive capacity is usually related to the level of genetic diversity. From the points of molecular ecology, genetic diversity can allow species or populations to adapt quickly to changing environment conditions and different habitats (Freeland et al., 2011). Similarly, from the perspective of conservation genetics, genetic diversity allows species or populations to tolerate a wider range of environmental changes, including bacteria, fungi and so on. Also, genetic diversity is helpful to maintain the evolutionary vigor (Frankham et al., 2010). In general, a higher genetic diversity enables the organism to respond better to new selection pressures (McDonald and Linde, 2002). When there was a selection pressure for exogenous antifungal agents, the more genetic diversity the fungal populations had, the higher the probability of survival. In other words, antifungal agents were the directional selection factors from Darwin's theory of Evolution. If the genetic diversity of the fungal population was high, there might be some individual death under the pressure of drug selection, but some individuals carrying different genes would survive. Therefore, it is reasonable to hypothesize that

microbial populations with higher genetic diversity are more likely to develop antimicrobial drug resistance.

However, to our best knowledge, no research targeting the genetic population features of *C. krusei* has been carried out to date. This is partly due to the lack of a flexible molecular typing method. Therefore, in this study, we (1) developed a novel set of microsatellite markers for molecular typing and population genetic analysis of *C. krusei*; (2) used the developed assay to type 48 multicenter collected *C. krusei* clinical strains; and (3) analyzed the correlation between genetic diversity and drug susceptibility among the studied strains.

MATERIALS AND METHODS

Ethics Statement

This study was reviewed and approved by the ethics committee of the National Institute for Communicable Disease Control and Prevention, Chinese CDC. Written informed consent was obtained from patients for use of the samples in research.

Isolate Collection and Identification

A total of 48 *C. krusei* isolates, each from a single patient, were collected from 15 hospitals distributed in 10 cities across China during the period 2009–2012, as part of the national surveillance program for invasive fungal infections (the

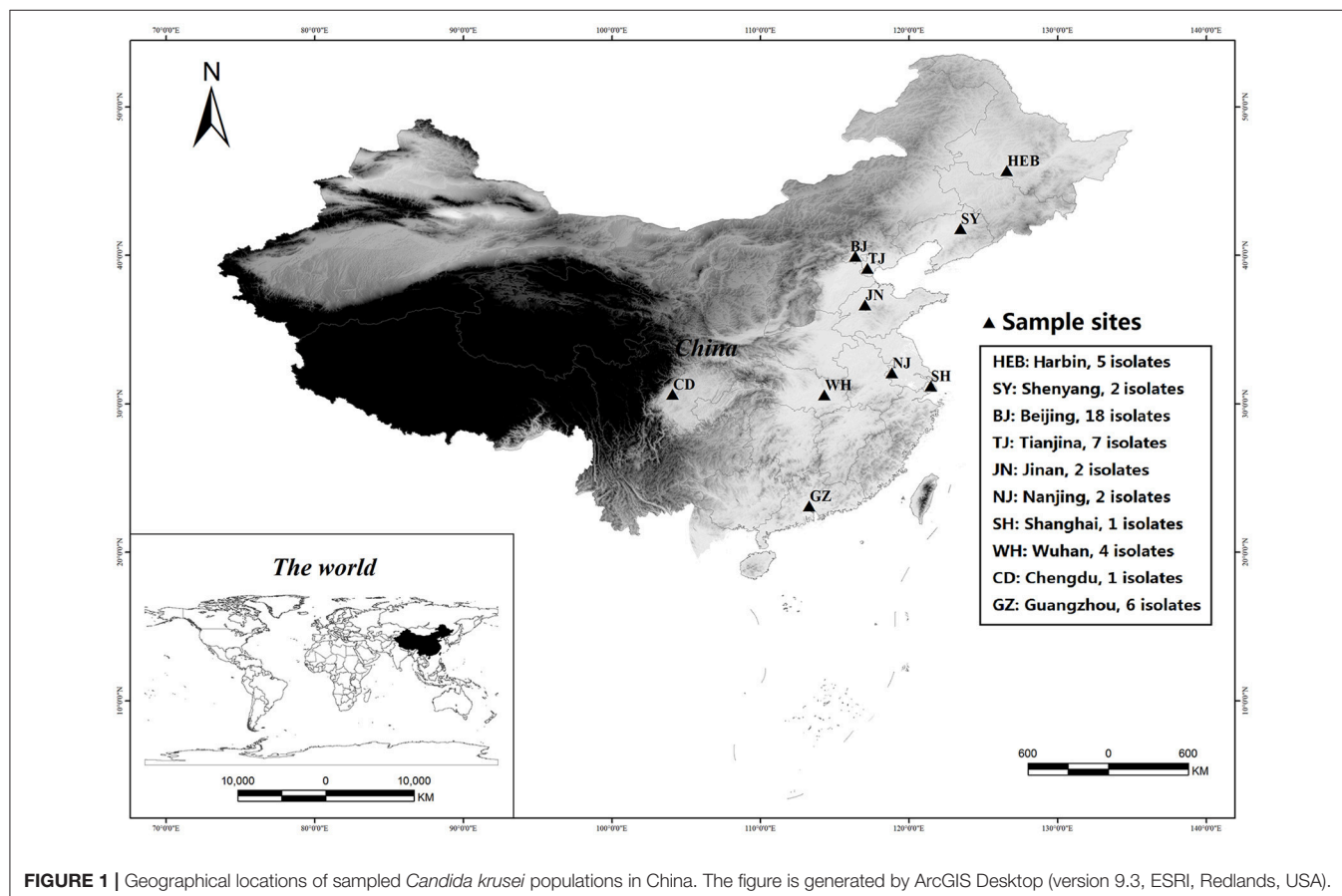


FIGURE 1 | Geographical locations of sampled *Candida krusei* populations in China. The figure is generated by ArcGIS Desktop (version 9.3, ESRI, Redlands, USA).

TABLE 1 | Characterization of *Candida krusei* microsatellite loci.

Locus	Primer sequences (5'–3')	Ta ^a (°C)	Repeat type	Size range (bp)	No. of alleles	PIC ^b	DP ^c	NCBI accession
Cakr001	ACGGACCCACAACATCAAC GAAGGGGAGGTAAGGAGA	56	(AT) ₁₁	381–394	7	0.663	0.701	MH079517
Cakr002	GTAGAACCCGTATGAGGAC GTAGAACCCGTATGAGGAC	52	(TA) ₁₃	293–303	6	0.708	0.750	MH079518
Cakr003	CATATCACTATGACATTCCA TCCATCTATCCGCAACAAG	52	(TCT) ₁₁	284–272	5	0.604	0.663	MH079519
Cakr004	AAGGACGGTGCTTTCAATC TTTACGACGGTTTCCAGTG	59	(TAT) ₁₂	365–401	11	0.739	0.768	MH079520
Cakr005	CAGTCAACTCGCCCTCCCT CAGTGTTTGTGCCTGTGCC	62	(AAT) ₁₇	311–362	16	0.867	0.878	MH079521
Cakr006	TAGTTTCGGGACTCTGTAT TCACGTTGTAACCGAGGTA	56	(TC) ₁₂	362–370	5	0.551	0.621	MH079522
Cakr007	GTAGGCGCGAAGGAAGAT TAACAACAGCAACCGAAAG	59	(TCA) ₁₁ T(CAT) ₉	174–261	8	0.803	0.826	MH079523
Cakr008	AGCACCCGTAAAACCTAC ATCTACAAGCGTTCTAAAT	52	(TA) ₁₂	245–257	6	0.665	0.716	MH079524
Cakr009	AGTATCCGAGTCTGGTTTA GGTAGGCTTCTCAGTTTTA	56	(AGA) ₁₀	223–256	9	0.561	0.586	MH079525
Cakr010	TTGTCGGATTGTGGTAAG CATCGTCAGCATTTTCACT	54	(GAA) ₁₀	278–323	7	0.586	0.640	MH079526
Cakr011	AGTTGGAGTTGTGGGGAGA GAGACGGGTTACCAAGGAT	62	(CTTGAC) ₁₃	357–453	13	0.822	0.837	MH079527
Cakr012	GCAATGTCGGAATGAAGTAG AAGGACGAGAACAGCAAGAA	59	(AT) ₁₁	346–356	6	0.711	0.750	MH079528
Cakr013	TTGGTAAGTTGGTGGGACG ACATTGGGAAGCGGAAGAA	59	(AT) ₁₀	246–252	4	0.335	0.356	MH079529
Cakr014	CCAAGGCAATGTCAGGAAC TTGTAGAGGACGGAATCTC	59	(TG) ₁₈	178–190	6	0.714	0.751	MH079530
Cakr015	CTCCTGGCATTGCCGTTAT AAGCGGGAAAGTTGTAGATT	59	(AC) ₁₁	295–305	5	0.696	0.742	MH079531
Cakr016	TAACTAAACACGTTTACCA TTTAGGATTGCTCTTTCA	54	(AT) ₁₀	193–199	4	0.313	0.350	MH079532
Cakr017	GACAAGAAATGCGGGAACC GGCGATGACAGCGATAGTG	59	(AT) ₁₀	284–314	7	0.661	0.703	MH079533
Cakr018	CATCGGAGGCTGGTAAATA TACGGAGTCGTCCTTGAT	59	(TA) ₁₁	284–294	6	0.604	0.658	MH079534
Cakr019	CGATTTCTAGTGTTAGT ATACTCTTAGCCCTGATACA	54	(TCA) ₁₁	225–264	11	0.695	0.717	MH079535
Cakr020	TCCACAAACACCGAAACACT ATAGACATGGCCAAATGAG	59	(AAC) ₁₁	275–311	9	0.735	0.771	MH079536
Cakr021	AGACCAACAGAGGAGGGACA ACGATAAATGATTTTCAAGC	56	(TA) ₁₁	343–365	9	0.789	0.814	MH079537
Cakr022	CGTTTATTCATGCCTTCCTC TAATGGTAATGCGGCTGATG	59	(AT) ₁₀	310–316	4	0.463	0.539	MH079538
Cakr023	GTTAGTGGCACCAAGAGGA GATGATGACTTCAAGGACGG	59	(TA) ₁₁	267–286	9	0.638	0.690	MH079539
Cakr024	CTGACACTACTATTTATTGGGATG TGTTTGGTATGATATCAATGTGC	56	(AAC) ₁₀	398–425	9	0.539	0.565	MH079540
Cakr025	AAACAGGGAAAGAATCATAA TGTATTGTAGCACCTAAAGC	54	(AC) ₁₀	263–321	11	0.683	0.728	MH079541

(Continued)

TABLE 1 | Continued

Locus	Primer sequences (5'–3')	Ta ^a (°C)	Repeat type	Size range (bp)	No. of alleles	PIC ^b	DP ^c	NCBI accession
Cakr026	GGCATGGTTTGTGTCGTGT GAGGGGACTTGGCAGAGGGA	59	(TA) ₁₀	294–314	11	0.699	0.720	MH079542
Cakr027	CGAAGTTTTGGTTCTTTAA CATTACCAATCCTTGTTAC	54	(AT) ₁₀	270–286	8	0.663	0.695	MH079543
Cakr028	TTGGAAGCAACTTAGAGTC TAGGTCTAAAGCAGAACGAG	56	(AT) ₁₀	248–254	4	0.652	0.708	MH079544
Cakr029	GTCTAGTCTCGCAATACCTC CTCTTTGGATTTCCTTTTAT	54	(CA) ₁₀ (CT) ₁₇	246–286	14	0.801	0.822	MH079545
Cakr030	AAACTCGGAATCTCCAAACG GTACCACTGGGCGAAAACAA	59	(CTT) ₁₁	147–168	8	0.557	0.581	MH079546
Cakr031	CCTGTGTGGTAATAGTTTTC CTAACGAGGAAGTTGTATGT	52	(TCT) ₁₀	347–392	10	0.636	0.659	MH079547
Cakr032	TGCGTTTCTCAGAGGCTGTT GTGGGGATAGGTGTTTGGTG	56	(TC) ₁₀	193–203	5	0.488	0.550	MH079548
Cakr033	GCGCTTCAGTGGTAGTCATA TTCCAGAACTTGAACTCGTC	56	(CAA) ₁₁	265–289	6	0.701	0.739	MH079549
Mean	–	–	–	–	7.848	0.647	–	–
Overall	–	–	–	–	–	–	1.000	–

^aAnnealing temperature; ^bPolymorphic information content; ^cdiscriminatory power.

CHIF-NET study, **Figure 1** and **Supplemental A**). The isolates were stored at -80°C until use at Peking Union Medical College Hospital, Beijing, China (PUMCH). Before testing, the isolates were inoculated on CHROMagarTM *Candida* medium (Difco Laboratories, Detroit, MI, USA) and incubated at 37°C for 24 h. Species identification of the isolates was confirmed by matrix-assisted laser desorption/ionization-time of flight mass spectrometry (MALDI-TOF MS, Vitek MS, bioMérieux, Marcy-l'Etoile, France) as per manufacturer's instructions, and by sequence analysis of their rDNA internal transcribed spacer (ITS) regions (Wang et al., 2012). The identities of all the isolates was confirmed by sequencing.

DNA Extraction, Microsatellite Development, and Genotyping

All the fungal isolates were grown on potato dextrose agar at 37°C for 24 h. DNA extraction was performed using a QIAamp DNA Mini Kit (Qiagen, Hilden, Germany).

The software SciRoKo was used to identify microsatellites in the *C. krusei* genome (GenBank assembly accession: GCA_001983325.1, Kofler et al., 2007; Cuomo et al., 2017). Primers were designed using Primer premier 5.0 (PREMIER Biosoft International, Palo Alto, CA, USA) in regions flanking microsatellite loci, and annealing temperatures were optimized with a gradient PCR. Polymorphic microsatellite loci were selected for molecular typing and population genetic analysis of *C. krusei*. There were two criteria used for selection of microsatellite loci: first, the locus had to have a relatively high genetic polymorphism (the number of alleles was >3); second, the locus could be amplified relatively stable. The microsatellite

loci would be abandoned if the loci was not amplified in more than two strains.

For the 33 selected microsatellite loci (**Table 1**), PCR was performed on 48 clinical isolates. Amplification was carried out using a *Taq* polymerase kit (Takara, Dalian, China). Each of the amplification reactions was composed of $1 \times$ PCR buffer, $0.2 \mu\text{M}$ dNTP, 0.5 U *Taq* polymerase, $0.2 \mu\text{M}$ each primer, and $2 \mu\text{l}$ genomic DNA ($20\text{--}50 \text{ ng}/\mu\text{l}$). The thermocycler conditions were as follows: initial denaturation at 95°C for 5 min, followed by 35 cycles of denaturation at 94°C for 30 s, annealing at an optimized primer-specific annealing temperature for 30 s (**Table 1**), extension at 72°C for 30 s and final extension at 72°C for 10 min. The primers for these selected loci were fluorescently labeled with 6-carboxy-fluorescein (6-FAM). Allele length was determined by migration of PCR products on an ABI 3,700 automated capillary DNA sequencer (Applied Biosystems). Allele sizes were assigned with GeneMapper software (version 3.7) according to an internal size standard (LIZ 500, Applied Biosystems).

Antifungal Susceptibility Testing

The *in vitro* susceptibility to nine antifungal drugs- fluconazole, voriconazole, itraconazole, posaconazole, caspofungin, micafungin, anidulafungin, amphotericin B, and 5-flucytosine, was determined for 48 isolates using the Clinical and Laboratory Standards Institute (CLSI) broth microdilution method²². Minimum inhibitory concentration (MIC) results for fluconazole, voriconazole, caspofungin, micafungin, and anidulafungin, were interpreted using clinical breakpoints in accordance with the CLSI guidelines (CLSI, 2017), and those for itraconazole, posaconazole, amphotericin B, and 5-flucytosine,

were interpreted using epidemiological cut-off values (Xiao et al., 2014). The quality control strains used were *C. krusei* ATCC 6,258 and *Candida parapsilosis* ATCC 22,019.

Data Analysis

Deviation from Hardy-Weinberg equilibrium was computed using GENEPOP version 4 (Rousset, 2008). Hardy-Weinberg equilibrium was tested using the score test for heterozygote deficiency and the significance was addressed by a Markov Chain algorithm (Markov chain parameters: dememorization number = 2,000, number of batches = 250, number of iterations per batch = 2,000).

The discriminatory power of markers was calculated according to the method of Hunter and Gaston (1988). Number of alleles (n_A), effective number of alleles (n_e), Shannon's Information Index (I), and Nei's unbiased gene diversity (H_S), were calculated using GENALEX 6.5 (Peakall and Smouse, 2012). Allelic Richness (AR) was calculated by FSTAT 2.9.3 (Goudet, 1995). Ne, I, H_S , and AR were used to measure genetic variability of populations.

Population composition was inferred for the *C. krusei* isolates using the program Structure 2.3 (Pritchard et al., 2000), which estimates the log probability of the data for each value of K (number of clusters or populations). A series of independent runs were performed by using K from 1 to 12 populations, a burn-in of 100,000 Markov chain Monte Carlo (MCMC) iterations, and a data collection period of 100,000 MCMC iterations. Each simulation of K was replicated 10 times. The method of Evanno et al. (2005) was used to estimate the most likely K given the data with Structure Harvester (Earl, 2012). The level of genetic differentiation at microsatellite loci among clusters was estimated as F_{ST} , which is simply a measure of how genetically similar populations are to one another. F_{ST} was calculated using Arlequin 3.5 (Excoffier and Lischer, 2010). Principal coordinates analysis (PCoA) of F_{ST} value among clusters was calculated using GenAlEx (Peakall and Smouse, 2012).

For antifungal susceptibility results, MIC₅₀, MIC₉₀, and geometric mean (GM) MIC values were calculated using WHONET software (version 5.6, WHO Collaborating Center for Surveillance of Antimicrobial Resistance, Boston, USA).

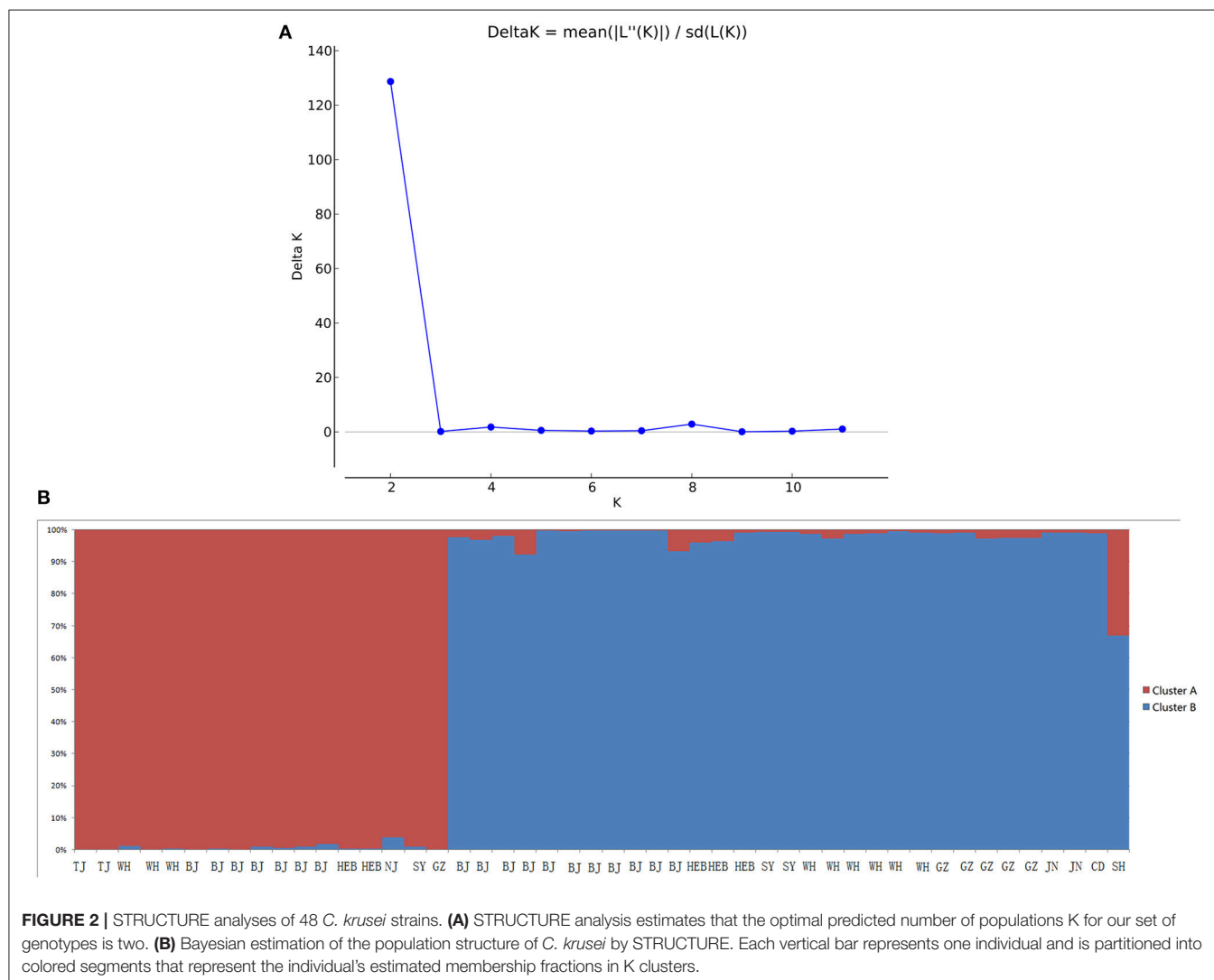


FIGURE 2 | STRUCTURE analyses of 48 *C. krusei* strains. **(A)** STRUCTURE analysis estimates that the optimal predicted number of populations K for our set of genotypes is two. **(B)** Bayesian estimation of the population structure of *C. krusei* by STRUCTURE. Each vertical bar represents one individual and is partitioned into colored segments that represent the individual's estimated membership fractions in K clusters.

RESULTS

Microsatellite Loci of *C. krusei*

Based on the genome of *C. krusei*, a total of 200 microsatellite loci were identified, and primers were designed (data not shown). Of these microsatellite loci, 33 polymorphic microsatellite loci (Cakr 001–Cakr 033) could be stably amplified in all *C. krusei* isolates (Table 1). The cumulative discriminatory power of the 33 loci was 1.000. If only 8 polymorphic sites with the highest polymorphism were selected (Cakr004, Cakr005, Cakr011, Cakr019, Cakr025, Cakr026, Cakr029, Cakr031), it was found that the cumulative discriminatory power would still be 1.000. This might mean that the molecular typing of strains

could be achieved effectively by using only these 8 microsatellite loci. All loci showed significant deviation from Hardy-Weinberg equilibrium ($P < 0.05$).

In addition, it must be noted that many isolates were heterozygote (Supplemental A).

Genetic Differentiation and Diversity

When performing STRUCTURE analyses, the clustering level $K = 2$ yielded the largest delta-K value (Figure 2A). At $K = 2$, individual isolates could be assigned to two clusters (Figure 2B). Cluster A included 17 strains and cluster B 31 strains. There was no clear relationship between cluster patterns and geographical source of the isolates, and between cluster patterns and disease

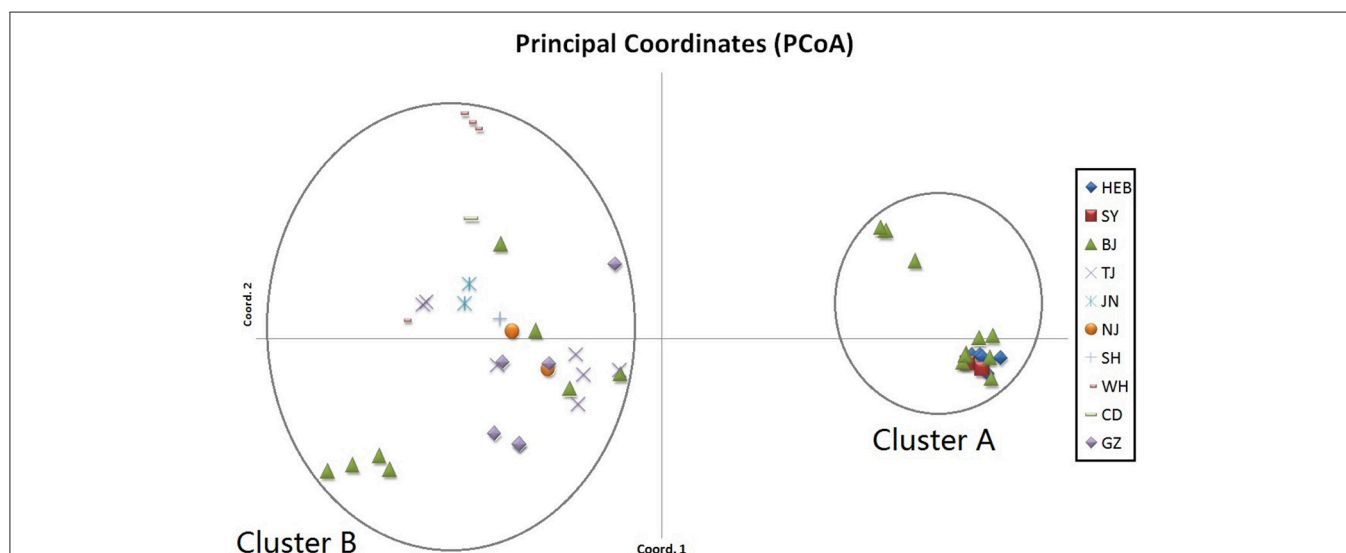


FIGURE 3 | Results of principal coordinate analysis (PCoA) of *C. krusei* clusters. Using estimates of Nei's unbiased genetic distance supports 2 main subgroups, which corresponded to the 2 clusters divided by STRUCTURE software.

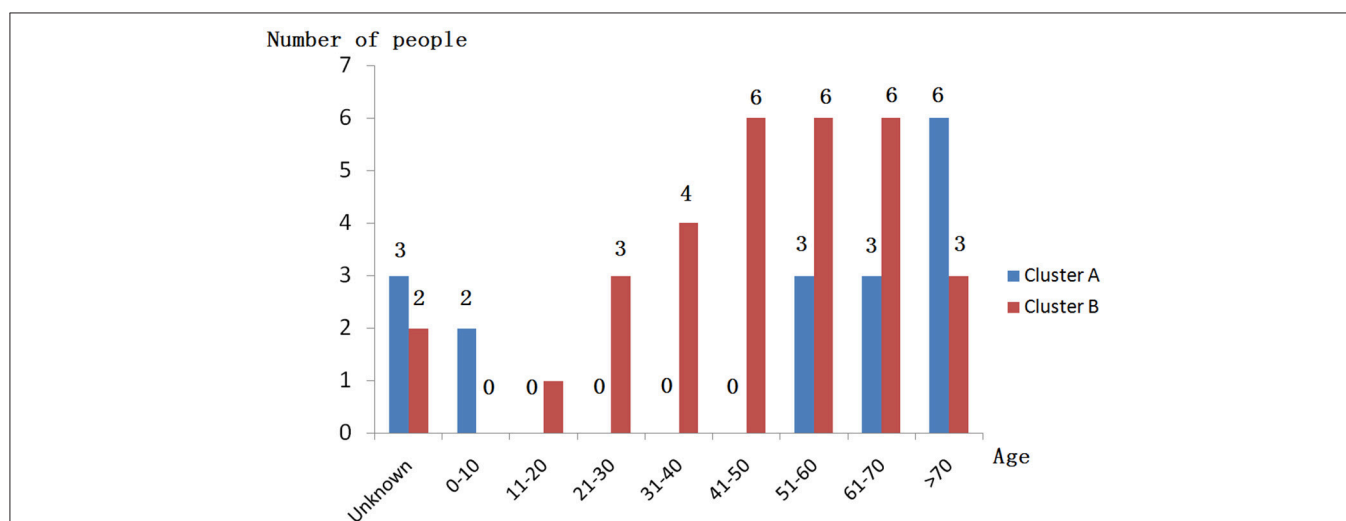


FIGURE 4 | Age distribution of patients isolated from strains of two clusters.

clinical manifestations. The F_{ST} between the two clusters was 0.188 ($P < 0.01$). The principal coordinate analysis (PCoA) supported the result of the STRUCTURE analyses (Figure 3), suggesting that the population of *C. krusei* was divided into two lineages. The PCoA also suggested that two lineages would both consist of strains from different geographical origins and clinical manifestations of disease. However, if patients from whom the isolates were obtained is considered, there appears to be some differences between the two clusters. The hosts of Cluster A strains were mainly children younger than 10 years old or aged people older than 50 years old. In contrast, the hosts of Cluster B covered almost all age groups (Figure 4). Furthermore, the specimen types of Cluster B are also more complex than Cluster A (Figure 5).

The genetic diversity of *C. krusei* was assessed by Shannon's Information Index, Nei's unbiased gene diversity and allelic richness. These indices are shown in Table 2. Four indices (Mean number of effective alleles, Shannon's Information Index, Nei's unbiased gene diversity, allelic richness), all showed that there was a higher genetic diversity in cluster B.

In vitro Susceptibilities

All isolates were intrinsically resistant to fluconazole (MICs ≥ 16 mg/L; Figure 6, Supplemental A). Of the other eight antifungal agents tested, all isolates were susceptible or of wild-type phenotype to voriconazole, itraconazole, posaconazole, anidulafungin, micafungin, 5-flucytosine, and amphotericin B. Only two of 48 isolates (4.2%) were interpreted as intermediate to caspofungin, both of which belonged to microsatellite cluster B, while the rest 95.8% (46/48) isolates remained susceptible to caspofungin (Figure 6, Supplemental A).

The Geometric mean (GM) MIC, MIC₅₀, and MIC₉₀ of the two clusters were generally similar, while the MIC range differed between the two clusters (Table 3, Figure 6). For most antifungal agents (6/9) (including caspofungin, posaconazole, voriconazole,

itraconazole, fluconazole, amphotericin B), cluster B had a wider MIC range. It is worth noting that the highest MIC values of all 6 antifungal agents were confined to cluster B.

DISCUSSION

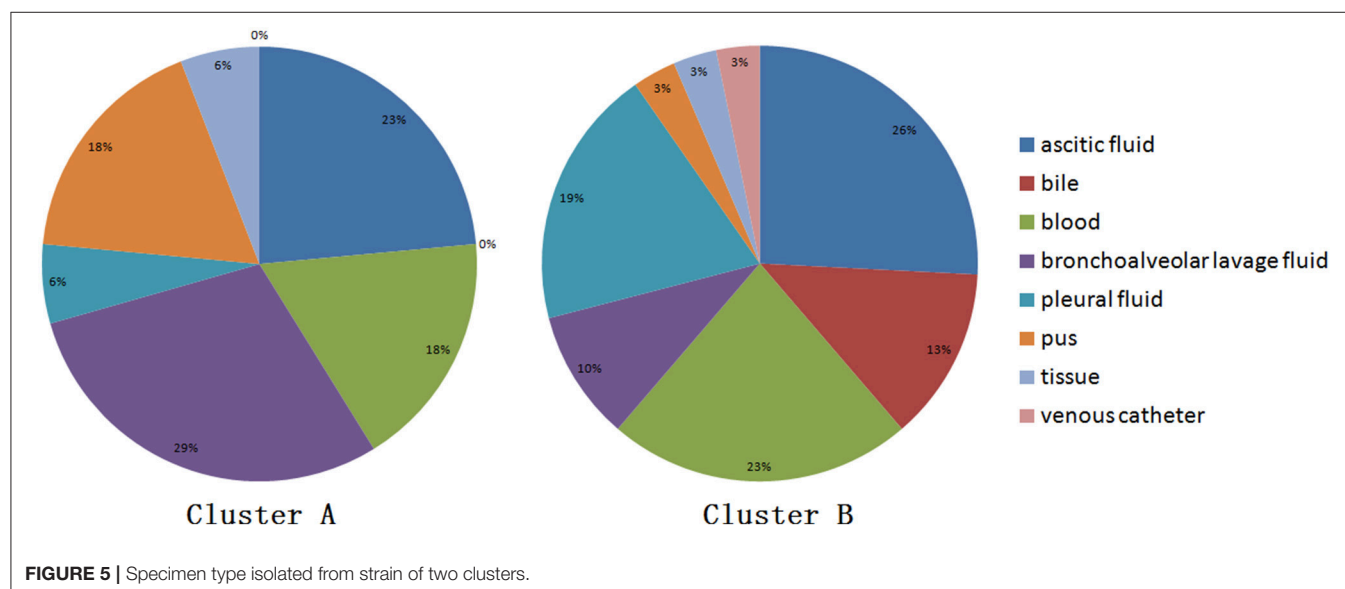
The correlation between genetic diversity and adaptive capacity of the population has long been studied in the field of molecular ecology. For example, it was found that the *Arabidopsis thaliana* population with higher genetic diversity had better colonization success (Crawford and Whitney, 2010). In principle, the process of fungal infection and clinical manifestation of disease is also considered a colonization success. Unfortunately, very few studies have been done on fungal infections and drug-resistance from the perspective of population genetics. In this study, we carried out a comprehensive analysis of the population genetic features and drug resistance, and attempted to elucidate the drug resistance of *C. krusei* from an evolutionary perspective.

Although an important pathogenic fungal species, the population genetic parameters of *C. krusei* have remained largely unknown. In this study, a novel array of microsatellite markers was developed for molecular typing and population genetic analysis of the species. The discriminatory index of the new

TABLE 2 | Genetic diversity of *Candida krusei* subgroups.

Subgroup	Number of strains	N_A^a	N_e^b	I^c	H_S^d	AR^e
Cluster A	17	2.545	1.865	0.645	0.416	2.527
Cluster B	31	7.667	4.186	1.583	0.737	6.659
Total	48	5.106	3.025	1.114	0.576	6.165

^aMean number of alleles; ^bMean number of effective alleles; ^cShannon's Information Index; ^dNei's unbiased gene diversity; ^eAllelic richness.



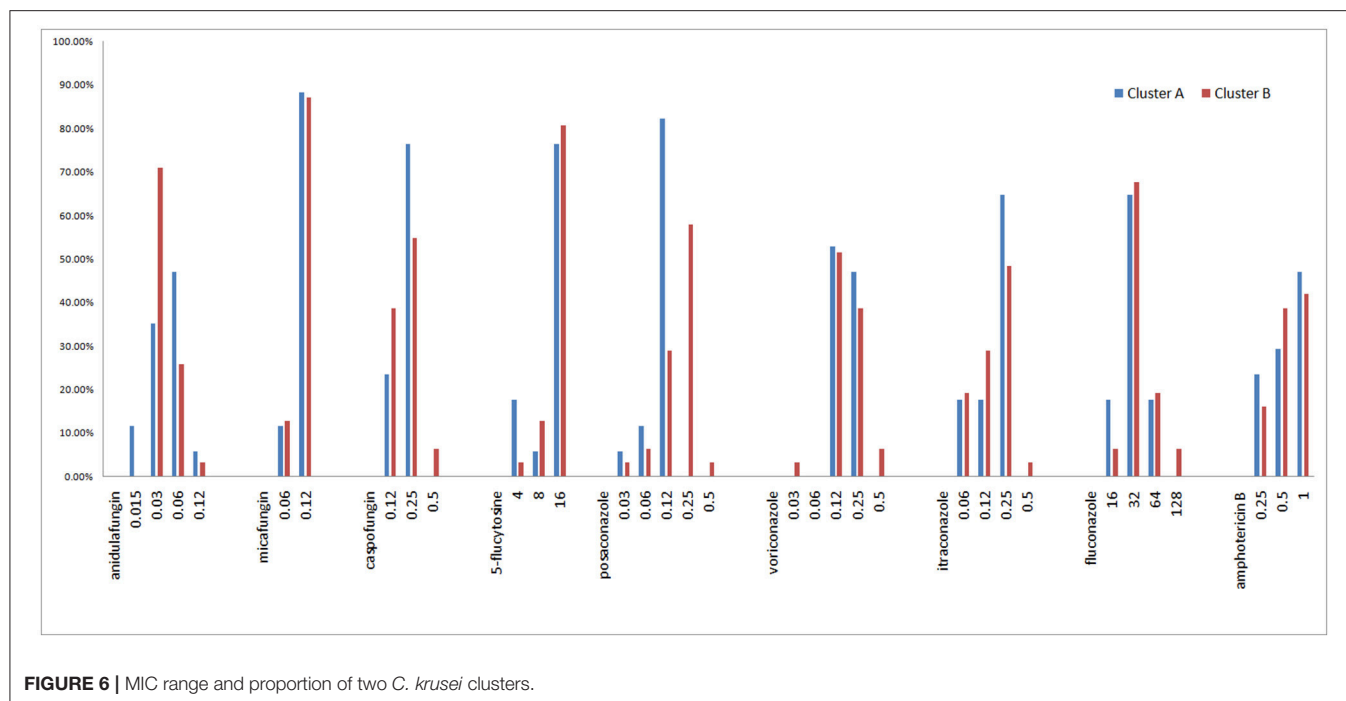


FIGURE 6 | MIC range and proportion of two *C. krusei* clusters.

TABLE 3 | GM MIC, MIC₅₀, MIC₉₀, and MIC range of *C. krusei* subgroups.

Subgroup		Anidulafungin (μg/ml)	Micafungin (μg/ml)	Caspofungin (μg/ml)	5-Flucytosine (μg/ml)	Posaconazole (μg/ml)	Voriconazole (μg/ml)	Itraconazole (μg/ml)	Fluconazole (μg/ml)	Amphotericin B (μg/ml)
Cluster A	GM MIC ^a	0.04	0.11	0.21	12.03	0.15	0.17	0.17	32.00	0.59
	MIC ₅₀ ^b	0.06	0.12	0.25	16	0.25	0.12	0.25	32	0.5
	MIC ₉₀ ^c	0.06	0.12	0.25	16	0.25	0.25	0.25	64	1
	MIC range	0.015–0.12	0.06–0.12	0.12–0.25	4–16	0.03–0.25	0.12–0.25	0.06–0.25	16–64	0.25–1
Cluster B	GM MIC	0.04	0.11	0.20	13.68	0.18	0.17	0.16	38.27	0.63
	MIC ₅₀	0.03	0.12	0.25	16	0.25	0.12	0.25	32	0.5
	MIC ₉₀	0.06	0.12	0.25	16	0.25	0.25	0.25	64	1
	MIC range	0.03–0.12	0.06–0.12	0.12–0.5	4–16	0.03–0.5	0.03–0.5	0.06–0.5	16–128	0.25–2
Overall	GM MIC	0.04	0.11	0.20	13.07	0.17	0.17	0.16	35.92	0.61
	MIC ₅₀	0.03	0.12	0.25	16	0.25	0.12	0.25	32	0.5
	MIC ₉₀	0.06	0.12	0.25	16	0.25	0.25	0.25	64	1
	MIC range	0.015–0.12	0.06–0.12	0.12–0.5	4–16	0.03–0.5	0.03–0.5	0.06–0.5	16–128	0.25–2

^aGeometric mean Minimum inhibitory concentration; ^bMean minimal inhibitory concentrations against 50 percent of strains; ^cMean minimal inhibitory concentrations against 90 percent of strains.

method (1.000) was slightly higher than MLST, which exhibited a discriminatory index of 0.998 (Jacobsen et al., 2007). It has been shown by Cuomo et al. (2017) that the genome of *C. krusei* is highly heterozygous, and this was also confirmed in the present study. For all microsatellite loci, there were some heterozygous individual isolates. As previously described in *Candida albicans*, a significant departure from Hardy-Weinberg equilibrium expectations was found (Sampaio et al., 2003). This finding supports the previous conclusions that reproduction in *C. krusei* is mainly clonal.

Based on the STRUCTURE software analysis, the *C. krusei* population in China appears to be divided into two clusters,

a result which was also supported by PCoA. The two clusters showed no obvious differences with respect to geographical distribution of the isolates. These findings are very similar to those of another pathogenic fungus, *Trichophyton rubrum*, which was also divided into two clusters with similar geographical distributions of the clusters (Gong et al., 2016). For pathogenic fungi, it might be a common phenomenon that different clusters of the same organism co-exist in the same geographical locale. Dispersal of pathogenic fungi is generally affected by host activity. It is highly possible that *C. krusei* strains of different clusters existed in different geographical areas and were carried to the same geographical area by hosts including humans. When the

survival capacity of different clusters is similar, it indicates that the different clusters co-existed in the same area. However, there were significant differences in host age between the two clusters, which might suggest that cluster B strains have a higher pathogenicity. Moreover, the type of specimens in Cluster B were also more complicated and seemed to confirm this. However, this is only a hypothesis, and more work needs to be done to demonstrate these findings in animal infection model experiments.

Cluster B had a higher genetic diversity which suggests a better adaptive capacity for survival in challenging conditions. As previously mentioned, the population with a higher genetic diversity is more likely to develop antimicrobial drug resistance. In our study, cluster B had a wider MIC range for 6 antifungal drugs, although there was no obvious difference in GM MIC, MIC₅₀, and MIC₉₀ between the two clusters. Specifically, the strains with the highest MIC value were either in the current group B (including 6 drugs: caspofungin, posaconazole, voriconazole, itraconazole, fluconazole, and amphotericin B), or both in group A and group B (including 3 drugs: anidulafungin, micafungin, and 5-flucytosine). Meanwhile, there was no strain with the highest MIC value was observed in Cluster A. These findings suggest that the population with higher genetic diversity may have more diverse phenotypes, including drug resistance. When subjected to selective pressure from antifungal drugs, cluster B might have a better adaptive capacity, and thus would be more likely to develop drug resistance. This suggests that the *C. krusei* population or lineage with higher genetic diversity needs more attention in terms of fungal drug resistance.

In conclusion, *C. krusei* was divided into two clusters by novel high-resolution microsatellite markers. The cluster with higher

genetic diversity had wider MIC ranges for six antifungal agents, and the highest MIC values of the six antifungal agents belonged to the cluster of higher genetic diversity. It is plausible that the *C. krusei* cluster with higher genetic diversity might have better adaptive capacity when under the selection pressure of antifungal agents.

AUTHOR CONTRIBUTIONS

JZ and Y-CX designed the experiments. JG, MX, HW, FZ, LH, and WW collected the samples and performed the experiments. JG, MX, TK, and YW analyzed data. JG, MX, and TK wrote the manuscript. All authors read and approved the final manuscript.

ACKNOWLEDGMENTS

This work was supported by a Peking Union Medical College Hospital Out-standing Young Talents Program (JQ201703), a Chinese Academy of Medical Sciences Innovation Fund for Medical Sciences (2016-I2M-1-014), a Beijing Innovation Base Cultivation and Development Special Fund (Z171100002217068), and the Major Infectious Diseases Such as AIDS and Viral Hepatitis Prevention and Control Technology Major Projects (2018ZX10712001).

SUPPLEMENTARY MATERIAL

The Supplementary Material for this article can be found online at: <https://www.frontiersin.org/articles/10.3389/fmicb.2018.02717/full#supplementary-material>

REFERENCES

- Akova, M., Akalin, H., Uzun, O., and Gür, D. (1991). Emergence of *Candida krusei* infections after therapy of oropharyngeal candidiasis with fluconazole. *Eur. J. Clin. Microbiol.* 10, 598–599.
- CLSI (2017). *Performance Standards for Antifungal Susceptibility Testing of Yeasts. Document M60Ed1E*. Wayne, PA: Clinical, and Laboratory Standards Institute.
- Crawford, K., and Whitney, K. (2010). Population genetic diversity influences colonization success. *Mol. Ecol.* 19, 1253–1263. doi: 10.1111/j.1365-294X.2010.04550.x
- Cuomo, C. A., Shea, T., Yang, B., Ra, R., and Forche, A. (2017). Whole genome sequence of the heterozygous clinical isolate *Candida krusei* 81-B-5. *G3* 7, 2883–2889. doi: 10.1534/g3.117.043547
- Earl, D. A. (2012). Structure harvester: a website and program for visualizing structure output and implementing the evanno method. *Conserv. Genet. Resour.* 4, 359–361. doi: 10.1007/s12686-011-9548-7
- Evanno, G., Regnaut, S., and Goudet, J. (2005). Detecting the number of clusters of individuals using the software structure: a simulation study. *Mol. Ecol.* 14, 2611–2620. doi: 10.1111/j.1365-294X.2005.02553.x
- Excoffier, L., and Lischer, H. E. (2010). Arlequin suite ver 3.5: a new series of programs to perform population genetics analyses under Linux and Windows. *Mol. Ecol. Resour.* 10, 564–567. doi: 10.1111/j.1755-0998.2010.02847.x
- Feng, W., Yang, J., Wang, Y., Chen, J., Xi, Z., and Qiao, Z. (2016). ERG11 mutations and upregulation in clinical itraconazole-resistant isolates of *Candida krusei*. *Can. J. Microbiol.* 62, 938–943. doi: 10.1139/cjm-2016-0055
- Forastiero, A., Garcia-Gil, V., Rivero-Menendez, O., Garcia-Rubio, R., Monteiro, M., Alastruey-Izquierdo, A., et al. (2015). Rapid development of *Candida krusei* echinocandin resistance during caspofungin therapy. *Antimicrob. Agents Chemother.* 59, 6975–6982. doi: 10.1128/AAC.01005-15
- Frankham, R., Ballou, J. D., and Briscoe, D. A. (2010). *Introduction to Conservation Genetics, 2nd Edn*. New York, NY: Cambridge University Press.
- Freeland, J. R., Kirk, H., and Peterson, S. (2011). *Molecular Ecology, 2nd Edn*. West Sussex: John Wiley & Sons, Ltd.
- Fukuoka, T., Johnston, D. A., Winslow, C. A., de Groot, M. J., Burt, C., Hitchcock, C. A., et al. (2003). Genetic basis for differential activities of fluconazole and voriconazole against *Candida krusei*. *Antimicrob. Agents Chemother.* 47, 1213–1219. doi: 10.1128/AAC.47.4.1213-1219.2003
- Gong, J., Wu, W., Ran, M., Wang, X., Liu, W., Wan, Z., et al. (2016). Population differentiation and genetic diversity of *Trichophyton rubrum* as revealed by highly discriminatory microsatellites. *Fungal. Genet. Biol.* 95, 24–29. doi: 10.1016/j.fgb.2016.08.002
- Goudet, J. (1995). FSTAT (version 1.2): a computer program to calculate F-statistics. *J. Hered.* 86, 485–486.
- Hakki, M., Staab, J. F., and Marr, K. A. (2006). Emergence of a *Candida krusei* isolate with reduced susceptibility to caspofungin during therapy. *Antimicrob. Agents Chemother.* 50, 2522–2524. doi: 10.1128/AAC.00148-06
- Hunter, P. R., and Gaston, M. A. (1988). Numerical index of the discriminatory ability of typing systems: an application of Simpson's index of diversity. *J. Clin. Microbiol.* 26, 2465–2466.
- Jacobsen, M. D., Gow, N. A., Maiden, M. C., Shaw, D. J., and Odds, F. C. (2007). Strain typing and determination of population structure of *Candida krusei* by multilocus sequence typing. *J. Clin. Microbiol.* 45, 317–323. doi: 10.1128/JCM.01549-06

- Jensen, R. H., Justesen, U. S., Rewes, A., Perlin, D. S., and Arendrup, M. C. (2014). Echinocandin failure case due to a previously unreported FKS1 mutation in *Candida krusei*. *Antimicrob. Agents Ch.* 58, 3550–3552. doi: 10.1128/AAC.02367-14
- Kofler, R., Schlötterer, C., and Lelley, T. (2007). SciRoKo: a new tool for whole genome microsatellite search and investigation. *Bioinformatics* 23, 1683–1685. doi: 10.1093/bioinformatics/btm157
- Kullberg, B. J., and Arendrup, M. C. (2015). Invasive candidiasis. *N. Engl. J. Med.* 373, 1445–1456. doi: 10.1056/NEJMra1315399
- Lamping, E., Ranchod, A., Nakamura, K., Tyndall, J. D., Niimi, K., Holmes, A. R., et al. (2009). Abc1p is a multidrug efflux transporter that tips the balance in favor of innate azole resistance in *Candida krusei*. *Antimicrob. Agents Chemother.* 53, 354–369. doi: 10.1128/AAC.01095-08
- McDonald, B. A., and Linde, C. (2002). Pathogen population genetics, evolutionary potential, and durable resistance. *Annu. Rev. Phytopathol.* 40, 349–379. doi: 10.1146/annurev.phyto.40.120501.101443
- Peakall, R., and Smouse, P. (2012). GenALEX 6.5: genetic analysis in Excel. Population genetic software for teaching and research: an update. *Bioinformatics* 28, 2537–2539. doi: 10.1093/bioinformatics/bts460
- Perlin, D. S., Rautemaa-Richardson, R., and Alastruey-Izquierdo, A. (2017). The global problem of antifungal resistance: prevalence, mechanisms, and management. *Lancet Infect. Dis.* 17, e383–e392. doi: 10.1016/S1473-3099(17)30316-X
- Pfaller, M. A., Diekema, D. J., Gibbs, D. L., Newell, V. A., Nagy, E., Dobiasova, S., et al. (2008). *Candida krusei*, a multidrug-resistant opportunistic fungal pathogen: geographic and temporal trends from the artemis disk antifungal surveillance program, 2001 to 2005. *J. Clin. Microbiol.* 46, 515–521. doi: 10.1128/JCM.01915-07
- Pritchard, J. K., Stephens, M., and Donnelly, P. (2000). Inference of population structure using multilocus genotype data. *Genetics* 155, 945–959.
- Ricardo, E., Miranda, I. M., Faria-Ramos, I., Silva, R. M., Rodrigues, A. G., and Pina-Vaz, C. (2014). *In vivo* and *in vitro* acquisition of resistance to voriconazole by *Candida krusei*. *Antimicrob. Agents Chemother.* 58, 4604–4611. doi: 10.1128/AAC.02603-14
- Rousset, F. (2008). Genepop'007: a complete re-implementation of the genepop software for Windows and Linux. *Mol. Ecol. Resour.* 8, 103–106. doi: 10.1111/j.1471-8286.2007.01931.x
- Salmond, G. P., and Welch, M. (2008). Antibiotic resistance: adaptive evolution. *Lancet* 372, S97–S103. doi: 10.1016/S0140-6736(08)61888-7
- Sampaio, P., Gusmão, L., Alves, C., Pina-Vaz, C., Amorim, A., and Pais, C. (2003). Highly polymorphic microsatellite for identification of *Candida albicans* strains. *J. Clin. Microbiol.* 41, 552–557. doi: 10.1128/JCM.41.2.552-557.2003
- Sanglard, D. (2016). Emerging threats in antifungal-resistant fungal pathogens. *Front. Med.* 3:11. doi: 10.3389/fmed.2016.00011
- Schuster, M. G., Meibohm, A., Lloyd, L., and Strom, B. (2013). Risk factors and outcomes of *Candida krusei* bloodstream infection: a matched, case-control study. *J. Infection* 66, 278–284. doi: 10.1016/j.jinf.2012.11.002
- Wang, H., Xiao, M., Chen, S. C., Kong, F., Sun, Z. Y., Liao, K., et al. (2012). *In vitro* susceptibilities of yeast species to fluconazole and voriconazole as determined by the 2010 national china hospital invasive fungal surveillance net (CHIF-NET) study. *J. Clin. Microbiol.* 50, 3952–3959. doi: 10.1128/JCM.01130-12
- Whaley, S. G., Berkow, E. L., Rybak, J. M., Nishimoto, A. T., Barker, K. S., and Rogers, P. D. (2017). Azole antifungal resistance in *Candida albicans* and emerging non-albicans *Candida* species. *Front. Microbiol.* 7:2173. doi: 10.3389/fmicb.2016.02173
- Xiao, M., Fan, X., Chen, S. C., Wang, H., Sun, Z. Y., Liao, K., et al. (2014). Antifungal susceptibilities of *Candida glabrata* species complex, *Candida krusei*, *Candida parapsilosis* species complex and *Candida tropicalis* causing invasive candidiasis in China: 3 year national surveillance. *J. Antimicrob. Chemother.* 70, 802–810. doi: 10.1093/jac/dku460

Conflict of Interest Statement: The authors declare that the research was conducted in the absence of any commercial or financial relationships that could be construed as a potential conflict of interest.

Copyright © 2018 Gong, Xiao, Wang, Kudinha, Wang, Zhao, Wu, He, Xu and Zhang. This is an open-access article distributed under the terms of the Creative Commons Attribution License (CC BY). The use, distribution or reproduction in other forums is permitted, provided the original author(s) and the copyright owner(s) are credited and that the original publication in this journal is cited, in accordance with accepted academic practice. No use, distribution or reproduction is permitted which does not comply with these terms.



Characterization of NDM-Encoding Plasmids From *Enterobacteriaceae* Recovered From Czech Hospitals

Veronika Paskova^{1,2}, Matej Medvecký^{3,4}, Anna Skalova^{1,2}, Katerina Chudejova^{1,2}, Ibrahim Bitar^{1,2}, Vladislav Jakubu⁵, Tamara Bergerova^{1,2}, Helena Zemlickova^{5,6}, Costas C. Papagiannitsis^{1,2*} and Jaroslav Hrabak^{1,2}

¹ Department of Microbiology, Faculty of Medicine and University Hospital in Plzen, Charles University, Plzen, Czechia,

² Faculty of Medicine, Biomedical Center, Charles University, Plzen, Czechia, ³ Veterinary Research Institute, Brno, Czechia,

⁴ Faculty of Science, National Centre for Biomolecular Research, Masaryk University, Brno, Czechia, ⁵ National Reference Laboratory for Antibiotics, National Institute of Public Health, Prague, Czechia, ⁶ Department of Clinical Microbiology, University Hospital and Faculty of Medicine in Hradec Kralove, Charles University, Hradec Kralove, Czechia

OPEN ACCESS

Edited by:

Simona Pollini,
Università degli Studi di Firenze, Italy

Reviewed by:

Remy A. Bonnin,
Université Paris-Saclay, France
Angela Novais,
Universidade do Porto, Portugal

*Correspondence:

Costas C. Papagiannitsis
c.papagiannitsis@gmail.com

Specialty section:

This article was submitted to
Evolutionary and Genomic
Microbiology,
a section of the journal
Frontiers in Microbiology

Received: 17 February 2018

Accepted: 21 June 2018

Published: 10 July 2018

Citation:

Paskova V, Medvecký M, Skalova A,
Chudejova K, Bitar I, Jakubu V,
Bergerova T, Zemlickova H,
Papagiannitsis CC and Hrabak J
(2018) Characterization of
NDM-Encoding Plasmids From
Enterobacteriaceae Recovered From
Czech Hospitals.
Front. Microbiol. 9:1549.
doi: 10.3389/fmicb.2018.01549

The aim of the present study was to characterize sporadic cases and an outbreak of NDM-like-producing *Enterobacteriaceae* recovered from hospital settings, in Czechia. During 2016, 18 *Enterobacteriaceae* isolates including 10 *Enterobacter cloacae* complex (9 *E. xiangfangensis* and 1 *E. asburiae*), 4 *Escherichia coli*, 1 *Kluyvera intermedia*, 1 *Klebsiella pneumoniae*, 1 *Klebsiella oxytoca*, and 1 *Raoultella ornithinolytica* that produced NDM-like carbapenemases were isolated from 15 patients. Three of the patients were colonized or infected by two different NDM-like producers. Moreover, an NDM-4-producing isolate of *E. cloacae* complex, isolated in 2012, was studied for comparative purposes. All isolates of *E. cloacae* complex, except the *E. asburiae*, recovered from the same hospital, were assigned to ST182. Additionally, two *E. coli* belonged to ST167, while the remaining isolates were not clonally related. Thirteen isolates carried *bla*_{NDM-4}, while six isolates carried *bla*_{NDM-1} ($n = 3$) or *bla*_{NDM-5} ($n = 3$). Almost all isolates carried *bla*_{NDM}-like-carrying plasmids being positive for the IncX3 allele, except ST58 *E. coli* and ST14 *K. pneumoniae* isolates producing NDM-1. Analysis of plasmid sequences revealed that all IncX3 *bla*_{NDM}-like-carrying plasmids exhibited a high similarity to each other and to previously described plasmids, like pNDM-QD28, reported from worldwide. However, NDM-4-encoding plasmids differed from other IncX3 plasmids by the insertion of a Tn3-like transposon. On the other hand, the ST58 *E. coli* and ST14 *K. pneumoniae* isolates carried two novel NDM-1-encoding plasmids, pKpn-35963cz, and pEsco-36073cz. Plasmid pKpn-35963cz that was an IncFIB(K) molecule contained an acquired sequence, encoding NDM-1 metallo- β -lactamase (M β L), which exhibited high similarity to the mosaic region of pS-3002cz from an ST11 *K. pneumoniae* from Czechia. Finally, pEsco-36073cz was a multireplicon A/C₂+R NDM-1-encoding plasmid. Similar to other type 1 A/C₂ plasmids, the *bla*_{NDM-1} gene was located within the ARI-A resistance island. These findings underlined that IncX3 plasmids have played a major role in the dissemination of *bla*_{NDM}-like genes in Czech hospitals. In combination with further evolution of NDM-like-encoding MDR plasmids through reshuffling, NDM-like producers pose an important public threat.

Keywords: NDM, metallo- β -lactamases, *Enterobacter xiangfangensis*, ST182, IncX3

INTRODUCTION

Acquired carbapenem-hydrolyzing β -lactamases are resistance determinants of increasing clinical importance in Gram-negative pathogens. Of these, NDM-1 metallo- β -lactamase (M β L) was first described in *Klebsiella pneumoniae* and *Escherichia coli* isolated in Sweden in 2008 from an Indian patient transferred from a New Delhi hospital (Yong et al., 2009). Since then, NDM-1-producing bacteria, including clinical isolates of *Enterobacteriaceae* and *Acinetobacter baumannii*, have been reported from the Indian subcontinent but also worldwide (Nordmann et al., 2011).

In Czechia, the occurrence of NDM-producing bacteria was rare, with only three sporadic cases being detected during 2011–2013. These cases included an NDM-1-producing *A. baumannii* isolated from a patient repatriated from Egypt (Hrabák et al., 2012), an NDM-4-producing strain of *Enterobacter cloacae* complex from a patient previously hospitalized in Sri Lanka (Papagiannitsis et al., 2013b) and a ST11 *K. pneumoniae* isolate carrying two NDM-1-encoding plasmids, from Slovakia (Studentova et al., 2015). However, an increase in the isolation frequency of NDM-like-producing *Enterobacteriaceae* from Czech hospitals was observed, during 2016.

Thus, the aim of the present study was to characterize the NDM-like producers detected in Czech hospitals, during 2016. Also, we describe the complete nucleotide sequences of representative *bla*_{NDM}-like-carrying plasmids harbored by the studied isolates.

MATERIALS AND METHODS

Bacterial Isolates and Confirmation of Carbapenemase Production

In 2016, Czech hospitals referred a total of 410 *Enterobacteriaceae* isolates with a meropenem MIC of $>0.125 \mu\text{g/ml}$ (EUCAST, 2012) to the National Reference Laboratory for Antibiotics. Species identification was confirmed by matrix-assisted laser desorption ionization-time of flight mass spectrometry (MALDI-TOF MS) using MALDI Biotyper software (Bruker Daltonics, Bremen, Germany). All isolates were tested for carbapenemase production by the MALDI-TOF MS meropenem hydrolysis assay (Rotova et al., 2017). Isolates that were positive by the MALDI-TOF MS meropenem hydrolysis assay were subjected to metallo- β -lactamase, KPC, and OXA-48 detection using the double-disc synergy test with EDTA, the phenylboronic acid disc test, and the temocillin disc test (Lee et al., 2003; Doi et al., 2008; Glupczynski et al., 2012), respectively. Additionally, carbapenemase genes (*bla*_{KPC}, *bla*_{VIM}, *bla*_{IMP}, *bla*_{NDM}, and *bla*_{OXA-48}-like) were detected by PCR amplification (Poirel et al., 2004; Ellington et al., 2007; Naas et al., 2008; Yong et al., 2009). PCR products were sequenced as described below. Isolates positive for *bla*_{NDM}-like genes were further studied. Moreover, the NDM-4-producing isolate of *E. cloacae* complex, recovered at the University Hospital Pilsen (Pilsen, Czechia) during 2012 (Papagiannitsis et al., 2013b), was included in this study for comparative purposes.

Susceptibility Testing

The MICs of piperacillin, piperacillin-tazobactam, cefotaxime, ceftazidime, cefepime, aztreonam, meropenem, ertapenem, gentamicin, amikacin, chloramphenicol, tetracycline, trimethoprim-sulfamethoxazole, ciprofloxacin, colistin, and tigecycline were determined by the broth dilution method (EUCAST, 2003). Data were interpreted according to the criteria of the European Committee on Antimicrobial Susceptibility Testing (EUCAST; www.eucast.org).

Typing

All isolates were typed by multilocus sequence typing (MLST) (Diancourt et al., 2005; Wirth et al., 2006; Miyoshi-Akiyama et al., 2013; Herzog et al., 2014). The databases at <https://pubmlst.org/ecloacae/>, <http://mlst.warwick.ac.uk/mlst/dbs/Ecoli>, <http://bigdb.web.pasteur.fr/klebsiella> and <https://pubmlst.org/koxytoca/> were used to assign STs.

Detection of β -Lactamases

The β -lactamase content of all *bla*_{NDM}-like-positive isolates was determined by isoelectric focusing (IEF). Bacterial extracts were obtained by sonication of bacterial cells suspended in 1% glycine buffer and clarified by centrifugation. Sonicated cell extracts were analyzed by IEF in polyacrylamide gels containing ampholytes (pH 3.5–9.5; AP Biotech, Piscataway, NJ). The separated β -lactamases were visualized by covering the gel with the chromogenic cephalosporin nitrocefin (0.2 mg/ml; Oxoid Ltd., Basingstoke, United Kingdom; Papagiannitsis et al., 2015).

On the basis of the IEF data, PCR detection of various *bla* genes was performed by the use of primers specific for *bla*_{TEM-1}, *bla*_{OXA-1}, *bla*_{SHV}, *bla*_{CTX-M}, and *bla*_{CMY}, as reported previously (Paľucha et al., 1999; Pérez-Pérez and Hanson, 2002; Woodford et al., 2006; Coque et al., 2008). Both strands of the PCR products were sequenced using an ABI 377 sequencer (Applied Biosystems, Foster City, CA).

Transfer of *bla*_{NDM}-Like Genes

Conjugal transfer of *bla*_{NDM}-like genes from the clinical strains was carried out in mixed broth cultures (Vatopoulos et al., 1990), using the rifampin-resistant *E. coli* A15 laboratory strain as a recipient. Transconjugants were selected on MacConkey agar plates supplemented with rifampin (150 mg/l) and ampicillin (50 mg/l). Plasmid DNA from clinical isolates, which failed to transfer *bla*_{NDM}-like by conjugation, was extracted using a Qiagen Maxi kit (Qiagen, Hilden, Germany) and used to transform *E. coli* DH5 α cells. The preparation and transformation of competent *E. coli* cells were done using calcium chloride (Cohen et al., 1972). Transformants were selected on Luria-Bertani agar plates with ampicillin (50 mg/l). Transconjugants or transformants were confirmed to be NDM-like producers by PCR (Yong et al., 2009) and the MALDI-TOF MS meropenem hydrolysis assay (Rotova et al., 2017).

Plasmid Analysis

To define the genetic units of the *bla*_{NDM}-like genes, the plasmid contents of all NDM-producing clinical and recombinant strains

were analyzed by pulsed-field gel electrophoresis (PFGE) of total DNA digested with S1 nuclease (Promega, Madison, WI, USA; Barton et al., 1995). Following PFGE, the DNA was transferred to a BrightStar-Plus positively charged nylon membrane (Applied Biosystems, Foster City, CA) and hybridized with digoxigenin-labeled *bla*_{NDM}-like probe.

Plasmid incompatibility (Inc) groups were determined by the PCR-based replicon typing (PBRT) method (Carattoli et al., 2005; Johnson et al., 2012), using total DNA from transconjugants or transformants. Additionally, the IncR replicon was detected as described previously (García-Fernández et al., 2009).

Detection of Characteristic Regions

Based on the results from Illumina sequencing (see below), six PCRs targeting characteristic regions of NDM-4-encoding IncX3 plasmids and genomes of ST182 isolates of *E. cloacae* complex sequenced during this study were designed. The selected regions included: (i) a Tn3-like transposon found in NDM-4-encoding IncX3 plasmids, and (ii) four insertions identified in the genome of Encl-922 (see section Comparative Analysis of *Enterobacter* Isolates). All NDM-producing clinical or recombinant strains were screened for the presence of the regions described above by the use of specific primers (see Table S1).

Plasmid and Chromosome Sequencing

Ten plasmids were selected for complete sequencing. These plasmids were selected as representatives of different origins, plasmid sizes and hospitals. Additionally, clinical isolates Encl-922 and Encl-44578 were also selected for whole genome sequencing. The selected isolates were isolated 4-year apart (2012 and 2016).

Plasmid DNAs from transconjugants or transformants were extracted using a Qiagen Large-Construct kit (Qiagen, Hilden, Germany). Additionally, the genomic DNAs of clinical Encl-922 and Encl-44578 isolates were extracted using a DNA-Sorb-B kit (Sacace Biotechnologies S.r.l., Como, Italy). Multiplexed DNA libraries were prepared, using the Nextera XT Library Preparation kit, and 300-bp paired-end sequencing was performed on the Illumina MiSeq platform (Illumina Inc., San Diego, CA, USA) using the MiSeq v3 600-cycle Reagent kit. Initial paired-end reads were quality trimmed using the Trimmomatic tool v0.33 (Bolger et al., 2014) with the sliding window size of 4 bp, required average base quality ≥ 17 and minimum read length of 48 bases. Genomic DNA reads of clinical isolates of *E. cloacae* complex were consequently assembled using the de Bruijn graph-based *de novo* assembler SPAdes v3.9.1 (Bankevich et al., 2012), using k-mer sizes 21, 33, 55, 77, 99, and 127. For assembly of the plasmids, reads were mapped to the reference *E. coli* K-12 substrain MG 1655 genome (GenBank accession no. U00096) using the BWA-MEM algorithm (Li, 2013), in order to filter out the chromosomal DNA. Then, all the unmapped reads were assembled in the same way as described above. The sequence gaps were filled by a PCR-based strategy and Sanger sequencing. For sequence analysis and annotation, the BLAST algorithm (www.ncbi.nlm.nih.gov/BLAST), the ISfinder database (www-is.biotoul.fr/), and the open reading frame (ORF) finder tool (www.bioinformatics.org/sms/) were utilized. Comparative

genome alignments were performed using the Mauve v2.3.1 program (Darling et al., 2010).

Antibiotic resistance genes were identified using the ResFinder 2.1 tool (<https://cge.cbs.dtu.dk/services/ResFinder/>) with an identity threshold of $>90\%$ (Zankari et al., 2012).

Comparative Analysis of Clinical Isolates of *E. cloacae* Complex

Comparative genomic analysis of clinical isolates of *E. cloacae* complex was based on statistics calculated by QUAST v4.5 (Gurevich et al., 2013) and VarScan v2.3.9 (Koboldt et al., 2012) tools. All quality trimmed Illumina reads of Encl-922 were mapped to contigs of Encl-44578, employing BWA-MEM algorithm v0.7.12 (Li, 2013) and SAMtools v1.3 (Li et al., 2009), for the format conversions and analysis of the results. Then, single nucleotide polymorphisms (SNPs) and indels were detected employing VarScan with parameters set as follows: minimum read depth at a position = 6, minimum base quality at a position = 20 and minimum variant allele frequency threshold of 0.45. Moreover, SNPs and indels located in a region within 127 bp from any edge of a contig, as well as SNPs and indels harbored by contigs smaller than 2 kb were excluded from further analysis. Remaining SNPs and indels were also manually checked and refined by visualization of mapped data via Tablet v1.14.04.10 (Milne et al., 2013). Differences in assembly of *E. cloacae* complex genomes were inspected using QUAST's Icarus viewer (Mikheenko et al., 2016). In order to examine whether SNPs and indels were located in intergenic or coding regions, as well as to find out what are the differences in genetic information between studied isolates, contigs of clinical strains were annotated using Prokka v1.10 (Seemann, 2014). Genes harboring SNPs were compared against NCBI's conserved domain database (Marchler-Bauer et al., 2017) via CD-Search (Marchler-Bauer and Bryant, 2004) to identify conserved domain hits. Finally, sequencing data of clinical strains were examined for the presence of prophage sequences using PHAST web server (Zhou et al., 2011).

Nucleotide Sequence Accession Numbers

The nucleotide sequences of the pEsco-5256cz, pEncl-922cz, pRor-30818cz, pKpn-35963cz, pEsco-36073cz, pEncl-44578cz, pEnas-80654cz, pEnin-51781cz, pEsco-4382cz, and pKlox-45574cz plasmids have been deposited in GenBank under accession numbers MG252891, MG252892, MG252893, MG252894, MG252895, MG833402, MG833403, MG833404, MG833405, and MG833406, respectively. Whole genome assemblies of isolates of *E. cloacae* complex were deposited in NCBI under accession number PRJNA432167.

RESULTS

Carbapenemase-Producing *Enterobacteriaceae*

A total of 40 *Enterobacteriaceae* isolates showing carbapenemase activity on MALDI-TOF MS meropenem hydrolysis assay were recovered from Czech hospitals during 2016. PCR screening showed that 18 of the isolates were positive for *bla*_{NDM}, 14 isolates

were positive for *bla*_{OXA-48}, while the remaining 8 isolates were positive for *bla*_{KPC}.

NDM-Like-Producing Isolates

Altogether, 18 nonrepetitive isolates producing NDM-like carbapenemases were isolated from 15 patients in 2016. Among them, 10 were presumptively identified as belonging to *E. cloacae* complex, 4 were identified to be *E. coli*, while the remaining isolates belonged to unique species (*Enterobacter intermedius*, *K. pneumoniae*, *Klebsiella oxytoca*, and *Raoultella ornithinolytica*). A previous study showed that 16S rRNA gene sequence of *E. intermedius* was included within the cluster of the genus *Kluyvera*, and therefore, the transfer of *E. intermedius* to the genus *Kluyvera* as *Kluyvera intermedia* was proposed (Pavan et al., 2005). Three of the patients were colonized or infected by two different NDM-like producers (Table 1).

NDM-like producers were collected from five Czech hospitals located in three different Czech cities. In hospital B1, an outbreak that included ten patients diagnosed with NDM-like-producing *Enterobacteriaceae* lasted the studied period. Additionally, two patients colonized or infected with NDM-like producers were reported in hospital B2. The three remaining cases were identified in three different hospitals. None of the patients, treated in hospital B1, had recently traveled abroad or had been previously hospitalized. The patient treated in hospital C was directly repatriated from a hospital in China, while clinical data weren't available for the remaining patients.

Additionally, the NDM-4-producing isolate of *E. cloacae* complex identified in 2012 (Papagiannitsis et al., 2013b), was studied.

All 19 NDM-like producers exhibited resistance to piperacillin, piperacillin-tazobactam, cephalosporins, and ertapenem (Table S2), while the observed variations in the MICs of aztreonam might reflect the presence of additional resistance mechanisms in some of the isolates. Seventeen of the NDM-like producers also exhibited resistance to ciprofloxacin; 15 were resistant to gentamicin, 13 were resistant to trimethoprim-sulfamethoxazole, 1 was resistant to amikacin, and 1 was resistant to colistin, whereas all isolates were susceptible to tigecycline.

The population structure of NDM-like-producing isolates studied by MLST is shown in Table 1. All isolates of *E. cloacae* complex, except the *E. asburiae* strain, which were recovered from hospital B1, belonged to ST182. Of note was that the NDM-4-producing isolate of *E. cloacae* complex that was isolated, in 2012, from the patient previously hospitalized in Sri Lanka (Papagiannitsis et al., 2013b) was also assigned to ST182. Two of *E. coli*, both of which were from hospital B2, belonged to ST167. *E. coli* ST167 was recently found among NDM-5-producing isolates from different healthcare institutions in China (Yang et al., 2014; Zhang et al., 2016). The two remaining *E. coli* isolates were not clonally related and belonged to different STs (ST58 and ST69). The *K. pneumoniae* isolate was assigned to the high risk clone ST14 (Woodford et al., 2011), while the *K. oxytoca* isolate was classified into ST2 that belongs to a growing international clonal complex (CC2) (Izdebski et al., 2015).

Sequencing of the PCR products revealed three *bla*_{NDM}-type genes encoding the NDM-1, NDM-4, and NDM-5 enzymes (Table 1; Yong et al., 2009; Hornsey et al., 2011; Nordmann et al., 2012). NDM-5 is an NDM-1-related MβL variant that differs from NDM-1 by two amino-acid substitutions, Val88Leu and Met154Leu, the former one being its only change with NDM-4. Thirteen of the isolates, all of which were from hospital B1, were found to produce the NDM-4 MβL (Table 1). The three isolates from hospital B2 produced the NDM-5 enzyme, while the three remaining isolates that were recovered from sporadic cases in three different hospitals expressed NDM-1 carbapenemase. Additionally, most of *bla*_{NDM}-like-positive isolates were confirmed to coproduce the extended-spectrum β-lactamase CTX-M-15 (*n* = 18) either alone or along with TEM-1 (*n* = 13) and/or OXA-1 (*n* = 13), whereas the *K. pneumoniae* and *R. ornithinolytica* isolates also expressed the SHV-12 enzyme. The ST58 NDM-1-producing *E. coli* isolate coproduced CMY-16, CTX-M-15, OXA-10, and TEM-1 β-lactamases.

*bla*_{NDM}-Like-Carrying Plasmids

The *bla*_{NDM}-like genes from all clinical strains were transferred by conjugation (*n* = 14) or transformation (*n* = 5) (Table 1). All *bla*_{NDM}-like-positive recombinants exhibited resistance to piperacillin, piperacillin-tazobactam, cephalosporins, and ertapenem, while they remained susceptible to meropenem (Table S2). The three NDM-1-producing recombinants also exhibited resistance to aztreonam. Additionally, most of *bla*_{NDM}-like-positive recombinants (*n* = 18) were susceptible to non-β-lactam antibiotics.

Plasmid analysis of NDM-4-producing donor and transconjugant strains revealed the transfer of plasmids, all of which were ~55 kb in size (Table 1). The three NDM-5-producing transformants harbored plasmids of ~45 kb, whereas the three remaining recombinants carried *bla*_{NDM-1}-positive plasmids of different sizes (~55, ~150, and ~300 kb). Replicon typing showed seventeen of the plasmids, including those sizing ~45 and ~55 kb, were positive for the IncX3 allele. The *bla*_{NDM-1}-positive plasmid of ~300 kb was positive for replicons R and A/C, whereas the one remaining *bla*_{NDM-1}-carrying plasmid was non-typeable by the PBRT method (Carattoli et al., 2005; Johnson et al., 2012).

Structure of *bla*_{NDM}-Like-Carrying Plasmids

The complete sequence of *bla*_{NDM}-like-carrying plasmids representative of different plasmid sizes, replicons, and resistance genes (*n* = 10) was determined (Table 1). Sequence analysis revealed that all IncX3 *bla*_{NDM}-like-carrying plasmids exhibited a high similarity to each other and to previously described NDM-like-encoding plasmids, belonging to IncX3 group, reported from worldwide (Krishnaraju et al., 2015; Zhu et al., 2016; Pál et al., 2017). The *bla*_{NDM-5}-positive plasmids, pEco-5256cz and pKlox-45574cz, were almost identical to NDM-5-encoding plasmid pNDM-QD28 (100% coverage, 99% identity) (GenBank accession no. KU167608) that was characterized from a ST167 *E. coli* in China (Zhu et al., 2016). Differences among these plasmids consisted in few SNPs (*n* = 5), almost all

TABLE 1 | Characteristics of NDM-like-producing *Enterobacteriaceae*.

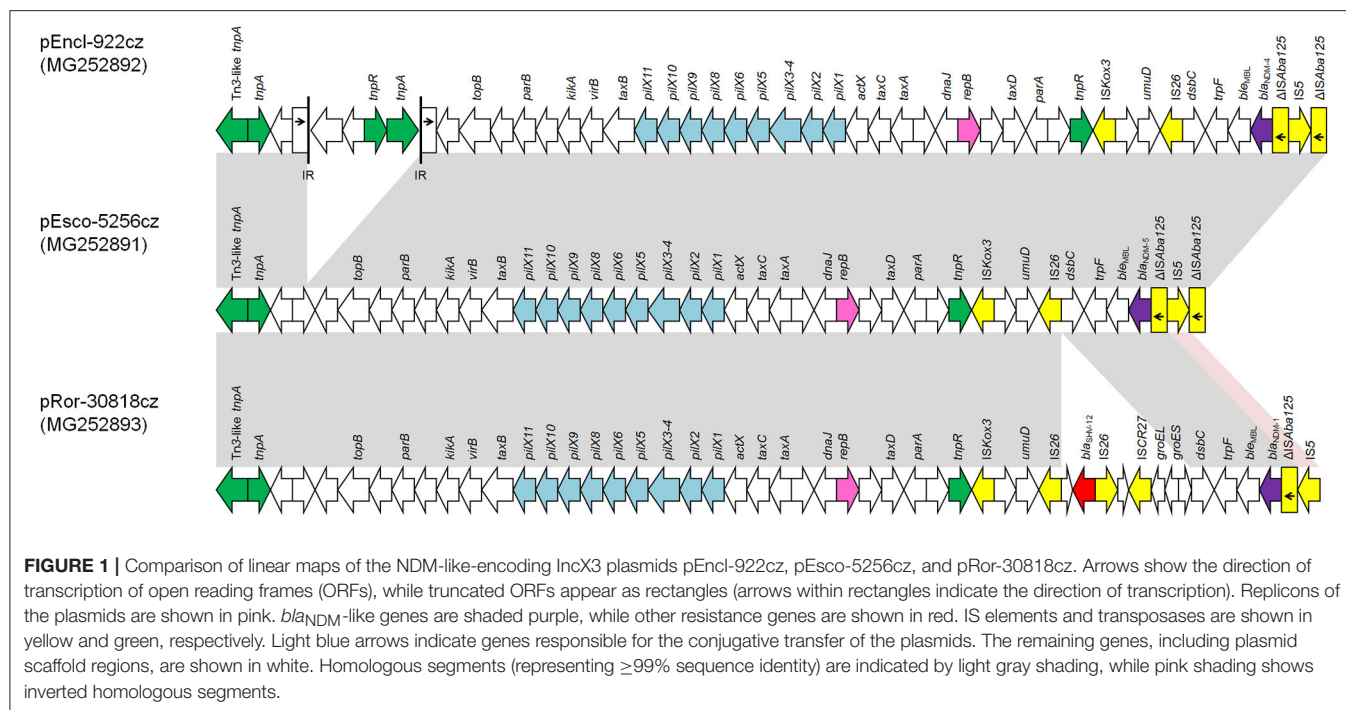
Isolate ^a	Isolation mn/yr (hospital)	Material (infection/colonization)	ST	β-Lactamase content	Size of NDM-encoding plasmid (kb) ^b	Replicon of NDM-encoding plasmid	Additional resistance markers
<i>E. xiangfangensis</i>							
Encl-922	09/2012 (B1)	Rectal swab (colonization)	ST182	NDM-4, CTX-M-15, OXA-1, TEM-1	~55 (53.683)	IncX3	
Encl-66918	04/2016 (B1)	Rectal swab (colonization)	ST182	NDM-4, CTX-M-15, OXA-1, TEM-1	~55	IncX3	
Encl-89040	06/2016 (B1)	Bile (infection)	ST182	NDM-4, CTX-M-15, OXA-1, TEM-1	~55	IncX3	
Encl-44578	07/2016 (B1)	Venous catheter (infection)	ST182	NDM-4, CTX-M-15, OXA-1, TEM-1	~55 (53.683)	IncX3	
Encl-89485○	07/2016 (B1)	Bile (infection)	ST182	NDM-4, CTX-M-15, OXA-1, TEM-1	~55	IncX3	
Encl-91221	09/2016 (B1)	Throat swab (colonization)	ST182	NDM-4, CTX-M-15, OXA-1, TEM-1	~55	IncX3	
Encl-93141	10/2016 (B1)	Peritoneal catheter (infection)	ST182	NDM-4, CTX-M-15, OXA-1	~55	IncX3	
Encl-98042	11/2016 (B1)	Rectal swab (colonization)	ST182	NDM-4, CTX-M-15, OXA-1	~55	IncX3	
Encl-98047■	11/2016 (B1)	Rectal swab (colonization)	ST182	NDM-4, CTX-M-15, OXA-1, TEM-1	~55	IncX3	
Encl-98546	12/2016 (B1)	Rectal swab (colonization)	ST182	NDM-4, CTX-M-15, OXA-1, TEM-1	~55	IncX3	
<i>E. asburiae</i>							
Enas-80654○	07/2016 (B1)	Bile (infection)	NA	NDM-4, CTX-M-15	~55 (53.683)	IncX3	
<i>K. intermedia</i>							
Enin-51781	10/2016 (B1)	Rectal swab (colonization)	NA	NDM-4, CTX-M-15, OXA-1	~55 (53.683)	IncX3	
<i>E. coli</i>							
Esco-14290	06/2016 (B2)	Nasal swab (colonization)	ST167	NDM-5, CTX-M-15, TEM-1	~45	IncX3	
Esco-5256▲	07/2016 (B2)	Bronchoalveolar lavage (infection)	ST167	NDM-5, CTX-M-15, TEM-1	~45 (46.161)	IncX3	
Esco-36073	09/2016 (A1)	Urine (infection)	ST58	NDM-1, CMY-16, OXA-10, CTX-M-15, TEM-1	~300 (300.958)	IncR, IncA/C ₂	<i>floR</i> , <i>tet(A)</i> , <i>strAB</i> , <i>sul2</i> , <i>aacA4</i> , <i>aphA7</i> , <i>dfrA14</i> , <i>arr-2</i> , <i>cmlA1</i> , <i>aadA1</i> , <i>aphA6</i> , <i>sul1</i>
Esco-4382■	12/2016 (B1)	Rectal swab (colonization)	ST69	NDM-4, CTX-M-15, TEM-1	~55 (53.683)	IncX3	
<i>K. oxytoca</i>							
Klox-45574▲	07/2016 (B2)	Rectal swab (colonization)	ST2	NDM-5	~45 (46.161)	IncX3	
<i>K. pneumoniae</i>							
Kpn-35963	09/2016 (A2)	Urine catheter (infection)	ST14	NDM-1, SHV-12, CTX-M-15, OXA-1	~150 (161.324)	IncFIB	<i>aacA4</i> , <i>dfrA14</i> , <i>mph(A)</i>
<i>Raoultella ornithinolytica</i>							
Ror-30818	09/2016 (C)	Rectal swab (colonization)	NA	NDM-1, SHV-12, CTX-M-15, OXA-1, TEM-1	~55 (53.051)	IncX3	

NA, not applicable.

^aWhite circles, black squares, and black triangles each indicate the NDM-like-producing isolates recovered from the same patient.^bData for plasmids found in transconjugants are shown in bold; data for plasmids observed in transformants are underlined.

located in mobile elements. Similar to pNDM-QD28, no other resistance genes were detected in these plasmids. Compared to other IncX3 NDM-encoding plasmids, all *bla*_{NDM-4}-encoding

plasmids differed by the insertion of a Tn3-like transposon (nt 7108-14624 in pEncl-44578cz) downstream *topB* gene (**Figure 1**). The Tn3-like sequence was composed by the 38-bp inverted



repeats (IR) of the transposon, *tnpA*, *tnpR*, and two ORFs encoding hypothetical proteins. Target site duplications of 5 bp (GTACC) at the boundaries of the Tn3-like element indicated insertion by transposition. Of note was that the sequence of pEncl-922cz, isolated in 2012 (Papagiannitsis et al., 2013b), was identical to the respective sequences of NDM-4-encoding plasmids recovered in the same hospital, during 2016. PCR screening confirmed the presence of the Tn3-like transposon in all NDM-4-encoding IncX3 plasmids, isolated in hospital B1, while Tn3-like wasn't detected in the remaining *bla*_{NDM}-like-positive plasmids that belonged to IncX3 group. Furthermore, the *bla*_{NDM-1}-positive plasmid, pRor-30818cz, harbored an additional 7875-bp sequence (nt 40617-48491 in pRor-30818cz) encoding the extended-spectrum β -lactamase SHV-12 (Figure 1). A similar SHV-12-encoding region was found in the IncX3 *bla*_{NDM-1}-positive plasmid pKP04NDM (100% coverage, 99% identity) (GenBank accession no. KU314941) described from a *K. pneumoniae* isolate in China.

The NDM-1-encoding plasmid pKpn-35963cz that was nontypeable by the PBRT method (Carattoli et al., 2005) was 161,324 bp in size. Plasmid pKpn-35963cz was composed of two distinct parts: a contiguous plasmid backbone of 115,998 bp (nt 1–58,655 and 103,982–161,324) and an acquired sequence of 45,326 bp (nt 58,656–103,981). The plasmid backbone, which shared similarities with the respective regions of plasmid p1605752FIB (GenBank accession no. CP022125) recovered from a pan-resistant isolate of *K. pneumoniae* from the United States, harbored regions responsible for replication [*repB* gene; IncFIB(K) replicon], conjugative transfer (*tra* and *trb* genes) and plasmid maintenance (*vagCD*, *psiAB*,

umuCD and *parAB* operons, and *ssb* gene; Figure 2). The acquired sequence of pKpn-35963cz contained a 17,836-bp segment (nt 77,360–95,195) encoding NDM-1, which was similar to the mosaic region of pS-3002cz (99% identity) (Studentova et al., 2015). The acquired sequence of pKpn-35963cz contained two additional segments that have also been described in pS-3002cz. The first segment (nt 65,518–72,935) included genes encoding an EcoRII methylase and EcoRII endonuclease, and the class 1 integron In191 carrying the *dfraA14* resistance gene. The second segment (nt 101,342–103,981) contained fragments of transposons Tn1000 (Δ Tn1000) and Tn1331 (Δ Tn1331). Δ Tn1331 comprised *tnpR* and *aacA4* resistance gene. Furthermore the acquired sequence of pKpn-35963cz carried a macrolide resistance operon [*mph*(A)], and regions encoding OXA-1 and CTX-M-15 β -lactamases (Figure 2). In the acquired sequence of pKpn-35963cz, intact and truncated copies of several mobile elements that may have been implicated in the formation of this region were found.

The plasmid pEsco-36073cz, which encoded the NDM-1 carbapenemase, is 300,958 bp in size. The plasmid showed a complex structure, being composed of sequences of diverse origin (Figure 3). A 170,314-bp sequence (nt 232,204–300,958 and 1–101,559) resembled the type 1 A/C₂ plasmid pRH-1238 (94% coverage, 99% identity; Figure 3), characterized from a *Salmonella enterica* serovar Corvallis strain isolated from a migratory wild bird in Germany (Villa et al., 2015). Analysis of A/C₂-associated sequence by the core gene PMLST (cgPMLST) scheme (Hancock et al., 2017) indicated that it belonged to cgST3.4. The A/C₂ backbone was composed of regions responsible for replication (*repA* gene), conjugative

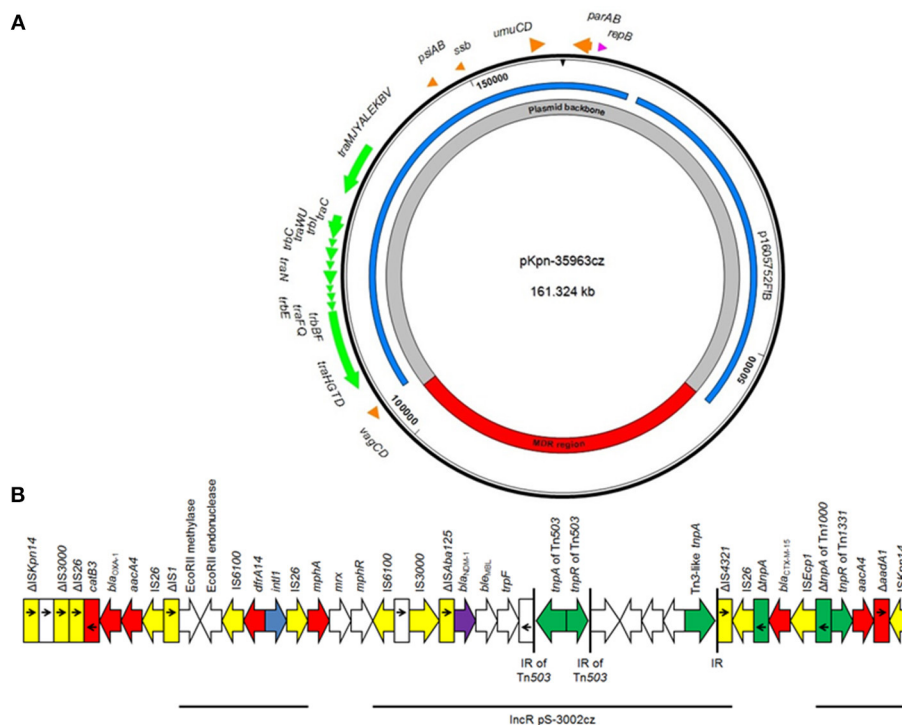


FIGURE 2 | (A) Overview of the plasmid pKpn-35963cz. The innermost circles show the main regions of the plasmids. Similarities with other plasmids are shown in the next circle; each color represents a unique plasmid. In the outer circle, indicative genes and the direction of transcription are shown by arrows. Replicons of the plasmid are indicated as pink arrows. Genes responsible for plasmid transfer and maintenance are shown in green and orange, respectively. **(B)** Linear map of the multidrug resistance region (MDR) of the plasmid pKpn-35963cz. Arrows show the direction of transcription of open reading frames (ORFs), while truncated ORFs appear as rectangles (arrows within rectangles indicate the direction of transcription). *bla*_{NDM}-like genes are shaded purple, while other resistance genes are shown in red. IS elements and transposases are shown in yellow and green, respectively. *int1* genes are shaded blue. The remaining genes are shown in white. Thin lines below the map correspond to highly similar sequences from other plasmids.

transfer (*Tra1* and *Tra2* regions), and plasmid maintenance (*higBA* and *parAB* operons and *xerD*- and *kfrA*-like genes). Apart from the backbone, pEsco-36073cz carried the *bla*_{CMY-2}-like-containing region, and the ARI-B and ARI-A resistance islands, as previously described in other type 1 A/C₂ MDR plasmids (Harmer and Hall, 2015; Papagiannitsis et al., 2016). The *bla*_{NDM-1} gene was located within ARI-A, in a genetic environment similar to those previously identified in pRH-1238 (Villa et al., 2015). However, unlike in pRH-1238, the ARI-A of pEsco-36073cz lacked the macrolide resistance determinant *mphA-mel-repAciN*. Furthermore, a class 1 integron with *aacA4* and *aphA1* gene cassettes was located between *resI* and *resII* sites of the Tn1696 module. The ARI-A of pEsco-36073cz also carried a new integron, In1459, whose variable region comprised the *dfrA14*, *arr-2*, *cmlA1*, *bla*_{OXA-10}, *aadA1* cassettes. Additionally, pEsco-36073cz included fragments resembling the backbone of the recently described IncR plasmid pKP1780 (Papagiannitsis et al., 2013a), and sequences previously found in the plasmid pPSP-a3e (Conlan et al., 2014) and in the chromosomes of several Gram-negative rods. Genes encoding for resistance to arsenate, cooper and mercury were identified in the three remaining acquired regions of pEsco-36073cz.

Comparative Analysis of *Enterobacter* Isolates

“*In silico*” *hsp60* typing of the genome sequences (Hoffmann and Roggenkamp, 2003) showed that both isolates belonged to the recently recognized *E. xiangfangensis* species (Gu et al., 2014).

Since all isolates of *E. cloacae* complex, except the *E. asburiae* isolate, belonged to the same ST and carried the same IncX3 *bla*_{NDM-4}-carrying plasmid, the WGS data of clinical strains Encl-922 and Encl-44578 were compared, using QUAST and VarScan tools, in order to examine the phylogenetic relationship of the isolates recovered in 2012 and 2016.

Comparative analysis of clinical isolates revealed that the genome of Encl-922 exhibited extensive similarity (99.87% identity) to the genome of Encl-44578. Sixteen SNPs were identified in the genome of Encl-922, compared to that of Encl-44578, five of which were located within prophage regions (Table 2). Interestingly, Encl-922 harbored three large insertions of 8,933 bp (nt 439,392–448,324 in node 2), of 17,903 bp (nt 17,786–35,688 in node 32) and of 13,165 bp (nt 1–13,165 in node 27; prophage sequence PHAGE_Salmon_SPN3UB_NC_019545). Additionally, Encl-922 harbored an insertion of 33-bp sequence (AACCCTCTCCCCAAGGGGAGAGG GGACGATTA) located in an intergenic region. Moreover,

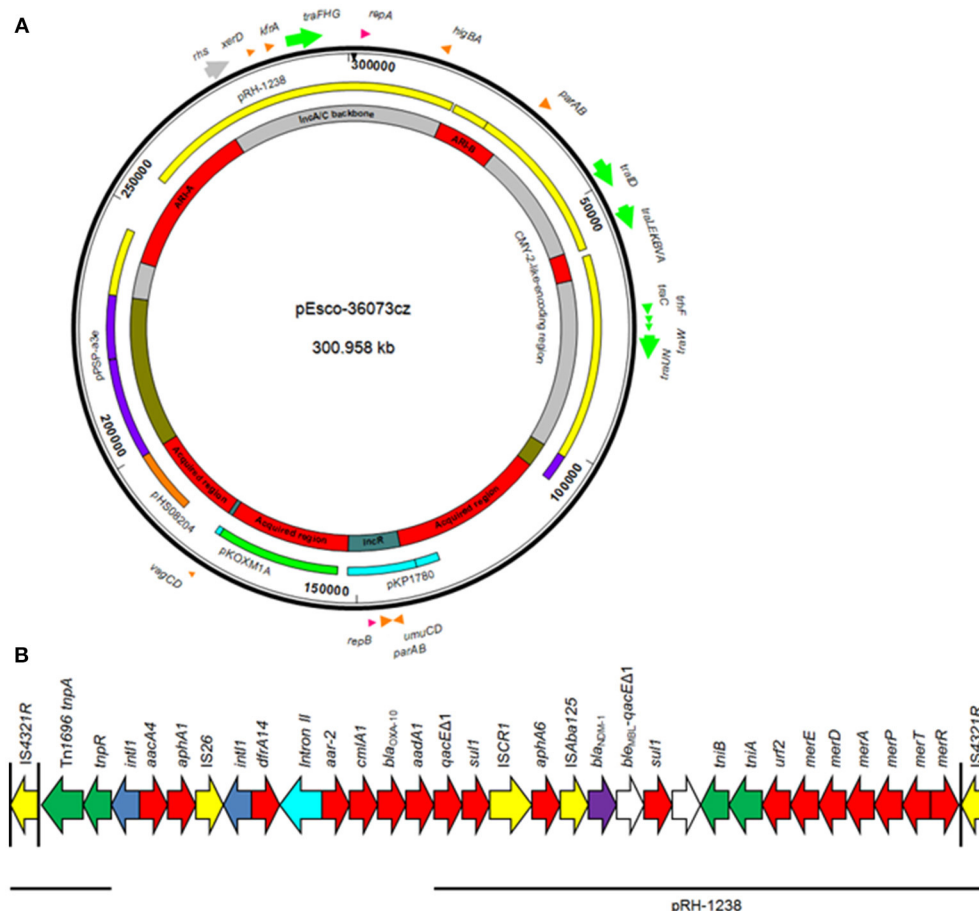


FIGURE 3 | (A) Overview of the plasmid pEsco-36073cz. The innermost circles show the main regions of the plasmids. Similarities with other plasmids are shown in the next circle; each color represents a unique plasmid. In the outer circle, indicative genes and the direction of transcription are shown by arrows. Replicons of the plasmid are indicated as pink arrows. Genes responsible for plasmid transfer and maintenance are shown in green and orange, respectively. **(B)** Linear map of the ARI-A resistance island of the plasmid pEsco-36073cz. Arrows show the direction of transcription of open reading frames (ORFs), while truncated ORFs appear as rectangles (arrows within rectangles indicate the direction of transcription). *bla*_{NDM}-like genes are shaded purple, while other resistance genes are shown in red. IS elements and transposases are shown in yellow and green, respectively. *int1* genes are shaded blue; teal blue arrow indicates the group II intron. The remaining genes are shown in white. Thin lines below the map correspond to highly similar sequences from other plasmids.

Encl-922 showed a single nucleotide (G) deletion leading to CDS annotation change of general stress protein 39 to putative oxidoreductase YghA. Analysis of whole genome sequencing (WGS) data by PHAST web server found five intact prophage sequences (PHAGE_Haemop_HP2_NC_003315, PHAGE_Salmon_SPN3UB_NC_019545, PHAGE_EnteromEp390_NC_019721, PHAGE_Pseudo_PPpW_3_NC_023006, and PHAGE_Salmon_SP_004_NC_021774) and one questionable prophage region (PHAGE_EnteromSfl_NC_027339), in both *E. xiangfangensis* isolates. However, Encl-922 included one additional incomplete prophage region (PHAGE_Salmon_SPN3UB_NC_019545), which was absent from the Encl-44578 genome.

Screening by PCR and sequencing identified that all *E. xiangfangensis* isolates, recovered during 2016, didn't harbor any of the four mentioned insertions. Thus, this finding indicated that *Enterobacter* isolates from 2016 differed from Encl-922.

DISCUSSION

The present study investigated sporadic cases and an outbreak of NDM-like-producing *Enterobacteriaceae* recovered from Czech hospitals, during 2016. Specifically, 12 NDM-4-producing isolates, which belonged to *E. xiangfangensis* ($n = 9$), *E. asburiae* ($n = 1$), *K. intermedius* ($n = 1$), and *E. coli* ($n = 1$) species, 3 NDM-5 producers of *E. coli* ($n = 2$) and *K. oxytoca* ($n = 1$) species, and one *E. coli*, one *K. pneumoniae* and one *R. ornithinolytica* producing NDM-1 MBL were characterized.

The setting that was most affected was hospital B1, in which an outbreak of NDM-4-producing ST182 *E. xiangfangensis* isolates took place. ST182 isolates of *E. cloacae* complex were previously identified in Mexico and were associated with the production of NDM-1 enzyme (Torres-González et al., 2015; Bocanegra-Ibarias et al., 2017). Of note was that the isolate of *E. cloacae* complex, isolated in 2012 from a

TABLE 2 | Summary table of 16 SNPs found between the genomes of *E. xiangfangensis* isolates Encl-44578 (reference) and Encl-922 (query).

PROKKA name	Conserved domain classification	Enzyme commission number	Contig	SNP	Gene length (aa)	aa substitution
_a	–	–	2	T64623G	–	–
_a	–	–	7	T88097G	–	–
Methyl viologen resistance protein SmvA	MFS transporter	–	8	T51220C	496	M293T
D-amino acid dehydrogenase small subunit	D-amino acid dehydrogenase	1.4.99.1	23	A46893G	432	S395S
NADP-dependent malic enzyme	NADP-dependent malic enzyme	1.1.1.40	2	A296564G	759	N584N
Glyoxylate/hydroxypyruvate reductase A	Glyoxylate/hydroxypyruvate reductase A	1.1.1.79	4	G113111A	312	R267H
Ribonuclease E	Ribonuclease E	3.1.26.12	4	T156395C	1035	H685R
Hypothetical protein	–	–	38	C784A	369	T239N
Hypothetical protein	Similar to protein YjaG	–	39	A24170G	196	I61V
Low-affinity gluconate transporter	Low-affinity gluconate transporter	–	6	T100479C	421	S277P
Arabinose operon regulatory protein	DNA-binding transcriptional regulator	–	12	A66284G	281	N193S
Anaerobic dimethyl sulfoxide reductase chain B	DMSO_dmsB family protein	–	35	T1976G	205	K120Q
Tail length tape measure protein	COG5281 and Phage_HK97_TLTM domain-containing protein	–	5	G24809A	1154	L824L
Tail length tape measure protein	COG5281 and Phage_HK97_TLTM domain-containing protein	–	5	T24845C	1154	A836A
Tail length tape measure protein	COG5281 and Phage_HK97_TLTM domain-containing protein	–	5	C24893A	1154	G852G
Terminase-like family protein	P family protein	–	26	G7615T	589	R485L

^a The first two SNPs are located in intergenic regions.

patient who had been previously hospitalized in Sri Lanka (Papagiannitsis et al., 2013b), also belonged to ST182 and harbored an IncX3 *bla*_{NDM-4}-positive plasmid being identical to respective plasmids characterized from isolates recovered from patients treated in hospital B1 (Table 1), during 2016. However, comparative genome analysis revealed the presence of four insertions in the genome of *E. xiangfangensis* Encl-922 isolate. These insertions were not found in the genomic DNA of *E. xiangfangensis* isolates from 2016, suggesting a second insertion event of NDM-4-producing *E. xiangfangensis* isolates in Czech hospitals.

In three of the patients, two different NDM-like producers were identified during their hospitalization, supposing the *in vivo* horizontal transfer of *bla*_{NDM}-like-carrying plasmids. Sequencing and PCR screening data revealed the presence of the same *bla*_{NDM-4}- or *bla*_{NDM-5}-carrying plasmid in these isolates (Table 1). These results confirmed the hypothesis of the *in vivo* horizontal transfer of *bla*_{NDM}-like-carrying plasmids.

Results from Illumina sequencing showed that IncX3 plasmids have played a major role in the dissemination of *bla*_{NDM}-like genes in Czech hospitals, which is in agreement with the findings from previous studies from worldwide (Krishnaraju

et al., 2015; Zhu et al., 2016; Pál et al., 2017). In the current study, three *bla*_{NDM}-type genes, encoding the NDM-1, NDM-4, and NDM-5 enzymes, were associated with IncX3 plasmids exhibiting high similarity to each other. Considering also the fact that NDM-1, NDM-4, and NDM-5 differ by one or two amino-acid substitutions may indicate the possibility that *bla*_{NDM}-like genes encoding NDM-1-related variants have evolved in the same plasmid type. Additionally, Illumina data showed the presence of a unique sequence, a Tn3-like transposon, in sequenced *bla*_{NDM-4}-carrying plasmids. PCR confirmed the presence of the Tn3-like sequence in all transconjugants, carrying *bla*_{NDM-4}-positive plasmids. Thus, the PCR targeting of the Tn3-like sequence was able to distinguish *bla*_{NDM-4}-positive plasmids from other IncX3 plasmids carrying *bla*_{NDM-1} or *bla*_{NDM-5}. On the other hand, two of the sporadic isolates carried novel NDM-1-encoding plasmids. Plasmid pKpn-35963cz that was an IncFIB(K) molecule contained an acquired sequence, encoding NDM-1 MβL, which exhibited high similarity to the mosaic region of pS-3002cz. pS-3002cs was characterized from an ST11 *K. pneumoniae* isolate, producing NDM-1 carbapenemase, identified in Czechia (Studentova et al., 2015). Whereas plasmid pEsco-36073cz was a multireplicon

A/C₂+R NDM-1-encoding plasmid, being a fusion derivative of sequences of diverse origin. Similar to other type 1 A/C₂ plasmids (Harmer and Hall, 2015; Villa et al., 2015), the *bla*_{NDM-1} gene was located within the ARI-A resistance island.

In conclusion, the data presented here contribute to the current knowledge of NDM-like-producing *Enterobacteriaceae*. In agreement with previous studies, our findings punctuate that NDM-like producers constitute an important public threat, mainly due to the rapid horizontal transfer of IncX3 *bla*_{NDM}-carrying plasmids but, also, due to further evolvement of NDM-like-encoding MDR plasmids via reshuffling.

AUTHOR CONTRIBUTIONS

CP and JH played an important role in interpreting the results and in writing the manuscript. VJ, TB, and HZ helped to acquired data. VP, MM, AS, KC, and IB carried out experimental work. CP supervised the experiments and revised the final manuscript, which was approved by all authors.

REFERENCES

- Bankevich, A., Nurk, S., Antipov, D., Gurevich, A. A., Dvorkin, M., Kulikov, A. S., et al. (2012). SPAdes: a new genome assembly algorithm and its applications to single-cell sequencing. *J. Comp. Biol.* 19, 455–477. doi: 10.1089/cmb.2012.0021
- Barton, B. M., Harding, G. P., and Zuccarelli, A. J. (1995). A general method for detecting and sizing large plasmids. *Anal. Biochem.* 226, 235–240. doi: 10.1006/abio.1995.1220
- Bocanegra-Ibarras, P., Garza-González, E., Morfin-Otero, R., Barrios, H., Villarreal-Treviño, L., and Rodríguez-Noriega, E., et al. (2017). Molecular and microbiological report of a hospital outbreak of NDM-1-carrying *Enterobacteriaceae* in Mexico. *PLoS ONE* 12:e0179651. doi: 10.1371/journal.pone.0179651
- Bolger, A. M., Lohse, M., and Usadel, B. (2014). Trimmomatic: a flexible trimmer for illumina sequence data. *Bioinformatics* 30, 2114–2120. doi: 10.1093/bioinformatics/btu170
- Carattoli, A., Bertini, A., Villa, L., Falbo, V., Hopkins, K. L., and Threlfall, E. J. (2005). Identification of plasmids by PCR-based replicon typing. *J. Microbiol. Methods* 63, 219–228. doi: 10.1016/j.mimet.2005.03.018
- Cohen, S. N., Chang, A. C. Y., and Hsu, L. (1972). Nonchromosomal antibiotic resistance in bacteria: genetic transformation of *Escherichia coli* by R-factor DNA. *Proc. Natl. Acad. Sci. U.S.A.* 69, 2110–2114. doi: 10.1073/pnas.69.8.2110
- Conlan, S., Thomas, P. J., Deming, C., Park, M., Lau, A. F., Dekker, J. P., et al. (2014). Single-molecule sequencing to track plasmid diversity of hospital-associated carbapenemase-producing *Enterobacteriaceae*. *Sci. Transl. Med.* 6:254ra126. doi: 10.1126/scitranslmed.3009845
- Coque, T. M., Novais, A., Carattoli, A., Poirel, L., Pitout, J., Peixe, L., et al. (2008). Dissemination of clonally related *Escherichia coli* strains expressing extended-spectrum β -lactamase CTX-M-15. *Emerging Infect. Dis.* 14, 195–200. doi: 10.3201/eid1402.070350
- Darling, A. E., Mau, B., and Perna, N. T. (2010). Progressivemaue: multiple genome alignment with gene gain, loss and rearrangement. *PLoS ONE* 5:e11147. doi: 10.1371/journal.pone.0011147
- Diancourt, L., Passet, V., Verhoef, J., Grimont, P. A., and Brisse, S. (2005). Multilocus sequence typing of *Klebsiella pneumoniae* nosocomial isolates. *J. Clin. Microbiol.* 43, 4178–4182. doi: 10.1128/JCM.43.8.4178-4182.2005
- Doi, Y., Potoski, B. A., Adams-Haduch, J. M., Sidjabat, H. E., Pasculle, A. W., and Paterson, D. L. (2008). Simple disk-based method for detection of *Klebsiella pneumoniae* carbapenemase-type beta-lactamase by use of a boronic acid compound. *J. Clin. Microbiol.* 46, 4083–4086. doi: 10.1128/JCM.01408-08

FUNDING

This work was supported by the Medical Research Foundation of the Czech Republic (grant numbers 15-28663A and 17-29239A); by the National Sustainability Program I (NPU I; grant number LO1503) provided by the Ministry of Education Youth and Sports of the Czech Republic; and the Charles University Research Fund- PROGRES (grant number Q39).

ACKNOWLEDGMENTS

We are very thankful to Dana Kralova for technical assistance during the present study. The authors also thank Thomas Jové for curating integron sequencing data.

SUPPLEMENTARY MATERIAL

The Supplementary Material for this article can be found online at: <https://www.frontiersin.org/articles/10.3389/fmicb.2018.01549/full#supplementary-material>

- Ellington, M. J., Kistler, J., Livermore, D. M., and Woodford, N. (2007). Multiplex PCR for rapid detection of genes encoding acquired metallo- β -lactamases. *J. Antimicrob. Chemother.* 59, 321–322. doi: 10.1093/jac/dkl481
- EUCAST (2003). European Committee on Antimicrobial Susceptibility Testing (EUCAST) of the European Society of Clinical Microbiology and Infectious Diseases (ESCMID), (2003). Determination of minimum inhibitory concentrations (MICs) of antibacterial agents by broth dilution. *Clin. Microbiol. Infect.* 9, ix–xv. doi: 10.1046/j.1469-0691.2003.00790.x
- EUCAST (European Committee on Antimicrobial Susceptibility Testing) (2012). *EUCAST Guidelines for Detection of Resistance Mechanism and Specific Resistances of Clinical and/or Epidemiological Importance*. Växjö: European Committee on Antimicrobial Susceptibility Testing. Available online at: http://www.eucast.org/fileadmin/src/media/PDFs/EUCAST_files/Consultation/EUCAST_guidelines_detection_of_resistance_mechanisms_121222.pdf
- García-Fernández, A., Fortini, D., Veldman, K., Mevius, D., and Carattoli, A. (2009). Characterization of plasmids harbouring *qnrS1*, *qnrB2* and *qnrB19* genes in *Salmonella*. *J. Antimicrob. Chemother.* 63, 274–281. doi: 10.1093/jac/dkn470
- Glupczynski, Y., Huang, T. D., Bouchahrouf, W., Rezende de Castro, R., Bauraing, C., Gérard, M., et al. (2012). Rapid emergence and spread of OXA-48-producing carbapenem-resistant *Enterobacteriaceae* isolates in Belgian hospitals. *Int. J. Antimicrob. Agents* 39, 168–172. doi: 10.1016/j.ijantimicag.2011.10.005
- Gu, C. T., Li, C. Y., Yang, L. J., and Huo, G. C. (2014). *Enterobacter xiangfangensis* sp. nov., isolated from Chinese traditional sourdough, and reclassification of *Enterobacter sacchari* Zhu et al. 2013 as *Kosakonia sacchari* comb. nov. *Int. J. Syst. Evol. Microbiol.* 64, 2650–2656. doi: 10.1099/ijss.0.064709-0
- Gurevich, A., Saveliev, V., Vyahhi, N., and Tesler, G. (2013). QUASt: quality assessment tool for genome assemblies. *Bioinformatics* 29, 1072–1075. doi: 10.1093/bioinformatics/btt086
- Hancock, S. J., Phan, M. D., Peters, K. M., Forde, B. M., Chong, T. M., Yin, W. F., et al. (2017). Identification of IncA/C plasmid replication and maintenance genes and development of a plasmid multilocus sequence typing scheme. *Antimicrob. Agents Chemother.* 61, e01740–e01816. doi: 10.1128/AAC.01740-16
- Harmer, C. J., and Hall, R. M. (2015). The A to Z of A/C plasmids. *Plasmid* 80, 63–82. doi: 10.1016/j.plasmid.2015.04.003
- Herzog, K. A., Schneditz, G., Leitner, E., Feiler, G., Hoffmann, K. M., Zollner-Schwetz, I., et al. (2014). Genotypes of *Klebsiella oxytoca* isolates from patients with nosocomial pneumonia are distinct from those of isolates from

- patients with antibiotic-associated hemorrhagic colitis. *J. Clin. Microbiol.* 52, 1607–1616. doi: 10.1128/JCM.03373-13
- Hoffmann, H., and Roggenkamp, A. (2003). Population genetics of the nomenspecies *Enterobacter cloacae*. *Appl. Environ. Microbiol.* 69, 5306–5318. doi: 10.1128/AEM.69.9.5306-5318.2003
- Hornsey, M., Phee, L., and Wareham, D. W. (2011). A novel variant, NDM-5, of the New Delhi metallo- β -lactamase in a multidrug-resistant *Escherichia coli* ST648 isolate recovered from a patient in the United Kingdom. *Antimicrob. Agents Chemother.* 55, 5952–5954. doi: 10.1128/AAC.05108-11
- Hrabak, J., Stolbová, M., Studentová, V., Fridrichová, M., Chudacková, E., and Zemlickova, H. (2012). NDM-1 producing *Acinetobacter baumannii* isolated from a patient repatriated to the Czech Republic from Egypt, July 2011. *Euro Surveill.* 17:20085.
- Izdebski, R., Fiett, J., Urbanowicz, P., Baraniak, A., Derde, L. P., Bonten, M. J., et al. (2015). Phylogenetic lineages, clones and β -lactamases in an international collection of *Klebsiella oxytoca* isolates non-susceptible to expanded-spectrum cephalosporins. *J. Antimicrob. Chemother.* 70, 3230–3237. doi: 10.1093/jac/dkv273
- Johnson, T. J., Bielak, E. M., Fortini, D., Hansen, L. H., Hasman, H., Debroy, C., et al. (2012). Expansion of the IncX plasmid family for improved identification and typing of novel plasmids in drug-resistant *Enterobacteriaceae*. *Plasmid* 68, 43–50. doi: 10.1016/j.plasmid.2012.03.001
- Koboldt, D. C., Zhang, Q., Larson, D. E., Shen, D., McLellan, M. D., Lin, L., et al. (2012). VarScan 2: somatic mutation and copy number alteration discovery in cancer by exome sequencing. *Genome Res.* 22, 568–576. doi: 10.1101/gr.129684.111
- Krishnaraju, M., Kamatchi, C., Jha, A. K., Devasena, N., Vennila, R., Sumathi, G., et al. (2015). Complete sequencing of an IncX3 plasmid carrying *bla*_{NDM-5} allele reveals an early stage in the dissemination of the *bla*_{NDM} gene. *Indian J. Med. Microbiol.* 33, 30–38. doi: 10.4103/0255-0857.148373
- Lee, K., Lim, Y. S., Yong, D., Yum, J. H., and Chong, Y. (2003). Evaluation of the Hodge test and the imipenem-EDTA double-disk synergy test for differentiating metallo- β -lactamase-producing isolates of *Pseudomonas* spp. and *Acinetobacter* spp. *J. Clin. Microbiol.* 41, 4623–4629. doi: 10.1128/JCM.41.10.4623-4629.2003
- Li, H. (2013). Aligning sequence reads, clone sequences and assembly contigs with BWA-MEM. *ArXiv*. e-Prints 1303, 3997.
- Li, H., Handsaker, B., Wysoker, A., Fennell, T., Ruan, J., Homer, N., et al. (2009). The sequence alignment/map format and SAMtools. *Bioinformatics* 25, 2078–2079. doi: 10.1093/bioinformatics/btp352
- Marchler-Bauer, A., Bo, Y., Han, L., He, J., Lanczycki, C. J., Lu, S., et al. (2017). CDD/SPARCLE: functional classification of proteins via subfamily domain architectures. *Nucl. Acids Res.* 45, D200–D203. doi: 10.1093/nar/gkw1129
- Marchler-Bauer, A., and Bryant, S. H. (2004). CD-Search: protein domain annotations on the fly. *Nucleic Acids Res.* 32, W327–W331. doi: 10.1093/nar/gkh454
- Mikheenko, A., Valin, G., Prjibelski, A., Saveliev, V., and Gurevich, A. (2016). Icarus: visualizer for de novo assembly evaluation. *Bioinformatics* 32, 3321–3323. doi: 10.1093/bioinformatics/btw379
- Milne, I., Stephen, G., Bayer, M., Cock, P. J. A., Pritchard, L., Cardle, L., et al. (2013). Using Tablet for visual exploration of second-generation sequencing data. *Brief. Bioinformatics* 14, 193–202. doi: 10.1093/bib/bbs012
- Miyoshi-Akiyama, T., Hayakawa, K., Ohmagari, N., Shimojima, M., and Kirikae, T. (2013). Multilocus sequence typing (MLST) for characterization of *Enterobacter cloacae*. *PLoS ONE* 8:e66358. doi: 10.1371/journal.pone.0066358
- Naas, T., Cuzon, G., Villegas, M. V., Lartigue, M. F., Quinn, J. P., and Nordmann, P. (2008). Genetic structure at the origin of acquisition of the beta-lactamase *bla*_{KPC} gene. *Antimicrob. Agents Chemother.* 52, 1257–1263. doi: 10.1128/AAC.01451-07
- Nordmann, P., Boulanger, A. E., and Poirel, L. (2012). NDM-4 metallo- β -lactamase with increased carbapenemase activity from *Escherichia coli*. *Antimicrob. Agents Chemother.* 56, 2184–2186. doi: 10.1128/AAC.05961-11
- Nordmann, P., Poirel, L., Walsh, T. R., and Livermore, D. M. (2011). The emerging NDM carbapenemases. *Trends Microbiol.* 19, 588–595. doi: 10.1016/j.tim.2011.09.005
- Pál, T., Ghazawi, A., Darwish, D., Villa, L., Carattoli, A., Hashmey, R., et al. (2017). Characterization of NDM-7 carbapenemase-producing *Escherichia coli* isolates in the Arabian Peninsula. *Microb. Drug Resist.* 23, 871–878. doi: 10.1089/mdr.2016.0216
- Pałucha, A., Mikiewicz, B., Hryniewicz, W., and Gniadkowski, M. (1999). Concurrent outbreaks of extended-spectrum beta-lactamase-producing organisms of the family *Enterobacteriaceae* in a Warsaw hospital. *J. Antimicrob. Chemother.* 44, 489–499. doi: 10.1093/jac/44.4.489
- Papagiannitsis, C. C., Dolejska, M., Izdebski, R., Giakkoupi, P., Skalova, A., Chudejova, K., et al. (2016). Characterisation of IncA/C² plasmids carrying an In416-like integron with the *bla*_{VIM-19} gene from *Klebsiella pneumoniae* ST383 of Greek origin. *Int. J. Antimicrob. Agents* 47, 158–162. doi: 10.1016/j.ijantimicag.2015.12.001
- Papagiannitsis, C. C., Miriagou, V., Giakkoupi, P., Tzouveleakis, L. S., and Vatopoulos, A. C. (2013a). Characterization of pKP1780, a novel IncR plasmid from the emerging *Klebsiella pneumoniae* ST147, encoding the VIM-1 metallo- β -lactamase. *J. Antimicrob. Chemother.* 68, 2259–2262. doi: 10.1093/jac/dkt196
- Papagiannitsis, C. C., Studentova, V., Chudackova, E., Bergerova, T., Hrabak, J., Radej, J., et al. (2013b). Identification of a New Delhi metallo- β -lactamase-4 (NDM-4)-producing *Enterobacter cloacae* from a Czech patient previously hospitalized in Sri Lanka. *Folia Microbiol.* 58, 547–549. doi: 10.1007/s12223-013-0247-5
- Papagiannitsis, C. C., Studentova, V., Jakubu, V., Spanelova, P., Urbaskova, P., Zemlickova, H., et al. (2015). High prevalence of ST131 among CTX-M-producing *Escherichia coli* from community-acquired infections, in the Czech Republic. *Microb. Drug Resist.* 21, 74–84. doi: 10.1089/mdr.2014.0070
- Pavan, M. E., Franco, R. J., Rodriguez, J. M., Gadaleta, P., Abbott, S. L., Janda, J. M., et al. (2005). Phylogenetic relationships of the genus *Kluyvera*: transfer of *Enterobacter intermedius* Izard et al. 1980 to the genus *Kluyvera* as *Kluyvera intermedia* comb. nov. and reclassification of *Kluyvera cochleae* as a later synonym of *K. intermedia*. *Int. J. Syst. Evol. Microbiol.* 55, 437–442. doi: 10.1099/ijs.0.63071-0
- Pérez-Pérez, F. J., and Hanson, N. D. (2002). Detection of plasmid-mediated AmpC beta-lactamase genes in clinical isolates by using multiplex PCR. *J. Clin. Microbiol.* 40, 2153–2162. doi: 10.1128/JCM.40.6.2153-2162.2002
- Poirel, L., Heritier, C., Tolun, V., and Nordmann, P. (2004). Emergence of oxacillinase-mediated resistance to imipenem in *Klebsiella pneumoniae*. *Antimicrob. Agents Chemother.* 48, 15–22. doi: 10.1128/AAC.48.1.15-22.2004
- Rotova, V., Papagiannitsis, C. C., Skalova, A., Chudejova, K., and Hrabak, J. (2017). Comparison of imipenem and meropenem antibiotics for the MALDI-TOF MS detection of carbapenemase activity. *J. Microbiol. Methods* 137, 30–33. doi: 10.1016/j.mimet.2017.04.003
- Seemann, T. (2014). Prokka: rapid prokaryotic genome annotation. *Bioinformatics* 30, 2068–2069. doi: 10.1093/bioinformatics/btu153
- Studentova, V., Dobiasova, H., Hedlova, D., Dolejska, M., Papagiannitsis, C. C., and Hrabak, J. (2015). Complete nucleotide sequences of two NDM-1-encoding plasmids from the same sequence type 11 *Klebsiella pneumoniae* strain. *Antimicrob. Agents Chemother.* 59, 1325–1328. doi: 10.1128/AAC.04095-14
- Torres-González, P., Bobadilla-Del Valle, M., Tovar-Calderón, E., Leal-Vega, F., Hernández-Cruz, A., Martínez-Gamboa, A., et al. (2015). Outbreak caused by *Enterobacteriaceae* harboring NDM-1 metallo- β -lactamase carried in an IncFII plasmid in a tertiary care hospital in Mexico City. *Antimicrob. Agents Chemother.* 59, 7080–7083. doi: 10.1128/AAC.00055-15
- Vatopoulos, A. C., Philippon, A., Tzouveleakis, L. S., Komninou, Z., and Legakis, N. J. (1990). Prevalence of a transferable SHV-5 type beta-lactamase in clinical isolates of *Klebsiella pneumoniae* and *Escherichia coli* in Greece. *J. Antimicrob. Chemother.* 26, 635–648. doi: 10.1093/jac/26.5.635
- Villa, L., Guerra, B., Schmoger, S., Fischer, J., Helmuth, R., Zong, Z., et al. (2015). IncA/C plasmid carrying *bla*_{NDM-1}, *bla*_{CMY-16}, and *fosA3* in a *Salmonella enterica* serovar corvallis strain isolated from a migratory wild bird in Germany. *Antimicrob. Agents Chemother.* 59, 6597–6600. doi: 10.1128/AAC.00944-15
- Wirth, T., Falush, D., Lan, R., Colles, F., Mensa, P., Wieler, L. H., et al. (2006). Sex and virulence in *Escherichia coli*: an evolutionary perspective. *Mol. Microbiol.* 60, 1136–1151. doi: 10.1111/j.1365-2958.2006.05172.x
- Woodford, N., Fagan, E. J., and Ellington, M. J. (2006). Multiplex PCR for rapid detection of genes encoding CTX-M extended-spectrum (beta)-lactamases. *J. Antimicrob. Chemother.* 57, 154–155. doi: 10.1093/jac/dki412
- Woodford, N., Turton, J. F., and Livermore, D. M. (2011). Multiresistant Gram-negative bacteria: the role of high-risk clones in the

- dissemination of antibiotic resistance. *FEMS Microbiol. Rev.* 35, 736–755. doi: 10.1111/j.1574-6976.2011.00268.x
- Yang, P., Xie, Y., Feng, P., and Zong, Z. (2014). *bla*_{NDM-5} carried by an IncX3 plasmid in *Escherichia coli* sequence type 167. *Antimicrob. Agents Chemother.* 58, 7548–7552. doi: 10.1128/AAC.03911-14
- Yong, D., Toleman, M. A., Giske, C. G., Cho, H. S., Sundman, K., Lee, K., et al. (2009). Characterization of a new metallo- β -lactamase gene, *bla*_{NDM-1}, and a novel erythromycin esterase gene carried on a unique genetic structure in *Klebsiella pneumoniae* sequence type 14 from India. *Antimicrob. Agents Chemother.* 53, 5046–5054. doi: 10.1128/AAC.00774-09
- Zankari, E., Hasman, H., Cosentino, S., Vestergaard, M., Rasmussen, S., Lund, O., et al. (2012). Identification of acquired antimicrobial resistance genes. *J. Antimicrob. Chemother.* 67, 2640–2644. doi: 10.1093/jac/dks261
- Zhang, L. P., Xue, W. C., and Meng, D. Y. (2016). First report of New Delhi metallo- β -lactamase 5 (NDM-5)-producing *Escherichia coli* from blood cultures of three leukemia patients. *Int. J. Infect. Dis.* 42, 45–46. doi: 10.1016/j.ijid.2015.10.006
- Zhou, Y., Liang, Y., Lynch, K., Dennis, J. J., and Wishart, D. S. (2011). PHAST: a fast phage search tool. *Nucleic Acids Res.* 39, W347–W352. doi: 10.1093/nar/gkr485
- Zhu, Y. Q., Zhao, J. Y., Xu, C., Zhao, H., Jia, N., and Li, Y. N. (2016). Identification of an NDM-5-producing *Escherichia coli* sequence type 167 in a neonatal patient in China. *Sci. Rep.* 6:29934. doi: 10.1038/srep29934

Conflict of Interest Statement: The authors declare that the research was conducted in the absence of any commercial or financial relationships that could be construed as a potential conflict of interest.

Copyright © 2018 Paskova, Medvecký, Skalová, Chudejová, Bitar, Jakubu, Bergerová, Zemlicková, Papagiannitsis and Hrabák. This is an open-access article distributed under the terms of the Creative Commons Attribution License (CC BY). The use, distribution or reproduction in other forums is permitted, provided the original author(s) and the copyright owner(s) are credited and that the original publication in this journal is cited, in accordance with accepted academic practice. No use, distribution or reproduction is permitted which does not comply with these terms.



Identification of a Novel Plasmid Lineage Associated With the Dissemination of Metallo- β -Lactamase Genes Among Pseudomonads

Vincenzo Di Pilato¹, Alberto Antonelli¹, Tommaso Giani^{1,2}, Lucia Henrici De Angelis³, Gian Maria Rossolini^{1,2} and Simona Pollini^{1,2*}

OPEN ACCESS

Edited by:

Raffaele Zarrilli,
University of Naples Federico II, Italy

Reviewed by:

Remy A. Bonnin,
Université Paris-Saclay, France
Stefano Gaiarsa,
Fondazione IRCCS Policlinico
San Matteo, Italy

*Correspondence:

Simona Pollini
simona.pollini@unifi.it

Specialty section:

This article was submitted to
Antimicrobials, Resistance
and Chemotherapy,
a section of the journal
Frontiers in Microbiology

Received: 08 April 2019

Accepted: 14 June 2019

Published: 02 July 2019

Citation:

Di Pilato V, Antonelli A, Giani T,
Henrici De Angelis L, Rossolini GM
and Pollini S (2019) Identification of a
Novel Plasmid Lineage Associated
With the Dissemination
of Metallo- β -Lactamase Genes
Among Pseudomonads.
Front. Microbiol. 10:1504.
doi: 10.3389/fmicb.2019.01504

Acquisition of metallo- β -lactamases (MBLs) represents one of most relevant resistance mechanisms to all β -lactams, including carbapenems, ceftolozane and available β -lactamase inhibitors, in *Pseudomonas* spp. VIM-type enzymes are the most common acquired MBLs in *Pseudomonas aeruginosa* and, to a lesser extent, in other *Pseudomonas* species. Little is known about the acquisition dynamics of these determinants, that are usually carried on integrons embedded into chromosomal mobile genetic elements. To date, few MBL-encoding plasmids have been described in *Pseudomonas* spp., and their diversity and role in the dissemination of these MBLs remains largely unknown. Here we report on the genetic features of the VIM-1-encoding plasmid pMOS94 from *P. mosselii* AM/94, the earliest known VIM-1-producing strain, and of related elements involved in dissemination of MBL. Results of plasmid DNA sequencing showed that pMOS94 had a modular organization, consisting of backbone modules associated with replication, transfer and antibiotic resistance. Plasmid pMOS94, although not typable according to the PBRT scheme, was classifiable either in MOB_{F11} or MPF_T plasmid families. The resistance region included the class I integron In70, carrying *bla*_{VIM-1}, in turn embedded in a defective Tn402-like transposon. Comparison with pMOS94-like elements led to the identification of a defined plasmid lineage circulating in different *Pseudomonas* spp. of clinical and environmental origin and spreading different MBL-encoding genes, including *bla*_{IMP-63}, *bla*_{BIM}, and *bla*_{VIM}-type determinants. Genetic analysis revealed that this plasmid lineage likely shared a common ancestor and had evolved through the acquisition and recombination of different mobile elements, including the MBL-encoding transposons. Our findings provide new insights about the genetic diversity of MBL-encoding plasmids circulating

among *Pseudomonas* spp., potentially useful for molecular epidemiology purposes, and revealed the existence and persistence of a successful plasmid lineage over a wide spatio-temporal interval, spanning over five different countries among two continents and over 20-years.

Keywords: metallo- β -lactamase, mobile genetic elements, integron, antibiotic resistance, plasmid

INTRODUCTION

Pseudomonas is a genetically and metabolically diverse genus of bacteria, which inhabit a wide variety of environments and can act as pathogens of humans, animals and plants. Among the wide variety of *Pseudomonas* species, only few have been recognized as human pathogens, with *Pseudomonas aeruginosa* being the most common cause of infections (Driscoll et al., 2007; Høiby et al., 2015; Peix et al., 2018).

The acquisition by pathogenic *Pseudomonas* species of β -lactamases able to degrade most anti-*pseudomonas* β -lactams and resistant to currently available β -lactamase inhibitors, such as the metallo- β -lactamases (MBLs), can provide a remarkable contribution to the emergence of strains with difficult-to-treat resistance (DTR) phenotypes (Hawkey et al., 2018). VIM-type enzymes are among the most widespread and prevalent acquired MBLs in *P. aeruginosa* (Hong et al., 2015), and have occasionally been reported also in other *Pseudomonas* spp. of clinical interest including *Pseudomonas putida*, *Pseudomonas mosselii*, *Pseudomonas monteilii*, *Pseudomonas stutzeri*, and *Pseudomonas mendocina* (Yan et al., 2001; Lombardi et al., 2002; Giani et al., 2012; Ocampo-Sosa et al., 2015; Almuzara et al., 2018).

Metallo- β -lactamase genes, and in particular *bla*_{VIM}- and *bla*_{IMP}-type genes, are typically carried on mobile gene cassettes inserted into integron platforms (Partridge et al., 2018). While among *Enterobacterales* MBL-encoding integrons are mostly associated with plasmid lineages of IncN-, IncI1- and IncHI2-type replicons (Carattoli, 2009; Villa et al., 2014), less is known about the genetic support of these elements among *Pseudomonas* spp. In these species, MBL-encoding integrons have been described both as chromosomal- (Lauretti et al., 1999; Perez et al., 2014; Di Pilato et al., 2015; Roy Chowdhury et al., 2016) and plasmid-borne, but only few plasmids have been completely sequenced (Li et al., 2008; Bonnin et al., 2013; Vilacoba et al., 2014; San Millan et al., 2015; Botelho et al., 2017, 2018; Partridge et al., 2018; Liapis et al., 2019), and information about prevalence and diversity of MBL-carrying plasmid lineages remains largely unknown.

In this study we have investigated the genetic support of the *bla*_{VIM-1} gene from a non-*aeruginosa* *Pseudomonas* strains of clinical origin, namely *Pseudomonas mosselii* AM/94, which represents the earliest known VIM-1-producing strain (Giani et al., 2012). In that strain, *bla*_{VIM-1} was previously shown to be carried on a gene cassette inserted into integron In70, but its genetic support was not further investigated. Here we report that in this strain the integron was plasmid-borne and describe the structure of the *bla*_{VIM-1}-carrying plasmid from AM/94, named pMOS94. The results of a comparative

genetic analysis with pMOS94, allowed the definition of a novel plasmid lineage involved in dissemination of MBL genes among *Pseudomonas* spp.

MATERIALS AND METHODS

Bacterial Strains and Antimicrobial Susceptibility Testing

Pseudomonas mosselii AM/94 was isolated in 1994 from the lower respiratory tract of an inpatient in Genoa, Italy (Giani et al., 2012). *P. aeruginosa* C/53 and C/57 were isolated in 2014 from bloodstream infections from intensive care patients from Milan, Italy, and the complete genome has been previously determined (Giani et al., 2018). Identification to the species level and Sequence Type (ST) of C/57 strain were carried out in silico on whole genome sequence data. Antimicrobial susceptibility testing was carried out by reference broth-microdilution method and results were interpreted according to EUCAST clinical breakpoints (EUCAST breakpoint tables version 9, 2019¹).

Plasmid Transfer and Typing

Electrotransformation experiments were performed with electrocompetent *E. coli* DH10B and *P. aeruginosa* PAO-1 using plasmid DNA preparations, obtained as described previously (Docquier et al., 2003). The broad-host range vector plasmid pME6001 (Blumer et al., 1999) was used as positive control in electrotransformation experiments. Transformants were selected on LB agar containing ceftazidime (10 mg/L for *E. coli* and 20 mg/L for *P. aeruginosa*) or gentamicin (30 mg/L) for the pME6001 vector. Conjugation experiments were performed in solid medium as previously described (Docquier et al., 2003), using *E. coli* J53 Azi^R as the recipient strain. Ceftazidime (10 mg/L) was used for the selection of transconjugants and sodium azide (150 mg/L) for counterselection of the donor. Plasmid incompatibility groups were determined following the previously described PCR-based replicon typing (PBRT) schemes (Carattoli et al., 2005; García-Fernández et al., 2009; Villa et al., 2010; Johnson et al., 2012). In silico typing using plasmid relaxases (MOB) regions (Garcillán-Barcia et al., 2009) and the mating pair formation (MPF) apparatus (Smillie et al., 2010) was performed according to the previously proposed classification scheme (Guglielmini et al., 2014; Orlek et al., 2017).

¹www.eucast.org/clinical_breakpoints/

DNA Sequencing and Bioinformatic Analysis

Genomic DNA was extracted as previously described (Johnson, 1994). Plasmid DNA was extracted using Wizard® Plus SV Minipreps DNA purification system (Promega, Madison, United States) according to manufacturer's instructions. Plasmid DNAs from strain AM/94 was subjected to complete sequencing with the Illumina MiSeq platform (Illumina Inc., San Diego, United States) with a 2×250 or 2×300 bp paired-end approach. A total of 171,952 high quality reads were generated and assembled using SPAdes 3.11 (Bankevich et al., 2012). Sequence annotation was performed using the RAST web-server (Aziz et al., 2008). Finishing of pMOS94 and pAER57 plasmid sequences was achieved through Sanger sequencing of PCR products spanning contigs' gaps. Sequence comparisons were performed using BLAST² and Mauve³ Core genome alignments were performed using Roary, using the non-paralog splitting method (Page et al., 2015; Rozwadowski et al., 2017). Plasmid circular and linear maps were generated using the CGView Server and EasyFig tools, respectively (Grant and Stothard, 2008; Sullivan et al., 2011). Comparator plasmid sequences were selected from the NCBI-NIH database (non-redundant) to include all circular molecules with 100% sequence identity at nucleotide level of the *repA-oriV* region of plasmid pMOS94. A tentative plasmid classification based on replicase (*rep*) homology was inferred through nucleotide sequence alignments of *rep* genes from representative members of the IncN (García-Fernández et al., 2011), IncW (Suzuki et al., 2010; Aoki et al., 2018), and IncP9 replicons (Sevastyanovich et al., 2008), collectively clustering into the MOB_{F11} relaxase family, to which pMOS94-like plasmids belong. Plasmids used in this analysis are reported in **Supplementary Table S1**. Sequences were aligned using the MAFFT v.7 server⁴ with the G-INS-1 progressive method, and the *rep* phylogeny was inferred using the Neighbor-joining method implemented by MAFFT. Phylogenetic trees were visualized and annotated through the Evolview software (He et al., 2016).

RESULTS

Mapping of *bla*_{VIM-1} in a Plasmid From *P. mosselii* AM/94

Pseudomonas mosselii AM/94 was previously shown to carry the *bla*_{VIM-1} gene cassette as part of an In70 integron platform (5'CS – *bla*_{VIM-1} – *aacA4* – *aphA15* – *aadA15* – 3'CS) (Giani et al., 2012).

To investigate the genetic support of the *bla*_{VIM-1} cassette and of its cognate integron in *P. mosselii* AM/94, an S1 nuclease assay and hybridization with a *bla*_{VIM}-specific probe were performed. Results mapped *bla*_{VIM} to a 50 kb plasmid (data not shown), hereafter referred to as pMOS94.

Gene transfer experiments failed in yielding transconjugants using *E. coli* J53 as recipient in conjugation experiments, and transformants using *E. coli* DH10B and *P. aeruginosa* PAO-1 as recipients in electrotransformation experiments.

The PBRT assay (Carattoli et al., 2005; García-Fernández et al., 2009; Villa et al., 2010; Johnson et al., 2012), performed on total DNA purified from AM/94, could not identify any plasmid replicon.

Sequence Analysis of pMOS94: General Features and Plasmid Backbone

In order to determine the genetic features of pMOS94, plasmid DNA was purified from AM/94 and completely sequenced. *De novo* sequence assembly yielded a single contig of 51,660 kb in length, which resulted in a 52,002 kb circular molecule, with a raw coverage of 380× and a mean G+C content of 59.6%, following sequence completion.

A total of 71 coding sequences (CDS) were identified by the RAST annotation pipeline, of which 37 had a predicted function consisting in: replication and stability ($n = 7$), transfer ($n = 14$), mobile genetic elements ($n = 9$) and antibiotic resistance ($n = 7$) (**Figure 1**).

Plasmid pMOS94 showed a modular organization associated with the following functions: (i) plasmid replication; (ii) conjugal transfer; (iii) antibiotic resistance.

The replication module included genes essential for plasmid replication (*repA*, *res*) and stability (*stbABC*), as well as a type II toxin-antitoxin system (*vapBC*) for stable maintenance. A putative replication origin (*oriV*) was identified immediately adjacent to *repA*, characterized by four 19-bp (TTCGTCCTCCAGGGACCG) and seven 9-bp (TTCGTCCT) iteron repeats, suggesting a theta-type replication mechanism for pMOS94 (Chattoraj, 2000).

The transfer module comprised a *trw*-type gene cluster encoding a T4SS machinery, composed by three structurally different components within the same segmented operon (Llosa and Alkorta, 2017) encoding: (i) the inner membrane complex (TrwMKIGB); (ii) the outer membrane core complex (TrwNHFE); (iii) the external pilus (TrwLJ). *In silico* analyses according to the MOB and MPF typing schemes, exploiting T4SS components for classification (Garcillán-Barcia et al., 2009; Smillie et al., 2010; Guglielmini et al., 2014; Orlek et al., 2017), revealed that pMOS94 was classifiable either in the MOB_{F11} or in the MPF_T families.

The resistance region was organized in two non-contiguous segments, of which one was represented by the In70 integron platform carried on a defective Tn402-like transposon, whereas the second included Tn5393c, a Tn3-family transposon carrying the *strA-strB* genes, coding for phosphotransferases able to confer high level resistance to streptomycin (Chiou and Jones, 1993; Sunde and Norström, 2005). These segments were located downstream of and within the transfer module, respectively. The interruption of the *trw* operon by insertion of Tn5393c, apparently related with a transposition event generating 5-bp direct repeats (DRs) (5'-GAATA-3') flanking the element, could explain the inability of pMOS94 for conjugal transfer.

²<http://blast.ncbi.nlm.nih.gov/>

³<http://darlinglab.org/mauve/mauve.html>

⁴<https://mafft.cbrc.jp/alignment/server/>

period (2014), and showed the same clonality (ST 532) and resistome (data not shown), C/57 was selected as representative for plasmid closure.

Interestingly, the analyzed plasmids were uniquely detected within members of the *Pseudomonas* genus, including strains of *P. aeruginosa*, *P. putida*, and *P. mosselii*. All of them carried an MBL-encoding gene (i.e., *bla_{VIM}*, *bla_{IMP}*, or *bla_{BIM}*) in association with additional antibiotic resistance determinants (Table 1). In most of cases (6/7) the *Pseudomonas* strains were from clinical sources, with the exception of *P. putida* IEC33019, which was from an environmental source. Overall these strains were from five different countries, belonging to two continents, and had been isolated over a prolonged time period spanning over 20-years (Table 1).

Sequence analysis and comparison of pMOS94 with the other plasmids revealed an overall conserved backbone structure, containing genes involved in stability, maintenance and, in some cases, encoding the T4SS or parts thereof (Figure 2). Except for pAMBL2, where the transfer operon and the cognate relaxase were fully lacking, all plasmids were found to belong to the MOB_{F11}/MPF_T families and were untypeable by the replicon typing scheme, as pMOS94.

Compared to pMOS94, pIEC33019 exhibited the closest conserved architecture, with major differences due to the acquisition of mobile genetic elements targeting a different backbone region (Figure 2). Conversely, the most diverging elements were pAMBL2, pPC9 and pAER57. Plasmid pAMBL2 was a small (24.1 kb) deletion derivative of pMOS94, where the entire *trw* locus was lacking, carrying only genes essential for replication processes and a multiresistance region (Figure 2; San Millan et al., 2015). Plasmid pPC9 was characterized by a mosaic architecture, carrying mobile genetic elements and multiple genes coding for metal (e.g., *merEA*) and antibiotic resistance (e.g., In860) (Figure 2 and Table 1; Molina et al., 2014). Plasmid pAER57 was the largest identified element of this lineage (>100 kb), and was characterized by a more complex chimeric arrangement, including a 43 kb segment sharing 87% nucleotide identity with the archetypal IncP-9

pWW0 catabolic plasmid from *P. putida* (GenBank Acc. No. AJ344068) (Greated et al., 2002; Sevastyanovich et al., 2008). The 43 kb segment, likely acquired through recombination with a pWW0-like plasmid, included genes coding for replication (e.g., *res-oriV-rep*), partitioning (e.g., *parABC*, *korA*), transfer (e.g., *mpfABCDEFGHIIJ*) and unknown functions. Therefore, pAER57 was classifiable as a multi-replicon plasmid, being characterized by an additional replication locus (i.e., *res-oriV-rep*) 91% identical to that of pWW0.

Analysis of SNPs evaluated on core orthologous genes of pMOS94-like plasmids showed an overall limited sequence diversity. In detail, all plasmids differed only by 1–2 SNPs from each other, with the exception of pAER57 that was the more divergent, showing 13–14 SNPs differences.

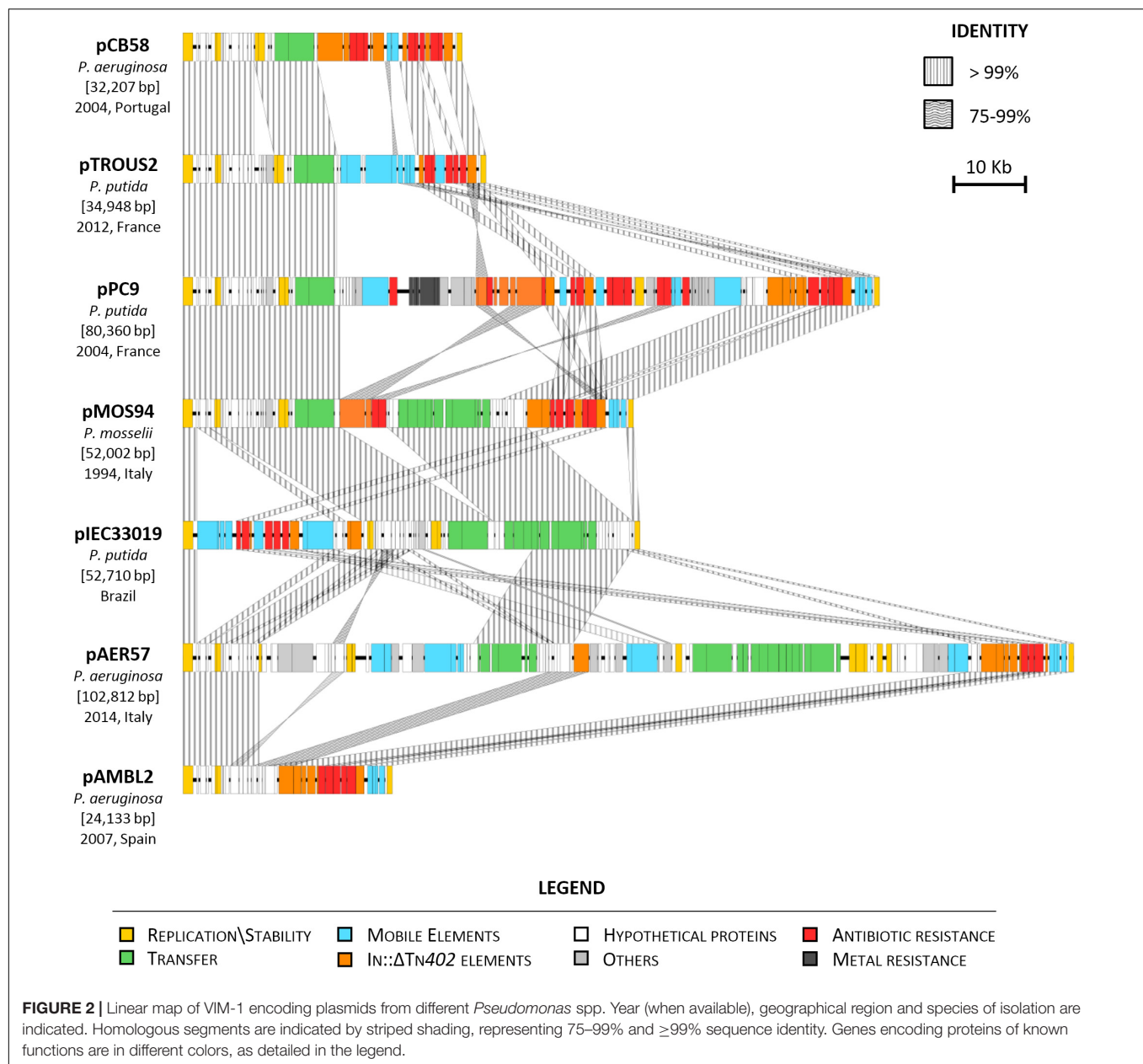
Further sequence analysis revealed that members of this plasmid lineage were also able to integrate into the host chromosome as linear elements. Evidences of integration came from a recent study reporting on the structure of a chromosomal genomic island carrying an MBL determinant from a *P. aeruginosa* strain of clinical origin isolated in Prague in 2015 (GenBank acc. no. KY860572). In this case, the integrated element was apparently a deletion-derivative of pMOS94 (carrying only backbone essential regions coding for replication functions) inserted within a Tn2 family transposon (Tn6162), in turn embedded into a genomic island (PACS171b) previously described in high risk clones of *P. aeruginosa* (i.e., ST 235) as chromosomal support of MBL-encoding genes (Martinez et al., 2012; Di Pilato et al., 2015).

Noteworthy, a plasmid lineage closely related (84–87% identity of the *repA-oriV* locus and belonging to the MOB_{F11} and MPF_T families) to the one identified in this study was detected in the NCBI non-redundant database and included elements preferentially circulating within the genus *Pseudomonas*. These elements included: (i) plasmid pCT14 encoding mercury resistance from *Pseudomonas veronii* (Bramucci et al., 2006); (ii) two unnamed plasmids from *P. aeruginosa* AR_0356 and 163940 producing a KPC-2 carbapenemase (GenBank acc. nos. CP027168.1 and CP029092.1); (iii) plasmid pTROUS1 from

TABLE 1 | General features of the *Pseudomonas* spp. strains and plasmids included in this study.

Organism (strain)	Isolation year	Geographical region	Plasmid	Resistance determinants ^a	References	Acc. No.
<i>P. mosselii</i> (AM/94)	1994	Italy, Genoa	pMOS94	<i>bla_{VIM-1}</i> , <i>aacA4</i> , <i>aadA1</i> , <i>aphA15</i> , <i>strA</i> , <i>strB</i> , <i>sul1</i>	This study and Giani et al., 2012	MK671725
<i>P. putida</i> (HB3267)	2004	France, Besançon	pPC9	<i>aadB</i> , <i>strA</i> , <i>strB</i> , <i>aphA15</i> , <i>aadA1</i> , <i>aacA4</i> , <i>bla_{VIM-1}</i> , <i>cmlA1</i> , <i>sul1</i> , <i>sul2</i> , <i>tet(A)</i>	Molina et al., 2014	CP003739
<i>P. aeruginosa</i>	2004	Portugal	pCB58	<i>bla_{VIM-2}</i> , <i>aacA7</i> , <i>aacC1</i> , <i>aacA4v</i> , <i>strA</i> , <i>strB</i>	Botelho et al., 2018	KY630469
<i>P. aeruginosa</i>	2007	Spain, Madrid	pAMBL2	<i>bla_{VIM-1}</i> , <i>aacA4</i> , <i>bla_{VIM-1}</i> , <i>bla_{VIM-1}</i> , <i>aadA1</i> , <i>sul1</i>	San Millan et al., 2015	KP873171
<i>P. putida</i> (12917)	2012	France	pTROUS2	<i>bla_{IMP-63}</i> , <i>bla_{OXA-19}</i> , <i>aacA4v</i>	Liapis et al., 2019	MK047611
<i>P. aeruginosa</i> (C/57)	2014	Italy, Milan	pAER57	<i>aacA4</i> , <i>bla_{VIM-1}</i> , <i>aacA4</i> , <i>aadA1</i> , <i>sul1</i>	This study and Giani et al., 2018	MK671726
<i>P. putida</i> (IEC33019)	–	Brazil	pIEC33019	<i>qnrVC1</i> , <i>bla_{BIM}</i> , <i>ΔaadA6v</i> , <i>sul1</i>	–	CP016446

^aUncharacterized gene variants are named according to the closest homolog plus “v”.

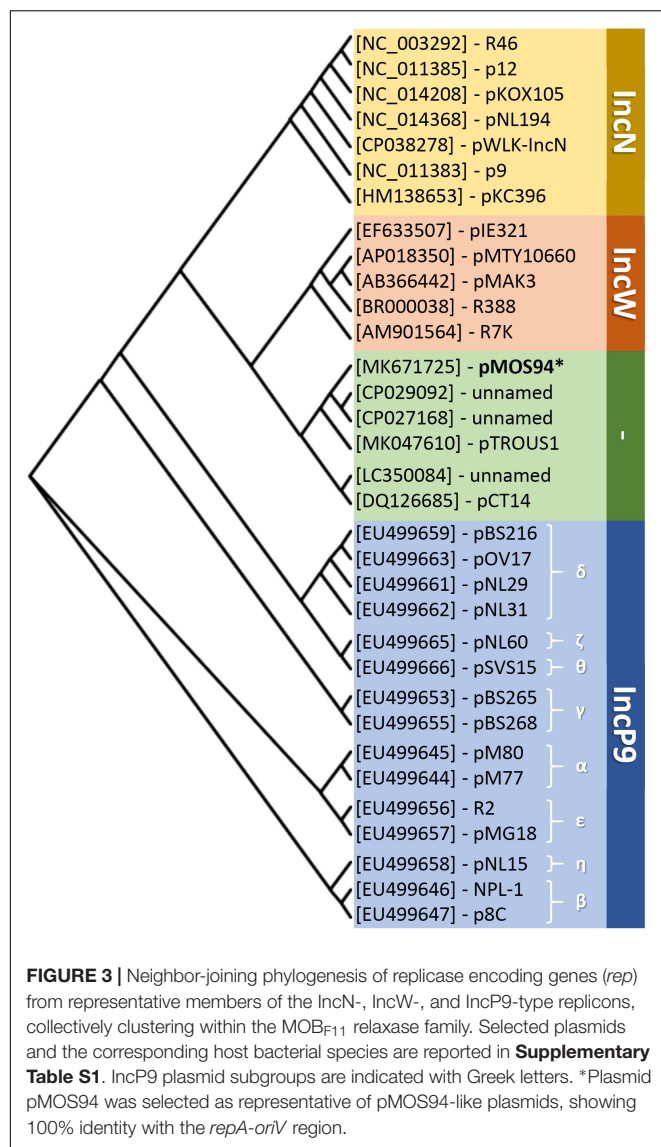


P. aeruginosa 163940 producing an IMP-63 carbapenemase (GenBank acc. no. MK047610.1), and (iv) a non-circular molecule resembling a plasmid element (GenBank acc. no. LC350084.1) coding for a VIM-2 carbapenemase. Notably, most of these elements were associated with clinically relevant resistance determinants and, according to available metadata, were of clinical (pTROUS1 and LC350084.1) or environmental (pCT14) origin. Using the *repA-oriV* locus as probe, at least 96 records were found among *Pseudomonas* spp. draft genome sequences in NCBI wgs database (i.e., showing 100–90% identity), highlighting a potential wide dissemination of pMOS94-related elements. Nevertheless, the plasmidic nature of such records could not be verified due to their fragmentation and unfinished status. In order to infer possible phylogenetic relationships between pMOS94,

pMOS94-related plasmids (i.e., those showing 84–87% identity of the *repA-oriV* locus) and known plasmid replicons belonging to the MOB_{F1} relaxase family, to which pMOS94-like plasmids belong, a classification according to the *rep* locus was attempted. The analysis showed that pMOS94 and related plasmids clustered in a separate branch, that appeared more closely related to IncW than IncN and IncP9 replicons (Figure 3).

Genetic Environment of the MBL-Encoding Genes in the pMOS94-Like Plasmids

All seven plasmids of the pMOS94-like lineage described above carried an MBL-encoding gene, embedded in a class



I integron platform (Figure 4), including *bla_{VIM-1}* in four plasmids, and the *bla_{VIM-2}*, *bla_{BIM}*, and *bla_{IMP-63}* in the remaining ones. The *bla_{VIM-1}* gene was found embedded in the In70 integron (in pMOS94) or in its derivatives (e.g., In110, In860, In1167) carrying a modified version of the typical gene cassette array of this element (i.e., in pAMBL2, pAER57, and pPC9). On the other hand, the other MBL genes were carried in integrons of different structure (e.g., In58, In1326, and In1297; Figure 4). Despite their heterogeneity, the MBL-encoding integrons always carried aminoglycosides resistance determinants, with *aacA4* variants being the most frequent (Figure 4). Most of the integrons carried typical 5'CS and 3'CS regions, except for In110 in pAER57, where the *intI1* gene was partially deleted (Figure 4).

The MBL-encoding integrons were always associated with defective Tn402-like transposons. In most cases (namely pAMBL2, pPC9, pMOS94, pAER57, and pCB58),

the Tn402 25 bp inverted repeats (IRi and IRt) were present at the boundaries of the defective transposons, while in the remaining plasmids (i.e., pTROUS2 and pIEC33019) IRi was present adjacent to the integrase gene, suggesting recombination events which deleted the IRt end. The Tn402 *tni* transposition module was present downstream the 3'CS region in a partially deleted form (in five plasmids), or completely absent (in the others) (Figure 4).

In some cases, additional mobile elements were found within the Tn402 elements, targeting the cassette array or other regions (Figure 4). The IS_{Psp7}-like and IS_{I10}-like insertion sequences, respectively targeting the cassette arrays of pTROUS2 and pIEC33019 were flanked by DRs, suggesting acquisition by transposition.

Evolutionary History of the Tn402-Like Transposons Carried by pMOS94-Like Plasmids

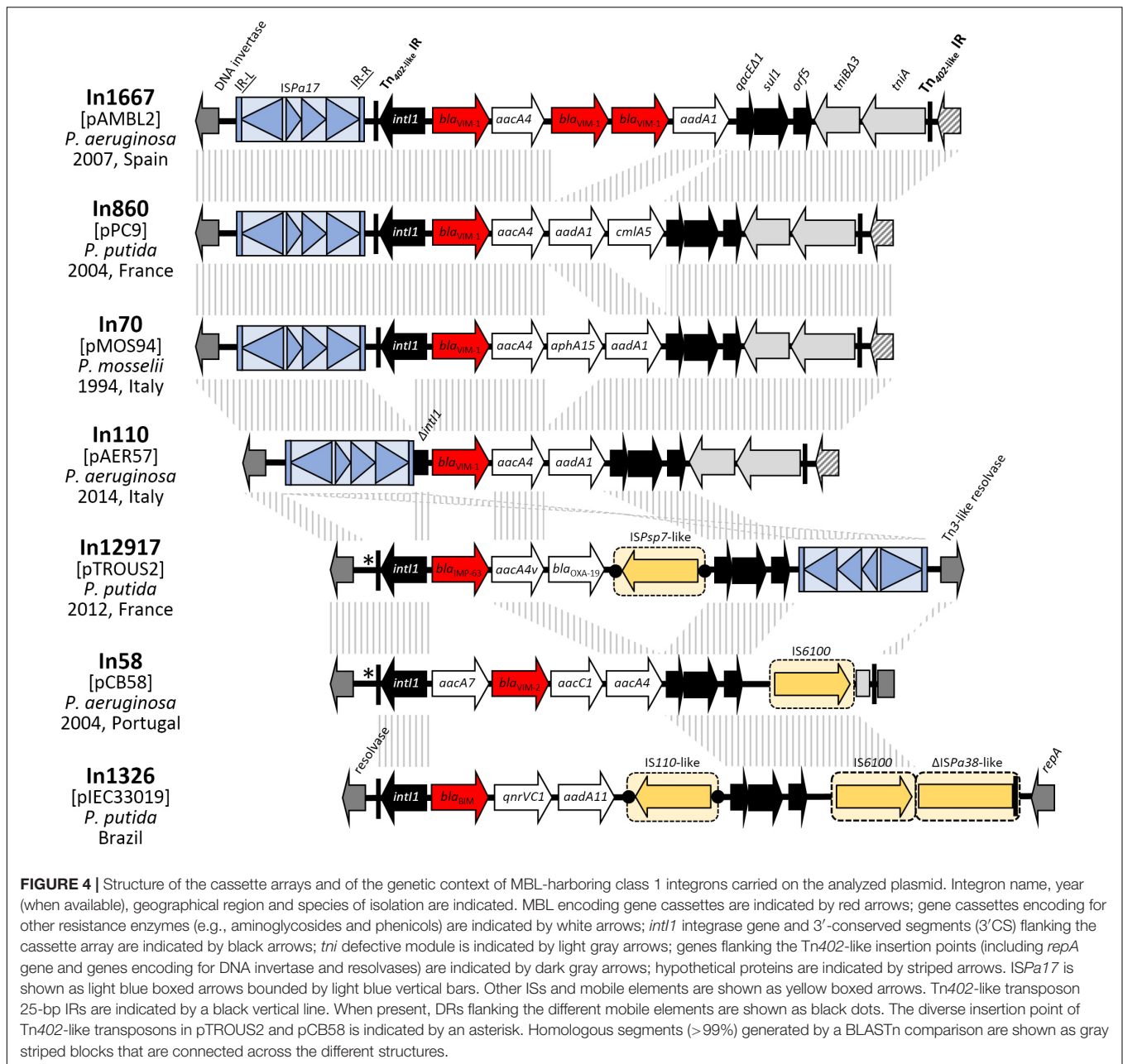
In all cases the Tn402-like elements carried by the pMOS94-like plasmids were not flanked by 5 bp DRs, that represent the molecular markers of the transposition of this kind of mobile elements, suggesting that acquisition had involved different recombination events, or that recombination events involving one transposon moiety had occurred after transposition.

In all plasmids but pIEC33019, the Tn402-like element was inserted into an A-T rich region located upstream of the locus coding for a DNA invertase. Within this region, all the Tn402-like elements carrying *bla_{VIM-1}* were inserted at the same site (i.e., 258 bp upstream of the DNA invertase gene), while the remaining ones were inserted slightly upstream (i.e., 281 bp upstream of the DNA invertase gene). On the other hand, in plasmid pIEC33019 the Tn402-like element was inserted in a different backbone region located downstream of *repA* (Figure 4).

Interestingly, all Tn402-like transposons carrying *bla_{VIM-1}* were flanked by a copy of the IS_{Pa17} insertion sequence (Haines et al., 2005), located upstream of the IRi end (Figure 4). Conversely, a different IS_{Pa17}/Tn402-like transposon assembly was found in plasmid pTROUS2, where the IS element was inserted downstream of the class I integron 3'CS region and disrupted the *tniA* gene (Figure 4). This IS was already described as associated to MBL-encoding Tn402-like transposons aboard plasmids from GNNFs, where it likely contributed to the MBL gene platform acquisition through a novel transposition mechanism exploiting the similarity between the Tn402 IRs and their counterparts in IS_{Pa17} (Di Pilato et al., 2014; Botelho et al., 2017; Liapis et al., 2019). Nevertheless, in pMOS94-like plasmids no evidence of an IS_{Pa17}-mediated mobilization was found, since no DRs bounding the IS_{Pa17} IR-L and the Tn402 IRt end were detected (Figure 4).

DISCUSSION

In this work we characterized the *bla_{VIM-1}*-carrying plasmid pMOS94 from *P. mosselii* AM/94 isolated in Italy in 1994,



which represents the earliest known VIM-producing strain (Giani et al., 2012). Analysis of the complete sequence of pMOS94 led to the identification of a novel plasmid lineage characterized by an original replication origin (i.e., *repA-oriv*) and included in the MOB_{F11} and MPF_T families, according to the typing schemes based on plasmid relaxases and on the MPF system, respectively (Guglielmini et al., 2014; Orlek et al., 2017). Interestingly, the MOB_{F11} family includes relaxases of plasmids belonging to IncW and IncN replicons, responsible for the spreading of antibiotic resistance determinants among enterobacteria, and to the IncP9 group, including metal-resistance and xenobiotic-biodegradation plasmids from *Pseudomonas* spp. (Garcillán-Barcia et al., 2009;

Shintani et al., 2015). Based on replicase sequence homology, pMOS94-like plasmids showed a closer relatedness with the IncW replicon family. Further transfer experiments will be needed to evaluate the incompatibility behavior of these plasmids.

Sequence analyses revealed that members of this novel plasmid lineage were involved in spread of MBL-encoding genes, and accounted for a broad dissemination of such resistance determinants among pseudomonads of clinical and environmental origin, spanning over a time period of at least 20 years, among at least five different countries from two continents. However, the association of pMOS94 and pMOS94-like plasmids with resistance genes could be somewhat biased by

the fact that the main purpose of bacterial sequencing focuses on antibiotic resistance.

The comparison of pMOS94-like plasmids highlighted a high phylogenetic relatedness within the lineage, which had likely evolved from a common ancestor. This point was also supported by the low sequence divergence observed among core backbone genes with the exception of pAER57, which was slightly more divergent. Nonetheless, the different insertion points of Tn402-like transposons and cognate integrons within the accessory region might represent a molecular marker of different evolutionary pathways for pMOS94 and pMOS94-like plasmids. In this scenario, different hypotheses could be made on the evolution of MGEs associated with this plasmid lineage: (i) the Tn402-like transposons could have been acquired following different insertion events that, in some cases (e.g., plasmids harboring blaVIM-1), occurred at the same site; (ii) at least three insertion events (occurring at different sites) led to the acquisition of the Tn402-like transposons, that subsequently evolved independently by genetic rearrangements and gene cassettes loss/acquisition. The number of the analyzed plasmids and sequence data publicly available for comparison, however, are limited and the chronological order of these events (i.e., the evolution of the backbone core genes and the acquisition of the accessory resistance regions) remains to be clarified.

Recently, a number of studies have described novel plasmid supports for different MBL genes among pseudomonads (Li et al., 2008; Bonnin et al., 2013; Vilacoba et al., 2014; San Millan et al., 2015; Botelho et al., 2017, 2018; Partridge et al., 2018; Liapis et al., 2019), reporting on the structure of single plasmids or on structures circulating in a restricted geographical area or within a relatively short time period.

The present study contributed to extend current knowledge about the diversity and phylogeny of plasmids circulating in *Pseudomonas* spp., reporting on a successful plasmid lineage carrying MBL genes. Although mobilization experiments were not successful under the experimental conditions used in this study, the heterogeneous range of species carrying pMOS94-like plasmids suggests that these elements are able to be transferred. Therefore, further experiments are needed to evaluate their mobilization potential among GNNFs and eventually *Enterobacteriales*, in order to better understand the possible contribution

in disseminating antibiotic resistance traits by this novel plasmid lineage.

NUCLEOTIDE SEQUENCE ACCESSION NUMBERS

The complete nucleotide sequence of pMOS94 from *P. mosselii* AM/94 and pAER57 from *P. aeruginosa* C/57 have been registered in GenBank under accession numbers MK671725 and MK671726, respectively.

DATA AVAILABILITY

The nucleotide sequences described for the first time in this study, namely pMOS94 and pAER57 sequences, have been deposited in GenBank database and will be made available to other researchers following publication. The remaining plasmid nucleotide sequences analyzed in this study are publicly available in the GenBank database under the accession numbers cited in the manuscript.

AUTHOR CONTRIBUTIONS

VDP and AA did plasmid sequencing, analyzed the data, and drafted the manuscript. TG and LHDA produced the phenotypic data and handled the samples. GR and SP coordinated the experiments, drafted and edited the manuscript.

FUNDING

This work was supported in part by EvoTAR (No. HEALTH-F3-2011-2011-123282004) to GR.

SUPPLEMENTARY MATERIAL

The Supplementary Material for this article can be found online at: <https://www.frontiersin.org/articles/10.3389/fmicb.2019.01504/full#supplementary-material>

REFERENCES

- Almuzara, M., Montaña, S., Carulla, M., Sly, G., Fernandez, J., Hernandez, M., et al. (2018). Clinical cases of VIM-producing *Pseudomonas mendocina* from two burned patients. *J. Glob. Antimicrob. Resist.* 14, 273–274. doi: 10.1016/j.jgar.2018.08.002
- Aoki, K., Harada, S., Yahara, K., Ishii, Y., Motooka, D., Nakamura, S., et al. (2018). Molecular Characterization of IMP-1-Producing *Enterobacter cloacae* Complex Isolates in Tokyo. *Antimicrob. Agents Chemother.* 23, e2091–17. doi: 10.1128/AAC.02091-2017
- Aziz, R. K., Bartels, D., Best, A. A., DeJongh, M., Disz, T., Edwards, R. A., et al. (2008). The RAST server: rapid annotations using subsystems technology. *BMC Genomics* 9:75. doi: 10.1186/1471-2164-9-75
- Bankevich, A., Nurk, S., Antipov, D., Gurevich, A. A., Dvorkin, M., Kulikov, A. S., et al. (2012). SPAdes: a new genome assembly algorithm and its applications to single-cell sequencing. *J. Comput. Biol.* 19, 455–477. doi: 10.1089/cmb.2012.0021
- Blumer, C., Heeb, S., Pessi, G., and Haas, D. (1999). Global GacA-steered control of cyanide and exoprotease production in *Pseudomonas fluorescens* involves specific ribosome binding sites. *Proc. Natl. Acad. Sci. U.S.A.* 96, 14073–14078. doi: 10.1073/pnas.96.24.14073
- Bonnin, R. A., Poirel, L., Nordmann, P., Eikmeyer, F. G., Wibberg, D., Pühler, A., et al. (2013). Complete sequence of broad-host-range plasmid pNOR-2000 harbouring the metallo- β -lactamase gene blaVIM-2 from *Pseudomonas aeruginosa*. *J. Antimicrob. Chemother.* 68, 1060–1065. doi: 10.1093/jac/dks526

- Botelho, J., Grosso, F., and Peixe, L. (2017). Characterization of the pJB12 plasmid from *Pseudomonas aeruginosa* reveals Tn6352, a novel putative transposon associated with mobilization of the *bla*_{VIM-2}-harboring In58 integron. *Antimicrob. Agents Chemother.* 61, e2532–16. doi: 10.1128/AAC.02532-16
- Botelho, J., Grosso, F., Quinteira, S., Brilhante, M., Ramos, H., and Peixe, L. (2018). Two decades of *bla*_{VIM-2}-producing *Pseudomonas aeruginosa* dissemination: an interplay between mobile genetic elements and successful clones. *J. Antimicrob. Chemother.* 73, 873–882. doi: 10.1093/jac/dkx517
- Bramucci, M., Chen, M., and Nagarajan, V. (2006). Genetic organization of a plasmid from an industrial wastewater bioreactor. *Appl. Microbiol. Biotechnol.* 71, 67–74. doi: 10.1007/s00253-005-0119-112
- Carattoli, A. (2009). Resistance Plasmid Families in *Enterobacteriaceae*. *Antimicrob. Agents Chemother.* 53, 2227–2238. doi: 10.1128/AAC.01707-1708
- Carattoli, A., Bertini, A., Villa, L., Falbo, V., Hopkins, K. L., and Threlfall, E. J. (2005). Identification of plasmids by PCR-based replicon typing. *J. Microbiol. Methods* 63, 219–228. doi: 10.1016/j.mimet.2005.03.018
- Chatteraj, D. K. (2000). Control of plasmid DNA replication by iterons: no longer paradoxical. *Mol. Microbiol.* 37, 467–476. doi: 10.1046/j.1365-2958.2000.01986.x
- Chiou, C. S., and Jones, A. L. (1993). Nucleotide sequence analysis of a transposon (Tn5393) carrying streptomycin resistance genes in *Erwinia amylovora* and other gram-negative bacteria. *J. Bacteriol.* 175, 732–740. doi: 10.1128/jb.175.3.732-740.1993
- Di Pilato, V., Pollini, S., and Rossolini, G. M. (2014). Characterization of plasmid pAX22, encoding VIM-1 metallo- β -lactamase, reveals a new putative mechanism of In70 integron mobilization. *J. Antimicrob. Chemother.* 69, 67–71. doi: 10.1093/jac/dkt311
- Di Pilato, V., Pollini, S., and Rossolini, G. M. (2015). Tn6249, a new Tn6162 transposon derivative carrying a double-integron platform and involved with acquisition of the *bla*_{VIM-1} metallo- β -lactamase gene in *Pseudomonas aeruginosa*. *Antimicrob. Agents Chemother.* 59, 1583–1587. doi: 10.1128/AAC.04047-4014
- Docquier, J.-D., Riccio, M. L., Mugnaioli, C., Luzzaro, F., Endimiani, A., Toniolo, A., et al. (2003). IMP-12, a new plasmid-encoded metallo- β -lactamase from a *Pseudomonas putida* clinical isolate. *Antimicrob. Agents Chemother.* 47, 1522–1528. doi: 10.1128/aac.47.5.1522-1528.2003
- Driscoll, J. A., Brody, S. L., and Kollef, M. H. (2007). The epidemiology, pathogenesis and treatment of *Pseudomonas aeruginosa* Infections. *Drugs* 67, 351–368. doi: 10.2165/00003495-200767030-200767033
- García-Fernández, A., Fortini, D., Veldman, K., Mevius, D., and Carattoli, A. (2009). Characterization of plasmids harbouring *qnrS1*, *qnrB2* and *qnrB19* genes in *Salmonella*. *J. Antimicrob. Chemother.* 63, 274–281. doi: 10.1093/jac/dkn470
- García-Fernández, A., Villa, L., Moodley, A., Hasman, H., Miriagou, V., Guardabassi, L., et al. (2011). Multilocus sequence typing of IncN plasmids. *J. Antimicrob. Chemother.* 66, 1987–1991. doi: 10.1093/jac/dkr225
- Garcillán-Barcia, M. P., Francia, M. V., and de La Cruz, F. (2009). The diversity of conjugative relaxases and its application in plasmid classification. *FEMS Microbiol. Rev.* 33, 657–687. doi: 10.1111/j.1574-6976.2009.00168.x
- Giani, T., Arena, F., Pollini, S., Di Pilato, V., D'Andrea, M. M., Henrici De Angelis, L., et al. (2018). Italian nationwide survey on *Pseudomonas aeruginosa* from invasive infections: activity of ceftolozane/tazobactam and comparators, and molecular epidemiology of carbapenemase producers. *J. Antimicrob. Chemother.* 73, 664–671. doi: 10.1093/jac/dkx453
- Giani, T., Marchese, A., Coppo, E., Kroumova, V., and Rossolini, G. M. (2012). VIM-1-producing *Pseudomonas mosselii* isolates in Italy, predating known VIM-producing index strains. *Antimicrob. Agents Chemother.* 56, 2216–2217. doi: 10.1128/AAC.06005-11
- Grant, J. R., and Stothard, P. (2008). The CGView Server: a comparative genomics tool for circular genomes. *Nucleic Acids Res.* 36, W181–W184. doi: 10.1093/nar/gkn179
- Greated, A., Lambertsen, L., Williams, P. A., and Thomas, C. M. (2002). Complete sequence of the IncP-9 TOL plasmid pWW0 from *Pseudomonas putida*. *Environ. Microbiol.* 4, 856–871. doi: 10.1046/j.1462-2920.2002.00305.x
- Guglielmini, J., Néron, B., Abby, S. S., Garcillán-Barcia, M. P., de la Cruz, F., and Rocha, E. P. C. (2014). Key components of the eight classes of type IV secretion systems involved in bacterial conjugation or protein secretion. *Nucleic Acids Res.* 42, 5715–5727. doi: 10.1093/nar/gku194
- Haines, A. S., Jones, K., Cheung, M., and Thomas, C. M. (2005). The IncP-6 Plasmid Rms149 consists of a small mobilizable backbone with multiple large insertions. *J. Bacteriol.* 187, 4728–4738. doi: 10.1128/JB.187.14.4728-4738.2005
- Hawkey, P. M., Warren, R. E., Livermore, D. M., McNulty, C. A. M., Enoch, D. A., Otter, J. A., et al. (2018). Treatment of infections caused by multidrug-resistant Gram-negative bacteria: report of the British society for antimicrobial chemotherapy/healthcare infection society/british infection association joint working party. *J. Antimicrob. Chemother.* 73, iii2–iii78. doi: 10.1093/jac/dky027
- He, Z., Zhang, H., Gao, S., Lercher, M. J., Chen, W. H., and Hu, S. (2016). Evolvview v2: an online visualization and management tool for customized and annotated phylogenetic trees. *Nucleic Acids Res.* 44, W236–W241. doi: 10.1093/nar/gkw370
- Hoiby, N., Ciofu, O., and Bjarnsholt, T. (2015). “*Pseudomonas*,” in *Manual of Clinical Microbiology*, Eleventh Edn, eds J. Jorgensen, M. A. Pfaller, K. C. Carroll, G. Funke, M. L. Landry, S. Richter, et al. (Washington, DC: ASM Press).
- Hong, D. J., Bae, I. K., Jang, I.-H., Jeong, S. H., Kang, H.-K., and Lee, K. (2015). Epidemiology and characteristics of metallo- β -lactamase-producing *Pseudomonas aeruginosa*. *Infect. Chemother.* 47, 81–97. doi: 10.3947/ic.2015.47.2.81
- Johnson, J. L. (1994). “Similarity analysis of DNAs,” in *Methods for General and Molecular Bacteriology*, eds P. Gerhardt, R. G. E. Murray, W. A. Wood, and N. R. Krieg (Washington, DC: American Society for Microbiology), 655–682.
- Johnson, T. J., Bielak, E. M., Fortini, D., Hansen, L. H., Hasman, H., Debroy, C., et al. (2012). Expansion of the IncX plasmid family for improved identification and typing of novel plasmids in drug-resistant *Enterobacteriaceae*. *Plasmid* 68, 43–50. doi: 10.1016/j.plasmid.2012.03.001
- Lauretti, L., Riccio, M. L., Mazzariol, A., Cornaglia, G., Amicosante, G., Fontana, R., et al. (1999). Cloning and characterization of *bla*_{VIM}, a new integron-borne metallo- β -lactamase gene from a *Pseudomonas aeruginosa* clinical isolate. *Antimicrob. Agents Chemother.* 43, 1584–1590. doi: 10.1128/aac.43.7.1584
- Li, H., Toleman, M. A., Bennett, P. M., Jones, R. N., and Walsh, T. R. (2008). Complete sequence of p07-406, a 24,179-base-pair plasmid harboring the *bla*_{VIM-7} metallo- β -lactamase gene in a *Pseudomonas aeruginosa* isolate from the United States. *Antimicrob. Agents Chemother.* 52, 3099–3105. doi: 10.1128/AAC.01093-1097
- Liapis, E., Bour, M., Triponney, P., Jové, T., Zahar, J.-R., Valot, B., et al. (2019). Identification of diverse integron and plasmid structures carrying a novel carbapenemase among *Pseudomonas* Species. *Front. Microbiol.* 10:404. doi: 10.3389/fmicb.2019.00404
- Llós, M., and Alkorta, I. (2017). Coupling proteins in type IV secretion. *Curr. Top. Microbiol. Immunol.* 413, 143–168. doi: 10.1007/978-3-319-75241-9_6
- Lombardi, G., Luzzaro, F., Docquier, J.-D., Riccio, M. L., Perilli, M., Coli, A., et al. (2002). Nosocomial infections caused by multidrug-resistant isolates of *Pseudomonas putida* producing VIM-1 metallo- β -Lactamase. *J. Clin. Microbiol.* 40, 4051–4055. doi: 10.1128/JCM.40.11.4051-4055.2002
- Martinez, E., Marquez, C., Ingold, A., Merlino, J., Djordjevic, S. P., Stokes, H. W., et al. (2012). Diverse mobilized class 1 integrons are common in the chromosomes of pathogenic *Pseudomonas aeruginosa* clinical isolates. *Antimicrob. Agents Chemother.* 56, 2169–2172. doi: 10.1128/AAC.06048-6011
- Molina, L., Udaondo, Z., Duque, E., Fernández, M., Molina-Santiago, C., Roca, A., et al. (2014). Antibiotic resistance determinants in a *Pseudomonas putida* strain isolated from a Hospital. *PLoS One* 9:e81604. doi: 10.1371/journal.pone.0081604
- Ocampo-Sosa, A. A., Guzmán-Gómez, L. P., Fernández-Martínez, M., Román, E., Rodríguez, C., Marco, F., et al. (2015). Isolation of VIM-2-producing *Pseudomonas monteilii* clinical strains disseminated in a tertiary Hospital in northern Spain. *Antimicrob. Agents Chemother.* 59, 1334–1336. doi: 10.1128/AAC.04639-14
- Orlek, A., Phan, H., Sheppard, A. E., Doumith, M., Ellington, M., Peto, T., et al. (2017). A curated dataset of complete *Enterobacteriaceae* plasmids compiled from the NCBI nucleotide database. *Data Brief* 12, 423–426. doi: 10.1016/j.dib.2017.04.024
- Page, A. J., Cummins, C. A., Hunt, M., Wong, V. K., Reuter, S., Holden, M. T. G., et al. (2015). Roary: rapid large-scale prokaryote pan genome analysis. *Bioinformatics* 31, 3691–3693. doi: 10.1093/bioinformatics/btv421

- Partridge, S. R., Kwong, S. M., Firth, N., and Jensen, S. O. (2018). Mobile genetic elements associated with antimicrobial resistance. *Clin. Microbiol. Rev.* 31, e88–17. doi: 10.1128/CMR.00088-17
- Peix, A., Ramírez-Bahena, M.-H., and Velázquez, E. (2018). The current status on the taxonomy of *Pseudomonas* revisited: an update. *Infect. Genet. Evol.* 57, 106–116. doi: 10.1016/j.meegid.2017.10.026
- Perez, F., Hujer, A. M., Marshall, S. H., Ray, A. J., Rather, P. N., Suwantarat, N., et al. (2014). Extensively drug-resistant *Pseudomonas aeruginosa* isolates containing *bla*_{VIM-2} and elements of *Salmonella* genomic island 2: a new genetic resistance determinant in Northeast Ohio. *Antimicrob. Agents Chemother.* 58, 5929–5935. doi: 10.1128/AAC.02372-2314
- Roy Chowdhury, P., Scott, M., Worden, P., Huntington, P., Hudson, B., Karagiannis, T., et al. (2016). Genomic islands 1 and 2 play key roles in the evolution of extensively drug-resistant ST235 isolates of *Pseudomonas aeruginosa*. *Open Biol.* 6:150175. doi: 10.1098/rsob.150175
- Rozwandowicz, M., Brouwer, M. S., Zomer, A. L., Bossers, A., Harders, F., Mevius, D. J., et al. (2017). Plasmids of Distinct IncK Lineages Show Compatible Phenotypes. *Antimicrob. Agents Chemother.* 61, e1954–16. doi: 10.1128/AAC.01954-1916
- San Millan, A., Toll-Riera, M., Escudero, J. A., Cantón, R., Coque, T. M., and Craig MacLean, R. (2015). Sequencing of plasmids pAMBL1 and pAMBL2 from *Pseudomonas aeruginosa* reveals a *bla*_{VIM-1} amplification causing high-level carbapenem resistance. *J. Antimicrob. Chemother.* 70, 3000–3003. doi: 10.1093/jac/dkv222
- Sevastyanovich, Y. R., Krasowiak, R., Bingle, L. E. H., Haines, A. S., Sokolov, S. L., Kosheleva, I. A., et al. (2008). Diversity of IncP-9 plasmids of *Pseudomonas*. *Microbiology* 154, 2929–2941. doi: 10.1099/mic.0.2008/017939-17930
- Shintani, M., Sanchez, Z. K., and Kimbara, K. (2015). Genomics of microbial plasmids: classification and identification based on replication and transfer systems and host taxonomy. *Front. Microbiol.* 6:242. doi: 10.3389/fmicb.2015.00242
- Smillie, C., Garcillan-Barcia, M. P., Francia, M. V., Rocha, E. P. C., and de la Cruz, F. (2010). Mobility of Plasmids. *Microbiol. Mol. Biol. Rev.* 74, 434–452. doi: 10.1128/MMBR.00020-10
- Sullivan, M. J., Petty, N. K., and Beatson, S. A. (2011). Easyfig: a genome comparison visualizer. *Bioinformatics* 27, 1009–1010. doi: 10.1093/bioinformatics/btr039
- Sunde, M., and Norström, M. (2005). The genetic background for streptomycin resistance in *Escherichia coli* influences the distribution of MICs. *J. Antimicrob. Chemother.* 56, 87–90. doi: 10.1093/jac/dki150
- Suzuki, H., Yano, H., Brown, C. J., and Top, E. M. (2010). Predicting plasmid promiscuity based on genomic signature. *J. Bacteriol.* 192, 6045–6055. doi: 10.1128/JB.00277-210
- Vilacoba, E., Quiroga, C., Pistorio, M., Famiglietti, A., Rodríguez, H., Kovensky, J., et al. (2014). A *bla*_{VIM-2} plasmid disseminating in extensively drug-resistant clinical *Pseudomonas aeruginosa* and *Serratia marcescens* isolates. *Antimicrob. Agents Chemother.* 58, 7017–7018. doi: 10.1128/AAC.02934-14
- Villa, J., Viedma, E., Brañas, P., Orellana, M. A., Otero, J. R., and Chaves, F. (2014). Multiclonal spread of VIM-1-producing *Enterobacter cloacae* isolates associated with In624 and In488 integrons located in an IncHI2 plasmid. *Int. J. Antimicrob. Agents* 43, 451–455. doi: 10.1016/j.ijantimicag.2014.02.006
- Villa, L., García-Fernández, A., Fortini, D., and Carattoli, A. (2010). Replicon sequence typing of IncF plasmids carrying virulence and resistance determinants. *J. Antimicrob. Chemother.* 65, 2518–2529. doi: 10.1093/jac/dkq347
- Yan, J.-J., Hsueh, P.-R., Ko, W.-C., Luh, K.-T., Tsai, S.-H., Wu, H.-M., et al. (2001). Metallo- β -lactamases in clinical *Pseudomonas* isolates in Taiwan and identification of VIM-3, a novel variant of the VIM-2 enzyme. *Antimicrob. Agents Chemother.* 45, 2224–2228. doi: 10.1128/AAC.45.8.2224-2228.2001

Conflict of Interest Statement: The authors declare that the research was conducted in the absence of any commercial or financial relationships that could be construed as a potential conflict of interest.

Copyright © 2019 Di Pilato, Antonelli, Giani, Henrici De Angelis, Rossolini and Pollini. This is an open-access article distributed under the terms of the Creative Commons Attribution License (CC BY). The use, distribution or reproduction in other forums is permitted, provided the original author(s) and the copyright owner(s) are credited and that the original publication in this journal is cited, in accordance with accepted academic practice. No use, distribution or reproduction is permitted which does not comply with these terms.



Characterization of a Multiresistance Plasmid Carrying the *optrA* and *cfr* Resistance Genes From an *Enterococcus faecium* Clinical Isolate

Gianluca Morroni¹, Andrea Brenciani^{2*}, Alberto Antonelli³, Marco Maria D'Andrea^{3,4}, Vincenzo Di Pilato³, Simona Fioriti², Marina Mingoia², Carla Vignaroli⁵, Oscar Cirioni¹, Francesca Biavasco⁵, Pietro E. Varaldo², Gian Maria Rossolini^{3,6} and Eleonora Giovanetti⁵

OPEN ACCESS

Edited by:

Teresa M. Coque,
Instituto Ramón y Cajal
de Investigación Sanitaria, Spain

Reviewed by:

Yoshikazu Ishii,
Toho University, Japan
Ana R. Freitas,
Universidade do Porto, Portugal

*Correspondence:

Andrea Brenciani
a.brenciani@univpm.it;
andreabrenciani@yahoo.it

Specialty section:

This article was submitted to
Evolutionary and Genomic
Microbiology,
a section of the journal
Frontiers in Microbiology

Received: 30 April 2018

Accepted: 27 August 2018

Published: 11 September 2018

Citation:

Morroni G, Brenciani A, Antonelli A,
D'Andrea MM, Di Pilato V, Fioriti S,
Mingoia M, Vignaroli C, Cirioni O,
Biavasco F, Varaldo PE, Rossolini GM
and Giovanetti E (2018)
Characterization of a Multiresistance
Plasmid Carrying the *optrA* and *cfr*
Resistance Genes From an
Enterococcus faecium Clinical Isolate.
Front. Microbiol. 9:2189.
doi: 10.3389/fmicb.2018.02189

¹ Infectious Diseases Clinic, Department of Biomedical Sciences and Public Health, Polytechnic University of Marche Medical School, Ancona, Italy, ² Unit of Microbiology, Department of Biomedical Sciences and Public Health, Polytechnic University of Marche Medical School, Ancona, Italy, ³ Department of Experimental and Clinical Medicine, University of Florence, Florence, Italy, ⁴ Department of Medical Biotechnologies, University of Siena, Siena, Italy, ⁵ Unit of Microbiology, Department of Life and Environmental Sciences, Polytechnic University of Marche, Ancona, Italy, ⁶ Microbiology and Virology Unit, Florence Careggi University Hospital, Florence, Italy

Enterococcus faecium E35048, a bloodstream isolate from Italy, was the first strain where the oxazolidinone resistance gene *optrA* was detected outside China. The strain was also positive for the oxazolidinone resistance gene *cfr*. WGS analysis revealed that the two genes were linked (23.1 kb apart), being co-carried by a 41,816-bp plasmid that was named pE35048-oc. This plasmid also carried the macrolide resistance gene *erm(B)* and a backbone related to that of the well-known *Enterococcus faecalis* plasmid pRE25 (identity 96%, coverage 65%). The *optrA* gene context was original, *optrA* being part of a composite transposon, named Tn6628, which was integrated into the gene encoding for the ζ toxin protein (*orf19* of pRE25). The *cfr* gene was flanked by two *ISEnfa5* insertion sequences and the element was inserted into an *Inu(E)* gene. Both *optrA* and *cfr* contexts were excisable. pE35048-oc could not be transferred to enterococcal recipients by conjugation or transformation. A plasmid-cured derivative of *E. faecium* E35048 was obtained following growth at 42°C, and the complete loss of pE35048-oc was confirmed by WGS. pE35048-oc exhibited some similarity but also notable differences from pEF12-0805, a recently described enterococcal plasmid from human *E. faecium* also co-carrying *optrA* and *cfr*; conversely it was completely unrelated to other *optrA*- and *cfr*-carrying plasmids from *Staphylococcus sciuri*. The *optrA*-*cfr* linkage is a matter of concern since it could herald the possibility of a co-spread of the two genes, both involved in resistance to last resort agents such as the oxazolidinones.

Keywords: multiresistance plasmid, *optrA* gene, *cfr* gene, oxazolidinone resistance, *Enterococcus faecium*

INTRODUCTION

Enterococci are members of the gut microbiota of humans and many animals, and are widespread in the environment. They are also major opportunistic pathogens, mostly causing healthcare-related infections. Among the reasons of their increasing role as nosocomial pathogens, the primary factor is their inherent ability to express and acquire resistance to several antimicrobial agents, with *Enterococcus faecium* emerging as the most therapeutically challenging species (Arias and Murray, 2012).

Oxazolidinones are among the few agents that retain activity against multiresistant strains of enterococci (Shaw and Barbachyn, 2011; Patel and Gallagher, 2015), and the emergence of resistance to these drugs is an issue of notable clinical relevance. Particularly worrisome, due to their potential for horizontal dissemination, are the oxazolidinone resistances caused by *cfr*, encoding a ribosome-modifying enzyme (Kehrenberg et al., 2005; Deshpande et al., 2015; Munita et al., 2015), and *optrA*, encoding a ribosome protection mechanism (Wang et al., 2015; Wilson, 2016; Sharkey et al., 2016). Both these genes were found to be associated with a number of different mobile genetic elements.

The *optrA* gene, in particular, was discovered in China in enterococci of human and animal origin isolated in 2005–2014 (Wang et al., 2015) where it was detected in different genetic contexts (He et al., 2016). Since then, *optrA*-positive enterococci have been reported worldwide (Mendes et al., 2016; Cavaco et al., 2017; Freitas et al., 2017; Pfaller et al., 2017a,b), including Italy, where *optrA* was found — the first report outside China — in two bloodstream isolates of *E. faecium* which were also positive for the *cfr* gene, which was not expressed (Brenciani et al., 2016b). By further investigating one of those isolates (strain E35048), we noticed that both *optrA* and *cfr* were capable of undergoing excision as minicircles (Brenciani et al., 2016b). It is worth noting that among the reported *optrA* protein variants (Morrone et al., 2017), the one detected in *E. faecium* E35048, named *optrA*_{E35048}, is the most divergent, differing by 21 amino acid substitutions from the firstly described *optrA* variant (Wang et al., 2015).

The goal of the present work was to investigate the locations, genetic environments, and transferability of the *optrA* and *cfr* resistance genes detected in *E. faecium* E35048. We characterized the genetic contexts and location of *optrA* and *cfr* in *E. faecium* E35048, and found that both genes were co-carried on a plasmid of original structure, named pE35048-oc. This plasmid, which also carried the macrolide resistance gene *erm(B)*, shared regions of homology with the well-characterized (Schwarz et al., 2001) and widely distributed (Rosvoll et al., 2010; Freitas et al., 2016) conjugative multiresistance enterococcal plasmid pRE25, but was unable to transfer. In pE35048-oc, the genetic context of *optrA* was different from those so far described in other *optrA*-carrying plasmids, underscoring the plasticity of these resistance regions.

MATERIALS AND METHODS

Bacterial Strain

optrA- and *cfr*-positive *E. faecium* E35048 (linezolid MIC, 4 µg/ml; tedizolid MIC, 2 µg/ml) was isolated in Italy in 2015 from a blood culture (Brenciani et al., 2016b).

WGS and Sequence Analysis

Genomic DNA was extracted using a commercial kit (Sigma-Aldrich, St. Louis, MO). WGS was carried out with the Illumina MiSeq platform (Illumina Inc., San Diego, CA, United States) by using a 2 × 300 paired end approach and a DNA library prepared using Nextera XT DNA Sample Prep Kit (Illumina, San Diego, CA, United States). *De novo* assembly was performed with SPAdes V 3.10.0 (Bankevich et al., 2012) using default parameters. Scaffolds characterized by a length ≤ 300 bp were filtered out. Raw reads were mapped to the filtered scaffolds by using bwa (Li and Durbin, 2009) to check the quality of the assembly. Tentative ordering of selected scaffolds of plasmid origin was performed by BLASTN comparisons of data from WGS to homologous plasmids, and eventually confirmed by PCR approach followed by Sanger sequencing. The ST was determined through the Center for Genomic Epidemiology¹. Analysis of insertion sequences was carried out using ISFinder online database² (Siguier et al., 2006).

PCR Mapping Experiments

PCR mapping with outward-directed primers topo-FW (5'-GAAGCGACAAGAGCAAGTAT-3') and *optrA*-RV (5'-TCTTGAAGTACTGATTCTCGG-3'), and Sanger sequencing were used to close the pE35048-oc plasmid sequence.

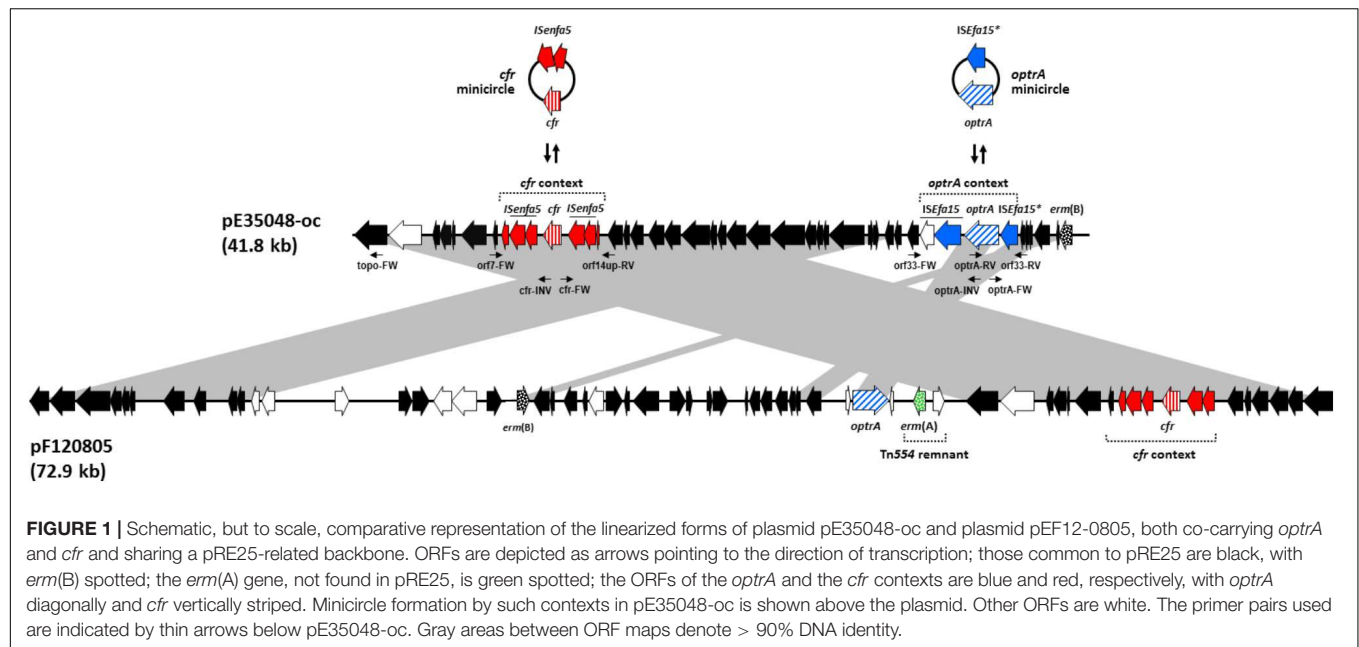
To investigate the excision of the *optrA* and *cfr* genetic contexts, PCR mapping and sequencing assays were performed using: (i) primer pairs targeting the regions flanking their insertion sites [*orf7*-FW (5'-ATTTTCTTTTGATTGGTA-3') and *orf14up*-RV (5'-AAGTAATCTTTTTTTGTTTT-3') for the *cfr* genetic context; and *orf33*-FW (5'-CTTGTTTTGGTGTTGCCCTGG-3') and *orf33*-RV (5'-CCACCAAGTAAAAAAGCGG-3') for the *optrA* genetic context]; (ii) outward-directed primer pairs designed from *cfr* and *optrA* genes [*cfr*-INV (5'-TTGATGACCTAATAAATGGAAGTA-3') and *cfr*-FW (5'-ACCTGAGATGTATGGAGAAG-3'); *optrA*-INV (5'-TTTTTCCACATCCATTTCTACC-3') and *optrA*-FW (5'-GAAAAATAACACAGTAAAAGGC-3')] (Figure 1).

S1-PFGE, Southern Blotting and Hybridization

Total DNA in agarose gel plugs was digested with S1 nuclease (Thermo Fisher Scientific, Milan, Italy) and separated by PFGE as previously described (Barton et al., 1995). After S1-PFGE, DNA was blotted onto positively charged nylon membrane (Ambion-Celbio, Milan, Italy) and hybridized with specific

¹<https://cge.cbs.dtu.dk/services/MLST/>

²<https://isfinder.biotoul.fr/>



probes (Brenciani et al., 2007). *cfr* and *optrA* probes were obtained by PCR as described elsewhere (Wang et al., 2015; Brenciani et al., 2016a).

Transformation and Conjugation Experiments

Purified plasmids extracted from *E. faecium* E35048 were transformed into the *E. faecalis* JH2-2 recipient by electrotransformation as described previously (Brenciani et al., 2016a). The transformants were selected on plates supplemented with florfenicol (10 µg/ml) or erythromycin (10 µg/ml).

In mating experiments, *E. faecium* E35048 was used as the donor. Two florfenicol-susceptible laboratory strains were used as recipients: *E. faecium* 64/3 (Werner et al., 1997), and *E. faecalis* JH2-2, both resistant to fusidic acid. Conjugal transfer was performed on a membrane filter. Transconjugants were selected on plates supplemented with florfenicol (10 µg/ml) or erythromycin (10 µg/ml) plus fusidic acid (25 µg/ml).

Curing Assays

Enterococcus faecium E35048 was grown overnight in brain heart agar (BHA) at 42°C for some passages. After each passage a few colonies were picked up, and their DNA was extracted and screened for the presence of the *optrA* and *cfr* genes by PCR with specific primers (Brenciani et al., 2016b). In case of negative testing, the strain was regarded as possibly cured and subjected to WGS for confirmation.

Nucleotide Sequence Accession Numbers

The complete nucleotide sequence of plasmid pE35048-oc has been assigned to GenBank accession no. MF580438, available under the BioProject ID PRJNA481862.

RESULTS AND DISCUSSION

Genome General Features and Resistome of *E. faecium* E35048

Assembly of the raw WGS data followed by filtering of low length contigs gave a total of 172 scaffolds (range: 310–137, 266 bp; N50: 41,930 bp; L50: 18; mean coverage: 92X). *E. faecium* E35048 was assigned to ST117, a globally disseminated hospital-adapted clone (Hegstad et al., 2014; Tedim et al., 2017). Resistome analysis revealed the presence of six acquired resistance genes in addition to the previously described *optrA* and *cfr* genes: *erm(B)* (resistance to macrolides, lincosamides and group B streptogramins), *msr(C)* (resistance to macrolides and group B streptogramins), *tet(M)* (resistance to tetracycline), *aphA* and *aadE* (resistance to aminoglycosides), and *sat4* (resistance to streptothricin).

Characterization of the *optrA*- and *cfr*-Carrying Plasmid pE35048-oc

The *optrA* and *cfr* genes were found to be linked, 23.1 kb apart in the linearized form, on the same contig, which also contained regions of high similarity (96% nucleotide identity) to the *E. faecalis* plasmid pRE25 (50 kb) (65% coverage) (Schwarz et al., 2001) (GenBank accession no. NC_008445).

PCR and Sanger sequencing using outward-directed primers targeting *orf1* and *optrA* demonstrated that the region containing *optrA* and *cfr* was part of a plasmid which was designated pE35048-oc (Figure 1). The plasmid was 41,816 bp in size, contained 42 open reading frames (ORFs), and had a G + C content of 35%.

S1-PFGE analysis of genomic DNA extracted from *E. faecium* E35048 showed four plasmids, ranging in size from ~10 to

~250 kb (data not shown). Both *optrA* and *cfr* probes hybridized with a plasmid of ~45 kb, in agreement with sequencing data.

The characteristics of the plasmid ORFs and of their products are detailed in **Table 1**. In particular, pE35048-oc carried (i) a *repS* gene (*orf6*, corresponding to *orf6* of pRE25), encoding a theta mechanism replication protein responsible for the plasmid replication; (ii) a putative origin of replication downstream of *orf6*; and (iii) a region containing the putative minimal conjugative unit of pRE25, consisting of 15 ORFs (*orf28* to *orf14*, corresponding to *orf24* to *orf39* of pRE25) and the origin of transfer (*oriT*) found upstream of *orf28* (Schwarz et al., 2001). BLASTN analysis showed that the *oriT* nucleotide sequence was shorter in pE35048-oc (only 15 bp vs. 38 bp in pRE25). Compared to pRE25, pE35048-oc lacked (i) the region spanning from *orf41* to *orf5* (two IS1216 elements probably involved in the rearrangement occurred during plasmid evolution); (ii) *orf10*, i.e., the chloramphenicol resistance *cat* gene; and (iii) *orf11*, another replication gene encoding a rolling-circle replication protein. In addition, compared to pRE25, pE35048-oc carried the *optrA* and *cfr* genes and their respective genetic environments.

The *optrA* context (5,850 bp) consisted of the *optrA*_{E35048} gene followed by a novel insertion sequence of the IS21 family, named ISEfa15. Consistently with other members of this family (Berger and Haas, 2001), ISEfa15 included two CDS encoding a transposase and a helper protein, and was bounded by 11-bp imperfect inverted repeats (IRL 5'-TGTTTATGATA-3' and IRR 5'-TGTATTTGTCA-3'). A truncated copy of ISEfa15, named ISEfa15*, was present also upstream of *optrA* gene. This *optrA* context was flanked by 5-bp target site duplications (5'-CTAAT-3') suggesting its mobilization as a composite transposon, named Tn6628 (**Figure 1**). This transposon was previously shown to form circular intermediate (3,350 bp) including *optrA* and the truncated copy of ISEfa15 (Brenciani et al., 2016b).

The proposed role of IS1216 in the dissemination of *optrA* among different types of enterococcal plasmids (He et al., 2016) is likely to be true also for other transposase genes. The *optrA* context was located downstream of the *erm(B)* gene (*orf15* of pRE25) and was integrated into *orf33* (*orf19* of pRE25, which encodes the ζ toxin protein of the ω - ϵ - ζ toxin/antitoxin system). This integration inactivates ζ toxin encoded by *orf33*, a condition that could prevent the correct partitioning of pE35048-oc and lead to the appearance of plasmid-free segregants (Magnuson, 2007).

The *cfr* context (6,098 bp) was located between *orf7* and *orf14* (*orf39* and *orf40* of pRE25) and consisted of the *cfr* gene flanked by two ISEnfa5 elements, inserted in turn into the *lnu(E)* gene. The same genetic context of *cfr* [including the direct repeats and the *lnu(E)* gene] has been reported in China in a plasmid from a *Streptococcus suis* isolate from an apparently healthy pig (Wang et al., 2013) and in Italy in an MRSA isolated from a patient with cystic fibrosis (Antonelli et al., 2016), with *cfr* being untransferable in both instances. Very recently, the *cfr* gene, flanked by only one ISEnfa5, inserted upstream, has been described in a chromosomal fragment shared by three pig isolates of *Staphylococcus sciuri* (Fan et al., 2017).

PCR assays, using primer pairs targeting regions flanking the *optrA* and the *cfr* contexts (**Figure 1**), and sequencing

experiments confirmed that both genes could be excised leaving one of the two flanking genes (ISEfa15 or ISEnfa5, respectively) at the excision sites.

Transferability of the *optrA* and *cfr* Genes and Curing of *E. faecium* E35048 From pE35048-oc

Repeated attempts of conjugation and transformation assays failed to demonstrate any *optrA* or *cfr* transfer from *E. faecium* E35048 to enterococcal recipients. The partial deletion of *oriT* and the lack of the rolling-circle replication protein might be responsible for the non-conjugative behavior of pE35048-oc compared to pRE25 (Schwarz et al., 2001).

An *optrA*- and *cfr*-negative isogenic strain of *E. faecium* E35048 was obtained after three passages on BHA at 42°C. It was subjected to WGS. Compared to the wild type, it disclosed complete loss of pE35048-oc.

pE35048-oc vs. Other Plasmids Sharing Co-carriage of *optrA* and *cfr*

Since this study was started, co-location of *optrA* and *cfr* has been reported in a few additional plasmids, some from pig isolates of *S. sciuri* (Li et al., 2016; Fan et al., 2017) and one, pEF12-0805, from a human isolate of *E. faecium* (Lazaris et al., 2017). Comparison of pE35048-oc with the *S. sciuri* plasmids revealed completely unrelated backbones and *optrA* and *cfr* contexts. On the other hand, pE35048-oc was related with pEF12-0805 (accession no. KY579372.1) although with significant differences (**Figure 1**). In particular:

(i) pE35048-oc and pEF12-0805 share a pRE25-related backbone (Schwarz et al., 2001), but pEF12-0805 is much larger (72,924 bp vs. 41,816 bp) due to the presence of a larger amount of pRE25-related regions, including the pRE25 region spanning from *orf51* to *orf5* (~12.5 kb) and a rearranged region of pRE25 containing antibiotic resistance genes *aphA*, *aadE*, and *lnu(B)* (~13 kb). (ii) A ~4-kb remnant of the *ermA*-carrying transposon Tn554 (Murphy et al., 1985) is found only in pEF12-0805. (iii) The *optrA* contexts of the two plasmids are completely different, only the *optrA* gene of pE35048-oc being part of a composite transposon. The absence of insertion sequences makes it unlikely that the *optrA* gene of pEF12-0805 is excisable. Moreover, whereas in pE35048-oc the *optrA* context is found downstream of *erm(B)*, the *optrA* gene of pEF12-0805 is associated with the *ermA*-carrying Tn554 remnant. (iv) Interestingly, the *cfr* contexts of the two plasmids are the same, including some plasmid backbone flanking regions on either side (**Figure 1**), suggesting that the two plasmids might be derived from a pRE25-related common ancestor that had initially acquired the mobile *cfr* element. (v) Repeated transfer assays were unsuccessful with both plasmids. Finally, (vi) whereas we obtained a pE35048-ocured derivative of our *E. faecium* isolate, curing assays were unsuccessful with *E. faecium* strain F120805 (Lazaris et al., 2017).

TABLE 1 | Amino acid sequence identities/similarities of putative proteins encoded by the pE35048-oc (GenBank accession no. [MF580438](#)).

ORF	Start (bp)	Stop (bp)	Size (amino Acid)	Predicted function	BLASTP analysis ^a		
					Most significant database match	Accession no.	% Amino acid identity (% amino acid similarity)
<i>orf1</i>	1833	1	610	DNA Topoisomerase III	Type 1 topoisomerase (plasmid) [<i>Enterococcus faecium</i>]	YP_976069.1	100 (100)
<i>orf1</i>	3,818	1,932	628	Group II intron	Group II intron reverse transcriptase/maturase [<i>Lactobacillales</i>]	WP_010718345.1	100 (100)
^b <i>Δorf3</i>	4,917	4,555	120	DNA Topoisomerase III	Topoisomerase [<i>Bacilli</i>]	WP_000108744.1	100 (100)
<i>orf4</i>	5,534	4,917	205	Resolvase	Resolvase (plasmid) [<i>E. faecalis</i>]	YP_003864109.1	99 (100)
<i>orf5</i>	5,718	5,548	56		Hypothetical protein pRE25p07 (plasmid) [<i>E. faecalis</i>]	YP_783891.1	98 (100)
<i>orf6</i>	7,557	6,067	496	Replication protein	Replication protein (plasmid) [<i>E. faecium</i>]	NP_044463.1	100 (100)
<i>orf7</i>	8,213	7,941	90	Transcriptional regulator	CopS (plasmid) [<i>Streptococcus pyogenes</i>]	YP_232751.1	100 (100)
<i>Δorf8</i>	8,901	8,446	151	Responsible for lincomycin resistance	Lincomycin nucleotidyltransferase (plasmid) [<i>E. faecium</i>]	ARQ19308.1	99 (100)
<i>orf9</i>	9,772	8,873	299	Transposase	Transposase [<i>Streptococcus suis</i>]	AGO02197.1	100 (100)
<i>orf10</i>	10,443	9,769	224	Transposase	IS3 family transposase [<i>E. faecalis</i>]	WP_013330754.1	100 (100)
<i>orf11</i>	11,867	10,809	352	23S ribosomal RNA methyltransferase	Cfr family 23S ribosomal RNA methyltransferase [<i>Staphylococcus aureus</i>]	WP_001835153.1	100 (100)
<i>orf12</i>	13,177	12,278	299	Transposase	Transposase [<i>S. suis</i>]	AGO02197.1	100 (100)
<i>orf13</i>	13,848	13,174	224	Transposase	IS3 family transposase [<i>E. faecalis</i>]	WP_013330754.1	100 (100)
<i>Δorf8</i>	13,921	14,061	47	Responsible for lincomycin resistance	Lincomycin resistance protein [synthetic construct]	AGT57825.1	100 (100)
<i>orf14</i>	15,391	14,531	289		Hypothetical protein [<i>S. suis</i>]	WP_079268203.1	96 (98)
<i>orf15</i>	15,822	15,451	123		Hypothetical protein [<i>Enterococcus casseliflavus</i>]	WP_032495652.1	99 (99)
<i>orf16</i>	16,546	15,809	245		Hypothetical protein [<i>E. faecalis</i>]	WP_012858057.1	100 (100)
<i>orf17</i>	17,768	16,836	310		Hypothetical protein [<i>Enterococcus</i> sp. HMSC063D12]	WP_070544061.1	100 (100)
<i>orf18</i>	18,693	17,770	307	Membrane protein insertase	Hypothetical protein [<i>Enterococcus</i> sp. HMSC063D12]	WP_070544063.1	99 (99)
<i>orf19</i>	20,366	18,711	551	Type IV secretory pathway, VirD4 component, TraG/TraD family ATPase	Hypothetical protein [<i>Enterococcus</i>]	WP_002325630.1	100 (100)
<i>orf20</i>	20,790	20,359	143		Ypsilon (plasmid) [<i>E. faecalis</i>]	YP_003864141.1	100 (100)
<i>orf21</i>	21,346	20,795	183		Hypothetical protein [<i>E. faecium</i>]	WP_029485693.1	99 (99)
<i>orf22</i>	22,468	21,359	369	Amidase	Putative lytic transglycosylase (plasmid) [<i>E. faecalis</i>]	YP_003864139.1	99 (99)
<i>orf23</i>	23,842	22,490	450		Conjugal transfer protein TraF [<i>E. faecium</i>]	WP_085837474.1	98 (99)
<i>orf24</i>	25,817	23,856	653	Type IV secretory pathway, VirB4 component	TrsE (plasmid) [<i>E. faecalis</i>]	YP_003864137.1	100 (100)

(Continued)

Table 1 | Continued

ORF	Start (bp)	Stop (bp)	Size (amino Acid)	Predicted function	BLASTP analysis ^a		
					Most significant database match	Accession no.	% Amino acid identity (% aminacid similarity)
<i>orf25</i>	26,457	25,828	209		Hypothetical protein [Enterococcus]	WP_002325627.1	99 (100)
<i>orf26</i>	26,857	26,474	127		AM21 (plasmid) [E. faecalis]	YP 003305365.1	100 (100)
<i>orf27</i>	27,208	26,876	110	T4SS_CagC	Hypothetical protein pRE25p25 (plasmid) [E. faecalis]	YP_783909.1	100 (100)
<i>orf28</i>	29,217	27,232	661	Nickase	Molybdopterin-guanine dinucleotide biosynthesis protein MobA [E. faecalis]	WP_025186512.1	99 (100)
<i>orf29</i>	29,509	29,808	99		Hypothetical protein pRE25p23 (plasmid) [E. faecalis]	YP_783907.1	100 (100)
<i>orf30</i>	29,811	30,068	85		Hypothetical protein [Enterococcus]	WP_021109234.1	100 (100)
<i>orf31</i>	30,927	30,430	165	Molecular chaperone DnaJ	Molecular chaperone DnaJ [Enterococcus]	WP_025481726.1	97 (98)
<i>orf32</i>	31,353	30,946	135		Hypothetical protein pRE25p20 (plasmid) [E. faecalis]	YP_783904.1	98 (99)
<i>Δorf33</i>	32,376	31,705	223	Zeta-toxin	Toxin zeta [E. faecium]	WP_002300569.1	97 (98)
<i>orf34</i>	33,173	32,412	253	DNA replication protein DnaC	AAA family ATPase [Proteiniborus ethanoligenes]	WP_091728780.1	94 (98)
<i>orf35</i>	34,750	33,170	526	ISEfa15 transposase	Transposase [P. ethanoligenes]	WP_091728892.1	70 (84)
<i>orf36</i>	36,973	35,006	655	ABC-F type ribosomal protection protein	ABC-F type ribosomal protection protein Optra [E. faecalis]	WP_078122475.1	97 (98)
<i>orf37</i>	38,100	37,078	340	ISEfa15 transposase (partial)	Transposase [Clostridium formicaceticum]	WP_070963420.1	64 (80)
<i>Δorf33</i>	38,423	39,199	75	Zeta-toxin	Zeta toxin [E. faecium]	WP_080440976.1	100 (100)
<i>orf38</i>	38,697	38,425	90	Epsilon-antitoxin	Antidote of epsilon-zeta post-segregational killing system (plasmid) [S. pyogenes]	YP_232758.1	100 (100)
<i>orf39</i>	38,929	38,714	71	Omega-repressor	Transcriptional repressor (plasmid) [S. pyogenes]	YP_232757.1	99 (100)
<i>orf40</i>	39,917	39,021	298	ParA putative ATPase	Chromosome partitioning protein ParA [S. suis]	WP_0023 87620.1	100 (100)
<i>orf41</i>	40,445	40,314	43		Hypothetical protein (plasmid) [Pediococcus acidilactici]	WP_002321978.1	100 (100)
<i>orf42</i>	41,187	40,450	245	23S rRNA (adenine(2058)-N(6))-methyltransferase	23S rRNA (adenine(2058)-N(6))-methyltransferase Erm(B) [S. suis]	WP_024418925.1	99 (100)

^aFor each ORF, only the most significant identity detected is listed. ^b Δ represents a truncated ORF.

The *E. faecium* hosts of the two plasmids belonged to different sequence types and were isolated from different sources. Strain E35048 was recovered in 2015 in Italy from a blood culture, belonged to ST117, exhibited no mutational mechanisms of oxazolidinone resistance, and was vancomycin susceptible. Strain F120805, recovered in 2013 in Ireland from feces and reported to have a linezolid MIC of 8 μg/ml, belonged to ST80, exhibited also mutational mechanisms of oxazolidinone resistance (involving both 23S rRNA and ribosomal protein L3), and was vancomycin resistant (*vanA*

genotype). Although belonging to different sequence types, ST80 and ST117 were part of the same clonal group, ST78.

CONCLUSION

Distinctive findings of the *optrA*- and *cfr*-carrying plasmid pE35048-oc are its relation to the well-known enterococcal plasmid pRE25, shared with plasmid pEF12-0805

(Lazaris et al., 2017); a unique *optrA* context, that has never been described before; and the fact that both the *optrA* and *cfr* contexts are capable of excising to form minicircles. This, in addition to the belonging of *E. faecium* E35048 to ST117, a globally disseminated clone recovered in many European health institutions (Hegstad et al., 2014; Tedim et al., 2017), might favor the spread of *optrA* and *cfr* in the hospital setting. Under this respect, the *in vitro* non-transferability of pE35048-oc is somehow reassuring, although transfer *in vivo* cannot be ruled out. Moreover, at the hospital level, it cannot be excluded that co-carriage of *optrA* and *cfr* by the same plasmid ends up turning into co-spread, as already highlighted with pheromone-responsiveness plasmids (Francia and Clewell, 2002), and also in consideration of the

very recent finding that, in enterococci, non-conjugative plasmids can be mobilized by co-resident, conjugative plasmids (Di Sante et al., 2017). Co-spread would be a cause for special concern, considering that both *optrA* and *cfr* encode resistance, through diverse mechanisms, to different antibiotics, including last resort agents such as oxazolidinones.

AUTHOR CONTRIBUTIONS

AB, PV, and EG designed the study and wrote the paper. FB, OC, and GR have contributed to critical reading of the manuscript. GM, AA, MD, VD, SF, MM, CV, and SF did the laboratory work.

REFERENCES

- Antonelli, A., D'Andrea, M. M., Galano, A., Borch, B., Brenciani, A., Vaggelli, G., et al. (2016). Linezolid-resistant *cfr*-positive MRSA, Italy. *J. Antimicrob. Chemother.* 71, 2349–2351. doi: 10.1093/jac/dkw108
- Arias, C. A., and Murray, B. E. (2012). The rise of the *Enterococcus*: beyond vancomycin resistance. *Nat. Rev. Microbiol.* 10, 266–278. doi: 10.1038/nrmicro2761
- Bankevich, A., Nurk, S., Antipov, D., Gurevich, A. A., Dvorkin, M., Kulikov, A. S., et al. (2012). SPAdes: a new genome assembly algorithm and its applications to single-cell sequencing. *J. Comput. Biol.* 19, 455–477. doi: 10.1089/cmb.2012.0021
- Barton, B. M., Harding, G. P., and Zuccarelli, A. J. (1995). A general method for detecting and sizing large plasmids. *Anal. Biochem.* 226, 235–240. doi: 10.1006/abio.1995.1220
- Berger, B., and Haas, D. (2001). Transposase and integrase: specialized transposition proteins of the bacterial insertion sequence IS21 and related elements. *Cell. Mol. Life Sci.* 58, 403–419. doi: 10.1007/PL00000866
- Brenciani, A., Bacciaglia, A., Vecchi, M., Vitali, L. A., Varaldo, P. E., and Giovanetti, E. (2007). Genetic elements carrying *erm(B)* in *Streptococcus pyogenes* and association with *tet(M)* tetracycline resistance gene. *Antimicrob. Agents Chemother.* 51, 1209–1216. doi: 10.1128/AAC.01484-06
- Brenciani, A., Morrone, G., Pollini, S., Tiberi, E., Mingoia, M., Varaldo, P. E., et al. (2016a). Characterization of novel conjugative multiresistance plasmids carrying *cfr* from linezolid-resistant *Staphylococcus epidermidis* clinical isolates from Italy. *J. Antimicrob. Chemother.* 71, 307–313. doi: 10.1093/jac/dkv341
- Brenciani, A., Morrone, G., Vincenzi, C., Manso, E., Mingoia, M., Giovanetti, E., et al. (2016b). Detection in Italy of two clinical *Enterococcus faecium* isolates carrying both the oxazolidinone and phenicol resistance gene *optrA* and a silent multiresistance gene *cfr*. *J. Antimicrob. Chemother.* 71, 1118–1119. doi: 10.1093/jac/dkv438
- Cavaco, L. M., Bernal, J. F., Zankari, E., Léon, M., Hendriksen, R. S., Perez-Gutierrez, E., et al. (2017). Detection of linezolid resistance due to the *optrA* gene in *Enterococcus faecalis* from poultry meat from the American continent (Colombia). *J. Antimicrob. Chemother.* 72, 678–683. doi: 10.1093/jac/dkw490
- Deshpande, L. M., Ashcraft, D. S., Kahn, H. P., Pankey, G., Jones, R. N., Farrell, D. J., et al. (2015). Detection of a new *cfr*-like gene, *cfr(B)*, in *Enterococcus faecium* isolates recovered from human specimens in the United States as part of the SENTRY antimicrobial surveillance program. *Antimicrob. Agents Chemother.* 59, 6256–6261. doi: 10.1128/AAC.01473-15
- Di Sante, L., Morrone, G., Brenciani, A., Vignaroli, C., Antonelli, A., D'Andrea, M. M., et al. (2017). pHT β -promoted mobilization of non-conjugative resistance plasmids from *Enterococcus faecium* to *Enterococcus faecalis*. *J. Antimicrob. Chemother.* 72, 2447–2453. doi: 10.1093/jac/dkx197
- Fan, R., Lia, D., Feßler, A. T., Wu, C., Schwarz, S., and Wang, Y. (2017). Distribution of *optrA* and *cfr* in florfenicol-resistant *Staphylococcus sciuri* of pig origin. *Vet. Microbiol.* 210, 43–48. doi: 10.1016/j.vetmic.2017.07.030
- Francia, M. V., and Clewell, D. B. (2002). Transfer origins in the conjugative *Enterococcus faecalis* plasmids pAD1 and pAM373: identification of the pAD1 nic site, a specific relaxase and a possible TraG-like protein. *Mol. Microbiol.* 45, 375–395. doi: 10.1046/j.1365-2958.2002.03007.x
- Freitas, A. R., Elghaieb, H., León-Sampedro, R., Abbassi, M. S., Novais, C., Coque, T. M., et al. (2017). Detection of *optrA* in the African continent (Tunisia) within a mosaic *Enterococcus faecalis* plasmid from urban wastewaters. *J. Antimicrob. Chemother.* 72, 3245–3251. doi: 10.1093/jac/dkx321
- Freitas, A. R., Tedim, A. P., Francia, M. V., Jensen, L. B., Novais, C., Peixe, L., et al. (2016). Multilevel population genetic analysis of *vanA* and *vanB* *Enterococcus faecium* causing nosocomial outbreaks in 27 countries (1986–2012). *J. Antimicrob. Chemother.* 71, 3351–3366. doi: 10.1093/jac/dkw312
- He, T., Shen, Y., Schwarz, S., Cai, J., Lv, Y., Li, J., et al. (2016). Genetic environment of the transferable oxazolidinone/phenicol resistance gene *optrA* in *Enterococcus faecalis* isolates of human and animal origin. *J. Antimicrob. Chemother.* 71, 1466–1473. doi: 10.1093/jac/dkw016
- Hegstad, K., Longva, J. Å., Hide, R., Aasnaes, B., Lunde, T. M., and Simonsen, G. S. (2014). Cluster of linezolid-resistant *Enterococcus faecium* ST117 in Norwegian hospitals. *Scand. J. Infect. Dis.* 46, 712–715. doi: 10.3109/00365548.2014.923107
- Kehrenberg, C., Schwarz, S., Jacobsen, L., Hansen, L. H., and Vester, B. (2005). A new mechanism for chloramphenicol, florfenicol and clindamycin resistance: methylation of 23S ribosomal RNA at A2503. *Mol. Microbiol.* 57, 1064–1073. doi: 10.1111/j.1365-2958.2005.04754.x
- Lazaris, A., Coleman, D. C., Kearns, A. M., Pichon, B., Kinnevey, P. M., Earls, M. R., et al. (2017). Novel multiresistance *cfr* plasmids in linezolid-resistant methicillin-resistant *Staphylococcus epidermidis* and vancomycin-resistant *Enterococcus faecium* (VRE) from a hospital outbreak: co-location of *cfr* and *optrA* in VRE. *J. Antimicrob. Chemother.* 72, 3252–3257. doi: 10.1093/jac/dkx292
- Li, D., Wang, Y., Schwarz, S., Cai, J., Fan, R., Li, J., et al. (2016). Co-location of the oxazolidinone resistance genes *optrA* and *cfr* on a multiresistance plasmid from *Staphylococcus sciuri*. *J. Antimicrob. Chemother.* 71, 1474–1478. doi: 10.1093/jac/dkw040
- Li, H., and Durbin, R. (2009). Fast and accurate short read alignment with burrows-wheeler transform. *Bioinformatics.* 25, 1754–1760. doi: 10.1093/bioinformatics/btp324
- Magnuson, R. D. (2007). Hypothetical functions of toxin-antitoxin systems. *J. Bacteriol.* 189, 6089–6092. doi: 10.1128/JB.00958-07
- Mendes, R. E., Hogan, P. A., Jones, R. N., Sader, H. S., and Flamm, R. K. (2016). Surveillance for linezolid resistance via the Zovox® annual appraisal of potency and spectrum (ZAAPS) programme (2014): evolving resistance mechanisms with stable susceptibility rates. *J. Antimicrob. Chemother.* 71, 1860–1865. doi: 10.1093/jac/dkw052
- Morrone, G., Brenciani, A., Simoni, S., Vignaroli, C., Mingoia, M., and Giovanetti, E. (2017). Commentary: nationwide surveillance of novel oxazolidinone resistance gene *optrA* in *Enterococcus* isolates in China from 2004 to 2014. *Front. Microbiol.* 8:1631. doi: 10.3389/fmicb.2017.01631
- Munita, J. M., Bayer, A. S., and Arias, C. A. (2015). Evolving resistance among gram-positive pathogens. *Clin. Infect. Dis.* 61, 48–57. doi: 10.1093/cid/civ523

- Murphy, E., Huwyler, L., and de Freire Bastos Mdo, C. (1985). Transposon Tn554: complete nucleotide sequence and isolation of transposition-defective and antibiotic-sensitive mutants. *EMBO J.* 4, 3357–3365.
- Patel, R., and Gallagher, J. C. (2015). Vancomycin-resistant enterococcal bacteremia pharmacotherapy. *Ann. Pharmacother.* 49, 69–85. doi: 10.1177/1060028014556879
- Pfaller, M. A., Mendes, R. E., Streit, J. M., Hogan, P. A., and Flamm, R. K. (2017a). Five-year summary of in vitro activity and resistance mechanisms of linezolid against clinically important gram-positive cocci in the United States from the LEADER surveillance program (2011 to 2015). *Antimicrob. Agents. Chemother.* 61:e00609-17. doi: 10.1128/AAC.00609-17
- Pfaller, M. A., Mendes, R. E., Streit, J. M., Hogan, P. A., and Flamm, R. K. (2017b). ZAAPS Program results for 2015: an activity and spectrum analysis of linezolid using clinical isolates from medical centres in 32 countries. *J. Antimicrob. Chemother.* 72, 3093–3099. doi: 10.1093/jac/dkx251
- Rosvoll, T. C. S., Pedersen, T., Sletvold, H., Johnsen, P. J., Sollid, J. E., Simonsen, G. S., et al. (2010). PCR-based plasmid typing in *Enterococcus faecium* strains reveals widely distributed pRE25-, pRUM-, pIP501- and pHT β -related replicons associated with glycopeptide resistance and stabilizing toxin-antitoxin systems. *FEMS Immunol. Med. Microbiol.* 58, 254–268. doi: 10.1111/j.1574-695X.2009.00633.x
- Schwarz, F. V., Perreten, V., and Teuber, M. (2001). Sequence of the 50-kb conjugative multiresistance plasmid pRE25 from *Enterococcus faecalis* RE25. *Plasmid* 46, 170–177. doi: 10.1006/plas.2001.1544
- Sharkey, L. K. R., Edwards, T. A., and O'Neill, A. J. (2016). ABC-F proteins mediate antibiotic resistance through ribosomal protection. *mBio* 7:e01975. doi: 10.1128/mBio.01975-15
- Shaw, K. J., and Barbachyn, M. R. (2011). The oxazolidinones: past, present, and future. *Ann. N. Y. Acad. Sci.* 1241, 48–70. doi: 10.1111/j.1749-6632.2011.06330.x
- Siguier, P., Perochon, J., Lestrade, L., Mahillon, J., and Chandler, M. (2006). ISfinder: the reference centre for bacterial insertion sequences. *Nucleic Acids Res.* 34, D32–D36. doi: 10.1093/nar/gkj014
- Tedim, A. P., Lanza, V. F., Manrique, M., Pareja, E., Ruiz-Garbajosa, P., Cantón, R., et al. (2017). Complete genome sequences of isolates of *Enterococcus faecium* sequence type 117, a globally disseminated multidrug-resistant clone. *Genome Announc.* 5:e01553-16. doi: 10.1128/genomeA.01553-16
- Wang, Y., Li, D., Song, L., Liu, Y., He, T., Liu, H., et al. (2013). First report of the multiresistance gene *cfr* in *Streptococcus suis*. *Antimicrob. Agents Chemother.* 57, 4061–4063. doi: 10.1128/AAC.00713-13
- Wang, Y., Lv, Y., Cai, J., Schwarz, S., Cui, L., Hu, Z., et al. (2015). A novel gene, *optrA*, that confers transferable resistance to oxazolidinones and phenicols and its presence in *Enterococcus faecalis* and *Enterococcus faecium* of human and animal origin. *J. Antimicrob. Chemother.* 70, 2182–2190. doi: 10.1093/jac/dkv116
- Werner, G., Klare, I., and Witte, W. (1997). Arrangement of the *vanA* gene cluster in enterococci of different ecological origin. *FEMS Microbiol. Lett.* 155, 55–61. doi: 10.1111/j.1574-6968.1997.tb12685.x
- Wilson, D. N. (2016). The ABC of ribosome-related antibiotic resistance. *mBio* 7:e00598-16. doi: 10.1128/mBio.00598-16

Conflict of Interest Statement: The authors declare that the research was conducted in the absence of any commercial or financial relationships that could be construed as a potential conflict of interest.

Copyright © 2018 Morrone, Brenciani, Antonelli, D'Andrea, Di Pilato, Fioriti, Mingoia, Vignaroli, Cirioni, Biavasco, Varaldo, Rossolini and Giovanetti. This is an open-access article distributed under the terms of the Creative Commons Attribution License (CC BY). The use, distribution or reproduction in other forums is permitted, provided the original author(s) and the copyright owner(s) are credited and that the original publication in this journal is cited, in accordance with accepted academic practice. No use, distribution or reproduction is permitted which does not comply with these terms.



Excision and Circularization of Integrative Conjugative Element Tn5253 of *Streptococcus pneumoniae*

Francesco Santoro, Alessandra Romeo, Gianni Pozzi and Francesco Iannelli*

Laboratory of Molecular Microbiology and Biotechnology, Department of Medical Biotechnologies, University of Siena, Siena, Italy

OPEN ACCESS

Edited by:

Simona Pollini,
Università degli Studi di Firenze, Italy

Reviewed by:

Marina Mingoia,
Università Politecnica delle Marche,
Italy
Filipa Grosso,
Universidade do Porto, Portugal

*Correspondence:

Francesco Iannelli
francesco.iannelli@unisi.it

Specialty section:

This article was submitted to
Evolutionary and Genomic
Microbiology,
a section of the journal
Frontiers in Microbiology

Received: 10 April 2018

Accepted: 16 July 2018

Published: 31 July 2018

Citation:

Santoro F, Romeo A, Pozzi G and
Iannelli F (2018) Excision
and Circularization of Integrative
Conjugative Element Tn5253
of *Streptococcus pneumoniae*.
Front. Microbiol. 9:1779.
doi: 10.3389/fmicb.2018.01779

The integrative conjugative element (ICE) Tn5253 of *Streptococcus pneumoniae*, conferring resistance to tetracycline and chloramphenicol, was found integrated at a 83-bp specific target site (*attB*) located in the *rbgA* gene of the pneumococcal chromosome. PCR analysis of Tn5253-carrying strains showed evidence of precise excision of Tn5253 from the pneumococcal chromosome with production of (i) circular forms of the ICE in which the ends were joined by a 84-bp sequence (*attTn*), and (ii) reconstituted chromosomal *attB*. When integrated into the chromosome, Tn5253 was flanked by *attL*, identical to *attB*, and *attR*, identical to *attTn*. Circular forms of Tn5253 were present at a concentration of 3.8×10^{-4} copies per chromosome, whereas reconstituted *attB* sites were at 3.0×10^{-4} copies per chromosome. Deletion of *int-xis* of Tn5253 abolished production of circular forms ($<7.1 \times 10^{-6}$ copies per chromosome) and was associated to the lack of Tn5253 conjugal transfer suggesting, as expected, that Tn5253 circular form acts as a conjugation intermediate.

Keywords: integrative conjugative element (ICE), circular form, attachment site, conjugative transposon, Tn5253, conjugation, mobile genetic elements

INTRODUCTION

Horizontal gene transfer, mediated by MGEs, significantly drives bacterial genome evolution including the acquisition and dissemination of new patterns of antibiotic resistance (Burrus and Waldor, 2004). Functional characterization of MGEs is essential to understand the evolution and spread of antibiotic resistance within a given bacterial species and also among different species (Frost et al., 2005). ICEs, which include CTs, are MGEs that integrate into the bacterial genome and are capable of intracellular transposition to a new genomic location or intercellular transposition to a new genome host upon conjugative transfer (Mullany et al., 2002). ICEs account for up to 25% of the genetic material in a bacterial genome (Paulsen et al., 2003) and are the major promoters of genetic diversity in bacteria (Burrus and Waldor, 2004; Johnson and Grossman, 2015).

The CT Tn916, carrying the *tet(M)* gene, is the prototype of the Tn916–Tn1545 family of ICEs, and one of the most studied ICEs of gram positive bacteria (Santoro et al., 2014). Tn916 was shown to excise from the bacterial chromosome producing a covalently closed circular form of the element which was called “CI.” Production of CIs of Tn916 was demonstrated to be essential for conjugative transposition of the element (Scott et al., 1988). Recombination processes of ICEs are catalyzed by

Abbreviations: CI: circular intermediate; CDS: coding sequence; CT: conjugative transposon; HGT: horizontal gene transfer; ICE: integrative conjugative element; MGE: mobile genetic element.

site specific recombinases (serine or tyrosine) or by DDE transposases (Ambroset et al., 2016). The Tn916 element carries the *int* and *xis* genes which code for a tyrosine site specific recombinase and an excisionase, respectively (Lu and Churchward, 1995). Excision and circularization require both Xis and Int, whereas Int alone is sufficient for integration (Storrs et al., 1991). Dosage of Tn916 CIs demonstrated that their number correlates with conjugation frequency and is variable among different strains (Manganelli et al., 1995).

Tn5253 is a 64,528-bp composite ICE of *Streptococcus pneumoniae* which contains integrated two distinct genetic elements: Tn5251, belonging to the Tn916–Tn1545 family of ICEs, and Ω cat(pC194) which carry *tet*(M) and *cat* resistance genes, respectively (Ayoubi et al., 1991; Provvedi et al., 1996; Santoro et al., 2010; Iannelli et al., 2014). Tn5253 contains two pairs of *xis/int* recombinase genes one of which is part of Tn5251 (Kiliç et al., 1994; Iannelli et al., 2014). Genomic sequence analysis and PCR genotyping studies demonstrated that Tn5253-like elements are very common in multidrug-resistant pneumococcal strains including pandemic isolates (Croucher et al., 2009; Henderson-Begg et al., 2009; Mingoia et al., 2011). A study on 240 different pneumococcal isolates of the multidrug-resistance 23F Spanish strain lineage, carrying the Tn5253-like element ICESpn23FST81, showed that the element is maintained among all derivative strains (Croucher et al., 2011). In this work, we investigated excision and circularization of the composite ICE Tn5253, including the respective contribution of each *xis/int* recombinase pair to the conjugal transfer of the genetic element.

MATERIALS AND METHODS

Bacterial Strains, Growth, and Mating Conditions

The bacterial strains used in this study and their relevant properties are described in Table 1. Bacterial growth and plate mating conjugation experiments were performed as reported (Santoro et al., 2010).

Pneumococcal Lysate Preparation

Pneumococcal cultures (1 ml) were harvested in exponential phase (OD₅₉₀ about 0.2, roughly corresponding to 5×10^8 CFU/ml) and centrifuged at $11,000 \times g$ for 2 min. Bacterial pellets were resuspended in 30 μ l of lysis solution (DOC 0.1%, SDS 0.008%) and incubated at 37°C until clarification (about 10 min). Two hundred and seventy micro liters of TE 1 \times , pH 8.0 were then added to the lysate.

PCR, Sequencing, and Sequence Analysis

PCR and direct PCR sequencing were carried out following an already described protocol (Iannelli et al., 1998; Santoro et al., 2010) and DNA sequence analysis was obtained with standard softwares. DNA sequence alignments were performed using Clustal Omega¹ and Lalign². Oligonucleotide primers and their characteristics are reported in Table 2.

PCR Mutagenesis

Isogenic deletion mutant strains were constructed transforming FR24 with linear PCR mutagenic constructs assembled by gene splicing by overlap extension as already described (Pearce et al., 2002; Iannelli and Pozzi, 2004). Deletion of Tn5251 *int* and *xis* CDS (*orf21* and *orf22* of Tn5253) was obtained with a mutagenic construct containing the *ami/aad9* spectinomycin resistance cassette flanked at the left by a 496-bp DNA fragment and at the right by a 569-bp fragment corresponding to nucleotides 16,810–17,305 and 18,780–19,348 of Tn5253 (GenBank EU351020), respectively. The primer pair IF100/IF101 was used to amplify the spectinomycin-resistance cassette from plasmid pR412 (Bergé et al., 2002), whereas IF517/IF681 and IF520/IF682 were used to amplify the flanking fragments from FR24.

The *xis* and *int* CDSs of Tn5253 (*orf78* and *orf79*) were deleted with a mutagenic construct containing the *ami/aphIII* kanamycin resistance cassette, flanked at the left by a 471-bp DNA fragment and at the right by a 603-bp corresponding

¹<https://www.ebi.ac.uk/Tools/msa/clustalo/>

²<http://vega.igh.cnrs.fr/bin/lalign-guess.cgi>

TABLE 1 | *Streptococcus pneumoniae* strains.

Strain	Relevant properties ^a	Origin (Reference)
D39	type 2 Avery's strain	Lanie et al., 2007
FP58	Conjugation recipient. <i>str-41</i> ; Sm ^R derivative of D39	Iannelli et al., 2004
Rx1	Unencapsulated derivative of D39	Pearce et al., 2002
FP10	Conjugation recipient. Δ comC, <i>str-41</i> ; Cm ^R , Sm ^R ; unencapsulated, competence deficient derivative of Rx1	Santoro et al., 2010
FP11	Conjugation recipient. Δ comC, <i>nov-1</i> ; Cm ^R , Nov ^R ; unencapsulated, competence deficient derivative of Rx1	Santoro et al., 2010
BM6001	Tn5253 donor; <i>cat</i> , <i>tet</i> (M); original clinical strain	Dang-Van et al., 1978
DP1322	Tn5253 donor; <i>cat</i> , <i>tet</i> (M); Cm ^R , Tc ^R ; Rx1 derivative transformed with BM6001 DNA	Smith et al., 1981
FR24	Tn5253; <i>cat</i> , <i>tet</i> (M); Cm ^R , Tc ^R , Sm ^R ; transconjugant from mating between DP1322 and FP10	This study
FR51	Tn5253; <i>cat</i> , <i>tet</i> (M), Δ <i>xis-int</i> of Tn5253; Cm ^R , Tc ^R , Sm ^R ; Km ^R ; recombinases (<i>orf78-orf79</i>) deletion mutant of FR24	This study
FR82	Tn5253; <i>cat</i> , <i>tet</i> (M), Δ <i>int-xis</i> of Tn5251; Cm ^R , Tc ^R , Sm ^R ; Spe ^R ; recombinases (<i>orf21-orf22</i>) deletion mutant of FR24	This study

^a*str-41* indicates a point mutation conferring resistance to streptomycin, while *nov-1* indicates a point mutation conferring resistance to novobiocin. Cm, chloramphenicol; Km, kanamycin; Nov, novobiocin; Sm, streptomycin; Tc, tetracycline; Spe, spectinomycin; R, resistance.

TABLE 2 | Oligonucleotide primers.

Name	Sequence (5' to 3')	Notes ^a	GenBank ID: nucleotides
IF327	CAA TAT AGC GTG ATG ATT GTA AT		EU351020: 1,103–1,081
IF328	AGT GAG AAT CAA ATC AGA GGT T		EU351020: 65,221–65,242
IF373	GAT GAT GAT TTG ACA CAA GAA TA		EU351020: 62,969–62,991
IF521	ATC AAA CGG ATC CCC AGC TTG TAT TCA TGT CAT CAT CCT TCC T	The first 21 nucleotides are complementary to IF149	EU351020: 63,439–63,418
IF522	ATA TTT TAC TGG ATG AAT TGT TTT AGT TTT GGT GTT CGC TTG GTG TTT AG	The first 26 nucleotides are complementary to IF210	EU351020: 65,260–65,283
IF523	CGG TGT ATC CAA GAT TTC CAG		EU351020: 65,862–65,842
IF517	ATT TCC TTG CGT GAT GTG TGA		EU351020: 16,810–16,830
IF681	GTA TCG CTC TTG AAG GGA ATA GTA CAA ATG AAT TTA CTA CTT	The first 19 nucleotides are complementary to IF101	EU351020: 17,305–17,283
IF682	GAT CCA CTA GTT CTA GAG CTC CCA AAT AGG AAT GTC AGT	The first 19 nucleotides are complementary to IF100	EU351020: 18,780–18,799
IF520	GTA TGG TCG TTG ATG AAG TCT		EU351020: 19,348–19,328
IF100	GCT CTA GAA CTA GTG GAT C		AY334020: 1–16
IF101	TTC CCT TCA AGA GCG ATA C		AY334020: 890–872
IF149	CAA GCT GGG GAT CCG TTT GAT		AY334018: 5–25
IF210	CTA AAA CAA TTC ATC CAG TAA AAT AT		AY334019: 880–855
IF496	GTT TGG ACA TCA TTC ATT TG		CP000410: 1,043,748–1,043,767
IF356	GAC TAG ATA GAG GCA AGC GT		CP000410: 1,043,962–1,043,943
IF138	CAG ATC AAG AAA TCA AAC TCC AA		CP000410: 725,024–725,046
IF139	CAG CAT CAT CTA CAG AAA CTC		CP000410: 725,194–725,174

^aNucleotides complementary to resistance cassettes primers are reported in italics.

to nucleotides 62,969–63,439 of Tn5253 and 65,260–65,862 of Tn5253, respectively. The primer pair IF149/IF210 was used to amplify the kanamycin-resistance cassette from plasmid pR410 (Bergé et al., 2002), while IF373/IF521 and IF522/IF523 were used to amplify the left and right fragments from FR24. Linear PCR constructs were used directly as donor DNA in transformation experiments. Mutant strains were selected for acquisition of spectinomycin or kanamycin resistance and the correct integration of constructs was confirmed by PCR and sequencing (Iannelli and Pozzi, 2004).

Real-Time PCR Quantification

Real-time PCR experiments were carried out with the KAPA SYBR FAST qPCR kit Master Mix Universal (2X) (Kapa Biosystems) on a LightCycler 1.5 apparatus (Roche). Real-time PCR mixture contained, in a final volume of 20 µl, 1× KAPA SYBR FAST qPCR reaction mix, 5 pmol of each primer and 1 µl of bacterial lysate as starting template. Thermal profile was an initial 3 min denaturation step at 95°C followed by 40 cycles of repeated denaturation (0 s at 95°C), annealing (20 s at 50°C), and polymerisation (10 s at 72°C). The temperature transition rate was 20°C/s in the denaturation and annealing step and 5°C/s in the polymerisation step. The primer pair IF327/IF328 amplified a 411 bp fragment used for CIs quantification, while IF496/IF356 amplified a 215 bp fragment used for free locus quantification, a 171 bp fragment of chromosomal *gyrB* gene obtained with primers IF138/IF139 was used to standardize results (Table 2). A standard curve for the *gyrB* gene was built plotting the threshold cycle against the number of chromosome copies using serial dilutions of chromosomal DNA with known

concentration. This external standard curve was used to quantify in each sample the number of (i) chromosome copies, (ii) CIs, and (iii) reconstituted *attB*. Lower limit of detection of the assay was 10 copies/reaction. The quantification was corrected for the primer efficiency. Melting curve analysis was performed to differentiate the amplified products from primer dimers.

RESULTS AND DISCUSSION

Excision of Tn5253 From the Pneumococcal Chromosome

PCR analysis of cell lysates of Tn5253-carrying pneumococcal strains showed evidence of precise excision of Tn5253 from its specific attachment site (*attB*) in the pneumococcal chromosome. This excision was investigated in liquid cultures of BM6001, the clinical isolate in which Tn5253 was originally found, and four other Tn5253-carrying laboratory strains all deriving from classic type 2 D39 (Table 1). Using divergent primers (IF327, IF328; Table 2) designed on the ends of the element, PCR analysis showed the presence of junctions between the left and right ends of Tn5253 (*attTn*), whereas with convergent primers (IF496, IF356; Table 2) designed on the regions flanking the insertion site it was possible to show the presence of chromosomes with reconstituted target sites for integration of Tn5253 (*attB*) (Figure 1). In all Tn5253-carrying pneumococci, DNA sequence analysis of PCR fragments indicated that: (i) *attTn* was 84 bp in size and was identical to *attR*, the 84-bp direct repeat present at the right end of the integrated element, whereas (ii) *attB* was 83 bp in size and was identical to *attL*, the direct repeat present

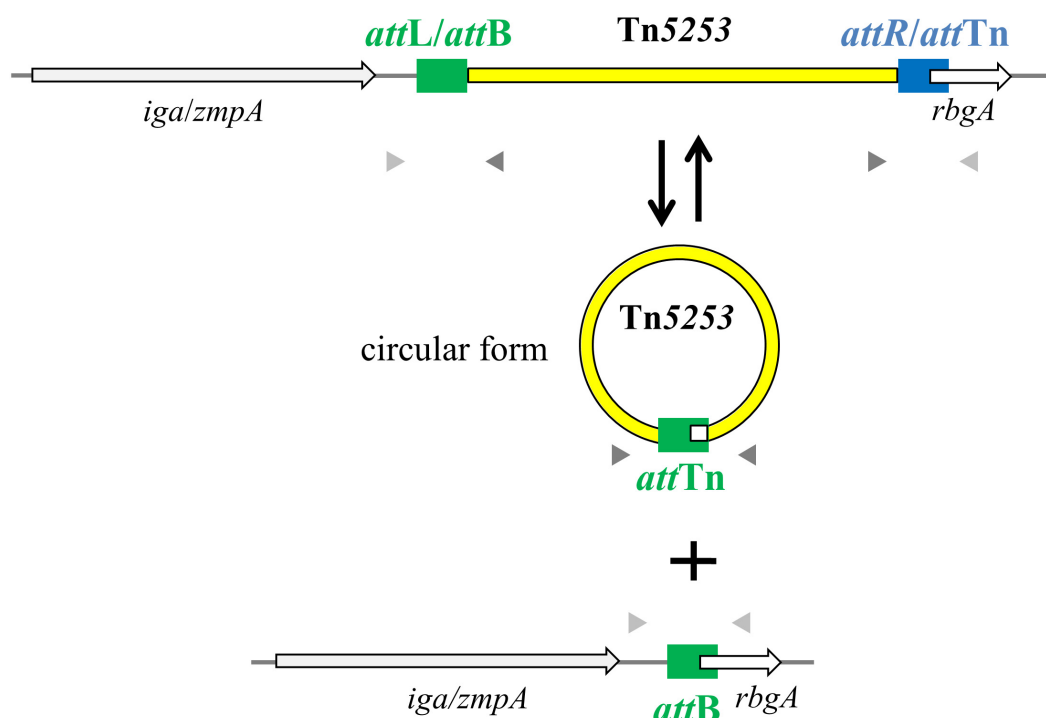


FIGURE 1 | Tn5253 excises from pneumococcal chromosome producing a circular form and a reconstitution of *attB* insertion site. In the circular form of Tn5253 the left and right ends are joined by *attTn* which is identical to *attR* whereas the reconstituted *attB* site is identical to *attL*. *att* sites are represented as filled rectangles, chromosomal genes as open arrows, Tn5253 as a yellow bar. Arrowheads represent PCR primers used for circular form (dark gray) and reconstituted *attB* site (light gray) detection.

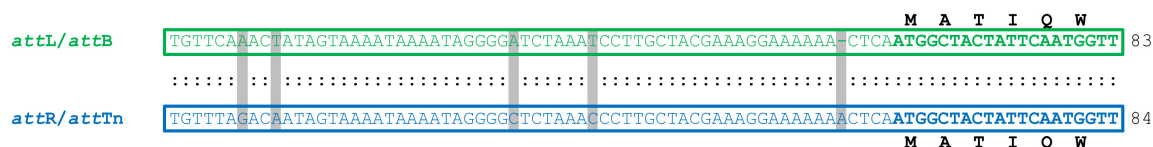


FIGURE 2 | Sequence alignment of Tn5253 attachment sites in *Streptococcus pneumoniae* D39 and derivatives. Upon integration into pneumococcal chromosome, Tn5253 is flanked by *attL* and *attR*. The element excises from chromosome producing a circular form where the left and right ends are joined by *attTn* and restoring the *attB* insertion site. *attB* is 83-bp long and is identical to *attL* while *attTn* is 84-bp long and is identical to *attR*. *attR-attTn* contain 4 nucleotide changes and 1 insertion compared to *attL-attB*. *attL-attB* contains the first 20 nucleotides of *rbgA* CDS, whose deduced amino acid sequence is reported, together with the 63 nucleotides upstream of the start codon. Within the sequences, identical nucleotides are indicated by colon, changes are shaded. Amino acids are indicated using one-letter code abbreviations. Lengths of attachment sites are reported on the right.

at the left end of the integrated element (Figure 2). The *attR-attTn* repeat contained 4 nucleotide changes and 1 insertion compared to *attL-attB* (Figure 2). These results suggest that in Tn5253-carrying strains, recombination occurs between the two imperfect direct repeats *attL* and *attR* leading to precise excision of the element from the chromosome, with production of circular forms of Tn5253 in which the ends are joined by *attR/attTn*, while the *attL/attB* repeat remains in the bacterial chromosome (Figure 1).

Quantification of Circular Forms and Reconstituted *attB* Sites

To obtain a quantitative estimate of Tn5253 excision from the *S. pneumoniae* chromosome, Real-time PCR was used to quantify

concentration of circular forms and reconstituted *attB* sites in liquid bacterial cultures. Different Tn5253-carrying laboratory strains of D39 ancestry, and BM6001 showed very homogeneous quantitative results (Table 3). In the laboratory strain DP1322 circular forms of Tn5253 were present at a concentration of 5.1×10^{-4} ($\pm 2.7 \times 10^{-4}$) copies per chromosome, whereas reconstituted *attB* sites were at 2.1×10^{-4} ($\pm 3.0 \times 10^{-5}$) copies per chromosome. These values were comparable to those obtained in the Tn5253-carrying laboratory strains (Table 3). Autonomous plasmid-like replication is common in ICEs and contributes to the stability and maintenance of these elements (Lee et al., 2010; Carraro et al., 2015; Johnson and Grossman, 2015). The hypothesis that also Tn5253 circular forms undergo few cycles of autonomous replication can explain why the copy

TABLE 3 | Real-time PCR quantification of Tn5253 circular form and reconstituted *attB*^a.

Strain	Circular forms	Reconstituted <i>attB</i> sites	Conjugation frequency ^b
BM6001	1.8×10^{-4} ($\pm 1.5 \times 10^{-5}$)	2.4×10^{-4} ($\pm 3.6 \times 10^{-5}$)	3.4×10^{-7}
DP1322	5.1×10^{-4} ($\pm 2.7 \times 10^{-4}$)	2.1×10^{-4} ($\pm 3.0 \times 10^{-5}$)	1.6×10^{-4}
FR24	5.4×10^{-4} ($\pm 3.1 \times 10^{-4}$)	3.7×10^{-4} ($\pm 3.3 \times 10^{-5}$)	2.0×10^{-4}
FR51	none ($\leq 7.1 \times 10^{-6}$)	none ($\leq 7.1 \times 10^{-6}$)	none ($< 9.9 \times 10^{-8}$)

^aConcentration was expressed as copies per chromosome. ^bFrequency refers to mating experiments where *S. pneumoniae* FP11 was the recipient.

number of circular forms is higher than the copy number of the reconstituted *attB* site.

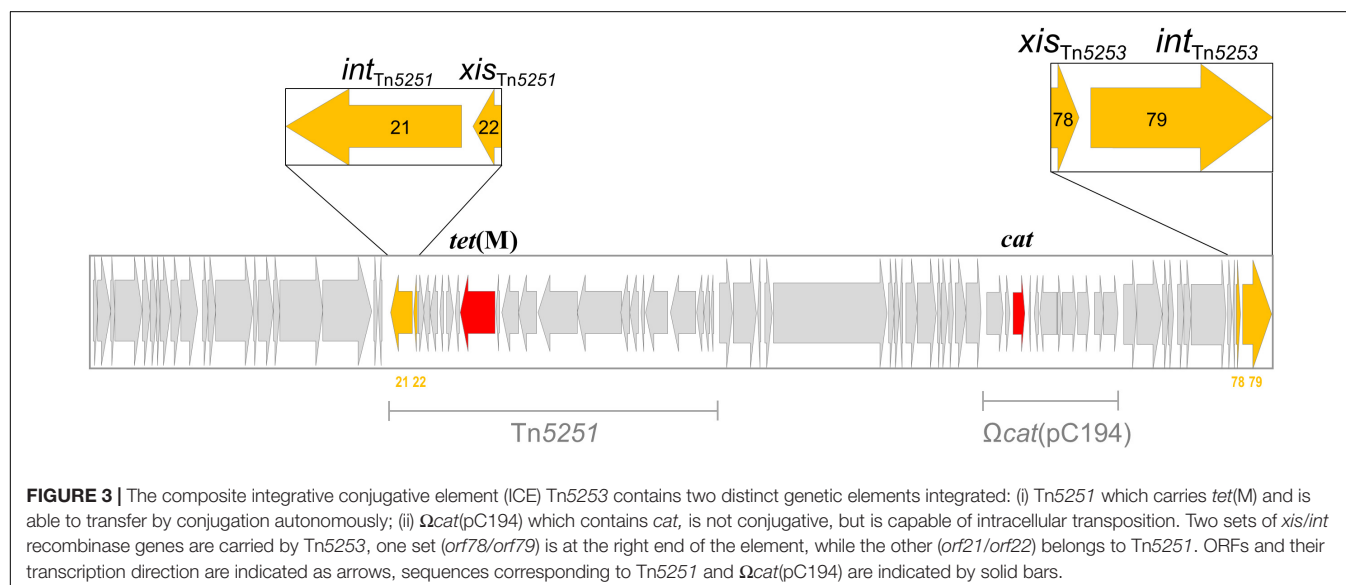
Site-Specific Integration of Tn5253 Into the *rbgA* Gene

In *S. pneumoniae* D39 and in its derivatives used as conjugation recipients (Table 1) DNA sequence analysis showed that *attB* of Tn5253 was 83 bp in size, and was always located within the *rbgA* gene (nucleotides 1,043,779 to 1,043,861, GenBank CP000410) (Figure 1). The ribosomal biogenesis GTPase A encoded by *rbgA* is a conserved, essential bacterial protein involved in the 50S ribosome subunit assembly (Uicker et al., 2006). The *attB* site contained the first 20 nucleotides of the *rbgA* CDS together with the 63 nucleotides upstream of the start codon (Figures 1, 2). The junction fragments of Tn5253 with the bacterial chromosome were investigated in a total of 12 transconjugants obtained in independent matings in which Tn5253 was transferred by conjugation from 2 pneumococcal donors (BM6001 and DP1322; Table 1) to 3 pneumococcal recipients (FP58, FP10, FP11; Table 1). Left and right junction fragments were amplified by PCR (using primer pairs IF496/IF327 and IF328/IF356) and sequenced in all transconjugants. DNA sequence analysis showed that in all cases Tn5253 integration occurred at the same site within *rbgA*, between the two direct repeats: (i) *attL*, corresponding to the *attB* of the recipient and (ii) *attR*, corresponding to the *attTn* of the circular forms of Tn5253

(Figure 2). These results indicated that *attR*, one of the two repeats flanking Tn5253 in the donor chromosome, was always transferred by conjugation to the recipients. Since the integrated form of Tn5253 was invariably flanked by *attB* at the left end (*attL*) and *attTn* at the right end (*attR*), we hypothesize a polarization in the DNA integration process. Site specific integration of MGEs often occurs at one end of essential and highly conserved genes, such as the 3' end of tRNA genes and the 3' or 5' end of genes coding for ribosomal proteins (Ambroset et al., 2016). Also for Tn5253 integration occurs at the 5' end of an essential gene, with target site duplication allowing restoration of an intact CDS. The use of essential and conserved genes as target sites guarantees the presence and conservation of *attB* in bacterial genomes favoring the spread of ICEs such as Tn5253, which can overpass the border of a single species and thus favor the dissemination of multiple antibiotic resistance genes. In fact, in other bacterial species such as *Streptococcus pyogenes* and *Streptococcus mitis*, Tn5253-like elements are found integrated at the 5' end of *rbgA* orthologous genes (Mingoia et al., 2014; Petrosyan et al., 2016).

Recombinase Genes Involved in Tn5253 Excision

Two sets of *xis/int* recombinase genes are present in the sequence of Tn5253, one set (*orf78/orf79*) is at the right end of the element,



while the other (*orf21/orf22*) belongs to Tn5251 (**Figure 3**). Excisionase Xis and tyrosine integrase Int are known to work in synergy, for this reason we decided to construct mutants where the *xis* and *int* genes were both deleted. For each set of *xis/int* recombinase genes, we constructed an isogenic deletion mutant in the Tn5253-carrying strain FR24. In FR51 a 1,820-bp DNA fragment (position 63,440–65,259, GenBank No. EU351020) encompassing *orf78/orf79* CDSs was deleted and replaced with the 876-bp *ami/aphIII* cassette. In FR82 a 1,474-bp DNA fragment (position 17,306–18,779, GenBank No. EU351020) encompassing *orf21/orf22* CDS was deleted and replaced with the 894-bp *ami/aad9* cassette (**Table 2**). The deletion of *xis/int* of Tn5251 abolished the production of circular forms and the conjugal transfer of Tn5251, but did not affect the frequencies of Tn5253 circular forms, of *attB* site reconstitution, and of Tn5253 conjugal transfer (data not shown). Deletion of *xis/int* of Tn5253 in FR51 abolished the circular forms generation and the reconstitution of *attB* site ($<7.1 \times 10^{-6}$ copies per chromosome for both genetic structures, **Table 3**). The absence of circular forms in FR51 was associated to the lack of Tn5253 conjugal transfer suggesting, that the circular form of Tn5253 acts as a conjugation intermediate as proposed for other characterized ICEs including Tn916. Data obtained using *xis/int* deletion mutants showed that the two recombinase pairs act independently and do not complement each other. This finding suggests that the association between the two elements is physical but not functional.

CONCLUSION

In this work we have shown that: (i) Tn5253 is capable of precise excision from the chromosome, producing circular forms of the

element, and leaving chromosomes with reconstituted *attB* sites; (ii) in the circular forms, the two ends of Tn5253 are joined by *attTn*, an 84-bp DNA fragment identical to the *attR* junction fragment flanking the element in its integrated form; (iii) *attR* is always transferred to the recipient strain during conjugation; (iv) production of Tn5253 circular forms and their conjugal transfer were abolished when *xis/int* of Tn5253 were deleted. Even if the importance of ICEs in shaping bacterial genomes is widely recognized and nucleotide sequences of ICEs are increasingly available, a functional characterization is available only for a few of these genetic elements. This work on Tn5253 contributes to elucidating the transfer functions of one of the prototypes of ICEs of gram positive bacteria.

AUTHOR CONTRIBUTIONS

FS, FI, and GP designed the experiments. FS and AR performed the experimental work. All authors analyzed and interpreted the data. FI, FS, and GP wrote the paper.

FUNDING

The research leading to these results has received funding from the European Union Seventh Framework Programme (FP7/2007-2013) under grant agreement no. 241446 (project ANTIRESEDEV).

ACKNOWLEDGMENTS

We are grateful to Marc Prudhomme and Jean-Pierre Claverys for kindly providing us plasmids pr410 and pr412.

REFERENCES

- Ambroset, C., Coluzzi, C., Guédon, G., Devignes, M. D., Loux, V., Lacroix, T., et al. (2016). New insights into the classification and integration specificity of *Streptococcus* integrative conjugative elements through extensive genome exploration. *Front. Microbiol.* 6:1483. doi: 10.3389/fmicb.2015.01483
- Ayoubi, P., Kilic, A. O., and Vijayakumar, M. N. (1991). Tn5253, the pneumococcal omega (cat tet) BM6001 element, is a composite structure of two conjugative transposons, Tn5251 and Tn5252. *J. Bacteriol.* 173, 1617–1622.
- Bergé, M., Moscoso, M., Prudhomme, M., Martin, B., and Claverys, J.-P. (2002). Uptake of transforming DNA in Gram-positive bacteria: a view from *Streptococcus pneumoniae*. *Mol. Microbiol.* 45, 411–421. doi: 10.1046/j.1365-2958.2002.03013.x
- Burrus, V., and Waldor, M. K. (2004). Shaping bacterial genomes with integrative and conjugative elements. *Res. Microbiol.* 155, 376–386. doi: 10.1016/j.resmic.2004.01.012
- Carraro, N., Poulin, D., and Burrus, V. (2015). Replication and active partition of integrative and conjugative elements (ICEs) of the SXT/R391 family: the line between ICEs and conjugative plasmids is getting thinner. *PLoS Genet.* 11:e1005298. doi: 10.1371/journal.pgen.1005298
- Croucher, N. J., Harris, S. R., Fraser, C., Quail, M. A., Burton, J., van der Linden, M., et al. (2011). Rapid pneumococcal evolution in response to clinical interventions. *Science* 331, 430–434. doi: 10.1126/science.1198545
- Croucher, N. J., Walker, D., Romero, P., Lennard, N., Paterson, G. K., Bason, N. C., et al. (2009). Role of conjugative elements in the evolution of the multidrug-resistant pandemic clone *Streptococcus pneumoniae* Spain23F ST81. *J. Bacteriol.* 191, 1480–1489. doi: 10.1128/JB.01343-08
- Dang-Van, A., Tiraby, G., Acar, J. F., Shaw, W. V., and Bouanchaud, D. H. (1978). Chloramphenicol resistance in *Streptococcus pneumoniae*: enzymatic acetylation and possible plasmid linkage. *Antimicrob. Agents Chemother.* 13, 577–583. doi: 10.1128/AAC.13.4.577
- Frost, L. S., Leplae, R., Summers, A. O., and Toussaint, A. (2005). Mobile genetic elements: the agents of open source evolution. *Nat. Rev. Microbiol.* 3, 722–732. doi: 10.1038/nrmicro1235
- Henderson-Begg, S. K., Roberts, A. P., and Hall, L. M. C. (2009). Diversity of putative Tn5253-like elements in *Streptococcus pneumoniae*. *Int. J. Antimicrob. Agents* 33, 364–367. doi: 10.1016/j.ijantimicag.2008.10.002
- Iannelli, F., Chiavolini, D., Ricci, S., Oggioni, M. R., and Pozzi, G. (2004). Pneumococcal surface protein C contributes to sepsis caused by *Streptococcus pneumoniae* in mice. *Infect. Immun.* 72, 3077–3080. doi: 10.1128/IAI.72.5.3077-3080.2004
- Iannelli, F., Giunti, L., and Pozzi, G. (1998). Direct sequencing of long polymerase chain reaction fragments. *Mol. Biotechnol.* 10, 183–185. doi: 10.1007/BF02760864
- Iannelli, F., and Pozzi, G. (2004). Method for introducing specific and unmarked mutations into the chromosome of *Streptococcus pneumoniae*. *Mol. Biotechnol.* 26, 81–86. doi: 10.1385/MB:26:1:81
- Iannelli, F., Santoro, F., Oggioni, M. R., and Pozzi, G. (2014). Nucleotide sequence analysis of integrative conjugative element Tn5253 of *Streptococcus pneumoniae*. *Antimicrob. Agents Chemother.* 58, 1235–1239. doi: 10.1128/AAC.01764-13

- Johnson, C. M., and Grossman, A. D. (2015). Integrative and conjugative elements (ICEs): what they do and how they work. *Annu. Rev. Genet.* 49, 577–601. doi: 10.1146/annurev-genet-112414-055018
- Kiliç, A. O., Vijayakumar, M. N., and al-Khaldi, S. F. (1994). Identification and nucleotide sequence analysis of a transfer-related region in the streptococcal conjugative transposon Tn5252. *J. Bacteriol.* 176, 5145–5150. doi: 10.1128/jb.176.16.5145-5150.1994
- Lanie, J. A., Ng, W.-L., Kazmierczak, K. M., Andrzejewski, T. M., Davidsen, T. M., Wayne, K. J., et al. (2007). Genome sequence of Avery's virulent serotype 2 strain D39 of *Streptococcus pneumoniae* and comparison with that of unencapsulated laboratory strain R6. *J. Bacteriol.* 189, 38–51. doi: 10.1128/JB.01148-06
- Lee, C. A., Babic, A., and Grossman, A. D. (2010). Autonomous plasmid-like replication of a conjugative transposon. *Mol. Microbiol.* 75, 268–279. doi: 10.1111/j.1365-2958.2009.06985.x
- Lu, F., and Churchward, G. (1995). Tn916 target DNA sequences bind the C-terminal domain of integrase protein with different affinities that correlate with transposon insertion frequency. *J. Bacteriol.* 177, 1938–1946. doi: 10.1128/jb.177.8.1938-1946.1995
- Manganelli, R., Romano, L., Ricci, S., Zazzi, M., and Pozzi, G. (1995). Dosage of Tn916 circular intermediates in *Enterococcus faecalis*. *Plasmid* 34, 48–57. doi: 10.1006/plas.1995.1032
- Mingoia, M., Morici, E., Morroni, G., Giovanetti, E., Del Grosso, M., Pantosti, A., et al. (2014). Tn5253 family integrative and conjugative elements carrying *mef(I)* and *catQ* determinants in *Streptococcus pneumoniae* and *Streptococcus pyogenes*. *Antimicrob. Agents Chemother.* 58, 5886–5893. doi: 10.1128/AAC.03638-14
- Mingoia, M., Tili, E., Manso, E., Varaldo, P. E., and Montanari, M. P. (2011). Heterogeneity of Tn5253-like composite elements in clinical *Streptococcus pneumoniae* isolates. *Antimicrob. Agents Chemother.* 55, 1453–1459. doi: 10.1128/AAC.01087-10
- Mullany, P., Roberts, A. P., and Wang, H. (2002). Mechanism of integration and excision in conjugative transposons. *Cell. Mol. Life Sci.* 59, 2017–2022. doi: 10.1007/s000180200001
- Paulsen, I. T., Banerjee, L., Myers, G. S. A., Nelson, K. E., Seshadri, R., Read, T. D., et al. (2003). Role of mobile DNA in the evolution of vancomycin-resistant *Enterococcus faecalis*. *Science* 299, 2071–2074. doi: 10.1126/science.1080613
- Pearce, B. J., Iannelli, F., and Pozzi, G. (2002). Construction of new unencapsulated (rough) strains of *Streptococcus pneumoniae*. *Res. Microbiol.* 153, 243–247. doi: 10.1016/S0923-2508(02)01312-8
- Petrosyan, V., Holder, M., Ajami, N. J., Petrosino, J. F., Sahasrabhojane, P., Thompson, E. J., et al. (2016). Complete genome sequence of *Streptococcus mitis* strain SVGS_061 isolated from a neutropenic patient with viridans group streptococcal shock syndrome. *Genome Announc.* 4:e00259-16. doi: 10.1128/genomeA.00259-16
- Provvedi, R., Manganelli, R., and Pozzi, G. (1996). Characterization of conjugative transposon Tn5251 of *Streptococcus pneumoniae*. *FEMS Microbiol. Lett.* 135, 231–236. doi: 10.1111/j.1574-6968.1996.tb07994.x
- Santoro, F., Oggioni, M. R., Pozzi, G., and Iannelli, F. (2010). Nucleotide sequence and functional analysis of the tet(M)-carrying conjugative transposon Tn5251 of *Streptococcus pneumoniae*. *FEMS Microbiol. Lett.* 308, 150–158. doi: 10.1111/j.1574-6968.2010.02002.x
- Santoro, F., Vianna, M. E., and Roberts, A. P. (2014). Variation on a theme; an overview of the Tn916/Tn1545 family of mobile genetic elements in the oral and nasopharyngeal streptococci. *Front. Microbiol.* 5:535. doi: 10.3389/fmicb.2014.00535
- Scott, J. R., Kirchman, P. A., and Caparon, M. G. (1988). An intermediate in transposition of the conjugative transposon Tn916. *Proc. Natl. Acad. Sci. U.S.A.* 85, 4809–4813. doi: 10.1073/pnas.85.13.4809
- Smith, M. D., Hazum, S., and Guild, W. R. (1981). Homology among tet determinants in conjugative elements of streptococci. *J. Bacteriol.* 148, 232–240.
- Storrs, M. J., Poyart-Salmeron, C., Trieu-Cuot, P., and Courvalin, P. (1991). Conjugative transposition of Tn916 requires the excisive and integrative activities of the transposon-encoded integrase. *J. Bacteriol.* 173, 4347–4352. doi: 10.1128/jb.173.14.4347-4352.1991
- Uicker, W. C., Schaefer, L., and Britton, R. A. (2006). The essential GTPase RbgA (YlqF) is required for 50S ribosome assembly in *Bacillus subtilis*. *Mol. Microbiol.* 59, 528–540. doi: 10.1111/j.1365-2958.2005.04948.x

Conflict of Interest Statement: The authors declare that the research was conducted in the absence of any commercial or financial relationships that could be construed as a potential conflict of interest.

Copyright © 2018 Santoro, Romeo, Pozzi and Iannelli. This is an open-access article distributed under the terms of the Creative Commons Attribution License (CC BY). The use, distribution or reproduction in other forums is permitted, provided the original author(s) and the copyright owner(s) are credited and that the original publication in this journal is cited, in accordance with accepted academic practice. No use, distribution or reproduction is permitted which does not comply with these terms.



The Versatile Mutational Resistome of *Pseudomonas aeruginosa*

Carla López-Causapé, Gabriel Cabot, Ester del Barrio-Tofiño and Antonio Oliver*

Servicio de Microbiología y Unidad de Investigación, Hospital Universitari Son Espases, Institut d'Investigació Sanitària Illes Balears, Palma de Mallorca, Spain

OPEN ACCESS

Edited by:

Gian Maria Rossolini,
Università degli Studi di Firenze, Italy

Reviewed by:

Daniel Pletzer,
The University of British Columbia,
Canada

Max Maurin,
Université Grenoble Alpes, France

*Correspondence:

Antonio Oliver
antonio.oliver@ssib.es

Specialty section:

This article was submitted to
Evolutionary and Genomic
Microbiology,
a section of the journal
Frontiers in Microbiology

Received: 24 January 2018

Accepted: 23 March 2018

Published: 06 April 2018

Citation:

López-Causapé C, Cabot G,
del Barrio-Tofiño E and Oliver A
(2018) The Versatile Mutational
Resistome of *Pseudomonas*
aeruginosa. *Front. Microbiol.* 9:685.
doi: 10.3389/fmicb.2018.00685

One of the most striking features of *Pseudomonas aeruginosa* is its outstanding capacity for developing antimicrobial resistance to nearly all available antipseudomonal agents through the selection of chromosomal mutations, leading to the failure of the treatment of severe hospital-acquired or chronic infections. Recent whole-genome sequencing (WGS) data obtained from *in vitro* assays on the evolution of antibiotic resistance, *in vivo* monitoring of antimicrobial resistance development, analysis of sequential cystic fibrosis isolates, and characterization of widespread epidemic high-risk clones have provided new insights into the evolutionary dynamics and mechanisms of *P. aeruginosa* antibiotic resistance, thus motivating this review. Indeed, the analysis of the WGS mutational resistome has proven to be useful for understanding the evolutionary dynamics of classical resistance pathways and to describe new mechanisms for the majority of antipseudomonal classes, including β -lactams, aminoglycosides, fluoroquinolones, or polymyxins. Beyond addressing a relevant scientific question, the analysis of the *P. aeruginosa* mutational resistome is expected to be useful, together with the analysis of the horizontally-acquired resistance determinants, for establishing the antibiotic resistance genotype, which should correlate with the antibiotic resistance phenotype and as such, it should be useful for the design of therapeutic strategies and for monitoring the efficacy of administered antibiotic treatments. However, further experimental research and new bioinformatics tools are still needed to overcome the interpretation limitations imposed by the complex interactions (including those leading to collateral resistance or susceptibility) between the 100s of genes involved in the mutational resistome, as well as the frequent difficulties for differentiating relevant mutations from simple natural polymorphisms.

Keywords: antibiotic resistance, resistome, *Pseudomonas aeruginosa*, multidrug resistance, evolution, resistance development, mutation

INTRODUCTION

Pseudomonas aeruginosa is one of the most frequent and severe causes of hospital-acquired infections, particularly affecting immunocompromised (especially neutropenic) and Intensive Care Unit (ICU) patients. Indeed, *P. aeruginosa* is the first cause of ventilator associated pneumonia (VAP) and burn wound infections, both associated with a very high mortality rate (Vincent, 2003; Bassetti et al., 2012). Likewise, *P. aeruginosa* is the most frequent driver of chronic respiratory infections in cystic fibrosis (CF) patients or other chronic underlying diseases (Döring et al., 2011).

One of the most striking features of *P. aeruginosa* is its outstanding capacity for developing antimicrobial resistance to nearly all available antipseudomonal agents through the selection of chromosomal mutations. Indeed, treatment failure caused by the development of antimicrobial resistance is a too frequent outcome of *P. aeruginosa* infections. The problem of mutation-mediated antibiotic resistance is further amplified in the chronic infection setting, due to the very high prevalence of hypermutable strains, showing greatly enhanced spontaneous mutation rates caused by defective DNA repair or error avoidance systems (Oliver et al., 2000; Maciá et al., 2005).

Beyond the obvious negative impact of resistance development for the treated patient, the accumulation of several of these chromosomal mutations leads to the emergence of multidrug resistant (MDR), extensively drug-resistant (XDR) or even pan-antibiotic-resistant (PDR) strains, which can be responsible for notable epidemics in the hospital setting (Deplano et al., 2005; Suarez et al., 2011). Moreover, recent studies have evidenced the existence of MDR/XDR global clones disseminated in different hospitals worldwide, and for that reason they have been denominated high-risk clones (Woodford et al., 2011; Oliver et al., 2015). Although high-risk clones are frequently associated with transferable antimicrobial resistance determinants, they also typically show a wide range of chromosomal mutations playing a major role in the resistance phenotype (Oliver et al., 2015). Likewise, recent reports have evidenced the interpatient spread of antimicrobial resistance mutations linked to the transmission of epidemic CF strains (López-Causapé et al., 2017).

Along with growing information from mechanistic studies on chromosomal resistance mechanisms and their complex regulatory pathways, involved in adaptive resistance (Lister et al., 2009; Muller et al., 2011; Skiada et al., 2011; Juan et al., 2017), the introduction of whole-genome sequencing (WGS) approaches is shaping up a new dimension for the mutational resistance landscape. The term resistome was first used to account for the set of primary antibiotic resistance genes that could be eventually transferred to human pathogens (D'Costa et al., 2006). Soon after the concept of intrinsic resistome was introduced to include all chromosomal genes that are involved in intrinsic resistance, and whose presence in strains of a bacterial species is independent of previous antibiotic exposure and is not due to horizontal gene transfer (HGT) (Fajardo et al., 2008). Finally, the term mutational resistome was more recently implemented to account for the set of mutations involved in the modulation of antibiotic resistance levels in the absence of HGT (Cabot et al., 2016b; López-Causapé et al., 2017). Recent WGS data obtained from *in vitro* assays on the evolution of antibiotic resistance, *in vivo* monitoring of antimicrobial resistance development, analysis of sequential CF isolates, and characterization of wide spread epidemic high-risk clones provide new insights into the evolutionary dynamics and mechanisms of *P. aeruginosa* antibiotic resistance (Cabot et al., 2016a; Feng et al., 2016; Del Barrio-Tofiño et al., 2017; Jaillard et al., 2017; López-Causapé et al., 2017). Indeed, the analysis of WGS mutational resistomes has proven to be useful for understanding the evolutionary dynamics of classical resistance mechanisms and to depict

new ones for the majority of antimicrobial classes, including β -lactams, aminoglycosides, fluoroquinolones, polymyxins and others, as reviewed in the following sections. **Table 1** summarizes the main genes and mutations known to increase resistance levels and therefore shaping up the *P. aeruginosa* mutational resistome.

β -LACTAM MUTATIONAL RESISTOME

The most frequent mutation-driven β -lactam resistance mechanism is likely the overproduction of the chromosomal cephalosporinase AmpC, involving a wide range of genes belonging to complex regulatory pathways of cell-wall recycling (Juan et al., 2017). Among them, the mutational inactivation of *dacB*, encoding the non-essential penicillin-binding protein (PBP) PBP4, and *ampD*, encoding a *N*-acetyl-muramyl-L-alanine amidase have been found to be the most frequent cause of *ampC* derepression and β -lactam resistance (Juan et al., 2005; Moya et al., 2009). The inactivation of PBP4 has also been shown to activate the BlrAB/CreBC regulatory system, further increasing resistance levels (Moya et al., 2009). Additionally, specific point mutations leading to a conformation change in the transcriptional regulator AmpR, causing *ampC* upregulation and β -lactam resistance, have been noted among clinical strains. They include the D135N mutation, described in several species besides *P. aeruginosa*, including *Stenotrophomonas maltophilia*, *Citrobacter freundii*, or *Enterobacter cloacae* (Juan et al., 2017) or the R154H mutation, linked to the widespread MDR/XDR ST175 high-risk clone. Mutation of many other genes, including those encoding other amidases (AmpDh2 and AmpDh3), other PBPs (such as PBP5 and PBP7), lytic transglycosylases (such as SltB1 and mltB), MPL (UDP-*N*-acetylmuramate:L-alanyl- γ -D-glutamyl-meso-diaminopimelate ligase), or NuoN (NADH dehydrogenase I chain N) have been shown to enhance *ampC* expression, either alone or combined with other mutations, although their impact on β -lactam resistance among clinical strains still needs to be further analyzed (Juan et al., 2017).

In addition to *ampC* overexpression, recent studies have revealed that β -lactam resistance development, including the novel combinations of β -lactam- β -lactamase inhibitors ceftolozane/tazobactam and ceftazidime/avibactam, may result from mutations leading to the structural modification of AmpC (Cabot et al., 2014; Lahiri et al., 2014; Fraile-Ribot et al., 2017a; Haidar et al., 2017). Likewise, recent studies identified diverse AmpC variants associated with high-level cephalosporin resistance, including ceftolozane/tazobactam and ceftazidime/avibactam, in a small proportion (around 1%) of clinical *P. aeruginosa* isolates (Berrazeg et al., 2015). Over 200 *Pseudomonas* Derived Cephalosporinase (PDC) variants have been described so far, including those associated with enhanced ceftolozane/tazobactam and ceftazidime/avibactam resistance (**Table 1**). An update database of PDC variants is maintained in our laboratory and is freely available at <https://arpbigdisba.com>. Additionally, resistance development to ceftolozane/tazobactam and/or ceftazidime/avibactam may involve mutations leading to the structural modification of narrow spectrum OXA-2 and OXA-10 acquired oxacillinases (Fraile-Ribot et al., 2017a,b).

TABLE 1 | Main genes and mutations known to be involved in increased *P. aeruginosa* antibiotic resistance.

Gene	Resistance mechanisms/ altered target	Antibiotics affected ^a	Type of mutation	Relevant examples of gain-of-function mutations	Reference
<i>gyrA</i>	DNA gyrase	FQ	Gain-of-function	G81D, T83A, T83I, Y86N, D87G, D87N, D87Y, Q106L	Bruchmann et al., 2013; Kos et al., 2015; Cabot et al., 2016b; Del Barrio-Tofiño et al., 2017; López-Causapé et al., 2017
<i>gyrB</i>	DNA gyrase	FQ	Gain-of-function	S466F, S466Y, Q467R, E468D	Bruchmann et al., 2013; Kos et al., 2015; Del Barrio-Tofiño et al., 2017; López-Causapé et al., 2017
<i>parC</i>	DNA topoisomerase IV	FQ	Gain-of-function	S87L, S87W	Bruchmann et al., 2013; Kos et al., 2015; Cabot et al., 2016b; Del Barrio-Tofiño et al., 2017
<i>parE</i>	DNA topoisomerase IV	FQ	Gain-of-function	S457G, S457T, E459D, E459K	Bruchmann et al., 2013; Kos et al., 2015; Del Barrio-Tofiño et al., 2017; López-Causapé et al., 2017
<i>pmrA</i>	Lipopolysaccharide (lipid A)	COL	Gain-of-function	L157Q	Lee and Ko, 2014
<i>pmrB</i>	Lipopolysaccharide (lipid A)	COL	Gain-of-function	L14P, A54V, R79H, R135Q, A247T, A248T, A248V, R259H, M292I, M292T	Barrow and Kwon, 2009; Moskowitz et al., 2012
<i>phoQ</i>	Lipopolysaccharide (lipid A)	COL	Loss-of-function		
<i>parR</i>	Lipopolysaccharide (lipid A)	COL	Gain-of-function	M59I, E156K	Muller et al., 2011; Guénard et al., 2014
	OprD downregulation	IMP, MER			
	MexEF-OprN hyperproduction	FQ			
	MexXY-OprM hyperproduction	FQ, AMG, CEF			
<i>parS</i>	Lipopolysaccharide (lipid A)	COL	Gain-of-function	L14Q, V101M, L137P, A138T, A168V Q232E, G361R	Muller et al., 2011; Fournier et al., 2013; Guénard et al., 2014
	OprD downregulation	IMP, MER			
	MexEF-OprN hyperproduction	FQ			
	MexXY-OprM hyperproduction	FQ, AMG, CEF			
<i>cprS</i>	Lipopolysaccharide (lipid A)	COL	Gain-of-function	R241C	Gutu et al., 2013
<i>colR</i>	Lipopolysaccharide (lipid A)	COL	Gain-of-function	D32N	Gutu et al., 2013
<i>colS</i>	Lipopolysaccharide (lipid A)	COL	Gain-of-function	A106V	Gutu et al., 2013
<i>mexR</i>	MexAB-OprM hyperproduction	FQ, CAZ, CEF, PPT, MER, CAZ/AVI	Loss-of-function		
<i>nalC</i>	MexAB-OprM hyperproduction	FQ, CAZ, CEF, PPT, MER, CAZ/AVI	Loss-of-function		
<i>nalD</i>	MexAB-OprM hyperproduction	FQ, CAZ, CEF, PPT, MER, CAZ/AVI	Loss-of-function		
<i>nfxB</i>	MexCD-OprJ hyperproduction	FQ, CEF	Loss-of-function		
<i>mexS</i>	MexEF-OprN hyperproduction	FQ	Loss-of-function		
	OprD downregulation	IMP, MER			
<i>mexT</i>	MexEF-OprN hyperproduction	FQ	Gain-of-function	G257S, G257A	Juarez et al., 2018
	OprD downregulation	IMP, MER			

(Continued)

TABLE 1 | Continued

Gene	Resistance mechanisms/altered target	Antibiotics affected ^a	Type of mutation	Relevant examples of gain-of-function mutations	Reference
<i>cmrA</i>	MexEF-OprN hyperproduction	MER, FQ	Gain-of-function	A68V, L89Q, H204L, N214K	Juarez et al., 2017
<i>mvaT</i>	MexEF-OprN hyperproduction	FQ	Loss-of-function		
<i>PA3271</i>	MexEF-OprN hyperproduction	FQ	Loss-of-function		
<i>mexZ</i>	MexXY-OprM hyperproduction	FQ, AMG, CEF	Loss-of-function		
<i>PA5471.1</i>	MexXY-OprM hyperproduction	FQ, AMG, CEF	Loss-of-function		
<i>amgS</i>	MexXY-OprM hyperproduction	FQ, AMG, CEF	Gain-of-function	V121G, R182C	Lau et al., 2015
<i>oprD</i>	OprD inactivation	IMP, MER	Loss-of-function		
<i>ampC</i>	AmpC structural modification	CAZ/AVI, C/T	Gain-of-function	T96I, G183D, E247K	Cabot et al., 2014; Fraile-Ribot et al., 2017a
<i>ampD</i>	AmpC hyperproduction	CAZ, CEF, PPT	Loss-of-function		
<i>ampDh2</i>	AmpC hyperproduction	CAZ, CEF, PPT	Loss-of-function		
<i>ampDh3</i>	AmpC hyperproduction	CAZ, CEF, PPT	Loss-of-function		
<i>ampR</i>	AmpC hyperproduction	CAZ, CEF, PPT	Gain-of-function	D135N, G154R	Bagge et al., 2002; Cabot et al., 2016b
<i>dacB</i>	AmpC hyperproduction	CAZ, CEF, PPT	Loss-of-function		
<i>ftsI</i>	Penicillin-binding-protein 3 (PBP3)	CAZ, CEF, PPT, MER, CAZ/AVI, C/T	Gain-of-function	R504C, R504H, P527T, F533L	Diaz Caballero et al., 2015; Cabot et al., 2016a,b; Del Barrio-Tofiño et al., 2017; López-Causapé et al., 2017
<i>fusA1</i>	Elongation factor G	AMG	Gain-of-function	I61M, V93A, E100G, K504E, Y552C, P554L, A555E, N592I, P618L, T671A, T671I	Feng et al., 2016; Bolard et al., 2017; Del Barrio-Tofiño et al., 2017; López-Causapé et al., 2017, 2018
<i>glpT</i>	Transporter protein GlpT	FOS	Loss-of-function		
<i>rpoB</i>	RNA polymerase β -chain	RIF	Gain-of-function	S517F, Q518R, Q518L, D521G, H531Y, H531L, S536F, L538I, S579F, S579Y, N629S, D636Y	Jatsenko et al., 2010

^aFQs, fluoroquinolones; COL, colistin; AMGs, aminoglycosides; CAZ, ceftazidime; CEF, cefepime; PPT, piperacillin-tazobactam; IMP, imipenem; MER, meropenem; CAZ/AVI, ceftazidime/avibactam; C/T, ceftolozane/tazobactam; FOS, fosfomycin; RIF, rifampicin.

Besides β -lactamases, there is increasing evidence on the role of target modification in *P. aeruginosa* β -lactam resistance. Particularly noteworthy are the mutations in *ftsI*, encoding PBP3, an essential high molecular class B PBP with transpeptidase activity (Chen et al., 2016). Indeed, data from CF patients (Diaz Caballero et al., 2015; López-Causapé et al., 2017), epidemic high-risk clones (Cabot et al., 2016b; Del Barrio-Tofiño et al., 2017) as well as from *in vitro* studies (Cabot et al., 2016a) have recently shown that PBP3 is under strong mutational pressure, and that specific mutations in this PBP contribute to β -lactam resistance development. R504C/H and F533L mutations are likely those most commonly reported, and are located within the protein domains implicated in the formation and stabilization of the inactivating complex β -lactam-PBP3 (Han et al., 2010). Moreover, these specific mutations have been documented to emerge *in vivo* during chronic respiratory infection in CF patients (Diaz Caballero et al., 2015; López-Causapé et al., 2017) and upon meropenem (Cabot et al., 2016a) and aztreonam (Jorth

et al., 2017) exposure *in vitro*. However, the precise contribution of PBP3 mutations to β -lactam resistance phenotypes needs to be further investigated using isogenic strains. Likewise, despite unique polymorphisms have also been detected in some clinical strains for other PBPs, their role in β -lactam resistance, if any, still needs to be experimentally addressed.

Other relevant components of the β -lactam mutational resistome are the porins and RND efflux pumps. Mutational inactivation of OprD is well-known to be the primary carbapenem resistance mechanisms in *P. aeruginosa* (Lister et al., 2009; Castanheira et al., 2014). OprD inactivation typically results from indels or nonsense mutations, including the Q142X mutation, characteristic of the widespread ST175 high-risk clone (Cabot et al., 2016b). Additionally, some amino acid substitutions have also been recently associated with OprD-driven resistance, particularly in the CF setting (Richardot et al., 2015). Finally, carbapenem resistance may also result from *oprD* repression caused by mutations in the MexEF-OprN efflux pump regulators

(*mexS/T*) or the ParRS two-component system (Li et al., 2015). Overexpression of MexAB-OprM, caused by mutation of several genes involved in its regulation (*mexR*, *nalC*, or *nalD*) increases MICs of most β -lactams except imipenem, whereas overexpression of MexXY (*mexZ*, *parSR*, *amgS* mutations) is particularly involved in cefepime resistance (Li et al., 2015). Additionally, sequence variations in unique residues are detected in the genes coding for the efflux pump (Del Barrio-Tofiño et al., 2017; López-Causapé et al., 2017); however, their contribution to resistance profiles, if any, still needs to be further explored.

Finally, another potentially relevant mutational β -lactam resistance mechanism is the selection of large (>200 kb) deletions affecting specific parts of the chromosome (Cabot et al., 2016a). Although the basis of the conferred resistance phenotype still needs to be further clarified, these mutants can be recognized by the characteristic brown pigment (pyomelanine) caused by the deletion of one of the affected genes, *hmgA*, coding for a homogentisate-1,2-dioxygenase. This type of deletion has been documented in both, *in vitro* evolved β -lactam-resistant mutants and CF isolates (Cabot et al., 2016a; Hocquet et al., 2016). However, the deletion of *hmgA* is not responsible for the resistance phenotype, which could be linked to the deletion of another of the affected genes, *galU*. This gene codes for a UDP-glucose pyrophosphorylase involved in the synthesis of the lipopolysaccharide (LPS) core. Indeed, analysis of transposon mutant libraries has shown that inactivation of *galU* increases ceftazidime and meropenem MICs (Dötsch et al., 2009; Alvarez-Ortega et al., 2010).

AMINOGLYCOSIDE MUTATIONAL RESISTOME

In the absence of horizontally-acquired aminoglycoside modifying enzymes, resistance to this antibiotic class has been particularly linked to the mutational overexpression of MexXY-OprM. Indeed, mutational overexpression of this pump, mainly caused by *mexZ*, *amgS*, or *parRS* mutations (Table 1), is very frequent among clinical isolates, from both, CF patients and nosocomial infections (Guénard et al., 2014; Prickett et al., 2017). Moreover, recent studies show that the epidemic high-risk clone ST175 overexpresses MexXY due to a specific mutation in *mexZ* (G195E) (Cabot et al., 2016b). However, recent studies have revealed that the aminoglycoside mutational resistome extends far beyond MexXY overexpression, and that high-level resistance may result from the accumulation of multiple mutations, and the involvement of several novel resistance determinants has been recently documented (El'Garch et al., 2007; Schurek et al., 2008; Feng et al., 2016). Among them is particularly noteworthy *fusA1*, coding for the elongation factor G. Indeed, specific *FusA1* mutations have been associated with aminoglycoside resistance *in vitro* (Feng et al., 2016; López-Causapé et al., 2018) and among clinical, particularly CF, strains (Chung et al., 2012; Markussen et al., 2014; Greipel et al., 2016; López-Causapé et al., 2017, 2018). Moreover, the implication of *fusA1* mutations in aminoglycoside resistance has been recently confirmed through site-directed mutagenesis (Bolard et al., 2017).

FLUOROQUINOLONE MUTATIONAL RESISTOME

The fluoroquinolone mutational resistome generally includes specific missense mutations in DNA gyrase (*gyrA* and/or *gyrB*) and topoisomerase IV (*parC* and/or *parE*) Quinolone Resistance-Determining Regions (QRDRs) (Table 1) (Bruchmann et al., 2013; Kos et al., 2015). High-level fluoroquinolone resistance in *P. aeruginosa* high-risk clones is nearly universal, and typically involves combinations of mutations in GyrA-T83 and ParC-S87 (Del Barrio-Tofiño et al., 2017). QRDR mutations involved in fluoroquinolone resistance in CF might be more variable (López-Causapé et al., 2017). It is also well-known that the mutational overexpression of efflux pumps modulate fluoroquinolone resistance (Table 1). While the overexpression of MexAB-OprM and MexXY-OprM is globally more frequent among clinical strains, its contribution to clinical fluoroquinolone resistance is likely more modest (Bruchmann et al., 2013). On the other hand, the mutational overexpression of MexEF-OprN or MexCD-OprJ is associated with high-level (clinical) fluoroquinolone resistance, and although their prevalence is considered low except in the CF chronic infection setting, recent data show that it might be higher than expected (Richardot et al., 2015).

POLYMYXIN MUTATIONAL RESISTOME

Whereas the prevalence of polymyxin (colistin and polymyxin B) resistance is still globally low (<5%), it has increased in the last years because of the frequent use of these last-resource antibiotics for the treatment of MDR/XDR nosocomial and CF strains. Polymyxin resistance results most frequently from the modification of the LPS caused by the addition of a 4-amino-4-deoxy-L-arabinose moiety in the lipid A structure (Olaitan et al., 2014; Jeannot et al., 2017). The involved mutations are frequently located in the PmrAB or PhoPQ two-component regulators, which lead to the activation of the *arnBCADTEF* operon (Barrow and Kwon, 2009). More recent studies have revealed that mutations in the ParRS two-component regulator, not only produce polymyxin resistance due to the activation of the *arnBCADTEF* operon, but also lead to a MDR phenotype determined by the overexpression of MexXY and the repression of OprD (Muller et al., 2011). Moreover, two additional two-component regulators, ColRS and CprRS, have been recently found to be involved in polymyxin resistance (Gutu et al., 2013). The analysis of colistin resistance mechanisms among clinical strains is not always straight forward, since the presence of mutations in these two-component regulators is not always associated with clinical colistin resistance, probably denoting partial complementation between the different regulators (Moskowitz et al., 2012; Gutu et al., 2013; López-Causapé et al., 2017). Moreover, recent *in vitro* evolution assays have revealed the implication of additional mutations in high level colistin resistance, facilitated by the emergence of mutator (*mutS* deficient) phenotypes (Döbelmann et al., 2017). Particularly noteworthy among them are those occurring in LptD, LpxC, or MigA.

OTHER ANTIBIOTICS

Even if not considered a classical antipseudomonal agent, fosfomycin has emerged in the last decade as a potentially useful antibiotic in urinary tract infections and combined therapy for MDR/XDR *P. aeruginosa* (Michalopoulos et al., 2011). However, fosfomycin resistance spontaneous mutation rates are high and the mechanism involved is typically the mutational inactivation of *glpT*, coding for a glycerol-3-phosphate permease required for fosfomycin uptake (Castañeda-García et al., 2009; Rodríguez-Rojas et al., 2010). *glpT* mutations, conferring high-level fosfomycin resistance are also frequently found among MDR/XDR high-risk clones (Del Barrio-Tofiño et al., 2017), and some specific mutations, such as T211P, have been fixed in some widespread lineages as described for ST175 (Cabot et al., 2016b). Another potentially useful antimicrobial for combined therapy against MDR/XDR *P. aeruginosa* is rifampicin (Cai et al., 2017). However, rifampicin resistance may emerge at high frequency due to the selection of specific missense mutations in *rpoB*, coding for the beta subunit of the RNA polymerase (Jatsenko et al., 2010). Another example of newer antibiotic families with antipseudomonal activity are the pacidamycins, uridyl peptide antibiotics, targeting translocase I, an essential enzyme in peptidoglycan biosynthesis (Mistry et al., 2013). Emergence of high-level resistance to this antibiotic class has been shown to involve the selection of mutations in the Opp transporter, a binding protein-dependent ABC transporter used for oligopeptide import. Finally, the *P. aeruginosa* mutational resistome, particularly in the CF setting, may also include resistance to other used antibiotics such as the frequent mutations of domain V of 23S rRNA, conferring macrolide resistance (Mustafa et al., 2017).

CONCLUDING REMARKS AND FUTURE PERSPECTIVES

The analysis of the *P. aeruginosa* mutational resistome, together with the analysis of the horizontally-acquired resistance determinants, should be useful for establishing the antibiotic resistance genotype, which should correlate with the antibiotic resistance phenotype and as such, it should permit the design of therapeutic strategies and for monitoring the efficacy of administered antibiotic treatments. However, the current applicability of the analysis of the mutational resistome is still limited by the large number of genes involved and the complexity of the resistance phenotypes generated, and, particularly, by the difficulties, in many cases, for differentiating relevant mutations from simple natural polymorphisms. Obviously, the evolution of the mutational resistome is a direct consequence of antimicrobial exposure and as such, it is not surprising that exposure to one antibiotic drives evolution of the mutational resistome for that antibiotic. However, the complexity of the actual resistance profile is further increased by the specificity and interactions among different resistance mechanisms. Indeed, a resistance mutation selected by one antibiotic may have a

variable effect among the different agents within the same antibiotic class or family. Likewise, cross resistance (or collateral resistance) implies that exposure to one antibiotic drives also the development of resistance to a different one from the same or other classes. Typically, this is caused by the developed resistance mechanism (such as efflux pump overexpression) affecting simultaneously different antibiotics. Indeed, potential development of cross resistance is a major issue to consider when using antibiotic combinations (Vestergaard et al., 2016). Moreover, cross resistance between antibiotics and antiseptics and other biocides may also occur (Li et al., 2015). Perhaps less obvious is collateral susceptibility, which implies that exposure to one antibiotic increases the susceptibility to a different one (Pál et al., 2015; Imamovic et al., 2017). This might be achieved through two mechanisms. One possible mechanism is that exposure to one antibiotic directly causes increased susceptibility to a different one, for example, mutations in the β -lactamase AmpC increases cephalosporin hydrolysis while reducing that of penicillins or carbapenems (Cabot et al., 2014). The second possibility is that the development of a resistance mechanism impairs the activity of another existing resistance mechanism. An example is competition between the different efflux pumps, since the overexpression of one may impair the expression of another (Mulet et al., 2011). Thus, the evolution of the mutational resistome for a given antibiotic is not only dependent on the exposure to this antibiotic, but it is also conditioned by the simultaneous or even previous exposures to other antibiotics. An illustrative example is provided in a recent *in vitro* study that demonstrated, for a broad range of antibiotic classes, that the history of exposure and resistance development to a given antibiotic, conditions the dynamics and mechanisms of resistance development when exposed to a second one (Yen and Papin, 2017). In summary, the comprehensive analysis of the mutational resistome of *P. aeruginosa* in CF and nosocomial infections is expected to become a useful tool for optimizing therapeutic strategies and monitoring the efficacy of administered antibiotic treatments in the near future.

AUTHOR CONTRIBUTIONS

CL-C and AO wrote the manuscript. CL-C, GC, EdB-T, and AO reviewed the literature.

FUNDING

The authors were supported by Plan Nacional de I+D+i 2013–2016 and Instituto de Salud Carlos III, Subdirección General de Redes y Centros de Investigación Cooperativa, Ministerio de Economía, Industria y Competitividad, Spanish Network for Research in Infectious Diseases (REIPI RD16/0016) and grant PI15/00088 (PI AO) and co-financed by European Development Regional Fund ERDF “A way to achieve Europe,” Operative program Intelligent Growth 2014–2020. AO was also supported by the European Union through the 11th Call of the Innovative Medicines Initiative (grant COMBACTE-MAGNET).

REFERENCES

- Alvarez-Ortega, C., Wiegand, I., Olivares, J., Hancock, R. E., and Martínez, J. L. (2010). Genetic determinants involved in the susceptibility of *Pseudomonas aeruginosa* to beta-lactam antibiotics. *Antimicrob. Agents Chemother.* 54, 4159–4167. doi: 10.1128/AAC.00257-10
- Bagge, N., Ciofu, O., Hentzer, M., Campbell, J. I., Givskov, M., and Høiby, N. (2002). Constitutive high expression of chromosomal beta-lactamase in *Pseudomonas aeruginosa* caused by a new insertion sequence (IS1669) located in ampD. *Antimicrob. Agents Chemother.* 46, 3406–3411. doi: 10.1128/AAC.46.11.3406-3411.2002
- Barrow, K., and Kwon, D. H. (2009). Alterations in two-component regulatory systems of phoPQ and pmrAB are associated with polymyxin B resistance in clinical isolates of *Pseudomonas aeruginosa*. *Antimicrob. Agents Chemother.* 53, 5150–5154. doi: 10.1128/AAC.00893-09
- Bassetti, M., Taramasso, L., Giacobbe, D. R., and Pelosi, P. (2012). Management of ventilator-associated pneumonia: epidemiology, diagnosis and antimicrobial therapy. *Expert Rev. Anti. Infect. Ther.* 10, 585–596. doi: 10.1586/eri.12.36
- Berrazeg, M., Jeannot, K., Ntsogo Enguéné, V. Y., Broutin, I., Loeffert, S., Fournier, D., et al. (2015). Mutations in β -Lactamase AmpC increase resistance of *Pseudomonas aeruginosa* isolates to antipseudomonal cephalosporins. *Antimicrob. Agents Chemother.* 59, 6248–6255. doi: 10.1128/AAC.00825-15
- Bolard, A., Plesiat, P., and Jeannot, K. (2017). Mutations in gene *fusA1* as a novel mechanism of aminoglycoside resistance in clinical strains of *Pseudomonas aeruginosa*. *Antimicrob. Agents Chemother.* 62, e01835-17. doi: 10.1128/AAC.01835-17
- Bruchmann, S., Dötsch, A., Nouri, B., Chaberny, I. F., and Häussler, S. (2013). Quantitative contributions of target alteration and decreased drug accumulation to *Pseudomonas aeruginosa* fluoroquinolone resistance. *Antimicrob. Agents Chemother.* 57, 1361–1368. doi: 10.1128/AAC.01581-12
- Cabot, G., Bruchmann, S., Mulet, X., Zamorano, L., Moyà, B., Juan, C., et al. (2014). *Pseudomonas aeruginosa* ceftolozane-tazobactam resistance development requires multiple mutations leading to overexpression and structural modification of AmpC. *Antimicrob. Agents Chemother.* 58, 3091–3099. doi: 10.1128/AAC.02462-13
- Cabot, G., Zamorano, L., Moyà, B., Juan, C., Navas, A., Blázquez, J., et al. (2016a). Evolution of *Pseudomonas aeruginosa* antimicrobial resistance and fitness under low and high mutation rates. *Antimicrob. Agents Chemother.* 60, 1767–1778. doi: 10.1128/AAC.02676-15
- Cabot, G., López-Causapé, C., Ocampo-Sosa, A. A., Sommer, L. M., Domínguez, M. Á., Zamorano, L., et al. (2016b). Deciphering the resistome of the widespread *Pseudomonas aeruginosa* Sequence Type 175 international high-risk clone through whole-genome sequencing. *Antimicrob. Agents Chemother.* 60, 7415–7423.
- Cai, Y., Yang, D., Wang, J., and Wang, R. (2017). Activity of colistin alone or in combination with rifampicin or meropenem in a carbapenem-resistant bioluminescent *Pseudomonas aeruginosa* intraperitoneal murine infection model. *J. Antimicrob. Chemother.* 73, 456–461. doi: 10.1093/jac/dkx399
- Castañeda-García, A., Rodríguez-Rojas, A., Guelfo, J. R., and Blázquez, J. (2009). The glycerol-3-phosphate permease GlpT is the only fosfomycin transporter in *Pseudomonas aeruginosa*. *J. Bacteriol.* 191, 6968–6974. doi: 10.1128/JB.00748-09
- Castanheira, M., Deshpande, L. M., Costello, A., Davies, T. A., and Jones, R. N. (2014). Epidemiology and carbapenem resistance mechanisms of carbapenem-non-susceptible *Pseudomonas aeruginosa* collected during 2009–11 in 14 European and Mediterranean countries. *J. Antimicrob. Chemother.* 69, 1804–1814. doi: 10.1093/jac/dku048
- Chen, W., Zhang, Y. M., and Davies, C. (2016). Penicillin-Binding Protein 3 is essential for growth of *Pseudomonas aeruginosa*. *Antimicrob. Agents Chemother.* 61, e01651-16. doi: 10.1128/AAC.01651-16
- Chung, J. C., Becq, J., Fraser, L., Schulz-Trieglaff, O., Bond, N. J., Foweraker, J., et al. (2012). Genomic variation among contemporary *Pseudomonas aeruginosa* isolates from chronically infected cystic fibrosis patients. *J. Bacteriol.* 194, 4857–4866. doi: 10.1128/JB.01050-12
- D'Costa, V. M., McGrann, K. M., Hughes, D. W., and Wright, G. D. (2006). Sampling the antibiotic resistome. *Science* 311, 374–377. doi: 10.1126/science.1120800
- Del Barrio-Tofiño, E., López-Causapé, C., Cabot, G., Rivera, A., Benito, N., Segura, C., et al. (2017). Genomics and susceptibility profiles of extensively drug-resistant *Pseudomonas aeruginosa* isolates from Spain. *Antimicrob. Agents Chemother.* 61, e01589-17. doi: 10.1128/AAC.01589-17
- Deplano, A., Denis, O., Poirel, L., Hocquet, D., Nonhoff, C., Byl, B., et al. (2005). Molecular characterization of an epidemic clone of panantibiotic-resistant *Pseudomonas aeruginosa*. *J. Clin. Microbiol.* 43, 1198–1204. doi: 10.1128/JCM.43.3.1198-1204.2005
- Diaz Caballero, J., Clark, S. T., Coburn, B., Zhang, Y., Wang, P. W., Donaldson, S. L., et al. (2015). Selective sweeps and parallel pathoadaptation drive *Pseudomonas aeruginosa* evolution in the cystic fibrosis lung. *mBio* 6, e00981-15. doi: 10.1128/mBio.00981-15
- Döring, G., Parameswaran, I. G., and Murphy, T. F. (2011). Differential adaptation of microbial pathogens to airways of patients with cystic fibrosis and chronic obstructive pulmonary disease. *FEMS Microbiol. Rev.* 35, 124–146. doi: 10.1111/j.1574-6976.2010.00237.x
- Dötsch, A., Becker, T., Pommerenke, C., Magnowska, Z., Jänsch, L., and Häussler, S. (2009). Genomewide identification of genetic determinants of antimicrobial drug resistance in *Pseudomonas aeruginosa*. *Antimicrob. Agents Chemother.* 53, 2522–2531. doi: 10.1128/AAC.00035-09
- Döselmann, B., Willmann, M., Steglich, M., Bunk, B., Nübel, U., Peter, S., et al. (2017). Rapid and consistent evolution of colistin resistance in extensively drug-resistant *Pseudomonas aeruginosa* during morbidostat culture. *Antimicrob. Agents Chemother.* 61, e00043-17. doi: 10.1128/AAC.00043-17
- El'Garch, F., Jeannot, K., Hocquet, D., Llanes-Barakat, C., and Plésiat, P. (2007). Cumulative effects of several nonenzymatic mechanisms on the resistance of *Pseudomonas aeruginosa* to aminoglycosides. *Antimicrob. Agents Chemother.* 51, 1016–1021. doi: 10.1128/AAC.00704-06
- Fajardo, A., Martínez-Martín, N., Mercadillo, M., Galán, J. C., Ghysels, B., Matthijs, S., et al. (2008). The neglected intrinsic resistome of bacterial pathogens. *PLoS One* 3:e1619. doi: 10.1371/journal.pone.0001619
- Feng, Y., Jonker, M. J., Moustakas, I., Brul, S., and Ter Kuile, B. H. (2016). Dynamics of mutations during development of resistance by *Pseudomonas aeruginosa* against five antibiotics. *Antimicrob. Agents Chemother.* 60, 4229–4236. doi: 10.1128/AAC.00434-16
- Fournier, D., Richardot, C., Müller, E., Robert-Nicoud, M., Llanes, C., Plésiat, P., et al. (2013). Complexity of resistance mechanisms to imipenem in intensive care unit strains of *Pseudomonas aeruginosa*. *J. Antimicrob. Chemother.* 68, 1772–1780. doi: 10.1093/jac/dkt098
- Fraille-Ribot, P. A., Cabot, G., Mulet, X., Periañez, L., Martín-Pena, M. L., Juan, C., et al. (2017a). Mechanisms leading to in vivo ceftolozane/tazobactam resistance development during the treatment of infections caused by MDR *Pseudomonas aeruginosa*. *J. Antimicrob. Chemother.* doi: 10.1093/jac/dkx424 [Epub ahead of print].
- Fraille-Ribot, P. A., Mulet, X., Cabot, G., Del Barrio-Tofiño, E., Juan, C., Pérez, J. L., et al. (2017b). In vivo emergence of resistance to novel cephalosporin- β -Lactamase inhibitor combinations through the duplication of amino acid D149 from OXA-2 β -Lactamase (OXA-539) in Sequence Type 235 *Pseudomonas aeruginosa*. *Antimicrob. Agents Chemother.* 61, e01117-17. doi: 10.1128/AAC.01117-17
- Greipel, L., Fischer, S., Klockgether, J., Dorda, M., Mielke, S., Wiehlmann, L., et al. (2016). Molecular epidemiology of mutations in antimicrobial resistance loci of *Pseudomonas aeruginosa* isolates from airways of Cystic Fibrosis patients. *Antimicrob. Agents Chemother.* 60, 6726–6734. doi: 10.1128/AAC.00724-16
- Guénard, S., Muller, C., Monlezun, L., Benas, P., Broutin, I., Jeannot, K., et al. (2014). Multiple mutations lead to MexXY-OprM-dependent aminoglycoside resistance in clinical strains of *Pseudomonas aeruginosa*. *Antimicrob. Agents Chemother.* 58, 221–228. doi: 10.1128/AAC.01252-13
- Gutu, A. D., Sgambati, N., Strasbourger, P., Brannon, M. K., Jacobs, M. A., Haugen, E., et al. (2013). Polymyxin resistance of *Pseudomonas aeruginosa* phoQ mutants is dependent on additional two-component regulatory systems. *Antimicrob. Agents Chemother.* 57, 2204–2215. doi: 10.1128/AAC.02353-12
- Haidar, G., Philips, N. J., Shields, R. K., Snyder, D., Cheng, S., Potoski, B. A., et al. (2017). Ceftolozane-Tazobactam for the treatment of multidrug-resistant *Pseudomonas aeruginosa* infections: clinical effectiveness and evolution of resistance. *Clin. Infect. Dis.* 65, 110–120. doi: 10.1093/cid/cix182

- Han, S., Zaniewski, R. P., Marr, E. S., Lacey, B. M., Tomaras, A. P., Evdokimov, A., et al. (2010). Structural basis for effectiveness of siderophore-conjugated monocarbams against clinically relevant strains of *Pseudomonas aeruginosa*. *Proc. Natl. Acad. Sci. U.S.A.* 107, 22002–22007. doi: 10.1073/pnas.1013092107
- Hocquet, D., Petitjean, M., Rohmer, L., Valot, B., Kulasekara, H. D., Bedel, E., et al. (2016). Pyomelanin-producing *Pseudomonas aeruginosa* selected during chronic infections have a large chromosomal deletion which confers resistance to pyocins. *Environ. Microbiol.* 18, 3482–3493. doi: 10.1111/1462-2920.13336
- Imamovic, L., Ellabaan, M. M. H., Dantas Machado, A. M., Citterio, L., Wulff, T., Molin, S., et al. (2017). Drug-driven phenotypic convergence supports rational treatment strategies of chronic infections. *Cell* 172, 121–134.e14. doi: 10.1016/j.cell.2017.12.012
- Jaillard, M., van Belkum, A., Cady, K. C., Creely, D., Shortridge, D., Blanc, B., et al. (2017). Correlation between phenotypic antibiotic susceptibility and the resistome in *Pseudomonas aeruginosa*. *Int. J. Antimicrob. Agents* 50, 210–218.
- Jatsenko, T., Tover, A., Tegova, R., and Kivisaar, M. (2010). Molecular characterization of Rif(r) mutations in *Pseudomonas aeruginosa* and *Pseudomonas putida*. *Mutat. Res.* 683, 106–114. doi: 10.1016/j.mrfmmm.2009.10.015
- Jeannot, K., Bolard, A., and Plésiat, P. (2017). Resistance to polymyxins in Gram-negative organisms. *Int. J. Antimicrob. Agents* 49, 526–535. doi: 10.1016/j.ijantimicag.2016.11.029
- Jorth, P., McLean, K., Ratjen, A., Secor, P. R., Bautista, G. E., Ravishanker, S., et al. (2017). Evolved aztreonam resistance is multifactorial and can produce hypervirulence in *Pseudomonas aeruginosa*. *mBio* 8, e00517–17. doi: 10.1128/mBio.00517-17
- Juan, C., Maciá, M. D., Gutiérrez, O., Vidal, C., Pérez, J. L., and Oliver, A. (2005). Molecular mechanisms of beta-lactam resistance mediated by AmpC hyperproduction in *Pseudomonas aeruginosa* clinical strains. *Antimicrob. Agents Chemother.* 49, 4733–4738. doi: 10.1128/AAC.49.11.4733-4738.2005
- Juan, C., Torrens, G., González-Nicolau, M., and Oliver, A. (2017). Diversity and regulation of intrinsic β -lactamases from non-fermenting and other Gram-negative opportunistic pathogens. *FEMS Microbiol. Rev.* 41, 781–815. doi: 10.1093/femsre/fux043
- Juarez, P., Broutin, I., Bordin, C., Plésiat, P., and Llanes, C. (2018). Constitutive activation of MexT by amino acid substitutions results in MexEF-OprN overproduction in clinical isolates of *Pseudomonas aeruginosa*. *Antimicrob. Agents Chemother.* doi: 10.1128/AAC.02445-17 [Epub ahead of print].
- Juarez, P., Jeannot, K., Plésiat, P., and Llanes, C. (2017). Toxic electrophiles induce expression of the multidrug efflux pump MexEF-OprN in *Pseudomonas aeruginosa* through a novel transcriptional regulator, CmrA. *Antimicrob. Agents Chemother.* 61, e00585–17. doi: 10.1128/AAC.00585-17
- Kos, V. N., Déraspe, M., McLaughlin, R. E., Whiteaker, J. D., Roy, P. H., Alm, R. A., et al. (2015). The resistome of *Pseudomonas aeruginosa* in relationship to phenotypic susceptibility. *Antimicrob. Agents Chemother.* 59, 427–436. doi: 10.1128/AAC.03954-14
- Lahiri, S. D., Johnstone, M., Ross, P. L., McLaughlin, R. E., Olivier, N. B., and Alm, R. A. (2014). Avibactam and class C β -lactamases: mechanism of inhibition, conservation of the binding pocket, and implications for resistance. *Antimicrob. Agents Chemother.* 58, 5704–5713. doi: 10.1128/AAC.03057-14
- Lau, C. H., Krahn, T., Gilmour, C., Mullen, E., and Poole, K. (2015). AmgRS-mediated envelope stress-inducible expression of the mexXY multidrug efflux operon of *Pseudomonas aeruginosa*. *Microbiol. Open* 4, 121–135. doi: 10.1002/mbo3.226
- Lee, J. Y., and Ko, K. S. (2014). Mutations and expression of PmrAB and PhoPQ related with colistin resistance in *Pseudomonas aeruginosa* clinical isolates. *Diagn. Microbiol. Infect. Dis.* 78, 271–276. doi: 10.1016/j.diagmicrobio.2013.11.027
- Li, X. Z., Plésiat, P., and Nikaido, H. (2015). The challenge of efflux-mediated antibiotic resistance in Gram-negative bacteria. *Clin. Microbiol. Rev.* 28, 337–418. doi: 10.1128/CMR.00117-14
- Lister, P. D., Wolter, D. J., and Hanson, N. D. (2009). Antibacterial-resistant *Pseudomonas aeruginosa*: clinical impact and complex regulation of chromosomally encoded resistance mechanisms. *Clin. Microbiol. Rev.* 22, 582–610. doi: 10.1128/CMR.00040-09
- López-Causapé, C., Rubio, R., Cabot, G., and Oliver, A. (2018). Evolution of the *Pseudomonas aeruginosa* aminoglycoside mutational resistome in vitro and in the cystic fibrosis setting. *Antimicrob. Agents Chemother.* doi: 10.1128/AAC.02583-17 [Epub ahead of print].
- López-Causapé, C., Sommer, L. M., Cabot, G., Rubio, R., Ocampo-Sosa, A. A., Johansen, H. K., et al. (2017). Evolution of the *Pseudomonas aeruginosa* mutational resistome in an international Cystic Fibrosis clone. *Sci. Rep.* 7:5555. doi: 10.1038/s41598-017-05621-5
- Maciá, M. D., Blanquer, D., Togores, B., Saulea, J., Pérez, J. L., and Oliver, A. (2005). Hypermutation is a key factor in development of multiple-antimicrobial resistance in *Pseudomonas aeruginosa* strains causing chronic lung infections. *Antimicrob. Agents Chemother.* 49, 3382–3386. doi: 10.1128/AAC.49.8.3382-3386.2005
- Markussen, T., Marvig, R. L., Gómez-Lozano, M., Aanæs, K., Burleigh, A. E., Høiby, N., et al. (2014). Environmental heterogeneity drives within-host diversification and evolution of *Pseudomonas aeruginosa*. *mBio* 5, e01592-14. doi: 10.1128/mBio.01592-14
- Michalopoulos, A. S., Livaditis, I. G., and Gougoutas, V. (2011). The revival of fosfomycin. *Int. J. Infect. Dis.* 15, e732–39. doi: 10.1016/j.ijid.2011.07.007
- Mistry, A., Warren, M. S., Cusick, J. K., Karkhoff-Schweizer, R. R., Lomovskaya, O., and Schweizer, H. P. (2013). High-level pacidamycin resistance in *Pseudomonas aeruginosa* is mediated by an opp oligopeptide permease encoded by the opp-fabI operon. *Antimicrob. Agents Chemother.* 57, 5565–5571. doi: 10.1128/AAC.01198-13
- Moskowitz, S. M., Brannon, M. K., Dasgupta, N., Pier, M., Sgambati, N., Miller, A. K., et al. (2012). PmrB mutations promote polymyxin resistance of *Pseudomonas aeruginosa* isolated from colistin-treated cystic fibrosis patients. *Antimicrob. Agents Chemother.* 56, 1019–1030. doi: 10.1128/AAC.05829-11
- Moya, B., Dötsch, A., Juan, C., Blázquez, J., Zamorano, L., Haussler, S., et al. (2009). Beta-lactam resistance response triggered by inactivation of a nonessential penicillin-binding protein. *PLoS Pathog.* 5:e1000353. doi: 10.1371/journal.ppat.1000353
- Mulet, X., Moyá, B., Juan, C., Maciá, M. D., Pérez, J. L., Blázquez, J., et al. (2011). Antagonistic interactions of *Pseudomonas aeruginosa* antibiotic resistance mechanisms in planktonic but not biofilm growth. *Antimicrob. Agents Chemother.* 55, 4560–4568. doi: 10.1128/AAC.00519-11
- Muller, C., Plésiat, P., and Jeannot, K. (2011). A two-component regulatory system interconnects resistance to polymyxins, aminoglycosides, fluoroquinolones, and β -lactams in *Pseudomonas aeruginosa*. *Antimicrob. Agents Chemother.* 55, 1211–1221. doi: 10.1128/AAC.01252-10
- Mustafa, M. H., Khandekar, S., Tunney, M. M., Elborn, J. S., Kahl, B. C., Denis, O., et al. (2017). Acquired resistance to macrolides in *Pseudomonas aeruginosa* from cystic fibrosis patients. *Eur. Respir. J.* 49:1601847. doi: 10.1183/13993003.01847-2016
- Olaitan, A. O., Morand, S., and Rolain, J. M. (2014). Mechanisms of polymyxin resistance: acquired and intrinsic resistance in bacteria. *Front. Microbiol.* 5:643. doi: 10.3389/fmicb.2014.00643
- Oliver, A., Cantón, R., Campo, P., Baquero, F., and Blázquez, J. (2000). High frequency of hypermutable *Pseudomonas aeruginosa* in cystic fibrosis lung infection. *Science* 288, 1251–1254. doi: 10.1126/science.288.5469.1251
- Oliver, A., Mulet, X., López-Causapé, C., and Juan, C. (2015). The increasing threat of *Pseudomonas aeruginosa* high-risk clones. *Drug Resist. Updat.* 2, 41–59. doi: 10.1016/j.drup.2015.08.002
- Pál, C., Papp, B., and Lázár, V. (2015). Collateral sensitivity of antibiotic-resistant microbes. *Trends Microbiol.* 23, 401–407. doi: 10.1016/j.tim.2015.02.009
- Prickett, M. H., Hauser, A. R., McColley, S. A., Cullina, J., Potter, E., Powers, C., et al. (2017). Aminoglycoside resistance of *Pseudomonas aeruginosa* in cystic fibrosis results from convergent evolution in the *mexZ* gene. *Thorax* 72, 40–47. doi: 10.1136/thoraxjnl-2015-208027
- Richardot, C., Plésiat, P., Fournier, D., Monlezun, L., Broutin, I., and Llanes, C. (2015). Carbapenem resistance in cystic fibrosis strains of *Pseudomonas aeruginosa* as a result of amino acid substitutions in porin OprD. *Int. J. Antimicrob. Agents* 45, 529–532. doi: 10.1016/j.ijantimicag.2014.12.029
- Rodríguez-Rojas, A., Maciá, M. D., Couce, A., Gómez, C., Castañeda-García, A., Oliver, A., et al. (2010). Assessing the emergence of resistance: the absence of biological cost in vivo may compromise fosfomycin treatments for *P. aeruginosa* infections. *PLoS One* 5:e10193. doi: 10.1371/journal.pone.0010193
- Schurek, K. N., Marr, A. K., Taylor, P. K., Wiegand, I., Semenec, L., Khaira, B. K., et al. (2008). Novel genetic determinants of low-level aminoglycoside resistance

- in *Pseudomonas aeruginosa*. *Antimicrob. Agents Chemother.* 52, 4213–4219. doi: 10.1128/AAC.00507-08
- Skiada, A., Markogiannakis, A., Plachouras, D., and Daikos, G. L. (2011). Adaptive resistance to cationic compounds in *Pseudomonas aeruginosa*. *Int. J. Antimicrob. Agents* 37, 187–193. doi: 10.1016/j.ijantimicag.2010.11.019
- Suarez, C., Peña, C., Arch, O., Dominguez, M. A., Tubau, F., Juan, C., et al. (2011). A large sustained endemic outbreak of multiresistant *Pseudomonas aeruginosa*: a new epidemiological scenario for nosocomial acquisition. *BMC Infect. Dis.* 11:272. doi: 10.1186/1471-2334-11-272
- Vestergaard, M., Paulander, W., Marvig, R. L., Clasen, J., Jochumsen, N., Molin, S., et al. (2016). Antibiotic combination therapy can select for broad-spectrum multidrug resistance in *Pseudomonas aeruginosa*. *Int. J. Antimicrob. Agents* 47, 48–55. doi: 10.1016/j.ijantimicag.2015.09.014
- Vincent, J. L. (2003). Nosocomial infections in adult intensive-care units. *Lancet* 361, 2068–2077. doi: 10.1016/S0140-6736(03)13644-6
- Woodford, N., Turton, J. F., and Livermore, D. M. (2011). Multiresistant Gram-negative bacteria: the role of high-risk clones in the dissemination of antibiotic resistance. *FEMS Microbiol. Rev.* 35, 736–755. doi: 10.1111/j.1574-6976.2011.00268.x
- Yen, P., and Papin, J. A. (2017). History of antibiotic adaptation influences microbial evolutionary dynamics during subsequent treatment. *PLoS Biol.* 15:e2001586. doi: 10.1371/journal.pbio.2001586

Conflict of Interest Statement: The authors declare that the research was conducted in the absence of any commercial or financial relationships that could be construed as a potential conflict of interest.

Copyright © 2018 López-Causapé, Cabot, del Barrio-Tofiño and Oliver. This is an open-access article distributed under the terms of the Creative Commons Attribution License (CC BY). The use, distribution or reproduction in other forums is permitted, provided the original author(s) and the copyright owner are credited and that the original publication in this journal is cited, in accordance with accepted academic practice. No use, distribution or reproduction is permitted which does not comply with these terms.



Genome Sequencing and Comparative Analysis of *Stenotrophomonas acidaminiphila* Reveal Evolutionary Insights Into Sulfamethoxazole Resistance

Yao-Ting Huang¹, Jia-Min Chen¹, Bing-Ching Ho², Zong-Yen Wu^{3,4}, Rita C. Kuo³ and Po-Yu Liu^{5,6,7*}

¹ Department of Computer Science and Information Engineering, National Chung Cheng University, Chiayi, Taiwan,

² Department of Clinical Laboratory Sciences and Medical Biotechnology, National Taiwan University Hospital, Taipei, Taiwan,

³ DOE Joint Genome Institute, Walnut Creek, CA, United States, ⁴ Department of Veterinary Medicine, National Chung Hsing University, Taichung, Taiwan, ⁵ The Department of Nursing, Shu-Zen Junior College of Medicine and Management, Kaohsiung, Taiwan, ⁶ Rong Hsing Research Center for Translational Medicine, College of Life Sciences, National Chung Hsing University, Taichung, Taiwan, ⁷ Division of Infectious Diseases, Department of Internal Medicine, Taichung Veterans General Hospital, Taichung, Taiwan

OPEN ACCESS

Edited by:

Silvia Buroni,
University of Pavia, Italy

Reviewed by:

Prabhu B. Patil,
Institute of Microbial Technology
(CSIR), India
Haitham Sghaier,
Centre National des Sciences et
Technologies Nucléaires, Tunisia

*Correspondence:

Po-Yu Liu
pyliu@vghtc.gov.tw;
liupoyu@gmail.com

Specialty section:

This article was submitted to
Evolutionary and Genomic
Microbiology,
a section of the journal
Frontiers in Microbiology

Received: 28 February 2018

Accepted: 30 April 2018

Published: 17 May 2018

Citation:

Huang Y-T, Chen J-M, Ho B-C,
Wu Z-Y, Kuo RC and Liu P-Y (2018)
Genome Sequencing
and Comparative Analysis
of *Stenotrophomonas acidaminiphila*
Reveal Evolutionary Insights Into
Sulfamethoxazole Resistance.
Front. Microbiol. 9:1013.
doi: 10.3389/fmicb.2018.01013

Stenotrophomonas acidaminiphila is an aerobic, glucose non-fermentative, Gram-negative bacterium that been isolated from various environmental sources, particularly aquatic ecosystems. Although resistance to multiple antimicrobial agents has been reported in *S. acidaminiphila*, the mechanisms are largely unknown. Here, for the first time, we report the complete genome and antimicrobial resistome analysis of a clinical isolate *S. acidaminiphila* SUNE0 which is resistant to sulfamethoxazole. Comparative analysis among closely related strains identified common and strain-specific genes. In particular, comparison with a sulfamethoxazole-sensitive strain identified a mutation within the sulfonamide-binding site of *folP* in SUNE0, which may reduce the binding affinity of sulfamethoxazole. Selection pressure analysis indicated *folP* in SUNE0 is under purifying selection, which may be owing to long-term administration of sulfonamide against *Stenotrophomonas*.

Keywords: genome sequencing, *Stenotrophomonas acidaminiphila*, sulfamethoxazole resistance, *Stenotrophomonas*, comparative genomics, dihydropteroate synthase

INTRODUCTION

Bacteria within the genus *Stenotrophomonas* species are aerobic, glucose non-fermentative, Gram-negative bacilli which inhabit diverse marine and terrestrial environments. The genus *Stenotrophomonas* currently comprises of 14 species¹. *Stenotrophomonas acidaminiphila* was identified in 2002 (Assih et al., 2002). Initially isolated from sewage sludge from wastewater treatment, it isolated mostly from aquatic environments. Reports of *S. acidaminiphila* human isolates are limited. To our best knowledge, no case of *S. acidaminiphila* infections has ever been reported to date. However, studies of environmental isolates revealed highly resistant to multiple antibiotics (Assih et al., 2002; Vinuesa and Ochoa-Sanchez, 2015).

¹ <http://www.bacterio.net/stenotrophomonas.html>

TABLE 1 | Overview of the *S. acidaminiphila* strains in this study.

Strain	Site of isolation	Country of origin	Reference
SUNEO	Human bile	Taiwan	This study
ZAC14D2_NAIMI4_2	Superficial sediments of polluted river	Mexico	Vinuesa and Ochoa-Sanchez, 2015
JCM 13310	Sludge from anaerobic chemical waste water reactor	Mexico	Assih et al., 2002

The antimicrobial options for *Stenotrophomonas* infections are limited because of its inherent resistance to most antibiotics, where trimethoprim-sulfamethoxazole (trimethoprim and sulfonamide combination in a 1:5 ratio) has long been regarded as the agent of choice (Sanchez, 2015). The main component, sulfamethoxazole interrupts the biosynthesis of tetrahydrofolic acid in both bacteria and primitive eukaryotes by targeting the dihydropteroate synthase (DHPS) catalyses, which catalyzes the condensation of 6-hydroxymethyl-7,8-dihydropterin monophosphate (DHPP) with p-aminobenzoic acid (PABA) (Skold, 2000). However, the resistance to sulfamethoxazole is increasing and is mainly caused by single amino acid mutations in the chromosomal gene encoding DHPS or by the acquisition of *sul* genes encoding alternative drug-resistance variants

of the DHP via mobile genetic elements (Toleman et al., 2007). To date, only two environmental strains of *S. acidaminiphila* genomes have been sequenced, all of which were isolated from river sediments (Assih et al., 2002; Vinuesa and Ochoa-Sanchez, 2015). However, the genome, pathogenome, and antimicrobial resistome of clinical isolate can still differ a lot in comparison with those of environmental strains, owing to the adaptation to host immune system and antibiotic pressure. Therefore, a complete genome from clinical isolates is valuable for designing effective treatment strategies. Here, we sequenced the genome of the *S. acidaminiphila* strain SUNEO, a first clinical isolate that possessed trimethoprim-sulfamethoxazole resistance. We propose a scenario for the origin and evolution of *S. acidaminiphila* SUNEO, based on its genomic features. Gene annotation and comparative analysis further revealed a unique profile of *folP* mutation that could play a role in drug resistance.

MATERIALS AND METHODS

Bacterial Strain Isolation, Identification, and Antimicrobial Susceptibility Testing

Strain SUNEO was isolated from the bile of a cholangiocarcinoma patient with obstructive jaundice and cholangitis. The bile

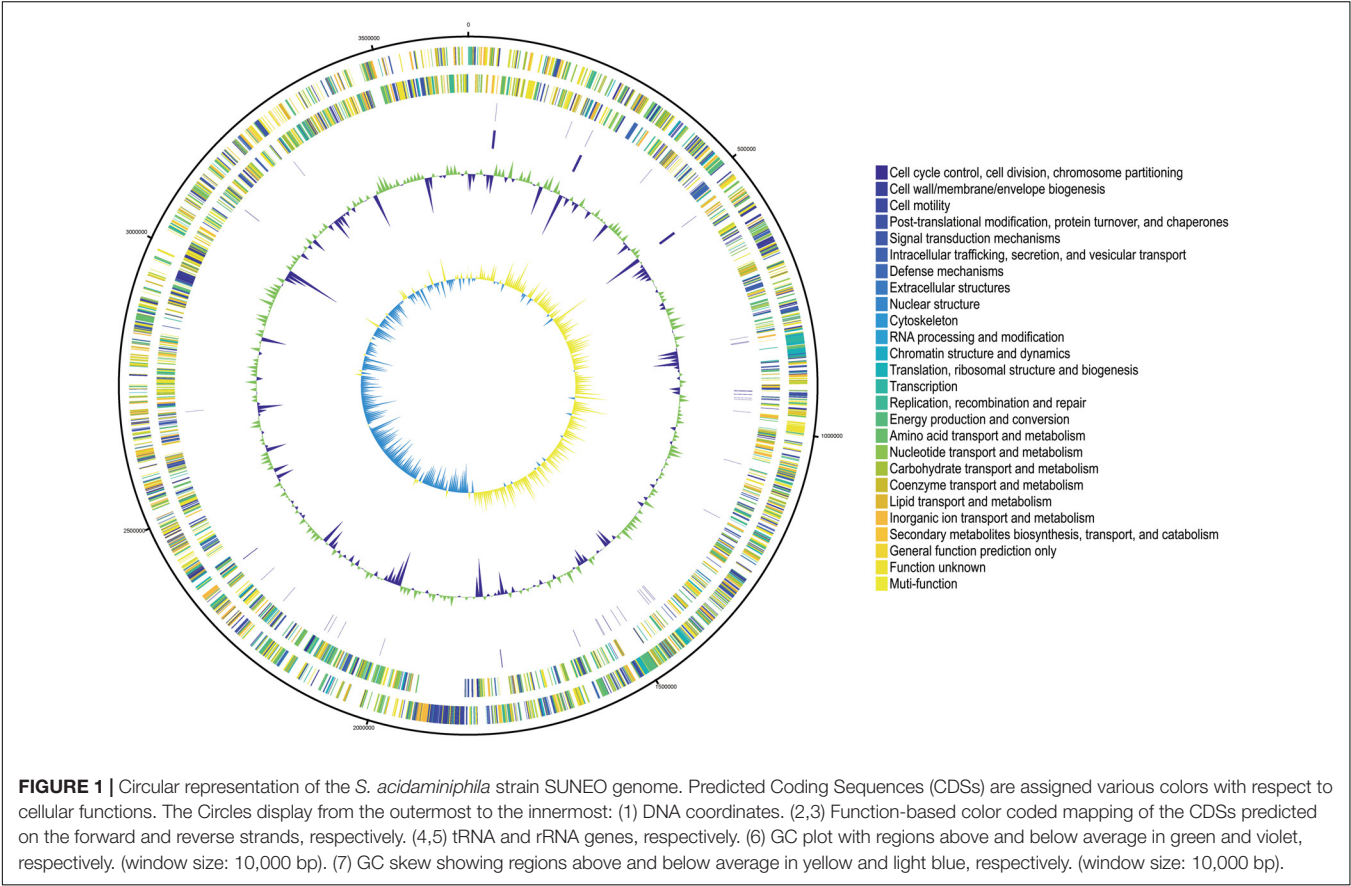


TABLE 2 | Genomic features of *S. acidaminiphila* strain SUNE0, ZAC14D2_NAIMI4_2, and JCM 13310.

Strain	Genome assembly status	Genome size (bp)	GC content (%)	Total Genes*1	Total CDS*2	Pseudo genes	Total proteins	rRNA	tRNA	Modify date
SUNE0	Complete	3,660,864	69.8	3,247	3,173	292	2,881	9	61	16 February, 2017
ZAC14D2_NAIMI4_2	Complete	4,138,297	68.5	3,709	3,635	65	3,570	9	61	11 April, 2017
JCM 13310	Draft	3,942,520	68.8	3,636	3,573	131	3,442	3	56	11 April, 2017

*1 Total genes = Total CDS + rRNA + tRNA + ncRNA. *2 Total CDS = Total Proteins + Pseudo genes.

sample was inoculated on trypticase soy agar with 5% sheep blood (Becton–Dickinson, Franklin Lakes, NJ, United States) and incubated aerobically at 37°C overnight. The isolate was identified through 16S rRNA gene sequencing as previously described (Assih et al., 2002; Mangwani et al., 2014). Antibiotic susceptibility tests for the strain SUNE0 was performed by the automated Vitek 2 system (bioMérieux, Inc., Durham, NC, United States) according to the manufacturer’s instructions.

Library Preparation and Whole-Genome Sequencing

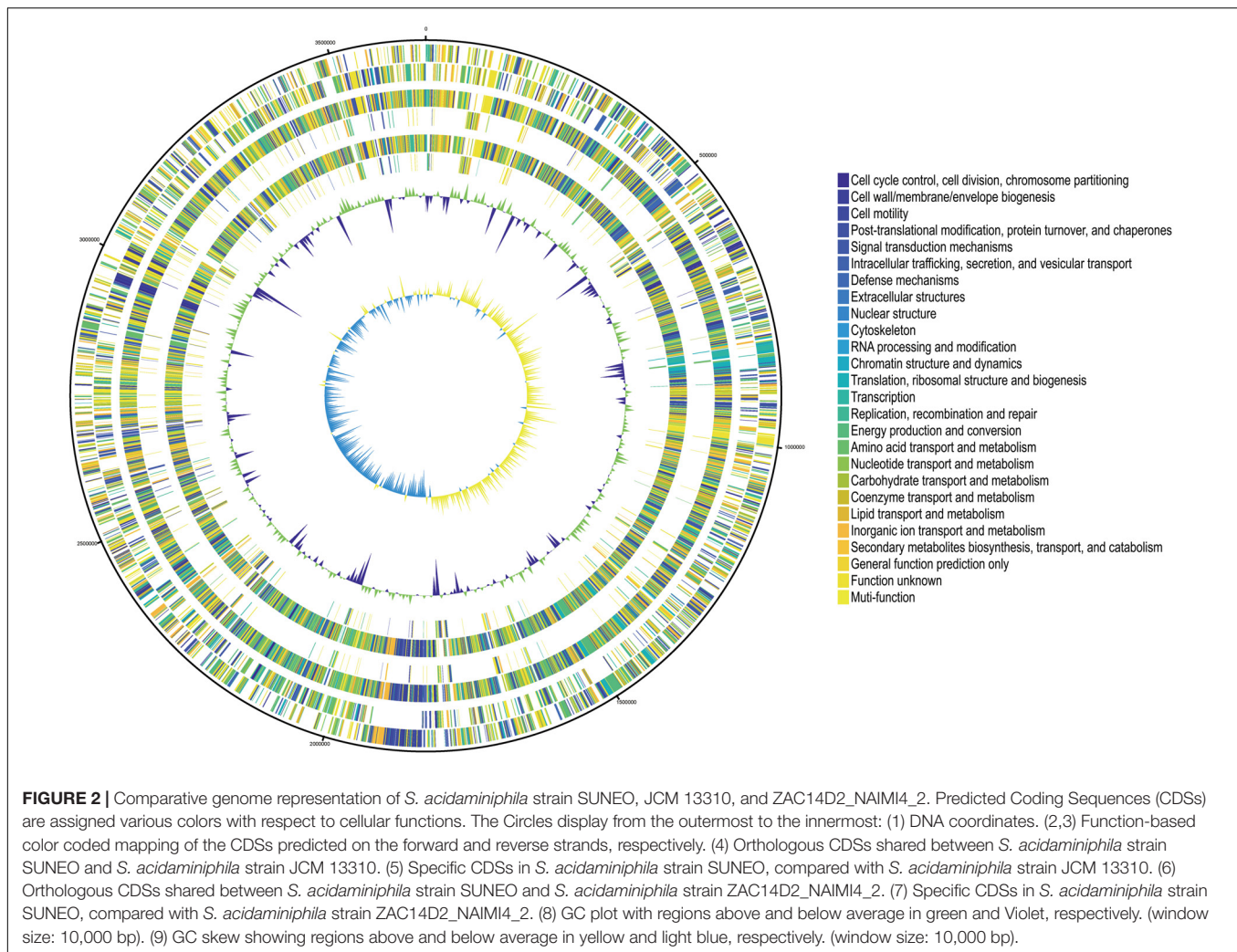
Overnight cultures were grown in Luria-Bertani broth overnight at 37°C. Genomic DNA was extracted using DNeasy blood and tissue kit (Qiagen, Valencia, CA, United States) as per the manufacturer’s instructions. High-molecular-weight gDNA was sheared to 10-kb lengths using g-TUBES (Covaris, Woburn, MA, United States). Sheared DNA was processed into PacBio sequencing library. DNA damage repair, end repair, and ligation of SMRT adapters were performed using PacBio SMRTbell Template Prep Kit (Pacific Biosciences). Whole genome sequencing was performed using PacBio sequencing platform (Pacific Biosciences, Menlo Park, CA, United States). Sequence runs of three single-molecule real-time (SMRT) cells were performed on the PacBio RS II sequencer with a 120-min movie time/SMRT cell. SMRT Analysis portal version 2.1 was used for read filtering and adapter trimming, with default parameters, and post-filtered data of 1.479 Gb (~404X coverage) with an average read length of ~6.2 kb was used for subsequent assembly (Supplementary Table 1).

Genome Assembly and Gene Annotation

The post-filtered genome reads were *de novo* assembled by Canu (v1.4) (Koren et al., 2017), which produced one single large contig (~3.6 Mb). Circlator was used to circularize this contig into a complete circular genome (Hunt et al., 2015). Protein-coding and non-coding genes in the SUNE0 genome were annotated using National Center for Biotechnology Information (NCBI) Prokaryotic Genomes Automatic Annotation Pipeline (PGAAP). Functional classification of these annotated genes was carried out by RPSBLAST version 2.2.15 in conjunction with Clusters of Orthologous Groups (COGs) of proteins databases (*E*-values < 0.001).

Comparative Genomics Analysis and Classification of Pan-Genomic Core Genes and Strain-Specific Genes

To study the comparative genomics of *S. acidaminiphila*, three whole genome sequences of *S. acidaminiphila* strains; *S. acidaminiphila* SUNE0, JCM 13310 (Assih et al., 2002), and ZAC14D2_NAIMI4_2 (Vinuesa and Ochoa-Sanchez, 2015) were downloaded from the NCBI database (Table 1). The protein sequences of all three strains were BLAST-aligned against each other (*E*-value < 0.001). However, BLAST may identify false homologs due to repeat sequences commonly shared by multiple genes. Thus, a gene is considered to be shared by both strains if the alignment coverage of both genes is at least 60%. The cutoff



was determined by the statistics of alignment coverage of all gene-pairs. We observed that 60% act as a good cutoff for balancing sensitivity and specificity. We consider each gene to be strain-specific if it is presented in only one strain and lost in all other strains. On the other hand, the genes shared by all strains are considered to be pan-genomic core genes.

16S rRNA Phylogenetic Analysis

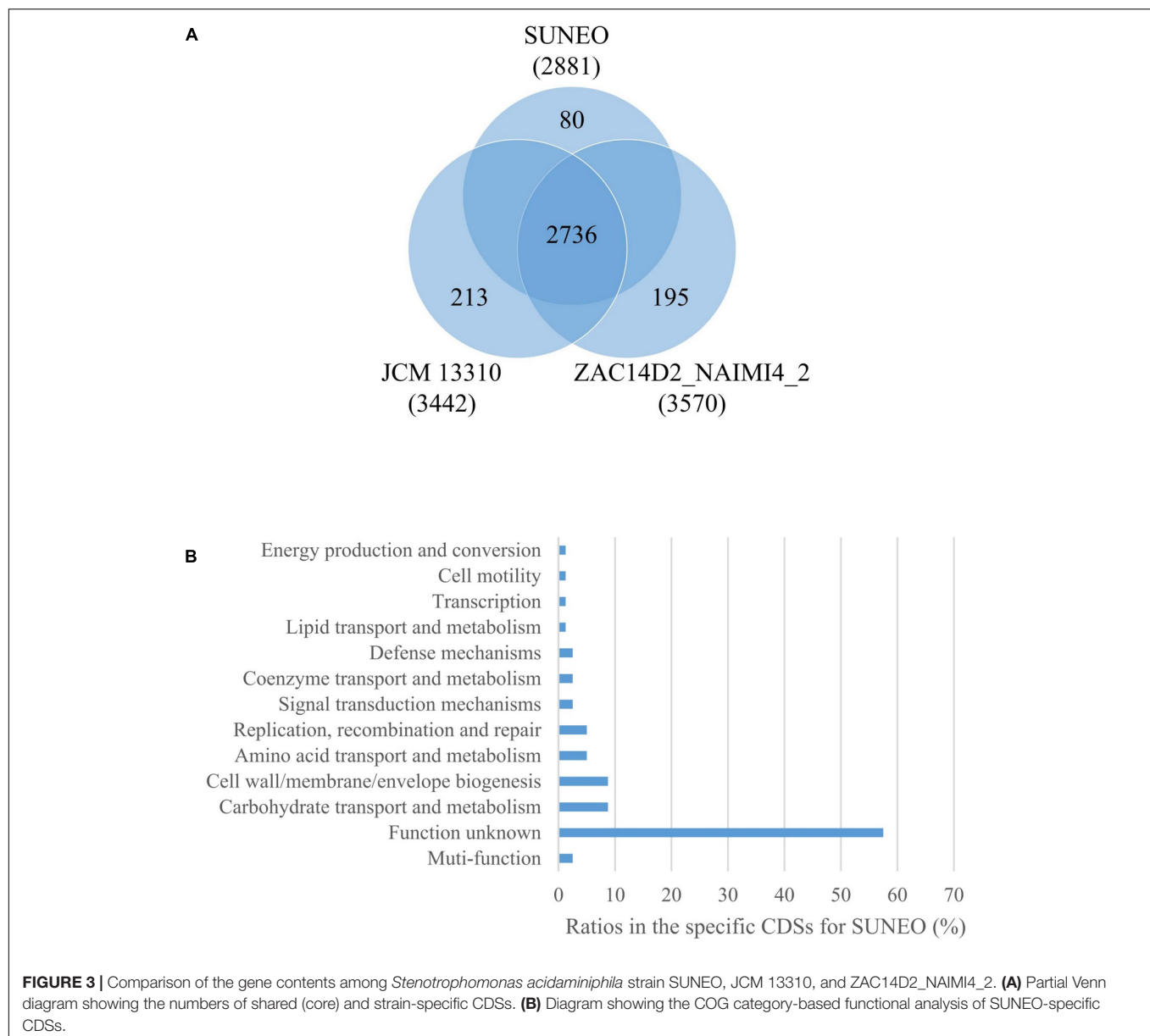
The publicly available 16S rRNA sequences of type strains of *Stenotrophomonas* spp. (including the *S. acidaminiphila* strain SUNE0) were retrieved from the National Center for Biotechnology Information (NCBI) nucleotide database (Supplementary Table 2) (Pruitt et al., 2007; Alavi et al., 2014; Davenport et al., 2014; Patil et al., 2016). In particular, two *S. acidaminiphila* strains (i.e., JCM 13310 and ZAC14D2 NAIMI4) were included in order to confirm the phylogenetic status of SUNE0. At first, multiple sequence alignment of the 16S rRNA gene sequences of all strains was first performed by MEGA (v7). Specifically, ClustalW was used for multiple sequence alignment. Evolution history was reconstructed using the built-in maximum-likelihood method with 1,000 bootstraps.

Multi-Locus Sequence Typing Using Multiple Housekeeping Genes

To further validate these clade assignments, multilocus sequence analysis (MLSA) was performed by concatenation of housekeeping genes: *atpD*, *guaA*, *mutM*, *nuoD*, *ppsA*, and *recA* (Kaiser et al., 2009). Multiple sequence alignment of these housekeeping genes in 15 *Stenotrophomonas* genomes was performed using MEGA in order to infer their phylogeny (Alavi et al., 2014; Davenport et al., 2014; Patil et al., 2016; Sanchez-Castro et al., 2017). Two conventional *gyrB* and *gapA* were not included because *gyrB* is completely absent in *S. acidaminiphila* JCM 13310 and only very short piece of *gapA* is found in *S. ginsengisoli* DSM 24757. Additional MLSA using the six housekeeping genes plus 16S rRNA is also performed using MEGA (v7) to confirm the phylogenetic position of SUNE0.

Whole-Genome Average Nucleotide Identity Analysis

To measure the nucleotide-level genomic similarity between SUNE0 and related *Stenotrophomonas* genomes



(Alavi et al., 2014; Davenport et al., 2014; Patil et al., 2016), the Average Nucleotide Identity (ANI) (Konstantinidis and Tiedje, 2005) was calculated by the USEARCH program (Yoon et al., 2017) based on modified OrthoANI algorithm (Lee et al., 2016). A radial phylogram was constructed using distance matrix computations using the Integrated Microbial Genomes pipeline (Chen et al., 2017).

Annotation of Antibiotic-Resistance Genes

The SUNE0 resistome is annotated by using both the Resistance Gene Identifier from the Comprehensive Antibiotic Resistance Database (McArthur et al., 2013) and the IMG database (Markowitz et al., 2012). RGI prediction of resistome is based on homology and SNP models, where the strict criteria were

chosen for prediction. In homolog models, BLAST is used to detect functional homologs of antimicrobial resistance genes. In contrast, SNP models identify candidate genes which acquire mutations conferring antimicrobial resistance genes based on curated SNP matrices. The SUNE0 resistome is predicted through alignment against the IMG database using BLASTN with a 95% sequence identity threshold.

Sequence, Structural, and Selection Analysis of *folP* Gene

The phylogeny of the DHPS protein was constructed by MEGA7. The publicly available *folP* homolog gene sequences of 18 *Stenotrophomonas* strains (including *S. acidaminiphila* strain SUNE0) were retrieved from the National Center for Biotechnology Information (NCBI) nucleotide database

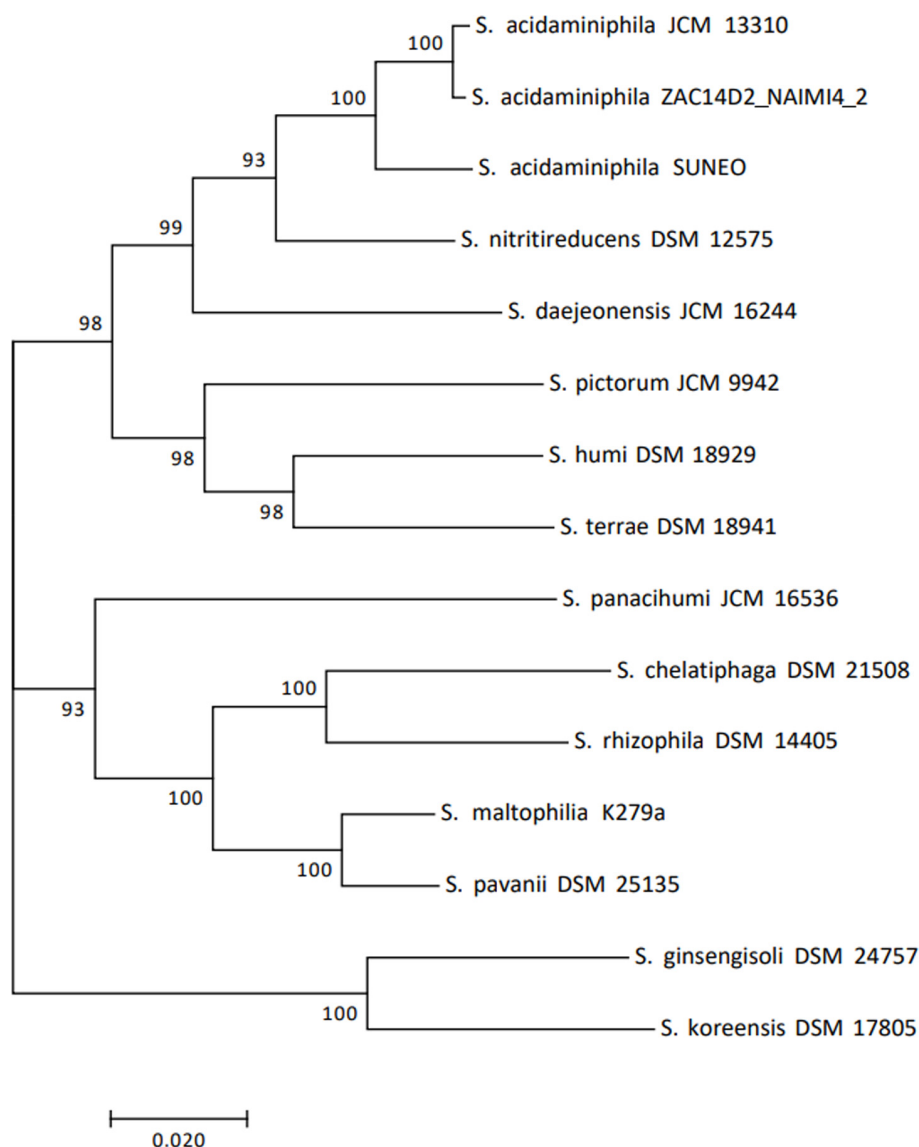


FIGURE 4 | Phylogenetic tree of *S. acidaminiphila* SUNE0 and related type strains of *Stenotrophomonas* species based on the phylogenetic analysis of seven housekeeping genes (16S rRNA, *atpD*, *guaA*, *mutM*, *nuoD*, *ppsA*, and *recA*).

(Supplementary Table 3). The amino acid sequences of DHPS from SUNE0 and JCM 13310 were BLAST-aligned against each other in order to identify the mutation loci and annotate the conservative loop regions. To probe its topological structure, the 3D structure of DHPS proteins were predicted by Robetta², and subsequently visualized by NOC 3.01³. In conjunction with the annotated loop regions in the sequence level, we were able to compare the local substructure of Loop2 between the two strains. The ratio of non-synonymous to synonymous substitutions (i.e., Ka/Ks) is used to estimate positive and purifying selection at each amino-acid site in *folP* for SUNE0, JCM 13310, and

ZAC14D2_NAIMI4_2. The M8 site model (with ω allowed to > 1) with intermediate precision level ($\epsilon = 0.1$, which defines when two likelihood values converged) is used to compute the Ka/Ks ratio⁴.

RESULTS

Genome Overview and Annotation

The total size of the genome is 3,660,864 bp with a G+C content of 69.8%. An illustration of the genomic contents in the genome of SUNE0 is shown in **Figure 1**. A total of 3,173 Coding Sequences (CDSs) were predicted (**Table 2**). In

²<http://robetta.bakerlab.org/>

³<http://noch.sourceforge.net>

⁴<http://selecton.tau.ac.il>

TABLE 3 | Antimicrobial susceptibility profiles of *S. acidaminiphila* SUNE0 and JCM 13310.

Class	Subclass	Antibiotics	SUNE0*	JCM 13310*
Aminoglycoside antibiotic	–	Amikacin	16, S	≤ 8, S
		Gentamicin	2, S	≤ 4, S
		Netilmicin		≤ 4, S
		Tobramycin		≤ 4, S
Fluoroquinolone antibiotic	–	Ciprofloxacin	≤ 0.25, S	≤ 1, S
		Ofloxacin		≤ 1, S
Lipopeptide antibiotic	Polymyxin antibiotic	Colistin		≤ 2, S
Diaminopyrimidine antibiotic	–	Trimethoprim Sulfamethoxazole	80(4/76), R	≤ 2/38, S
Sulfonamide antibiotic				
β-lactam antibiotic	Carbapenem	Imipenem	≥ 16, R	> 8, R
		Cefalotin		> 32, R
	Cephem	Cefepime	≤ 1, S	
		Cefotaxime		> 32, R
		Ceftriaxone	16, I	
		Ceftazidime	≤ 1, S	≤ 4, S
		Amoxicillin		> 16, R
		Piperacillin		≤ 16, S
	Penam	Ticarcillin		≥ 16–64, I
		Amoxicillin Clavulanic acid		> 16, R
β-lactam combination agents	Penam β-lactamase inhibitor	Ampicillin Sulbactam	≤ 2, S	
		Piperacillin Tazobactam	≤ 4, S	≤ 16, S
Tetracycline derivative	Glycylcycline	Tigecycline	≤ 0.5, S	

*R, resistant; S, susceptible; I, intermediate.

addition, 70 RNAs including rRNA and tRNA were identified. No extrachromosomal elements were found in SUNE0.

Comparative Genomic Study and Identification of Core and Strain-Specific Genes of *S. acidaminiphila* Genomes

General genomic features of *S. acidaminiphila* SUNE0 were compared to the *S. acidaminiphila* JCM 13310 and ZAC14D2_NAIMI4_2 (Table 2). The genome size of the *S. acidaminiphila* strain ZAC14D2_NAIMI4_2 was the largest (4,138,297 bp) amongst all genomes (ranging from 3,660,864 to 3,942,520 bp). The highest genomic G+C content (69.8%) was from the *S. acidaminiphila* strain SUNE0 followed by the *S. acidaminiphila* strain JCM 13310 (68.8%), and the *S. acidaminiphila* strain ZAC14D2_NAIMI4_2 (68.5%).

The protein-coding genes of SUNE0 were compared with those of *S. acidaminiphila* JCM 13310 and ZAC14D2_NAIMI4_2, in order to identify orthologous core genes which are shared across all strains and strain-specific genes. Figure 2 depicts both the positions and the color-coded functions of *S. acidaminiphila* SUNE0 genes in comparison with all other strains, whereas the number of orthologous and strain-specific genes is shown in Figure 3. In summary, the core genome of *S. acidaminiphila* consisted of 2,736 core genes shared across all strains, whereas 807 genes are specific only to *S. acidaminiphila* SUNE0 (Figure 3A). Functional analysis of SUNE0-specific genes revealed that, in addition to hypothetical proteins, a relative abundance of the gene is involved in carbohydrate transport, along

with metabolism and cell wall/membrane/envelop biogenesis (Figure 3B). DHPS encoding *folP* homologs genes are presented in all strains.

Phylogenetic Analysis of *S. acidaminiphila*

A maximum-likelihood tree of the three *S. acidaminiphila* genomes and 12 reported *Stenotrophomonas* strains (comprising of *S. daejeonensis*, *S. humi*, *S. pictorum*, *S. terrae*, *S. nitritireducens*, *S. ginsengisoli*, *S. koreensis*, *S. maltophilia*, *S. pavanii*, *S. chelatiphaga*, *S. panacihumi*, and *S. rhizophila*) was created based on 16S rRNA gene sequences (Supplementary Figure 1). This phylogenetic tree shows *S. acidaminiphila* SUNE0, JCM 13310, and ZAC14D2_NAIMI4_2 grouped together. The result was further supported by Alignment Fraction analysis, which showed SUNE0 was included in the *S. acidaminiphila* JCM 13310 and ZAC14D2_NAIMI4_2 phylogenetic subgroup (Supplementary Figure 2).

The MLSA using conventional housekeeping genes (with or without 16S RNA) both revealed high phylogenetic similarities higher than 99% among SUNE0, JCM 13310, and ZAC14D2_NAIMI4_2 (Figure 4 and Supplementary Figure 3), which was the accepted species threshold (Kaiser et al., 2009). Genomic-wide relatedness comparison was calculated with the OrthoANI program using publicly available genomes from type strains of *Stenotrophomonas* species (Alavi et al., 2014; Davenport et al., 2014; Patil et al., 2016; Sanchez-Castro et al., 2017). As the ANI value of SUNE0 to *S. acidaminiphila* strain is 92.94–92.83% (Supplementary Table 4), indicated a taxonomic

TABLE 4 | Summary of the antibiotic resistance genes among the three strains of *S. acidaminiphila* and their related locus tag.

	SUNEO	ZAC14D2_NAIMI4_2	JCM 13310
β-lactam resistance gene			
Class A β -lactamase L2	B1L07_04670	AOT14_RS05350	ABB33_RS08520
Class B metallo- β -lactamase L1	B1L07_11340	AOT14_RS12805	ABB33_RS04665
VEB β -lactamase			
VEB-5	B1L07_15655	AOT14_RS07520	ABB33_RS15710
Aminoglycoside resistance gene			
AAC(6')			
AAC(6')-Ic	B1L07_09660	AOT14_RS11055	ABB33_RS07955
Fluoroquinolone resistance gene			
Quinolone resistance gene			
QnrB27	B1L07_15000	AOT14_RS17045	ABB33_RS01740
Efflux pump			
RND efflux pump			
AcrAB-TolC RND system			
acrR	B1L07_02745	AOT14_RS03270	ABB33_RS01685
acrA	B1L07_02750	AOT14_RS03275	ABB33_RS01690
acrB	B1L07_02755	AOT14_RS03280	ABB33_RS01695
SmeDEF RND system			
smeD	B1L07_07555	AOT14_RS08230	ABB33_RS10360
smeE	B1L07_07560	AOT14_RS08235	ABB33_RS10365
smeF	B1L07_07570	AOT14_RS08245	ABB33_RS10375
SmeOP-TolC RND system			
smeO	B1L07_03315	AOT14_RS03840	ABB33_RS09950
smeP	B1L07_03320	AOT14_RS03845	ABB33_RS09945
MFS efflux pump			
NorA MFS system			
norA	B1L07_03630	ABB33_RS16160	AOT14_RS06550
arlR	B1L07_05940	ABB33_RS10760	AOT14_RS06670
arlS	B1L07_05945	ABB33_RS10755	AOT14_RS06675
mgrA	B1L07_12295	ABB33_RS03745	AOT14_RS13715
EmrAB-TolC MFS system			
emrA	B1L07_10580	AOT14_RS12025	ABB33_RS05915
emrB	B1L07_10575	AOT14_RS12020	ABB33_RS05920
tolC	B1L07_03300	AOT14_RS03825	ABB33_RS09965

outlier (Gomila et al., 2015). Together, all these analysis (from single gene, multiple genes, to entire genome) concordantly concluded that the phylogenetic position of SUNEO is indeed belonging to *S. acidaminiphila*.

Comparative Analysis of Antibiotic Resistance Genes in SUNEO

Antimicrobial susceptibility test showed that SUNEO is resistant to both imipenem and trimethoprim/sulfamethoxazole (Table 3). Comparative analysis was performed on the three *S. acidaminiphila* genomes, among which JCM 13310 is trimethoprim/sulfamethoxazole susceptible (Table 3). All three strains harbor similar resistance genes. There are Ambler class B β -lactamase L1 and Ambler class A β -lactamase L2 in all of the three strains. The resistance-nodulation-division (RND) family efflux pump, consisting of the *smeDEF* and *smeOP* genes, along with the efflux pumps genes that are homologous to efflux pumps encoded in *S. maltophilia* and

Escherichia coli were also identified in all of the tested strains (Table 4).

Phylogeny of *folP* Homologs in *Stenotrophomonas* Strains

Comparative genomic analysis has revealed the gene *folP* is commonly presented among *S. maltophilia* strains. *folP* encodes DHPS and is the target of sulfonamides, to which SUNEO is resistant. A BLASTP search in *Stenotrophomonas* strains with *folP* as the primer sequence returned a collection of related homologs with the annotation of DHPS (Baker and Sali, 2001). We retrieved 18 protein sequence candidates with available MIC data for each strain. The phylogeny of the DHPS protein constructed by MEGA7 (Kumar et al., 2016) clearly presented two distinct groups: one denotes a family of *folP* homologs from *S. maltophilia* whereas the other comprises a series of *folP* homologs from non-maltophilia *Stenotrophomonas* strains (Figure 5). Of particular note, *folP* homologs between

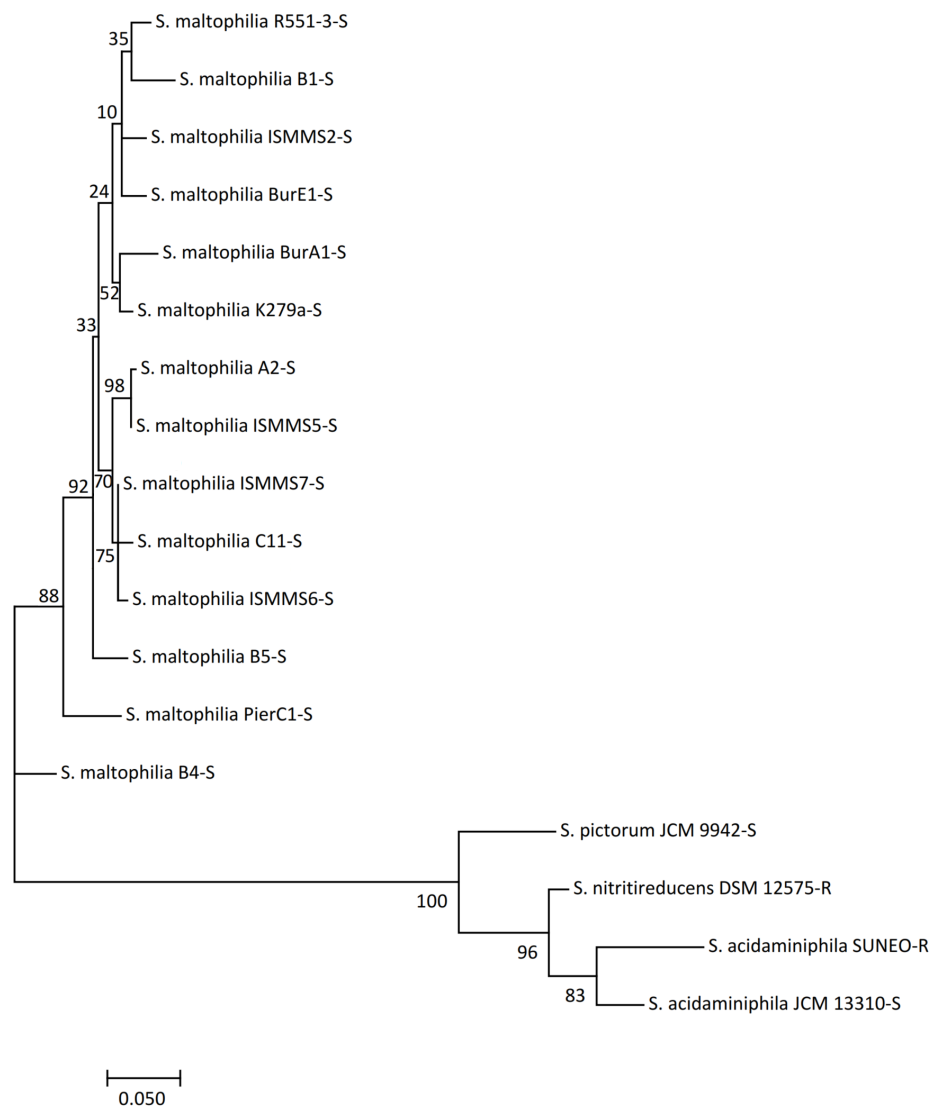


FIGURE 5 | Phylogenetic tree of the amino acid sequences of dihydropteroate synthase homologs from *Stenotrophomonas* strains. Evolutionary history was inferred by using the maximum likelihood method. The bootstrap consensus tree inferred from 1,000 replicates is taken to represent the evolutionary history of the taxa analyzed. R: resistant to TMP-SMX. S: susceptible to TMP-SMX.

SUNE0 and JCM 13310 are highly similar in comparison with other distant-related strains. This implies that the resistance of SUNE0 to sulfonamides is due to few/key mutations acquired occasionally instead of continual accumulation of resistant alleles after speciation.

Sulfonamide-Binding Site Mutation Revealed by Structural Analysis

In order to identify key mutation in *folP* leading to resistance of SUNE0, sequence composition of DHPS between JCM 13310 and SUNE0 was compared, which exhibited an amino acid change (Gly⁷² → Glu⁷²) in one highly conservative region (termed Loop2) (Figure 6). Structural modeling allows us to visualize the difference in DHPS architecture between these

two strains. This conservative region stabilizes the binding of PABA and variation at this region has been shown to contribute to resistance to sulfonamide (Yun et al., 2012). We further reconstruct their protein 3D structures to verify the difference of DHPS architecture between these two strains. The protein substructure at Loop2 in SUNE0 appears disordered in comparison with that of JCM 13310 (Figure 7), which may reduce the binding stability of sulfonamide and lead to resistance.

The selection pressure (Ka/Ks) was measured along the entire *folP* (Figure 8). The results indicated that strong signals of purifying selection (Ka/Ks < 0.08) are widely spread in *folP*. This implies evolution of *folP* in SUNE0 is probably constrained by high selection pressure from long-term exposure of sulfonamide.






				
SUNE0	MFDIAPVLDCAGRLLRLDRPRVMGIVNVT	PDPS	SDGGRHFSAEAAVAHALALVEQGADVL	60
JCM 13310	MFDTSPPVDCAGRPLRLDRPRVMGIVNVT	PDPS	SDGGRHFSTDAIAHALALVEQGADIL	60
	***	: ** :	*****	***** : ** : ***** *
				
SUNE0	DIGGESTRPGAEQVSAQQEIERVVPVIEALVARTPVPVSDTFKPDVMRAALAAGAGMVN			120
JCM 13310	DIGGESTRPGAGQVSAQQEIERVAPVIEALAARVPVPLSVDTFKEVPMRAAVAAGAGMVN			120
	*****	*****	: ***** *	***** *
				
SUNE0	DVQALRQPGALETVADAGAAVVLMAHVGGPYDAGVAWASDDVAGDVQRFLAERLFAAEMA			180
JCM 13310	DVQALRQPGALEVVAGSGAAVVLMAHVGGPHDAGVAWSDSDVAGDVQRFLAERLFAAEMA			180
	*****	: ** :	***** *	***** *
				
SUNE0	GIARNRLVDPGYGFNKDDTTQNFALLAAQEKLLALGVPLLAGLSRKRCIGDVTGRAVAEE			240
JCM 13310	GIARNRLVDPGYGFNKDTAQNFALLAAQEKLLALGVPLLAGLSRKRCIGEVTRTVVAE			240
	*****	: ***** *	***** *	***** *
				
SUNE0	RVAGSVA AHL LAVQRGARIVRVHDVAATVDALKVLAALDAVPAGRSERAQPPRPDED			298
JCM 13310	RVAGSVA AHL LAVQRGAGIVRVHDVAATVDALKVLAALDAVPAPRADRVAPRPDED			298
	*****	*****	* . *	*****

FIGURE 6 | Alignment result of the *folP*s in the *S. acidaminiphila* strain SUNE0 and JCM 13310. Residues marked with red dots are sites of common sulfa drug (sulfonamide) resistance mutations. The last line in the data means the consensus amino acid symbol of the residue in the corresponding position for all strains: an asterisk indicates positions which have a single, fully conserved residue; a colon indicates conservation between groups of strongly similar properties; a period indicates conservation between groups of weakly similar properties.

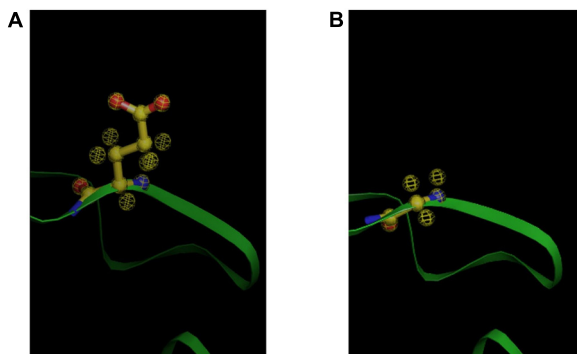


FIGURE 7 | Structure predication for the *folP* gene products (dihydropteroate synthase) of *S. acidaminiphila* SUNE0 and JCM 13310. **(A)** Glu72 in the SUNE0 dihydropteroate synthase. **(B)** Gly72 in the JCM 13310 dihydropteroate synthase.

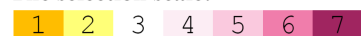
DISCUSSION

The data we present represents a first glimpse into the evolution and mechanism for sulfamethoxazole resistance in *S. acidaminiphila*. Our discovery of novel mutations in DHPS offers new insight into the newly emerging field of *Stenotrophomonas* infections, furthering our understanding of the diversity in the dissemination of sulfamethoxazole resistance. Sulfamethoxazole interrupt the essential folate pathway in bacteria by targeting the enzyme DHPS, which in turn catalyzes the condensation of DHPP with PABA in the production of

the folate intermediate. The locus of the mutation is consistent with earlier observations that many sulfamethoxazole resistance mutations are located within two conserved loops (called Loop1 and Loop2) of DHPS, which creates a specific binding pocket for PABA (Estrada et al., 2016).

To gain further structural insight of the DHPS homologs in SUNE0 and JCM 13319, structural modeling was performed, where the ribbon structures of their DHPS were generated. The 3D structural DHPS proteins in SUNE0 illustrated that the substructure at Loop2 is disordered. Further structural comparisons of DHPS also indicated that the resistant (SUNE0) and sensitive (JCM 13310) strains display a different substructure around the PABA-binding pockets. In agreement with the earlier proposal by Yun et al. (2012), sulfonamide resistance is associated with the Loop2 mutation and subsequent DHPS substructure disorder affected the binding of PABA. It was also reported that mutations in DHPS were associated with sulfamethoxazole resistance in both prokaryotes (Huovinen, 2001) and primitive eukaryotes (Triglia et al., 1997), where associated structural changes in Loop1–Loop2 PABA binding sites occurred (Capasso and Supuran, 2014). As sulfa drugs interrupt the folate pathway by competing with PABA as DHPS substrates, mutation at both the sequence and the structure of DHPS in SUNE0 could be attributed to its resistance to sulfamethoxazole.

The selection pressure measured along the DHPS-encoding gene *folP* reveals strong signals of purifying selection, implying the evolution of *folP* is constrained by high selection pressure. Sulfamethoxazole has been the first-line antibiotic agent against *Stenotrophomonas* for decades and is widely use in agriculture. The usage of specific antibiotic agent has been shown to result in

**Legend:****The selection scale:**

Positive selection Purifying selection

FIGURE 8 | Selection pressure (Ka/Ks) measured along *folP* among *S. acidaminiphila* strains. The strong signals of purifying selection are defined as the loci with Ka/Ks < 0.8. Overall, 72 loci of strong signals of purifying selection is wide-spread across the entire gene sequence.

purifying selection in certain genes of resistant strains (Mortimer et al., 2018), because purifying selection on a subset of genes can be intensified in the setting of resistance. After sufficiently long-term usage of the same antibiotic agent, resistance may even reach a point of stabilizing evolution, completely reducing or invalidating the efficiency of the drug (Cornick et al., 2014). As *folP* in *S. acidaminiphila* already exhibited purifying selection, the administration of sulfamethoxazole for *S. acidaminiphila* infections in the future should be taken with caution.

Stenotrophomonas acidaminiphila SUNE0 is also resistant to various antibiotics, suggesting multiple resistance mechanisms. Current understanding of the resistance determinants of *S. acidaminiphila* is limited. Vinuesa and Ochoa-Sanchez (2015) reported on predicted antibiotic resistant genes (without phenotypic resistance) in *S. acidaminiphila* ZAC14D2_NAIMI4_2 isolated from river sediment in Mexico, while Assih et al. (2002) reported on phenotypic resistance (without genotypic changes) in *S. acidaminiphila* JCM 13310. To address this concern, we conducted resistome analysis of *S. acidaminiphila* SUNE0 and predicted multiple efflux pumps, which have also been detected in *S. maltophilia* strains (Crossman et al., 2008). In particular, we identified the RND efflux pump genes *smeDEF*, which was associated with trimethoprim/sulfamethoxazole resistance (Sanchez and Martinez, 2015). The resistance of trimethoprim/sulfamethoxazole in SUNE0 could be a combination effect related to DHPS mutation and efflux pumps.

Stenotrophomonas acidaminiphila is able to degrade a number of organic pollutants, including Fomesafen [5-(2-

chloro-4-[trifluoromethyl]phenoxy)-N-methylsulfonyl-2-nitro-benzamide] (Huang et al., 2017), Diuron [3-(3,4-dichlorophenyl)-1,1-dimethylurea] (Egea et al., 2017), and azo dye crystal violet (Kim et al., 2002). Our comparative analysis of resistome in *S. acidaminiphila* revealed that the efflux pumps genes presented in all examined *S. acidaminiphila* strains. Efflux pumps play a major role in both solvent tolerance and bioremediation (Fernandes et al., 2003), which is consistent with recent observations of the biodegradation of sulfonamide (Liao et al., 2016) and aminoglycoside (Selvaraj et al., 2018) in *S. acidaminiphila*. The mechanistic insight we gained further raises the possibility of cross-resistance to both environmental toxic compounds and antibiotics which would have a major impact on the use of disinfectants and disinfecting procedures.

Currently, most of the reported *Stenotrophomonas* infections are caused by *S. maltophilia* which is frequently recovered from clinical samples and is an emerging opportunistic pathogen associated with substantial morbidity and mortality, particularly in immunocompromised patients (Falagas et al., 2009). Incidences of human infection appear to have increased recently, where a variety of clinical syndromes have been described, including pneumonia, bacteremia, and peritonitis (Denton and Kerr, 1998; Sattler et al., 2000). However, biliary tract infections remain uncommon. Our report outlines the first human biliary infection caused by *S. acidaminiphila*. The virulence factors of *S. acidaminiphila* are largely unknown. Our data has revealed RND pump homologs of the *acrAB* in SUNE0. *acrAB* encodes a bile-induced efflux system and is expressed in both animal models and infected patients

(Gunn, 2000; Piddock, 2006). Additional studies are required in order to clarify its role in *S. acidaminiphila* pathogenesis.

CONCLUSION

Our analysis reveals a possible core genome of *S. acidaminiphila*, along with accessory genomes specific to each strain, providing insights into the resistant potential of the clinical isolate. We propose a scenario for the origin and evolution of *S. acidaminiphila*, based on its genomic features. Gene annotation and comparative analysis further revealed a unique profile of *folP* mutation. The mechanism for sulfonamide resistance in *S. acidaminiphila* SUNE0 appears to involve the mutation of the Loop2 region of DHPS, thereby leading to alterations in the structural conformation of the site and the multi-drug efflux pumps.

DATA AVAILABILITY

This genome project, which includes the raw read data, assembly, and annotation, has been deposited at NCBI/GenBank as BioProject PRJNA374779. The assembly is available under accession CP019797; the version described in this paper is the first version.

REFERENCES

- Alavi, P., Starcher, M. R., Thallinger, G. G., Zachow, C., Muller, H., and Berg, G. (2014). *Stenotrophomonas* comparative genomics reveals genes and functions that differentiate beneficial and pathogenic bacteria. *BMC Genomics* 15:482. doi: 10.1186/1471-2164-15-482
- Assih, E. A., Ouattara, A. S., Thierry, S., Cayol, J. L., Labat, M., and Macarie, H. (2002). *Stenotrophomonas acidaminiphila* sp. nov., a strictly aerobic bacterium isolated from an upflow anaerobic sludge blanket (UASB) reactor. *Int. J. Syst. Evol. Microbiol.* 52(Pt 2), 559–568. doi: 10.1099/00207713-52-2-559
- Baker, D., and Sali, A. (2001). Protein structure prediction and structural genomics. *Science* 294, 93–96. doi: 10.1126/science.1065659
- Capasso, C., and Supuran, C. T. (2014). Sulfa and trimethoprim-like drugs - antimetabolites acting as carbonic anhydrase, dihydropteroate synthase and dihydrofolate reductase inhibitors. *J. Enzyme. Inhib. Med. Chem.* 293, 379–387. doi: 10.3109/14756366.2013.787422
- Chen, I. A., Markowitz, V. M., Chu, K., Palaniappan, K., Szeto, E., Pillay, M., et al. (2017). IMG/M: integrated genome and metagenome comparative data analysis system. *Nucleic Acids Res.* 45, D507–D516. doi: 10.1093/nar/gkw929
- Cornick, J. E., Harris, S. R., Parry, C. M., Moore, M. J., Jassi, C., Kamng'ona, A., et al. (2014). Genomic identification of a novel co-trimoxazole resistance genotype and its prevalence amongst *Streptococcus pneumoniae* in Malawi. *J. Antimicrob. Chemother.* 69, 368–374. doi: 10.1093/jac/dkt384
- Crossman, L. C., Gould, V. C., Dow, J. M., Vernikos, G. S., Okazaki, A., Sebahia, M., et al. (2008). The complete genome, comparative and functional analysis of *Stenotrophomonas maltophilia* reveals an organism heavily shielded by drug resistance determinants. *Genome Biol.* 9:R74. doi: 10.1186/gb-2008-9-4-r74
- Davenport, K. W., Daligault, H. E., Minogue, T. D., Broomall, S. M., Bruce, D. C., Chain, P. S., et al. (2014). Complete genome sequence of *Stenotrophomonas maltophilia* type strain 810-2 (ATCC 13637). *Genome Announc.* 25, e00974-14. doi: 10.1128/genomeA.00974-14
- Denton, M., and Kerr, K. G. (1998). Microbiological and clinical aspects of infection associated with *Stenotrophomonas maltophilia*. *Clin. Microbiol. Rev.* 11, 57–80.

AUTHOR CONTRIBUTIONS

Y-TH, J-MC, and P-YL designed and coordinated the study and carried out the data analysis. Y-TH, J-MC, and P-YL performed the bioinformatics analysis. Z-YW, B-CH, and P-YL carried out the experiments and interpreted data for the work. Y-TH, Z-YW, RK, and P-YL wrote the manuscript. Y-TH, RK, and P-YL checked and edited the manuscript. All authors have read and approved the manuscript.

FUNDING

Y-TH was supported in part by the Ministry of Science and Technology (MOST) with 106-2221-E-194-056-MY3. P-YL was supported by the Taichung Veterans General Hospital with TCVGH-1073901B and TCVGH-NK1079003.

SUPPLEMENTARY MATERIAL

The Supplementary Material for this article can be found online at: <https://www.frontiersin.org/articles/10.3389/fmicb.2018.01013/full#supplementary-material>

- Egea, T. C., da Silva, R., Boscolo, M., Rigonato, J., Monteiro, D. A., Grunig, D., et al. (2017). Diuron degradation by bacteria from soil of sugarcane crops. *Heliyon* 3:12:e00471. doi: 10.1016/j.heliyon.2017.e00471
- Estrada, A., Wright, D. L., and Anderson, A. C. (2016). Antibacterial antifolates: from development through resistance to the next generation. *Cold Spring Harb. Perspect. Med.* 68:a028324. doi: 10.1101/cshperspect.a028324
- Falagas, M. E., Kastoris, A. C., Vouloumanou, E. K., Rafailidis, P. I., Kapaskelis, A. M., and Dimopoulos, G. (2009). Attributable mortality of *Stenotrophomonas maltophilia* infections: a systematic review of the literature. *Future Microbiol.* 4, 1103–1109. doi: 10.2217/fmb.09.84
- Fernandes, P., Ferreira, B. S., and Cabral, J. M. (2003). Solvent tolerance in bacteria: role of efflux pumps and cross-resistance with antibiotics. *Int. J. Antimicrob. Agents* 22, 211–216.
- Gomila, M., Pena, A., Mulet, M., Lalucat, J., and Garcia-Valdes, E. (2015). Phylogenomics and systematics in *Pseudomonas*. *Front. Microbiol.* 6:214. doi: 10.3389/fmicb.2015.00214
- Gunn, J. S. (2000). Mechanisms of bacterial resistance and response to bile. *Microbes Infect.* 28, 907–913.
- Huang, X., He, J., Yan, X., Hong, Q., Chen, K., He, Q., et al. (2017). Microbial catabolism of chemical herbicides: microbial resources, metabolic pathways and catabolic genes. *Pestic. Biochem. Physiol.* 143, 272–297. doi: 10.1016/j.pestbp.2016.11.010
- Hunt, M., Silva, N. D., Otto, T. D., Parkhill, J., Keane, J. A., and Harris, S. R. (2015). Circlator: automated circularization of genome assemblies using long sequencing reads. *Genome Biol.* 16:294. doi: 10.1186/s13059-015-0849-0
- Huovinen, P. (2001). Resistance to trimethoprim-sulfamethoxazole. *Clin. Infect. Dis.* 32, 1608–1614. doi: 10.1086/320532
- Kaiser, S., Biehler, K., and Jonas, D. (2009). A *Stenotrophomonas maltophilia* multilocus sequence typing scheme for inferring population structure. *J. Bacteriol.* 191, 2934–2943. doi: 10.1128/JB.00892-08
- Kim, J.-D., Yoon, J.-H., Park, Y.-H., Fusako, K., Kim, H.-T., Lee, D.-W., et al. (2002). Identification of *Stenotrophomonas maltophilia* LK-24 and its degradability of crystal violet. *J. Microbiol. Biotechnol.* 12, 437–443.

- Konstantinidis, K. T., and Tiedje, J. M. (2005). Genomic insights that advance the species definition for prokaryotes. *Proc. Natl. Acad. Sci. U.S.A.* 102, 2567–2572. doi: 10.1073/pnas.0409727102
- Koren, S., Walenz, B. P., Berlin, K., Miller, J. R., Bergman, N. H., and Phillippy, A. M. (2017). Canu: scalable and accurate long-read assembly via adaptive k-mer weighting and repeat separation. *Genome Res.* 27, 722–736. doi: 10.1101/gr.215087.116
- Kumar, S., Stecher, G., and Tamura, K. (2016). MEGA7: molecular evolutionary genetics analysis version 7.0 for bigger datasets. *Mol. Biol. Evol.* 33, 1870–1874. doi: 10.1093/molbev/msw054
- Lee, I., Ouk Kim, Y., Park, S. C., and Chun, J. (2016). OrthoANI: an improved algorithm and software for calculating average nucleotide identity. *Int. J. Syst. Evol. Microbiol.* 66, 1100–1103. doi: 10.1099/ijsem.0.000760
- Liao, X., Li, B., Zou, R., Xie, S., and Yuan, B. (2016). Antibiotic sulfanilamide biodegradation by acclimated microbial populations. *Appl. Microbiol. Biotechnol.* 100, 2439–2447. doi: 10.1007/s00253-015-7133-9
- Mangwani, N., Shukla, S. K., Kumari, S., Rao, T. S., and Das, S. (2014). Characterization of *Stenotrophomonas acidaminiphila* NCW-702 biofilm for implication in the degradation of polycyclic aromatic hydrocarbons. *J. Appl. Microbiol.* 117, 1012–1024. doi: 10.1111/jam.12602
- Markowitz, V. M., Chen, I.-M. A., Palaniappan, K., Chu, K., Szeto, E., Grechkin, Y., et al. (2012). IMG: the integrated microbial genomes database and comparative analysis system. *Nucleic Acids Res.* 40, D115–D122. doi: 10.1093/nar/gkr1044
- McArthur, A. G., Wagglechner, N., Nizam, F., Yan, A., Azad, M. A., Baylay, A. J., et al. (2013). The comprehensive antibiotic resistance database. *Antimicrob. Agents Chemother.* 57, 3348–3357. doi: 10.1128/AAC.00419-13
- Mortimer, T. D., Weber, A. M., and Pepperell, C. S. (2018). Signatures of selection at drug resistance loci in *Mycobacterium tuberculosis*. *mSystems* 3, e108–e117. doi: 10.1128/mSystems.0010817
- Patil, P. P., Midha, S., Kumar, S., and Patil, P. B. (2016). Genome sequence of type strains of genus *Stenotrophomonas*. *Front. Microbiol.* 7:309. doi: 10.3389/fmicb.2016.00309
- Piddock, L. J. (2006). Multidrug-resistance efflux pumps - not just for resistance. *Nat. Rev. Microbiol.* 4, 629–636. doi: 10.1038/nrmicro1464
- Pruitt, K. D., Tatusova, T., and Maglott, D. R. (2007). NCBI reference sequences (RefSeq): a curated non-redundant sequence database of genomes, transcripts and proteins. *Nucleic Acids Res.* 35, D61–D65. doi: 10.1093/nar/gkl842
- Sanchez, M. B. (2015). Antibiotic resistance in the opportunistic pathogen *Stenotrophomonas maltophilia*. *Front. Microbiol.* 6:658. doi: 10.3389/fmicb.2015.00658
- Sanchez, M. B., and Martinez, J. L. (2015). The efflux pump SmeDEF contributes to trimethoprim-sulfamethoxazole resistance in *Stenotrophomonas maltophilia*. *Antimicrob. Agents Chemother.* 59, 4347–4348. doi: 10.1128/AAC.00714-15
- Sanchez-Castro, I., Bakkali, M., and Merroun, M. L. (2017). Draft Genome Sequence of *Stenotrophomonas bentonitica* BII-R7(T), a selenite-reducing bacterium isolated from Spanish bentonites. *Genome Announc.* 5, e00719-17. doi: 10.1128/genomeA.00719-17
- Sattler, C. A., Mason, E. O. Jr., and Kaplan, S. L. (2000). Nonrespiratory *Stenotrophomonas maltophilia* infection at a children's hospital. *Clin. Infect. Dis.* 31, 1321–1330. doi: 10.1086/317473
- Selvaraj, G. K., Tian, Z., Zhang, H., Jayaraman, M., Yang, M., and Zhang, Y. (2018). Culture-based study on the development of antibiotic resistance in a biological wastewater system treating stepwise increasing doses of streptomycin. *AMB Express* 8:12. doi: 10.1186/s13568-018-0539-x
- Skold, O. (2000). Sulfonamide resistance: mechanisms and trends. *Drug Resist. Updat.* 3, 155–160. doi: 10.1054/drup.2000.0146
- Toleman, M. A., Bennett, P. M., Bennett, D. M., Jones, R. N., and Walsh, T. R. (2007). Global emergence of trimethoprim/sulfamethoxazole resistance in *Stenotrophomonas maltophilia* mediated by acquisition of sul genes. *Emerg. Infect. Dis.* 13, 559–565. doi: 10.3201/eid1304.061378
- Triglia, T., Menting, J. G., Wilson, C., and Cowman, A. F. (1997). Mutations in dihydropteroate synthase are responsible for sulfone and sulfonamide resistance in *Plasmodium falciparum*. *Proc. Natl. Acad. Sci. U.S.A.* 94, 13944–13949.
- Vinuesa, P., and Ochoa-Sanchez, L. E. (2015). Complete genome sequencing of *Stenotrophomonas acidaminiphila* ZAC14D2_NAIMI4_2, a multidrug-resistant strain isolated from sediments of a polluted river in Mexico, uncovers new antibiotic resistance genes and a novel class-II lasso peptide biosynthesis gene cluster. *Genome Announc.* 3, e1433-1415. doi: 10.1128/genomeA.01433-15
- Yoon, S. H., Ha, S. M., Lim, J., Kwon, S., and Chun, J. (2017). A large-scale evaluation of algorithms to calculate average nucleotide identity. *Antonie Van Leeuwenhoek* 110, 1281–1286. doi: 10.1007/s10482-017-0844-4
- Yun, M. K., Wu, Y., Li, Z., Zhao, Y., Waddell, M. B., Ferreira, A. M., et al. (2012). Catalysis and sulfa drug resistance in dihydropteroate synthase. *Science* 335, 1110–1114. doi: 10.1126/science.1214641

Conflict of Interest Statement: The authors declare that the research was conducted in the absence of any commercial or financial relationships that could be construed as a potential conflict of interest.

Copyright © 2018 Huang, Chen, Ho, Wu, Kuo and Liu. This is an open-access article distributed under the terms of the Creative Commons Attribution License (CC BY). The use, distribution or reproduction in other forums is permitted, provided the original author(s) and the copyright owner are credited and that the original publication in this journal is cited, in accordance with accepted academic practice. No use, distribution or reproduction is permitted which does not comply with these terms.



Mutational Evolution of *Pseudomonas aeruginosa* Resistance to Ribosome-Targeting Antibiotics

Fernando Sanz-García, Sara Hernando-Amado* and José L. Martínez*

Centro Nacional de Biotecnología, Consejo Superior de Investigaciones Científicas, Madrid, Spain

OPEN ACCESS

Edited by:

Elena Perrin,
Università degli Studi di Firenze, Italy

Reviewed by:

Antonio Oliver,
Hospital Universitario Son Dureta,
Spain
Michael L. Vasil,
University of Colorado, United States

*Correspondence:

Sara Hernando-Amado
shernando@cnb.csic.es
José L. Martínez
jlmtnz@cnb.csic.es

Specialty section:

This article was submitted to
Evolutionary and Genomic
Microbiology,
a section of the journal
Frontiers in Genetics

Received: 26 July 2018

Accepted: 18 September 2018

Published: 18 October 2018

Citation:

Sanz-García F,
Hernando-Amado S and Martínez JL
(2018) Mutational Evolution
of *Pseudomonas aeruginosa*
Resistance to Ribosome-Targeting
Antibiotics. *Front. Genet.* 9:451.
doi: 10.3389/fgene.2018.00451

The present work examines the evolutionary trajectories of replicate *Pseudomonas aeruginosa* cultures in presence of the ribosome-targeting antibiotics tobramycin and tigecycline. It is known that large number of mutations across different genes – and therefore a large number of potential pathways – may be involved in resistance to any single antibiotic. Thus, evolution toward resistance might, to a large degree, rely on stochasticity, which might preclude the use of predictive strategies for fighting antibiotic resistance. However, the present results show that *P. aeruginosa* populations evolving in parallel in the presence of antibiotics (either tobramycin or tigecycline) follow a set of trajectories that present common elements. In addition, the pattern of resistance mutations involved include common elements for these two ribosome-targeting antimicrobials. This indicates that mutational evolution toward resistance (and perhaps other properties) is to a certain degree deterministic and, consequently, predictable. These findings are of interest, not just for *P. aeruginosa*, but in understanding the general rules involved in the evolution of antibiotic resistance also. In addition, the results indicate that bacteria can evolve toward higher levels of resistance to antibiotics against which they are considered to be intrinsically resistant, as tigecycline in the case of *P. aeruginosa* and that this may confer cross-resistance to other antibiotics of therapeutic value. Our results are particularly relevant in the case of patients under empiric treatment with tigecycline, which frequently suffer *P. aeruginosa* superinfections.

Keywords: antibiotic resistance, *Pseudomonas aeruginosa*, tobramycin, tigecycline, mutation, evolution

INTRODUCTION

Antibiotic resistance has been a major public health concern since the dawn of the antibiotic era, but in recent decades there has been an alarming increase in the number and type of antibiotic-resistant bacteria (Appelbaum, 2012), posing a threat to health worldwide (Roca et al., 2015). Predicting the mechanisms by which bacteria may acquire resistance is therefore important in the prevention and treatment of infections (Martinez et al., 2007; Martinez et al., 2011).

Resistance can be acquired via horizontal transfer of antibiotic resistance genes (HGT), or through mutation (Hernando-Amado et al., 2017). While exhaustive information is available on the mechanisms of antibiotic resistance at the basic science and epidemiological levels, the evolutionary trajectories leading to high level antimicrobial resistance, as well as the reproducibility of these trajectories among populations evolving concurrently, have been studied in less detail. It is worth mentioning, however, that the reconstruction of mutants that are selected in patients

under treatment have shown that fitness costs and the selection of compensatory mutations are critical for the success of some specific antibiotic resistance mutations (Shcherbakov et al., 2010; Brandis et al., 2015; Meftahi et al., 2016; Huseby et al., 2017). Nevertheless, this type of retrospective analyses is useful just for studying already known mechanisms of resistance, not for predicting new ones (Pietsch et al., 2017).

Strategies to predict the emergence of resistance mutations (Martinez et al., 2007) were implemented soon after the discovery of antibiotics (Bryson and Szybalski, 1952), one of the most useful of which is experimental evolution. Since the seminal work of Richard Lenski, experimental evolution has been used to analyze different bacterial traits, including the development of resistance to antibiotics (Bryson and Szybalski, 1952; Toprak et al., 2011; Turrientes et al., 2013; Feng et al., 2016; Ibacache-Quiroga et al., 2018). Recent research has shown experimental evolution able to predict the emergence of resistance against different antimicrobial agents, including colistin (Jochumsen et al., 2016), beta-lactams, quinolones and aminoglycosides (Cabot et al., 2016; Feng et al., 2016; Ibacache-Quiroga et al., 2018; Lopez-Causape et al., 2018b). In recent years, the potential of experimental evolution has been further boosted by the development of technologies that allow the fast and affordable sequencing of whole bacterial genomes.

Pseudomonas aeruginosa, an opportunistic pathogen widely distributed in nature (Silby et al., 2011), commonly causes lung, airway and other infections in hospitalized patients. It is the main cause of chronic infections in patients with cystic fibrosis (CF) and chronic obstructive pulmonary disease (Martinez-Solano et al., 2008; Tummeler et al., 2014). These infections are usually fought using aminoglycosides, β -lactams and polymyxins (Palmer and Whiteley, 2015). Unfortunately, *P. aeruginosa* intrinsically shows low-level susceptibility to a number of drugs, even against the recently developed glycolcycline tigecycline (Pankey, 2005), which works via tightly binding to the ribosome and thus evading the most common tetracycline resistance mechanisms. In addition, mutants presenting increased levels of antibiotic resistance are selected along chronic infections. Indeed, while resistance to aminoglycosides in *P. aeruginosa* isolates from acute infections has been largely attributed to the acquisition of antibiotic resistance genes, mutation plays a major role for the acquisition of resistance by *P. aeruginosa* causing chronic infections (Vogne et al., 2004; Guenard et al., 2014; Bolard et al., 2018).

In the present work, experimental evolution and whole-genome sequencing (WGS) were used to examine evolutionary trajectories of *P. aeruginosa* toward resistance against two ribosome-targeting antimicrobials: tobramycin and tigecycline. The aim was to determine whether the mechanisms that impair the actions of different drugs targeting the same cell machinery are shared (at least in part), or whether resistance to each drug is specific via a different mechanism. Tigecycline binds to the 30S ribosomal subunit, thereby blocking the interaction of aminoacyl-tRNA with the A site of the ribosome, whereas tobramycin prevents the formation of the 70S complex (Kotra et al., 2000). While tobramycin forms part of usual therapy regimens against *P. aeruginosa* (Cheer et al., 2003), the pathogen

is intrinsically resistant to tigecycline (following the clinical definition of antibiotic resistance) (Martinez et al., 2015). One cause of this phenotype is the capability of the multidrug efflux pump MexXY, also involved in intrinsic *P. aeruginosa* tobramycin resistance (Westbrock-Wadman et al., 1999), to extrude tigecycline (Dean et al., 2003). Nonetheless, tigecycline was used in the present study since it provides an opportunity to examine whether or not bacterial pathogens can acquire clinically relevant characteristics when challenged with the antibiotics to which they are considered to be intrinsically resistant. In this regard, it is worth mentioning that *P. aeruginosa* has emerged as a major cause of superinfection in nosocomial patients treated with tigecycline (Garcia-Cabrera et al., 2010; Ulu-Kilic et al., 2015; Katsiari et al., 2016). Knowing whether or not the empirical use of tigecycline for treating Gram-negative hospital infections might challenge *P. aeruginosa*, affecting its susceptibility to other antibiotics commonly used for treating *P. aeruginosa* infections, is of relevance for developing a rational approach for treating such superinfections. The results showed that even for microorganisms dubbed intrinsically resistant to an antibiotic, the challenge with this antibiotic selects mutants presenting reduced susceptibility to antibiotics of clinical value.

Experimental evolution studies allow one to determine whether evolutionary trajectories are reproducible, i.e., whether the process of evolution is mainly deterministic and hence predictable (Martinez et al., 2007), or whether it is largely stochastic. The present work provides a predictive analysis of the potential mutational causes of resistance in *P. aeruginosa* against two ribosome-targeting antibiotics belonging to different structural families, as well as the different evolutionary trajectories taken toward this resistance. This information may allow new strategies to be designed for predicting, managing, and eventually reducing resistance in this important nosocomial pathogen. In addition, the results throw light on whether bacterial evolution is largely stochastic or presents some deterministic features, and thus whether the emergence and spread of antibiotic resistance can be predicted to a certain extent (Martinez et al., 2007, 2011).

MATERIALS AND METHODS

Growth Conditions and Determination of Susceptibility to Antibiotics

Unless otherwise stated, bacteria were grown in Mueller Hinton Broth (MHB, Pronadisa) at 37°C with agitation at 250 rpm. The initial concentrations of tigecycline (Pfizer) and tobramycin (Normon, S. L.) that inhibit the growth of *P. aeruginosa* PA14 under the culture conditions used in the evolution experiments were determined at 37°C.

General susceptibility to a wide range of antibiotics – tigecycline, tetracycline, aztreonam, ceftazidime, imipenem, ciprofloxacin, levofloxacin, norfloxacin, tobramycin, streptomycin, amikacin, colistin, polymyxin B, chloramphenicol, fosfomycin and erythromycin – was examined by disk diffusion in Mueller Hinton Agar (MHA) (Sigma) at 37°C.

The MICs of different antibiotics were determined for the bacterial populations over the evolution period at 37°C in MHA using *E*-test strips (MIC Test Strip, Liofilchem®). MICs of colistin and polymyxin B were determined in MHB II by double dilution in microtiter plates. The MICs to the antibiotics of selection and to fosfomycin were repeated twice and in all cases, the results were the same in the replicated assays.

Experimental Evolution

Twelve independent bacterial populations (four controls without antibiotics, four populations challenged with tigecycline, and four populations challenged with tobramycin) were grown in parallel in MHB for 35 consecutive days. All replicates were established from a stock culture of the *P. aeruginosa* PA14 strain. Each day, the cultures were diluted (1/250) with fresh MHB: 8 µl of bacterial culture in 2 ml of medium. The concentrations of tigecycline and tobramycin used for selection increased over the evolution period from the initial MIC up to 32MIC, doubling them every 5 days. Every 5 days, samples from each culture were taken and preserved at −80°C for future investigation.

Whole-Genome Sequencing

Genomic DNA was extracted at the end of the evolution assays from all 12 populations using the Gnome® DNA kit (MP Biomedicals). Whole-genome sequencing was performed by Sistemas Genómicos S.L. Libraries were obtained without amplification following Illumina protocols and recommendations. The quality of the extracted material was analyzed via a 4200 TapeStation High Sensitivity assay, and the DNA concentration determined by real-time PCR using a LightCycler 480 device (Roche). The pool of libraries was pair-end sequenced (100 × 2) in an Illumina HiSeq 2500 sequencer. The average number of reads per sample was 8646177, which represents a coverage of 200x on average. Short reads used in this publication are deposited in SRA database¹ with accession PRJNA490803.

Bioinformatic Analysis

Mutations in the evolved bacteria were detected using CLC Genomics Workbench 9.0 (QIAGEN) software. WGS data were trimmed and the reads aligned with the *P. aeruginosa* UCBPP-PA14 reference chromosome (NC_008463.1). The single nucleotide polymorphisms (SNPs) present in the populations kept under selective pressure were identified and filtered against those present in the populations maintained in the absence of such pressure. The cut-off threshold of a mutation to be included in the analysis was ≥15%.

Confirmation of SNPs

Sanger sequencing was used to verify the mutations found via WGS (Supplementary Table S1) and to ascertain the order of appearance of these modifications. Twenty-four pairs of primers, which amplified 100–200 base pair regions containing each putative mutation, were designed (Supplementary Table S2). After PCR amplification, the corresponding amplicons were

purified using the QIAquick PCR Purification Kit (QIAGEN) and sequenced at GATC Biotech.

RNA Extraction and Real-Time RT-PCR

One flask containing 20 ml of MHB was inoculated with an overnight culture of the selected clones and *P. aeruginosa* PA14 to a final O.D.₆₀₀ = 0.01, and they were incubated until exponential phase was reached (O.D.₆₀₀ = 0.6). 10 ml of each culture were centrifuged at 7000 rpm for 15 min and at 4°C. This process was performed with three independent biological replicates.

Then, RNeasy mini Kit (QIAGEN) extraction protocol was followed: 570 µl of TE buffer (10 mM Tris-HCl, 1 mM EDTA [pH 8.0]) and 30 µl of lysozyme (Sigma), for a final concentration of 1 mg/ml of the latter, were added to each sample. Afterward, the samples were mixed by vortexing for 10 s and were incubated at room temperature for 10 min with regular vortexing. A volume of 2100 µl of buffer RLT (QIAGEN) was added, and samples were sonicated at 0.45 Hz for 20 s. Next, 1410 µl of ethanol (Merck) was added and the protocol continued according to the manufacturer's instructions. In order to remove any residual DNA, two DNase treatments were carried out, with DNase I (QIAGEN) and TURBO DNase (Ambion). Finally, a PCR with *rplU* primers (Supplementary Table S2) was performed to check that no residual DNA was present in the RNA samples. High Capacity cDNA Reverse Transcription Kit (Applied Biosystems) was used to synthesize cDNA from 5 µg of RNA. Then, real-time RT-PCR was performed using 50 ng of cDNA and the Power SYBR green PCR Master Mix (Applied Biosystems) in the ABI PRISM 7500 real-time PCR system (Applied Biosystems). Gene expression data were normalized using the gene *rplU* (Supplementary Table S2). Differences in the relative amounts of mRNA were obtained following the 2^{−ΔΔCt} method (Livak and Schmittgen, 2001).

RESULTS AND DISCUSSION

Different publications have shown that the genes that contribute to antibiotic resistance (intrinsic resistance) comprise around 3% of the genome of a given bacterial species (Breidenstein et al., 2008; Fajardo et al., 2008; Tamae et al., 2008; Alvarez-Ortega et al., 2010; Blake and O'Neill, 2013; Fernandez et al., 2013). In the case of *P. aeruginosa* the search of a comprehensive transposon-tagged library has shown that the inactivation of 135 genes renders low-level tobramycin resistance (Schurek et al., 2008). Even if we do not take into consideration gain of function mutations (which are not considered in transposon insertion libraries studies), neither that different mutations might be selectable in each of these genes (Martinez and Baquero, 2000), hence increasing the number of potential antibiotic resistance mutants (Lopez-Causape et al., 2018a), the number of possible combinations of these 135 genes is 2.7E230. It can be argued that the number of mutations that a single bacterium can accumulate is likely low. However, even if only five mutations are accumulated as reported in the present work (see below), the number of combinations of these 135 potential mutations, taken five by five, is 4.1E10 if the order of

¹<https://www.ncbi.nlm.nih.gov/sra>

selection is taken into consideration and 3.4×10^8 if the order of selection of each of the mutations along evolution is not taken into consideration. If all possible combinations were equivalent in terms of antibiotic resistance, these numbers would mean that mutation-driven antibiotic resistance should be unpredictable.

Stepwise Evolution of *P. aeruginosa* Toward Antibiotic Resistance

To determine whether similar potential evolutionary trajectories are followed by different populations, four biological replicates were allowed to evolve in parallel under selective pressure from tobramycin (populations 1–4), tigecycline (populations 5–8) and in the absence of any selective pressure (populations 9–12). In populations 1–8 the antibiotic concentration was doubled every 5 days, from 0.5 µg/ml for tobramycin and 4 µg/ml for tigecycline, up to 32MIC. At 64MIC no growth was seen after 5 days incubation, suggesting this concentration to be beyond limits of *P. aeruginosa* when evolving toward tobramycin and tigecycline resistance in these experimental conditions.

To monitor the evolution of resistance over the selection period, the susceptibility of each population to the selecting antibiotic was determined every 5 days by *E*-test. When bacteria are confronted to increased concentrations of antibiotics, two different phenotypic trajectories can be foreseen. Sudden selection of high-level resistance at the first steps of evolution or stepwise selection of mutants presenting increasing resistance levels. As shown in **Figure 1**, a stepwise evolutionary trajectory was observed for both antibiotics, suggesting either accumulation of sequential mutations after each evolution step (i.e., each change in antibiotic concentration), or the displacement of low-level resistance mutants by higher-level resistance ones as the selection pressure increased. It is important to note that the evolutionary trajectory was similar in all replicated experiments (**Figure 1**). This suggests the number of evolutionary trajectories possible (at least at phenotypic level) is limited, although the amount of genotypic evolutionary trajectories can be larger (Lässig et al., 2017).

An increase in the MIC of an antibiotic after experimental evolution does not, however, necessarily mean that antibiotic-resistant mutants have been selected for: resistance may be due to a phenotypic adaptation to the presence of an antibiotic rather than to mutations (Levin and Rozen, 2006; Martinez et al., 2009; Martinez and Rojo, 2011). To address this possibility, the evolved populations were sub-cultured in the absence of selection pressure (three sequential passages in MHB) and the MICs again determined. These were found not to change, indicating that the observed modifications were mainly due to the selection of stable mutants.

Cross-Resistance and Collateral Sensitivity of Evolved Populations

To determine whether the development of resistance was specific to the selecting antibiotic or also affected susceptibility to other antimicrobials, a range of representative antibiotics was tested (beta-lactams, quinolones, tetracyclines, macrolides, aminoglycosides, polymyxins, and chloramphenicol) by disk

diffusion (**Supplementary Table S4**). Despite it has been shown macrolides as azithromycin can select *mexCD-oprJ* overexpressing mutants in *P. aeruginosa* biofilms (Mulet et al., 2009), no differences in susceptibility to imipenem and erythromycin were detected between the wild-type parental *P. aeruginosa* PA14 strain and the evolved populations. Whether these differences can be due to the different experimental model (biofilm or planktonic cells) or the different genetic background where mutants are selected (PAO1 or PA14) remains to be established. Nevertheless, almost every evolved population developed resistance against other antibiotics belonging to the different structural families, implying that at least some resistance mutations are not tigecycline- or tobramycin-specific (**Table 1**). Notably, in all cases the evolved populations were more susceptible to fosfomycin than the wild-type strain, and it is important to know whether this is related to the development of resistance to ribosome-targeting agents. In this regard, it is worth mentioning that *Listeria monocytogenes* is more susceptible to fosfomycin when growing intracellularly than when growing extracellularly. The reason for this lies in the overexpression of a hexose-phosphate transporter when the bacteria are grown intracellularly, which provides an entry route for this antibiotic (Scortti et al., 2006). These results indicate that the resistance to ribosome-targeting drugs may correlate with increasing susceptibility to fosfomycin, although the underlying mechanisms remain obscure. Given that these types of drug are widely used clinically, it is important to determine whether this trade-off occurs commonly, and whether the combined or sequential use of both types of antibiotic offers a better alternative to current therapies.

Mutations Selected in the Presence of Antibiotics

To gain insight into the genetic events associated with the development of resistance in the evolved populations, the genomes of each, as well as that of the original population (for which a frozen sample was available), were sequenced on the last day of the experiment (when the antibiotic concentration was 32MIC). Different mutations can appear by chance or because of the *P. aeruginosa* adaptation for growing in MHB. Consequently, only those mutations present in the populations evolving under antibiotic selective pressure and not in the control populations evolving in absence of selection were taken into consideration. In other words, only those mutations that are enriched (and hence have been selected) under antibiotic selective pressure were taken into consideration. Indeed, all mutant alleles selected in the presence of antibiotics and not present in the populations grown without antibiotics present always a coverage >50% and typically >90% (**Supplementary Table S1**) in the whole population, indicating that they are under positive selection when *P. aeruginosa* grows in presence of antibiotics. **Supplementary Table S1** shows the locations of all 35 confirmed genetic changes potentially associated with the development of resistance. A total of 31 single-nucleotide variants (SNVs) and 4 multi-nucleotide variants (MNVs; deletions and substitutions of various nucleotides and one transposition) were found, 31 located in genes and 4 in intergenic regions. The majority of the

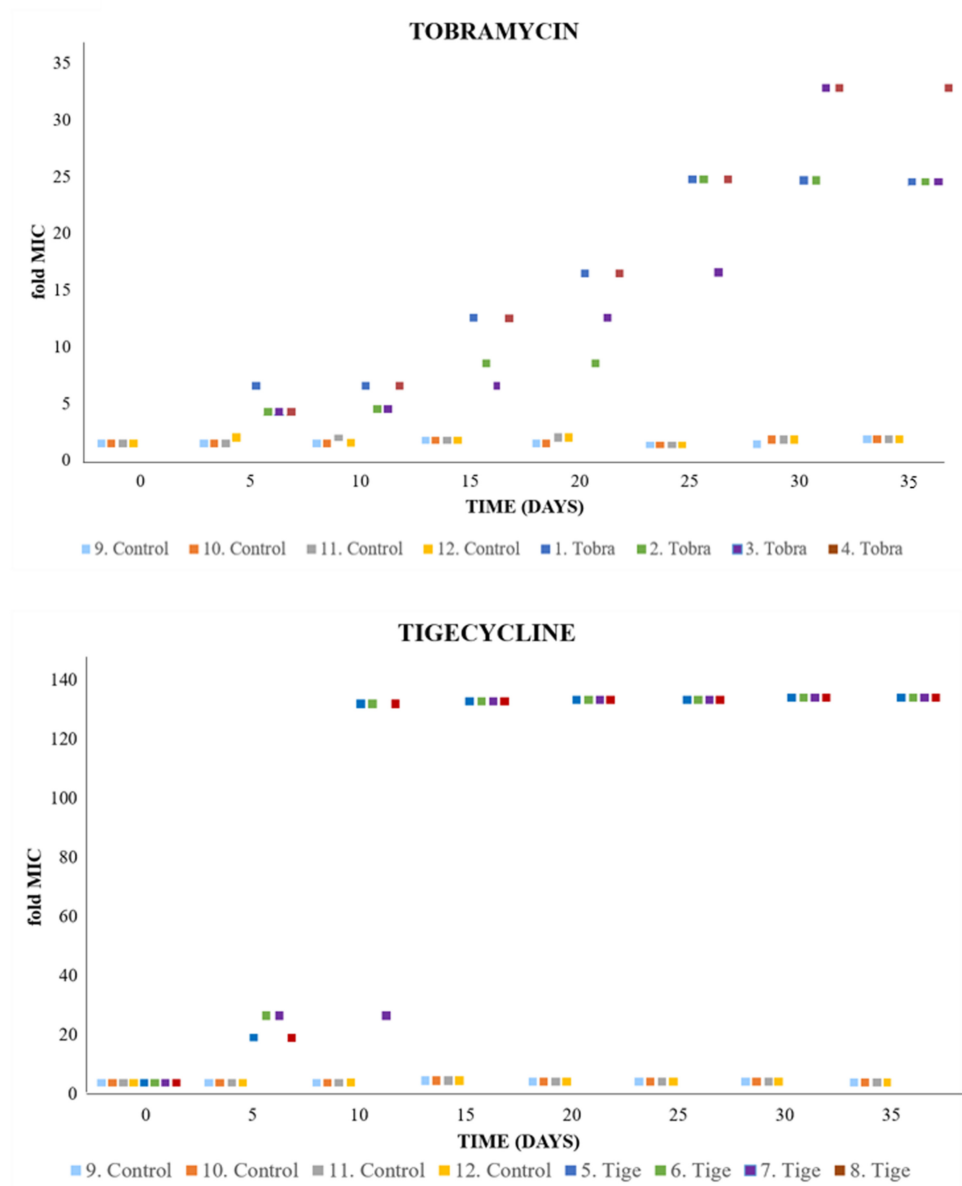


FIGURE 1 | Evolution of *P. aeruginosa* under antibiotic selective pressure. Graphs show the rise of the MICs over the evolution period, from the value corresponding to the wild-type strain (tobramycin [Tobra], 1 $\mu\text{g/ml}$; tigecycline [Tige], 2 $\mu\text{g/ml}$) to high levels of tobramycin/tigecycline resistance (doubling the antibiotic concentration every 5 days). The detection limit of the tigecycline E-test was 256 $\mu\text{g/ml}$, limiting the assessment of resistance levels from day 15 to the end of the experiment. MIC values for each replicate are provided in **Supplementary Table S3**.

mutations located in genes resulted in amino acid alterations, frameshifts or stop codons. In addition, the coverage of the obtained reads was mapped to the *P. aeruginosa* genome to search for gene amplifications and deletions. One 377 bp deletion was detected in the tigecycline-treated population 8, comprising part of the gene coding for the transcriptional repressor of the multidrug efflux pump *mexCD-oprJ*, *nfxB*, plus a small region of the adjacent gene *morA*.

To further verify the presence in the evolved populations of the mutations identified by WGS (**Supplementary Table S1**),

the regions containing these mutations were amplified and the amplicons Sanger-sequenced.

Common Aspects of the Evolution of *P. aeruginosa* Toward Resistance to Tobramycin or Tigecycline

The present results shed light on the development of resistance to ribosome-targeting antibiotics in *P. aeruginosa*. Although this opportunistic pathogen is already intrinsically resistant to

TABLE 1 | MICs ($\mu\text{g/ml}$) of antibiotics of different structural families in the populations evolved at 32MIC tobramycin and tigecycline.

Replicate	Tgc	Tet	Atm	Caz	Cip	Tob	S	Ak	C	F	Cs	PB
PA14	1.5	16	1.5	1	0.094	1	16	2	24	24	1.5	0.75
Tobramycin 32MIC												
1	64	48	3	1.5	0.5	32	192	≥ 256	24	1	6	2.5
2	24	32	4	1.5	0.5	24	256	192	32	1	6	2.5
3	12	24	4	1.5	0.19	8	64	128	24	1	4	3
4	32	24	3	1.5	0.5	32	192	≥ 256	24	1.5	5	2.5
Tigecycline 32MIC												
5	≥ 256	192	8	4	0.75	4	96	32	128	2	2.5	1
6	≥ 256	192	8	3	0.5	1.5	64	16	64	1.5	2.5	1
7	≥ 256	≥ 256	6	3	0.25	2	128	16	96	1	5	2
8	≥ 256	192	6	2	0.75	8	192	32	128	2	5	1.5
Controls												
9	2	12	2	1.5	0.094	1	12	4	24	32	1.5	0.75
10	2	8	2	1	0.19	1	12	2	16	32	1.5	0.75
11	1.5	12	2	1	0.094	1	12	3	32	32	1.5	1
12	2	12	2	1.5	0.125	0.75	12	3	16	32	1.5	0.75

Tgc, tigecycline; tet, tetracycline; atm, aztreonam; caz, ceftazidime; cip, ciprofloxacin; tob, tobramycin; s, streptomycin; ak, amikacin; c, chloramphenicol; f, fosfomycin; cs, colistin; pb, polymyxin B. All MICs were obtained by E-test, excepting for polymyxin B and colistin, which were analyzed via double dilution in a microtiter plate.

TABLE 2 | Previously described role on antibiotic resistance of genes presenting mutations in the evolved populations.

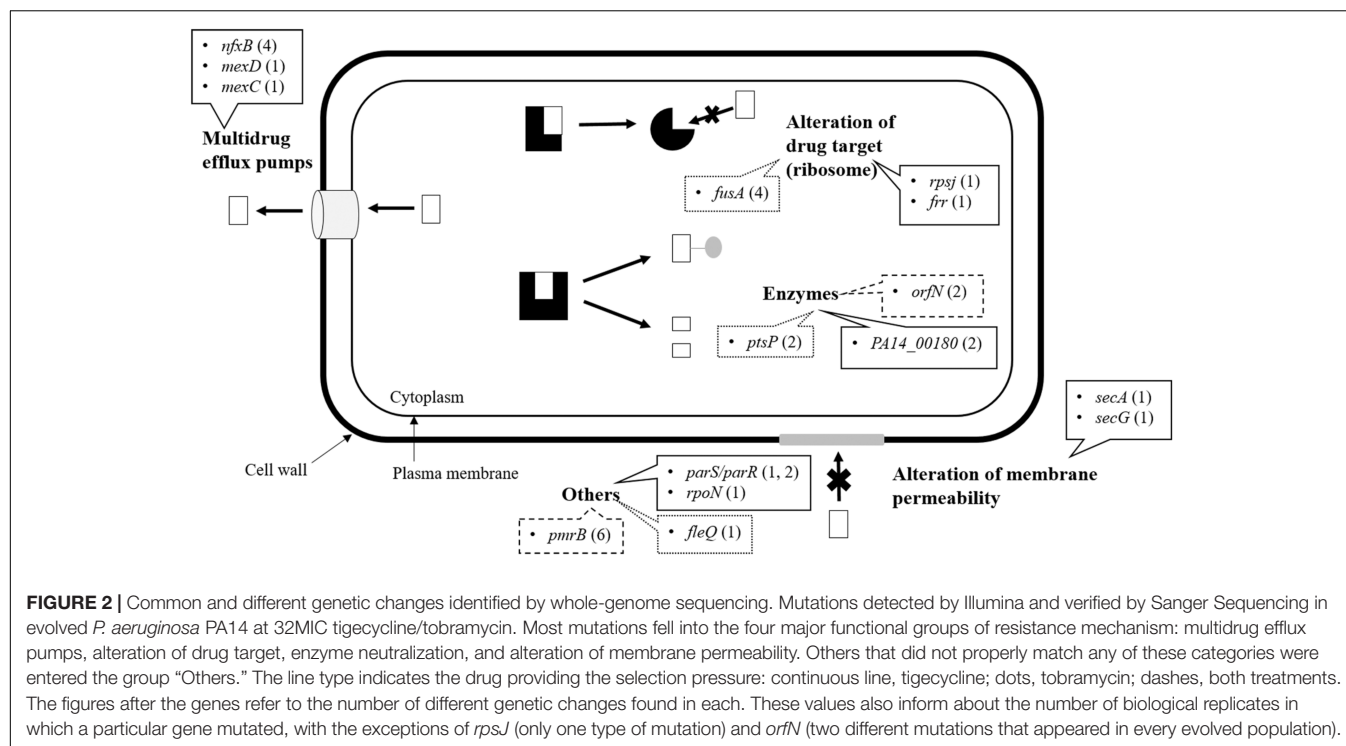
Gene name	Tobramycin replicates	Tigecycline replicates	Previously described role in resistance	References
<i>orfN</i>	4	4	Ciprofloxacin	Wong et al., 2012
<i>pmrB</i>	4	2	Cationic peptides, quinolones, tigecycline, tobramycin	Muller et al., 2011; Moskowitz et al., 2012; Lopez-Causape et al., 2018b
<i>fusA</i>	4	–	Aminoglycosides	Wang et al., 2015; Feng et al., 2016; Bolard et al., 2018; Lopez-Causape et al., 2018b
<i>ptsP</i>	2	–	Tobramycin	Schurek et al., 2008
<i>fleQ</i>	1	–	–	–
<i>nfxB</i>	–	4	Quinolones, tetracyclines, β -lactams, chloramphenicol	Masuda et al., 2000b
<i>mexCD</i>	–	2; 1 <i>mexC</i> , 1 <i>mexD</i>	Quinolones, tetracyclines, β -lactams, chloramphenicol	Masuda et al., 2000b
<i>PA14_00180</i>	–	2	–	–
<i>rpsJ</i>	–	2	Tetracycline, tigecycline	Hu et al., 2005; Ahn et al., 2016
<i>parRS</i>	–	3; 2 <i>parR</i> , 1 <i>parS</i>	Cationic peptides, aminoglycosides	Fernández et al., 2010; Muller et al., 2011
<i>secAG</i>	–	2; 1 <i>secA</i> , 1 <i>secG</i>	–	–
<i>frr</i>	–	1	–	–
<i>rpoN</i>	–	1	Carbenicillin, quinolones, tobramycin	Viducic et al., 2007, 2016, 2017

tigecycline, highly resistant populations with MICs several times higher than that seen for the wild-type strain were selected for in the experimental evolution assays (**Figure 1**).

Overall, the results indicate that increased resistance to tigecycline and tobramycin comes about via distinguishable evolutionary trajectories but which show some similarities (**Table 2**). In particular, mutations in *orfN* (selected in all eight replicates) and *pmrB* (selected in 6 out of 8 replicates) were selected under pressure from either antibiotic (**Figure 2**). It should be noted that all populations evolved in the presence of antibiotic, and none of those evolved in unexposed control populations show mutants in *orfN* during the first step in evolution (i.e., after the first change in antibiotic concentration). This gene codes for a putative glycosyl transferase needed for the

glycosylation of type A flagellins (Schirm et al., 2004). Six of the studied mutants carried a single base pair deletion in a poly-G repeat in *orfN*, and two contained a single base pair insertion in the same region (**Supplementary Table S1**), all of them leading to a Val50fs mutation. Similar mutations have been found in *P. aeruginosa* when exposed to ciprofloxacin under experimental evolution conditions (Wong et al., 2012). The fact that these mutations are located in a poly-G repeat region supports that this gene might have a specific high mutation rate as the consequence of polymerase slippage (Moxon et al., 2006). We hypothesize that this might be the reason why *orfN* mutants are detected in all replicates.

pmrAB is a two-component system involved in polymyxin resistance (Moskowitz et al., 2012). The system regulates the



expression of operons involved in the biosynthesis of lipid A with 4-aminoarabinose, which produces a more positively charged lipopolysaccharide, thus reducing the binding and the activity of cationic peptides (Gunn et al., 2000). Gain-of-function mutants with lipid A modifications can be selected for and are resistant to colistin (Fernández et al., 2010). Moreover, a recent evolution study of *P. aeruginosa* involving colistin gave rise to the selection of mutations in *pmrB* (Jochumsen et al., 2016), and it has been proposed that mutations in such regulatory elements may potentiate the effect of other mutations (Lind et al., 2015). Indeed, *pmrB* is involved in a wide range of antibiotic resistances, including those to quinolones, tigecycline, tobramycin and cationic peptides (Muller et al., 2011; Lopez-Causape et al., 2018b). In agreement with these data, the populations selected in our evolution experiment present a reduced susceptibility to colistin and polymyxin B (Table 1).

Evolutionary Pathways Toward Tobramycin Resistance in *P. aeruginosa*

Having shown the common features of the evolutionary trajectories toward resistance to both test antibiotics, the specific pathways toward resistance to each were sought. Mutations in *fusA* and *ptsP* were found to be involved in evolution toward tobramycin resistance (Schurek et al., 2008; Wang et al., 2015; Feng et al., 2016). Together with the above mentioned *orfN* mutants, mutations in *fusA*, which codes for elongation factor G, may be envisaged as a first response to aminoglycosides (Wang et al., 2015; Feng et al., 2016) since they were observed in all evolved populations (Figure 2). Further, recent works have shown this type of mutations to be present in clinical

isolates as well as in *in vitro* selected aminoglycoside resistant mutants (Bolard et al., 2018; Ibacache-Quiroga et al., 2018; Lopez-Causape et al., 2018b), reinforcing its role in the acquisition of aminoglycosides resistance. Although *mexXY* overexpression is considered a hallmark of aminoglycoside resistance development of CF chronic infections (Guenard et al., 2014), our data using PA14, as well as a recent experimental study using PAO1 (Lopez-Causape et al., 2018b), show that this does not necessarily always occurs, at least *in vitro*.

Consistent with a proposed role of *ptsP* in low-level tobramycin resistance (Schurek et al., 2008), the present results indicate that its mutation might also be important, because of its presence in 2 out of 4 tobramycin replicates. In fact, the MIC clearly increased when this mutation appeared alone (population 2, 8–24 µg/ml; Figure 3 and Supplementary Table S3). Whether or not this type of mutation is selected for in clinical settings deserves further investigation. Finally, FleQ is a major flagellar regulator that has been found responsive to c-di-GMP and plays a role in biofilm formation (Hickman and Harwood, 2008; Jimenez et al., 2012; Matsuyama et al., 2016), although it has not been previously described to be involved in antibiotic resistance in planktonic cells.

It has been previously shown that mutations in at least 135 genes can render low-level aminoglycoside resistance in *P. aeruginosa* (Schurek et al., 2008). Despite the large number of possible combinations that might be selected along evolution under antibiotic selective pressure, we found that all four evolved populations contained mutants in *orfN*, *fusA* and *pmrB* and two of these evolved populations also presented mutants in *ptsP*. Further, recent work performed independently in another laboratory has also shown that *fusA* and *pmrB* mutants are

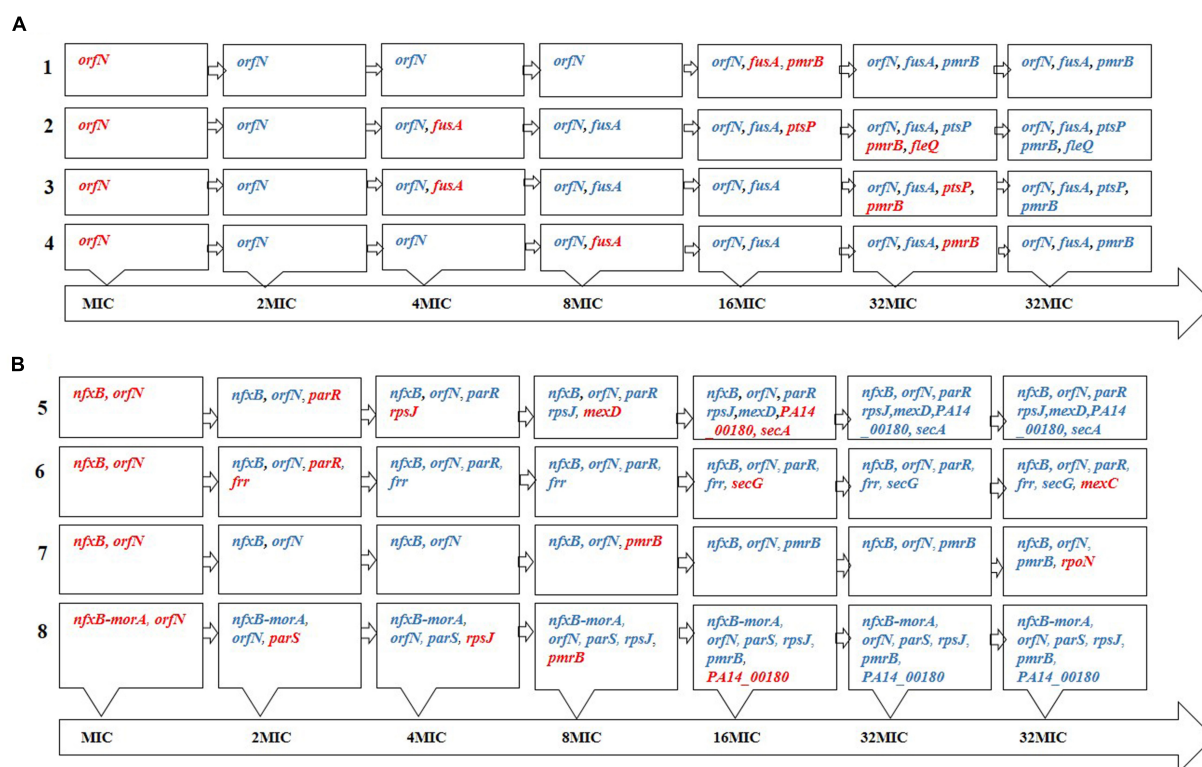


FIGURE 3 | Order of appearance of genetic changes. Order of appearance of (A) tobramycin and (B) tigecycline resistance mutations during the evolution process, as determined by PCR amplifications of known SNVs/MNVs in 32MIC populations. The names of the genes in red indicate that these mutations appeared in this step. Once a mutation appears it remains in the population until the end of the evolutionary period. We cannot discard that other mutations may have appeared and not fixed over the 35 days evolution period.

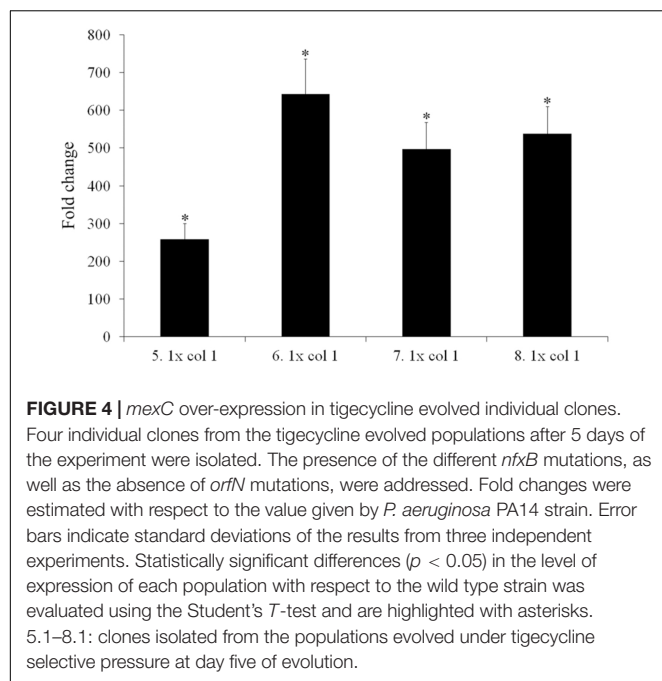
frequently selected in presence of aminoglycosides (Lopez-Causape et al., 2018b). Taking into consideration that the number of possible combinations of five mutations from the above mentioned 135 genes exceeds 3.4E8, our results indicate that *P. aeruginosa* mutation-driven resistance to tobramycin displays a certain degree of predictability.

Evolutionary Pathways Toward Tigecycline Resistance in *P. aeruginosa*

Pseudomonas aeruginosa PA14 evolving under selective pressure from tigecycline accumulated resistance mutations, indicating that, even in intrinsically resistant microorganisms, resistance may increase. Among the selected mutated genes, three – *rpsJ*, *parRS* and *nfxB* – have already been described involved in antibiotic resistance (a result that validates the present experimental strategy). The Val57 change in the 30S ribosomal protein S10 (*rpsJ*), which was present in two out of four replicates, is commonly seen in tetracycline-resistant clinical isolates of pathogens such as *Neisseria gonorrhoeae*, (Hu et al., 2005) while in *Klebsiella pneumoniae* different mutations in this gene have been related to tigecycline resistance (Ahn et al., 2016). Further, the two-component *parRS* system has been extensively examined in association with resistance to various drugs. In our experimental evolution assay, three out of the four tigecycline

evolved populations presented mutations in this two-component system (Figure 3), which may be indicative of its importance in resistance. *ParRS* may promote multidrug resistance via three mechanisms: by inducing the expression of efflux pumps (such as MexXY-OprM), by repressing the expression of porins, and via LPS alteration (Muller et al., 2011).

The transcriptional repressor of the multidrug efflux pump MexCD-OprJ (Purcell and Poole, 2013), one of the most clinically important of all efflux pumps in *P. aeruginosa*, is coded for by *nfxB*. Loss-of-function mutations in this gene result in the pump's overexpression. Different mutations in *nfxB* were selected in all four replicates of the evolving populations, and most were fully inactivating mutations (a 377 bp deletion leading to a truncated protein; a transposition; and an 11 bp deletion). Although it has been suggested that the main efflux pump contributing to tigecycline resistance in *P. aeruginosa* is MexXY-OprM (Masuda et al., 2000a; Dean et al., 2003), the first step along the path to resistance in the present work was seen to be the selection of mutants able to extrude tigecycline via MexCD-OprJ. To ascertain whether or not *nfxB* selected mutations inactivate the repressor, hence allowing MexCD overexpression, one individual clone from each 5 days tigecycline evolved population was isolated in MHA. The presence of their corresponding *nfxB* mutations and the absence of *orfN* modification were confirmed by Sanger-sequencing. Expression



of *mexC* was measured in comparison with the one of the wild-type strain. As shown in **Figure 4**, all clones carrying *nfxB* mutations overexpressed *mexC*, confirming that these mutations inactivate, in different degree, the NfxB repressor. Two further mutations in each of the genes coding for the subunits of this efflux pump (*mexC* and *mexD*) were then selected for in populations 5 and 6 respectively. It may be that these mutations alter the specificity of MexCD-OprJ improving the capacity of the pump to extrude tigecycline. The MexD SNV (Phe608Cys) is located in one of the two large periplasmic loops known to be involved in substrate specificity (Elkins and Nikaido, 2002). In agreement with this, it has been described that mutations in AcrB, the *Enterobacteriaceae* ortholog of MexD, alter the pump's substrate profile (Blair et al., 2015). While a role for these mutations in reducing the susceptibility to tigecycline is a compelling hypothesis, it cannot be ruled out that mutations in *mexD* or *mexC* may compensate for any increased non-physiological extrusion of some important cellular metabolite by those mutants that overexpress this pump.

The present results indicate that tigecycline resistance might also come about through changes in the Sec system (*SecA* and *SecE*), likely via the modification of the permeability of the membrane and the impairment of tigecycline uptake. It has also been suggested that the Sec pathway could be involved in the translocation of components of multidrug efflux pumps across the bacterial membranes (Yoneyama et al., 2010; Akiba et al., 2013; Chaudhary et al., 2015), but it is unclear how changes in this translocation could increase resistance in the selected mutants. Tigecycline increased resistance may also come about through modifications of the σ_{54} RpoN factor that has been found to modulate *P. aeruginosa* virulence (Kazmierczak et al., 2005), bacterial tolerance to carbapenems (Viducic et al., 2016), susceptibility to quinolones (Viducic et al., 2007) and

survival in the presence of tobramycin (Viducic et al., 2017). Both the Sec pathway and RpoN have been proposed as excellent targets in the search of novel antibiotics (Jin et al., 2016; Lloyd et al., 2017). Our findings suggest that tigecycline might select mutants presenting cross-resistance to these potential inhibitors, still under development. Mutations in the gene encoding the ribosome recycling factor *frr* are likely related to modifications in the tigecycline target (ribosome). Indeed, this particular mutation is located in the start codon (**Supplementary Table S1**), so it may affect the level of *frr*, impairing the steady state amount of active ribosomes. A similar situation might arise with *PA14_00180*, which codes for a putative rRNA small subunit methyltransferase, hence likely able to modify the ribosome.

All the changes seen during the evolution of the populations subjected to selective pressure from tigecycline indicate that evolutionary pathways toward tigecycline resistance present some common features. All four replicates present mutations in *orfN* and *nfxB* and mutations in *parRS* were selected in three out of the four populations. Mutations at *secAG*, *PA14_00180*, *rpsJ* or *mexCD* were selected in half (two) of the populations. This indicates that *P. aeruginosa* can develop resistance to tigecycline by following a limited number of different evolutionary trajectories, which share some specific type of mutations, suggesting a certain degree of determinism.

In addition of conferring resistance to the selecting antibiotics, the respective mutants also showed resistance to antibiotics belonging to other structural categories and with different targets. This might be explained, at least in part, via the important role that efflux pumps seem to play in the development of resistance. Indeed, all mutants selected in the presence of tigecycline showed mutations in *nfxB*, which would lead to the overexpression of MexCD-OprJ. In turn this might reduce susceptibility to quinolones, tetracyclines, beta-lactams and chloramphenicol (De Kievit et al., 2001) – phenotypes in agreement with the present data (**Table 1**). Moreover, all four population replicates analyzed showed reduced susceptibility to aminoglycosides. This phenotype may be explained in three populations as a result of the mutations selected for in the ParRS system, which is involved in modification of the lipopolysaccharide and in the regulation of the expression of MexXY-OprM, an efflux pump that contributes to aminoglycoside resistance in *P. aeruginosa* (Masuda et al., 2000a), and which is described as being regulated by the two-component system ParRS (Muller et al., 2011).

CONCLUSION

Experimental evolution approaches may allow determining basic aspects of evolution, among which knowing to what extent evolution (in our case of asexual organisms) can be predictable and hence deterministic or is basically stochastic (non-predictable) (Lässig et al., 2017), is notably interesting. This is particularly relevant in the case of antibiotic resistance, a field in which the implementation of novel therapeutic approaches is based in the assumption that evolution of antibiotic resistance can be largely predictable (Martinez et al., 2007), a feature that goes against most common views on evolution.

The present work provides information on the evolutionary trajectories leading to resistance to antibiotics belonging to different structural families but targeting the ribosome in *P. aeruginosa*. The results suggest that, although mutations in several genes may contribute to the development of antibiotic resistance (Fajardo et al., 2008; Tamae et al., 2008; Alvarez-Ortega et al., 2011; Martinez, 2012; Vestergaard et al., 2016; Lopez-Causape et al., 2018a), which may imply a large degree of stochasticity in the evolutionary trajectories, mutation-driven evolution toward resistance is partially deterministic, at least when bacteria grow in the same conditions. This opens up the possibility of predicting the appearance of antibiotic resistance (Martinez et al., 2007).

The selection of specific mutations depends primarily on the fitness of each mutant before/after selection and the rate of mutation supply for each of the mutations (Huseby et al., 2017; Hughes and Andersson, 2017). Recent work has shown that a high generalized mutation supply does not alter the types of mutations selected upon experimental evolution (Ibacache-Quiroga et al., 2018), in which case fitness costs, together with population bottlenecks (Vogwill et al., 2016), will be the main constraints for selecting some mutants over other mutations able of providing the same resistance phenotype. However, the situation might be different in the case of gene-specific high mutation rates, a situation that might have happened in the case of *orfN*. To note here that all mutations in *orfN* have been selected in a poly-G region, present in the *P. aeruginosa* PA14 strain, a situation that might increase the mutation rate as the consequence of polymerase slippage (Moxon et al., 2006). We hypothesize that this gene-specific high mutational supply might be in the basis of the presence of *orfN* mutants in all replicates. However, *OrfN* sequence is highly polymorphic in *P. aeruginosa* (Arora et al., 2004) becoming doubtful if these results can be extrapolated to strains with different *orfN* alleles.

The present results clearly show that challenging *P. aeruginosa* with tigecycline has clinically relevant consequences, despite this bacterial pathogen is considered to be intrinsically resistant to this antibiotic. Tigecycline is used for empiric treatment of Gram-negative infections, and in this type of patients, the main agent causing superinfection is *P. aeruginosa* (García-Cabrera et al., 2010; Ulu-Kilic et al., 2015; Katsiari et al., 2016), which is most likely under tigecycline selection during treatment. Our results indicate that tigecycline selects mutants presenting reduced susceptibility to antibiotics of clinical value as aztreonam, ceftazidime, ciprofloxacin or aminoglycosides. Notably, these mutants also display an increased susceptibility to fosfomycin. Our results suggest that fosfomycin might be an antibiotic of choice for treating superinfections by *P. aeruginosa* in tigecycline treated patients. A recent work has shown that

most antibiotic resistance mutations display strain-independent phenotypes (Knopp and Andersson, 2018). Nevertheless, it is also true that the current work has been performed with a single, model strain and, because of the diversity of *P. aeruginosa*, it would be important to examine additional strains to establish whether this phenotype depends on the genomic context or can be extrapolated to other *P. aeruginosa* clinical isolates.

Antibiotic resistance can be acquired by the acquisition of antibiotic resistance genes, which usually confer resistance to members of the same family of antibiotics. However, particularly relevant in the case of chronic infections is the selection of antibiotic resistant mutants. Our results indicate that antibiotic resistance mutations frequently have a pleiotropic effect, altering susceptibility to other drugs. In agreement with this is the fact that some of the mutations selected for by exposure to tobramycin or tigecycline have previously been described to confer resistance to other antibiotics belonging to different structural families.

AUTHOR CONTRIBUTIONS

FS-G and SH-A performed the experiments. JM and SH-A designed the work. All the authors participated in the interpretation of the results and in writing the article.

FUNDING

Work in our laboratory is supported by grants from the Instituto de Salud Carlos III (Spanish Network for Research on Infectious Diseases [RD16/0016/0011]), from the Spanish Ministry of Economy and Competitiveness (BIO2017-83128-R and BIO2014-54507-R) CNB, and from the Autonomous Community of Madrid (B2017/BMD-3691). FS-G is the recipient of an FPU fellowship from the Spanish Ministry of Education. The funders had no role in study design, data collection and interpretation, or the decision to submit the work for publication.

ACKNOWLEDGMENTS

We thank Adrian Burton (www.physicalevidence.es) for editing the manuscript.

SUPPLEMENTARY MATERIAL

The Supplementary Material for this article can be found online at: <https://www.frontiersin.org/articles/10.3389/fgene.2018.00451/full#supplementary-material>

REFERENCES

- Ahn, C., Yoon, S. S., Yong, T. S., Jeong, S. H., and Lee, K. (2016). The resistance mechanism and clonal distribution of tigecycline-nonsusceptible *Klebsiella pneumoniae* isolates in Korea. *Yonsei Med. J.* 57, 641–646. doi: 10.3349/ymj.2016.57.3.641
- Akiba, K., Ando, T., Isogai, E., Nakae, T., and Yoneyama, H. (2013). Tat pathway-mediated translocation of the Sec pathway substrate OprM, an outer membrane subunit of the resistance nodulation division xenobiotic extrusion pumps, in *Pseudomonas aeruginosa*. *Chemotherapy* 59, 129–137. doi: 10.1159/000353894
- Alvarez-Ortega, C., Wiegand, I., Olivares, J., Hancock, R. E., and Martinez, J. L. (2010). Genetic determinants involved in the susceptibility of *Pseudomonas*

- aeruginosa* to beta-lactam antibiotics. *Antimicrob. Agents Chemother.* 54, 4159–4167. doi: 10.1128/AAC.00257-10
- Alvarez-Ortega, C., Wiegand, I., Olivares, J., Hancock, R. E., and Martinez, J. L. (2011). The intrinsic resistome of *Pseudomonas aeruginosa* to beta-lactams. *Virulence* 2, 144–146.
- Appelbaum, P. C. (2012). 2012 and beyond: potential for the start of a second pre-antibiotic era? *J. Antimicrob. Chemother.* 67, 2062–2068. doi: 10.1093/jac/dks213
- Arora, S. K., Wolfgang, M. C., Lory, S., and Ramphal, R. (2004). Sequence polymorphism in the glycosylation island and flagellins of *Pseudomonas aeruginosa*. *J. Bacteriol.* 186, 2115–2122.
- Blair, J. M., Bavro, V. N., Ricci, V., Modi, N., Cacciottio, P., Kleinekathfer, U., et al. (2015). AcrB drug-binding pocket substitution confers clinically relevant resistance and altered substrate specificity. *Proc. Natl. Acad. Sci. U.S.A.* 112, 3511–3516. doi: 10.1073/pnas.1419939112
- Blake, K. L., and O'Neill, A. J. (2013). Transposon library screening for identification of genetic loci participating in intrinsic susceptibility and acquired resistance to antistaphylococcal agents. *J. Antimicrob. Chemother.* 68, 12–16. doi: 10.1093/jac/dks373
- Bolard, A., Plesiat, P., and Jeannot, K. (2018). Mutations in gene *fusA1* as a novel mechanism of aminoglycoside resistance in clinical strains of *Pseudomonas aeruginosa*. *Antimicrob. Agents Chemother.* 62:e01835-17. doi: 10.1128/aac.01835-17
- Brandis, G., Pietsch, F., Alemayehu, R., and Hughes, D. (2015). Comprehensive phenotypic characterization of rifampicin resistance mutations in *Salmonella* provides insight into the evolution of resistance in *Mycobacterium tuberculosis*. *J. Antimicrob. Chemother.* 70, 680–685. doi: 10.1093/jac/dku434
- Breidenstein, E. B., Khaira, B. K., Wiegand, I., Overhage, J., and Hancock, R. E. (2008). Complex ciprofloxacin resistome revealed by screening a *Pseudomonas aeruginosa* mutant library for altered susceptibility. *Antimicrob. Agents Chemother.* 52, 4486–4491. doi: 10.1128/AAC.00222-08
- Bryson, V., and Szybalski, W. (1952). Microbial selection. *Science* 116, 45–51. doi: 10.1126/science.116.3003.45
- Cabot, G., Zamorano, L., Moya, B., Juan, C., Navas, A., Blázquez, J., et al. (2016). Evolution of *Pseudomonas aeruginosa* antimicrobial resistance and fitness under low and high mutation rates. *Antimicrob. Agents Chemother.* 60, 1767–1778. doi: 10.1128/AAC.02676-15
- Chaudhary, A. S., Chen, W., Jin, J., Tai, P. C., and Wang, B. (2015). SecA: a potential antimicrobial target. *Future Med. Chem.* 7, 989–1007. doi: 10.4155/fmc.15.42
- Cheer, S. M., Waugh, J., and Noble, S. (2003). Inhaled tobramycin (TOBI): a review of its use in the management of *Pseudomonas aeruginosa* infections in patients with cystic fibrosis. *Drugs* 63, 2501–2520.
- De Kievit, T. R., Parkins, M. D., Gillis, R. J., Srikumar, R., Ceri, H., Poole, K., et al. (2001). Multidrug efflux pumps: expression patterns and contribution to antibiotic resistance in *Pseudomonas aeruginosa* biofilms. *Antimicrob. Agents Chemother.* 45, 1761–1770.
- Dean, C. R., Visalli, M. A., Projan, S. J., Sum, P. E., and Bradford, P. A. (2003). Efflux-mediated resistance to tigecycline (GAR-936) in *Pseudomonas aeruginosa* PAO1. *Antimicrob. Agents Chemother.* 47, 972–978.
- Elkins, C. A., and Nikaido, H. (2002). Substrate specificity of the RND-type multidrug efflux pumps AcrB and AcrD of *Escherichia coli* is determined predominantly by two large periplasmic loops. *J. Bacteriol.* 184, 6490–6498.
- Fajardo, A., Martinez-Martin, N., Mercadillo, M., Galan, J. C., Ghysels, B., Matthijs, S., et al. (2008). The neglected intrinsic resistome of bacterial pathogens. *PLoS One* 3:e1619. doi: 10.1371/journal.pone.0001619
- Feng, Y., Jonker, M. J., Moustakas, I., Brul, S., and Ter Kuile, B. H. (2016). Dynamics of mutations during development of resistance by *Pseudomonas aeruginosa* against five antibiotics. *Antimicrob. Agents Chemother.* 60, 4229–4236. doi: 10.1128/AAC.00434-16
- Fernandez, L., Alvarez-Ortega, C., Wiegand, I., Olivares, J., Kocincova, D., Lam, J. S., et al. (2013). Characterization of the polymyxin B resistome of *Pseudomonas aeruginosa*. *Antimicrob. Agents Chemother.* 57, 110–119. doi: 10.1128/AAC.01583-12
- Fernández, L., Gooderham, W. J., Bains, M., McPhee, J. B., Wiegand, I., and Hancock, R. E. (2010). Adaptive resistance to the “last hope” antibiotics polymyxin B and colistin in *Pseudomonas aeruginosa* is mediated by the novel two-component regulatory system ParR-ParS. *Antimicrob. Agents Chemother.* 54, 3372–3382. doi: 10.1128/AAC.00242-10
- García-Cabrera, E., Jimenez-Mejias, M. E., Gil Navarro, M. V., Gomez-Gomez, M. J., Ortiz-Leyba, C., Cordero, E., et al. (2010). Superinfection during treatment of nosocomial infections with tigecycline. *Eur. J. Clin. Microbiol. Infect. Dis.* 29, 867–871. doi: 10.1007/s10096-010-0942-y
- Guenard, S., Muller, C., Monlezun, L., Benas, P., Broutin, L., Jeannot, K., et al. (2014). Multiple mutations lead to MexXY-OprM-dependent aminoglycoside resistance in clinical strains of *Pseudomonas aeruginosa*. *Antimicrob. Agents Chemother.* 58, 221–228. doi: 10.1128/aac.01252-13
- Gunn, J. S., Ryan, S. S., Van Velkinburgh, J. C., Ernst, R. K., and Miller, S. I. (2000). Genetic and functional analysis of a PmrA-PmrB-regulated locus necessary for lipopolysaccharide modification, antimicrobial peptide resistance, and oral virulence of *Salmonella enterica* serovar typhimurium. *Infect. Immun.* 68, 6139–6146.
- Hernando-Amado, S., Sanz-Garcia, F., Blanco, P., and Martinez, J. L. (2017). Fitness costs associated with the acquisition of antibiotic resistance. *Essays Biochem.* 61, 37–48. doi: 10.1042/ebc20160057
- Hickman, J. W., and Harwood, C. S. (2008). Identification of FleQ from *Pseudomonas aeruginosa* as a c-di-GMP-responsive transcription factor. *Mol. Microbiol.* 69, 376–389. doi: 10.1111/j.1365-2958.2008.06281.x
- Hu, M., Nandi, S., Davies, C., and Nicholas, R. A. (2005). High-level chromosomally mediated tetracycline resistance in *Neisseria gonorrhoeae* results from a point mutation in the *rpsJ* gene encoding ribosomal protein S10 in combination with the *mtrR* and *penB* resistance determinants. *Antimicrob. Agents Chemother.* 49, 4327–4334. doi: 10.1128/AAC.49.10.4327-4334.2005
- Hughes, D., and Andersson, D. I. (2017). Evolutionary trajectories to antibiotic resistance. *Annu. Rev. Microbiol.* 71, 579–596. doi: 10.1146/annurev-micro-090816-093813
- Huseby, D. L., Pietsch, F., Brandis, G., Garoff, L., Tegehall, A., and Hughes, D. (2017). Mutation supply and relative fitness shape the genotypes of ciprofloxacin-resistant *Escherichia coli*. *Mol. Biol. Evol.* 34, 1029–1039. doi: 10.1093/molbev/msx052
- Ibacache-Quiroga, C., Oliveros, J. C., Couce, A., and Blázquez, J. (2018). Parallel evolution of high-level aminoglycoside resistance in *Escherichia coli* under low and high mutation supply rates. *Front. Microbiol.* 9:427. doi: 10.3389/fmicb.2018.00427
- Jimenez, P. N., Koch, G., Thompson, J. A., Xavier, K. B., Cool, R. H., and Quax, W. J. (2012). The multiple signaling systems regulating virulence in *Pseudomonas aeruginosa*. *Microbiol. Mol. Biol. Rev.* 76, 46–65. doi: 10.1128/MMBR.05007-11
- Jin, J., Hsieh, Y. H., Cui, J., Damera, K., Dai, C., Chaudhary, A. S., et al. (2016). Using chemical probes to assess the feasibility of targeting *secA* for developing antimicrobial agents against gram-negative bacteria. *ChemMedChem* 11, 2511–2521. doi: 10.1002/cmdc.201600421
- Jochimsen, N., Marvig, R. L., Damkiaer, S., Jensen, R. L., Paulander, W., Molin, S., et al. (2016). The evolution of antimicrobial peptide resistance in *Pseudomonas aeruginosa* is shaped by strong epistatic interactions. *Nat. Commun.* 7:13002. doi: 10.1038/ncomms13002
- Katsiari, M., Ntoulis, K., Nteves, I., Roussou, Z., Platsouka, E. D., and Maguina, A. (2016). Characteristics of superinfections during treatment with tigecycline. *J. Chemother.* 28, 110–115. doi: 10.1080/1120009x.2015.1118184
- Kazmierczak, M. J., Wiedmann, M., and Boor, K. J. (2005). Alternative sigma factors and their roles in bacterial virulence. *Microbiol. Mol. Biol. Rev.* 69, 527–543. doi: 10.1128/MMBR.69.4.527-543.2005
- Knopp, M., and Andersson, D. I. (2018). Predictable phenotypes of antibiotic resistance mutations. *mBio* 9:e00770-18. doi: 10.1128/mBio.00770-18
- Kotra, L. P., Haddad, J., and Mobashery, S. (2000). Aminoglycosides: perspectives on mechanisms of action and resistance and strategies to counter resistance. *Antimicrob. Agents Chemother.* 44, 3249–3256.
- Lässig, M., Mustonen, V., and Walczak, A. M. (2017). Predicting evolution. *Nat. Ecol. Evol.* 1:77. doi: 10.1038/s41559-017-0077
- Levin, B. R., and Rozen, D. E. (2006). Non-inherited antibiotic resistance. *Nat. Rev. Microbiol.* 4, 556–562.
- Lind, P. A., Farr, A. D., and Rainey, P. B. (2015). Experimental evolution reveals hidden diversity in evolutionary pathways. *eLife* 4:e07074. doi: 10.7554/eLife.07074
- Livak, K. J., and Schmittgen, T. D. (2001). Analysis of relative gene expression data using real-time quantitative PCR and the 2^{-ΔΔC_T} Method. *Methods* 25, 402–408.

- Lloyd, M. G., Lundgren, B. R., Hall, C. W., Gagnon, L. B., Mah, T. F., Moffat, J. F., et al. (2017). Targeting the alternative sigma factor RpoN to combat virulence in *Pseudomonas aeruginosa*. *Sci. Rep.* 7:12615. doi: 10.1038/s41598-017-12667-y
- Lopez-Causape, C., Cabot, G., Del Barrio-Tofino, E., and Oliver, A. (2018a). The versatile mutational resistome of *Pseudomonas aeruginosa*. *Front. Microbiol.* 9:685. doi: 10.3389/fmicb.2018.00685
- Lopez-Causape, C., Rubio, R., Cabot, G., and Oliver, A. (2018b). Evolution of the *Pseudomonas aeruginosa* aminoglycoside mutational resistome in vitro and in the cystic fibrosis setting. *Antimicrob. Agents Chemother.* 62:e02583-17. doi: 10.1128/aac.02583-17
- Martinez, J. L. (2012). The antibiotic resistome: challenge and opportunity for therapeutic intervention. *Future Med. Chem.* 4, 347–359. doi: 10.4155/fmc.12.2
- Martinez, J. L., and Baquero, F. (2000). Mutation frequencies and antibiotic resistance. *Antimicrob. Agents Chemother.* 44, 1771–1777.
- Martinez, J. L., Baquero, F., and Andersson, D. I. (2007). Predicting antibiotic resistance. *Nat. Rev. Microbiol.* 5, 958–965.
- Martinez, J. L., Baquero, F., and Andersson, D. I. (2011). Beyond serial passages: new methods for predicting the emergence of resistance to novel antibiotics. *Curr. Opin. Pharmacol.* 11, 439–445. doi: 10.1016/j.coph.2011.07.005
- Martinez, J. L., Coque, T. M., and Baquero, F. (2015). What is a resistance gene? Ranking risk in resistomes. *Nat. Rev. Microbiol.* 13, 116–123. doi: 10.1038/nrmicro3399
- Martinez, J. L., Fajardo, A., Garmendia, L., Hernandez, A., Linares, J. F., Martinez-Solano, L., et al. (2009). A global view of antibiotic resistance. *FEMS Microbiol. Rev.* 33, 44–65. doi: 10.1111/j.1574-6976.2008.00142.x
- Martinez, J. L., and Rojo, F. (2011). Metabolic regulation of antibiotic resistance. *FEMS Microbiol. Rev.* 35, 768–789. doi: 10.1111/j.1574-6976.2011.00282.x
- Martinez-Solano, L., Macia, M. D., Fajardo, A., Oliver, A., and Martinez, J. L. (2008). Chronic *Pseudomonas aeruginosa* infection in chronic obstructive pulmonary disease. *Clin. Infect. Dis.* 47, 1526–1533. doi: 10.1086/593186
- Masuda, N., Sakagawa, E., Ohya, S., Gotoh, N., Tsujimoto, H., and Nishino, T. (2000a). Contribution of the MexX-MexY-oprM efflux system to intrinsic resistance in *Pseudomonas aeruginosa*. *Antimicrob. Agents Chemother.* 44, 2242–2246.
- Masuda, N., Sakagawa, E., Ohya, S., Gotoh, N., Tsujimoto, H., and Nishino, T. (2000b). Substrate specificities of MexAB-OprM, MexCD-OprJ, and MexXY-oprM efflux pumps in *Pseudomonas aeruginosa*. *Antimicrob. Agents Chemother.* 44, 3322–3327.
- Matsuyama, B. Y., Krasteva, P. V., Baraquet, C., Harwood, C. S., Sondermann, H., and Navarro, M. V. (2016). Mechanistic insights into c-di-GMP-dependent control of the biofilm regulator FleQ from *Pseudomonas aeruginosa*. *Proc. Natl. Acad. Sci. U.S.A.* 113, E209–E218. doi: 10.1073/pnas.1523148113
- Meftahi, N., Namouchi, A., Mhenni, B., Brandis, G., Hughes, D., and Mardassi, H. (2016). Evidence for the critical role of a secondary site rpoB mutation in the compensatory evolution and successful transmission of an MDR tuberculosis outbreak strain. *J. Antimicrob. Chemother.* 71, 324–332. doi: 10.1093/jac/dkv345
- Moskowitz, S. M., Brannon, M. K., Dasgupta, N., Pier, M., Sgambati, N., Miller, A. K., et al. (2012). PmrB mutations promote polymyxin resistance of *Pseudomonas aeruginosa* isolated from colistin-treated cystic fibrosis patients. *Antimicrob. Agents Chemother.* 56, 1019–1030. doi: 10.1128/AAC.05829-11
- Moxon, R., Bayliss, C., and Hood, D. (2006). Bacterial contingency loci: the role of simple sequence DNA repeats in bacterial adaptation. *Annu. Rev. Genet.* 40, 307–333. doi: 10.1146/annurev.genet.40.110405.090442
- Mulet, X., Maciá, M. D., Mena, A., Juan, C., Pérez, J. L., and Oliver, A. (2009). Azithromycin in *Pseudomonas aeruginosa* biofilms: bactericidal activity and selection of nfxB mutants. *Antimicrob. Agents Chemother.* 53, 1552–1560. doi: 10.1128/aac.01264-08
- Muller, C., Plesiat, P., and Jeannot, K. (2011). A two-component regulatory system interconnects resistance to polymyxins, aminoglycosides, fluoroquinolones, and beta-lactams in *Pseudomonas aeruginosa*. *Antimicrob. Agents Chemother.* 55, 1211–1221. doi: 10.1128/aac.01252-10
- Palmer, G. C., and Whiteley, M. (2015). Metabolism and pathogenicity of *Pseudomonas aeruginosa* infections in the lungs of individuals with cystic fibrosis. *Microbiol. Spectr.* 3. doi: 10.1128/microbiolspec.MBP-0003-2014
- Pankey, G. A. (2005). Tigecycline. *J. Antimicrob. Chemother.* 56, 470–480. doi: 10.1093/jac/dki248
- Pietsch, F., Bergman, J. M., Brandis, G., Marcusson, L. L., Zorzet, A., Huseby, D. L., et al. (2017). Ciprofloxacin selects for RNA polymerase mutations with pleiotropic antibiotic resistance effects. *J. Antimicrob. Chemother.* 72, 75–84. doi: 10.1093/jac/dkw364
- Purssell, A., and Poole, K. (2013). Functional characterization of the NfxB repressor of the mexCD-oprJ multidrug efflux operon of *Pseudomonas aeruginosa*. *Microbiology* 159(Pt 10), 2058–2073. doi: 10.1099/mic.0.069286-0
- Roca, I., Akova, M., Baquero, F., Carlet, J., Cavaleri, M., Coenen, S., et al. (2015). The global threat of antimicrobial resistance: science for intervention. *New Microbes New Infect.* 6, 22–29. doi: 10.1016/j.nmni.2015.02.007
- Schirm, M., Arora, S. K., Verma, A., Vinogradov, E., Thibault, P., Ramphal, R., et al. (2004). Structural and genetic characterization of glycosylation of type a flagellin in *Pseudomonas aeruginosa*. *J. Bacteriol.* 186, 2523–2531.
- Schurek, K. N., Marr, A. K., Taylor, P. K., Wiegand, I., Semenc, L., Khaira, B. K., et al. (2008). Novel genetic determinants of low-level aminoglycoside resistance in *Pseudomonas aeruginosa*. *Antimicrob. Agents Chemother.* 52, 4213–4219. doi: 10.1128/AAC.00507-08
- Scortti, M., Lacharme-Lora, L., Wagner, M., Chico-Calero, I., Losito, P., and Vázquez-Boland, J. A. (2006). Coexpression of virulence and fosfomycin susceptibility in *Listeria*: molecular basis of an antimicrobial in vitro-in vivo paradox. *Nat. Med.* 12, 515–517.
- Shcherbakov, D., Akbergenov, R., Matt, T., Sander, P., Andersson, D. I., and Böttger, E. C. (2010). Directed mutagenesis of *Mycobacterium smegmatis* 16S rRNA to reconstruct the in-vivo evolution of aminoglycoside resistance in *Mycobacterium tuberculosis*. *Mol. Microbiol.* 77, 830–840. doi: 10.1111/j.1365-2958.2010.07218.x
- Silby, M. W., Winstanley, C., Godfrey, S. A., Levy, S. B., and Jackson, R. W. (2011). *Pseudomonas* genomes: diverse and adaptable. *FEMS Microbiol. Rev.* 35, 652–680. doi: 10.1111/j.1574-6976.2011.00269.x
- Tamae, C., Liu, A., Kim, K., Sitz, D., Hong, J., Becket, E., et al. (2008). Determination of antibiotic hypersensitivity among 4,000 single-gene-knockout mutants of *Escherichia coli*. *J. Bacteriol.* 190, 5981–5988. doi: 10.1128/JB.01982-07
- Toprak, E., Veres, A., Michel, J. B., Chait, R., Hartl, D. L., and Kishony, R. (2011). Evolutionary paths to antibiotic resistance under dynamically sustained drug selection. *Nat. Genet.* 44, 101–105. doi: 10.1038/ng.1034
- Tummler, B., Wiehlmann, L., Klockgether, J., and Cramer, N. (2014). Advances in understanding *Pseudomonas*. *F1000Prime Rep.* 6:9. doi: 10.12703/P6-9
- Turrientes, M. C., Baquero, F., Levin, B. R., Martinez, J. L., Ripoll, A., Gonzalez-Alba, J. M., et al. (2013). Normal mutation rate variants arise in a Mutator (Mut S) *Escherichia coli* population. *PLoS One* 8:e72963. doi: 10.1371/journal.pone.0072963
- Ulu-Kilic, A., Alp, E., Altun, D., Cevahir, F., Kalın, G., and Demiraslan, H. (2015). Increasing frequency of *Pseudomonas aeruginosa* infections during tigecycline use. *J. Infect. Dev. Ctries.* 9, 309–312. doi: 10.3855/jidc.4700
- Vestergaard, M., Leng, B., Haaber, J., Bojer, M. S., Vegge, C. S., and Ingmer, H. (2016). Genome-wide identification of antimicrobial intrinsic resistance determinants in *Staphylococcus aureus*. *Front. Microbiol.* 7:2018. doi: 10.3389/fmicb.2016.02018
- Viducic, D., Murakami, K., Amoh, T., Ono, T., and Miyake, Y. (2016). RpoN modulates carbapenem tolerance in *Pseudomonas aeruginosa* through *Pseudomonas* quinolone signal and PqsE. *Antimicrob. Agents Chemother.* 60, 5752–5764. doi: 10.1128/aac.00260-16
- Viducic, D., Murakami, K., Amoh, T., Ono, T., and Miyake, Y. (2017). RpoN promotes *Pseudomonas aeruginosa* survival in the presence of tobramycin. *Front. Microbiol.* 8:839. doi: 10.3389/fmicb.2017.00839
- Viducic, D., Ono, T., Murakami, K., Katakami, M., Susilowati, H., and Miyake, Y. (2007). rpoN gene of *Pseudomonas aeruginosa* alters its susceptibility to quinolones and carbapenems. *Antimicrob. Agents Chemother.* 51, 1455–1462. doi: 10.1128/AAC.00348-06
- Vogne, C., Aires, J. R., Bailly, C., Hocquet, D., and Plesiat, P. (2004). Role of the multidrug efflux system MexXY in the emergence of moderate resistance to aminoglycosides among *Pseudomonas aeruginosa* isolates from patients with cystic fibrosis. *Antimicrob. Agents Chemother.* 48, 1676–1680.
- Vogwill, T., Phillips, R. L., Gifford, D. R., and MacLean, R. C. (2016). Divergent evolution peaks under intermediate population bottlenecks during bacterial experimental evolution. *Proc. Biol. Sci.* 283:20160749. doi: 10.1098/rspb.2016.0749

- Wang, D., Dorosky, R. J., Han, C. S., Lo, C. C., Dichosa, A. E., Chain, P. S., et al. (2015). Adaptation genomics of a small-colony variant in a *Pseudomonas chlororaphis* 30-84 biofilm. *Appl. Environ. Microbiol.* 81, 890–899. doi: 10.1128/AEM.02617-14
- Westbrock-Wadman, S., Sherman, D. R., Hickey, M. J., Coulter, S. N., Zhu, Y. Q., Warrener, P., et al. (1999). Characterization of a *Pseudomonas aeruginosa* efflux pump contributing to aminoglycoside impermeability. *Antimicrob. Agents Chemother.* 43, 2975–2983.
- Wong, A., Rodrigue, N., and Kassen, R. (2012). Genomics of adaptation during experimental evolution of the opportunistic pathogen *Pseudomonas aeruginosa*. *PLoS Genet.* 8:e1002928. doi: 10.1371/journal.pgen.1002928
- Yoneyama, H., Akiba, K., Hori, H., Ando, T., and Nakae, T. (2010). Tat pathway-mediated translocation of the sec pathway substrate protein MexA, an inner membrane component of the MexAB-OprM xenobiotic extrusion pump in *Pseudomonas aeruginosa*. *Antimicrob. Agents Chemother.* 54, 1492–1497. doi: 10.1128/aac.01495-09
- Conflict of Interest Statement:** The authors declare that the research was conducted in the absence of any commercial or financial relationships that could be construed as a potential conflict of interest.
- Copyright © 2018 Sanz-García, Hernando-Amado and Martínez. This is an open-access article distributed under the terms of the Creative Commons Attribution License (CC BY). The use, distribution or reproduction in other forums is permitted, provided the original author(s) and the copyright owner(s) are credited and that the original publication in this journal is cited, in accordance with accepted academic practice. No use, distribution or reproduction is permitted which does not comply with these terms.



Insights Into the Evolution of *Staphylococcus aureus* Daptomycin Resistance From an *in vitro* Bioreactor Model

Erica Lasek-Nesselquist^{1*}, Jackson Lu², Ryan Schneider³, Zhuo Ma², Vincenzo Russo², Smruti Mishra², Manjunath P. Pai⁴, Janice D. Pata^{1,3}, Kathleen A. McDonough^{1,3} and Meenakshi Malik²

¹ Wadsworth Center, New York State Department of Health, Albany, NY, United States, ² Albany College of Pharmacy and Health Sciences, Albany, NY, United States, ³ Department of Biomedical Sciences, University at Albany, School of Public Health, Albany, NY, United States, ⁴ Department of Clinical Pharmacy, University of Michigan, Ann Arbor, MI, United States

OPEN ACCESS

Edited by:

Simona Pollini,
Università degli Studi di Firenze, Italy

Reviewed by:

Soojin Yang,
Chung-Ang University, South Korea
Juan M. Pericas,
University Hospital Arnau de Vilanova,
Spain

*Correspondence:

Erica Lasek-Nesselquist
erica.lasek-nesselquist@health.ny.gov

Specialty section:

This article was submitted to
Evolutionary and Genomic
Microbiology,
a section of the journal
Frontiers in Microbiology

Received: 24 July 2018

Accepted: 08 February 2019

Published: 28 February 2019

Citation:

Lasek-Nesselquist E, Lu J, Schneider R, Ma Z, Russo V, Mishra S, Pai MP, Pata JD, McDonough KA and Malik M (2019) Insights Into the Evolution of *Staphylococcus aureus* Daptomycin Resistance From an *in vitro* Bioreactor Model. *Front. Microbiol.* 10:345. doi: 10.3389/fmicb.2019.00345

The extensive use of daptomycin for treating complex methicillin-resistant *Staphylococcus aureus* infections has led to the emergence of daptomycin-resistant strains. Although genomic studies have identified mutations associated with daptomycin resistance, they have not necessarily provided insight into the evolution and hierarchy of genetic changes that confer resistance, particularly as antibiotic concentrations are increased. Additionally, plate-dependent *in vitro* analyses that passage bacteria in the presence of antibiotics can induce selective pressures unrelated to antibiotic exposure. We established a continuous culture bioreactor model that exposes *S. aureus* strain N315 to increasing concentrations of daptomycin without the confounding effects of nutritional depletion to further understand the evolution of drug resistance and validate the bioreactor as a method that produces clinically relevant results. Samples were collected every 24 h for a period of 14 days and minimum inhibitory concentrations were determined to monitor the acquisition of daptomycin resistance. The collected samples were then subjected to whole genome sequencing. The development of daptomycin resistance in N315 was associated with previously identified mutations in genes coding for proteins that alter cell membrane charge and composition. Although genes involved in metabolic functions were also targets of mutation, the common route to resistance relied on a combination of mutations at a few key loci. Tracking the frequency of each mutation throughout the experiment revealed that mutations need not arise progressively in response to increasing antibiotic concentrations and that most mutations were present at low levels within populations earlier than would be recorded based on single-nucleotide polymorphism (SNP) filtering criteria. In contrast, a serial-passaged population showed only one mutation in a gene associated with resistance and provided limited detail on the changes that occur upon exposure to higher drug dosages. To conclude, this study demonstrates the successful *in vitro* modeling of antibiotic resistance in a bioreactor and highlights the evolutionary paths associated with the acquisition of daptomycin non-susceptibility.

Keywords: *Staphylococcus aureus*, bioreactor culture, daptomycin, whole-genome sequencing analysis, evolution of resistance

INTRODUCTION

Staphylococcus aureus is one of the pathogens most commonly associated with both community and hospital acquired infections (Chambers and DeLeo, 2009; Leclercq, 2009; Patel, 2009). Antibiotic management of infections caused by *S. aureus* is complicated by the emergence of methicillin resistant *S. aureus* (MRSA), vancomycin intermediate *S. aureus* (VISA), and vancomycin resistant *S. aureus* (VRSA) (Chambers and DeLeo, 2009; Howden et al., 2010; Bayer et al., 2013). More recently, daptomycin nonsusceptible (according to Clinical Laboratory Standards Institute 2016 guidelines) strains of *S. aureus* (herein referred to as DAP resistant or DAP-R) have emerged as daptomycin increasingly becomes the drug of choice for infections caused by MRSA and VISA strains (Marty et al., 2006; Skiest, 2006; Fowler et al., 2007; Jones et al., 2008; Stryjewski and Corey, 2014).

Previous studies have described the acquisition of DAP-R by *S. aureus* as a complex multifactorial process (Chen et al., 2015; Tran et al., 2015; Kang et al., 2017), with contributions from expression changes and mutations in genes involved in cell wall and cell membrane homeostasis (Friedman et al., 2006; Camargo et al., 2008; Yang et al., 2009; Fischer et al., 2011; Patel et al., 2011; Bayer et al., 2014, 2015; Capone et al., 2016; Kang et al., 2017; Ma et al., 2018; Sabat et al., 2018). The majority of these studies characterized transcriptional changes and/or genetic mutations in clinical DAP-R isolates of *S. aureus* that emerged as a result of prolonged treatment with (1) daptomycin alone, (2) other antibiotics (typically vancomycin) followed by the administration of daptomycin, or (3) other antibiotics with no daptomycin treatment (Friedman et al., 2006; Murthy et al., 2008; Mishra et al., 2009, 2011, 2014; Yang et al., 2009; Howden et al., 2010; Boyle-Vavra et al., 2011; Fischer et al., 2011; Cameron et al., 2012; Hafer et al., 2012; Peleg et al., 2012; Bayer et al., 2014, 2015; Cafiso et al., 2014; Berti et al., 2015; Gaupp et al., 2015; Capone et al., 2016; Kang et al., 2017; Sabat et al., 2018). Serial passaging of *S. aureus* on plates or liquid culture by exposing the bacteria to fixed concentrations of antibiotic and identifying the associated molecular and/or phenotypic changes represents another strategy employed to elucidate the mechanisms of daptomycin resistance (Silverman et al., 2001; Friedman et al., 2006; Mishra et al., 2009, 2012; Patel et al., 2011; Peleg et al., 2012; Berti et al., 2015; Müller et al., 2018). While these studies identify targets of mutation associated with killing by antibiotics, they only provide a snapshot of the evolutionary process after all mutations have been acquired. In the case of clinical isolates there is no knowledge of which mutations accumulate in response to specific levels of treatment while *in vitro* studies involving serial passage often characterize the response to only a single dose of antibiotic or describe the final DAP-R strain. Similarly, mutations selected in response to vancomycin treatment or other antibiotics do not necessarily represent predominant mutations that would emerge after daptomycin treatment alone. It has been reported that *S. aureus* strains can develop vancomycin heteroresistance which makes them DAP-R despite never having been exposed to daptomycin (Pillai et al., 2007). Therefore, isolates of *S. aureus* that were resistant to other antibiotics prior to acquisition of

DAP-R do not provide the details of DAP-R evolution in a DAP-S population. Better understanding of the evolution of DAP-R in *S. aureus* would derive from a system, such as a bioreactor, where a DAP-S bacterial population grown at a steady state is exposed to increasing concentrations of daptomycin, with mutations responsible for daptomycin resistance identified at each step (Toprak et al., 2011, 2013).

The goals of our study were to establish the bioreactor as a tool for realistically modeling the emergence of drug resistance and to use the bioreactor to further elucidate the evolution of daptomycin resistance in susceptible *S. aureus* populations by overcoming some of the limitations of alternative methods. Our results demonstrate that a continuous culture bioreactor maintains bacterial growth at a steady state while also maintaining the concentration of daptomycin at desired levels. We recovered single nucleotide polymorphisms (SNPs) in genes previously implicated in DAP-R as well as mutations in possible new targets of resistance. In comparison, the serial passaged culture showed only one mutation potentially associated with daptomycin resistance and did not offer the level of insight into mutation frequency fluctuations that the bioreactor populations provided. Our bioreactor results support the hypothesis that resistance at higher daptomycin concentrations requires only a few key changes and that these mutations often emerge much earlier in the history of the population, underscoring the need to examine the path to high minimum inhibitory concentrations (MICs), not just the endpoint.

MATERIALS AND METHODS

Bacteria Parental Strain

Staphylococcus aureus strain N315 (ATCC 29213) obtained from BEI Resources (Catalog No. NR-45898), Manassas, VA, United States (Biodefense and Emerging Infections Research Resources)¹ served as the parental DAP-S strain and was propagated in Mueller Hinton Broth (MHB) (BD BBL™) and frozen in 15% glycerol in 1 ml aliquots for further use. Daptomycin resistant isolates were derived from the parent N315 strain which was consistently exposed to increasing doses of daptomycin in MHB in a bioreactor or in serial passaged flask culture. For every experiment, blood agar plates (Trypticase Soy Agar II with 5% sheep blood, BD Biosciences) were streaked with bacteria from frozen glycerol stocks. After overnight incubation at 37°C with 5% CO₂, a single colony was used to seed the bioreactor or flask culture populations. Three bioreactor replicates (populations A–C) and one serial passaged flask culture experiment (population P) were performed with populations B and C being exposed to 0, 6, 10, and 14 µg/ml daptomycin and populations A and P being exposed to 6 and 10 µg/ml of daptomycin.

Daptomycin

Clinical grade Cubicin® (injectable daptomycin) from a single lot was purchased from Albany Medical Center Outpatient

¹<https://www.beiresources.org/>

Pharmacy, Albany NY, United States. The daptomycin was supplied as 500 mg vials and was reconstituted in sterile water to achieve desired concentrations to be used in various experiments.

Serial Passage Flask Culture

Bacterial flask cultures were grown overnight in MHB supplemented with 50 mg/L calcium and 12.5 mg/L magnesium and adjusted to 10^7 CFU/ml concentration. This served as the 0-h time point. After two hours, the concentration of bacteria was roughly 10^8 CFU/ml at which time 6 μ g/ml daptomycin was added. Both treated and untreated flasks were grown overnight and subsequently plated on 6 μ g/ml daptomycin drug plates. Colonies were isolated, grown overnight, and frozen for further analysis. This process was repeated at 10 μ g/ml daptomycin with the colonies from 6 μ g/ml drug exposure serving as the seed populations.

Bioreactor Culture and Adaptation Conditions

The bioreactor system is a continuous culture system in which the rate of inflow (fresh medium) and outflow (spent medium containing culture) is equal, resulting in a constant volume of 400 ml culture in the vessel. The system maintains the bacterial population in exponential growth at a constant density (except after initial additions of antibiotic), as confirmed by CFU counts and optical densities (ODs) of cultures sampled at different time points. MHB was inoculated with a single colony of *S. aureus* N315 strain and maintained for a period of 14 days at a constant OD₆₀₀ of 0.045 (equivalent to 1×10^7 CFU/ml) in a 400 ml volume by automated dilution of the culture from feed reservoirs in a Sartorius Stedim Biostat A plus bioreactor. Briefly, thawed glycerol stock of N315 was streaked out on blood agar plates. A single colony was picked to inoculate 20 ml of MHB, which was incubated overnight in an orbital shaker at 37°C. The next day, the inoculum was diluted 1:1 to make a 40 ml starting culture of 0.4 OD₆₀₀. The starting culture was added to 360 ml in the bioreactor and then maintained at an OD₆₀₀ of 0.45. Daptomycin was added in step-wise increments at a concentration of 6 μ g/ml after 24 h, 10 μ g/ml after 120 h, and 14 μ g/ml after 220/320 h of growth.

Isolation of DAP-S and DAP-R Isolates

Samples were collected from the bioreactor at 24, 120, and 220/320 h following exposure to 0, 6, 10, and 14 μ g/ml of daptomycin. Samples from population P were collected after exposure to 0, 6, and 10 μ g/ml of daptomycin after 24 h of growth. Stocks of both population-based and single colony-based resistant isolates were made in 15% glycerol and stored at -80°C for further analysis. Colonies were isolated by streaking Mueller-Hinton agar plates supplemented with 50 mg/ml calcium and 6 μ g/ml daptomycin.

Measurement of Bacterial Growth Rate

Isolates were grown in a shaking incubator at 37°C. Aliquots were collected at 2 h intervals for a period of 6–8 h for populations

A–C. Samples from population P were collected at 0, 2, 4, 6, and 24 h starting from the 0-h time point. The aliquots were serially diluted and plated on sheep blood agar plates to quantify bacterial numbers. The plates were incubated at 37°C overnight. The colonies were counted and the results were expressed as log₁₀ CFU/ml.

Antimicrobial Susceptibility Studies

The MIC values were determined for isolates using either Epsilometer test (E test) or broth microdilution method. The MIC was considered to be the lowest concentration of daptomycin required to inhibit the growth of *S. aureus* N315. All susceptibility testing was performed using samples in triplicate and each experiment was repeated at least twice. For E tests, bacterial cultures of isolates were grown to OD₆₀₀ of 0.08–0.09 in 5 ml cation-adjusted MHB (CAMHB) containing 25 mg/ml calcium and 12.5 mg/ml magnesium. Sterile cotton swabs were used to uniformly streak a lawn of each sample on trypticase soy agar plates containing 5% sheep blood. The cultures were allowed to be completely adsorbed. Using sterile tweezers, the E test strips containing varying concentrations of daptomycin (BioMérieux Inc.) were placed on the streaked agar plates. The plates were incubated at 37°C for 18–20 h. The elliptical zones of inhibitions were read to determine the MIC values.

The broth dilution method was performed according to the Clinical Laboratory Standards Institute (CLSI) guidelines. Blood agar plates streaked with bioreactor-derived isolates and a control N315 strain were grown overnight. Single colonies were picked, inoculated in 5 ml CAMHB and grown to achieve an OD₆₀₀ of 0.08–0.09, which corresponds to 1×10^8 CFU/ml. Daptomycin with a starting concentration of 32 μ g/ml was serially diluted two-fold in a sterile 96-well plate to achieve a final concentration of 16, 8, 4, 2, 1, 0.5, 0.25, and 0 μ g/ml. In accordance with the CLSI standards, bacterial suspension diluted to a final concentration of 5.5×10^5 CFU/ml was added to each well of the plate containing varying concentrations of daptomycin. The 96-well plate was incubated for 24 h after which the results were recorded.

DNA Extraction and Whole Genome Sequencing

Bacterial pellets from overnight cultures of the reference *S. aureus* N315 strain, bioreactor-derived isolates and colonies, and serial passaged isolates and colonies were treated with lysostaphin and lysozyme to disrupt the peptidoglycan layer of the cell wall. Genomic DNA was purified using PureLink Genomic DNA Mini Kit (Invitrogen) and samples were sent for whole genome DNA sequencing at Wadsworth Center, New York State Department of Health, Albany, NY, United States. Whole genome sequencing libraries were prepared with the Nextera DNA library preparation kit (Illumina) and sequenced using the standard 500 cycle V2 protocol on an Illumina MiSeq. Whole genome sequences were required to have an average depth of coverage of at least $60 \times$ before analysis.

Identification of Mutations Associated With Daptomycin Resistance

The subroutine BBDuk from BBtools v36.38² quality trimmed raw reads and removed any remaining adaptors with the following parameters: qin = 33, ktrim = r, mink = 11, trimq = 20, minlength = 100, tbp = t, and tpe = t. Sequence libraries for our parent N315 genome and all subsequent populations and clones were reference aligned to the N315 genome from NCBI (Refseq accession number NC_002745.2) with BWA mem v.0.7.5 (Li and Durbin, 2009). SAMtools and BCFtools 0.1.19 (Li and Durbin, 2009; Li, 2011) detected single nucleotide polymorphisms (SNPs) from each reference alignment – considering only base positions with a Phred score ≥ 20 and reads with a minimum mapping score of 20. We further filtered the list of SNPs for each population by only examining mutations at positions covered by a depth of 20 or more reads and where 5% or more of the reads supported the alternative nucleotide. We considered a SNP to be present in colonies if positions were covered by 20 or more reads and 95% or more of the reads supported the alternative nucleotide. The presence of each potential SNP and its quality were confirmed in IGV v.2.3.78 (Robinson et al., 2011; Thorvaldsdóttir et al., 2013) and mutations that occurred in highly variable regions (such as phage insertions) were discarded. Custom designed Python scripts associated mutations with coding or non-coding regions to identify changes potentially involved in daptomycin resistance and to translate codons into amino acids.

Accession numbers for sequence data generated from this project have been deposited in GenBank under the BioProject PRJNA446060 <http://www.ncbi.nlm.nih.gov/bioproject/446060> and SRA accession SRP136646.

RESULTS

Staphylococcus aureus N315 Acquires Resistance to Daptomycin in a Bioreactor

A 35-fold reduction in bacterial viability was observed following the addition of 6 $\mu\text{g/ml}$ concentration of daptomycin that was corroborated by a sudden drop in the OD₆₀₀ values (Figures 1A,B). Bacterial numbers returned to the starting concentration of 1×10^8 CFUs within the next 24 h of growth (Figure 1B) at which time the second bolus of daptomycin at 10 $\mu\text{g/ml}$ was added. The second treatment resulted in a moderate 10-fold drop in bacterial viability, which remained at the same level for next 96–120 h of growth (Figure 1B). An identical pattern for OD₆₀₀ values was also observed (Figure 1A). The addition of the third bolus of 14 $\mu\text{g/ml}$ of daptomycin after 220 h of growth did not reduce bacterial viability. On the contrary, a 5–10-fold increase in bacterial numbers was observed (Figure 1B). Corresponding increases in the MIC values were observed in association with enhanced bacterial viability in response to increasing doses of daptomycin (Figure 1C). In

summary, the parent *S. aureus* was initially sensitive to the smallest dose (6 $\mu\text{g/ml}$) of daptomycin but DAP resistant *S. aureus* emerged, which progressively exhibited an enhanced resistance to increasing exposures of daptomycin.

The Bioreactor Recovers Clinically Relevant Mutations Associated With Daptomycin Resistance

Our parental N315 genome (sequenced after acquisition from BEI but before introduction to the bioreactor or serial passage) deviated from the NCBI N315 strain (NC_002745.2) by eight SNPs, which were present in all bioreactor passaged populations (A–C) and clonal lines (Supplementary Table S1) and the serial passaged population P and its clonal lines (with the exception of the absence of the substitution at position 939485 in population C; Supplementary Table S1).

All three bioreactor populations (A–C) evolved mutations at the phosphatidylglycerol lysyl-transferase *mprF* gene (SA1193) after exposure to daptomycin. Populations B and C also exhibited mutations at the cardiolipin synthase *cls2* locus (SA1891; Table 1). These mutations, as well as the SNPs retrieved from the CDP-diaclycerol-glycerol-3-phosphate 3-phosphatidyltransferase *pgsA* gene (SA0828) and the PAS sensor histidine kinase *walk* (previously *ycgG*) gene (SA0018), have been recorded in clinical or laboratory DAP-R strains (Friedman et al., 2006; Howden et al., 2011; Peleg et al., 2012; Bayer et al., 2015; Chen et al., 2015; Kang et al., 2017). We also detected mutations in the *clpX* gene (SA1498) and the ABC transporter permease gene *vraG* gene (SA0617), which have been shown to vary in response to daptomycin exposure (Cameron et al., 2012; Peleg et al., 2012; Song et al., 2013).

The bioreactor also recovered new mutations that might be candidates for contributing to daptomycin resistance but require further exploration, including the nonsynonymous substitutions in the genes coding for an ATP-dependent helicase and the *pur* operon repressor and an intergenic mutation near the DNA-3-methyladenine glycosylase locus (Table 1). Serial passaged population P showed only three mutations after exposure to 10 $\mu\text{g/ml}$ daptomycin and only the SNP in the *pgsA* gene occurred at a locus previously associated with daptomycin resistance in laboratory strains (Table 1; Peleg et al., 2012).

Frequency Profiles Reveal Early Appearance of Mutations in Bioreactor Experiments

Tracking the frequency of mutations throughout the course of the bioreactor experiments revealed that many SNPs appeared earlier than were identified by our filtering criteria (See example: Figure 2). Mutations present at very low frequencies at no or low daptomycin concentrations were often observed reaching high frequencies at 10 or 14 $\mu\text{g/ml}$ daptomycin in population B. This suggests that variants observed in less than 5% of the population, which did not pass our reporting threshold, actually represent real mutants present in earlier populations (Supplementary Table S2).

²<https://sourceforge.net/projects/bbmap>

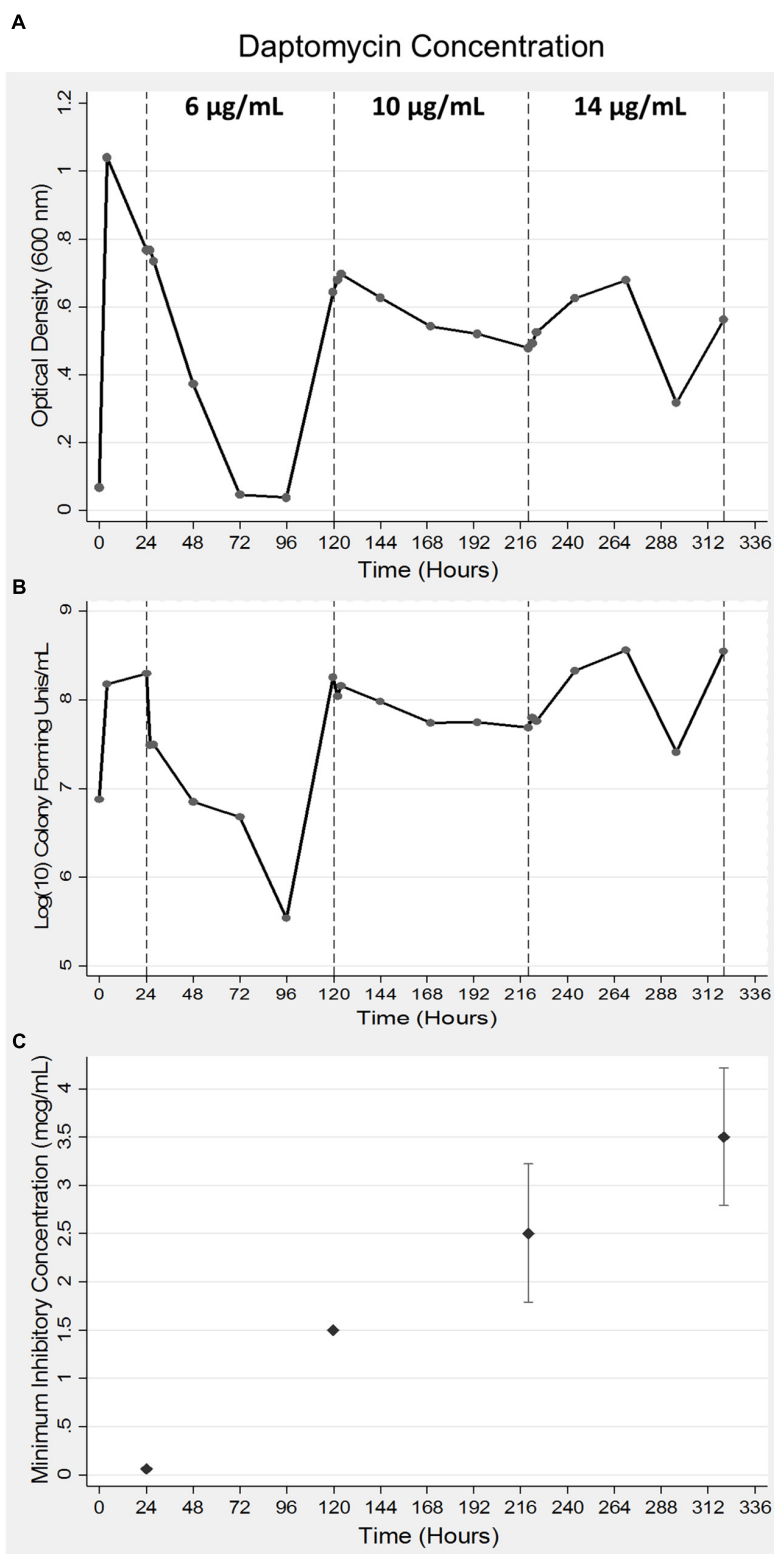


FIGURE 1 | Acquisition of daptomycin resistance in *S. aureus* using a bioreactor model. Bacteria were grown for a period of 24 h after which daptomycin was added at indicated concentrations at 24, 120, and 220 h of growth in a bioreactor. Samples were collected at 24 h intervals to measure optical density at 600 nm (**A**) and bacterial viability was determined by counting CFUs (**B**). The data shown are representative of three independent experiments conducted (**A–C**). The MICs of the bacterial aliquots collected at the indicated times were determined as described in the Methods section (**C**). The data are presented as mean \pm SD and are representative of three independent experiments conducted with two replicates each.

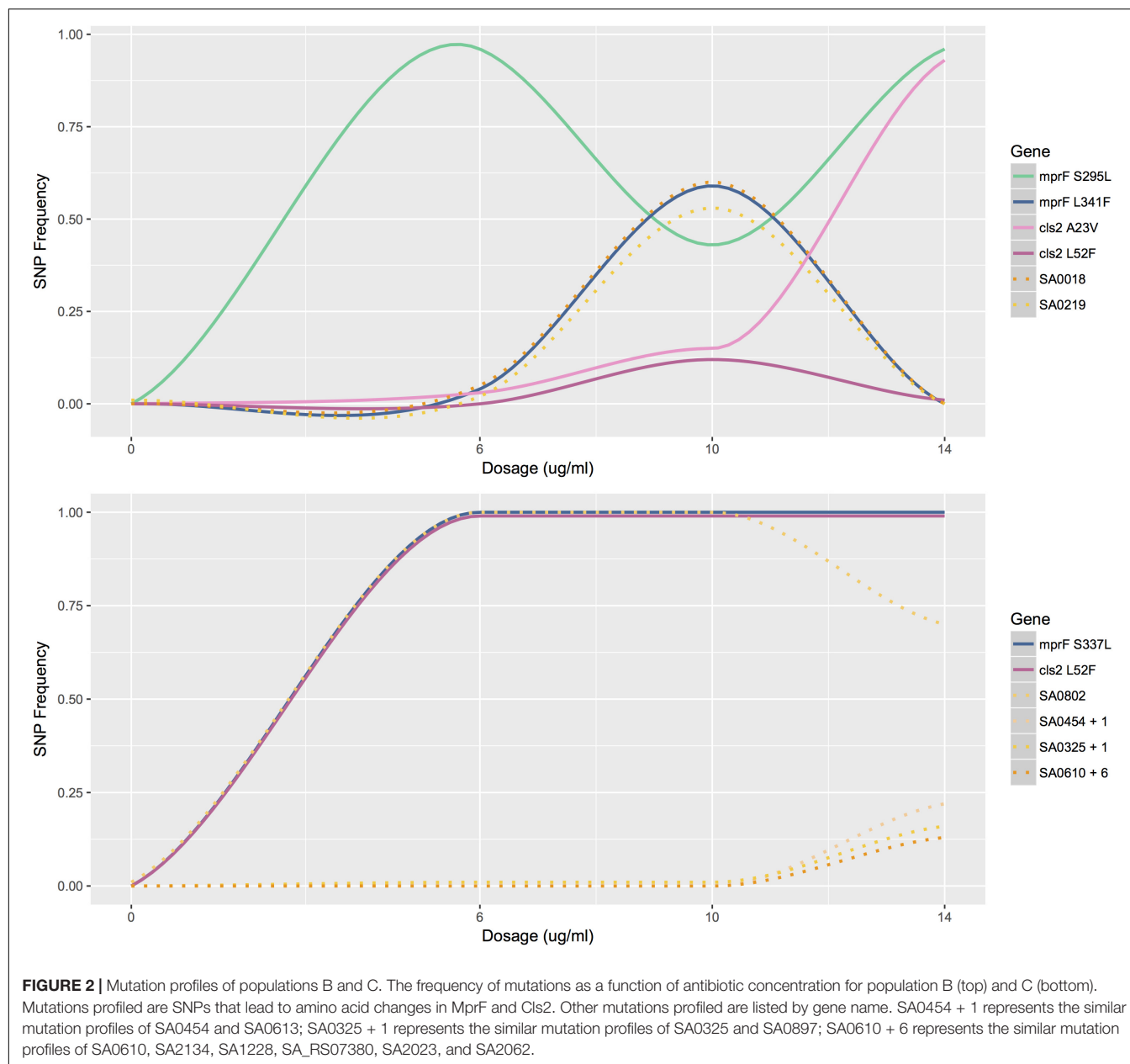
TABLE 1 | SNP acquisition in bioreactor and serial passaged *Staphylococcus aureus* populations exposed to daptomycin.

Pop ^a	DAP exposure ^c	Genome position	Sequence type	Amino acid change	Gene name ^e	Protein product ^f
A	6, 10	1278854	Coding	K135E	SA1126/pgsA	CDP-diacylglycerol-glycerol-3-phosphate 3-phosphatidyltransferase
A	6, 10	1364495	Coding	S295L	SA1193/mprF	phosphatidylglycerol lysyltransferase
A ^b	6	2288162	Noncoding	NA	SA_RS11590	hypothetical protein
B	10	26957	Coding	S437F	SA0018/walK	PAS domain-containing sensor histidine kinase
B	10	261590	Coding	N151N	SA0219	pyruvate formate-lyase-activating enzyme
B	6, 10, 14	863920	Coding	Q221* ^d	SA0756	3-dehydroquinase
B	6, 10, 14	1364495	Coding	S295L	SA1193/mprF	phosphatidylglycerol lysyltransferase
B	6, 10	1364634	Coding	L341F	SA1193/mprF	phosphatidylglycerol lysyltransferase
B	10	1706314	Coding	R364C	SA1498	ATP-dependent Clp protease ATP-binding subunit ClpX
B ^b	10, 14	2143178	Coding	A23V	SA1891/cls2	cardiolipin synthase
B ^b	10	2143266	Coding	L52F	SA1891/cls2	cardiolipin synthase
B	10	2399255	Noncoding	NA	SA2134	DNA-3-methyladenine glycosylase
C ^b	14	382426	Noncoding	NA	SA0325	glycerol-3-phosphate transporter
C	14	525203	Coding	F33V	SA0454	pur operon repressor
C ^b	14	705637	Coding	N320N	SA0610	lipase LipA
C	14	708186	Coding	Q294R	SA0613	3-beta hydroxysteroid dehydrogenase
C ^b	0	710848	Coding	M1R	SA0617/vraG	bacitracin ABC transporter permease
C ^b	14	730798	Noncoding	NA	SA0638	undecaprenyl-diphosphatase
C	6, 10, 14	906481	Coding	G170D	SA0802	NADH dehydrogenase
C	14	1018829	Coding	A223G	SA0897	2-succinyl-6-hydroxy-2,4-cyclohexadiene-1-carboxylate synthase
C	6, 10, 14	1364621	Coding	S337L	SA1193/mprF	phosphatidylglycerol lysyltransferase
C ^b	14	1493152	Coding	D857G	SA1288	ATP-dependent helicase DinG
C ^b	14	1510280	Coding	M25I	SA_RS07380	hypothetical protein
C	6, 10, 14	2143266	Coding	L52F	SA1891/cls2	cardiolipin synthase
C ^b	14	2295261	Coding	C265W	SA2023	DNA-directed RNA polymerase subunit alpha
C ^b	14	2325759	Coding	T106I	SA2062	transcriptional regulator
C ^b	0	2550881	Coding	T142S	SA2275	hypothetical protein
P	10	1278981	Coding	S177F	SA1126/pgsA	CDP-diacylglycerol-glycerol-3-phosphate 3-phosphatidyltransferase
P	10	1295864	Coding	S64I	SA1139	glycerol-3-phosphate-responsive antiterminator
P ^b	10	1300305	Coding	W338* ^d	SA1142	glycerol-3-phosphate dehydrogenase

^aPop, Bioreactor and serial passaged populations; ^bmutations detected in > 5% but < 20% of population as assessed by read depth; ^cDap exposure, the concentration of daptomycin at which the mutation was recorded to have occurred in the population – 0, 0 μ g/ml daptomycin; 6, 6 μ g/ml daptomycin; 10, 10 μ g/ml daptomycin; 14, 14 μ g/ml daptomycin; ^dchange to a stop codon; ^eGene abbreviations included with the gene names highlight genes with previously determined associations to DAP resistance in clinical and/or laboratory strains of *S. aureus*; ^fProtein product descriptions for intergenic mutations represent the closest gene to the intergenic SNP

For example, the SNP at position 2143178 (in *cls2*) in population B was present in 3% of the reads at 6 μ g/ml daptomycin (Figure 2), but was not recorded at this time point because it did not pass our 5% reporting threshold. However, this SNP increased to 15% at 10 μ g/ml and almost reached fixation at 14 μ g/ml (represented in 93% of the population; Supplementary Table S2 and Figure 2). Similarly, the SNPs at positions 26957, 261590, 1364495, and 2399255 in population B (in genes *walK*, SA0219, *mprF*, and the noncoding region near SA2134, respectively) reached

intermediate frequencies at 10 μ g/ml daptomycin but were actually present earlier in < = 5% of population (Supplementary Table S2). Although population C appeared relatively stable until 14 μ g/ml, some SNPs were already present at low frequencies at 0, 6, and 10 μ g/ml daptomycin concentrations (Supplementary Table S2 and Figure 2). In contrast, serial passaged population P showed no indication of mutations until after the highest drug exposure of 10 μ g/ml (Supplementary Table S2). Thus, sampling throughout drug exposures in the bioreactor revealed that mutations relevant to resistance at high



antibiotic concentrations often appeared much earlier in the history of the population.

Colonies Confirm Presence of Low Frequency Variants

The three colonies sequenced from population A at 6 $\mu\text{g/ml}$ and populations B and P 10 $\mu\text{g/ml}$ daptomycin exposure helped to confirm the presence of several SNPs in the populations from which they derived (**Supplementary Table S3**). Mutations present in the two populations but absent in their colonies most likely reflect the heterogeneous composition of the populations, but could also indicate poor recovery of mutant cells on plates or represent false-positive SNPs. For example, the nonsynonymous

mutation in the *pgsA* gene was detected in 68% of the reads in population A at 6 $\mu\text{g/ml}$ DAP (**Supplementary Table S2**) but did not appear in any of the three colonies derived from this population (**Supplementary Tables S2, S3**). The relatively high number of reads with this SNP, the fact that the same mutation occurred in population A at 10 $\mu\text{g/ml}$ DAP exposure, and the fact that this SNP has been documented in other DAP resistant *S. aureus* strains (Peleg et al., 2012) all suggest that this mutation is real but inhibited growth on plates or was not represented by the small sampling size in the colonies. The SNP at position 1706314 was present in only 8% of population B but occurred in 100% of the reads for two of the three colonies (**Supplementary Table S2**). Similarly, a mutation present at position 352545 in the ABC transporter permease gene SA0296 occurred in only 5% of

the reads for population P (not reaching our cutoff threshold) but was present in 100% of the reads for colony 3 from this population (**Supplementary Table S2**).

DISCUSSION

We describe a novel approach to studying the accumulation of genetic mutations that leads to enhanced daptomycin resistance in *S. aureus* N315, a highly DAP-S strain. We employed a continuous culture model using a bioreactor which eliminates the conditions of nutrient limitation and allows bacterial replication to occur unhindered except for antibiotic exposure. Thus, growth of DAP-S strains in a bioreactor continuously exposes the bacteria to a known increasing concentration of daptomycin that constantly challenges the bacterial population and selects for changes related to antibiotic pressure (Toprak et al., 2011, 2013). Additionally, the bioreactor model allows us to continuously monitor bacterial growth in a way that is not possible with hollow fiber or plate dependent methods. The consistently increasing concentration of daptomycin in a bioreactor simulates clinical situations where the bacteria are present in a nutritionally rich environment in pockets where the drug concentration may not reach lethal bactericidal levels. This differential distribution of antibiotic allows some bacteria to persist and selects for DAP-R *S. aureus* strains that are refractory to killing when exposed to higher concentrations of antibiotics.

S. aureus populations subjected to increasing concentrations of daptomycin in the bioreactor displayed mutations at loci associated with resistance in clinically and laboratory-derived isolates (Friedman et al., 2006; Howden et al., 2011; Peleg et al., 2012; Bayer et al., 2015; Chen et al., 2015; Kang et al., 2017; Sabat et al., 2018), thereby demonstrating the utility of the bioreactor for studying the *in vivo* and *in vitro* evolution of daptomycin resistance. The three experimental replicates (populations A–C) revealed that the bioreactor yields consistent, reproducible results as evidenced by the repeated evolution of several genetic mutations in more than one population. This supports the hypothesis that daptomycin resistance can occur through multiple routes but evolution converges on and targets a few main pathways.

We also detected SNPs at or near new loci that might contribute to daptomycin resistance, such as a nonsynonymous change in a DNA helicase and a mutation in the noncoding region near DNA-3-methyladenine glycosylase (**Table 1**). These two genes code for proteins that have DNA repair functions and could either assist in mediating mutational load or facilitate mutation depending on gain or loss of function. Mutations in genes that code for proteins involved in oxidative phosphorylation or electron transport might contribute to the altered metabolic activities that accompany the acquisition of antibiotic resistance in *S. aureus* (Somerville and Proctor, 2009; Proctor et al., 2014). In population C, amino acid changes to NADH dehydrogenase (coded for by SA0802), which transfers electrons to menaquinone in the electron transport chain, and MenH (coded for by SA0897), which functions in menaquinone synthesis, could reflect the presence of small-colony variants that we isolated

from the bioreactor. These small-colony variants display deficient electron transport chains and are associated with persistent, antibiotic resistant infections (Somerville and Proctor, 2009; Proctor et al., 2014). Metabolic shifts in DAP-R strains were associated with a decrease in the TCA cycle and an increased production of pyrimidines and purines that diverted carbon to the synthesis of cell wall components such as teichoic acid and peptidoglycan (Gaupp et al., 2015). Transcriptomic profiling revealed that the *pur* operon – responsible for purine synthesis – was strongly regulated in DAP-R strains (Müller et al., 2018). Correspondingly, we observed mutations in a transcription factor that controls purine biosynthesis (SA0454) as well as changes in metabolic genes involved in glucose metabolism (SA0219), amino acid synthesis (SA0756), and steroid biosynthesis and degradation (SA0613; **Table 1**). While serial passaged population P evolved resistance to daptomycin, the SNP in *pgsA* – the only mutation associated with this condition – arose after exposure to the highest concentration of daptomycin. This suggests that transcriptional changes mediated resistance at lower concentrations and illustrates the different results produced by the two culture methods.

Although populations A–C independently acquired many of the same SNPs or mutations at the same loci, the evolutionary landscapes explored were varied and the mutation profiles were distinct (e.g., **Figure 2**). However, all three populations converged upon a combination of changes – either at *pgsA* and *mprF* or *mprF* and *cls2* – supporting our hypothesis that the presence of only a few key adaptations drives daptomycin resistance in *S. aureus* N315. Both cardiolipin synthase (coded for by *cls2*) and CDP-diacylglycerol-glycerol-3-phosphatidyltransferase (coded for by *pgsA*) are involved in the production of membrane phospholipids (Peleg et al., 2012; Bayer et al., 2013). Thus, modifications to these enzymes could influence daptomycin binding and/or translocation across the membrane via compositional changes or changes to membrane fluidity or charge (Peleg et al., 2012; Bayer et al., 2013). The MprF enzyme lysinylates PG – a major cell membrane component for *S. aureus* – and translocates it to the outer membrane, which influences the charge of the membrane and could ultimately cause repulsion of the DAP-Ca²⁺ complex (Ernst et al., 2009). The presence of mutations in phospholipid biosynthesis genes also represented the unifying characteristic across 21 clinical and 12 laboratory DAP-R isolates, underscoring the importance of a few key genes in providing initial resistance as well as the genomic background capable of surviving increased antibiotic exposure (Peleg et al., 2012). While mutations at *mprF*, *rpoB/C*, and *yycG* (*walK*) loci consistently arose in (varying) sequential order from serial passage experiments (Friedman et al., 2006) and mutations also accumulated sequentially in vancomycin resistant clinical isolates (Mwangi et al., 2007), our results highlight the fact that the evolution of daptomycin resistance does not necessarily rely on a linear addition of genomic mutations. Furthermore, the bioreactor revealed that most mutations arose in the population at an earlier time point than might be recorded from sequencing only the final DAP-R population, a level of detail that our serial passage experiment could not provide. For example, some SNPs

present in less than 5% of the population, reached fixation by the end of the experiment. Additionally, the presence of low frequency variants in colonies plated from the DAP-R populations supports the hypothesis that most low-frequency variants were likely real and could be selected for in subsequent generations. The discrepancies between our results and past experiments could reflect strain specific responses or the effects of bioreactor versus plate-dependent growth. Additional bioreactor experiments with different *S. aureus* strains would help to clarify whether the trends we observed are more generalizable. The early appearance of low frequency variants suggests that there could be pre-existing mutations within the population that are selected for at higher concentrations of daptomycin. However, the appearance of additional low frequency variants at later time points, such as in Population C, presents the possibility that mutagenesis induced by drug exposure also plays a role in generating variation, a hypothesis that requires further experimentation as well.

While bioreactor populations consistently evolved pairs of mutations affiliated with daptomycin resistance, not all mutation combinations appear to be created equally as demonstrated by the different fates of mutations at *mprF* and *cls2* loci in populations B and C. At 10 µg/ml, population B contained two SNPs at the *mprF* locus (herein referred to as *mprF* S295L and L341F) represented in approximately equal proportions and two SNPs at the *cls2* locus (herein referred to as *cls2* A23V and L52F) also represented in equal proportions (Figure 2). However, after increasing the antibiotic concentration, *mprF* S295L and *cls2* A23V were represented in almost 100% of the population while *mprF* L341F and *cls2* L52F were essentially extinct (Figure 2). The simultaneous rise of *mprF* S295L and *cls2* A23V with the corresponding extinction of *mprF* L341F and *cls2* L52F suggests that two DAP-R subpopulations existed with the first conferring a selective advantage (Figure 2). Population C displayed the same *cls2* L52F mutation as Population B and an S337L *mprF* mutation (which resides in the same transmembrane domain as position 341). Interestingly, it required an additional 24 h for population C to rebound to the same CFU levels reached by population B at 14 µg/ml. A fourth bioreactor experiment produced a DAP-R population with the same *mprF* and *cls2* mutations as Population C with a nearly identical mutational profile (i.e., SNPs appearing at the same time points with changes in SNP frequencies occurring at the same rates at the same dosages; Supplementary Figure S1) and confirmed the delayed rebound in growth after 14 µg/ml daptomycin exposure. Thus, it is tempting to speculate that the behavior of population C would represent the behavior of the *mprF* L341F/*cls2* L52F subpopulation in population B in the absence of competition. However, validation of fitness differences requires additional experiments that directly test the competition among populations with varying mutation combinations.

CONCLUSION

In conclusion, the bioreactor model represents a novel, effective method for recapitulating *in vivo* conditions and inducing DAP-R mutations typically observed in clinical isolates. The

bioreactor model reveals that certain key mutations are most likely required to be present to confer daptomycin resistance but the combination of key mutations can vary and mutations do not necessarily arise in a progressive fashion. Furthermore, the competitive advantages of mutation combinations do not appear to be equal even if the mutations arise in the same gene combinations (such as *mprF* and *cls2*). To our knowledge, this study is the first to unveil a possible hierarchical dominance to mutation combinations, although additional experimental confirmation is required. The bioreactor model illustrates that the evolution of DAP-R is a dynamic process, a characteristic often not reflected when examining static cultures or isogenic strains. Tracking the collective evolutionary fates of genomic mutations over the course of antibiotic treatment will assist in identifying early signs of resistance and might provide knowledge of which mutations will be more responsive to treatment.

AUTHOR CONTRIBUTIONS

KM, JP, MP, and MM conceived of the study. MM, JL, ZM, VR, and SM maintained the bioreactor and all cultures. ZM performed DNA extractions while RS submitted DNA for sequencing and contributed to data interpretations. MP generated Figure 1. EL-N and MM wrote the manuscript and EL-N performed all whole-genome sequencing analyses. All authors read and approved the final manuscript.

FUNDING

This work was supported by funding from an “Investment in Collaborative Research at the Wadsworth Center and Albany College of Pharmacy and Health Sciences Grant.” JP was supported by NIH R01-GM-080573.

ACKNOWLEDGMENTS

The following reagent was provided by the Network on Antimicrobial Resistance in *Staphylococcus aureus* (NARSA) for distribution by BEI Resources, NIAID, NIH: *Staphylococcus aureus*, Strain N315, NR-45898. The authors acknowledge the assistance of Wadsworth Center Applied Genomic Technologies and Bioinformatics and Statistics Cores.

SUPPLEMENTARY MATERIAL

The Supplementary Material for this article can be found online at: <https://www.frontiersin.org/articles/10.3389/fmicb.2019.00345/full#supplementary-material>

FIGURE S1 | Mutation profiles of population C and a fourth bioreactor experiment (population D). The frequency of mutations as a function of antibiotic concentration for population C (top) and population D (bottom). Mutations highlighted are SNPs that lead to amino acid changes in MprF and Cls2 and lower frequency variants NADH (NADH dehydrogenase, SA0802), menH (2-succinyl-6-hydroxy-2,

4-cyclohexadiene-1-carboxylate synthase, SA0897), and *rpoA* (DNA-directed RNA polymerase subunit alpha, SA2023). SNPs are identical between the populations and display the same dynamics (i.e., SNPs appear at the same time and change in frequency at the same rate and at the same dosages).

TABLE S1 | SNPs present in the parental DAP-S isolate of N315 in comparison to the NCBI Refseq N315 isolate. These changes were detected in our BEI parental N315 strain and all descendant populations, except for the mutation at position 939485, which is not present in Population C. Annotations associated with noncoding SNPs are for the nearest coding sequence.

REFERENCES

- Bayer, A. S., Mishra, N. N., Chen, L., Kreiswirth, B. N., Rubio, A., and Yang, S. J. (2015). Frequency and distribution of single-nucleotide polymorphisms within *mprF* in methicillin-resistant *Staphylococcus aureus* clinical isolates and their role in cross-resistance to daptomycin and host defense antimicrobial peptides. *Antimicrob. Agents Chemother.* 59, 4930–4937. doi: 10.1128/AAC.00970-15
- Bayer, A. S., Mishra, N. N., Sakoulas, G., Nonejuie, P., Nast, C. C., Pogliano, J., et al. (2014). Heterogeneity of *mprF* sequences in methicillin-resistant *Staphylococcus aureus* clinical isolates: role in cross-resistance between daptomycin and host defense antimicrobial peptides. *Antimicrob. Agents Chemother.* 58, 7462–7467. doi: 10.1128/AAC.03422-14
- Bayer, A. S., Schneider, T., and Sahl, H.-G. (2013). Mechanisms of daptomycin resistance in *Staphylococcus aureus*: role of the cell membrane and cell wall. *Ann. N. Y. Acad. Sci.* 1277, 139–158. doi: 10.1111/j.1749-6632.2012.06819.x
- Berti, A. D., Baines, S. L., Howden, B. P., Sakoulas, G., Nizet, V., Proctor, R. A., et al. (2015). Heterogeneity of genetic pathways toward daptomycin nonsusceptibility in *Staphylococcus aureus* determined by adjunctive antibiotics. *Antimicrob. Agents Chemother.* 59, 2799–2806. doi: 10.1128/AAC.04990-14
- Boyle-Vavra, S., Jones, M., Gourley, B. L., Holmes, M., Ruf, R., Balsam, A. R., et al. (2011). Comparative genome sequencing of an isogenic pair of USA800 clinical methicillin-resistant *Staphylococcus aureus* isolates obtained before and after daptomycin treatment failure. *Antimicrob. Agents Chemother.* 55, 2018–2025. doi: 10.1128/AAC.01593-10
- Cafiso, V., Bertuccio, T., Purrello, S., Campanile, F., Mammina, C., Sartor, A., et al. (2014). *dltA* overexpression: a strain-independent keystone of daptomycin resistance in methicillin-resistant *Staphylococcus aureus*. *Int. J. Antimicrob. Agents* 43, 26–31. doi: 10.1016/j.ijantimicag.2013.10.001
- Camargo, I. L., Neoh, H. M., Cui, L., and Hiramatsu, K. (2008). Serial daptomycin selection generates daptomycin-nonsusceptible *Staphylococcus aureus* strains with a heterogeneous vancomycin-intermediate phenotype. *Antimicrob. Agents Chemother.* 52, 4289–4299. doi: 10.1128/AAC.00417-08
- Cameron, D. R., Ward, D. V., Kostoulas, X., Howden, B. P., Moellering, R. C., Eliopoulos, G. M., et al. (2012). Serine/threonine phosphatase *Stp1* contributes to reduced susceptibility to vancomycin and virulence in *Staphylococcus aureus*. *J. Infect. Dis.* 205, 1677–1687. doi: 10.1093/infdis/jis252
- Capone, A., Cafiso, V., Campanile, F., Parisi, G., Mariani, B., Petrosillo, N., et al. (2016). In vivo development of daptomycin resistance in vancomycin-susceptible methicillin-resistant *Staphylococcus aureus* severe infections previously treated with glycopeptides. *Eur. J. Clin. Microbiol. Infect. Dis.* 35, 625–631. doi: 10.1007/s10096-016-2581-4
- Chambers, H. F., and DeLeo, F. R. (2009). Waves of resistance: *Staphylococcus aureus* in the antibiotic era. *Nat. Rev. Microbiol.* 7, 629–641. doi: 10.1038/nrmicro2200
- Chen, C.-J., Huang, Y.-C., and Chiu, C.-H. (2015). Multiple pathways of cross-resistance to glycopeptides and daptomycin in persistent MRSA bacteraemia. *J. Antimicrob. Chemother.* 70, 2965–2972. doi: 10.1093/jac/dkv225
- Ernst, C. M., Staibitz, P., Mishra, N. N., Yang, S. J., Hornig, G., Kalbacher, H., et al. (2009). The bacterial defensin resistance protein *MprF* consists of separable domains for lipid lysinylation and antimicrobial peptide repulsion. *PLoS Pathog* 5:e1000660. doi: 10.1371/journal.ppat.1000660
- Fischer, A., Yang, S. J., Bayer, A. S., Vaezzadeh, A. R., Herzig, S., Stenz, L., et al. (2011). Daptomycin resistance mechanisms in clinically derived *Staphylococcus aureus* strains assessed by a combined transcriptomics and proteomics approach. *J. Antimicrob. Chemother.* 66, 1696–1711. doi: 10.1093/jac/dkr195
- TABLE S2** | Allele Frequencies of SNPs for populations 6–8, population P and colonies 1–3 derived from population 6 at 6 µg/ml and populations 7 and P at 10 µg/ml daptomycin. Alt, Alternative (SNP) nucleotide frequency; Reads, total number of reads at a position. All concentrations are of daptomycin. No colonies were sequenced from Population C.
- TABLE S3** | SNPs present in colonies from Population A taken at 6 µg/ml daptomycin and populations B and P at 10 µg/ml daptomycin. Three colonies were sequenced from each population. SNPs present in the ancestral population are not shown.
- Fowler, V. G., Nelson, C. L., McIntyre, L. M., Kreiswirth, B. N., Monk, A., Archer, G. L., et al. (2007). Potential associations between hematogenous complications and bacterial genotype in *Staphylococcus aureus* infection. *J. Infect. Dis.* 196, 738–747. doi: 10.1086/520088
- Friedman, L., Alder, J. D., and Silverman, J. A. (2006). Genetic changes that correlate with reduced susceptibility to daptomycin in *Staphylococcus aureus*. *Antimicrob. Agents Chemother.* 50, 2137–2145. doi: 10.1128/AAC.00039-06
- Gaupp, R., Lei, S., Reed, J. M., Peisker, H., Boyle-Vavra, S., Bayer, A. S., et al. (2015). *Staphylococcus aureus* metabolic adaptations during the transition from a daptomycin susceptibility phenotype to a daptomycin nonsusceptibility phenotype. *Antimicrob. Agents Chemother.* 59, 4226–4238. doi: 10.1128/AAC.00160-15
- Hafer, C., Lin, Y., Kornblum, J., Lowy, F. D., and Uhlemann, A. C. (2012). Contribution of selected gene mutations to resistance in clinical isolates of vancomycin-intermediate *Staphylococcus aureus*. *Antimicrob. Agents Chemother.* 56, 5845–5851. doi: 10.1128/AAC.01139-12
- Howden, B. P., Davies, J. K., Johnson, P. D. R., Stinear, T. P., and Grayson, M. L. (2010). Reduced vancomycin susceptibility in *Staphylococcus aureus*, including vancomycin-intermediate and heterogeneous vancomycin-intermediate strains: resistance mechanisms, laboratory detection, and clinical implications. *Clin. Microbiol. Rev.* 23, 99–139. doi: 10.1128/CMR.00042-09
- Howden, B. P., McEvoy, C. R., Allen, D. L., Chua, K., Gao, W., Harrison, P. F., et al. (2011). Evolution of multidrug resistance during *Staphylococcus aureus* infection involves mutation of the essential two component regulator *WalK*. *PLoS Pathog.* 7:e1002359. doi: 10.1371/journal.ppat.1002359
- Jones, T., Yeaman, M. R., Sakoulas, G., Yang, S. J., Proctor, R. A., Sahl, H. G., et al. (2008). Failures in clinical treatment of *Staphylococcus aureus* infection with daptomycin are associated with alterations in surface charge, membrane phospholipid asymmetry, and drug binding. *Antimicrob. Agents Chemother.* 52, 269–278. doi: 10.1128/AAC.00719-07
- Kang, K.-M., Mishra, N. N., Park, K. T., Lee, G.-Y., Park, Y. H., Bayer, A. S., et al. (2017). Phenotypic and genotypic correlates of daptomycin-resistant methicillin-susceptible *Staphylococcus aureus* clinical isolates. *J. Microbiol.* 55, 153–159. doi: 10.1007/s12275-017-6509-1
- Leclercq, R. (2009). Epidemiological and resistance issues in multidrug-resistant staphylococci and enterococci. *Clin. Microbiol. Infect.* 15, 224–231. doi: 10.1111/j.1469-0691.2009.02739.x
- Li, H. (2011). A statistical framework for SNP calling, mutation discovery, association mapping and population genetical parameter estimation from sequencing data. *Bioinformatics* 27, 2987–2993. doi: 10.1093/bioinformatics/btr509
- Li, H., and Durbin, R. (2009). Fast and accurate short read alignment with Burrows-Wheeler transform. *Bioinformatics* 25, 1754–1760. doi: 10.1093/bioinformatics/btp324
- Ma, Z., Lasek-Nesselquist, E., Lu, J., Schneider, R., Shah, R., Oliva, G., et al. (2018). Characterization of genetic changes associated with daptomycin nonsusceptibility in *Staphylococcus aureus*. *PLoS One* 13:e0198366. doi: 10.1371/journal.pone.0198366
- Marty, F. M., Yeh, W. W., Wennersten, C. B., Venkataraman, L., Albano, E., Alyea, E. P., et al. (2006). Emergence of a clinical daptomycin-resistant *Staphylococcus aureus* isolate during treatment of methicillin-resistant *Staphylococcus aureus* bacteremia and osteomyelitis. *J. Clin. Microbiol.* 44, 595–597. doi: 10.1128/JCM.44.2.595-597.2006
- Mishra, N. N., Bayer, A. S., Weidenmaier, C., Grau, T., Wanner, S., Stefani, S., et al. (2014). Phenotypic and genotypic characterization of daptomycin-resistant

- methicillin-resistant *Staphylococcus aureus* strains: relative roles of *mprF* and *dlt* operons. *PLoS One* 9:e107426. doi: 10.1371/journal.pone.0107426
- Mishra, N. N., McKinnell, J., Yeaman, M. R., Rubio, A., Nast, C. C., Chen, L., et al. (2011). In vitro cross-resistance to daptomycin and host defense cationic antimicrobial peptides in clinical methicillin-resistant *Staphylococcus aureus* isolates. *Antimicrob. Agents Chemother.* 55, 4012–4018. doi: 10.1128/AAC.00223-11
- Mishra, N. N., Rubio, A., Nast, C. C., and Bayer, A. S. (2012). Differential adaptations of methicillin-resistant *Staphylococcus aureus* to serial in vitro passage in daptomycin: evolution of daptomycin resistance and role of membrane carotenoid content and fluidity. *Int. J. Microbiol.* 2012:683450. doi: 10.1155/2012/683450
- Mishra, N. N., Yang, S. J., Sawa, A., Rubio, A., Nast, C. C., Yeaman, M. R., et al. (2009). Analysis of cell membrane characteristics of in vitro-selected daptomycin-resistant strains of methicillin-resistant *Staphylococcus aureus*. *Antimicrob. Agents Chemother.* 53, 2312–2318. doi: 10.1128/AAC.01682-08
- Müller, A., Grein, F., Otto, A., Gries, K., Orlov, D., Zarubaev, V., et al. (2018). Differential daptomycin resistance development in *Staphylococcus aureus* strains with active and mutated *gra* regulatory systems. *Int. J. Med. Microbiol.* 308, 335–348. doi: 10.1016/j.ijmm.2017.12.002
- Murthy, M. H., Olson, M. E., Wickert, R. W., Fey, P. D., and Jalali, Z. (2008). Daptomycin non-susceptible methicillin-resistant *Staphylococcus aureus* USA 300 isolate. *J. Med. Microbiol.* 57, 1036–1038. doi: 10.1099/jmm.0.2008/000588-0
- Mwangi, M. M., Wu, S. W., Zhou, Y., Sieradzki, K., de Lencastre, H., Richardson, P., et al. (2007). Tracking the in vivo evolution of multidrug resistance in *Staphylococcus aureus* by whole-genome sequencing. *Proc. Natl. Acad. Sci. U.S.A.* 104, 9451–9456. doi: 10.1073/pnas.0609839104
- Patel, D., Husain, M., Vidaillac, C., Steed, M. E., Rybak, M. J., Seo, S. M., et al. (2011). Mechanisms of in-vitro-selected daptomycin-non-susceptibility in *Staphylococcus aureus*. *Int. J. Antimicrob. Agents* 38, 442–446. doi: 10.1016/j.ijantimicag.2011.06.010
- Patel, M. (2009). Community-associated methicillin-resistant *Staphylococcus aureus* infections: epidemiology, recognition and management. *Drugs* 69, 693–716. doi: 10.2165/00003495-200969060-00004
- Peleg, A. Y., Miyakis, S., Ward, D. V., Earl, A. M., Rubio, A., Cameron, D. R., et al. (2012). Whole genome characterization of the mechanisms of daptomycin resistance in clinical and laboratory derived isolates of *Staphylococcus aureus*. *PLoS One* 7:e28316. doi: 10.1371/journal.pone.0028316
- Pillai, S. K., Gold, H. S., Sakoulas, G., Wennersten, C., Moellering, R. C., and Eliopoulos, G. M. (2007). Daptomycin nonsusceptibility in *Staphylococcus aureus* with reduced vancomycin susceptibility is independent of alterations in *MprF*. *Antimicrob. Agents Chemother.* 51, 2223–2225. doi: 10.1128/AAC.00202-07
- Proctor, R. A., Kriegeskorte, A., Kahl, B. C., Becker, K., Löffler, B., and Peters, G. (2014). *Staphylococcus aureus* Small Colony Variants (SCVs): a road map for the metabolic pathways involved in persistent infections. *Front. Cell Infect. Microbiol.* 4:99. doi: 10.3389/fcimb.2014.00099
- Robinson, J. T., Thorvaldsdóttir, H., Winckler, W., Guttman, M., Lander, E. S., Getz, G., et al. (2011). Integrative genomics viewer. *Nat. Biotechnol.* 29, 24–26. doi: 10.1038/nbt.1754
- Sabat, A. J., Tinelli, M., Grundmann, H., Akkerboom, V., Monaco, M., Del Grosso, M., et al. (2018). Daptomycin resistant *Staphylococcus aureus* clinical strain with novel non-synonymous mutations in the *mprF* and *vraS* genes: a new insight into daptomycin resistance. *Front. Microbiol.* 9:2705. doi: 10.3389/fmicb.2018.02705
- Silverman, J. A., Oliver, N., Andrew, T., and Li, T. (2001). Resistance studies with daptomycin. *Antimicrob. Agents Chemother.* 45, 1799–1802. doi: 10.1128/AAC.45.6.1799-1802.2001
- Skiest, D. J. (2006). Treatment failure resulting from resistance of *Staphylococcus aureus* to daptomycin. *J. Clin. Microbiol.* 44, 655–656. doi: 10.1128/JCM.44.2.655-656.2006
- Somerville, G. A., and Proctor, R. A. (2009). At the crossroads of bacterial metabolism and virulence factor synthesis in staphylococci. *Microbiol. Mol. Biol. Rev.* 73, 233–248. doi: 10.1128/MMBR.00005-09
- Song, Y., Rubio, A., Jayaswal, R. K., Silverman, J. A., and Wilkinson, B. J. (2013). Additional routes to *Staphylococcus aureus* daptomycin resistance as revealed by comparative genome sequencing, transcriptional profiling, and phenotypic studies. *PLoS One* 8:e58469. doi: 10.1371/journal.pone.0058469
- Stryjewski, M. E., and Corey, G. R. (2014). Methicillin-resistant *Staphylococcus aureus*: an evolving pathogen. *Clin. Infect. Dis.* 58(Suppl. 1), S10–S19. doi: 10.1093/cid/cit613
- Thorvaldsdóttir, H., Robinson, J. T., and Mesirov, J. P. (2013). Integrative Genomics Viewer (IGV): high-performance genomics data visualization and exploration. *Brief. Bioinform.* 14, 178–192. doi: 10.1093/bib/bbs017
- Toprak, E., Veres, A., Michel, J. B., Chait, R., Hartl, D. L., and Kishony, R. (2011). Evolutionary paths to antibiotic resistance under dynamically sustained drug stress. *Nat. Genet.* 44, 101–105. doi: 10.1038/ng.1034
- Toprak, E., Veres, A., Yildiz, S., Pedraza, J. M., Chait, R., Paulsson, J., et al. (2013). Building a Morbidostat: an automated continuous-culture device for studying bacterial drug resistance under dynamically sustained drug inhibition. *Nat. Protoc.* 8, 555–567. doi: 10.1038/nprot.nprot.2013.021
- Tran, T. T., Munita, J. M., and Arias, C. A. (2015). Mechanisms of drug resistance: daptomycin resistance. *Ann. N. Y. Acad. Sci.* 1354, 32–53. doi: 10.1111/nyas.12948
- Yang, S. J., Kreiswirth, B. N., Sakoulas, G., Yeaman, M. R., Xiong, Y. Q., Sawa, A., et al. (2009). Enhanced expression of *dltABCD* is associated with the development of daptomycin nonsusceptibility in a clinical endocarditis isolate of *Staphylococcus aureus*. *J. Infect. Dis.* 200, 1916–1920. doi: 10.1086/648473

Conflict of Interest Statement: The authors declare that the research was conducted in the absence of any commercial or financial relationships that could be construed as a potential conflict of interest.

Copyright © 2019 Lasek-Nesselquist, Lu, Schneider, Ma, Russo, Mishra, Pai, Pata, McDonough and Malik. This is an open-access article distributed under the terms of the Creative Commons Attribution License (CC BY). The use, distribution or reproduction in other forums is permitted, provided the original author(s) and the copyright owner(s) are credited and that the original publication in this journal is cited, in accordance with accepted academic practice. No use, distribution or reproduction is permitted which does not comply with these terms.



Construction and Characterization of Synthetic Bacterial Community for Experimental Ecology and Evolution

Johannes Cairns^{1†}, Roosa Jokela^{1‡}, Jenni Hultman^{1§}, Manu Tamminen^{2||}, Marko Virta^{1¶} and Teppo Hiltunen^{1,2*}

¹ Department of Microbiology, University of Helsinki, Helsinki, Finland, ² Department of Biology, University of Turku, Turku, Finland

OPEN ACCESS

Edited by:

Elena Perrin,
Università degli Studi di Firenze, Italy

Reviewed by:

Henning Seedorf,
Temasek Life Sciences Laboratory,
Singapore
Vasvi Chaudhry,
Institute of Microbial Technology
(CSIR), India

*Correspondence:

Teppo Hiltunen
teppo.hiltunen@helsinki.fi
orcid.org/0000-0001-7206-2399

[†]orcid.org/0000-0003-1329-2025

[‡]orcid.org/0000-0002-4144-6573

[§]orcid.org/0000-0002-3431-1785

^{||}orcid.org/0000-0001-5891-7653

[¶]orcid.org/0000-0001-5981-7566

Specialty section:

This article was submitted to
Evolutionary and Genomic
Microbiology,
a section of the journal
Frontiers in Genetics

Received: 27 April 2018

Accepted: 23 July 2018

Published: 14 August 2018

Citation:

Cairns J, Jokela R, Hultman J,
Tamminen M, Virta M and Hiltunen T
(2018) Construction
and Characterization of Synthetic
Bacterial Community for Experimental
Ecology and Evolution.
Front. Genet. 9:312.
doi: 10.3389/fgene.2018.00312

Experimental microbial ecology and evolution have yielded foundational insights into ecological and evolutionary processes using simple microcosm setups and phenotypic assays with one- or two-species model systems. The fields are now increasingly incorporating more complex systems and exploration of the molecular basis of observations. For this purpose, simplified, manageable and well-defined multispecies model systems are required that can be easily investigated using culturing and high-throughput sequencing approaches, bridging the gap between simpler and more complex synthetic or natural systems. Here we address this need by constructing a completely synthetic 33 bacterial strain community that can be cultured in simple laboratory conditions. We provide whole-genome data for all the strains as well as metadata about genomic features and phenotypic traits that allow resolving individual strains by amplicon sequencing and facilitate a variety of envisioned mechanistic studies. We further show that a large proportion of the strains exhibit coexistence in co-culture over serial transfer for 48 days in the absence of any experimental manipulation to maintain diversity. The constructed bacterial community can be a valuable resource in future experimental work.

Keywords: microbial community, model system, synthetic ecology, experimental evolution, whole-genome sequencing

INTRODUCTION

Testing ecological and evolutionary theory in a highly controlled manner using simple laboratory setups with one or two microbial species (Fraser and Keddy, 1997; Buckling et al., 2009) has produced important insights into ecological interactions—e.g., competition, cooperation, and cross-feeding interactions (Helling et al., 1987; Treves et al., 1998; Rozen and Lenski, 2000; Shou et al., 2007; Harcombe, 2010); the role of cheaters (MacLean and Gudelj, 2006); predator–prey interactions (Shertzer et al., 2002); and host–parasite interactions (Morgan et al., 2005)—and evolutionary processes—e.g., the evolution of coexistence (Good et al., 2017), coevolution between species (Hall et al., 2011; Brockhurst and Koskella, 2013), and eco-evolutionary feedback dynamics (Yoshida et al., 2003; Hiltunen and Becks, 2014). However, there is an increasing awareness that ecological and evolutionary processes can be fundamentally altered in more complex multispecies communities owing to several features such as altered competitive interactions and multiple selection pressures (Dunham, 2007). Recent empirical findings show, for example, that pairwise

interactions can be strongly altered in the presence of other species (Kastman et al., 2016) and the rate of adaptation of species can differ between monocultures and communities (Lawrence et al., 2012). Even a basic understanding of certain characteristics of microbial life such as horizontal gene transfer (Smillie et al., 2011), metabolic interactions and spatial heterogeneity (Elias and Banin, 2012; van Gestel et al., 2014) requires investigation of multispecies settings integral to them. Furthermore, several key ecological features are specific to multispecies communities, such as diversity, stability, succession and high-order (e.g., four-way) species interactions (Bailey et al., 2016). There is therefore a profound need to expand the biotic complexity of study systems used in the fields of experimental microbial ecology and evolution.

The design of multispecies model communities in experimental ecology and evolution is part of the emerging field of synthetic ecology where synthetic communities are used for a plethora of basic and applied purposes. Several research attempts have sought mechanistic understanding of specific natural systems, such as methane consuming communities (Yu et al., 2017), plant root colonizing bacteria (Lebeis et al., 2015), the human gut microbiota (Goodman et al., 2011), and cheese rind communities (Wolfe et al., 2014), by complementing observational findings with findings from controlled *in vitro* or *in vivo* studies using synthetic communities. These studies focus on designing synthetic communities that capture the essential features of the natural system being investigated. A typical approach is to determine the prevalent taxa in the natural system or in the core microbiome (Shade and Handelsman, 2012) common to similar systems, to construct a synthetic community of taxonomically representative strains isolated from the natural system, and to culture the community in conditions mimicking the natural system. The limitations of this approach include the potentially important role in ecological functions or evolutionary processes of low-abundance taxa (Liu et al., 2017), microdiversity (Chase et al., 2017), or interactions between bacteria and members of other taxonomic groups such as viruses, unicellular eukaryotic predators or fungi, as well as technical difficulties in mimicking natural conditions in the laboratory (Wolfe, 2018). Likely owing to such limitations, among these studies, cases have been observed both where simple synthetic communities representing predominant taxa in natural systems recapitulate the dynamics in natural systems (Goodman et al., 2011; Wolfe et al., 2014; Lebeis et al., 2015) and where major differences are observed between synthetic and natural systems (Yu et al., 2016).

Compared with studies employing synthetic communities to understand specific natural systems, more applied studies focusing, among others, on medical therapeutics (Petrof et al., 2013; Sheth et al., 2016), bioremediation (Dejonghe et al., 2003; Zomorodi and Segre, 2016), or biofuel production (Wang et al., 2015), rely even more heavily on a detailed understanding of the characteristics and functions of specific bacterial taxa in natural systems to engineer communities that can successfully perform desired functions. In contrast, studies attempting to investigate highly general ecological or evolutionary processes, similar to traditional experimental microbial ecology and evolution

using one- or two-species model systems, do not necessarily seek to, or prefer simple culture conditions over the ability to, accurately represent a particular natural community. For instance, a synthetic community of 72 bacterial strains isolated from tree-hole bacterial communities—but limited to aerobic heterotrophs cultivable in simple laboratory conditions—has been used to investigate several key ecological questions, including the relationship between diversity and ecosystem productivity (Bell et al., 2005) and the success of multispecies invasions during different stages of ecological succession (Rivett et al., 2018). Celiker and Gore (2014), in turn, used a completely synthetic model community comprising six apparently random soil bacterial strains from culture collections to examine the repeatability of change in community composition over time.

In simplified synthetic communities, verisimilitude is sacrificed to obtain relative ease of analysis and modeling, and control of species interactions, non-linear effects from added traits and strains, and evolutionary change (Widder et al., 2016). There is ongoing debate about the utility of simple microcosm setups to understand ecological and evolutionary phenomena (Carpenter, 1996, 1999; Fraser and Keddy, 1997; Drenner and Mazumder, 1999; Benton et al., 2007; Buckling et al., 2009), yet the approach continues to produce major scientific discoveries (van Houte et al., 2016; Good et al., 2017; Betts et al., 2018; Frickel et al., 2018). Similarly, the definition of, need for, and necessary level of representativeness of synthetic communities remain matters of debate (Dolinsek et al., 2016; Widder et al., 2016; Zomorodi and Segre, 2016; Wolfe, 2018), and are likely strongly dependent on the research questions. Although debated, completely synthetic communities composed of strains isolated from different habitats can also be used to study general questions as well as having special use in studying questions such as community assembly and the evolution of coexistence in newly formed communities.

In this context, the detailed, mechanistic understanding of simpler, less representative synthetic communities can be thought to inform, or even be a prerequisite to, understanding more complex synthetic systems, and ultimately, natural systems. It has been argued that such efforts should focus on understanding a limited set of well-defined model synthetic communities, which would make results comparable between studies and allow collaborative efforts toward mechanistic understanding (Widder et al., 2016). However, not many such systems exist to our knowledge despite the general boom in synthetic ecology. Furthermore, the highly general level studies that exist primarily focus on simple phenotypic analyses (Bell et al., 2005; Foster and Bell, 2012; Celiker and Gore, 2014; Rivett et al., 2016, 2018; Rivett and Bell, 2018), although high-throughput molecular methods, such as amplicon sequencing, (meta)genomics, (meta)transcriptomics, proteomics and metabolomics, which have been promisingly utilized in studies focusing on synthetic systems mimicking natural systems (Goodman et al., 2011; Wolfe et al., 2014; Lebeis et al., 2015; Stopnisek et al., 2016; Yu et al., 2017), could provide valuable insights into the mechanisms behind observed phenotypic and community level features.

To address these needs, we here constructed a simplified experimental system comprising a completely synthetic

community of 33 bacterial strains representing two phyla and six classes that can be cultured individually and in co-culture in highly simple laboratory conditions, and that can be individually resolved based on amplicon sequencing. Furthermore, we present draft-level whole genome sequence data as well as information regarding genomic features and phenotypic traits for all strains in the community, facilitating further mechanistic studies. We also present proof of concept for coexistence of a large proportion (14/33) of the strains in co-culture after serial passage of cultures for 48 days. Such a community can be a highly useful resource for experimental microbial ecology and evolution. For instance, we recently used a closely related model system to track the mobility of antibiotic resistance genes in a complex bacterial community (Cairns et al., 2018). For future studies, we envision, for example, exploration of the trajectories of ecosystem composition and genetic structure in response to environmental perturbations or variability in functional trait space. We are also considering using the community as an internal control for improving high-throughput microbial single cell genome sequencing techniques such as epicPCR (Spencer et al., 2016) or metagenome assemblies.

MATERIALS AND METHODS

Constructing Model Community

Strains from the University of Helsinki culture collection (HAMBI) representing diverse taxa were initially screened for the ability to grow individually at 28°C in two complex liquid media: the nutrient-rich proteose peptone yeast extract (PPY: 20 g proteose peptone and 2.5 g yeast extract in 1 l deionized H₂O) medium or a custom lower-nutrient-level medium containing M9 salt solution and King's B (KB) nutrients at a 1% concentration compared with full-strength medium (concentrations used: 0.2 g peptone number 3 and 0.1 ml of 85% glycerol in 1 l of dH₂O), and 0.2 g l⁻¹ protozoan pellets (Carolina Biological Supply Co., Burlington, United States). Protozoan pellets were prepared by dissolving in dH₂O, bringing to boil and filtering through 40 µm to remove particulate matter. Notably, the strains were not selected based on being representative of any particular natural system but rather as a collection of strains, each representing a different taxonomic group, that can grow in simple, uniform laboratory conditions and therefore be easily used to test general ecological and evolutionary theory or techniques (Wolfe, 2018).

Previously, we performed a serial transfer experiment with an initial version of the model community consisting of 62 strains, including the *Escherichia coli* K-12 strain JE2571(RP4) harboring the multidrug resistance plasmid RP4 (Bradley, 1980; Cairns et al., 2018). The study demonstrates the ability of dozens of the strains to coexist in culture over 40 days, as well as a method for manipulating the level of spatial heterogeneity (biofilm mass) in community cultures. For tracking strain abundance over time in the study, we Sanger sequenced the near-full-length 16S rRNA gene sequences of the strains for use as a reference database for mapping high-throughput sequencing amplicons from experimental samples (Cairns et al., 2018). Based on these

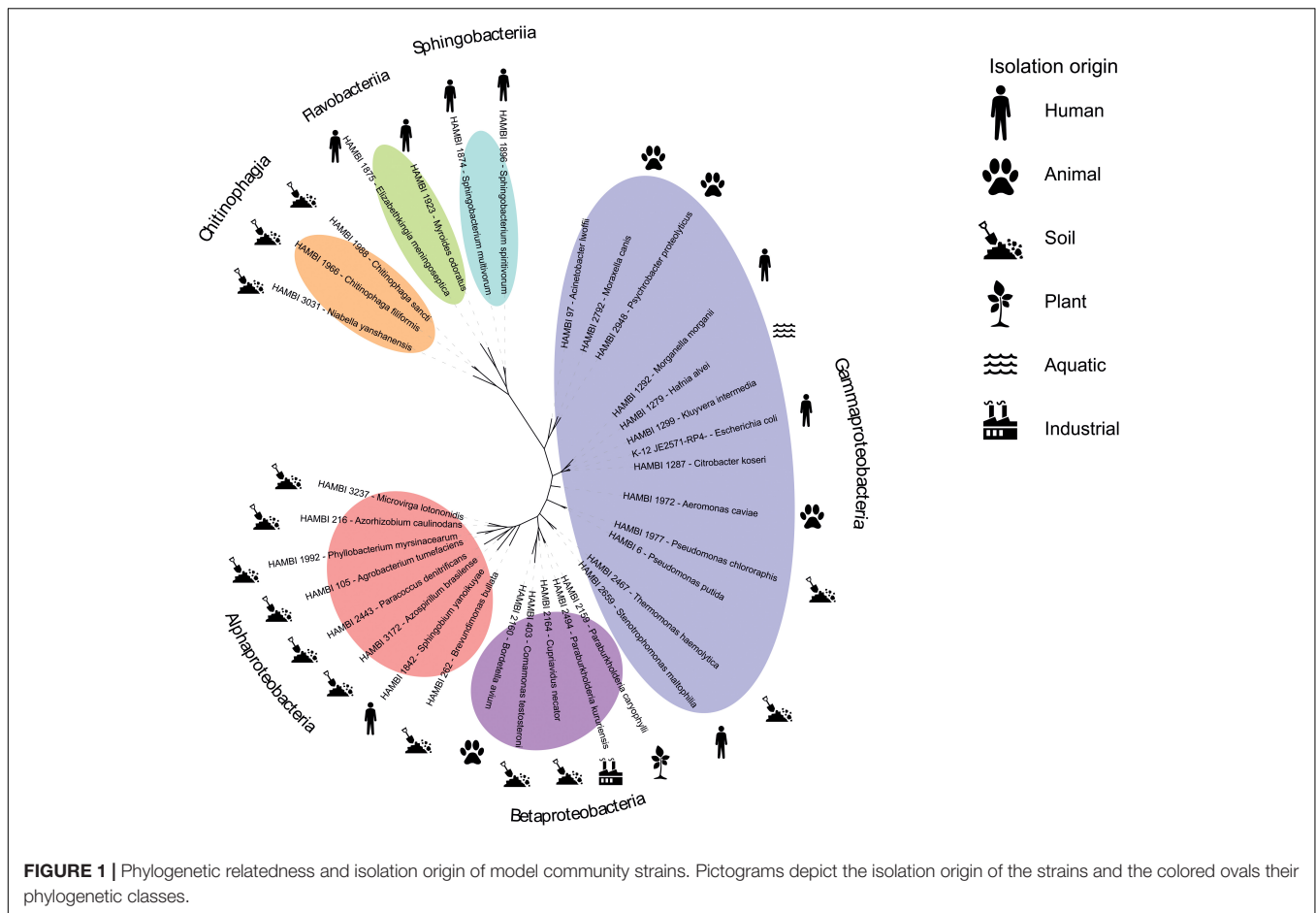
previous data, we refined the model community, removing strains with > 97% identity of 16S rRNA gene sequence with another strain in the community or uncertain strain identity. This resulted in a set of 33 gram-negative strains with confirmed culture collection identity that can be tracked at strain-level resolution through amplicon sequencing (**Supplementary Tables S1, S2**). The community was given the acronym HMC 33.1 (standing for HAMBI Mock Community containing 33 strains, version 1). The strains represent three classes in the phylum Proteobacteria (Alpha-, Beta- and Gammaproteobacteria) and three classes in the phylum Bacteroidetes (Chitinophagia, Flavobacteriia and Sphingobacteriia) (**Figure 1**). Each class contains a minimum of two strains, with the most representatives (13 strains) for the class Gammaproteobacteria. The strains have been isolated from diverse environments across the globe (**Supplementary Table S2**). Most of the strains originate from the soil, and the second highest group is human associated bacteria. Other sources include animals, aquatic environments, plants and the industry.

We further refined the co-culture medium to contain 1 g l⁻¹ R2A solution and 0.5 g l⁻¹ of cereal grass medium (Ward's Science, St. Catharines, ON, Canada) in M9 salt solution. Cereal grass medium stock was prepared by autoclaving in dH₂O and removing particulate matter by filtering through 5 µm.

To provide proof of concept for the coexistence of the strains in the medium, we performed a 48-day serial transfer experiment. The strains were grown separately for 4 days at 28°C with constant rotation at 50 rpm in the new medium and pooled together at equal volumes for the serial transfer experiment. The growth curves of strains when grown separately for 4 days are shown in **Supplementary Figure S1**. The stock community was stored in 30% glycerol at -80°C. The experiment was started by adding 10 µl of 100-fold diluted freeze-stored stock community to wells in a ABgene™ 96 Well 2.2 ml Polypropylene Deepwell Storage Plate (Thermo Fisher Scientific, Waltham, MA, United States) containing 550 µl of medium. The community was grown at 28°C with constant rotation at 100 rpm. The experiment was maintained every 96 h by transferring 10% to fresh medium. To determine bacterial density, optical density values at 600 nm were obtained for undiluted grown cultures after each growth cycle (Tecan Infinite M200 well-plate reader), and samples were frozen in glycerol for further analysis.

Phenotypic Analyses

Minimum inhibitory concentration (MIC) was determined for each strain for six antibiotics representing different antibiotic classes: ampicillin (class: penam), erythromycin (macrolide), kanamycin (aminoglycoside), nalidixic acid (fluoroquinolone), rifampicin (rifamycin), and streptomycin (aminoglycoside). For MIC determination, bacterial inoculum from an individual colony was suspended in M9 salt solution to 0.5 McFarland standard turbidity. Subsequently, 100 µl was spread-plated on 50% PPY agar medium containing a Liofilchem® MIC test strip (Liofilchem, Italy) for a specific antibiotic. The MIC was interpreted according to manufacturer's instructions after culturing at 28°C for 2 days, or for slow-growing strains, 6 days. Therefore, MICs were estimated in customized standard



conditions rather than strain-specific optimal growth conditions or standard conditions recommended by the European Committee on Antimicrobial Susceptibility Testing (EUCAST) for clinical bacterial isolates (Kahlmeter et al., 2006), and the data might therefore not be comparable with clinical MIC data.

The ability of the strains to utilize 31 different carbon sources was assessed using the Biolog EcoPlate system (Biolog, Inc., Hayward, CA, United States), with the exception of HAMBI 2948 which grew poorly in experimental conditions. The experimental procedure was modified from MacLean et al. (2004). Strains were precultured in liquid PPY medium for 48 or 96 h, depending on strain growth ability, at 28°C with constant rotation. Subsequently, cells were spun down, resuspended in M9 salt solution and nutrient-starved for 48–72 h. Starved cells were spun down to remove any carryover nutrients in the supernatant, and resuspended in fresh M9 salt solution. Following 100-fold dilution into M9 salt solution, 150 µl of the culture was pipetted to wells in an EcoPlate (one EcoPlate per strain) containing three technical replicate wells for each carbon source and a negative control. The ability of a strain to utilize a particular carbon source was interpreted as a significantly higher optical density, based on a *t*-test, at 590 nm (measured with Tecan Infinite M200 well-plate reader) compared to the negative control after culturing for 7 days at 28°C.

DNA Extraction and Sequencing for 16S rRNA Amplicon Analysis

DNA from three technical replicates from the original pooled bacterial community and three replicate communities from days 16, 32, and 48 in the serial transfer experiment was extracted using DNeasy 96 Blood & Tissue Kit (Qiagen, Hilden, Germany). DNA extraction was performed according to the manufacturer's instructions using 400–600 µl of sample. DNA concentrations were measured using the Qubit® 3.0 fluorometer (Thermo Fisher Scientific, Waltham, MA, United States).

Paired-end sequencing was performed using the Illumina MiSeq platform at the Institute for Molecular Medicine Finland (FIMM) amplifying the V3 and V4 regions of ribosomal RNA with Phusion High Fidelity PCR Master Mix (Thermo Fisher Scientific, Waltham, MA, United States). Reactions were done with a 2-step PCR method with primers carrying Illumina adapter tails (PCR1: forward 5'-ACACTCTTTCCCTACACGACGCTCTTCCGATCTCTCTACGGGAGGCAGCAG-3', reverse 5'-AGACGTGTGCTCTTCCGATCTTCTRCGMATTYCACYKCTACAC-3'; PCR2: forward 5'-ACACTCTTTCCCTACACGACGCTCTTCCGATCTGACTACHVGGGTATCTAATC-3', reverse 5'-AGACGTGTGCTCTTCCGATCTCCTACGGGNGGCWGCAG-3'). For PCR2, the primers are the same but the locus-specific part and adapter part have been paired vice versa

to create more diversity in the final sequencing library. Products from PCR1 and PCR2 were pooled together and indexed with two Illumina P5/P7 index primers (every sample had their own unique combination).

PCR amplification was performed in a volume of 20 μ l containing approx. 20 ng of sample DNA, 1 μ l (5 μ M) of each locus-specific primer (final concentration 0.25 μ M), and 10 μ l of 2 \times Phusion High-Fidelity PCR Master Mix, and the reaction mix was brought to a final volume with laboratory grade water. The cycling conditions were as follows: 98°C for 30 s, 27 cycles of 98°C for 10 s, 62°C for 30 s, and 72°C for 15 s, with a final extension at 72°C for 10 min, followed by hold at 10°C.

Sample indexing was performed in a volume of 20 μ l containing 1.5 μ l (5 μ M) of each index primer (final concentration 0.375 μ M), 10 μ l of 2 \times Phusion High-Fidelity PCR Master Mix (Thermo Fisher Scientific, Waltham, MA, United States) and 1 μ l of pooled PCR product. The reaction mix was brought to a final volume with laboratory grade water. The cycling conditions were as follows: 98°C for 30 s, 8 cycles of 98°C for 10 s, 65°C for 30 s, and 72°C for 20 s, with a final extension at 72°C for 5 min, followed by hold at 10°C.

After PCR, random samples were measured with LabChip GX Touch HT DNA High Sensitivity Reagent Kit (Perkin Elmer, Waltham, MA, United States) to check that the PCR was successful with the correct product size. The same run was repeated after indexing. Samples were pooled together in equal volumes and purified with Agencourt® AMPure® XP beads (Beckman Coulter, Brea, CA, United States) twice using 0.8 \times volume of beads compared to the sample pool volume (40 μ l). The ready amplicon library was diluted to 1:10 and 1:20 and quantified with the Agilent 2100 Bioanalyzer High Sensitivity DNA Analysis Kit (Agilent Genomics, Santa Clara, CA, United States). The 16S rRNA gene amplicon pool was sequenced with Illumina MiSeq System using the Illumina MiSeq Reagent Kit v3 600 cycles kit (Illumina, San Diego, CA, United States). The read length for the paired-end run was 2 \times 300 bp.

DNA Extraction and Sequencing for Whole-Genome Analysis

For this study, 16 of the 33 model community strains were whole-genome sequenced (Table 1). For the remaining 17 strains, 16 assembled genomes were obtained from the NCBI Reference Sequence Database (RefSeq) and 1 raw sequence dataset was obtained from the Joint Genome Institute Genomes OnLine Database (JGI GOLD; Supplementary Table S1). For the strains sequenced, DNA was extracted from 1 ml of liquid culture using the DNeasy 96 Blood & Tissue Kit (Qiagen, Hilden, Germany) according to manufacturer's instructions. DNA concentrations were measured using the Qubit® 3.0 fluorometer (Thermo Fisher Scientific, Waltham, MA, United States). High-throughput sequencing was performed by the Next Generation Sequencing Services, Institute for Molecular Medicine Finland (FIMM). For this, 2.5 ng of dsDNA was prepared according to the Nextera XT DNA Library Prep Kit Reference Guide (Illumina, San Diego, GA, United States) with the following modifications: All reactions

were performed in half of the normal volume, and normalization was done according to the concentration measured on LabChip GX Touch HT (PerkinElmer, United States). 530–670 bp fragments were size selected from the pool using BluePippin (Sage Science, United States). Sequencing was performed with the Illumina HiSeq2500 system in the HiSeq high output mode using v4 kits (Illumina, San Diego, CA, United States). The read length for the paired-end run was 2 \times 101 bp.

16S rRNA Amplicon Analysis

Sequencing adapters were removed from unpaired sequence data using Cutadapt 1.12 (Martin, 2011), with the parameter –minimum-length 100. Sequence pairing was done with Pear 0.9.11 (Zhang et al., 2014). Quality was assessed before and after Cutadapt and Pear with FASTQC¹, and further trimming was done with PRINSEQ (Schmieder and Edwards, 2011) using the parameters –trim_left 5 and –trim_right 40 to obtain better quality. Quality filtering was done with the USEARCH 10 (Edgar, 2013) command –fastq_filter with fastq_maxee setting 1.0 (to discard all reads with > 1.0 total expected errors). The command –usearch_global was used to align the sequences to the 16S rRNA fragment database of the strains with > 97% identity. The Shannon diversity index was computed using the USEARCH 10 command –alpha_div. Difference in community composition between days 16–48 (disregarding initial stock at time point 0 that might not represent viable cell counts for each strain) was assessed in R 3.4.0 (R Core Team, 2017) using permutational multivariate analysis of variance (PERMANOVA) as implemented in the adonis function in the vegan package (Anderson, 2001; Oksanen et al., 2016).

Genome Assembly and Annotation

Prior to genome assembly, Cutadapt 1.12 (Martin, 2011) was used to remove sequencing adapters and quality trim sequence data, with the parameters –O 10 (minimum overlap for an adapter match) and –q 28 (quality cutoff for the 3' end of each read). Sequence data quality before and after Cutadapt was assessed using FASTQC¹ and multiQC (Ewels et al., 2016). Genome assembly was performed using SPAdes 3.11.1 (Bankevich et al., 2012) with default settings (i.e., no specified parameters since SPAdes performs estimation of e.g., k-mer sizes, coverage cutoff value and PHRED quality offset for input reads). Following assembly, contigs were filtered by minimum coverage 30 and minimum length 1000 bp. Genome assembly quality was assessed using QUAST 4.0 (Gurevich et al., 2013), and by mapping reads back to the assembly using Bowtie 2 with default settings (Langmead and Salzberg, 2012) combined with the Picard² command CollectWgsMetrics performed for alignment files after sorting with SAMtools (Li et al., 2009) and marking duplicates with Picard (Table 1). Subsequently, all assemblies, including those obtained from databases, were annotated using Prokka 1.12 (Seemann, 2014), providing genus and species names, with the parameters –centre X, –compliant, and –usegenus.

¹<http://www.bioinformatics.babraham.ac.uk/projects/fastqc>

²<http://broadinstitute.github.io/picard>

TABLE 1 | Genome sequencing and assembly metrics.

Strain	Raw sequence yield (Gb)	Length (bp)	Coverage \pm SD	% reads mapped	Largest contig (bp)	No. contigs	GC%	N50
HAMBI 6	0.76	6,425,774	88.4 \pm 32.6	98.8	459,923	99	61.80	167,218
HAMBI 97	1.36	3,256,685	213 \pm 63.1	97.4	201,770	162	41.41	32,660
HAMBI 105	0.79	5,387,408	110 \pm 31.4	99.7	1,656,016	35	59.42	689,457
HAMBI 262	0.70	3,407,715	147 \pm 49.7	98.6	203,726	88	67.02	103,424
HAMBI 1287	0.91	4,685,430	142 \pm 40.2	99.7	540,344	31	53.81	453,729
HAMBI 1874	—*	5,845,984	219 \pm 36.4	94.9	337,658	94	39.90	117,696
HAMBI 1972	1.02	4,463,252	160 \pm 54.3	99.2	404,185	61	61.77	179,321
HAMBI 1977	0.74	6,621,816	83.0 \pm 31.5	99.4	675,539	57	63.08	355,467
HAMBI 1992	0.86	5,412,359	119 \pm 35.6	99.6	544,523	57	59.33	262,180
HAMBI 2159	0.86	6,527,402	96.1 \pm 30.2	99.0	590,902	59	64.73	222,449
HAMBI 2160	0.89	3,679,287	172 \pm 49.3	99.2	544,789	48	61.65	278,194
HAMBI 2467	0.77	2,584,354	200 \pm 48.3	98.5	519,133	29	70.03	174,888
HAMBI 2494	0.90	6,648,385	102 \pm 32.1	98.9	781,864	68	65.45	259,448
HAMBI 2792	1.28	2,116,559	245 \pm 22.5	95.7	118,108	103	45.03	51,649
HAMBI 2948	1.23	3,031,855	218 \pm 55.3	100	1,099,313	22	42.82	657,030
HAMBI 3031	1.09	5,519,621	147 \pm 55.8	99.9	1,089,344	28	42.70	633,609
HAMBI 3172	0.79	7,139,720	78.4 \pm 29.8	97.7	230,491	186	68.98	71,229

*HAMBI 1874 was assembled but not sequenced in this study.

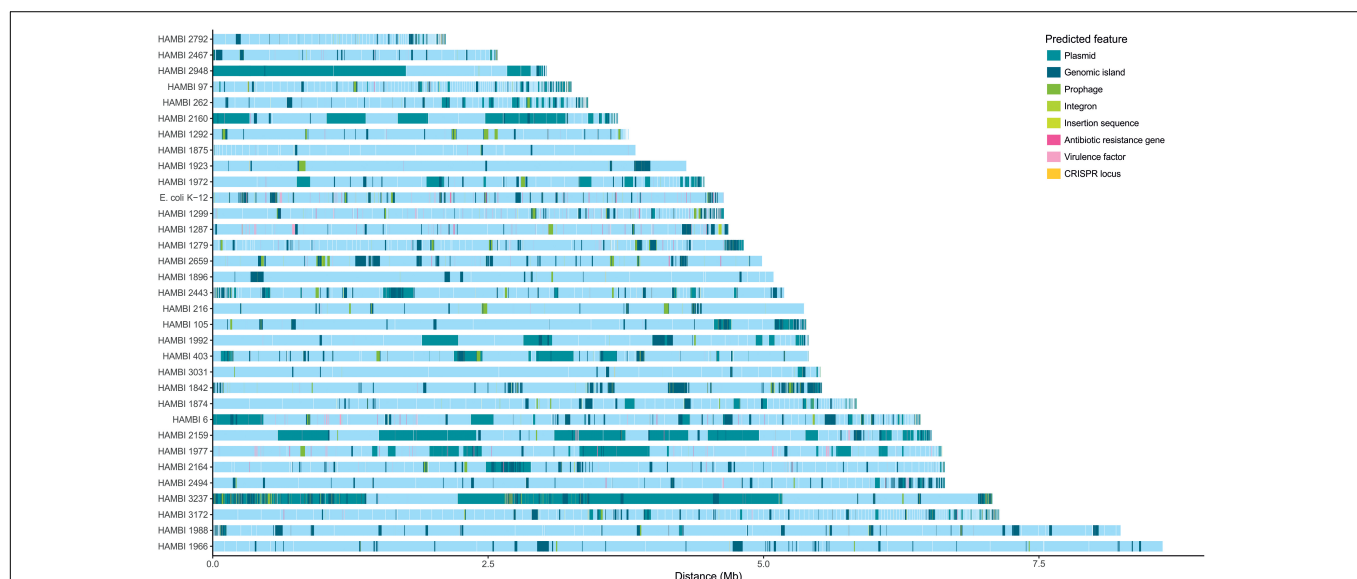


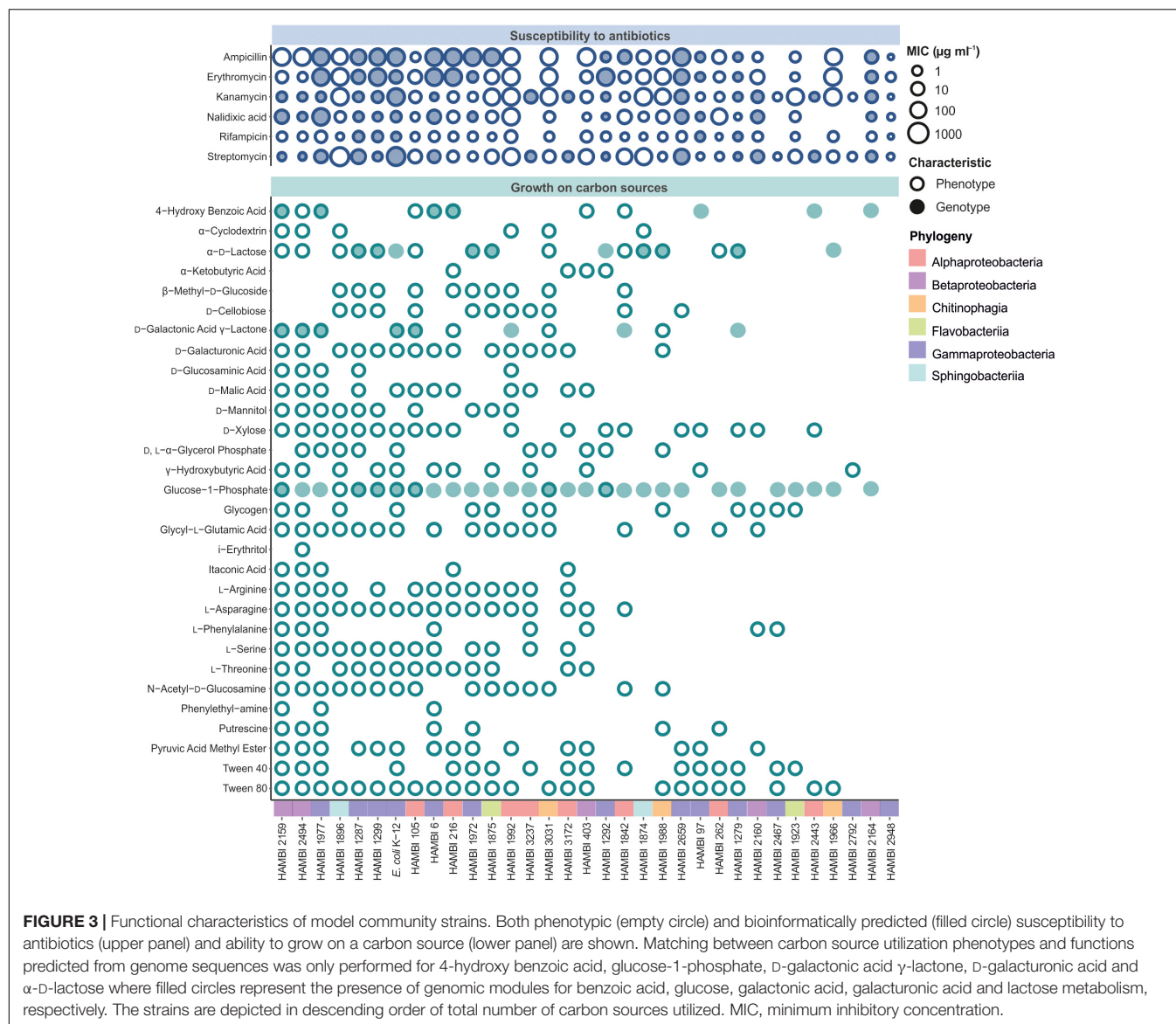
FIGURE 2 | Genomic features of model community strains. *E. coli* K-12, HAMBI 216, HAMBI 1923 and HAMBI 2659 are closed genomes composed of a single chromosome. Other genomes are composed of blocks of adjacent contigs whose order may not reflect genomic position. Contigs are ordered by size for genomes assembled in this study and by order of appearance in assembly file for genomes obtained from databases. Predicted features are depicted by colored blocks along the genome. These include plasmid-derived sequences, genomic islands, prophages, integrons, insertion sequences, antibiotic resistance genes, virulence factors, and CRISPR loci.

Phylogenetic Analysis

We identified and aligned genes conserved among all community members using Roary 3.8.0-0 (Page et al., 2015) with minimum BLASTp identity set to 65% and protein group limit set to 200,000 to account for high diversity in the community. The core gene alignment, consisting of four ribosomal proteins (*rplN*, *rpmA*, *rpsL*, and *rpsS*) and the ATP synthase subunit beta (*atpD*), was used to create a phylogenetic tree with PhyML (Guindon et al., 2010), visualized in iTol (Letunic and Bork, 2016).

Characterization of Genomic Features

To generate comprehensive genomic metadata for model community strains, the genome assemblies were scanned for genomic elements using several tools, with default parameters unless otherwise specified. The Metabolic And Physiological potential Evaluator (MAPLE) 2.3.0 (Takami et al., 2016) was used to map genes in assemblies to functional modules as defined by the Kyoto Encyclopedia of Genes and Genomes (KEGG) and for calculating module completion ratios (MCR).



Genomic islands, i.e., large genomic regions assumed to have horizontal origins, were predicted using IslandViewer 4 (Bertelli et al., 2017). For strains other than *E. coli* K-12, HAMBI 216, HAMBI 1923 and HAMBI 2659 which have closed genomes, genomic island predictions were obtained for incomplete genomes with contigs ordered against closely related reference genomes (**Supplementary Table S3**) using the Mauve contig orderer (Rissman et al., 2009; Bertelli et al., 2017).

Plasmid-derived sequences were predicted using cBar 1.2 (Zhou and Xu, 2010) and PlasmidFinder 1.3 (Carattoli et al., 2014), which was implemented through ABRicate³ using databases dated 2018-01-02. In addition, for genomes assembled for this study, plasmidSPAdes (Antipov et al., 2016) implemented in SPAdes 3.11.1 (Bankevich et al., 2012) was used, with

assignment of plasmid annotation to > 1000 bp regions in genome assembly contigs displaying 100% BLASTn (Altschul et al., 1990) identity with plasmid assemblies generated by plasmidSPAdes.

Antibiotic resistance and virulence genes were predicted with ABRicate (<https://github.com/tseemann/abricate>, databases dated 2018-01-02) using ResFinder 3.0 (Zankari et al., 2012), the comprehensive antibiotic resistance database (CARD) (Jia et al., 2017), and the virulence factors database (VFDB) (Chen et al., 2016), discarding hits with proportion of gene covered < 50%. Prophages, integrons, insertion sequences, and clustered regularly interspaced short palindromic repeats (CRISPR) were predicted using the PHAGE Search Tool – Enhanced Release (PHASTER; accessed 2018-01-08) (Arndt et al., 2016), Integron Finder 1.5.1 (Cury et al., 2016), ISEScan 1.5.4.3 (Xie and Tang, 2017) and CRISPRFinder (accessed 2018-02-01) (Grissa et al., 2007), respectively.

³<https://github.com/tseemann/abricate>

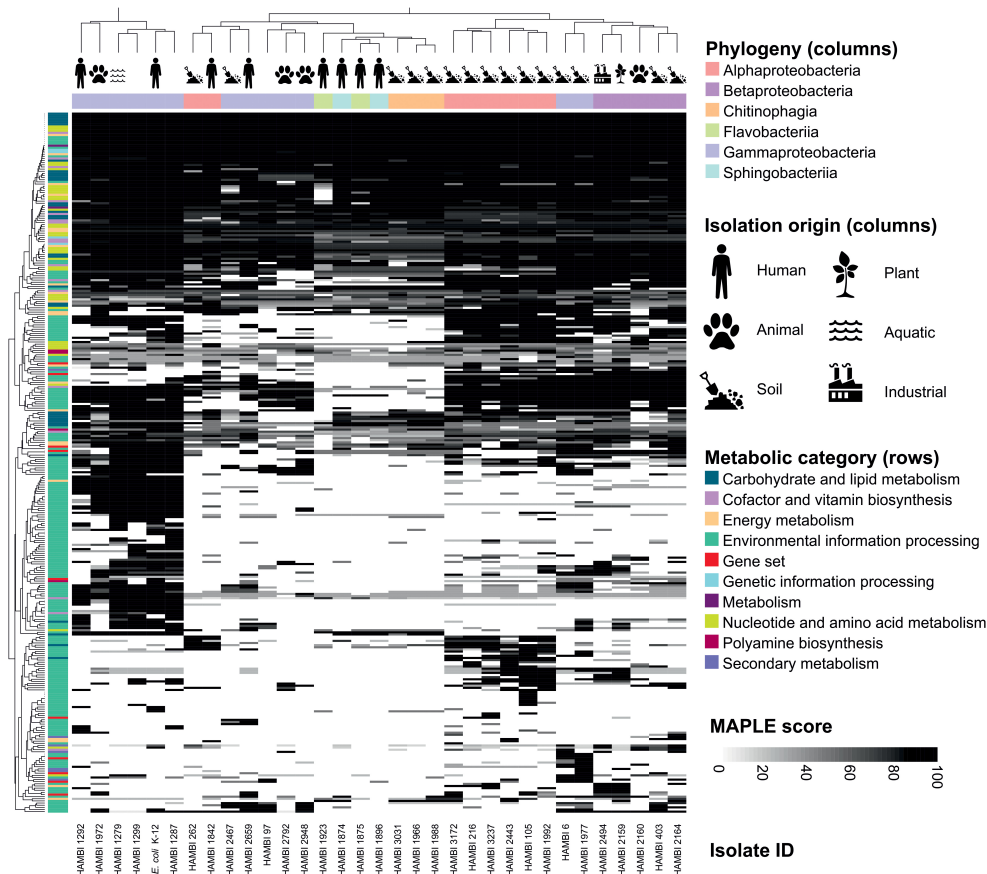


FIGURE 4 | Metabolic pathways of model community strains. The pathways were predicted from genome sequences using MAPLE. Pathway completeness (MAPLE score) is depicted as shades of gray in a heat map organized by the phylogenetic class and isolation origin of model community strains (columns) and by the presence of metabolic pathways predicted by MAPLE (rows). The metabolic characteristics display hierarchical clustering by the phylogenetic class and isolation origin of the isolates.

Notably, in the absence of further validation steps, plasmid predictions obtained with cBar or plasmidSPAdes have low accuracy (Arredondo-Alonso et al., 2017), and genomic island predictions for draft level genomes may contain errors (Bertelli et al., 2017), and the predicted loci must therefore be considered as regions of interest rather than high-confidence predictions.

RESULTS

Genomic Composition

The strains display high variability in genome size and genomic content, including the resistome, mobilome and functionome (Figure 2). Antibiotic resistance and virulence genes are particularly prevalent among strains in the Gammaproteobacteria class (Figures 1, 2). Genomic elements associated with horizontal gene transfer, including plasmids, genomic islands, prophages, integrons, and insertion sequences, occur frequently among the strains, as do CRISPR arrays that might be associated with CRISPR/Cas

systems conferring adaptive immunity against mobile genetic elements.

Metabolic and Physiological Characteristics

The strains display diverse antibiotic susceptibility and carbon source utilization phenotypes (Figure 3). Antibiotic resistance phenotypes are variably associated with the presence of bioinformatically predicted resistance factors to the antibiotic class. The number of carbon sources on which the strains can grow displays high variability, with a maximum of 25 out of 31 carbon sources (HAMBI 2159 and 2494, which both belong to the genus *Paraburkholderia*), indicating large differences between strains in metabolic capacity and fastidiousness. Furthermore, the presence of genomic functional modules for benzoic acid, galactonic acid, galacturonic acid or lactose metabolism is frequently associated with the ability of a strain to grow with a corresponding compound as the sole carbon source (Figure 3).

The metabolic characteristics predicted from the genome sequences by MAPLE display hierarchical clustering by

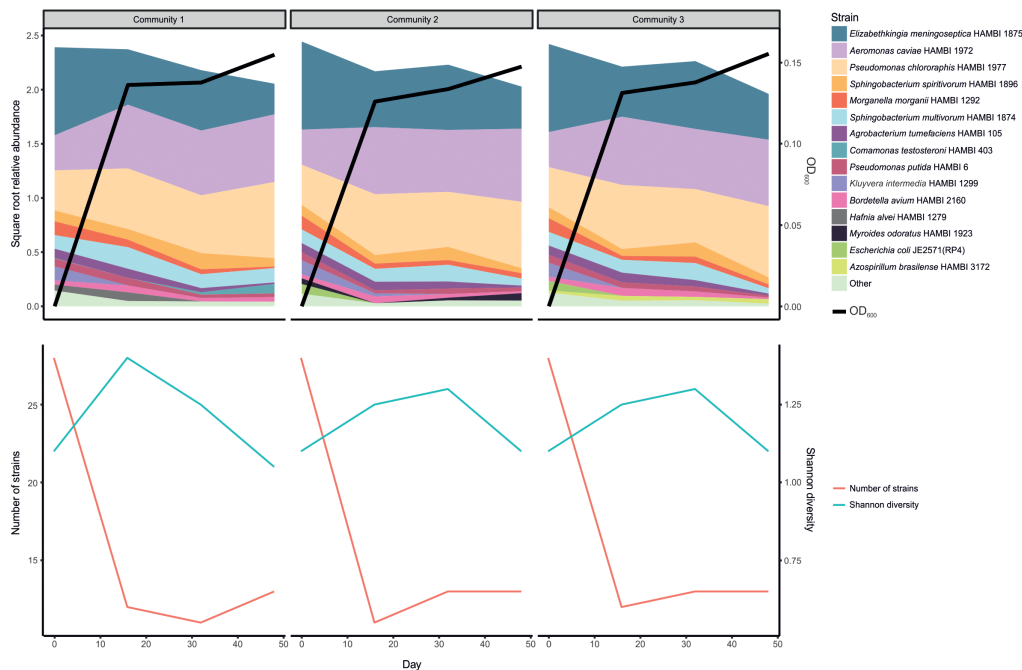


FIGURE 5 | Persistence of strains in model community when serially transferred for 48 days (three replicate communities). The upper panel shows the relative abundance of the 15 most abundant taxa and a proxy for total cell density (optical density, OD, at 600 nm). The lower panel shows two diversity indices, richness (strain count) and the Shannon index.

phylogenetic classes of the isolates as well as by their isolation origin (Figure 4). Soil isolates typically cluster separately from isolates from humans and animals. Most of this clustering is driven by metabolic functions related to environmental information processing. Core metabolic pathways such as the tricarboxylic acid cycle are present across all isolates while specialized metabolic features, such as utilization of less common carbohydrates, exhibit differences in their distribution across the isolates.

Coexistence of Strains in Co-culture

Serially transferring the 33 strain community for 48 days seemingly led to a loss of over half of the strains within the first 16 days, although the initial number of viable strains is uncertain owing to different growth dynamics of individual strains prior to initiating the experiment (Supplementary Figure S1 and Figure 5). After these transient dynamics, there was only a marginally significant change in community composition over time between days 16 and 48 (PERMANOVA: $F_{1,7} = 3.018$, $r^2 = 0.301$, $p = 0.074$). Furthermore, the apparent initial loss in richness (strain count) was accompanied by an increase in evenness, seen as a relatively small temporal change in Shannon diversity, which accounts for both factors. There were three dominant strains: *Elizabethkingia meningoseptica* HAMBI 1875, *Aeromonas caviae* HAMBI 1972 and *Pseudomonas chlororaphis* HAMBI 1977. However, the degree to which the dominance of these strains is caused by their relative abundance or viability in the input community (strain mix) or competitive ability during co-culture is uncertain.

DISCUSSION AND CONCLUSION

We developed a multispecies synthetic bacterial community, which was characterized at the genomic and phenotypic levels, revealing high diversity in the resistome, mobilome and functionome of the community. Furthermore, we demonstrated the utility of the community by showing coexistence of a large proportion (14/33) of the strains in co-culture over serial transfer for 48 days. These observations indicate that the community is suitable for use as a cultivated model community to ask a wide range of biological questions.

Along with characterizing the community, we produced comprehensive genomic and phenotypic metadata for the community members. This facilitates future mechanistic work with the community. For instance, our pipeline allows the use of amplicon sequencing to track community composition over time at strain-level resolution. Moreover, the genome assemblies provide a reference database for (meta)genomic and (meta)transcriptomic studies. Isolation of individual colonies combined with colony PCR, in turn, allows the rapid identification of substrains possessing mutations or horizontal gene transfer events of interest.

Our model community is composed of diverse bacterial strains isolated from different environments and hence does not mimic any specific natural community. Therefore, the community is more suited to study general questions about ecology and evolution such as community assembly and response to environmental perturbations rather than to explain patterns in any particular natural microbial community (Wolfe, 2018).

The ability of the community to answer general questions may be limited by the potential absence of focal taxonomic groups or high-order interactions that occur in more complex communities. The community is composed of bacteria alone, while interactions between bacteria and fungi, protozoa or bacteriophages often play a key role in natural microbial communities. In a separate study, however, we have introduced a method for incorporating protozoa in the community (Cairns et al., 2018).

The utility of the 33-strain model community and its predecessor is demonstrated in the current and previous work by us (Cairns et al., 2018). Here we present the community and a collection of methods and metadata to the scientific community. A previous version of the community has already been successfully used for tracking the mobility of antibiotic resistance genes (Cairns et al., 2018), and as prominent cases of future use we envision, for instance, replicated ecosystem microcosms to explore the trajectories of ecosystem composition and genetic structure in response to various environmental perturbations. We also envision the community as an efficient spike-in control to increase the statistical rigor of high-throughput microbial single cell assays such as epicPCR (Spencer et al., 2016) or as a test system for validating metagenome assemblers.

DATA AVAILABILITY

Raw fastq files and genome assemblies for the genomes sequenced or assembled in this study ($N = 17$) have been deposited in the National Center for Biotechnology Information (NCBI) Sequence Read Archive (SRA) and GenBank, respectively, under the BioProject Accession Number PRJNA476209. Accession numbers for raw fastq files or genome assemblies obtained for this study from databases are listed in **Supplementary Table S1**. Previously Sanger sequenced near-full-length 16S rRNA gene sequences for all strains are available in the European Nucleotide Archive (ENA) under the Accession Number PRJEB21728 (<https://www.ebi.ac.uk/ena/data/view/PRJEB21728>). The complete sequence for the plasmid RP4 harbored by *E. coli* K-12 JE2571(RP4) is available from GenBank under the accession BN000925 (Pansegrau et al., 1994). Genome annotations, including those obtained in this study for previously sequenced or assembled genomes, are available upon request.

The following community metadata is available via Dryad (doi: 10.5061/dryad.53b6n5f): Genomic predictions for functional modules obtained using MAPLE 2.3.0 (Takami et al.,

2016); genomic feature data collated into a single data frame, using custom R scripts (R Core Team, 2017), displaying strain, contig, locus, and genomic feature information; antibiotic MICs; and carbon source utilization phenotypes. Raw output files for each strain from all genomic feature prediction tools are available upon request.

The model community strains, except for *E. coli* K-12 strain JE2571(RP4), are available individually from the HAMBI culture collection at the University of Helsinki, Finland (<http://www.helsinki.fi/hambi/>). For further requests concerning the use of the model community, please contact the corresponding author.

AUTHOR CONTRIBUTIONS

JC and TH designed the experiments. RJ contributed to phenotypic measurements, proof of concept experiments, and performed sequence analyses for 16S rRNA amplicon data. TH, JH, and MV provided sequencing resources. JC and JH designed the sequence analyses. JC performed sequence analyses for whole-genome data and drafted the manuscript. JC, MT, and RJ contributed to data visualization. RJ, JH, MT, MV, and TH edited and commented on the manuscript. All authors gave final approval for publication and accept accountability for the content and work performed.

FUNDING

This work was supported by Academy of Finland projects (Grant Nos. 308128 and 314114 to JH and 307213 to TH), University of Helsinki (3-year Grant to JH), and Doctoral Programme in Microbiology and Biotechnology, University of Helsinki (funding to JC).

ACKNOWLEDGMENTS

We thank Anna Hartikainen and Liisa Ruusulehto for technical assistance, and acknowledge CSC – IT Center for Science Ltd., for the allocation of computational resources.

SUPPLEMENTARY MATERIAL

The Supplementary Material for this article can be found online at: <https://www.frontiersin.org/articles/10.3389/fgene.2018.00312/full#supplementary-material>

REFERENCES

- Altschul, S. F., Gish, W., Miller, W., Myers, E. W., and Lipman, D. J. (1990). Basic local alignment search tool. *J. Mol. Biol.* 215, 403–410. doi: 10.1016/S0022-2836(05)80360-2
- Anderson, M. J. (2001). A new method for non-parametric multivariate analysis of variance. *Austral Ecol.* 26, 32–46. doi: 10.1111/j.1442-9993.2001.01070.pp.x
- Antipov, D., Hartwick, N., Shen, M., Raiko, M., Lapidus, A., and Pevzner, P. A. (2016). plasmidSPAdes: assembling plasmids from whole genome sequencing data. *Bioinformatics* 32, 3380–3387. doi: 10.1093/bioinformatics/btw493
- Arndt, D., Grant, J. R., Marcu, A., Sajed, T., Pon, A., Liang, Y. J., et al. (2016). PHASTER: a better, faster version of the PHAST phage search tool. *Nucleic Acids Res.* 44, W16–W21. doi: 10.1093/nar/gkw387
- Arredondo-Alonso, S., Willems, R. J., van Schaik, W., and Schürch, A. C. (2017). On the (im)possibility of reconstructing plasmids from whole-genome short-read sequencing data. *Microb. Genom.* 3:e000128. doi: 10.1099/mgen.0.000128
- Bairey, E., Kelsic, E. D., and Kishony, R. (2016). High-order species interactions shape ecosystem diversity. *Nat. Commun.* 7:12285. doi: 10.1038/ncomms12285

- Bankevich, A., Nurk, S., Antipov, D., Gurevich, A. A., Dvorkin, M., Kulikov, A. S., et al. (2012). SPAdes: a new genome assembly algorithm and its applications to single-cell sequencing. *J. Comput. Biol.* 19, 455–477. doi: 10.1089/cmb.2012.0021
- Bell, T., Newman, J. A., Silverman, B. W., Turner, S. L., and Lilley, A. K. (2005). The contribution of species richness and composition to bacterial services. *Nature* 436, 1157–1160. doi: 10.1038/nature03891
- Benton, T. G., Solan, M., Travis, J. M. J., and Sait, S. M. (2007). Microcosm experiments can inform global ecological problems. *Trends Ecol. Evol.* 22, 516–521. doi: 10.1016/j.tree.2007.08.003
- Bertelli, C., Laird, M. R., Williams, K. P., Lau, B. Y., Hoar, G., Winsor, G. L., et al. (2017). IslandViewer 4: expanded prediction of genomic islands for larger-scale datasets. *Nucleic Acids Res.* 45, W30–W35. doi: 10.1093/nar/gkx343
- Betts, A., Gray, C., Zelek, M., MacLean, R. C., and King, K. C. (2018). High parasite diversity accelerates host adaptation and diversification. *Science* 360, 907–911. doi: 10.1126/science.aam9974
- Bradley, D. E. (1980). Morphological and serological relationships of conjugative pili. *Plasmid* 4, 155–169. doi: 10.1016/0147-619X(80)90005-0
- Brockhurst, M. A., and Koskella, B. (2013). Experimental coevolution of species interactions. *Trends Ecol. Evol.* 28, 367–375. doi: 10.1016/j.tree.2013.02.009
- Buckling, A., MacLean, R. C., Brockhurst, M. A., and Colegrave, N. (2009). The Beagle in a bottle. *Nature* 457, 824–829. doi: 10.1038/nature07892
- Cairns, J., Ruokolainen, L., Hultman, J., Tamminen, M., Virta, M., and Hiltunen, T. (2018). Ecology determines how low antibiotic concentration impacts community composition and horizontal transfer of resistance genes. *Commun. Biol.* 1:35. doi: 10.1038/s42003-018-0041-7
- Carattoli, A., Zankari, E., Garcia-Fernandez, A., Larsen, M. V., Lund, O., Villa, L., et al. (2014). *In silico* detection and typing of plasmids using PlasmidFinder and plasmid multilocus sequence typing. *Antimicrob. Agents Chemother.* 58, 3895–3903. doi: 10.1128/AAC.02412-14
- Carpenter, S. R. (1996). Microcosm experiments have limited relevance for community and ecosystem ecology. *Ecology* 77, 677–680. doi: 10.2307/2265490
- Carpenter, S. R. (1999). Microcosm experiments have limited relevance for community and ecosystem ecology: reply. *Ecology* 80, 1085–1088. doi: 10.1890/0012-9658(1999)080[1085:MEHLRF]2.0.CO;2
- Celiker, H., and Gore, J. (2014). Clustering in community structure across replicate ecosystems following a long-term bacterial evolution experiment. *Nat. Commun.* 5:4643. doi: 10.1038/ncomms5643
- Chase, A. B., Karaoz, U., Brodie, E. L., Gomez-Lunar, Z., Martiny, A. C., and Martiny, J. B. H. (2017). Microdiversity of an abundant terrestrial bacterium encompasses extensive variation in ecologically relevant traits. *mBio* 8:e1809-17. doi: 10.1128/mBio.01809-17
- Chen, L. H., Zheng, D. D., Liu, B., Yang, J., and Jin, Q. (2016). VFDB 2016: hierarchical and refined dataset for big data analysis-10 years on. *Nucleic Acids Res.* 44, D694–D697. doi: 10.1093/nar/gkv1239
- R Core Team (2017). *R: A Language and Environment for Statistical Computing*. Vienna: R Foundation for Statistical Computing.
- Cury, J., Jove, T., Touchon, M., Neron, B., and Rocha, E. P. C. (2016). Identification and analysis of integrons and cassette arrays in bacterial genomes. *Nucleic Acids Res.* 44, 4539–4550. doi: 10.1093/nar/gkw319
- Dejonghe, W., Berteloot, E., Goris, J., Boon, N., Crul, K., Maertens, S., et al. (2003). Synergistic degradation of linuron by a bacterial consortium and isolation of a single linuron-degrading *Variovorax* strain. *Appl. Environ. Microbiol.* 69, 1532–1541. doi: 10.1128/AEM.69.3.1532-1541.2003
- Dolinsek, J., Goldschmidt, F., and Johnson, D. R. (2016). Synthetic microbial ecology and the dynamic interplay between microbial genotypes. *FEMS Microbiol. Rev.* 40, 961–979. doi: 10.1093/femsre/fuw024
- Drenner, R. W., and Mazumder, A. (1999). Microcosm experiments have limited relevance for community and ecosystem ecology: comment. *Ecology* 80, 1081–1085. doi: 10.1890/0012-9658(1999)080[1081:MEHLRF]2.0.CO;2
- Dunham, M. J. (2007). Synthetic ecology: a model system for cooperation. *Proc. Natl. Acad. Sci. U.S.A.* 104, 1741–1742. doi: 10.1073/pnas.0611067104
- Edgar, R. C. (2013). UPARSE: highly accurate OTU sequences from microbial amplicon reads. *Nat. Methods* 10, 996–998. doi: 10.1038/nmeth.2604
- Elias, S., and Banin, E. (2012). Multi-species biofilms: living with friendly neighbors. *FEMS Microbiol. Rev.* 36, 990–1004. doi: 10.1111/j.1574-6976.2012.00325.x
- Ewels, P., Magnusson, M., Lundin, S., and Kaller, M. (2016). MultiQC: summarize analysis results for multiple tools and samples in a single report. *Bioinformatics* 32, 3047–3048. doi: 10.1093/bioinformatics/btw354
- Foster, K. R., and Bell, T. (2012). Competition, not cooperation, dominates interactions among culturable microbial species. *Curr. Biol.* 22, 1845–1850. doi: 10.1016/j.cub.2012.08.005
- Fraser, L. H., and Keddy, P. (1997). The role of experimental microcosms in ecological research. *Trends Ecol. Evol.* 12, 478–481. doi: 10.1016/S0169-5347(97)01220-2
- Frickel, J., Feulner, P. G. D., Karakoc, E., and Becks, L. (2018). Population size changes and selection drive patterns of parallel evolution in a host-virus system. *Nat. Commun.* 9:1706. doi: 10.1038/s41467-018-03990-7
- Good, B. H., McDonald, M. J., Barrick, J. E., Lenski, R. E., and Desai, M. M. (2017). The dynamics of molecular evolution over 60,000 generations. *Nature* 551, 45–50. doi: 10.1038/nature24287
- Goodman, A. L., Kallstrom, G., Faith, J. J., Reyes, A., Moore, A., Dantas, G., et al. (2011). Extensive personal human gut microbiota culture collections characterized and manipulated in gnotobiotic mice. *Proc. Natl. Acad. Sci. U.S.A.* 108, 6252–6257. doi: 10.1073/pnas.1102938108
- Grissa, I., Vergnaud, G., and Pourcel, C. (2007). CRISPRFinder: a web tool to identify clustered regularly interspaced short palindromic repeats. *Nucleic Acids Res.* 35, W52–W57. doi: 10.1093/nar/gkm360
- Guindon, S., Dufayard, J. F., Lefort, V., Anisimova, M., Hordijk, W., and Gascuel, O. (2010). New algorithms and methods to estimate maximum-likelihood phylogenies: assessing the performance of PhyML 3.0. *Syst. Biol.* 59, 307–321. doi: 10.1093/sysbio/syq010
- Gurevich, A., Saveliev, V., Vyahhi, N., and Tesler, G. (2013). QUAST: quality assessment tool for genome assemblies. *Bioinformatics* 29, 1072–1075. doi: 10.1093/bioinformatics/btt086
- Hall, A. R., Scanlan, P. D., Morgan, A. D., and Buckling, A. (2011). Host-parasite coevolutionary arms races give way to fluctuating selection. *Ecol. Lett.* 14, 635–642. doi: 10.1111/j.1461-0248.2011.01624.x
- Harcombe, W. (2010). Novel cooperation experimentally evolved between species. *Evolution* 64, 2166–2172. doi: 10.1111/j.1558-5646.2010.00959.x
- Helling, R. B., Vargas, C. N., and Adams, J. (1987). Evolution of *Escherichia coli* during growth in a constant environment. *Genetics* 116, 349–358.
- Hiltunen, T., and Becks, L. (2014). Consumer co-evolution as an important component of the eco-evolutionary feedback. *Nat. Commun.* 5:5226. doi: 10.1038/ncomms6226
- Jia, B. F., Raphenya, A. R., Alcock, B., Waglechner, N., Guo, P. Y., Tsang, K. K., et al. (2017). CARD 2017: expansion and model-centric curation of the comprehensive antibiotic resistance database. *Nucleic Acids Res.* 45, D566–D573. doi: 10.1093/nar/gkw1004
- Kahlmeter, G., Brown, D. F. J., Goldstein, F. W., MacGowan, A. P., Mouton, J. W., Odenholt, I., et al. (2006). European Committee on Antimicrobial Susceptibility Testing (EUCAST) Technical Notes on antimicrobial susceptibility testing. *Clin. Microbiol. Infect.* 12, 501–503. doi: 10.1111/j.1469-0691.2006.01454.x
- Kastman, E. K., Kamelamela, N., Norville, J. W., Cosetta, C. M., Dutton, R. J., and Wolfe, B. E. (2016). Biotic interactions shape the ecological distributions of *Staphylococcus* species. *mBio* 7:e1157-16. doi: 10.1128/mBio.01157-16
- Langmead, B., and Salzberg, S. L. (2012). Fast gapped-read alignment with Bowtie 2. *Nat. Methods* 9, 357–359. doi: 10.1038/nmeth.1923
- Lawrence, D., Fiegna, F., Behrends, V., Bundy, J. G., Phillimore, A. B., Bell, T., et al. (2012). Species interactions alter evolutionary responses to a novel environment. *PLoS Biol.* 10:e1001330. doi: 10.1371/journal.pbio.1001330
- Lebeis, S. L., Paredes, S. H., Lundberg, D. S., Breakfield, N., Gehring, J., McDonald, M., et al. (2015). Salicylic acid modulates colonization of the root microbiome by specific bacterial taxa. *Science* 349, 860–864. doi: 10.1126/science.aaa8764
- Letunic, I., and Bork, P. (2016). Interactive tree of life (iTOL) v3: an online tool for the display and annotation of phylogenetic and other trees. *Nucleic Acids Res.* 44, W242–W245. doi: 10.1093/nar/gkw290
- Li, H., Handsaker, B., Wysoker, A., Fennell, T., Ruan, J., Homer, N., et al. (2009). The sequence alignment/map format and SAMtools. *Bioinformatics* 25, 2078–2079. doi: 10.1093/bioinformatics/btp352
- Liu, W. Z., Russel, J., Roder, H. L., Madsen, J. S., Burmolle, M., and Sorensen, S. J. (2017). Low-abundant species facilitates specific spatial organization that promotes multispecies biofilm formation. *Environ. Microbiol.* 19, 2893–2905. doi: 10.1111/1462-2920.13816

- MacLean, R. C., Bell, G., and Rainey, P. B. (2004). The evolution of a pleiotropic fitness tradeoff in *Pseudomonas fluorescens*. *Proc. Natl. Acad. Sci. U.S.A.* 101, 8072–8077. doi: 10.1073/pnas.0307195101
- MacLean, R. C., and Gudelj, I. (2006). Resource competition and social conflict in experimental populations of yeast. *Nature* 441, 498–501. doi: 10.1038/nature04624
- Martin, M. (2011). Cutadapt removes adapter sequences from high-throughput sequencing reads. *EMBnet J.* 17, 10–12. doi: 10.14806/ej.17.1.200
- Morgan, A. D., Gandon, S., and Buckling, A. (2005). The effect of migration on local adaptation in a coevolving host-parasite system. *Nature* 437, 253–256. doi: 10.1038/nature03913
- Oksanen, J., Blanchet, G. F., Kindt, R., et al. (2016). *vegan: Community Ecology package. R Package version 2.3-5*. Available at: <http://CRAN.R-project.org/package=vegan>
- Page, A. J., Cummins, C. A., Hunt, M., Wong, V. K., Reuter, S., Holden, M. T., et al. (2015). Roary: rapid large-scale prokaryote pan genome analysis. *Bioinformatics* 31, 3691–3693. doi: 10.1093/bioinformatics/btv421
- Pansegau, W., Lanka, E., Barth, P. T., Figurski, D. H., Guiney, D. G., Haas, D., et al. (1994). Complete nucleotide sequence of Birmingham IncPα plasmids: compilation and comparative analysis. *J. Mol. Biol.* 239, 623–663. doi: 10.1006/jmbi.1994.1404
- Petrof, E. O., Gloor, G. B., Vanner, S. J., Weese, S. J., Carter, D., Daigneault, M. C., et al. (2013). Stool substitute transplant therapy for the eradication of *Clostridium difficile* infection: ‘RePOOPulating’ the gut. *Microbiome* 1:3. doi: 10.1186/2049-2618-1-3
- Rissman, A. I., Mau, B., Biehl, B. S., Darling, A. E., Glasner, J. D., and Perna, N. T. (2009). Reordering contigs of draft genomes using the Mauve Aligner. *Bioinformatics* 25, 2071–2073. doi: 10.1093/bioinformatics/btp356
- Rivett, D. W., and Bell, T. (2018). Abundance determines the functional role of bacterial phylotypes in complex communities. *Nat. Microbiol.* 3, 767–772. doi: 10.1038/s41564-018-0180-0
- Rivett, D. W., Jones, M. L., Ramoneda, J., Mombrikotb, S. B., Ransome, E., and Bell, T. (2018). Elevated success of multispecies bacterial invasions impacts community composition during ecological succession. *Ecol. Lett.* 21, 516–524. doi: 10.1111/ele.12916
- Rivett, D. W., Scheuerl, T., Culbert, C. T., Mombrikotb, S. B., Johnstone, E., Barracough, T. G., et al. (2016). Resource-dependent attenuation of species interactions during bacterial succession. *ISME J.* 10, 2259–2268. doi: 10.1038/ismej.2016.11
- Rozen, D. E., and Lenski, R. E. (2000). Long-term experimental evolution in *Escherichia coli*. VIII. Dynamics of a balanced polymorphism. *Am. Nat.* 155, 24–35. doi: 10.1086/303299
- Schmieder, R., and Edwards, R. (2011). Quality control and preprocessing of metagenomic datasets. *Bioinformatics* 27, 863–864. doi: 10.1093/bioinformatics/btr026
- Seemann, T. (2014). Prokka: rapid prokaryotic genome annotation. *Bioinformatics* 30, 2068–2069. doi: 10.1093/bioinformatics/btu153
- Shade, A., and Handelsman, J. (2012). Beyond the Venn diagram: the hunt for a core microbiome. *Environ. Microbiol.* 14, 4–12. doi: 10.1111/j.1462-2920.2011.02585.x
- Shertzer, K. W., Ellner, S. P., Fussmann, G. F., and Hairston, N. G. (2002). Predator-prey cycles in an aquatic microcosm: testing hypotheses of mechanism. *J. Anim. Ecol.* 71, 802–815. doi: 10.1046/j.1365-2656.2002.00645.x
- Sheth, R. U., Cabral, V., Chen, S. P., and Wang, H. H. (2016). Manipulating bacterial communities by in situ microbiome engineering. *Trends Genet.* 32, 189–200. doi: 10.1016/j.tig.2016.01.005
- Shou, W. Y., Ram, S., and Vilar, J. M. G. (2007). Synthetic cooperation in engineered yeast populations. *Proc. Natl. Acad. Sci. U.S.A.* 104, 1877–1882. doi: 10.1073/pnas.0610575104
- Smillie, C. S., Smith, M. B., Friedman, J., Cordero, O. X., David, L. A., and Alm, E. J. (2011). Ecology drives a global network of gene exchange connecting the human microbiome. *Nature* 480, 241–244. doi: 10.1038/nature10571
- Spencer, S. J., Tamminen, M. V., Preheim, S. P., Guo, M. T., Briggs, A. W., Brito, I. L., et al. (2016). Massively parallel sequencing of single cells by epicPCR links functional genes with phylogenetic markers. *ISME J.* 10, 427–436. doi: 10.1038/ismej.2015.124
- Stopnisek, N., Zuhlke, D., Carlier, A., Barberan, A., Fierer, N., Becher, D., et al. (2016). Molecular mechanisms underlying the close association between soil *Burkholderia* and fungi. *ISME J.* 10, 253–264. doi: 10.1038/ismej.2015.73
- Takami, H., Taniguchi, T., Arai, W., Takemoto, K., Moriya, Y., and Goto, S. (2016). An automated system for evaluation of the potential functionome: MAPLE version 2.1.0. *DNA Res.* 23, 467–475. doi: 10.1093/dnares/dsw030
- Treves, D. S., Manning, S., and Adams, J. (1998). Repeated evolution of an acetate-crossfeeding polymorphism in long-term populations of *Escherichia coli*. *Mol. Biol. Evol.* 15, 789–797. doi: 10.1093/oxfordjournals.molbev.a025984
- van Gestel, J., Weissing, F. J., Kuipers, O. P., and Kovacs, A. T. (2014). Density of founder cells affects spatial pattern formation and cooperation in *Bacillus subtilis* biofilms. *ISME J.* 8, 2069–2079. doi: 10.1038/ismej.2014.52
- van Houte, S., Ekroth, A. K. E., Broniewski, J. M., Chabas, H., Ashby, B., Bondy-Denomy, J., et al. (2016). The diversity-generating benefits of a prokaryotic adaptive immune system. *Nature* 532, 385–388. doi: 10.1038/nature17436
- Wang, H., Luo, H., Fallgren, P. H., Jin, S., and Ren, Z. J. (2015). Bioelectrochemical system platform for sustainable environmental remediation and energy generation. *Biotechnol. Adv.* 33, 317–334. doi: 10.1016/j.biotechadv.2015.04.003
- Widder, S., Allen, R. J., Pfeiffer, T., Curtis, T. P., Wiuf, C., Sloan, W. T., et al. (2016). Challenges in microbial ecology: building predictive understanding of community function and dynamics. *ISME J.* 10, 2557–2568. doi: 10.1038/ismej.2016.45
- Wolfe, B. E. (2018). Using cultivated microbial communities to dissect microbiome assembly: challenges, limitations, and the path ahead. *mSystems* 3:e161-17. doi: 10.1128/mSystems.00161-17
- Wolfe, B. E., Button, J. E., Santarelli, M., and Dutton, R. J. (2014). Cheese rind communities provide tractable systems for in situ and in vitro studies of microbial diversity. *Cell* 158, 422–433. doi: 10.1016/j.cell.2014.05.041
- Xie, Z. Q., and Tang, H. X. (2017). ISEScan: automated identification of insertion sequence elements in prokaryotic genomes. *Bioinformatics* 33, 3340–3347. doi: 10.1093/bioinformatics/btx433
- Yoshida, T., Jones, L. E., Ellner, S. P., Fussmann, G. F., and Hairston, N. G. (2003). Rapid evolution drives ecological dynamics in a predator-prey system. *Nature* 424, 303–306. doi: 10.1038/nature01767
- Yu, Z., Beck, D. A. C., and Chistoserdova, L. (2017). Natural selection in synthetic communities highlights the roles of *Methylococcaceae* and *Methylophilaceae* and suggests differential roles for alternative methanol dehydrogenases in methane consumption. *Front. Microbiol.* 8:2392. doi: 10.3389/fmicb.2017.02392
- Yu, Z., Krause, S. M. B., Beck, D. A. C., and Chistoserdova, L. (2016). A synthetic ecology perspective: how well does behavior of model organisms in the laboratory predict microbial activities in natural habitats? *Front. Microbiol.* 7:946. doi: 10.3389/fmicb.2016.00946
- Zankari, E., Hasman, H., Cosentino, S., Vestergaard, M., Rasmussen, S., Lund, O., et al. (2012). Identification of acquired antimicrobial resistance genes. *J. Antimicrob. Chemother.* 67, 2640–2644. doi: 10.1093/jac/dks261
- Zhang, J., Kobert, K., Flouri, T., and Stamatakis, A. (2014). PEAR: a fast and accurate Illumina Paired-End reAd mergeR. *Bioinformatics* 30, 614–620. doi: 10.1093/bioinformatics/btt593
- Zhou, F. F., and Xu, Y. (2010). cBar: a computer program to distinguish plasmid-derived from chromosome-derived sequence fragments in metagenomics data. *Bioinformatics* 26, 2051–2052. doi: 10.1093/bioinformatics/btq299
- Zomorodi, A. R., and Segre, D. (2016). Synthetic ecology of microbes: mathematical models and applications. *J. Mol. Biol.* 428, 837–861. doi: 10.1016/j.jmb.2015.10.019

Conflict of Interest Statement: The authors declare that the research was conducted in the absence of any commercial or financial relationships that could be construed as a potential conflict of interest.

Copyright © 2018 Cairns, Jokela, Hultman, Tamminen, Virta and Hiltunen. This is an open-access article distributed under the terms of the Creative Commons Attribution License (CC BY). The use, distribution or reproduction in other forums is permitted, provided the original author(s) and the copyright owner(s) are credited and that the original publication in this journal is cited, in accordance with accepted academic practice. No use, distribution or reproduction is permitted which does not comply with these terms.

Advantages of publishing in Frontiers



OPEN ACCESS

Articles are free to read
for greatest visibility
and readership



FAST PUBLICATION

Around 90 days
from submission
to decision



HIGH QUALITY PEER-REVIEW

Rigorous, collaborative,
and constructive
peer-review



TRANSPARENT PEER-REVIEW

Editors and reviewers
acknowledged by name
on published articles

Frontiers

Avenue du Tribunal-Fédéral 34
1005 Lausanne | Switzerland

Visit us: www.frontiersin.org

Contact us: info@frontiersin.org | +41 21 510 17 00



REPRODUCIBILITY OF RESEARCH

Support open data
and methods to enhance
research reproducibility



DIGITAL PUBLISHING

Articles designed
for optimal readership
across devices



FOLLOW US

@frontiersin



IMPACT METRICS

Advanced article metrics
track visibility across
digital media



EXTENSIVE PROMOTION

Marketing
and promotion
of impactful research



LOOP RESEARCH NETWORK

Our network
increases your
article's readership